VOLUME 64
NUMBER 1 / NUMÉRO 1
JANUARY / JANVIER
2007

An NRC Research Press
JOURNAL
Une REVUE des
Presses scientifiques du CNRC

Canadian Journal of FISHERIES AND AQUATIC SCIENCES

cjfas.nrc.ca

Journal canadien des SCIENCES HALIEUTIQUES ET AQUATIQUES

jcsha.cnrc.ca

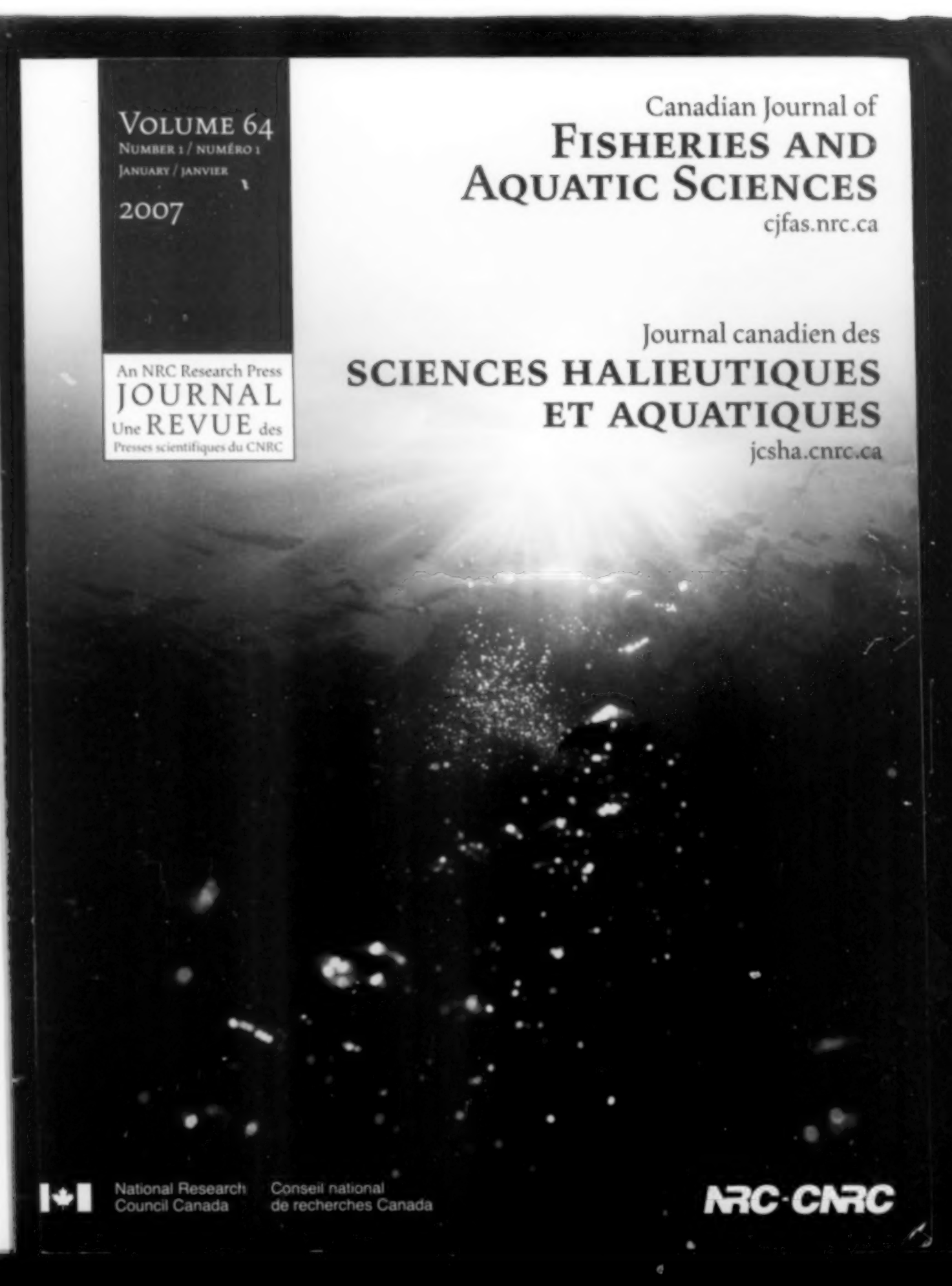

National Research Council Canada
Conseil national de recherches Canada

NRC·CNRC

ISSN 0706-652X / CJFSDX 64(1) 1–180 (2007)

The *Canadian Journal of Fisheries and Aquatic Sciences*, previously published as *Contributions to Canadian Biology* 1901–1925, *Contributions to Canadian Biology and Fisheries* 1926–1934, *Journal of the Biological Board of Canada* 1934–1937, and *Journal of the Fisheries Research Board of Canada* 1938–1979, is issued monthly to form annual volumes of 12 numbers plus supplements.

Editorial policy. The Journal publishes original research articles, perspectives (syntheses, critiques, reevaluations), discussions (comment and reply), and rapid communications. Manuscripts may concern cells, organisms, populations, communities, ecosystems, or processes that affect aquatic systems. They may cover a range of disciplines including biology and ecology of marine and freshwater organisms, limnology, oceanography, physiology, toxicology, genetics, economics, disease, and management. Preference will be given to manuscripts that emphasize understanding of observed phenomena and interpretation of experimental results. The Journal encourages papers that lead from clearly stated purpose or rationale and from testable hypotheses, concepts, or questions to identifiable conclusions or syntheses. Such papers may amplify, modify, question, or redirect accumulated knowledge embodied in contemporary perceptions of a particular state of aquatic sciences. The Journal discourages papers that are essentially descriptive, except in emerging disciplines; have only site-specific or local applications (a certain year, place, taxon, chemical compound, etc.); only confirm previously established principles; or apply standard techniques without breaking new methodological ground.

Manuscripts for publication should be submitted to the Editorial Office via NRC Research Press' online submission and peer review system (**OSPREY**) at http://pubs.nrc-cnrc.gc.ca/cjfas/osprey. Alternatively, manuscripts may be submitted to the Senior Editor, *Canadian Journal of Fisheries and Aquatic Sciences*, Department of Integrative Biology, Building #006, Room 118, University of Guelph, Guelph, ON N1G 2W1, Canada (519-824-4120 ext. 52646; fax: 519-767-9798; e-mail: cjfas@uoguelph.ca).

Submissions in either English or French are acceptable. The information must be original, that is, not copyrighted, published, or submitted elsewhere except in abstract form or unless by written consent of the Editor.

Correspondence concerning accepted manuscripts and corrected proofs should be sent to NRC Research Press, National Research Council of Canada, Ottawa, ON K1A 0R6, Canada (fax: 613-952-7656; e-mail: pubs@nrc-cnrc.gc.ca).

Instructions to Authors are published once a year in the first issue of each volume. Copies are available from NRC Research Press or at cjfas.nrc.ca. The **Publication Policy** of NRC Research Press is available at pubs.nrc-cnrc.gc.ca.

Microfilm. Issues from 1934 through the current volume can be purchased on 16- or 35-mm microfilm. Photocopies of individual articles or issues can be purchased from University Microfilms International, 330 North Zeeb Road, Ann Arbor, MI 48106, USA.

The *Canadian Journal of Fisheries and Aquatic Sciences*, ISSN 0706-652X, is published monthly, 12 times per year, by NRC Research Press, c/o USACAN Media Dist. Srv. Corp. at 26 Power Dam Way, Suite S1-S3, Plattsburgh, NY 12901, USA. Periodicals postage paid at Plattsburgh, NY. POSTMASTER: Send address changes to *Canadian Journal of Fisheries and Aquatic Sciences*, c/o NRC, P.O. Box 2888, Plattsburgh, NY 12901, USA.

Publié sans interruption depuis 1901, le *Journal canadien des sciences halieutiques et aquatiques* a paru sous plusieurs titres : *Contributions to Canadian Biology* 1901–1925, *Contributions to Canadian Biology and Fisheries* 1926–1934, *Journal of the Biological Board of Canada* 1934–1937, et *Journal of the Fisheries Research Board of Canada* 1938–1979. Le Journal paraît tous les mois, formant ainsi un volume de 12 numéros, et offre en plus jusqu'à deux suppléments par année.

Politique éditoriale. On publie, dans le Journal, des articles rendant compte de recherche originale, des perspectives (synthèses, critiques et réévaluations), des discussions (commentaires et réponses) et des communications rapides. Les documents peuvent porter sur les cellules, organismes, populations, communautés, écosystèmes ou processus qui affectent les systèmes aquatiques. Ils peuvent relever de divers domaines y compris la biologie et l'écologie des organismes marins et d'eau douce, la limnologie, l'océanographie, la physiologie, la toxicologie, la génétique, l'économie, la pathologie et la gestion. On accorde la préséance aux articles qui contribuent à la compréhension de phénomènes observés et à l'interprétation de résultats expérimentaux. On invite les auteurs à soumettre des articles ayant des objectifs précis ou relevant d'hypothèses, de concepts ou de questions vérifiables et se terminant par de solides conclusions ou d'utiles synthèses. Ces articles enrichissent, changent, mettent en question ou réorientent les connaissances acquises sur divers aspects des sciences aquatiques. On décourage toutefois la soumission d'articles simplement descriptifs (à moins qu'il ne s'agisse de nouvelles disciplines), d'application très limitée (applicables à une seule année, une seule région ou un seul taxon, portant sur un unique composé chimique, etc.); d'articles qui ne font que reprendre les principes énoncés dans des articles précédents; et d'articles rendant compte de l'application de normes sans gain de méthodologie.

Les auteurs sont invités à soumettre leur **manuscrit** au Bureau de la rédaction par le truchement du Système de soumission et d'examen en direct des articles (**OSPREY**) des Presses scientifique du CNRC à http://pubs.nrc-cnrc.gc.ca/jcsha/osprey. Sinon, ils peuvent transmettre leur manuscrit par la poste à la directrice scientifique principale, *Journal canadien des sciences halieutiques et aquatiques*, Département de biologie intégrative, édifice 006, bureau 118, University of Guelph, Guelph, ON N1G 2W1, Canada (519-824-4120 poste 52646; télécopieur : 519-767-9798; courriel : cjfas@uoguelph.ca).

Les contributions peuvent être en anglais ou en français. Elles doivent être originales, c.-à.-d. qu'elles ne doivent pas avoir fait l'objet d'un copyright, avoir été publiées ou soumises ailleurs, sauf sous forme abrégée ou avec le consentement du rédacteur. Le CNRC ne se tient en aucune façon responsable des opinions exprimées par un collaborateur ou des déclarations qui pourrait faire ce dernier.

La correspondance ayant trait aux manuscrits acceptés et les **épreuves corrigés** doivent être envoyées aux Presses scientifiques du CNRC, Conseil national de recherches du Canada, Ottawa, ON K1A 0R6, Canada (télécopieur : 613-952-7656; courriel : pubs@nrc-cnrc.gc.ca).

Les Recommandations aux auteurs sont publiées une fois par année dans le premier numéro de chaque volume. Des copies sont disponibles auprès du Bureau de la rédaction aux Presses scientifiques du CNRC ou au jcsha.cnrc.ca. **La Politique de publication** est disponible auprès des Presses scientifiques du CNRC ou au pubs.nrc-cnrc.gc.ca.

Microfilms. On peut acheter sur microfilms de 16 ou 35 mm tous les numéros depuis 1934. Des photocopies d'articles ou de numéros individuels sont aussi en vente auprès de University Microfilms International, 330 North Zeeb Road, Ann Arbor, MI 48106, É.-U.

This Journal is indexed or abstracted in / Cette revue est signalée ou résumée dans

ABSEARCH; Applied Science and Technology Index and Abstracts; Aquatic Sciences and Fisheries Abstracts; Biological Abstracts; Biological and Agricultural Abstracts; CAB Abstracts; Chemical Abstracts; Current Contents; Elsevier BIOBASE; Environmental Abstracts; ETDE Energy Database; General Science Index and Abstracts; GEOBASE; GeoRef; Life Sciences Collection; Meteorological and Geoastrophysical Abstracts; Oceanic Abstracts; PASCAL Database; Science Citation Index.

Volume 64, Number 1, January 2007

Canadian Journal of Fisheries and Aquatic Sciences

Published by the National Research Council of Canada

Volume 64, numéro 1, janvier 2007

Journal canadien des sciences halieutiques et aquatiques

Publié par le Conseil national de recherches du Canada

Senior Editor / Directrice scientifique principale **Moira M. Ferguson**

Editors / Directeurs

Jeffrey A. Hutchings, *Dalhousie University, Halifax*
Pierre Pepin, *Northwest Atlantic Fisheries Centre, DFO/MPO, St. John's, Newfoundland*
W. Gary Sprules, *University of Toronto at Mississauga*
Assistant to the Editors / Adjointe aux directeurs scientifiques **Holly Foster**

Associate Editors / Directeurs scientifiques associés

D. Boisclair, *Université de Montréal*
U. Borgmann, *Environment Canada, Burlington*
M.J. Bradford, *DFO/MPO and Simon Fraser University*
S.E. Campana, *DFO/MPO, Dartmouth*
R. Carignan, *Université de Montréal*
K.T. Frank, *DFO/MPO, Dartmouth*
J.W.A. Grant, *Concordia University*
M.M. Hansen, *Danish Institute for Fisheries Research, Silkeborg, Denmark*
R. Hilborn, *University of Washington*
D.F. Houlihan, *University of Aberdeen*
F.A. Huntingford, *University of Glasgow*
J.M. Jech, *NFSC/NOAA, Woods Hole, Mass.*
B. Jonsson, *Norwegian Institute for Nature Research, Oslo, Norway*
K.A. Kidd, *University of New Brunswick*
D.L. MacLatchy, *University of New Brunswick, Saint John*
P. Magnan, *Université du Québec à Trois Rivières*
C.T. Marshall, *University of Aberdeen*
R.B. Millar, *University of Auckland, New Zealand*
W.P. Patterson, *University of Saskatchewan*
Y.T. Prairie, *Université du Québec à Montréal*
T.J. Quinn II, *University of Alaska–Fairbanks, Juneau, Alaska*
T.P. Quinn, *University of Washington*
C.W. Ramcharan, *Laurentian University*
J.S. Richardson, *The University of British Columbia*
B. Sainte-Marie, *DFO/MPO, Mont-Joli*
R.E.H. Smith, *University of Waterloo*
S.J. Smith, *DFO/MPO, Dartmouth*
E.B. Taylor, *The University of British Columbia*
W.F. Vincent, *Université Laval*
R.D. Vinebrooke, *University of Alberta*
C.J. Walters, *The University of British Columbia*
B. de Young, *Memorial University of Newfoundland*

NRC Research Press / Presses scientifiques du CNRC

Fax / Télécopieur : 613-952-7656; e-mail / courriel : pubs@nrc-cnrc.gc.ca; URL / URL : pubs.nrc-cnrc.gc.ca
Editor-in-Chief / Directeur scientifique en chef **Bruce P. Dancik**
Assistant Editor-in-Chief / Adjoint au directeur scientifique en chef **Donald S. Mavinic**
Director / Directeur **Cameron D. Macdonald**

Business Manager / Gestionnaire des affaires commerciales **Jason Charron**
Advertising and reprints / Annonces publicitaires et tirés à part **Roxanne Landriault** 613-990-2254
Subscriptions / Abonnements **Eileen Evans-Nantais** 613-990-7873, **André Séguin** 613-993-9084

Manager, Journals Program / Gestionnaire du Programme des revues **Carolyn Brown**
Managing Editor / Rédactrice administrative **Cecily M. Pearson** 613-993-9099
Publication Officers / Agents de publication **Jennifer McColl, Thad Costigan**
Editorial Publication Assistant / Adjointe à la publication **Diana Leck**

Production Manager / Gestionnaire de la production **Brad Stoppa**
Production Application Support Technician / Technicienne au soutien de la production **Judy Hum**
Desktop Publishing Technician / Technicienne en éditique **Lisette Séguin**
Graphics Technician / Technicien en graphisme **Jeff Wisking**
Web Technician / Technicien Web **Dennis Cafferty**

The National Research Council of Canada accepts no responsibility for statements or opinions expressed by a contributor. Acceptance of an advertisement, announcement, or other material does not imply endorsement by either the Journal's Senior Editor or the National Research Council.

© National Research Council of Canada 2007. All rights reserved.

No part of this publication may be reproduced, stored, or transmitted in any form or by any means, without the written permission of the publisher, except as stated below.

The National Research Council of Canada grants **permission*** to individuals to make single copies of articles for personal use. Any person may reproduce short excerpts from articles in the journal for any purpose that respects the moral rights of authors, provided that the source is fully acknowledged. As a courtesy, the consent of authors of such material should be obtained directly from the author.

Authorization to reproduce items for other than personal use, as stated above, is granted by the National Research Council of Canada provided that the copyright fee of $7.00 per copy is paid directly to Access Copyright, The Canadian Copyright Licensing Agency, One Yonge Street, Suite 800, Toronto, ON M5E 1E5, Canada.

*The above permission does not extend to other kinds of copying, such as copying for general distribution, for advertising, or promotional purposes, for creating new collective works, or for resale. For such copying, arrangements must be made with the publisher, National Research Council of Canada, Ottawa, ON K1A 0R6, Canada.

Subscription information

The *Canadian Journal of Fisheries and Aquatic Sciences* (ISSN 0706-652X) is published monthly by the National Research Council of Canada. The 2007 annual subscription rates (second class postage) for Canada are $1051CAN institutional and $325CAN personal, for US & foreign $1051US institutional and $325US personal. For air mail add $150US to foreign rate. Canadian customers please include 6% GST (business no. 12149 1807 RT 0275). Subscriptions are entered for the calendar year. Remittances should be made payable to the Receiver General for Canada, credit NRC. Price for regular single issues: institutional, $110.00; personal, $35.00. Supplements will be priced separately. Special rates apply to members of Canadian scientific and engineering societies if they subscribe through their respective societies.

There are no refunds on cancelled subscriptions once delivery has begun. Claims for missing issues should be made within four months (North America) or six months (outside North America) following the date of publication. The publisher expects to supply missing issues only when losses have occurred in transit and when the reserve stock will permit. For change of address and subscription enquiries: Subscription Office, NRC Research Press, National Research Council of Canada, Ottawa, ON K1A 0R6, Canada; tel.: 613-993-9084; fax: 613-952-7656; e-mail: pubs@nrc-cnrc.gc.ca.

Microform backfiles are available from UMI, P.O. Box 1346, Ann Arbor, MI 48106-1346, USA, and Micromedia Ltd., 20 Victoria St., Toronto, ON M5C 2N8, Canada.

All issues of the *Canadian Journal of Fisheries and Aquatic Sciences* since 1996 are available on the Web. Pricing information can be found at pubs.nrc-cnrc.gc.ca.

Le Conseil national de recherches du Canada ne se tient en aucune façon responsable des opinions exprimées par un collaborateur ou des déclarations que pourrait faire ce dernier. La publication d'annonces publicitaires, d'avis et autres n'implique pas l'endossement de leur contenu par la directrice principale de la Revue ou le CNRC.

© Conseil national de recherches du Canada 2007. Tous droits réservés.

Il est interdit de reproduire, de sauvegarder ou de transmettre quelque partie de la présente publication dans quelque format ou de quelque façon sans le consentement écrit de l'éditeur, à l'exception des conditions suivantes.

Le Conseil national de recherches du Canada accorde aux particuliers le droit de faire des copies individuelles pour leur usage personnel. Toute personne peut reproduire de courts extraits des articles de la Revue pour autant que les droits moraux de l'auteur soient respectés et que la mention de provenance soit clairement indiquée. Il est de convenance de demander le consentement de l'auteur avant de faire mention de son travail.

On obtiendra l'autorisation de reproduire des articles à d'autres fins que l'usage personnel (tel qu'on l'a décrit ci-dessus) auprès du Conseil national de recherches du Canada pour autant que des redevances de droits d'auteurs de 7,00 $/copie soient versées au Access Copyright, The Canadian Copyright Licensing Agency, 1, rue Yonge, bureau 800, Toronto, ON M5E 1E5, Canada.

*La permission ci-dessus ne s'applique pas à la reproduction à grande échelle, telle que la reproduction aux fins de distribution générale, publicitaire ou promotionnelle, de compilation de nouveaux ouvrages collectifs ou de revente. Dans de tels cas, il faudra ratifier une entente particulière avec l'éditeur, le Conseil national de recherches du Canada, Ottawa, ON K1A 0R6, Canada.

Renseignements sur l'abonnement

Journal canadien des sciences halieutiques et aquatiques (ISSN 0706-652X) est une publication mensuelle du Conseil national de recherches du Canada. Le prix de l'abonnement annuel en 2007 au Canada (courrier de deuxième classe) est de 1051 $CAN pour les organismes et de 325 $CAN pour les particuliers. À l'étranger (y compris les É.-U.), le prix de l'abonnement est de 1051 $US pour les organismes et de 325 $US pour les particuliers. L'expédition par avion exige des frais de 150 $US en sus du prix d'abonnement à l'étranger. Les clients du Canada doivent ajouter la TPS de 6 % (numéro d'entreprise 12149 1807 RT 0275). Les abonnements sont pour l'année civile. Tout paiement doit être adressé au Receveur général du Canada, crédit du CNRC. Le prix par numéro est de 110 $ pour les organismes et de 35 $ pour les particuliers. Le prix des hors-série varie. Les membres des sociétés canadiennes de sciences et de génie bénéficient de taux préférentiels en s'abonnant via leurs sociétés respectives.

Aucun remboursement ne sera accordé ni aucune annulation acceptée une fois que les livraisons auront commencé. Les réclamations de numéros manquants devront être soumises dans les quatre mois (Amérique du Nord) ou dans les six mois (à l'extérieur de l'Amérique du Nord) suivant la date de publication. L'éditeur ne fournira de numéros manquants que si le document a été perdu pendant l'expédition et que si le stock le permet. Adressez tout changement d'adresse ou toute question quant à l'abonnement au : Bureau des abonnements, Presses scientifiques du CNRC, Conseil national de recherches Canada, Ottawa, ON K1A 0R6, Canada; téléphone : 613-993-9084; télécopieur : 613-952-7656; courriel : pubs@nrc-cnrc.gc.ca.

On peut obtenir les fichiers rétrospectifs sur **microforme** auprès de UMI, P.O. Box 1346, Ann Arbor, MI 48106-1346, É.-U., et auprès de Micromedia Ltée, 20, rue Victoria, Toronto, ON M5C 2N8, Canada.

À partir de 1996, tous les numéros de *Journal canadien des sciences halieutiques et aquatiques* sont accessibles sur le Web. On trouvera des renseignements sur les tarifs à pubs.nrc-cnrc.gc.ca.

RAPID COMMUNICATION / COMMUNICATION RAPIDE

Shaking and moving: low rates of sediment transport trigger mass drift of stream invertebrates

Chris Gibbins, Damià Vericat, Ramon J. Batalla, and Carlos M. Gomez

Abstract: During floods, river invertebrates may be swept downstream in large numbers. This so-called "catastrophic drift" leads to a major redistribution of animals, as well as reduced fitness and increased mortality among drifters. We present the first field evidence of the role of sediment movement in triggering catastrophic drift. Experiments indicate that the loss of invertebrates from the bed becomes exponential when shear stress reaches the threshold that entrains bedload. However, we found that low rates of bedload are sufficient to rapidly denude patches of riverbed of their invertebrates and so trigger mass drift. Such low bedload rates occur during small floods. As small floods occur frequently, our results suggest that episodes of catastrophic drift are frequent. This conclusion is counterintuitive, as the persistence of invertebrate communities on riverbeds suggests that such events cannot be truly catastrophic. Moreover, the drift losses that we observed occurred in the absence of significant geomorphic disturbance; this is inconsistent with the notion of catastrophic drift being a response to hydrological disturbance events. We argue that a new definition of catastrophic drift is needed, a definition based not on drift magnitude or the triggering role of sediment movement, but on the population consequences of downstream displacement.

Résumé : Durant les crues, les invertébrés des rivières peuvent être entraînés en grand nombre vers l'aval. Cette prétendue « dérive catastrophique » cause une redistribution importante des animaux, tout en réduisant la fitness et augmentant la mortalité des organismes dans la dérive. Nous présentons les premières données de terrain sur le rôle du déplacement des sédiments dans le déclenchement de la dérive catastrophique. Nos expériences indiquent que la perte d'invertébrés dans le lit de la rivière devient exponentielle lorsque la force d'arrachement atteint le seuil au-delà duquel se produit un entrainement de la charge de fond. Cependant, des valeurs faibles de charge de fond suffisent à dégarnir rapidement certaines surfaces de fond de rivière de leurs invertébrés et ainsi à déclencher une dérive massive. De telles faibles valeurs de charge de fond se produisent lors de crues de moindre importance. Comme ces petites crues ont lieu fréquemment, nos résultats indiquent que la dérive catastrophique est un phénomène commun. Une telle conclusion semble contredire la perception courante, puisque la persistance des communautés d'invertébrés dans le lit des rivières laisse croire que de tels événements ne peuvent être vraiment catastrophiques. De plus, les pertes dues à la dérive que nous observons se produisent en l'absence d'importantes perturbations géomorphologiques; cela ne s'accorde pas avec l'idée que la dérive catastrophique est une réaction à des événements de perturbation hydrologique. Nous croyons qu'il est nécessaire de redéfinir la notion de dérive catastrophique et de donner une définition qui ne soit pas basée sur l'importance de la dérive, ni sur le rôle déclencheur des déplacements des sédiments, mais sur les conséquences démographiques des mouvements vers l'aval.

[Traduit par la Rédaction]

Flood disturbances and catastrophic drift

Periodic extreme events, whether they are hurricanes, fires, or avalanches, play an important role in structuring ecosystems (Sousa 1984). Depending on their magnitude, frequency, duration, and timing, such "disturbance" events influence diversity across a number of spatial and temporal scales. Floods are an obvious source of disturbance for river animals. Conse-

Received 15 September 2006. Accepted 15 December 2006. Published on the NRC Research Press Web site at http://cjfas.nrc.ca on 13 January 2007.
J19538

C. Gibbins.[1] Department of Geography and Environment, University of Aberdeen, Aberdeen, Scotland.
D. Vericat. Forestry and Technology Centre of Catalonia, Solsona, Spain.
R.J. Batalla. Department of Environment and Soil Sciences, University of Lleida, Lleida, Spain.
C.M. Gomez. Department of Economics and Economic History, University of Alcalá, Madrid, Spain.

[1]Corresponding author (e-mail: c.gibbins@abdn.ac.uk).

 doi:10.1139/F06-181 © 2007 NRC Canada

quently, there has been much interest in trying to understand the links between the frequency of flood events of different magnitude and patterns in diversity (Resh et al. 1988).

For small animals such as invertebrates, the implications of a major flood are not difficult to envisage: individuals may be scoured from the riverbed and carried downstream in large numbers (Bond and Downes 2003). The term "catastrophic drift" is used widely to characterise this phenomenon (Giller and Malmqvist 1998). The movement of sediment that occurs during large floods (its entrainment and downstream transport) is thought to be the trigger that initiates catastrophic drift (Brittain and Eikeland 1988). Although this is not a controversial hypothesis, the difficulty of undertaking detailed experiments during flood conditions has meant that empirical supporting evidence is lacking. Many studies have monitored drift during periods of elevated discharge and correlated drift rates or densities to either reach discharge or velocity at drift net positions. Because the point on the streambed from which the drifting animals originate is not known, such studies cannot be used to make inferences about the processes triggering their entry into the water column. Understanding these processes is important because it helps distinguish between hydrological events that represent ecological disturbances (those resulting in so-called catastrophic drift) and those that do not. We designed a set of field experiments using a novel portable flume to assess (*i*) whether sediment movement triggers a sudden and dramatic increase in drift and (*ii*) the rates of sediment transport sufficient to cause this increase.

Experimental design

We constructed a portable flume that permits manipulation of flow hydraulics in situ within natural river channels (Fig. 1; also see caption for details of flume operation). The flume allowed us to recreate the conditions found during small floods, but over carefully selected patches of riverbed. We used the flume to manipulate hydraulics over 27 patches of relatively fine bed material (sands and fine gravels) distributed across a 150 m reach of an upland gravel-bed river (Ribera Salada, northeastern Spain). These patches are the principal source of bedload material transported in gravel-bed rivers during the low-magnitude, high-frequency flood events (e.g., Garcia et al. 1999), whose hydraulics we recreated in the flume.

Experiments were undertaken on four dates between January and April 2006. On each date, discharge was always stable and less than the reach median flow. We first placed the flume over a selected patch, with the doors in their normal position (doors parallel with flume sides; no manipulation of hydraulic conditions inside the flume). Hydraulic conditions (depth and velocity at 0.2 and 0.4 × depth), bedload transport rate, and drift losses were then measured inside the flume over a 15-min period. Bedload and any animals mobilised from the bed were captured in a drift net fixed to the downstream end of the flume. The doors were then opened, manipulating hydraulic conditions inside the flume; depth, velocity, loss of animals, and bedload transport were monitored again. We also sampled drift 2 m upstream from the flume during each experiment; this was the closest possible distance upstream from the flume for positioning a drift net without reducing the velocity of the water entering the flume. These samples provided data on the number of animals entering the flume from upstream and so allowed us to calculate the loss of invertebrates from the bed of the flume for each experiment (loss from flume bed per minute = number captured in the net at the downstream end of the flume minus the number captured at the upstream net). Velocity data were used to calculate boundary shear stress using the equation given by Whiting and Dietrich (1990). Across the 27 experimental patches, the mean increase in velocity resulting from opening the flume doors was 80% at 0.4 × depth and 120% at 0.2 × depth. The average increment in shear stress was almost 400%, with a maximum value of 40.57 dynes·cm^{-2}.

To set the loss of animals from the bed in the context of benthic density, we sampled the benthos at 14 random points across the reach using a Surber sampler. Results from flume experiments were also compared with long-term data on discharge and bedload transport in the study reach (Helley-Smith sampler; 76 mm intake) (Batalla et al. 2005). A small flood occurred in the Ribera Salada during the period of flume experiments (5 m^3·s^{-1}, the flow equalled or exceeded 10% of time in the river). Data on discharge, bedload transport rate, and size of bedload material transported during this flood were also collected at an upstream monitoring site (bedload sampled using two pit traps) and compared with those from the flume experiments.

Statistical analysis

To avoid zero values in the bedload data, a value of 10^{-9} was added to each value. This transformed zeros into positive values without distorting observations. In addition, to avoid the negative values in the observations of number of animals (i.e., more animals entering the flume from upstream than were lost from it) and to guarantee the existence of logarithms, data were rescaled by adding a constant of 3. Apart from making possible the estimation of the exponential model, this transformation does not have any effect on the regression coefficients; an upward movement of the dependent variable does not affect the marginal effects of changes in the explanatory variable over the dependent variable or any other statistical property of the model.

The goodness of fit of statistical relations between boundary shear stress, bedload rates, and number of animals lost from the flume bed was assessed using maximum likelihood estimators (MLEs) and *P* values (NLOGIT software, version 3.0; Econometric Software Inc. 2003). In each case, exponentials provided the best fit to the data (significant *P* and highest MLEs).

To find a critical value of the boundary shear stress above which the number of animals increases in a significant way (i.e., the breakpoint), we used a method based on spline regressions of the exponential model (see Marsh and Cormier (2002) for more details on spline regressions). As the breakpoint is unknown, the usual procedure consists of trying all alternatives available in the range of the spline variable and, once robust regression coefficients are obtained, selecting the proper model by using the MLE as the goodness of fit criteria.

© 2007 NRC Canada

Fig. 1. Flume used to manipulate hydraulic conditions over patches of streambed in the study reach. Flow is from left to right. The wooden doors used to manipulate hydraulic conditions inside the flume are shown here in their open position. In their normal position, these doors lay parallel to the transparent side walls. The drift net (1 mm mesh) attached at the downstream end of the flume is visible. The flume dimensions (1 m length × 0.5 m width) resulted in hydraulics over a 0.5 m^2 area of bed being manipulated. The stage board used to measure water depth inside the flume and the disk weights used to secure the flume in place can be seen in the photograph. A Valeport electromagnetic flow meter, positioned over the centre of the manipulated area and secured using brackets across the top of the flume, was used to measure velocities inside the flume.

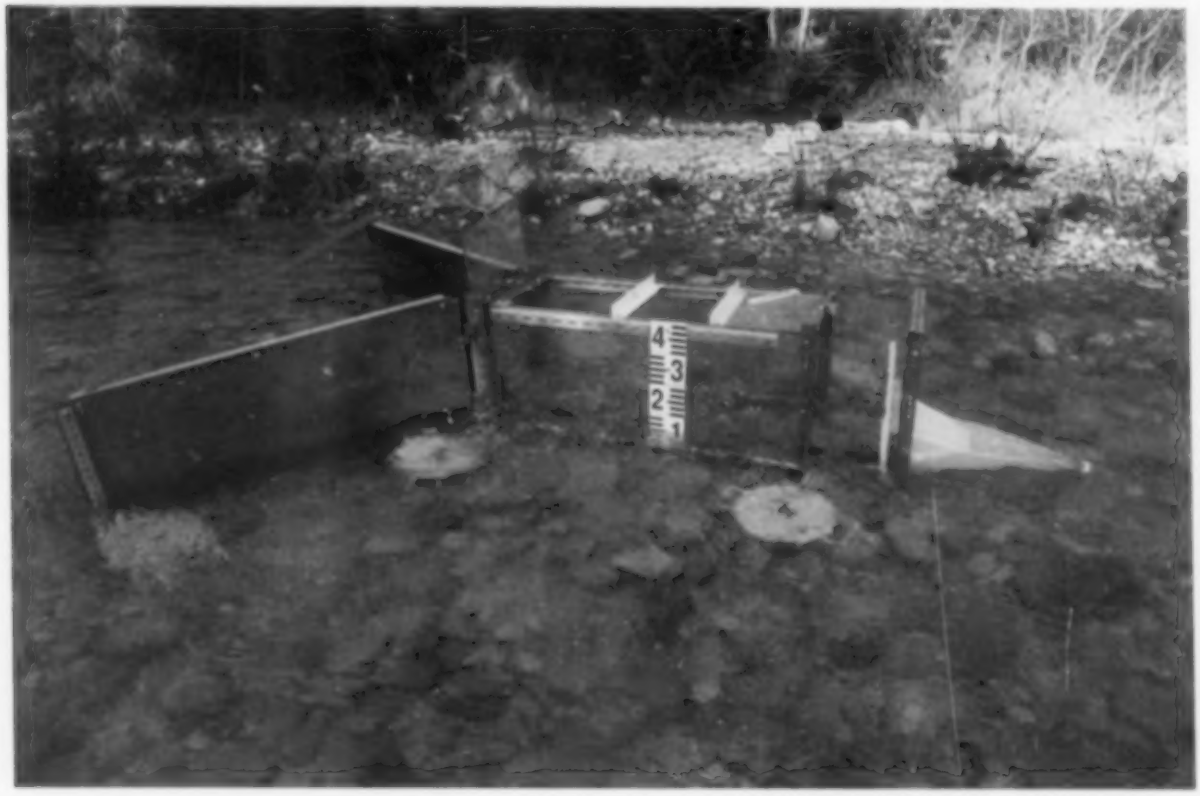

Hydraulics and the loss of sediment and invertebrates from the bed

An exponential curve best represented the relationship between the loss of animals from the experimental patches and boundary shear stress (Fig. 2). The spline regression procedure indicated that the breakpoint of the curve occurred at a value between 8.88 and 9.13 dynes·cm^{-2}; greater precision is not possible because of the lack of sample observations between these values. Thus, data indicate that invertebrate drift became exponential once shear stress reached a value of ~9 dynes·cm^{-2}. This shear value is coincident with the critical shear stress for entrainment of sediment from the patches (at <9 dynes·cm^{-2}, bedload was consistently 0; at >9 dynes·cm^{-2}, it was consistently >0). An exponential curve also provided the best fit to the relation between bedload transport and loss of animals (Fig. 2, inset). The break in this relation occurred as soon as sediment transport was initiated (i.e., at the minimum significant measured bedload rate (0.02 g·m^{-1}·s^{-1})). Results of the experiments therefore indicate that once boundary shear stress reaches a critical value, the process of sediment transport begins and the loss of invertebrates from the streambed becomes exponential. As species differ in their susceptibility to dislodgement, the species composition of the benthos may influence the precise statistical form of a drift – shear stress relationship. Dominant taxa in particular may shape the drift response curve. Thus, we do not anticipate the exponents for the equation given in the caption to Fig. 2 to be directly transferable to other locations with other faunas.

Although the existence of strong relationships between boundary shear stress, bedload transport, and invertebrate drift was not surprising, the very low rate of sediment transport that was sufficient to trigger a large-scale loss of animals from the bed was unexpected. The maximum instantaneous bedload transport rate that we created in the flume (6.6 g·m^{-1}·s^{-1}) represents a very low rate (e.g., Parker et al. 1982). At this rate, we found entrainment of invertebrates equivalent to a loss from the bed of 80 animals·m^{-2}·min^{-1} compared with the average benthic density of 882 (standard deviation, SD = 617) animals·m^{-2} across the reach. This indicates that complete depletion of invertebrates from a typical patch could occur within approximately 10 min. This depletion results in high and exponentially increasing drift

© 2007 NRC Canada

Fig. 2. Bedload transport rate (□) and the loss of animals (■) from experimental patches of streambed across the range of boundary shear stress values. The inset shows the relation between bedload transport and the loss of animals from the bed. Exponential curves best represented the relation between shear and the loss of animals (number lost per minute = $(2.12e^{0.08\text{shear}}) - 3$, $r^2 = 0.51$, $P < 0.0001$) and between bedload and the loss of animals (number lost per minute = $(3.04e^{0.43\text{bedload}}) - 3$, $r^2 = 0.33$, $P < 0.0001$). Note that the "– 3" in the equations is related to the transformation of the number of aanimals used to avoid negative values (see Statistical analysis for more details). An exponential curve also best represented the relation between shear stress and bedload transport rate (bedload = $0.235e^{0.08\text{shear}}$, $r^2 = 0.67$, $P < 0.0001$), although for clarity this curve is not shown in the figure. The break in slope of the exponential fitted to the shear stress vs loss of animals data is shown by the dotted vertical line in the main part of the figure.

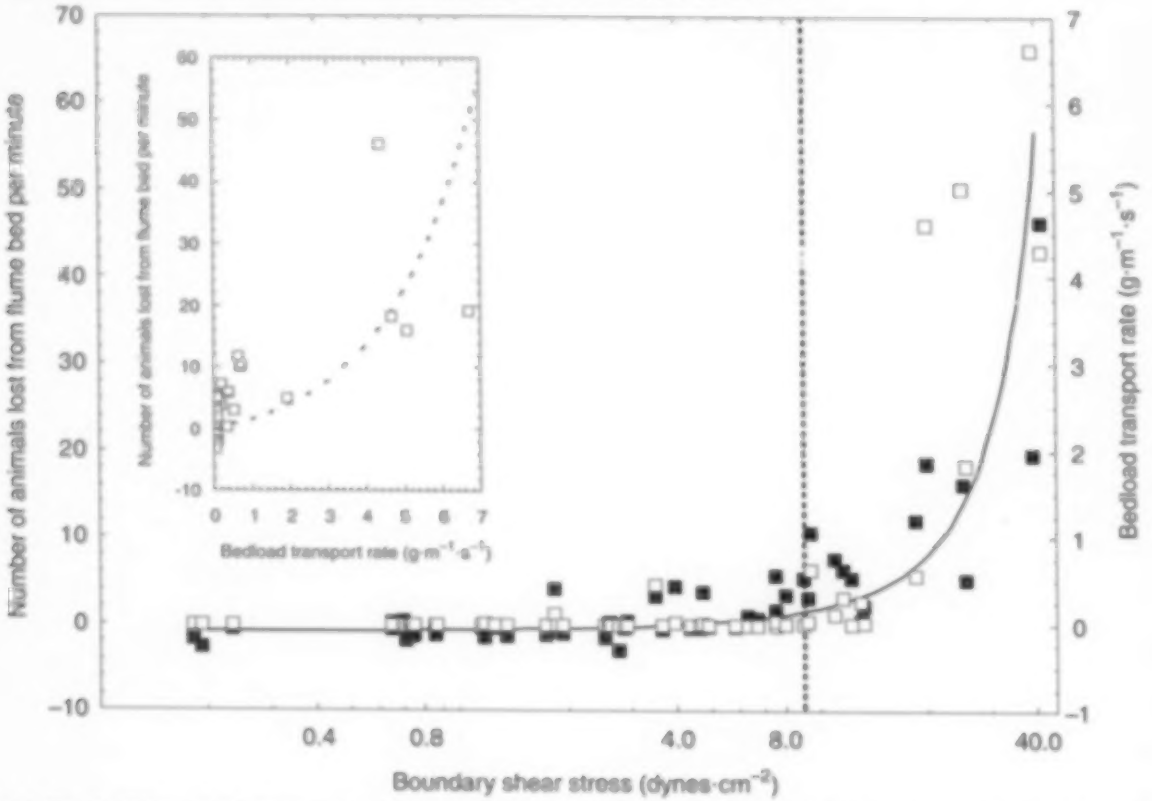

(as per Fig. 2). This and the trigger of sediment movement are consistent with current definitions of catastrophic drift (Brittain and Eikeland 1988).

Fortuitously, the flood that occurred during the period of experimentation produced hydraulic conditions and bedload transport rates similar to those of the flume manipulations. Manipulated flume velocities (0.4 × depth) averaged 0.96 m·s^{-1}, with a maximum of 2.14 m·s^{-1}; during the flood, velocities averaged 1.5 m·s^{-1}. Bedload transport rates during the flood were measured at 9.7 and 2.04 g·m^{-1}·s^{-1} in the two pit traps; material in the traps had median sizes of 1.1 and 4.6 mm compared with a mean of 1.4 mm in the flume experiments. On this basis, we conclude that conditions and associated drift losses created by the flume are typical of small, frequent floods in the reach. In turn, this suggests that large-scale loss of animals from patches of fine material occurs regularly, rather than being a rare phenomenon associated only with major floods.

Is this drift catastrophic?

At low shear stresses (<9 dynes·cm^{-2}), we observed little drift loss from the bed; here we assume that drift losses represent voluntary or background drift. A number of processes may have contributed to the increased drift at >9 dynes·cm^{-2}. Animals on exposed surfaces may have been sheared from the bed, whereas those on sediments being transported downstream may have been unable to hold on and so were thrown into the water column. However, as rates of sediment transport were so low, the latter process seems unlikely to be able to account for the high drift losses from the bed. When shear stress reaches the critical threshold for entraining the fine material present in a given patch, larger particles shake and, in some cases, "dance" on the bed. We observed this in the flume, and it is well known from previous studies (Carling et al. 1992). The likelihood of animals losing their foothold on sediment that is shaking or dancing is increased. Consequently, even though larger material may not be experiencing motion, its instability is likely to contribute to drift. This may explain why such high drift losses occurred from the patches; losses resulted from sediment instability created by a combination of the shaking and transport of material. Imbert and Perry (2000) found large (30-fold) increments in drift at discharges that were insufficient to result in sediment

© 2007 NRC Canada

transport. However, they made no reference to whether sediment was being agitated at these discharges. Our results indicate not only that drift losses from patches are correlated with rates of sediment transport (where transport is defined as the net downstream movement of material), but also that drift can also occur when sediment is being agitated rather than being transported downstream.

The principal contribution of our work is to show the precise form of the relations between shear stress, sediment loss, and drift from the bed of a natural, gravel-bed river, and the flood magnitude necessary to initiate mass drift. The results raise some fundamental questions as to the meaning of catastrophic drift and, in terms of river invertebrate communities, ideas of "catastrophe" and "disturbance". Low-magnitude, high-frequency flood events appear to be sufficient to trigger a dramatic loss of animals from the patches of fine sediment characteristic of gravel-bed rivers around the world. Hence, at the patch scale, episodes of drift of this magnitude are likely to be occurring frequently in such rivers. Bankfull discharge (the discharge high enough to inundate the full width and depth of a river channel) is generally needed before the coarse layer is entrained from the bed surface. In the study reach, this discharge is approximately 10 $m^3 \cdot s^{-1}$ (Batalla et al. 2005), twice as high as the natural flood that occurred during the flume experiments. Once the coarse surface layer is removed, geomorphic disturbance of a river reach results from the high rates of sediment transport that occur across the reach as a whole. Our results indicate that what is routinely labelled as catastrophic drift can occur at discharges well below those that result in such reach-scale geomorphic disturbance. Thus, there appears to be a mismatch in the relation between disturbance and catastrophe as used to represent the geomorphic (sediment transport) and associated ecological (invertebrate drift) impacts of floods.

For invertebrates entrained in the water column along with mobilised sediment, the risk of injury is likely to be much greater than that experienced by those drifting for behavioural reasons in low-flow conditions. Consequently, sediment movement may be more important than simply the physical mechanism that triggers a dramatic increase in drift: it may affect the survival or subsequent reproductive capacity of animals carried downstream. Current definitions of catastrophic drift (Brittain and Eikeland 1988; Giller and Malmqvist 1998) are based on the role of physical disturbance processes such as sediment movement and focus on drift magnitude to distinguish between catastrophic drift and non-catastrophic drift. Our results illustrate problems with such definitions: they show that extremely high drift losses can occur in conditions that hydrologists and geomorphologists would not consider to be disturbance.

Catastrophic drift is better defined in terms of the fate of those animals swept downstream. This requires long-term population studies, studies that present some very difficult methodological problems. Until such studies can be undertaken, the term "mass drift" is more appropriately used to describe the increases in drift associated with periods of elevated discharge, because it is not dependent on a theoretical match between disturbance and catastrophe. The results of our experiments raise sufficiently important questions to suggest that similar work should be undertaken in other river types, types in which sediment size characteristics and discharge – sediment transport relations differ from those of the Ribera Salada. Such studies should monitor simultaneously the drift losses from patches of fine sediments and those with a coarse surface layer.

Acknowledgements

The authors acknowledge the Leverhulme Trust for funding the work described in this paper. Damià Vericat was employed by research grants from the Spanish Ministry of Education and the Catalan Foundation for Research and Innovation during 2005 and 2006, respectively. Pit traps for bedload were constructed and are operated in the framework of the SESAM Project funded by the DGF German Science Foundation. We thank Dubrovka Pokrajac and Lorna Campbell for suggestions that helped improve the operation of the flume. The revisions of two anonymous reviewers greatly improved the final version of the manuscript.

References

Batalla, R.J., Garcia, C., and Balasch, J.C. 2005. Total sediment load in a Mediterranean mountainous catchment (the Ribera Salada River, Catalan Pre-Pyrenees, NE Spain). Z. Geomorphol. **49**(4): 495–514.

Bond, N.R., and Downes, B.J. 2003. The independent and interactive effects of fine sediment and flow on benthic invertebrate communities characteristic of small upland streams. Freshw. Biol. **48**: 455–465

Brittain, J., and Eikeland, T.J. 1988. Invertebrate drift — a review. Hydrobiologia, **166**: 77–93.

Carling, P., Kelsey, A., and Glaister, M.S. 1992. Effect of bed roughness, particle shape and orientation on initial motion criteria. *In* Dynamics of gravel-bed rivers. *Edited by* P. Billi, R.D. Hey, C.R. Thorne, and P. Tacconi. Wiley and Sons, Chichester, UK. pp. 23–41.

Econometric Software Inc. 2003. NLOGIT software. Version 3.0. Econometric Software Inc., Plainview, N.Y.

Garcia, C., Laronne, J.B., and Sala, M. 1999. Variable source areas of bedload in a gravel-bed stream. J. Sed. Res. **69**(1): 27–31.

Giller, P.S., and Malmqvist, B. 1998. The biology of streams and rivers. Oxford University Press, Oxford, UK.

Imbert, J.B., and Perry, J.A. 2000. Drift and benthic responses to stepwise and abrupt increases in non-scouring flow. Hydrobiologia, **436**: 191–208.

Marsh, L., and Cormier, D. 2002. Spline regression models. Sage Publications Inc., Thousand Oaks, California.

Parker, G., Klingeman, P.C., and McLean, D.G. 1982. Bedload and size distribution in paved gravel bed streams. J. Hydr. Div. ASCE, **108**: 544–571.

Resh, V.H., Brown, A.V., Covich, A.P., Gurtz, M.E., Li, H.W., Minshall, G.W., Reice, S.E., Sheldon, A.L., Wallace, J.B., and Wizmar, R. 1988. The role of disturbance in stream ecology. J. North Am. Benthol. Soc. **7**: 433–455

Sousa, W.P. 1984. The role of disturbance in natural communities. Annu. Rev. Ecol. Syst. **15**: 353–391.

Whiting, P.J., and Dietrich, W.E. 1990. Boundary shear stress and roughness over mobile alluvial beds. J. Hydr. Eng. **116**: 1495–1511.

© 2007 NRC Canada

Tracking seasonal migrations of redfish (*Sebastes* spp.) in and around the Gulf of St. Lawrence using otolith elemental fingerprints

Steven E. Campana, Alexandra Valentin, Jean-Marie Sévigny, and Don Power

Abstract: Large concentrations of beaked redfish (*Sebastes mentella* and *Sebastes fasciatus*) overwinter in the Cabot Strait and the approaches of the Gulf of St. Lawrence each year. Synoptic research vessel surveys indicate that redfish are distributed more widely in the summer than in the winter, particularly within the Gulf. Significant differences in the trace element composition of the otolith ("otolith elemental fingerprint") were observed among summer aggregations, indicating that the aggregations maintained some degree of separation while in the Gulf. *Sebastes mentella* and *S. fasciatus* were readily distinguished based on otolith elemental fingerprints. Using the elemental fingerprints of the summer samples as a natural tag, we found that *S. mentella* tended to move out of the Gulf in the winter. Aggregations of *S. mentella* found in the east during the summer were not found in our winter collections. The elemental fingerprints of *S. mentella* from the Saguenay Fjord were clearly distinct from redfish further east in the Gulf of St. Lawrence, indicating that this group had been separated from other redfish for much of their life. The implications of our findings extend not only to the fisheries management of redfish, but also to the extent of movement expected of deep-water fish species.

Résumé : Chaque année, de grands rassemblements de sébastes (« beaked redfish », *Sebastes mentella* et *S. fasciatus*) passent l'hiver dans le détroit de Cabot et les abords du golfe du Saint-Laurent. Des inventaires synoptiques faits par des navires de recherche indiquent que les sébastes ont une répartition plus étendue en été qu'en hiver, particulièrement dans le golfe. On observe des différences significatives dans la composition en éléments en traces des otolithes (« signature des éléments dans les otolithes ») dans les regroupements d'été, ce qui indique que ces regroupements maintiennent un certain degré de séparation pendant leur séjour dans le golfe. *Sebastes mentella* et *S. fasciatus* se distinguent clairement d'après la signature des éléments en traces dans leurs otolithes. En utilisant la signature des éléments des échantillons d'été comme étiquettes naturelles, nous découvrons que *S. mentella* a tendance à quitter le golfe pendant l'hiver. Les regroupements de *S. mentella* trouvés dans l'est durant l'été ne se retrouvent pas dans nos récoltes d'hiver. Les signatures des éléments des *S. mentella* du fjord du Saguenay sont nettement distinctes de celles des sébastes vivant plus à l'est dans le golfe du Saint-Laurent, ce qui indique que les sébastes du Saguenay ont été séparés des autres sébastes pour une grande partie de leur vie. Les conséquences de nos observations affectent non seulement la gestion des pêches de sébastes, mais elles concernent aussi l'importance des déplacements attendus chez les espèces de poissons d'eau profonde.

[Traduit par la Rédaction]

Introduction

The migration patterns of marine fish populations are less understood than the spawning migrations of anadromous fish such as salmon, but the influence on their population dynamics may be just as important. In response to spawning, feeding, or predator avoidance cues, marine fish migrations can extend over scales as small as a few kilometres in the case of flatfish moving offshore to overwinter (MacDonald et al. 1984) to thousands of kilometres for bluefin tuna crossing the North Atlantic (Lutcavage et al. 1999). The extent and timing of these often-annual migrations are generally both consistent and predictable within a given population, suggesting an evolutionary advantage. However, the exact nature of the survival advantage, as well as the migratory route and destination, are often poorly understood, in

Received 22 March 2006. Accepted 29 September 2006. Published on the NRC Research Press Web site at http://cjfas.nrc.ca on 10 January 2007.
J19239

S.E. Campana.[1] Bedford Institute of Oceanography, Fisheries and Oceans Canada, P.O. Box 1006, Dartmouth, NS B2Y 4A2, Canada.
A. Valentin. Institut des sciences de la mer de Rimouski, Université du Québec à Rimouski, 310, Allée des Ursulines, Rimouski, QC G5L 3A1, Canada.
J.-M. Sévigny. Institut Maurice-Lamontagne, Pêches et Océans Canada, 850 Route de la Mer, Mont-Joli, QC G5H 3Z4, Canada.
D. Power. Science Branch, Fisheries and Oceans Canada, P.O. Box 5667, St. John's, NL A1C 5X1, Canada.

[1]Corresponding author (e-mail: campanas@mar.dfo-mpo.gc.ca).

 doi:10.1139/F06-162 © 2007 NRC Canada

part due to the technical limitations associated with tracking the movements of millions of fish deep beneath the ocean's surface.

Although our understanding of marine fish migrations in the surface layers of the ocean requires improvement, it is immensely better than our understanding of the movements of deep-sea fishes. Excluding diel vertical migrations, which have been well documented (Gauthier and Rose 2002), large-scale seasonal migrations have not been reported in deep-sea fishes (Beamish et al. 2005). The absence of reports could be due to the sedentary nature of deep-sea fishes, but a more likely cause is the lack of study. Deep-sea fishes are very difficult to track in situ, largely because of the difficulties involved in bringing deepwater fishes to the surface for tagging (Starr et al. 2000). In the handful of studies reporting deep-sea migrations, reproduction and (or) feeding have been suggested as proximal causes in most (Kuo and Tanaka 1984; Duarte et al. 2001).

Acadian redfish (*Sebastes fasciatus*) and deepwater redfish (*S. mentella*) are members of a species complex of beaked redfish that form large aggregations in cold, deep water off the eastern coast of Canada, particularly in the Gulf of Maine, along the Scotian Shelf, off the shelf edge of Newfoundland, and into the Gulf of St. Lawrence (Atkinson 1987). The species can be exceedingly difficult to identify, requiring either dissection of the swimbladder musculature or genetic assay or both for confident identification (Ni 1981; Gascon 2003; Valentin et al. 2006). Hybridization of the sympatric species has also been reported (Rubec et al. 1991; Desrosiers et al. 1999; Roques et al. 2001). *Sebastes fasciatus* and *S. mentella* are common in the Gulf of St. Lawrence, where they often form large sympatric aggregations that are the targets for a year-round mixed-species commercial fishery (Atkinson 1987; Gascon 2003).

Unlike many marine fishes, redfish are internally fertilized and ovoviviparous, mating in late fall or early winter and extruding their live young in late spring and early summer (Atkinson 1987; St-Pierre and de Lafontaine 1995). The locations of mating and extrusion are not necessarily the same. Although extruded larvae of both species are known to be numerous in the Gulf of St. Lawrence and the intraspecies distribution of these larvae is known to be heterogeneous (Sévigny et al. 2000), the population structure of redfish in the Gulf is unknown. Population genetic studies of redfish in the Gulf of St. Lawrence and their approaches based on microsatellite DNA assays are also equivocal, suggesting weak structure in *S. fasciatus* and negligible structure in *S. mentella* (Roques et al. 2001; A. Valentin, unpublished data).

Many of the fish species in the Gulf of St. Lawrence are known to migrate to the warm, deep waters of the Laurentian Channel (near the mouth of the Gulf) to overwinter, presumably to avoid near-freezing water temperatures and ice cover over much of their summer habitat (Templeman 1962; D'Amours et al. 1994; Campana et al. 1999). It is unlikely that *Sebastes* spp. need to migrate to avoid cold temperatures, as temperature at their typical depth ranges of 150–300 m (for *S. fasciatus*) and 350–500 m (for *S. mentella*) are reasonably constant all year round (Atkinson 1984). However, based on a comparison of summer and winter research surveys and the historical distribution of the fishing fleet, there is some indication that redfish change their distribution between summer and winter, moving to the southeast for the winter (Morin et al. 1994; Gascon 2003). A substantial proportion of the biomass of Gulf of St. Lawrence *Sebastes* spp. apparently overwinters in a relatively circumscribed area in the Laurentian Channel close to the Cabot Strait. However, the line separating the two redfish management units that encompass the Gulf of St. Lawrence and Laurentian Channel areas bisects what appears to be a continuous distribution in the overwintering area (Morin et al. 1994). Both mixed-population catches and distributions of populations outside of management units can introduce serious error into the stock assessment of any fish species, thus degrading efforts at optimal management (Wood et al. 1989).

Conventional tagging studies are seldom carried out on deepwater species such as redfish because of the difficulties in bringing them to the surface without fatal decompression of the swimbladder, compounded by low recapture rates (Starr et al. 2000). Therefore, we used the trace element composition of the otolith as a more highly resolved natural tag. The otolith is well suited to this application because it grows without resorption throughout the life of the fish (Campana and Neilson 1985) and it accretes trace elements from the environment in a temperature-sensitive manner (Campana 1999). Thus the elemental composition of the whole otolith ("elemental fingerprint") serves as an environmentally induced natural tag of fish that have spent at least part of their lives in different habitats, independent of genetic identity. Recent studies have demonstrated not only that the elemental fingerprint of species such as cod is population-specific, but also that otolith growth and environmental shifts over periods of up to a year have a negligible effect on the whole-otolith fingerprint (Campana et al. 1999, 2000). Given the slow growth and extended life span of redfish (up to 75 years) (Campana et al. 1990), the elemental fingerprint of redfish otoliths would be expected to be even more stable. By using the whole-otolith elemental fingerprint of redfish on summer grounds as a short-term natural tag, it should be possible to track and identify those same groups of fish on the overwintering grounds with no more assumptions than those associated with genetic markers (Campana et al. 1999).

In this paper, we start by using the results of synoptic research vessel surveys to document the distribution and density of redfish on their summer grounds in the Gulf of St. Lawrence and Laurentian Channel. We then apply otolith elemental fingerprints as natural tags to test the hypothesis that redfish move out of the Gulf of St. Lawrence to overwinter in the Laurentian Channel, where they potentially mix with another redfish population. We conclude by assessing the implications of the findings for migration theory and fisheries management.

Materials and methods

Sample collection

The density and distribution of redfish in the Gulf of St. Lawrence and the Laurentian Channel were surveyed as part of three separate stratified random surveys in July and

© 2007 NRC Canada

Table 1. Summary of redfish samples analyzed by species and season.

Sample label	Season	Date	Latitude (N)	Longitude (W)	Depth (m)	*S. mentella*			*S. fasciatus*		
						N	Length, cm (SE)	Otolith weight, mg (SE)	*N*	Length, cm (SE)	Otolith weight, mg (SE)
3PN1	Summer	3 Aug. 2002	46°53.3′	58°50.0′	434	30	33.5 (0.4)	281 (7)			
4S44	Summer	7 Aug. 2002	48°03.6′	60°34.2′	447	32	34.7 (0.4)	316 (10)			
4R48	Summer	7 Aug. 2002	48°07.3′	59°46.0′	315	30	33.6 (0.5)	289 (10)			
3PS1	Summer	30 July 2002	45°08.2′	55°10.2′	202				31	28.6 (0.4)	218 (8)
4VS13	Summer	13 Aug. 2002	44°13.8′	58°02.8′	515	31	34.7 (0.4)	348 (11)			
4VS36	Summer	3 Aug. 2002	45°16.3′	57°42.2′	217				32	29.3 (0.4)	217 (8)
4VN77	Summer	27 July 2002	46°22.8′	58°55.4′	348	31	33.8 (0.4)	293 (9)			
4R107	Summer	12 Aug. 2001	49°45.5′	59°10.8′	217				32	31.6 (0.5)	265 (10)
3PS4*	Summer	30 July 2002	44°56.4′	55°39.9′	203	2	36.5 (0.5)	348 (11)	2	34.0 (2.0)	257 (25)
3PS4*	Summer	31 July 2002	44°53.1′	55°44.1′	306	1	43.0 (0)	458 (0)	1	32.0 (0)	178 (0)
3PS4*	Summer	31 July 2002	44°48.7′	55°40.8′	623	11	37.3 (1.6)	335 (41)	1	31.0 (0)	207 (0)
3PS4*	Summer	31 July 2002	44°51.0′	55°46.7′	485	2	36.5 (2.5)	397 (119)	11	33.5 (0.8)	274 (10)
4VN2	Winter	9 Nov. 2002	45°42.8′	57°53.0′	425	31	35.1 (0.4)	311 (9)			
4VN5	Winter	9 Nov. 2002	45°47.1′	58°07.0′	245				32	31.2 (0.5)	224 (9)
4VN12	Winter	10 Nov. 2002	46°58.3′	59°37.2′	431	32	34.3 (0.5)	312 (10)			
4S35	Winter	11 Nov. 2002	48°19.5′	60°50.5′	429	31	35.8 (0.5)	357 (12)			
4R51	Winter	12 Nov. 2002	48°19.1′	59°58.9′	392	32	34.3 (0.4)	314 (10)			
4R53	Winter	12 Nov. 2002	48°17.8′	59°44.3′	248				32	28.4 (0.5)	197 (7)
3PN77	Winter	13 Nov. 2002	47°08.3′	58°24.0′	390	32	33.0 (0.3)	296 (9)			
3PS133	Winter	15 Nov. 2002	45°32.0′	56°49.2′	394	31	34.3 (0.5)	319 (11)			
3PS138	Winter	18 Nov. 2002	44°51.9′	56°01.8′	448				32	29.9 (0.5)	246 (10)
Saguenay	Winter	Jan.–Feb. 2003	48°07′	69°40′		48	29.4 (0.1)	204 (3)	2	28.0 (0.6)	204 (4)
Total						407			208		

Note: *N*, number of fish used in the analysis. SE, standard error.
*Pooled as one sample.

© 2007 NRC Canada

Fig. 1. Map of study area contoured to show the relative distribution of *Sebastes* spp. in the summer of 2002 (kg/standardized set). Yellow circles show summer collection sites for *S. fasciatus*; yellow stars show summer collection sites of *S. mentella*. The 100 and 200 m bathymetric contours are shown.

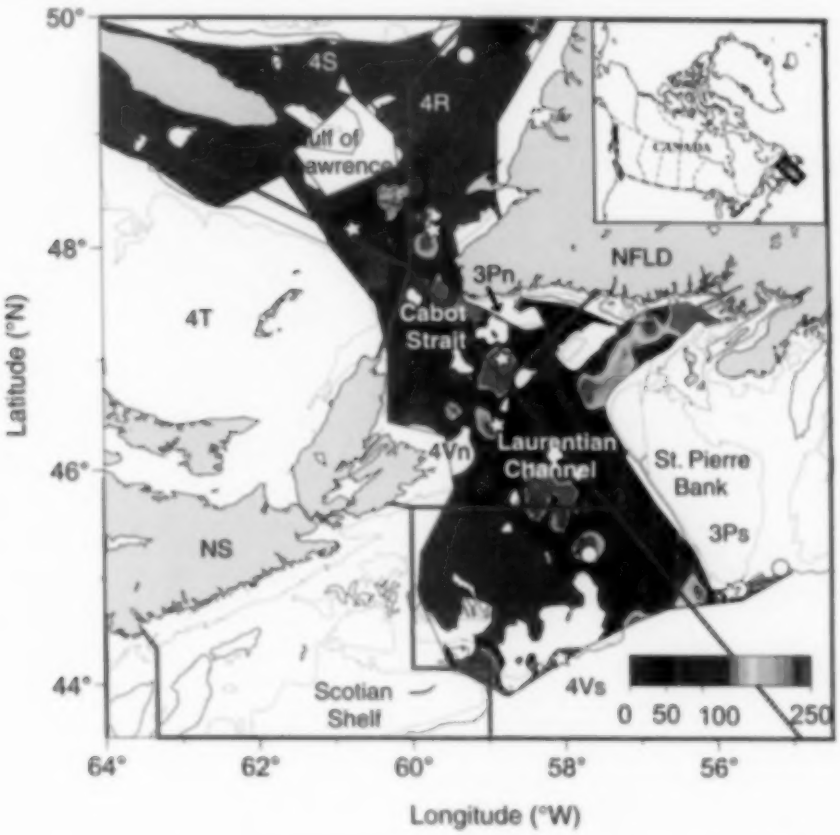

August of 2002 (Table 1). The mean distance between survey samples was 20–30 km, although some areas were surveyed at 5 km intervals. Standardized catch weight per set was contoured using Delauney triangles in the spatial analysis program ACON (available at http://www.mar.dfo-mpo.gc. ca/science/acon/index.html).

To characterize the otolith elemental fingerprint of the major redfish aggregations in and around the Gulf of St. Lawrence, samples of primarily adult redfish (25–45 cm) were collected with otter trawls aboard research vessels in the summers of 2001 and 2002 from previously documented major aggregations (Gascon 2003). Sets in which the catch exceeded 100 kg were considered to be representative of each of the major aggregations (Table 1; Fig. 1). A minimum of 30 redfish was selected from each set for a total of 110 *S. fasciatus* and 170 *S. mentella*. The specimens were frozen immediately after capture. After thawing in the laboratory, the fork length, weight, and sex were recorded. The sagittal otolith pair was then removed from each fish and stored dry in paper envelopes until the time of elemental analysis. The species identity of individual fish was unknown at the time of collection (when fin clips were taken) but was subsequently assigned on the basis of the genotype at 13 microsatellite loci (A. Valentin, unpublished data). The otolith elemental fingerprints of these nine summer samples were considered as our reference collection against which our winter samples were subsequently compared.

Winter aggregations of both species of redfish were sampled in the fall and winter of 2002 (Table 1). A total of nine sets were sampled for otoliths, yielding 98 *S. fasciatus* and 189 *S. mentella*. An additional 48 *S. mentella* were collected by handline from the Saguenay Fjord in the winter of 2003. Sample processing was as described for the summer samples.

Elemental analysis

Before elemental analysis, all otoliths were decontaminated using a modification of the protocol described in Fowler et al. (1995). Briefly, this involved a 5-min sonification of each otolith in an acid-washed 50 ml polypropylene vial containing Super Q water (distilled, millipore-filtered, reverse-osmosis water), followed by a 1-min scrubbing with an acid-washed toothbrush, triple rinsing in Super Q water, a 3-min sonification in Super Q, and a final triple rinse in Super Q. Decontaminated otoliths were air-dried in acid-washed polypropylene caps under a Class 100 laminar-flow, positive-pressure fume hood for 24 h before weighing to the nearest 0.1 mg. Decontaminated otoliths were subsequently stored

© 2007 NRC Canada

dry in sealed, acid-washed polypropylene vials to await assay. Blank vials were similarly prepared for blank corrections and calculations of limits of detection. At all stages of the decontamination process, otoliths were exposed only to acid-washed plastic materials, and all steps other than sonification were carried out in the laminar-flow fume hood.

Decontaminated otoliths were dissolved in subboiling, redistilled nitric acid and brought to 0.1% *w/v* with Super Q water. A suite of seven trace elements (Li, K, Mg, Mn, Sr, Cd, and Ba) was assayed with inductively coupled plasma mass spectrometry (ICP-MS), of which five were suitable for quantification by isotope dilution. Isotope dilution was the preferred method of quantification owing to superior accuracy and precision in otolith assays (Campana et al. 1995). The enriched isotopes used in the spiking procedure were ^{6}Li, ^{25}Mg, ^{67}Zn, ^{86}Sr, and ^{136}Ba, whereas the remaining more abundant isotopes were used for quantification. The remaining elements were referenced to an internal standard (In) for assay by conventional ICP-MS and quantified using matrix-matched external standards. Because of concerns over possible isobaric interferences or proximity to detection limits, significant assay results for B, Cu, Zn, Pb, and U were not carried forward to the statistical analyses.

An additional three elements (Ca, Na, and Sr) were assayed with inductively coupled plasma emission spectrometry (ICP-ES) after a 300-fold dilution of the original dissolved otolith. Quantification was through matrix-matched external standards. Fe was also assayed, but mean concentrations were too close to detection limits to be useful.

Differences in otolith elemental composition among groups of fish may be statistically significant, but they will not necessarily be large. Two protocols were adopted to minimize the possibility for artifactual differences and to reduce the variance: (*i*) the assay sequence was systematically randomized across sample sites to insure that instrument drift did not artifactually inflate the assay results of one sample site over another, and (*ii*) a pooled sample solution, consisting of aliquots of solution of 150 otoliths, was analyzed at regular intervals throughout the ICP-ES and ICP-MS analytical sequences. Analytical batches were subsequently normalized to the mean pooled-sample concentration (element by element). The effect of this normalization was to remove the effect of instrument drift and interbatch differences from all assays and therefore reduce the variance of the assays.

Limits of detection (calculated as 3 standard deviations (SD) of the blank; $\mu g \cdot g^{-1}$) for the elements of interest were as follows: 0.1 for Ba, 0.003 for Cd, 154 for Ca, 0.005 for Cu, 0.02 for Li, 0.09 for Mg, 0.01 for Mn, 7.0 for K, 0.8 for Na, and 0.6 for Sr.

Statistical analysis

The two redfish species were analyzed independently of each other. The within-group distributions of Li, Mg, and Mn concentrations were skewed and thus were ln-transformed prior to statistical analysis. To insure that differences in fish size or age among samples were not confused with site-specific differences, the effect of otolith weight was statistically removed from those elemental concentrations in which a significant size effect was evident (Campana 1999). The effect of otolith weight was removed from the elemental concentration of Na, K, Li, Mn, Mg, and Sr in each species by subtracting the product of the otolith weight and the common, within-group slope (from an analysis of covariance (ANCOVA)) from each observed concentration. The main effect in the ANCOVA was sample location, with otolith weight as the covariate. The interaction term between location and otolith weight was also tested for significance; elements with a significant interaction term were evaluated with and without size detrending to insure that statistical artifacts did not confound the analysis.

Each otolith was characterized by a suite of several elements; therefore multivariate statistics were used to distinguish among samples. Multivariate analysis of variance (MANOVA) was used to test for significant differences among samples, whereas discriminant function analysis (DFA) was used to prepare two-factor elemental fingerprints for illustrative purposes. Discriminant analysis was not used to classify the samples of unknown stock affinity (those collected in the winter). Principal component analysis (PCA) was also used to display the multivariate fingerprint, but unlike in DFA, this type of analysis does not attempt to maximize the distance between groups of fish.

Stock composition analysis of each sample location in the winter collection was carried out using the maximum likelihood based stock mixture analysis described in Campana et al. (1999). The reference groups for all stock mixture analyses were the species-specific, set-by-set summer samples of redfish. Conceptually, the stock composition analysis uses the multivariate distribution of the elemental fingerprints in each reference (summer) sample to estimate the proportion of each reference population in the unknown (winter) mixture. As long as all of the possible groups contributing to the winter group mixture have been represented in the summer samples, the analysis will produce an unbiased estimate of group proportions, with no more assumptions than those associated with genetic markers (Wood et al. 1987, 1989; Campana et al. 1999). The product of the analysis was the proportions of each summer reference sample in each winter sample. Note that the true spawning origin of each summer samples was unknown. Therefore, the classification of the winter samples is in terms of summer groups (samples), not of spawning populations. This approach is well suited to determining the relative movement of redfish collected in winter compared with where they were in the summer.

Results

Redfish distribution in the summer was concentrated in deep water along the shelf edge in the outer Gulf of St. Lawrence and approaches (Fig. 1). Relatively few redfish were collected west of 61°W. Redfish aggregations tended to be discontinuous, except on the outer Scotian Shelf and along St. Pierre Bank.

Although some of the collection sets included redfish of both species, most sets selected were dominantly or exclusively one species or the other (Table 1). Fish length differed slightly but significantly among sets and species ($p < 0.05$). The mean (±1 standard error (SE)) fork length of *S. fasciatus* in summer and winter was 30.3 ± 0.3 cm and 29.8 ± 0.3 cm, respectively, whereas that for *S. mentella* was 34.4 ± 0.2 cm in both winter and summer (excluding the fish from the Saguenay Fjord). *Sebastes mentella* from the winter

© 2007 NRC Canada

Fig. 2. Examples of the relationship between elemental concentration and otolith weight in *Sebastes mentella* collected in the Gulf of St. Lawrence. There was a significant relationship in the case of (*a*) Na but not (*b*) Ba. Each symbol type denotes a different sample location. The common within-group slope from the analysis of covariance is shown and was removed statistically from all elements with a significant relationship.

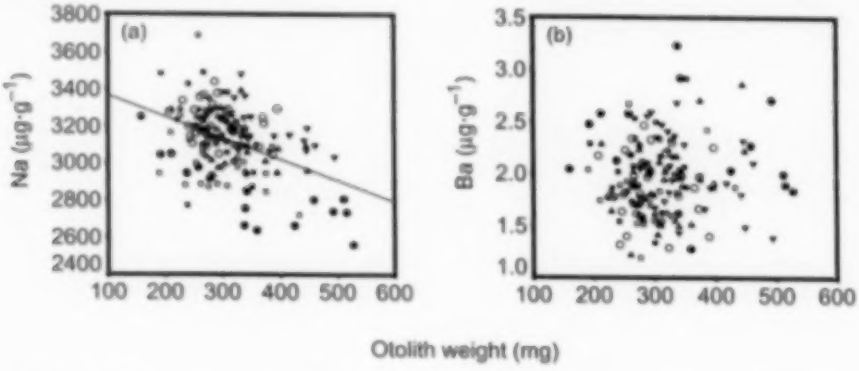

Table 2. Differences in elemental concentration among species and sample locations in the summer reference collections based on analysis of covariance with otolith weight as the covariate.

Species	Element	Slope parameter	Otolith weight × location	Location
S. fasciatus	Cd		ns	ns
	Na	–0.326	0.02	<0.01
	K	–0.328	0.01	<0.01
	ln Li	–0.00248	<0.01	<0.01
	Sr		ns	ns
	ln Mn	–0.00179	ns	<0.01
	ln Mg	–0.0010	ns	<0.01
	Ba		ns	<0.01
S. mentella	Cd	5.00×10^{-6}	ns	ns
	Na	–1.059	ns	<0.01
	K	–0.09	0.04	<0.01
	ln Li		ns	0.02
	Sr	1.486	ns	0.01
	ln Mn	–0.00259	ns	<0.01
	ln Mg	–0.00092	ns	ns
	Ba		ns	<0.01

Note: Where significant, the common within-group slope that was used to statistically remove the effect of otolith weight from elemental concentration is shown. ns, not significant.

Saguenay Fjord collection were significantly smaller at 29.4 ± 0.1 cm ($p < 0.05$), whereas those from summer 3PS4 were significantly larger at 37.4 ± 1.2 cm ($p < 0.05$) than any of the other summer sets.

All of the elements except Ba and Cd showed a significant relationship between concentration and fish length or otolith weight (Fig. 2). To insure that differences in fish size among sample locations did not confound any real differences in elemental concentration, the effect of otolith weight was statistically removed from the elemental concentrations through ANCOVA where significant (Table 2). In most but not all cases, the interaction term between location and otolith weight was not significant, making the common within-group slope of the ANCOVA the best measure of the size-specific effect. Where the interaction term was significant but limited to a single location, the common within-group slope was still used for detrending. However, stronger interactions were not detrended. In all cases, relative differences among detrended samples tended to be ranked similarly to those based on the original data.

Analysis of the summer (reference) samples of each species indicated that the concentrations of most elements differed substantially among locations (Fig. 3). All elements but Cd differed significantly among locations within at least one species (Table 2). Elements such as Ba (both species) and K (*S. mentella* only) showed a generally increasing gradient moving out of the Gulf of St. Lawrence, whereas elements such as Li, Mn, and Sr differed substantially among locations, but with no obvious gradient (Fig. 3). Although there was only one location where both redfish species were analyzed (3PS4) there seemed to be little overall correspondence in elemental concentration between the species at that

© 2007 NRC Canada

Fig. 3. Variation in mean (±95% confidence interval) elemental concentration between species and summer locations. Concentrations for all elements except Ba and Cd have been weight-detrended; however, the differences among locations changed relatively little as a result of the detrending. Solid symbols, *Sebastes mentella*; open symbols, *S. fasciatus*. Sample sites have been ordered from northwest (left) to southeast (right).

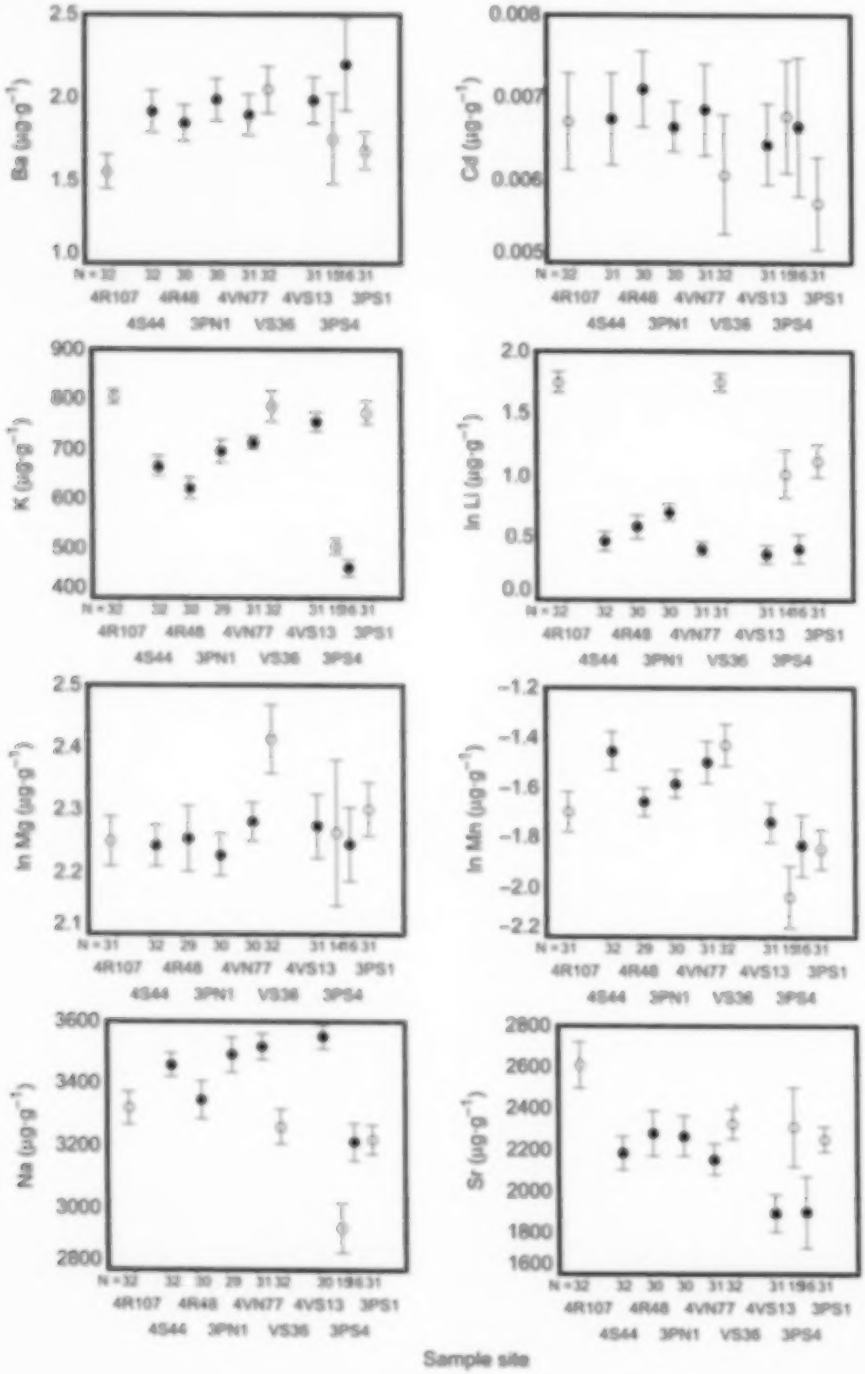

© 2007 NRC Canada

Fig. 4. The elemental fingerprints of (*a*) *Sebastes fasciatus* and (*b*) *S. mentella* as markers of summer samples in a discriminant analysis. Each data point represents a fish, and each colour represents a sample location. The centroids of each location are located below each label. Winter Saguenay samples (open circles) do not lie in the discriminant space defined by the summer samples of *S. mentella*, indicating that none of the summer samples represents the source group for the Saguenay sample.

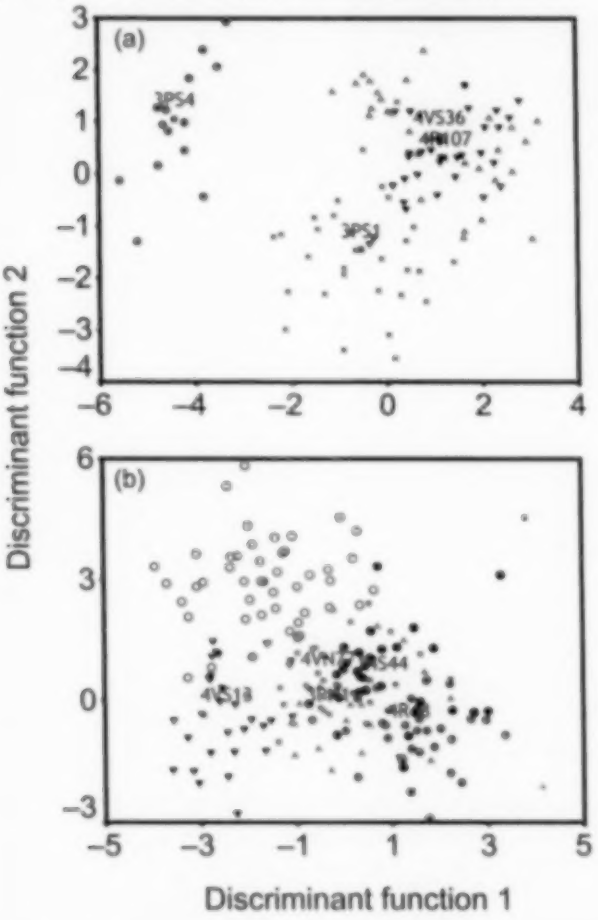

site, perhaps because this sample comprised several closely spaced but independent sets (Table 1).

Although it may be possible to use the concentration of a single element to distinguish between and track groups of redfish, it is preferable to use a multivariate approach, which uses all elements at once. A MANOVA demonstrated that the differences among summer sample locations were highly significant within each species ($p < 0.001$). DFA proved to be an excellent way to visualize those differences (Fig. 4). Four elements entering into the stepwise DFA (Li, Mn, Sr, and K) were common to both species, with Ba also entering into the DFA for *S. mentella*. In both species, the first two discriminant functions explained more than 90% of the variance. The DFA for *S. fasciatus* showed that two of the summer samples (3PS1 and 3PS4) were easily distinguished from all others in discriminant space, whereas the remaining

Fig. 5. Plot of the first two principal components (PC) of otolith elemental composition for locations containing both *Sebastes fasciatus* (in red) and *S. mentella* (in blue) in summer (▼) and winter (●). The two species tend to be easily identifiable based only on otolith elemental composition, irrespective of season.

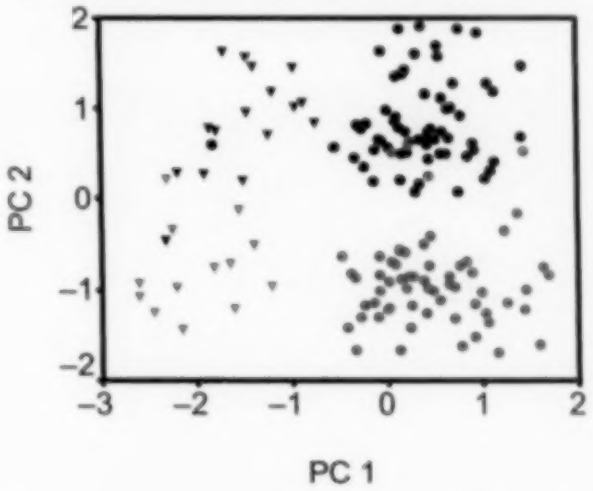

two samples were similar to each other (Fig. 4). When the discriminant scores for the winter samples were overlaid on the summer scores for *S. fasciatus* (using a DFA where only the summer samples were entered as reference groups), all of the winter samples seemed to be well represented by the space described by the summer samples (not shown). In other words, there was no reason to believe that the source groups for the winter samples included groups other than those represented by the existing summer samples.

A comparable DFA for *S. mentella* also showed that sample 3PS4 was isolated in discriminant space (not shown). When the DFA scores for the winter samples were overlaid on the summer scores, none of the winter samples lay in the discriminant space defined by sample 3PS4. Because this result implies that sample 3PS4 could not have been a source group for any of the winter samples, the DFA was repeated without using sample 3PS4 as a reference group. The resulting DFA showed clear and significant separation between two of the groups and overlapping but significant separation among all groups except 4VN77 and 3PN1 ($p < 0.05$) (Fig. 4). The discriminant space defined by these summer samples appeared to describe that of the winter samples very well, with the exception of the Saguenay redfish. The discriminant scores of the Saguenay redfish lay well outside the summer discriminant space, indicating that there were no appropriate source groups for the winter Saguenay redfish among any of the summer samples (Fig. 4).

The objective of this study was to differentiate among locations within a species, not to discriminate between species. However, given the difficulties in differentiating between species, elemental differences between species collected at the same location could help with the species identification. *Sebastes fasciatus* and *S. mentella* collected at similar locations (winter samples 4R53 vs 4R51 and 4VN2 vs 4VN5; summer sample 3PS4) in the same season were easily identified based only on a PCA of the otolith elemental composi-

© 2007 NRC Canada

Fig. 6. Stock mixture analysis of winter collections of (*a*) *Sebastes mentella* and (*b*) *S. fasciatus* of unknown origin classified using the otolith elemental fingerprints of summer collections as reference sources. The locations of the summer reference collections are shown as large coloured circles, the winter collections are indicated by small open circles. The proportional stock composition of each unknown winter collection is shown as a pie chart, with each colour referring to a specific summer source location.

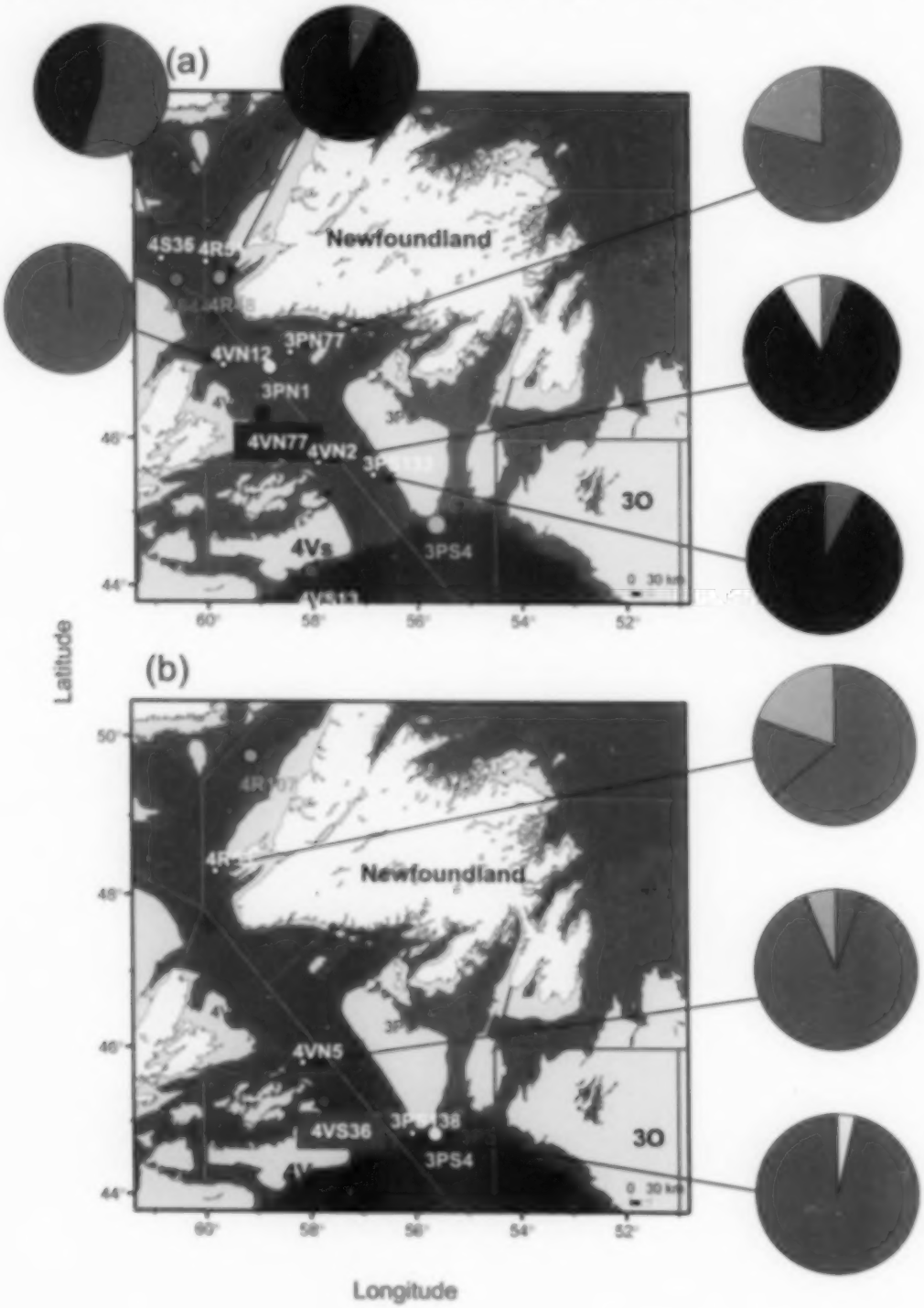

© 2007 NRC Canada

tion (Fig. 5). Indeed, the differentiation between species was so complete that it raises the possibility that the few individuals plotted in the factor space of the other species may have been misidentified. Summer and winter collections of each species were also distinguished, although the sole summer location where both species were collected (3PS4) was one that was isolated in discriminant space from all other summer samples.

Stock mixture analysis was used to determine the stock origin (in terms of summer reference samples) of each of the winter samples. Based on the elements that entered into the DFA, five elements were selected for entry into the mixture analysis: Li, Mn, Sr, Ba, and K. The accuracy of the resulting mixture estimates could not be directly measured. However, a jackknifed classification of each of the summer reference samples resulted in a mean accuracy of 96.5%, with no sample being classified with less than 92% accuracy.

More than half of each *S. mentella* winter sample was classified as having originated from a single summer reference sample, and in most cases, the single summer sample contributed more than 80% to the mixture (Fig. 6*a*). In four of the six winter samples, the summer sample that contributed most to a given winter sample was that closest and upstream (into the Gulf). Thus the mixture analysis indicated that *S. mentella* moved slightly to the southeast, towards the mouth of the Gulf, for the winter. The only samples that appeared to show a different pattern (4R51 and 4S35) were classified as having a large component from 4VN77. Although initially counterintuitive, this result may also be consistent with a winter outmigration from the Gulf; none of the summer reference samples was as far north in the Gulf as 4R51 and 4S35, suggesting that a more appropriate source group was not available from our summer sampling. There was no evidence of substantive contribution by the Scotian Shelf sample (4VS13) to any of the winter Gulf mixtures.

As was the case with *S. mentella*, all of the *S. fasciatus* winter samples were dominated by a single summer source (Fig. 6*b*), and once again, the source group for the winter mixtures was usually identified as a nearby summer sample. However, with this species, there was only one summer sample collected north of the Newfoundland – Cape Breton line, which is insufficient to determine the presence of any winter outmigration. The poor summer sample coverage of *S. fasciatus* may also explain the rather diverse mixture predicted for 4R53; if outmigration did occur, there were no nearby summer samples that could have served as a source, implying that the mixture analysis could only draw on incorrect summer sources for classification of this sample.

Discussion

The distribution of redfish in the 2002 summer surveys was broadly consistent with surveys carried out in the 1976–1993 period: most deep areas in the Gulf of St. Lawrence west of Anticosti Island contained redfish, although the distribution was patchy rather than continuous. Most of the *S. mentella* were captured at depths of 300–500 m, and most of the *S. fasciatus* were captured at depths of 200–250 m, similar to what was reported by Atkinson (1984). However, in contrast to summer surveys before 1994, *Sebastes* spp. were most concentrated in the Laurentian Channel and its approaches, rather than in the Gulf (Atkinson 1984; Morin et al. 1994; Gascon 2003). Presumably, the scarcity of redfish in the Gulf is due to the population collapse and subsequent fishery closure of Gulf of St. Lawrence (Management Unit 1) redfish (Department of Fisheries and Oceans (DFO) 2004). The winter distribution of *Sebastes* was not mapped as part of this project but has been well documented in previous summaries of winter research vessel surveys and fishing fleet distributions (Atkinson 1987; Morin et al. 1994; Gascon 2003). In all cases and in all years, redfish were concentrated in the southern Gulf of St. Lawrence – northern Laurentian Channel area during the winter, with relatively low numbers further west within the Gulf of St. Lawrence.

Does the winter concentration of *Sebastes* spp. in the Laurentian Channel and its approaches represent a simple movement out of the Gulf of St. Lawrence for overwintering, or is the winter concentration the focus of movement from all surrounding areas into one optimal overwintering ground? The stock mixture analyses provided clear evidence of southeasterly movement by *S. mentella* out of the Gulf and rejected the hypothesis that more easterly aggregations also joined the mixture. Indeed, summer *S. mentella* from the eastern edge of the Laurentian Channel (both south and north) were poorly represented in the winter samples, indicating that they overwintered somewhere else. These results are consistent with inferred movements based on research vessel surveys and fishing fleet distributions (Atkinson 1987; Morin et al. 1994; Gascon 2003). The movement demonstrated for *Sebastes* is also similar to that reported for cod (*Gadus morhua*) and other species in the Gulf of St. Lawrence, which also move out of the Gulf to overwinter (Swain et al. 1998; Campana et al. 1999; Castonguay et al. 1999). The difference between these species, though, lies in terms of evolutionary advantage: whereas cod and other species in the shallower waters of the Gulf would be exposed to a seasonal temperature range of >12 °C between summer and winter (Swain and Kramer 1995), redfish remaining in the deep waters of the Gulf would experience seasonal temperature differentials of less than 1 °C (Atkinson 1984). Therefore, temperature is unlikely to be the major cue for redfish outmigration in the winter. Food availability is a possibility, particularly as redfish vertically migrate to shallower depths on a diurnal basis, presumably to feed on euphausids and myctophids. Equally plausible is the possibility that winter outmigration occurs in response to endocrine-driven cues leading eventually to spawning, as has been observed in cod (Comeau et al. 2002). With redfish copulation occurring in late fall or early winter (Ni and Templeman 1985), overwintering aggregations may represent mating aggregations. If this is the case, the fact that few eastern Scotian Shelf (Unit 2) *S. mentella* were identified in the overwintering mixture may indicate that they constitute a population that is distinct from that in the Gulf of St. Lawrence and Laurentian Channel.

The overall absence of genetic structure observed within the Gulf of St. Lawrence *S. mentella* indicates that either there is only one spawning group or there is sufficient mixing among spawning groups to mask any genetic differentiation (Roques et al. 2001; A. Valentin, unpublished data). However, these mixing rates need not have been high; mixing on the order of 1% or less is enough to prevent genetic

© 2007 NRC Canada

differentiation (Bentzen et al. 1996). In contrast, the significant differences among otolith elemental fingerprints of the summer samples indicates that the groups remained in different environments through some portion of their lives, irrespective of their genetic origin. Although it is possible that distinct populations existed at all life history stages and that a small amount of genetic mixing occurred at the spawning stage, a more likely scenario is that distinct spawning groups of redfish contributed to a single, well-mixed larval pool in and around the Gulf of St. Lawrence. Redfish juveniles and larvae are undoubtedly more mobile than the adults, which suggests that the early life history stage is the one in which mixing occurs. As the redfish get older and settle into deeper waters, their aggregations are likely to become more structured and sedentary, mixing very little with other adult aggregations. Such a life history pattern would explain both the observed genetic homogeneity and the accumulated differences in otolith composition among groups.

Elemental fingerprints change very slowly in whole otoliths of long-lived fishes, and thus they serve as stable and accurate natural tags of groups of fish (Campana et al. 2000). Therefore, the basic limitation of the stock mixture analysis was the spacing of the summer reference samples. As with stock mixture analyses based on genetics, elemental stock mixture analyses classify an unknown sample (e.g., winter samples) in terms of proportions of each reference (summer) group. Thus it is important that all possible source groups be represented in the reference samples. The summer reference samples were reasonably well spaced for *S. mentella*, so the movement of most of the winter samples could be tracked with reasonable precision. An exception was the most westerly of the winter samples; if they originated further to the west, as was the case with the other winter samples, our analysis would have classified that sample incorrectly, owing to the absence of any reference group further to the west. A similar limitation was in effect for the classification of the *S. fasciatus* winter samples; the summer reference samples were widely spaced in the Gulf, implying that any movements of winter samples could only be detected at similar or larger scales.

Our conclusion that deepwater *Sebastes* undertake annual migrations, perhaps in the context of reproduction, seems plausible, but tracking studies on deepwater species are scarce (Starr et al. 2000). Virtually all studies on the distribution of adult *Sebastes* in the Atlantic have been confounded by difficulties in distinguishing among species and thus have been focused on the zoogeography of the congeneric species rather than within-species movements (Misra 1985; Stransky and MacLellan 2005; Valentin et al. 2006). Nevertheless, broad categories of deepwater fish migrations have become increasingly well documented. Diel vertical migrations in response to the day–night cycle are well established among deep-sea fishes (Butler et al. 2001; Gauthier and Rose 2002), as are ontogenetic migrations towards deeper water as the fish grows (Jacobson et al. 2001; Allain et al. 2003). However, the large-scale seasonal migrations so commonly observed in pelagic fishes have not been reported in deep-sea fishes (Beamish et al. 2005). For example, orange roughy (*Hoplostethus atlanticus*) are often associated with specific seamounts and do not venture far from their settling location (Smith et al. 2002). Edmonds et al. (1991) also reported minimal movements by deepwater aggregations of orange roughy. In contrast, smaller-scale migrations associated with reproduction and (or) feeding have been reported both for deep-sea angler (*Lophius budegassa*) (Duarte et al. 2001) and hoki (*Macruronus novaezelandidae*) (Kuo and Tanaka 1984). In the latter case, the scale of the migration (50–500 km) was on the same scale as was seen in our study on *Sebastes* spp.

The *S. mentella* collected from the Saguenay Fjord were characterized by elemental fingerprints that were completely unlike any of the other summer or winter samples. This fact indicates that the Saguenay redfish must have spent a portion of their lives separated from other redfish in the Gulf. Although it is not possible to determine from whole-otolith composition exactly how long different groups may have remained isolated from each other, the very distinct nature of the Saguenay fingerprints suggests a large portion of their lives must have been spent in isolation from the other groups. Microsatellite DNA assays indicate that the Saguenay redfish are genetically indistinguishable from *S. mentella* in the Gulf of St. Lawrence (Roques et al. 2002; A. Valentin, unpublished data). Therefore, Saguenay redfish appear to represent a population sink: a recruitment pulse of Gulf redfish that settled away from the bulk of the population and have since grown up in isolation from other redfish.

The interspecies difference in elemental fingerprints of *S. mentella* and *S. fasciatus* probably reflects an interspecies difference in life history and habitat more than an intrinsic difference in trace element incorporation into the otolith. Otolith composition is largely a product of the environment, both physical and chemical, as modified by growth rate and physiology (Campana 1999). It is unlikely that the water chemistry differed appreciably between the depths occupied by the two redfish species, even though *S. fasciatus* is found somewhat closer to shore. However, the temperature environment presumably differed, with *S. fasciatus* being found in shallower, warmer water (Atkinson 1984; Gascon 2003). The fact that *S. mentella* grows larger and, presumably, has a different growth rate would also contribute to differences in the elemental fingerprint. Environmental and physiological causes of the differences in otolith elemental fingerprints between *Sebastes* species are also consistent with the findings of Stransky et al. (2005), who reported significant differences in otolith elemental fingerprints between *S. mentella* and *S. marinus* collected at the same location.

The implications of our findings extend to the fisheries management of *Sebastes* spp. in both the Gulf of St. Lawrence and the Laurentian Channel areas. The current management of redfish in these areas assumes the presence of two populations based largely on biological characteristics and distribution: a population in the Gulf of St. Lawrence (Unit 1, NAFO divisions 4RST (January–December) and 3Pn4Vn (January–May)) and a population in the Laurentian Channel (Unit 2, NAFO divisions 3Ps4VsWfgj (January–December) and 3Pn4Vn (June–December)). These two populations are managed as if they overlap in a mixing area in 3Pn and 4Vn but are segregated by season (Atkinson 1987). Our results strongly support the interpretation that the 3Pn4Vn region is occupied by Laurentian Channel redfish (Unit 2) in the summer and by overwintering Gulf (Unit 1) redfish in the winter. There are also indications that southeasterly movements of redfish occur throughout the Gulf and

© 2007 NRC Canada

Laurentian Channel regions between summer and winter. Our results indicated that the southeasterly movement from the Gulf into the 3Pn area extended to at least the 3Ps border. This suggests that the mixing area may be more extensive than what is currently defined by the management units, which leaves open the possibility that overwintering Gulf (Unit 1) redfish could be fished as part of the Unit 2 quota. Because Unit 1 redfish are now under a fishing moratorium (DFO 2004), this mismatch between management areas and population mixing areas may be exacerbating its current low population numbers. With the likelihood that both the timing of migrations and the extent of the mixing area are variable from year to year, additional management measures (seasonal and (or) area closures) could be required as a precautionary measure for Unit 1 redfish, at least during the moratorium. More broadly, the limited movement of redfish observed in our study would suggest that large-scale management areas for redfish may be at risk of locally overfishing what are essentially semi-isolated redfish aggregations, even if they share a genetic origin. If future work confirms the limited movement of redfish in other areas, optimal management may require smaller management areas than now exist.

Acknowledgements

We thank Brigitte Bernier, Linda Marks, Warren Joyce, Arianne Savoie, Thomas Joly-Mischlich, Jean-Yves Carrier, Nancy Otis, Caroline Laporte, and Éric Parent for technical assistance and Jerry Black for expert advice on the mapping. Bruce Leaman and an anonymous referee provided helpful suggestions on the manuscript.

References

Allain, V., Biseau, A., and Kergoat, B. 2003. Preliminary estimates of French deepwater fishery discards in the Northeast Atlantic Ocean. Fish. Res. **60**: 185–192.

Atkinson, D.B. 1984. Distribution and abundance of beaked redfish in the Gulf of St. Lawrence, 1976–81. J. Northw. Atl. Fish. Sci. **5**: 189–197.

Atkinson, D.B. 1987. The redfish resources off Canada's east coast. *In* Proceedings of the International Rockfish Symposium. Lowell Wakefield Fisheries Symposium Series, Alaska Sea Grant College Program Report No. 97-2. pp. 15–33.

Beamish, R.J., McFarlane, G.A., and King, J.R. 2005. Migratory patterns of pelagic fishes and possible linkages between open ocean and coastal ecosystems off the Pacific coast of North America. Deep-Sea Res. **52**: 739–755.

Bentzen, P., Taggart, C.T., Ruzzante, D.E., and Cook, D. 1996. Microsatellite polymorphism and the population structure of Atlantic cod (*Gadus morhua*) in the Northwest Atlantic. Can. J. Fish. Aquat. Sci. **53**: 2706–2721.

Butler, M., Bollens, S.M., Burkhalter, B., Madin, L.P., and Horgan, E. 2001. Mesopelagic fishes of the Arabian Sea: distribution, abundance and diet of *Chauliodus pammelas*, *Chauliodus sloani*, *Stomias affinis*, and *Stomias nebulosus*. Deep-Sea Res. **48**: 1369–1383.

Campana, S.E. 1999. Chemistry and composition of fish otoliths: pathways, mechanisms and applications. Mar. Ecol. Prog. Ser. **188**: 263–297.

Campana, S.E., and Neilson, J.D. 1985. Microstructure of fish otoliths. Can. J. Fish. Aquat. Sci. **42**: 1014–1032.

Campana, S.E., Zwanenburg, K.C.T., and Smith, J.N. 1990. $^{210}Pb/^{226}Ra$ determination of longevity in redfish. Can. J. Fish. Aquat. Sci. **47**: 163–165.

Campana, S.E., Gagné, J.A., and McLaren, J.W. 1995. Elemental fingerprinting of fish otoliths using ID-ICPMS. Mar. Ecol. Prog. Ser. **122**: 115–120.

Campana, S.E., Chouinard, G.A., Hanson, J.M., and Fréchet, A. 1999. Mixing and migration of overwintering cod stocks near the mouth of the Gulf of St. Lawrence. Can. J. Fish. Aquat. Sci. **56**: 1873–1881.

Campana, S.E., Chouinard, G.A., Hanson, M., Fréchet, A., and Brattey, J. 2000. Otolith elemental fingerprints as biological tracers of fish stocks. Fish. Res. **46**: 343–357.

Castonguay, M., Rollet, C., Fréchet, A., Gagnon, P., Gilbert, D., and Bréthes, J.-C. 1999. Distribution changes of Atlantic cod (*Gadus morhua*) in the northern Gulf of St. Lawrence in relation to an oceanic cooling. ICES J. Mar. Sci. **56**: 333–344.

Comeau, L.A., Campana, S.E., and Chouinard, G.A. 2002. Timing of Atlantic cod (*Gadus morhua*) seasonal migrations in the southern Gulf of St. Lawrence: interannual variability and proximate control. ICES J. Mar. Sci. **59**: 333–351.

D'Amours, D., Frank, K.T., and Bugden, G. 1994. Report of the Working Group on Oceanographic Effects on Stock Migration and Mixing — reviewed by the Fisheries Oceanography Committee (FOC). DFO Atl. Fish. Res. Doc. No. 94/54.

Department of Fisheries and Oceans. 2004. Unit 1 redfish — 2003 update. DFO Can. Sci. Advis. Sec. Stock Status Rep. No. 2004/015.

Desrosiers, B., Sévigny, J.-M., and Chanut, J.-P. 1999. Restriction fragment length polymorphism of rDNA in the redfishes *Sebastes fasciatus* and *S. mentella* (Scorpaenidae) from the Gulf of St. Lawrence. Can. J. Zool. **77**: 267–277.

Duarte, R., Azevedo, M., Landa, J., and Pereda, P. 2001. Reproduction of anglerfish (*Lophius budegassa* and *Lophius piscatorius*) from the Atlantic Iberian coast. Fish. Res. **51**: 349–361.

Edmonds, J.S., Caputi, N., and Morita, M. 1991. Stock discrimination by trace-element analysis of otoliths of orange roughy (*Hoplostethus atlanticus*), a deep-water marine teleost. Aust. J. Mar. Freshw. Res. **42**: 383–389.

Fowler, A.J., Campana, S.E., Jones, C.M., and Thorrold, S.R. 1995. Experimental assessment of the effect of temperature and salinity on elemental composition of otoliths using solution-based ICPMS. Can. J. Fish. Aquat. Sci. **52**: 1421–1430.

Gascon, D. (*Editor*). 2003. Redfish Multidisciplinary Research Zonal Program (1995–1998): final report. Can. Tech. Rep. Fish. Aquat. Sci. No. 2462.

Gauthier, S., and Rose, G.A. 2002. Acoustic observation of diel vertical migration and shoaling behaviour in Atlantic redfishes. J. Fish Biol. **61**: 1135–1153.

Jacobson, L.D., Brodziak, J., and Rogers, J. 2001. Depth distributions and time-varying bottom trawl selectivities for dover sole (*Microstomus pacificus*), sablefish (*Anoplopoma fimbria*), and thornyheads (*Sebastolobus alascanus* and *S. altivelis*) in a commercial fishery. Fish. Bull. **99**: 309–327.

Kuo, C., and Tanaka, S. 1984. Distribution and migration of *Holi macrurosus novaezelandiae* in waters around New Zealand. Nipp. Suisan Gakkaishi, **50**: 391–396.

Lutcavage, M.E., Brill, R.W., Skomal, G.B., Chase, B.C., and Howey, P.W. 1999. Results of pop-up satellite tagging of spawning size class fish in the Gulf of Maine: do North Atlantic bluefin tuna spawn in the mid-Atlantic? Can. J. Fish. Aquat. Sci. **56**: 173–177.

© 2007 NRC Canada

MacDonald, J.S., Dadswell, M.J., Appy, R.G., Melvin, G.D., and Methven, D.A. 1984. Fishes, fish assemblages, and their seasonal movements in the lower Bay of Fundy and Passamaquoddy Bay, Canada. Fish. Bull. **82**: 121–139.

Misra, R.K. 1985. Quadratic discriminant analysis with covariance for stock delineation and population differentiation: a study of beaked redfishes (*Sebastes mentella* and *S. fasciatus*). Can. J. Fish. Aquat. Sci. **42**: 1672–1676.

Morin, B., Power, D., and Gagnon, P. 1994. Distribution of redfish (*Sebastes* spp.) in the Gulf of St. Lawrence and in the Laurentian Channel based on RV surveys and commercial fishery catch rates. DFO Atl. Fish. Res. Doc. No. 94/91.

Ni, I.-H. 1981. Separation of sharp-beaked redfish, *Sebastes fasciatus* and *S. mentella*, from northeastern Grand Bank by morphology of extrinsic gasbladder musculature. J. Northw. Atl. Fish. Sci. **2**: 7–12.

Ni, I.-H., and Templeman, W. 1985. Reproductive cycles of redfishes (*Sebastes*) in southern Newfoundland waters. J. Northw. Atl. Fish. Sci. **6**: 57–64.

Roques, S., Sévigny, J.-M., and Bernatchez, L. 2001. Evidence for broadscale introgressive hybridization between two redfish (genus *Sebastes*) in the Northwest Atlantic: a rare marine example. Mol. Ecol. **10**: 149–165.

Roques, S., Sévigny, J.-M., and Bernatchez, L. 2002 Genetic structure of deep-water redfish, *Sebastes mentella*, populations across the North Atlantic. Mar. Biol. **140**: 297–307.

Rubec, P.J., McGlade, J.M., Trottier, B.L., and Ferron, A. 1991. Evaluation of methods for separation of Gulf of St. Lawrence beaked redfishes, *Sebastes fasciatus* and *S. mentella*: malate dehydrogenase mobility patterns compared with extrinsic gasbladder muscle passages and anal fin ray counts. Can. J. Fish. Aquat. Sci. **48**: 640–660.

Sévigny, J.-M., Gagné, P., Lafontaine, Y., and Dodson, J. 2000. Identification and distribution of larvae of redfish (*Sebastes fasciatus* and *S. mentella*: Scorpaenidae) in the Gulf of St. Lawrence. Fish. Bull. **98**: 375–388.

Smith, P.J., Robertson, S.G., Horn, P.L., Bull, B., Anderson, O.F., Stanton, B.R., and Oke, C.S. 2002. Multiple techniques for determining stock relationships between orange roughy, *Hoplostethus atlanticus*, fisheries in the eastern Tasman Sea. Fish. Res. **58**: 119–140.

Starr, R.M., Heine, J.N., and Johnson, K.A. 2000. Techniques for tagging and tracking deepwater rockfishes. N. Am. J. Fish. Manag. **20**: 597–609.

St-Pierre, J.-F., and de Lafontaine, Y. 1995. Fecundity and reproduction characteristics of beaked redfish (*Sebastes fasciatus* and *S. mentella*) in the Gulf of St. Lawrence. Can. Tech. Rep. Fish. Aquat. Sci. No. 2059.

Stransky, C., and MacLellan, S.E. 2005. Species separation and zoogeography of redfish and rockfish (genus *Sebastes*) by otolith shape analysis. Can. J. Fish. Aquat. Sci. **62**: 2265–2276.

Stransky, C., Garbe-Schonberg, C.-D., and Gunther, D. 2005. Geographic variation and juvenile migration in Atlantic redfish inferred from otolith microchemistry. Mar. Freshw. Res. **56**: 677–691.

Swain, D.P., and Kramer, D.L. 1995. Annual variation in temperature selection by Atlantic cod (*Gadus morhua*) in the southern Gulf of St. Lawrence, Canada, and its relation to population size. Mar. Ecol. Prog. Ser. **116**: 11–23.

Swain, D.P., Chouinard, G.A., Morin, R., and Drinkwater, K.F. 1998. Seasonal variation in the habitat associations of Atlantic cod (*Gadus morhua*) and American plaice (*Hippoglossoides platessoides*) from the southern Gulf of St. Lawrence. Can. J. Fish. Aquat. Sci. **55**: 2548–2561.

Templeman, W. 1962. Divisions of cod stocks in the Northwest Atlantic. ICNAF Redbook, **III**: 79–123.

Valentin, A., Sévigny, J.-M., Power, D., Branton, R.M., and Morin, B. 2006. Extensive sampling and concomitant use of meristic characteristics and variation at the MDH-A* locus reveal new information on redfish species distribution and spatial pattern of introgressive hybridization in the Northwest Atlantic. J. Northwest Atl. Fish. Sci. **36**: 1–16.

Wood, C.C., McKinnell, S., Mulligan, T.J., and Fournier, D.A. 1987. Stock identification with the maximum-likelihood mixture model: sensitivity analysis and application to complex problems. Can. J. Fish. Aquat. Sci. **44**: 866–881.

Wood, C.C., Rutherford, D.T., and McKinnell, S. 1989. Identification of sockeye salmon (*Oncorhynchus nerka*) stocks in mixed-stock fisheries in British Columbia and southeast Alaska using biological markers. Can. J. Fish. Aquat. Sci. **46**: 2108–2120.

© 2007 NRC Canada

Changes in baseline growth and maturation parameters of Northwest Atlantic porbeagle, *Lamna nasus*, following heavy exploitation

Rachel M. Cassoff, Steven E. Campana, and Sigmund Myklevoll

Abstract: We tested for density-dependent changes in growth and maturation of Northwest Atlantic porbeagle (*Lamna nasus*) after the population declined by 75%–80% from fishing. Vertebrae and reproductive data collected from the virgin (1961–1966) and exploited (1993–2004) populations were analysed to test for differences in growth rate and age and length at maturity between the time periods. We detected significant differences between reparameterized von Bertalanffy growth models for each period, using likelihood ratio tests. Beyond an age of 7 years, mean length at age was greater during 1993–2004 than during 1961–1966. Between 1961–1963 and 1999–2001, length at maturity decreased in males (from 179 to 174 cm curved fork length (CFL)) and was invariant in females (216 cm CFL), whereas age at maturity declined in both males (from 8 to 7 years) and females (from 19 to 14 years). An analysis of porbeagle temperature associations indicated that sharks occupied comparable temperature conditions during the mid-1960s and 1990s, ruling out the possibility of temperature-induced growth changes. The observed increase in growth rate and decrease in age at maturity following exploitation support the hypothesis of a compensatory density-dependent growth response.

Résumé : Après que la population de maraîches (*Lamna nasus*) du nord-ouest de l'Atlantique eût décliné de 75–80 % à cause de la pêche, nous avons recherché l'existence de changements reliés à la densité dans la croissance et la maturation. Nous avons analysé des données sur les vertèbres et la reproduction récoltées dans la population non exploitée (1961–1966) et la population exploitée (1993–2004) afin de vérifier les différences de taux de croissance et d'âges et longueurs à la maturité durant ces deux périodes. Des tests de rapports de vraisemblance indiquent des différences significatives entre les modèles de croissance de Bertalanffy reparamétrisés durant les deux périodes. Au-delà de l'âge de 7 ans, la longueur moyenne en fonction de l'âge est plus grande en 1993–2004 qu'en 1961–1966. Entre 1961–1963 et 1999–2001, la longueur à la maturité a diminué chez les mâles (de 179 à 174 cm de longueur courbée à la fourche, CFL), mais elle est demeurée la même chez les femelles (216 cm CFL); cependant, l'âge à la maturité a décliné, tant chez les mâles (de 8 à 7 ans) que chez les femelles (de 19 à 14 ans). Une analyse des associations des maraîches avec la température indique que ces requins ont vécu dans des conditions thermiques comparables durant le milieu des années 1960 et les années 1990, ce qui élimine la possibilité que les changements de croissance aient été causés par la température. L'accroissement du taux de croissance et le déclin de l'âge à la maturité observés après l'exploitation est compatible avec l'hypothèse d'une réaction de croissance dépendante de la densité.

[Traduit par la Rédaction]

Introduction

The porbeagle, *Lamna nasus*, is a large, cold-temperate, pelagic shark species found in the eastern and western North Atlantic and more broadly throughout the oceans of the southern hemisphere (Svetlov 1978; Compagno 2001). Porbeagles residing in the Northwest Atlantic are considered to be members of a single population (Campana et al. 1999) ranging from northern Newfoundland to at least New Jersey and perhaps to South Carolina (Templeman 1963; Campana et al. 1999). Porbeagles in this population are most abundant on and along the continental shelves in the area encompassing the Gulf of Maine (off New England) to the Grand Banks (off southern Newfoundland). However, distribution varies seasonally across this region as a result of size and sex-specific north–south migrations (Aasen 1963; Campana et al. 2001).

In the Northwest Atlantic, porbeagle abundance has declined by an estimated 75%–80% since the early 1960s (Department of Fisheries and Oceans (DFO) 2005), warranting

Received 13 March 2006. Accepted 8 November 2006. Published on the NRC Research Press Web site at http://cjfas.nrc.ca on 16 January 2007.
J19223

R.M. Cassoff.[1,2] Department of Biology, Dalhousie University, 1355 Oxford Street, Halifax, NS B3H 4J1, Canada.
S.E. Campana. Department of Fisheries and Oceans, Bedford Institute of Oceanography, P.O. Box 1006, Dartmouth, NS B2Y 4A2, Canada.
S. Myklevoll. Institute of Marine Research, P.O. Box 1870, Nordnes, N-5817 Bergen, Norway.

[1]Corresponding author (e-mail: rcassoff@hotmail.com).
[2]Present address: 413 Maple Lane, Sewickley, PA 15143, USA.

 doi:10.1139/f06-167 © 2007 NRC Canada

their recent designation as endangered by the Committee on the Status of Endangered Wildlife in Canada (COSEWIC 2004). Several independent lines of evidence strongly implicate exploitation in commercial target fisheries as the cause of this decline (Campana et al. 2003). Commercial harvesting of porbeagles started in 1961, when Norwegian longliners began exploratory fishing on the virgin (previously unexploited) population. Historically, exploitation was most intense during the first few years of the fishery. From 1961 to 1964, total reported annual landings in the Northwest Atlantic rose from 1900 to 9000 tonnes (t) (Campana et al. 2002*a*). These intense fishing efforts precipitated the collapse of the Norwegian fishery in the late 1960s and reduced the population to an estimated 50% of the virgin abundance (DFO 2005). A modest recovery of porbeagle numbers occurred throughout the 1970s and 1980s, as landings averaged less than 350 t·year^{-1} (Campana et al. 2002*a*). However, annual catches increased to 1000–2000 t during the 1990s, and the abundance of porbeagles once again fell sharply (Campana et al. 2003). Subsequent catch restrictions, implemented under a Canadian Shark Management Plan, reduced annual landings to less than 250 t by 2002 (Campana et al. 2003). A recent stock assessment indicated that these measures were effective in stabilizing the population at its current low level (DFO 2005).

Given the magnitude of the decline in porbeagle abundance since the early 1960s, a density-dependent compensatory response would be expected. One process that could potentially lead to compensation in depleted shark populations is a density-dependent increase in somatic growth rates owing to reduced prey limitation and a concomitant decrease in the age at sexual maturity (as maturation is largely size-dependent) (Holden 1973). Demographic analyses have demonstrated that a compensatory growth response may be one of the main mechanisms of population regulation in sharks (Smith et al. 1998; Cortés 2002; Frisk et al. 2005). Compensatory changes in growth have been observed in a large number of teleost populations (see Rose et al. (2001) and references therein). However, because reliable, long-term biological and fisheries data are lacking for the majority of elasmobranch species (Compagno 1990; Stevens et al. 2000), few rigorous empirical investigations have addressed compensatory processes in sharks.

Two recent studies have provided the only empirical evidence to date of density-dependent growth in sharks. Carlson and Baremore (2003) reported increased juvenile growth rates and earlier sexual maturation of Atlantic sharpnose sharks (*Rhizoprionodon terraenovae*) in the Gulf of Mexico after a period of intensified exploitation. Similarly, off the southeastern US, Sminkey and Musick (1995) observed faster growth in juvenile sandbar sharks (*Carcharhinus plumbeus*) following declines in population size. Although density-dependent effects were strongly implicated in these changes, neither study was able to evaluate the relative influence of other factors that affect rates of growth, such as changes in environmental conditions. Furthermore, sampling occurred well after the onset of exploitation in both studies. Therefore, the documented changes in life history likely do not represent the full scope for compensatory response in either shark species.

The biology of the porbeagle in the Northwest Atlantic has been the subject of research since the commencement of commercial harvesting in the early 1960s. As a result, vertebral samples and reproductive data were available from the periods 1961–1966 and 1993–2004, providing us with the opportunity to examine possible density-dependent changes in baseline growth and maturation parameters. As far as we are aware, this is the only shark population for which pre-exploitation life history data are available. The first objective of our study was to reconstruct porbeagle growth rate and estimate age and length at maturity in order to test for differences between the time periods. If porbeagle growth was responsive to changes in density, then we would expect an increase in growth rate, as well as a decline in the age at maturity between the sampling periods. In addition to evaluating density-dependent effects, we also considered the effects of variation in ambient water temperature on porbeagle growth as an alternative explanation of observed growth rate changes. Finally, we evaluate the implications of our findings to the understanding of life history theory in sharks.

Materials and methods

Two sets of porbeagle vertebrae were used for age and growth analysis: one taken after three to four decades of heavy exploitation in the Northwest Atlantic and one taken from the virgin (previously unfished) population. Collectively, 615 samples were available from the recent past: 558 prepared vertebrae available from 1993–1999, which were used for a previous age determination study (Natanson et al. 2002), and 57 additional vertebrae obtained in 2004. Sampling took place primarily in the spring and fall on commercial and research vessels operating with longline gear in an area encompassing the Gulf of Maine to the Grand Banks (off southern Newfoundland) and Gulf of St. Lawrence (Fig. 1). Captured individuals were considered to be members of a single population, an assumption strongly supported by long-term tagging studies by Canada, the US, and Norway (Campana et al. 1999). Vertebrae were taken from sharks between the head and the branchial chamber (numbers 10–15) and stored frozen or in 70% ethanol. Body lengths were reported to the nearest centimetre as curved fork length (CFL; over the body distance from the tip of the snout to the fork in the tail) (CFL = straight fork length, r^2 = 0.998; Campana et al. 1999). Reproductive information, including maturity status and length of reproductive organs, was available for the years 1999–2001 (Jensen et al. 2002).

Vertebral samples collected in 1961–1966 were analyzed to reconstruct the growth rate of the virgin porbeagle population. A total of 229 samples were acquired from the archives of the Institute of Marine Research (IMR) in Bergen, Norway. Most of the vertebrae (99%) were collected in the first 2 years of the fishery. Sampling was carried out between May and August by Olav Aasen (IMR) onboard the Norwegian longliners that first targeted porbeagles in the Northwest Atlantic. Vertebrae were taken on the same fishing grounds as the more recent samples (with the exception of one shark captured off North Carolina) and with comparable fishing gear (Joyce 1999). Four to six vertebrae were reportedly removed midway between the head and the caudal

© 2007 NRC Canada

Fig. 1. Map of the Northwest Atlantic showing the distribution of porbeagle (*Lamna nasus*) catch recorded in the 1965 and 1966 fishing logs of the Norwegian longliner *M.S. Volstad*. Fishing locations for the remainder of the sampling period (1961–1964) are not shown. Expanding circles are proportional in size to the number of sharks captured, and xs represent zero catch. The principal porbeagle fishing grounds, where historical and recent vertebral samples were collected, are delineated by the rectangle. The 100 m (broken lines) and 200 m (solid lines) depth contours are shown.

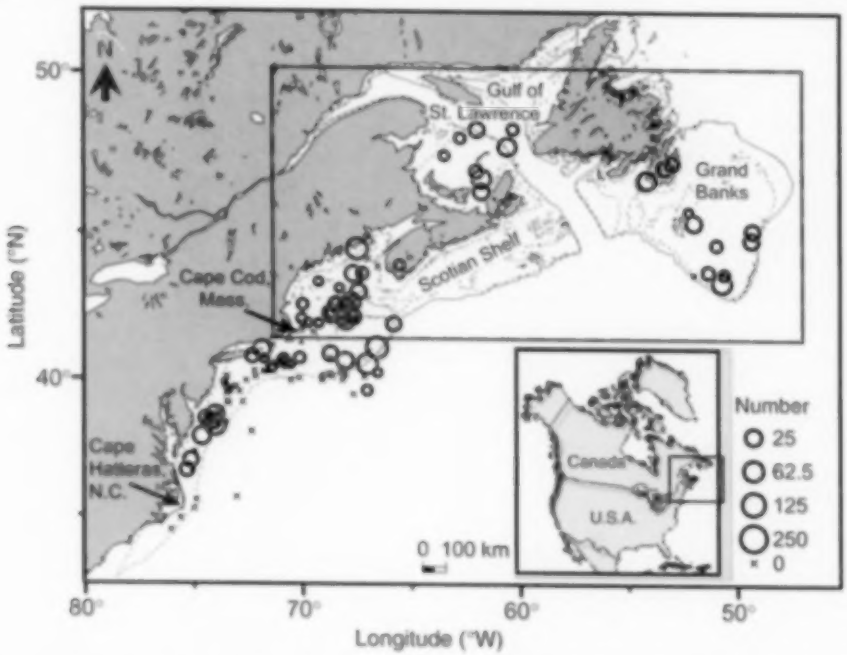

fin of each shark (numbers 50–60) (S. Myklevoll, personal communication, 2005) and stored either dry or in formalin. Aasen (1963) recorded exterior clasper and uterus lengths to the nearest millimetre and either a nonstandard total length (TL) or dorsal length (DL; distance from the anterior edge of the first dorsal fin to the anterior precaudal pit) to the nearest centimetre. The following regression models were used to convert Aasen's body length measurements to CFL (Campana et al. 1999, 2001):

$$\mathrm{CFL} = 0.947\,\mathrm{TL} + 3.64 \quad (n = 361, r^2 = 0.99)$$

$$\mathrm{CFL} = 3.03\,\mathrm{DL}^{0.934} \quad (n = 356, r^2 = 0.99)$$

One vertebra from each shark was processed according to the methods of Natanson et al. (2002). This entailed removing excess tissue and measuring medial dorso-ventral centrum diameter (CD) with calipers to the nearest millimetre. A sagittal (bow tie) cross section of each centrum was made through the center with a diamond-bladed Isomet saw. Digital images of sections were taken using an image analysis system under reflected light (1280 × 1024 resolution). To increase the contrast between adjacent growth bands, images were digitally enhanced using Adobe Photoshop 7.0® (Adobe Systems Inc. 2002). Centrum radius (CR) was measured to the nearest millimetre on these images with Optimas 5.2® (Meyer Instruments Inc. 2000), unless both section halves were broken during processing. Measurements were taken on each half bow tie from the base, which is located just above the isthmus, to the distal edge along the intersection of the corpus calcareum with the intermedialia.

Rigorous validation studies, using several techniques, have confirmed that deposition of a single pair of opaque and translucent bands (growth increment) occurs annually in porbeagles from birth to an age of at least 26 years (Campana et al. 2002*b*; Natanson et al. 2002). To ensure the accuracy of age determinations in the present study, interpretation of annuli was calibrated with a reference collection of more than 500 sectioned vertebrae of known or consensus-derived ages, used in the aforementioned studies. Samples from both time periods were then aged twice by the senior author, in a random order, following a double-blind procedure. Those deemed unreadable (recent sample, $n = 31$; historical sample, $n = 26$) were excluded from further analysis. The consistency of the new age interpretations with those published previously was evaluated using age-bias plots, and the coefficient of variation (CV) was used as a measure of precision (Campana et al. 1995).

Some of the sample tags attached to dried, historical vertebrae had deteriorated, making it impossible to link these samples to Aasen's recorded data. To estimate the lengths of these sharks, CFL was derived from a regression model fitted to the CFL–CR data or, in the absence of CR measurements, from the calculated relationship between CFL and CD. Both of these regressions were generated from a subsample of Aasen's vertebrae for which TL was recorded.

To compare growth characteristics between the virgin and exploited porbeagle populations, the von Bertalanffy growth

© 2007 NRC Canada

function (VBGF), as well as a reparameterized version of this model, were fitted to each set of length at age data using nonlinear least squares in Systat 10.0® (Systat Software Inc. 2002). The conventional VBGF (von Bertalanffy 1938; Ricker 1979) is expressed as

$$L_t = L_\infty[1 - e^{-K(t-t_0)}]$$

where L_t is the mean length at age t, L_∞ is the mean asymptotic length, K is the Brody growth coefficient, which determines how rapidly the horizontal asymptote is approached, and t_0 is the mean age at length zero. The alternative parameterization was formulated by Francis (1988) as

$$L = l_\phi + (l_\psi - l_\phi)(1 - r^{2(T-\phi)/(\psi-\phi)})/(1 - r^2)$$

where

$$r = (l_\psi - l_\chi)/(l_\chi - l_\phi)$$

The parameter L represents the mean length at age T, and l_ϕ, l_χ, and l_ψ represent the mean lengths at ages ϕ, $(\phi + \psi)/2$, and ψ, respectively, which were selected to fall within the range of both data sets. In addition, locally weighted least squares regression (lowess) curves were used to describe patterns of growth during each time period and were fitted to length at age data using the Lowess function in SPSS 11.5.0® (SPSS Inc. 2002).

Both the reparameterized and traditional von Bertalanffy growth models were used to test for statistical differences between the virgin and exploited length at age data sets. The reparameterized model was selected, because it overcomes two of the shortfalls of the conventional VBGF: the L_∞ and K parameters tend to be strongly correlated and the estimation of some parameter values involves extrapolation (Francis 1988). Likelihood ratio tests were employed to test for differences in growth curves between the time periods (Kimura 1980). Of the most commonly used statistical procedures for growth curve comparison, this approach is considered to be the most accurate on the basis of empirical analyses conducted by Cerrato (1990). This test assumes a normal, additive error structure and equal variances between data sets. The validity of the latter assumption was assessed using a Bartlett's test (Zar 1996).

Male length at maturity in porbeagles is associated with a distinct inflection in clasper growth (Jensen et al. 2002). Differences in male length at maturity between time periods were evaluated by fitting a logistic growth model to each set of clasper length (CL) – CFL data using nonlinear least squares and comparing their inflection points, which were used as a common reference point. The model was formulated following Piner et al. (2005):

$$\hat{y} = y_{min} + k[1 + \exp(b(a - x))]^{-1}$$

with fixed parameters y = CL, y_{min} = the minimum observed CL, and x = CFL and estimated parameters k = maximum observed CL – minimum observed CL, a = inflection point, and b = shape parameter. Length at female maturity, which corresponds with a marked increase in uterus development (Jensen et al. 2002), was clearly visible from graphs of uterus length versus CFL. The length at maturity for the virgin population, estimated from a plot of uterus growth, was compared with the reproductive information from more recent years reported by Jensen et al. (2002).

An analysis of historical porbeagle temperature associations was carried out using catch (number of sharks), effort (number of hooks per set), and fishing locations obtained from the 1965 logs of the Norwegian longliner *M.S. Volstad*. Vessel positions were given as Loran-A readings (to the nearest 5 µs) and were converted to latitude and longitude with LoranGPS 6.0® (Andren Software Co. 2005). Analyses were limited to the principal porbeagle fishing grounds extending north of Cape Cod, Mass. (Fig. 1).

To estimate the temperature at the depth of the longline gear associated with each fishing location, we extracted temperature profiles from the year 1965 from the Atlantic Fisheries Adjustment Program database (Bedford Institute of Oceanography, Dartmouth, Nova Scotia). Temperatures were averaged over the depth range (10–30 m) at which the Norwegian fleet set the longline hooks (Aasen 1963). Contour maps displaying temperature at mean gear depth, overlaid with catch per unit effort, were then produced for each month and area (e.g., Grand Banks) in which porbeagles were caught. Temperatures at fishing locations were estimated from these maps only if fishing sites were bounded on all sides by temperature contours.

The same set of contour maps was used to determine the range of temperatures available to porbeagles in areas surrounding fishing sets (environmental temperature). Broad fishing areas, which included the Gulf of Maine, Grand Banks, and Gulf of St. Lawrence, were delineated on the maps by polygons enclosing all of the 1965 fishing locations. Temperature observations lying within these polygons were drawn from the maps along a 30′ latitude × 30′ longitude grid pattern.

To identify porbeagle temperature associations, we compared cumulative distribution functions (CDFs) of two variables: temperature at fishing locations, weighted by catch per unit effort, and environmental temperature (Perry and Smith 1994). Cumulative distribution functions were generated with temperatures pooled across months (May–August) and areas because of limited data availability. Disparities between CDFs imply that porbeagles prefer a particular temperature range, whereas similarities suggest a lack of association between porbeagle catch and specific temperature conditions within the range available in the environment. Results were compared with findings from a similar analysis of temperature profiles from 1994 to 2000 (Campana and Joyce 2004).

Results

Aged specimens from the exploited population consisted of 291 males, 290 females, and 3 of unknown sex ranging in size from 77 to 261 cm CFL (Table 1). Those collected from the virgin population included 34 males, 43 females, and 126 samples that could not be matched to Aasen's recorded data and, therefore, were of unknown sex and body length (Table 1). These sharks had a CFL range of 70 to 245 cm. The coefficient of variation for the replicated age readings was 7%.

The modeled CFL–CR and CFL–CD relationships were used to reconstruct body lengths of 107 and 19 historical

© 2007 NRC Canada

Table 1. Summary of vertebral samples used to reconstruct growth in the virgin (1961–1966) and exploited (1993–2004) porbeagle (*Lamna nasus*) populations.

			Sample size				CFL of males (cm)		CFL of females (cm)	
Area	Season	Year	Males	Females	Unknown sex	Total	Min	Max	Min	Max
Virgin										
Gulf of Maine	Summer	1961	13	10	0	23	112	176	103	164
		1962	17	20	0	37	132	220	125	216
Scotian Shelf	Summer	1961	3	11	0	14	96	226	90	245
Grand Banks	Summer	1961	0	0	126	126*	92	231	92	231
Southeastern US	Spring	1966	0	1	0	1	—	—	146	146
Unknown	Unknown	1965	1	1	0	2	70	70	72	72
Total	—	—	34	43	126	203	70	226	72	245
Exploited										
Gulf of Maine	Summer	1999	3	0	0	3	182	219	—	—
	Spring	1994	17	16	0	33	104	239	101	203
		1999	75	66	0	141	77	232	97	241
	Summer	1997	1	1	0	2	156	156	193	193
		1999	3	6	0	9	105	144	128	228
		2004	31	17	0	48	113	202	110	181
	Autumn	1993	19	19	0	38	89	216	90	192
		1999	13	15	0	28	92	226	101	240
	Winter	1999	0	2	0	2	—	—	95	167
Grand Banks	Spring	1999	7	4	0	11	135	208	167	220
	Autumn	1993	9	15	1	25	170	232	113	236
		1997	0	1	0	1	—	—	169	169
		1999	64	80	0	144	95	246	94	256
	Winter	1999	7	13	0	20	107	240	200	261
Gulf of St. Lawrence	Autumn	1993	1	0	0	1	148	148	—	—
		1999	28	26	0	54	99	230	100	242
Unknown	Spring	1997	10	3	0	13	162	201	184	221
		1999	1	0	0	1	97	97	—	—
	Summer	1993	0	1	0	1	—	—	183	183
		1997	1	1	0	2	159	159	202	202
		1999	0	0	1	1	236	236	236	236
	Autumn	1996	1	1	0	2	189	189	139	139
		1997	0	1	0	1	—	—	100	100
	Winter	1996	0	1	0	1	—	—	224	224
	Unknown	—	0	1	1	2	97	102	97	102
Total	—	—	291	290	3	584	77	246	90	261

Note: Sample size and curved fork length (CFL) range are given separately for each sex by sampling area, season, and year. Seasons: spring, March–May; summer, June–August; autumn, September–November; winter, December–February. Min, minimum; max, maximum.
*Fork lengths were reconstructed from vertebral size.

samples, respectively, for which only centrum measurements were available. CFL and CR displayed a moderately curvilinear relationship, which was linearized by applying a $\log_e$–$\log_e$ transformation (Fig. 2). The least squares equation calculated from the transformed data was

$$\log_e(\mathrm{CFL}) = 0.74 \log_e(\mathrm{CR}) + 3.21 \quad (n = 76, r^2 = 0.95)$$

In the case of the CFL and CD data, the untransformed relationship provided a better fit:

$$\mathrm{CFL} = 5.08\mathrm{CD} + 24.05 \quad (n = 74, r^2 = 0.94)$$

Both linear regressions were highly significant ($P < 0.0001$), and neither differed significantly between the sexes (analysis of covariance, ANCOVA, $P > 0.7$).

Plots of length at age data for the sexes combined (Figs. 3 and 4) indicated that porbeagles from the virgin population grew more slowly throughout most of the observed age range. Age estimates ranged from 0 to 23 years in 1961–1966 and from 0 to 24 years in 1993–2004. In the virgin population, the youngest age classes (<3 years) displayed slightly higher growth rates. However, the growth curves for the two time periods overlapped between the ages of 4 and 7 years and then diverged as the relative growth in the virgin population slowed. Although differences in length at age were less pronounced beyond an age of about 20 years, few

© 2007 NRC Canada

Fig. 2. Least squares relationship between $\log_e$-transformed curved fork length and $\log_e$-transformed centrum radius for the virgin (1961–1966) porbeagle (*Lamna nasus*) population, which was used to reconstruct curved fork length of samples when body length data were missing. Observed values for males (◆, $n = 34$) and females (□, $n = 42$) are shown separately.

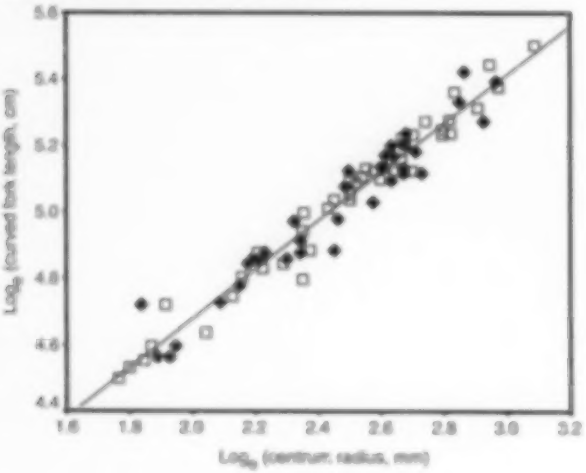

Fig. 3. Observations of porbeagle (*Lamna nasus*) length at age for the sexes combined based on vertebral ages from 1961–1966 (○) and 1993–2004 (△). Fitted lowess curves are shown (historical sample, broken line; recent sample, solid line). Historical data points have been jittered slightly to improve visibility.

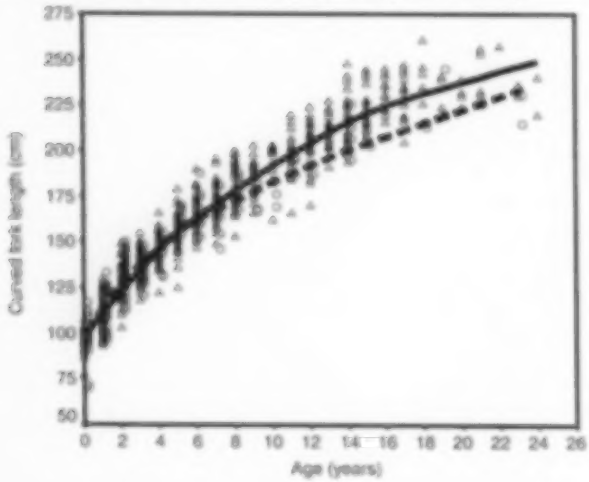

observations lay within this portion of the data range, particularly in the historical sample. Low sample sizes of known-sex sharks from the 1960s precluded the examination of sex-specific growth differences between the sampling periods. However, disparities in growth patterns between the sexes were considered to be minor on the basis of findings from a previous study on Northwest Atlantic porbeagle growth (Natanson et al. 2002).

Comparisons of both the fitted von Bertalanffy and reparameterized growth models revealed that differences in

Fig. 4. Observations of porbeagle (*Lamna nasus*) length at age for the sexes combined based on vertebral ages from 1961–1966 (○) and 1993–2004 (△). Fitted von Bertalanffy growth models are shown (historical sample, broken line; recent sample, solid line). Historical data points have been jittered slightly to improve visibility.

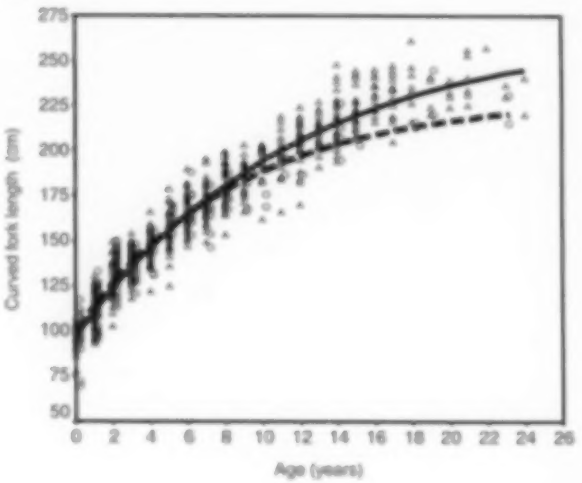

age–length data between the virgin and exploited porbeagle populations were significant ($P < 0.01$) (Table 2). Because the largest size classes were poorly represented in the historical data set (Figs. 3 and 4), the length range over which both types of growth curves were fitted and compared was limited to CFLs less than the maximum observed size in the historical sample (245 cm). The reference ages selected for the reparameterized model ($\phi = 0$, $\chi = 11.5$, and $\psi = 23$) spanned 99.7% (exploited) and 100% (virgin) of the observations lying within the restricted data range. The reparameterized growth models yielded a significantly larger predicted mean CFL at age 0 for the 1961–1966 sample ($l_0 = 102.8$ cm) compared with the 1993–2004 sample ($l_0 = 97.2$ cm) (Tables 2 and 3). The remaining parameter values for the virgin population ($l_{11.5} = 196.0$ cm, $l_{23} = 220.5$ cm) were significantly smaller than those for the exploited population ($l_{11.5} = 202.6$ cm, $l_{23} = 242.8$ cm) (Tables 2 and 3). Pronounced differences, likewise, were observed between values of the VBGF parameter L_∞: virgin, 229.2 cm; exploited, 267.6 cm (Tables 2 and 3). The variance assumption of the likelihood ratio approach for comparing growth curves was met ($\chi^2 = 0.316$, $P = 0.574$). Likelihood ratio tests detected significant differences in the overall reparameterized growth models and in all three of its parameters between the sampling periods ($P < 0.01$) (Table 3).

Comparisons of porbeagle reproductive data indicated a small shift in the male length at maturity but no change in the female length at maturity between the sampling periods 1961–1963 and 1999–2001. Clasper measurements were available for 285 and 365 males from the virgin and exploited populations, respectively. These data covered a similar range of fork lengths: virgin, 84–253 cm; exploited, 86–246 cm (Fig. 5). The estimated inflection points of the logistic growth models used to describe clasper development

© 2007 NRC Canada

Table 2. von Bertalanffy and reparameterized growth model parameter estimates for porbeagles (*Lamna nasus*) (sexes combined) collected in 1961–1966 and 1993–2004.

		von Bertalanffy parameters			Francis parameters			
Time period	n	L_∞ (cm)	K (year^{-1})	t_0 (years)	l_0 (cm)	$l_{11.5}$ (cm)	l_{23} (cm)	R^2
1961–1966	203	229.2±11.9	0.116±0.021	–5.12±0.75	102.8±3.0	196.0±3.1	220.5±7.4	0.90
1993–2004	577	267.6±9.3	0.084±0.009	–5.39±0.47	97.2±2.3	202.6±1.1	242.8±3.5	0.94

Note: 95% confidence intervals are given directly to the right of parameter values.

Table 3. Outcome of likelihood ratio tests comparing traditional and reparameterized von Bertalanffy growth curves between virgin (1961–1966) and exploited (1993–2004) porbeagle (*Lamna nasus*) populations.

Hypothesis	RSS	χ^2	df	P
H_1: No parameters are equal	77 973	—	—	—
H_{0a}: All parameters are equal	83 063	49.32	3	<0.001
von Bertalanffy growth parameters				
H_{0b}: L_∞s are equal	79 516	15.28	1	<0.001
H_{0c}: Ks are equal	78 720	7.44	1	<0.01
H_{0d}: t_0s are equal	78 004	0.31	1	0.578 ns
Reparameterized growth parameters				
H_{0e}: l_0s are equal	78 764	7.87	1	<0.01
H_{0f}: $l_{11.5}$s are equal	79 493	15.06	1	<0.001
H_{0g}: l_{23}s are equal	80 282	22.76	1	<0.001

Note: ns, not significant. Growth models containing parameter constraints (H_0s) were tested against a base model (H_1), in which all parameter values differed between data sets. The residual sum of squares (RSS) for each is given.

in the virgin (a = 148.3 ± 1.5 cm CFL) and exploited (a = 143.6 ± 1.1 cm CFL) populations indicated a significant decline in male length at maturity of about 5 cm between 1961–1963 and 1999–2001 (Fig. 5). Therefore, we assumed that the body lengths corresponding with the onset of male sexual maturity in the virgin and exploited populations were also offset by 5 cm. Jensen et al. (2002) estimated the median length at maturity in recently captured male porbeagles as 174 cm, based on clasper condition. Therefore, median length at maturity in males captured in 1961–1963 was estimated as 179 cm. In contrast, females from the virgin (n = 165) and exploited (n = 243) populations displayed very similar relationships between uterus length and body length (Fig. 6). A rapid increase in uterus growth, associated with sexual maturation, occurred in both samples at a CFL of approximately 216 cm. This value is comparable to the female length at 50% maturity (218 cm FL) reported by Jensen et al. (2002) for the more recent sampling period.

The temperature range occupied by porbeagles in 1965 was comparable to that reported by Campana and Joyce (2004) for the years 1994–2000. The 1965 catch-weighted (n = 34) and environmental (n = 82) temperature CDFs indicated that porbeagle catch rates were moderately enhanced at intermediate temperatures (Fig. 7). About 97% of captured sharks occupied a temperature range of 4–12 °C, which encompassed less than 80% of the environmental temperature observations. Published CDFs for more recent years showed that most porbeagles were caught in temperatures of 4–12 °C in the spring and 6–10 °C in the fall (Campana and Joyce 2004).

Discussion

We found an increase in growth rate and a decrease in the age at maturity of Northwest Atlantic porbeagles following large declines in abundance. Our results showed that recently collected sharks grew at a faster rate throughout most of their life span compared with sharks in the unfished population. Beyond an age of 7 years, the mean length of sharks captured in 1993–2004 was greater than that of sharks captured in 1961–1966. We also found that male length at maturity declined and female length at maturity remained unchanged following exploitation, and there was a reduction in the age at maturity in both sexes. Based on the reparameterized growth models for the sexes combined, age at maturity decreased from 8 to 7 years in males and from 19 to 14 years in females between 1961–1963 and 1999–2001. These observed changes in porbeagle growth and maturity are consistent with a compensatory growth response to reduced porbeagle abundance, whereby greater per capita food availability resulting from relaxed intraspecific competition promoted faster growth and thus enabled individuals to attain maturity earlier.

Juvenile porbeagles experienced declines in abundance of comparable magnitude to those of adults over the course of the commercial fishery (about 75% and 85%, respectively; DFO 2005). Surprisingly, though, our results indicate that the mean length of individuals in the first few age classes (0–3 years) decreased slightly between the sampling periods 1961–1966 and 1993–2004. This is reflected by the significantly higher mean length at age 0 predicted by the virgin

© 2007 NRC Canada

Fig. 5. Relationship between right outer clasper length and curved fork length for porbeagles (*Lamna nasus*) captured in (*a*) 1961–1963 and (*b*) 1999–2001 and associated estimates of the inflection point (broken lines) of fitted logistic growth curves (solid lines).

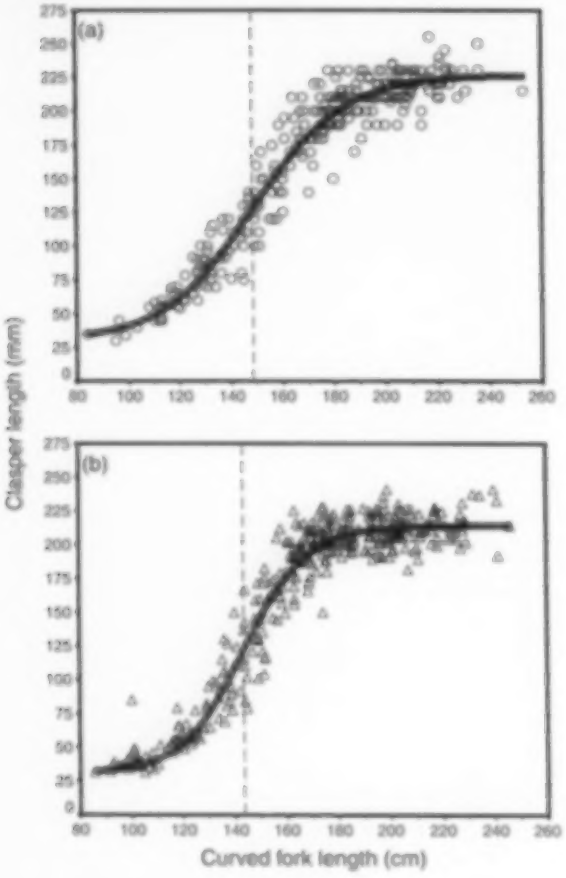

Fig. 6. Relationship between uterus length and curved fork length for porbeagles (*Lamna nasus*) captured in (*a*) 1961–1963 and (*b*) 1999–2001 and associated estimates of length at maturity (broken lines). The maturity status of individuals is indicated in the bottom plot: immature, ▲; mature, △.

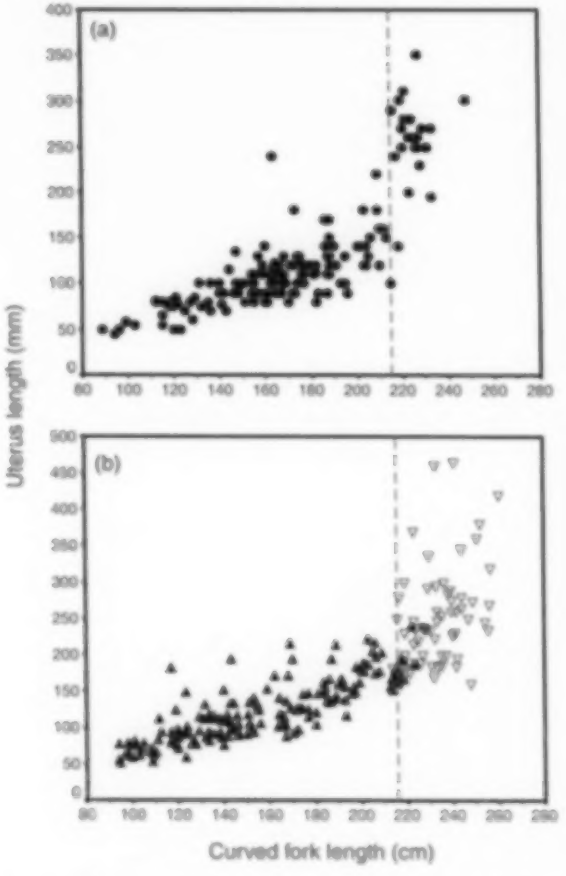

population's reparameterized VBGF than by the exploited population's reparameterized VBGF. We believe that this apparent decrease in relative growth following exploitation is attributable to sampling bias. The age at recruitment to the porbeagle fishery declined substantially after 1993, from 6–7 years to 2–3 years (Campana et al. 2002*a*). Smaller, slower-growing individuals in the youngest age classes would have been less vulnerable to capture by the longline gear during the earlier sampling period and, therefore, were most likely underrepresented in our historical sample.

Our results also showed that earlier maturation in recently collected male porbeagles was associated with a smaller length at maturity (1961–1963, 179 cm; 1999–2001, 174 cm), whereas in females, length at maturity was invariant (216 cm). This pattern is in contrast to that reported by Carlson and Baremore (2003) for the Atlantic sharpnose shark, in which faster growth and earlier maturation were accompanied by reduced length at maturity in both sexes. That female porbeagles did not experience a shift in length at maturity may reflect the importance of a large length at birth to fitness in this species. Survival of newborns in a pelagic environment is most likely highly dependent on their ability to capture prey and, in turn, on their body size (Smith et al. 1998). Therefore, the option for female porbeagles to begin breeding at a smaller length may be constrained by their ability to accommodate large embryos.

Several alternative hypotheses can be invoked to explain the observed increase in growth rates and decrease in age at maturity between the sampling periods 1961–1966 and 1993–2004. These include methodology or sampling, variation in ambient water temperature, genetic changes owing to size-selective fishing, and reductions in interspecific competition. We evaluate the plausibility of each in turn.

Variation in length at age data resulting from methodology or sample collection can give rise to differences in growth curves that are apparent rather than real. While evaluating previously reported differences in growth between two *Mustelus manazo* populations, Cailliet et al. (1990) identified several sources of variation that could bias growth curves: vertebral preparation techniques, reader accuracy and precision, sample size, and sample bias. These sources of

© 2007 NRC Canada

Fig. 7. Cumulative distribution functions of temperature at the mean depth of the longline gear based on data from 1965 for months and fishing areas combined. The broken line represents temperatures at porbeagle (*Lamna nasus*) fishing locations, weighted by catch per unit effort (number per hook), and the solid line represents temperatures in areas surrounding fishing sets.

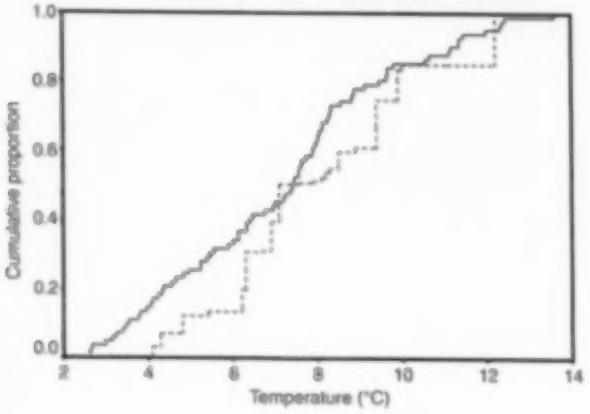

variability most likely produced spurious growth parameter estimates for two populations of blue shark (*Prionace glauca*), resulting in apparent interpopulation differences (Tanaka et al. 1990). In the present study, we were able to minimize these sources of variability by using a standardized preparation technique and a single, experienced age reader for both historic and recent samples. Interpretation of growth increments was calibrated before aging and was based on criteria validated for all age classes included in our study. The level of precision between our replicated age readings was high relative to that reported in other aging studies utilizing shark vertebrae (reviewed by Campana 2001). Furthermore, potential problems related to sample size and bias were addressed by using a reparameterized VBGF and restricting the statistical comparison of growth curves to a body length range where sample sizes were adequate. Therefore, we are confident that the observed increase in porbeagle growth rate between the time periods 1961–1966 and 1993–2004 is not just an artifact of methodology or sampling.

Another possible explanation for the increase in growth rate between the sampling periods is variation in the ambient water temperature of porbeagles. Temperature is a major factor controlling physiological rates in fish, and its effects on growth rate have been documented for many teleosts (Brett 1979). Based on our analyses of porbeagle temperature associations and those of Campana and Joyce (2004), porbeagles occupied a very similar range of temperatures during the mid-1960s and 1990s. Although these analyses provide only a snapshot of temperature conditions, they do suggest that variation in ambient water temperature did not contribute substantially to the differences in growth rate observed between the sampling periods. Porbeagles, like other members of the family Lamnidae, possess an efficient countercurrent heat exchange system and, therefore, are able to maintain body temperatures more than 7 °C warmer than the surrounding water (Carey and Teal 1969; Carey et al. 1981). This thermoregulatory ability would most likely eliminate the effect of any changes in water temperature on growth.

Adaptive evolution in response to fishing is another possible explanation of the changes in growth rate and maturity observed in our study. Prolonged and heavy exploitation has the potential to cause genetic changes in growth rates and maturity, because of the size-selective nature of fishing gear (Hutchings and Reynolds 2004). Such changes have been reported for populations of grayling (*Thymallus thymallus*) (Haugen and Vøllestad 2001) and northern Atlantic cod (*Gadus morhua*) (Olsen et al. 2004). Although porbeagles were subjected to intensive fishing pressure, the evolution of life history traits is likely to be slow relative to the period of commercial exploitation, which spanned less than three generations (generation time = 18 years) (Campana et al. 2003). Furthermore, the tendency of longline gear to preferentially capture the faster-growing members of the youngest age groups (Ricker 1979) would favor a reduction in mean length at age, which is contrary to the trend we observed. Therefore, it seems very doubtful that the observed changes in porbeagle life history represent a genetic response to fishing.

Another possible explanation for the observed increase in growth rate and decrease in age at maturity between the sampling periods is a reduction in interspecific competition for prey owing to the depletion of other large, pelagic predators in the temperate Northwest Atlantic. Porbeagles are tertiary consumers (Cortés 1999), feeding on a wide array of pelagic and demersal teleosts, as well as small elasmobranchs (Joyce et al. 2002). Since the general expansion of pelagic longline fisheries in the 1960s, many other tertiary predators have experienced substantial declines in response to exploitation (Ward and Myers 2005). Large temperate pelagic sharks, including threshers (*Alopias vulpinus*), great whites (*Carcharodon carcharias*), and blues (*Prionace glauca*), in the Northwest Atlantic declined by 60%–80% between 1986 and 2000 (Baum et al. 2003). If these predators exert top-down effects, their removal could have led to an increased abundance of porbeagle prey. Ward and Myers (2005) analyzed survey and observer data for the tropical Pacific pelagic community and found relatively little increase in the biomass of small fish species following pronounced declines in large predatory fishes. Nevertheless, top-down effects are difficult to assess in marine communities (Jennings and Kaiser 1998) and have not been quantified for the temperate Northwest Atlantic. Therefore, the possibility that porbeagle growth rate increased in response to reduced interspecific competition cannot be ruled out.

Holden (1973) advanced two mechanisms, in addition to compensatory growth, that might regulate population size in elasmobranchs: increased fecundity at lower densities owing to increased food availability, and decreased natural mortality at lower densities owing to reduced predation, cannibalism, or competition for food. Density-dependent fecundity is believed to play a minor role in regulating most shark populations (Stevens et al. 2000); the capacity of sharks to augment litter size is likely to be greatly constrained by the amount of space within the maternal body cavity (Holden 1973) and perhaps by the size of the maternal liver (Bone and Roberts 1969; Roff 1992). This may be particularly true of porbeagles, given their large length at birth relative to

© 2007 NRC Canada

maximum adult body length (about 25%). The available reproductive information from the Northwest Atlantic suggests that porbeagle fecundity has not increased since the onset of commercial exploitation. Jensen et al. (2002) reported a litter size of 3–6 pups with an average of 4, which is comparable to that observed prior to exploitation (range of 1–5 pups, but more commonly 2–4 pups; Bigelow and Schroeder 1948). Furthermore, the duration of the porbeagle reproductive cycle (1 year) has remained unchanged since the early 1960s (Aasen 1963; Jensen et al. 2002). In the case of natural mortality rates, only estimates for juvenile porbeagles were available for both the virgin and exploited populations. Estimates for the years 1961 (0.10) and 1998–2000 (0.12), based on catch curves and tag-recapture studies, respectively, were comparable (Campana et al. 2001). Further research is needed to more rigorously evaluate the relative importance of various density-dependent mechanisms in regulating population size. However, based on the available information, porbeagle fecundity and natural mortality appear to be relatively insensitive to changes in density, lending support to the hypothesis that population regulation in porbeagles occurs through compensatory changes in growth.

In conclusion, this is the first study to document changes in baseline growth and maturation parameters in an elasmobranch population following exploitation. In addition, our findings represent the only evidence of temporal changes in both growth rate and maturity in a large, long-lived shark species. Our results showed an increase in growth rates and a decrease in the age at maturity in porbeagles, associated with pronounced declines in abundance. Although we cannot dismiss the possibility that reduced interspecific competition contributed to these changes, results from our study provide strong support for the hypothesis of a compensatory growth response. Because estimates of growth and maturity parameters are used to model population growth, information from this investigation should reduce uncertainty surrounding the current recovery trajectory of the porbeagle population and, in turn, better inform management decisions in the future, as the population rebuilds.

Acknowledgements

The authors thank Lisa Natanson for providing the recent collection of vertebral samples and Christopher Jensen for providing the reproductive data from his research. The authors also thank Warren Joyce for help with sample collection, Linda Marks for advice in the lab, Patty Gray for allowing us to sample his catches at sea, David Gray for assistance with the Loran conversions, and Ole Mikkelson for help with the Norwegian translations. Paul Bentzen, Sandra Wakie, John Carlson, Malcolm Francis, and two anonymous reviewers provided helpful comments on an earlier draft of this manuscript. This research was partially funded by a Patrick Lett Graduate Student Bursary from Dalhousie University (to R.M.C.).

References

Aasen, O. 1963. Length and growth of the porbeagle (*Lamna nasus*, Bonnaterre) in the North West Atlantic. Fiskeridir. Skr. Ser. Havunders. **13**(6): 20–37.

Adobe Systems Inc. 2002. Adobe Photoshop 7.0®. Adobe Systems Inc., San Jose, California.

Andren Software Co. 2005. LoranGPS 6.0®. Andren Software Co., Indialantic, Florida.

Baum, J.K., Myers, R.A., Kehler, D.G., Worm, B., Harley, S.J., and Doherty, P.A. 2003. Collapse and conservation of shark populations in the Northwest Atlantic. Science (Washington, D.C.), **299**: 389–392.

Bigelow, H.B., and Schroeder, W.C. 1948. Fishes of the western North Atlantic. Part 1. Sears Foundation for Marine Research, Yale University, New Haven, Connecticut.

Bone, Q., and Roberts, B.L. 1969. The density of elasmobranchs. J. Mar. Biol. Assoc. U.K. **49**: 913–937.

Brett, J.R. 1979. Environmental factors and growth. *In* Fish physiology. Vol. 8. Bioenergetics and growth. *Edited by* W.S. Hoar, D.J. Randall, and J.R. Brett. Academic Press, New York. pp. 599–677.

Cailliet, G.M., Yudin, K.G., Tanaka, S., and Taniuchi, T. 1990. Growth characteristics of two populations of *Mustelus manazo* from Japan based upon cross-readings of vertebral bands. NOAA Tech. Rep. NMFS, **90**: 167–176.

Campana, S.E. 2001. Accuracy, precision and quality control in age determination, including a review of the use and abuse of age validation methods. J. Fish Biol. **59**: 197–242.

Campana, S.E., and Joyce, W.N. 2004. Temperature and depth associations of porbeagle shark (*Lamna nasus*) in the Northwest Atlantic. Fish. Oceanogr. **13**(1): 52–64.

Campana, S.E., Annand, M.C., and McMillan, J.I. 1995. Graphical and statistical methods for determining the consistency of age determinations. Trans. Am. Fish. Soc. **124**: 131–138.

Campana, S.E., Marks, L., Joyce, W., Hurley, P., and Showell, M. 1999. An analytical assessment of the porbeagle shark (*Lamna nasus*) population in the Northwest Atlantic. Can. Stock Assessment Secretariat Res. Doc. No. 99/158.

Campana, S.E., Marks, L., Joyce, W., and Harley, S. 2001. Analytical assessment of the porbeagle shark (*Lamna nasus*) population in the Northwest Atlantic, with estimates of long-term sustainable yield. Can. Sci. Advisory Secretariat Res. Doc. No. 2001/067.

Campana, S.E., Joyce, W., Marks, L., Natanson, L.J., Kohler, N.E., Jensen, C.F., Mello, J.J., Pratt, H.L., Jr., and Myklevoll, S. 2002*a*. Population dynamics of the porbeagle in the Northwest Atlantic Ocean. North Am. J. Fish. Manag. **22**: 106–121.

Campana, S.E., Natanson, L.J., and Myklevoll, S. 2002*b*. Bomb dating and age determination of large pelagic sharks. Can. J. Fish. Aquat. Sci. **59**: 450–455.

Campana, S.E., Joyce, W., and Marks, L. 2003. Status of the porbeagle shark (*Lamna nasus*) population in the Northwest Atlantic in the context of species at risk. Can. Sci. Advisory Secretariat Res. Doc. No. 2003/007.

Carey, F.G., and Teal, J.M. 1969. Mako and porbeagle: warm-bodied sharks. Comp. Biochem. Physiol. **28**(1): 199–204.

Carey, F.G., Teal, J.M., and Kanwisher, J.W. 1981. The visceral temperatures of mackerel sharks (Lamnidae). Physiol. Zool. **54**: 334–344.

Carlson, J.K., and Baremore, I.E. 2003. Changes in biological parameters of Atlantic sharpnose shark *Rhizoprionodon terraenovae* in the Gulf of Mexico: evidence for density-dependent growth and maturity? Mar. Freshw. Res. **54**: 227–234.

Cerrato, R.M. 1990. Interpretable statistical tests for growth comparisons using parameters in the von Bertalanffy equation. Can. J. Fish. Aquat. Sci. **47**: 1416–1426.

Compagno, L.J.V. 1990. Shark exploitation and conservation. NOAA Tech. Rep. NMFS, **90**: 391–414.

© 2007 NRC Canada

Compagno, L.J.V. 2001. Sharks of the world: an annotated and illustrated catalogue of shark species known to date. Vol. 2. FAO, Rome, Italy.

Cortés, E. 1999. Standardized diet compositions and trophic levels of sharks. ICES J. Mar. Sci. **56**: 707–717.

Cortés, E. 2002. Incorporating uncertainty into demographic modeling: application to shark populations and their conservation. Conserv. Biol. **16**(4): 1048–1062.

Committee on the Status of Endangered Wildlife in Canada. 2004. COSEWIC assessment and status report on the porbeagle shark *Lamna nasus* in Canada. Committee on the Status of Endangered Wildlife in Canada, Ottawa, Ontario.

Department of Fisheries and Oceans. 2005. Stock assessment report on NAFO subareas 3–6 porbeagle shark. Can. Sci. Advisory Secretariat Sci. Advisory Rep. No. 2005/044.

Francis, R.I.C.C. 1988. Are growth parameters estimated from tagging and age–length data comparable? Can. J. Fish. Aquat. Sci. **45**: 936–942.

Frisk, M.G., Miller, T.J., and Dulvy, N.K. 2005. Life histories and vulnerability to exploitation of elasmobranchs: inferences from elasticity, perturbation and phylogenetic analyses. J. Northw. Atl. Fish. Sci. **35**: 27–45.

Haugen, T.O., and Vøllestad, L.A. 2001. A century of life-history evolution in grayling. Genetica, **112–113**: 475–491.

Holden, M.J. 1973. Are long-term sustainable fisheries for elasmobranchs possible? Rapp. P.-V. Reun. Cons. Int. Explor. Mer, **164**: 360–367.

Hutchings, J.A., and Reynolds, J.D. 2004. Marine fish population collapses: consequences for recovery and extinction risk. Bioscience, **54**(4): 297–309.

Jennings, S., and Kaiser, M.J. 1998. The effects of fishing on marine ecosystems. Adv. Mar. Biol. **34**: 201–352.

Jensen, C.F., Natanson, L.J., Pratt, H.L., Jr., Kohler, N.E., and Campana, S.E. 2002. The reproductive biology of the porbeagle shark (*Lamna nasus*) in the western North Atlantic Ocean. Fish. Bull. **100**(4): 727–738.

Joyce, W.N. 1999. Management of shark fisheries in Atlantic Canada. FAO Fish. Tech. Pap. **378** (1): 74–108.

Joyce, W.N., Campana, S.E., Natanson, L.J., Kohler, N.E., Pratt, H.L., Jr., and Jensen, C.F. 2002. Analysis of stomach contents of the porbeagle shark (*Lamna nasus* Bonnaterre) in the Northwest Atlantic. ICES J. Mar. Sci. **59**: 1263–1269.

Kimura, D.K. 1980. Likelihood methods for the von Bertalanffy growth curve. Fish. Bull. **77**(4): 765–774.

Myers Instruments Inc. 2000. Optimas 5.2®. Myers Instruments Inc., Houston, Texas.

Natanson, L.J., Mello, J.J., and Campana, S.E. 2002. Validated age and growth of the porbeagle shark (*Lamna nasus*) in the western North Atlantic Ocean. Fish. Bull. **100**(2): 266–278.

Olsen, E.M., Heino, M., Lilly, G.R., Morgan, M.J., Brattey, J., Ernande, B., and Dieckmann, U. 2004. Maturation trends indicative of rapid evolution preceded the collapse of northern cod. Nature (London), **428**: 932–935.

Perry, R.I., and Smith, S.J. 1994. Identifying habitat associations of marine fishes using survey data: an application to the Northwest Atlantic. Can. J. Fish. Aquat. Sci. **51**: 589–602.

Piner, K.R., Hamel, O.S., Menkel, J.L., Wallace, J.R., and Hutchinson, C.E. 2005. Age validation of canary rockfish (*Sebastes pinniger*) from off the Oregon coast (USA) using the bomb radiocarbon method. Can. J. Fish. Aquat. Sci. **62**: 1060–1066.

Ricker, W.E. 1979. Growth rates and models. *In* Fish physiology. Vol. 8. Bioenergetics and growth. *Edited by* W.S. Hoar, D.J. Randall, and J.R. Brett. Academic Press, New York. pp. 678–743.

Roff, D.A. 1992. The evolution of life histories. Chapman & Hall, New York.

Rose, K.A., Cowan, J.H., Jr., Winemiller, K.O., Myers, R.A., and Hilborn, R. 2001. Compensatory density dependence in fish populations: importance, controversy, understanding and prognosis. Fish Fish. (Oxf.), **2**: 293–327.

Sminkey, T.R., and Musick, J.A. 1995. Age and growth of the sandbar shark, *Carcharhinus plumbeus*, before and after population depletion. Copeia, 1995: 871–883.

Smith, S.E., Au, D.W., and Show, C. 1998. Intrinsic rebound potential of 26 species of Pacific sharks. Mar. Freshw. Res. **49**: 663–678.

SPSS Inc. 2002. SPSS 11.5.0®. SPSS Inc., Chicago, Illinois.

Stevens, J.D., Bonfil, R., Dulvy, N.K., and Walker, P.A. 2000. The effects of fishing on sharks, rays, and chimaeras (chondrichthyans), and the implications for marine ecosystems. ICES J. Mar. Sci. **57**: 476–494.

Svetlov, M.F. 1978. The porbeagle, *Lamna nasus*, in Antarctic waters. J. Ichthyol. **18**(5): 850–851.

Systat Software Inc. 2002. Systat 10.0®. Systat Software Inc., Point Richmond, California.

Tanaka, S., Cailliet, G.M., and Yudin, K.G. 1990. Differences in growth of the blue shark, *Prionace glauca*: technique or population? NOAA Tech. Rep. NMFS, **90**: 177–187.

Templeman, W. 1963. Distribution of sharks in the Canadian Atlantic (with special reference to Newfoundland waters). Bull. Fish. Res. Board Can. No. 140.

von Bertalanffy, L. 1938. A quantitative theory of organic growth (inquiries on growth laws II). Hum. Biol. **10**: 181–213.

Ward, P., and Myers, R.A. 2005. Shifts in open-ocean fish communities coinciding with the commencement of commercial fishing. Ecology, **86**(4): 835–847.

Zar, J.H. 1996. Biostatistical analysis. Prentice-Hall International, Inc., Upper Saddle River, N.J.

© 2007 NRC Canada

Assessing genetic diversity of protected coho salmon (*Oncorhynchus kisutch*) populations in California

Katherine A. Bucklin, Michael A. Banks, and Dennis Hedgecock

Abstract: California coho salmon (*Oncorhynchus kisutch*) are under legal protection owing to significant declines in abundance over the last decades. Previously, California coho salmon were characterized as having low genetic diversity and weak population subdivision, attributable potentially to homogenization by out-of-basin hatchery releases. Here, diversity at seven highly polymorphic microsatellite DNA markers is assessed within and among 32 collections of coho salmon from 16 California watersheds. In 71% of local populations, genotypic composition deviates significantly from that expected under the assumption of random mating. We develop and apply methods to adjust for two potential causes of deviation from random mating expectations: (*i*) Wahlund effects, owing to heterogeneous collections of individuals, and (*ii*) the "Allendorf–Phelp's effect", owing to closely related juveniles in samples. Such population-level "adjustments" reduce within-region and increase among-region variance; after adjustment, we find strong concordance of genetic and geographic distances. We conclude that stock transfers have had minimal impact on population structure and that California coho salmon populations likely comprise small numbers of endemic breeders, potentially experiencing high levels of genetic drift and inbreeding.

Résumé : Les saumons coho (*Oncorhynchus kisutch*) de la Californie bénéficient d'une protection légale à cause de leur déclin significatif au cours des dernières décennies. Dans le passé, on caractérisait les saumons coho de la Californie par une faible diversité génétique et de faibles subdivisions de la population, à cause potentiellement de l'homogénéisation résultant d'empoissonnements à partir de pisciculturesses situées dans d'autres bassins versants. Nous évaluons ici la diversité à sept marqueurs microsatellites de l'ADN fortement polymorphes dans 32 récoltes de saumons coho de 16 bassins versants de la Californie et entre ces récoltes. Chez 71 % des populations locales, la composition génotypique diffère significativement de celle qu'on attendrait si les accouplements se faisaient au hasard. Nous mettons au point et utilisons des méthodes pour tenir compte de deux causes potentielles de déviation de l'accouplement au hasard : (*i*) les effets Wahlund par suite de collections hétérogènes d'individus et (*ii*) « l'effet Allendorf–Phelp » par suite d'échantillonnage comprenant des jeunes fortement apparentés. De tels « ajustements » au niveau de la population réduisent la variance à l'intérieur des régions et augmente celle qui existe entre les régions; après l'ajustement, il existe une forte concordance entre les distances génétiques et géographiques. Nous concluons que les transferts de stocks ont eu un impact minimal sur la structure de population et que les populations de saumons coho de la Californie contiennent vraisemblablement un petit nombre de reproducteurs endémiques et qu'elles subissent potentiellement un fort degré de dérive génétique et de consanguinité.

[Traduit par la Rédaction]

Introduction

Salmonid conservation requires identification of appropriate management units in complex, geographically structured hierarchies of populations. The challenges are to identify how biodiversity is influenced by geography (Carney et al. 1994; Waples et al. 2001), life history and ecology (Waples et al. 2001), hatchery production (Duchesne and Bernatchez 2002; Nickelson 2003; Saisa et al. 2003), and environmental degradation (Beechie et al. 1994; Nickelson and Lawson 1998; Pess et al. 2002). Under the US Endangered Species Act (ESA), the National Marine Fisheries Service grants protection to populations or "distinct population segments" called evolutionarily significant units (ESU), which are entities below the species level that can be listed under the ESA if (*i*) they are substantially reproductively isolated from other conspecific populations and (*ii*) represent an important component in the evolutionary legacy of the species (Waples 1991; Waples et al. 2001). The homing fidelity of salmon to natal spawning streams increases the potential for reproduc-

Received 6 February 2006. Accepted 15 November 2006. Published on the NRC Research Press Web site at http://cjfas.nrc.ca on 19 January 2007.
J19152

K.A. Bucklin[1] and M.A. Banks. Coastal Oregon Marine Experiment Station, Hatfield Marine Science Center, Department of Fisheries and Wildlife, Oregon State University, Newport, OR 97365, USA.
D. Hedgecock. Department of Biological Sciences, University of Southern California, Los Angeles, CA 90089-0371, USA.

[1]Corresponding author (e-mail: kbucklin@sbcglobal.net).

 doi:10.1139/F06-171 © 2007 NRC Canada

tive isolation among populations and local adaptation over evolutionary time. If local adaptation is an important factor in maintaining genetic diversity among populations or groups of populations, then declining populations are at greater probability of experiencing local extinctions, which are permanent losses of diversity and evolutionary potential (Waples et al. 2001).

In the Pacific Northwest, endemic coho salmon (*Oncorhynchus kisutch*) populations have recently undergone significant reductions in population census size (Brown et al. 1994; Weitcamp et al. 1995; Frankham et al. 2002). In California, the census number of wild coho salmon spawning today is less than 6% of what it was in the 1940s (which was already smaller than historical abundance), with most spawning populations consisting of fewer than 100 individuals (Brown et al. 1994). Small numbers of breeders, combined with homing fidelity to natal spawning streams, may increase the rate of genetic drift, reducing within-population genetic variation and increasing the likelihood of inbreeding and inbreeding depression (Wright 1931; Reed et al. 2002; England et al. 2003). However, accurate sampling and identification of population units and assessment of within- and among-population diversity become problematic when spawner densities are very low. Previous allozyme studies of California and Oregon coho salmon have reported low levels of genetic variation and population subdivision (Olin 1984; Bartley et al. 1992). These findings may simply reflect small sample sizes or lower levels of protein polymorphism compared with those of other Pacific salmon (Wehrhahn and Powell 1987), high straying rates, invariant life history traits (Waples et al. 2001), or stock transfers.

Until recently, out-of-basin and even out-of-state transfers of salmon stocks were routine across much of the Pacific Northwest. In California, for example, a coastal coho salmon stock from the Noyo River was planted in at least 27 northern California watersheds (Weitcamp et al. 1995; L. Weitcamp, Northwest Fisheries Science Center, 2725 Montlake Boulevard East, Seattle, WA 98112-2097, USA, unpublished data). Widespread planting of hatchery stocks can homogenize genetic differences among populations and ESUs (Reisenbichler and Phelps 1989; Krueger and May 1991; but see Utter 2004). The extent to which transfers may disrupt adaptations to local environmental conditions, especially at the southern end of the coho salmon range, is unknown.

Here, we take a novel approach in our attempt to describe genetic diversity within and among 32 collections of coho salmon from 16 California watersheds. We identify and grapple with profound problems that arise from attempting to identify and classify units of diversity in very small populations. We develop new methods for partitioning diversity within a stream into within- and among-deme components using a suite of highly polymorphic microsatellite markers. We also develop methods to utilize juvenile collections (in many cases, the only adequate population sample available), in spite of Allendorf and Phelps' (1981) cautionary advice that spawners provide more accurate estimates of among-population diversity. Our approach is an advance over previous work, which typically had the luxury of sampling adults and could identify collections only to stream and year. Our main goals were to test the efficacy of current ESU designations, using markers more polymorphic than those used previously, to determine if declining run sizes have affected population structure, or if past stock transfers have reduced genetic diversity among populations or regions. To identify the geographic scale of coho salmon population structure, we (*i*) employ environmental and biological data to partition genetic diversity within collections, (*ii*) determine relatedness in samples comprised of juveniles, (*iii*) examine temporal genetic variation among year classes, (*iv*) estimate genetic divergence among spawning runs, drainages, and regions, and finally (*v*) assess influence of hatchery plantings and reductions in abundance.

Materials and methods

Population samples

The 1483 individuals included in this analysis were collected from 32 sites in 16 watersheds or tributaries of major watersheds (Table 1) representing the southern end of the species range from the southern end of the northern California – southern Oregon (NC/SO) ESU and the central California coast (CCC) ESU, which extends south to Santa Cruz County (Weitcamp et al. 1995) (Fig. 1). Nine sites were sampled more than once in different years (Table 1), permitting study of temporal genetic variation. When breeding adults were not numerous, juvenile samples were acquired by seining or electrofishing. When high numbers of juveniles were encountered, a majority of individuals from each pool was sampled, a subset of which was later selected for genetic analyses to ensure random representation. Tissue samples for genetic analyses were obtained from juvenile caudal fins (nonlethal), caudal or operculum punches of hatchery adults, and caudal, operculum, or dorsal muscle tissue of wild adult carcasses. The data accompanying each sample varied but always included watershed, tributary, and location collected, collector, and date collected. In some cases, sex (adults), fork length, hatchery identification mark, and river mile were also included (see Table 1). Permits for tissue collection and holding were obtained from the California Department of Fish and Game (CDFG) and National Marine Fisheries Service (NMFS) for populations listed as threatened under the Endangered Species Act.

Microsatellite markers and molecular methods

Sixty-nine published salmonid microsatellite DNA markers were surveyed to determine candidate loci with high information content for California coho salmon. The screening process used samples from Scott Creek (Santa Cruz County), Noyo River (Mendocino County), Eel River (Humboldt County), and Smith River (Del Norte County) to examine variability and assess potential diagnostic power. Thirty-six markers were discarded because they did not amplify product or were not adequately polymorphic in the populations screened. Eighteen of the remaining 33 candidate markers amplified product. From these, we selected six loci with high numbers of alleles that amplified well in multiplexed reactions and achieved an assignment stringency of over 90% in the four populations screened. A preliminary analysis suggested that these six loci did not make greater than average contribution to population structure compared with the 18 variable candidate loci. Additionally, the microsatellite *iso-Ots-2*, which is known to have species-specific

© 2007 NRC Canada

Table 1. Samples of coho salmon (*Oncorhynchus kisutch*) collected from 16 California watersheds.

Watershed (population)	Tributary or site	*N*	Stage	Year collected	Name code	Criteria
1. Klamath River	Iron Gate Hatchery	45	A	1997/1998	KIHA97ANL	Ad, No, Left clip, FL 41–78 cm
Klamath River	Iron Gate Hatchery	36	A	1997/1998	KIHA97ML	Left clip, FL > 56 cm
2. Trinity River	Trinity River Hatchery	17	A	1997/1998	TRHA97S	FL < 45 cm
Trinity River	Trinity River Hatchery	77	A	1997/1998	TRHA97L	FL > 53 cm
3. Little River (Humboldt)	Little River Delta	72	S	2000	LRS00E	3–6 April 2000
Little River	Little River Delta	22	S	2000	LRS00L	20 April – 29 May 2000
4. SF Eel River	Hollowtree Creek	16	A	1997/1998	EHOLA97	—
5. SF Eel River	Redwood Creek	88	S	1997	EREDS97	3
6. SF Eel River	Redwood Creek	20	A	1998/1999	EREDA98	—
7. SF Eel River	SF Sproul Creek	34	S	1999	ESPRS99	—
8. Mattole River	Mattole River Delta	91	S	1998	MATS98	2, 3
9. Pudding Creek	Pudding Creek	78	Y	1998	PUDY98	3, 4
10. SF Noyo River	Egg-taking station	42	A	1997/1998	NOYA97	—
11. SF Noyo River	Egg-taking station	42	A	1999/2000	NOYA99	—
12. Albion	Albion Mainstem	20	A	1998/1999	ALBA98	2, 4
13. Albion River	Marsh Creek	18	Y	1998	ALBY98	—
14. Russian River	Warm Springs Hatchery	33	A	1995/1996	RRHA95	—
15. Russian River	Warm Springs Hatchery	25	A	1996/1997	RRHA96	—
16. Russian River	Warm Springs Hatchery	7	Y	1997	RRHY97	—
17. Russian River	Green Valley Creek	7	Y	1997	RRGV97	—
18. Russian River	Green Valley Creek	73	Y	1998	RRGV98	4
19. Russian River	Green Valley Creek	8	Y	2000	RRGV00	—
20. Lagunitas Creek	Lagunitas, San Geronimo	40	A	1996/1997	LAGA96	2, 3, 4, 5
21. Lagunitas Creek	Lagunitas, San Geronimo	71	A	1997/1998	LAGA97	2, 3, 4, 5
22. Lagunitas Creek	San Geronimo, Arroyo	30	Y	1998	LAGY98	4
23. Olema Creek	Mainstem	66	A	1996/1997	OLEA96	2, 3, 4, 5
24. Olema Creek	Mainstem	32	A	1997/1998	OLEA97	2, 3, 4, 5
25. Olema Creek	Mainstem	88	Y	1998	OLEY98	4
26. Redwood (Marin)	Mainstem	13	A	1997/1998	RWMA97	2, 3, 4, 5
27. Redwood (Marin)	Mainstem	24	Y	1998	RWMY98	4
28. Waddell Creek	Mainstem	42	Y	1999	WADY99L	RM 3.1 – 3.9
Waddell Creek	Mainstem	17	Y	1999	WADY99U	RM 4.7
29. Scott Creek	Hatchery	40	A	1995/1996	SCA95	—
30. Scott Creek	Hatchery	57	A	1997/1998	SCA97	—
31. Scott Creek	Hatchery	32	A	1998/1999	SCA98	—
32. Scott Creek	Mainstem, Big and Mill creeks	40	Y	1999	SCY99L	RM 2.55–3.55 B&M
Scott Creek	Mainstem at RM 4.9	10	Y	1999	SCY994.9	RM 4.9
Scott Creek	Upper Fork	10	Y	1999	SCY99UF	RM UF

Note: SF, South Fork. Initial populations are numbered (1–32) and designated by their name codes in subsequent tables and figures. Stages: A, adults; S, smolts; Y, young of the year. Subdividing criteria: (1) clip type (adipose (Ad.), No, Left); (2) fork length (FL); (3) date collected; (4) river mile (RM); (5) sex. When the above criteria were variable but not significant, the above numbers are shown (1–5); —, locations with no data.

differences, was included to ensure species identity (Greig et al. 2002), yielding a total of seven variable loci.

DNA was extracted using the Puregene™ DNA isolation kit (Gentra Systems Inc., Minneapolis, MN 55441, USA) in a 96-well format. Using a thermocycler (PTC-100; MJ Research, Inc., Hercules, CA 94547, USA), we amplified genomic DNA in three multiplexed reactions: (*i*) *Ots-103* (Nelson and Beacham 1999), *Ots-2* (Banks et al. 1999), and *iso-Ots-2* (Greig et al. 2002); (*ii*) *Ots-3* (Banks et al. 1999) and *One-13* (Scribner et al. 1996); and (*iii*) *P-53* (Park et al. 1996) and *Oki-1* (Smith. et al. 1998), each with a total volume of 10 µL. Reaction conditions for all primer combinations were 94° for 2 min, 94° for 30 s, 60° for 30 s, and 72° for 30 s for 34 cycles. Polymerase chain reaction (PCR) products were size-fractionated by polyacrylamide gel electrophoresis (PAGE) on a 45.0 cm wide × 22.5 cm high 8% denaturing gel at 50 W for 150 min. The forward PCR primer was labeled with a fluorescent phosphoamidite (HEX, FAM, or fluorescein). DNA fragments were visualized on the FMBIO® fluorescent imaging system (Hitachi

© 2007 NRC Canada

Fig. 1. Map of northern California, USA, showing the 16 watersheds from which coho salmon (*Oncorhynchus kisutch*) were collected for population genetic analyses. Numbers correspond to the following watershed or hatchery locations, ordered from north to south based on river mouth: (1) Klamath River, Iron Gate Hatchery; (2) Trinity River, Trinity River Hatchery; (3) Little River; (4) Eel River, Hollowtree Creek; (5) Eel River, Redwood Creek; (6) Eel River, Sproul Creek; (7) Mattole River; (8) Noyo River; (9) Pudding Creek; (10) Albion River; (11) Russian River, Warm Springs Hatchery; Russian River, Green Valley Creek; (12) Lagunitas Creek; (13) Olema Creek; (14) Redwood Creek; (15) Waddell Creek; (16) Scott Creek, Scott Creek Hatchery. NC/SO, northern California – southern Oregon evolutionarily significant unit (ESU); CCC, central California coast.

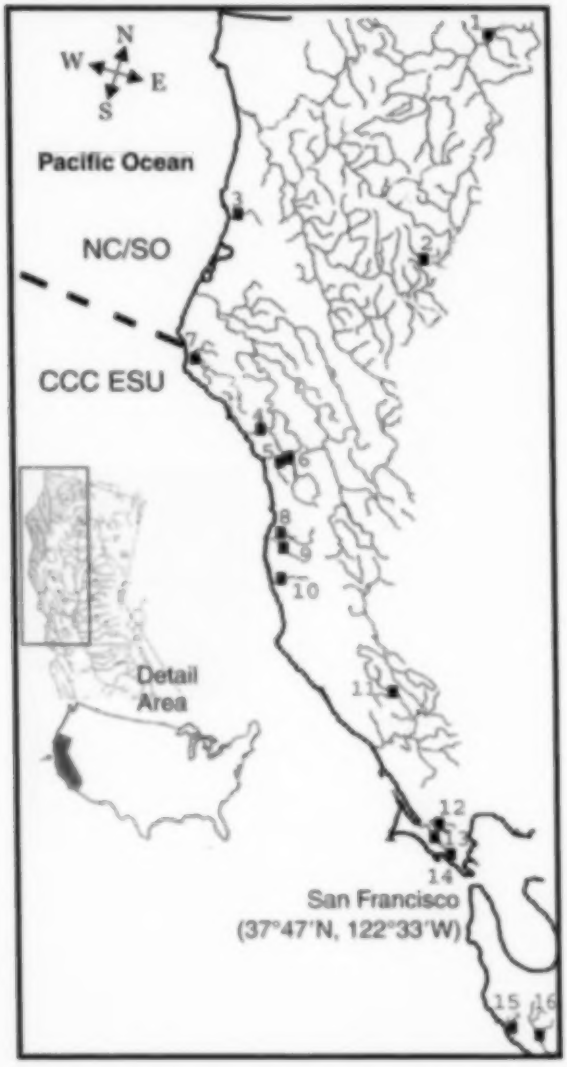

Software Engineering America Ltd., South San Francisco, CA 94080, USA). The sizes of individual bands were scored relative to MapMarker® standards (70–400 bp; BioVentures, Inc., Murfreesboro, TN 37133-2561, USA) and analyzed with Bio Image software (Bio Image Systems, Inc., Jackson, MI 49203, USA), or by eye. To minimize genotype-scoring errors, individuals were genotyped twice from two independent PCR reactions, and among-tray scoring variation was controlled by co-electrophoresing eight individuals from each of the 20 trays in two sets of gels. The genotype scores were double-checked for accuracy and independently verified by at least one other researcher.

Loci were ranked by number of alleles, from most polymorphic to least, to identify the most informative loci to detect family structure within collections of individuals taken from a watershed in a single year. Individuals with "sufficient" data were those for which (*i*) separate electrophoretic analyses produced repeatable genotypes and (*ii*) the four most polymorphic loci (*Ots-103*, *iso-Ots-2*, *One-13*, *Oki-1*) amplified, or five loci successfully amplified, including three of the above most polymorphic loci. For juvenile kinship analyses, amplification of three of the four most polymorphic loci was the minimal requirement.

Statistical methods

Population genetic parameters

We tested Hardy–Weinberg genotypic proportions (HWE) for each locus in each population using GENEPOP (version 3.3; Raymond and Rousset 1995). A Markov chain method was used to determine, without bias, the exact *P* value of the test (Guo and Thompson 1992).

Allele frequencies, observed and expected proportions of heterozygotes, linkage disequilibrium (LD), and *F* statistics were calculated using GENETIX (version 4.02; Laboratoire Génome et Populations, Université de Montpellier II, http://www.univ-montp2.fr/~genetix/index.htm). Within-population (F_{IS}) and among-population (F_{ST}) significance was determined by random permutation of alleles. Homogeneity of populations was determined by testing the significance of F_{ST} between all pairs of sites within major watersheds. For each test, the data set was permuted 10 000 times, and the threshold significance ($\alpha = 0.05$) was adjusted for n simultaneous tests using Sidak's correction $(1 - (1 - \alpha)^{1/n})$. LD was judged to be significant when more than three pairs of 21 (19%) were significant at the 5% α level, a proportion reached only three times in 100 simulated samples of size 20 drawn from a pooled baseline population of CCC coho salmon.

The computer program PHYLIP (version 3.57c; Felsenstein 1993) was used to evaluate the spatial distribution of genetic diversity among California coho salmon populations. Cavalli-Sforza and Edwards (1967) chord measures (CSE) were calculated using GENDIST. For fitting trees to the CSE distance matrices, the program NEIGHBOR was used to construct an unrooted tree by the neighbor-joining method (Saitou and Nei 1987). To assess the significance of the nodes in the tree, bootstrap results were obtained using SEQBOOT and CONSENSE with 1000 replicates. Trees were visualized using TreeView (Page 1996).

Adjustments of samples for microgeographic structure

Heterozygote deficiency can result artificially from unwitting admixture of individuals collected from genetically differentiated demes (Wahlund effect). Adult and juvenile

© 2007 NRC Canada

collections that departed significantly from single- or multiple-locus random mating equilibria were examined for evidence of admixture. Subdivision of samples was based on genotype-independent data collected prior to analysis, such as size (fork length), clip type (hatchery release identification), collection date (day of smolt outmigration), or collection site (young of the year; river mile) (see Table 1). We tested whether partitioning of population samples produced genetically different subgroups by the significance of F_{ST}.

Partitioning of juveniles into sibships

Fifteen of the 32 collections comprised juveniles collected as young of the year or smolts. We first checked for admixture in 11 juvenile samples for which independent criteria permitted subdivision, as described above. One sample was subdivided, making 12 juvenile samples. We next applied a family adjustment procedure developed by Banks et al. (2000) to identify and remove full sibships, replacing them with their hypothetical parents. Finally, in some cases, we tested whether adjusted subpopulations could be repooled, using nonsignificance of F_{ST} as a guide.

Twelve juvenile samples with high levels of LD and (or) significant departures from HWE were adjusted for family structure. The odds of two individuals being full siblings (vs unrelated) were calculated using the program KINSHIP 1.2 (Goodnight and Queller 1999) and baseline allelic frequencies of adult samples from this study (in HWE) from the same ESU as the sample of interest. Putative family groups were partitioned by hand from the sorted KINSHIP output matrix following the rule that the majority of KINSHIP relatedness coefficients were significant at the 0.01 or 0.001 level of significance. Putative sibling groups of size 3 or greater (with the exception of the 1998 Russian River Green Valley population for which we allowed families of size 2) were examined by the computer program SIBLINGS (K.A. Bucklin, W.F. Eichert, and D. Hedgecock, unpublished data) to test for gross violations of diploid Mendelian inheritance (e.g., more than four alleles at any locus or impossible combinations of genotypes). Individuals causing such violations were discarded from the group; discards of three or more individuals were then treated as a putative sibgroup. Once Mendelian sibling groups were identified, the possible mating types for the sibship were identified (see Table 2; Banks et al. 2000). The likelihoods of all possible mating pairs were calculated and ranked. The top-ranked mating type provided the putative genotypes of the parents. After forming full-sib groups, SIBLINGS looked for families having a common parent (half siblings). All individuals in each sibling group were then removed from the data set and replaced by their putative parents.

Russian River Green Valley samples represent a special case. Samples from 70 young-of-the-year coho salmon were collected from Green Valley Creek (RRGV98), a tributary to the Russian River, on 20 July 1998. A further 58 samples were collected from the same locations on 13 October 1998. Samples taken in July could have been resampled in October. Indeed, 49 pairs of individuals (one from each of the two sampling times) had identical multilocus genotypes; we deleted one member of each pair. Twenty-four other individuals collected on either date had unique genotypes, yielding a sample of 73 unique individuals. After partitioning the sample into 16 full-sibling families, we estimated the variance effective number of breeders from the mean and variance of parent contributions following the methods of Hedrick et al. (1995).

Pooling of temporally or spatially homogeneous subpopulations

After adjustments for admixture and family structure in collections of juveniles, we tested for temporal and spatial homogeneity among collections from the same watershed using pairwise F_{ST} with significance adjusted for n populations. Populations that did not significantly differ within the same basin were combined.

Isolation by distance

A Mantel test (Mantel 1967) implemented in GENETIX (Belkhir et al. 1998) was used to test for genetic isolation by distance between all 406 adjusted population pairs (29 populations). Genetic distance was measured as F_{ST} (Weir and Cockerham 1984). Geographic distance was measured as the shortest nearshore coastal route between river mouths (N. California Gazeteer; 1 mile = 1 inch). The genetic distance matrix was permuted 1000 times, and the correlation was quantified by Pearson's coefficient (r).

Results

Genetic diversity within coho salmon populations

Genotypes at seven microsatellite DNA markers for 1483 individuals from 32 samples, representing 16 watersheds partitioned by major tributary and year class, provide the basis for initial analyses (Table 1; Fig. 1). Nine watersheds are represented by samples from multiple years; in two cases, collections represent different tributaries of the same watershed. Ten of the 32 collections represent hatchery populations, the rest are from the wild. In 15 cases for which adults were not available or not numerous enough to provide an adequate sample, we used data from juvenile samples. Average sample size per collection is 46, although it is highly variable, with the three smallest collections having only seven or eight individuals (RRGVY97, RRGVY00, and RRHY97). However, after adjustments for family structure, small samples are pooled into larger samples (see below).

We observe widespread departures from random mating expectations in 23 of 32 sample collections (71%), as measured by tests of single-locus Hardy–Weinberg equilibria (HWE) and multiloci equilibria or LD (Table 2, values in bold). These deviations occur in 11 of the 15 juvenile population samples in which departures from random mating expectations might be expected because of relatedness. However, all nine collections of hatchery adults and three out of eight wild adult collections also depart from random mating equilibrium. Adult and juvenile populations differ in the proportion of single-locus or multiloci deviations. Of the 17 adult samples noted (Table 2), eight (47%) have significant F_{IS} and nine (52%) have more than three significant pairwise LD tests. Adult hatchery collections have significantly more deviations than do wild adult collections (12 instances of high LD or significant F_{IS} in nine hatchery collections compared with four instances in the eight wild collections). By contrast, of the 15 juvenile samples listed

© 2007 NRC Canada

Table 2. Deviations from random mating genotypic proportions for 32 samples of coho salmon (*Oncorhynchus kisutch*).

Population	*N*	H_{obs}	*Ots-103*	*Ots-2*	*iso-Ots-2*	*Ots-3*	*One-13*	*P-53*	*Oki-1*	F_{IS}	LD
KIGHA97	81	0.73			*					**0.070*** **	**7/21**
TRHA97	94	0.72	***		***			*		**0.045** **	1/21
LRS00	94	0.80	***		**	**		*	*	0.014	**12/21**
EREDA98	20	0.70	***							0.061	2/21
EREDS97	88	0.72		*						0.020	2/21
EHOLA97	16	0.68	*							0.064	3/21
ESPRS99	34	0.74	*							–0.020	**4/21**
MATS98	91	0.76								0.000	**9/21**
PUDY98	78	0.70	*							**0.057** **	**4/21**
NOYA97	42	0.70	*			**				**0.064***	2/21
NOYA99	42	0.73	*							**0.080** **	1/21
ALBA98	20	0.78					**			–0.036	**6/21**
ALBY98	18	0.78						*	*	–0.023	3/21
RRHA96	33	0.75	***							**0.057***	**4/21**
RRHA97	25	0.83								–0.046	**5/21**
RRHY97	7	0.67						*		**0.120***	**5/21**
RRGV97	7	0.71							**	–0.116	0/19
RRGV98	73	0.76	***	*	**		***	*	***	**–0.040***	**15/21**
RRGV00	8	0.78							*	**–0.257** **	1/15
LAGA96	40	0.78								0.017	1/21
LAGA97	71	0.79	*							–0.001	**4/21**
LAGY98	30	0.79						**		–0.024	**8/21**
OLEA96	66	0.66				***	*			**0.099** **	**6/21**
OLEA97	32	0.77				*		**		–0.005	3/21
OLEY98	88	0.73		*	**					0.002	**4/21**
RWMA97	13	0.69	**		**					0.099	1/18
RWMY98	24	0.66	*							–0.002	0/21
WADY99	59	0.65	*		**	***				0.011	**8/21**
SCA95	40	0.71								–0.049	**4/21**
SCA97	57	0.72	*		*	**	*			**–0.047***	**16/21**
SCA98	32	0.62	***		**	*	*	**	*	**0.097** **	**12/21**
SCY99	60	0.62								–0.008	**5/21**
No. of alleles/locus			31	9	23	18	19	15	19		

Note: Observed heterozygosity by population (H_{obs}), single-locus HWE (*, $P < 0.05$; **, $P < 0.01$; ***, $P < 0.001$, shown in bold), and over all loci (F_{IS}, *P*), and fraction of loci pairs showing linkage disequilibrium (LD), fractions ≥ 19% shown in bold.

© 2007 NRC Canada

Table 3. Samples of coho salmon (*Oncorhynchus kisutch*) adjusted for (*a*) subdivision and (*b*) kinship with subsequent (*c*) homogeneity testing.

(*a*) Subdividing admixed population samples.

Collection	Subpopulation	*N*	F_{ST}, *P*	F_{IS}, *P*
KIGHA97	KIGHA97ANL	45	0.0259***	0.053*
	KIGHA97ML	36		0.062*
TRHA97	TRHAL	77	0.0121*	0.053**
	TRHAS	17		–0.009
LRS00	LRS00E	72	0.0111**	0.019
	LRS00L	22		–0.015
MATS98	MATS98E	70	0.0091*	0.014
	MATS98L	21		–0.061
WADY99	WADY99L	42	0.0521***	0.011
	WADY99U	17		–0.085
SCY99	SCY99L (to UF)	40	0.0774***	–0.028
	SCY99UF (to 4.9)	10	0.0436***	–0.092
	SCY994.9 (to L)	10	0.0701**	–0.055

(*b*) Sibling groups in juvenile collections.

	No. of sibling groups of size							
Population	2	3	4	5	6	≥7	No. of FS removed	No. of parents added
LRS00E		6	2				26	18
LRS00L		1					3	2
ESPRS99		2	2				14	8
MATS98E		5	3	1			32	18
MATS98L		4					12	8
PUDY98		2	1				10	6
RRHY97	1						2	2
RRGV98	3	2	3		1	2	68	22
RRGV00			1				4	2
LAGY98			1				4	2
OLEY98		4	2			1	28	14
WADY99L		1	5	1			28	14
WADY99U			1			1	11	4
SCY99L		1		2	1		19	7
Total no. of individuals	8	84	84	20	12	53	261	127

(*c*) Pooling of homogeneous subpopulations.

Subpopulation 1	Subpopulation 2	Final population	F_{ST}	F_{IS}
LRS00E	LRS00L	LRS00	0.0045	0.0110
MATS98E	MATS98L	MATS98	0.0014	–0.0100
RRHA96	RRHA97	RRHA	0.0128	0.0249
RRHA96	RRHY97	—	–0.0033	—
RRHA97	RRHY97	—	0.0077	—
LAGA96	LAGA97	LAGA	0.0049	0.0104
RRGV97	RRGV00	RRGV9700	0.1485	–0.0118
OLEA97	OLEY98	OLEAY	0.0003	0.0224
SCA97	SCA98	SCA9798	0.0077	0.0025
SCY99L	SCY994.9	SCY99	0.0205	–0.0146

Note: *, $P < 0.05$; **, $P < 0.01$; ***, $P < 0.001$. FS, full sibs.

(Table 2), only four (27%) have significant F_{IS}, but 10 (66%) have more than three significant pairwise LD tests.

We first investigate the possibility that departures from random mating equilibrium within samples result from admixture of fish from genetically different subpopulations. Two adult (KIGHA97 and TRHA97) and four juvenile (LRS00, MATS 98, WADY98, SCY99) populations with significant F_{IS} or LD have significant pairwise F_{ST} after subdivision on the basis of independent collection data (Table 3*a*; see Table 1 for criteria).

We further investigate the possibility that departures from random mating expectations in juvenile collections with significant F_{IS} ($P < 0.05$) or LD (>19% possible pairwise loci combinations) are caused by family structure. Fifteen juve-

© 2007 NRC Canada

Table 4. Observed (Obs.) and expected (Exp.) Mendelian proportions of microsatellite genotypes in a full-sib coho salmon (*Oncorhynchus kisutch*) family from Green Valley Creek, Russian River.

Locus	Inferred P1 genotype	Inferred P2 genotype	F_1 genotype	Obs.	Exp.	Total	χ^2	*P*
Ots-103	224 236	228 232	224 228	6	7	28	1.43	0.699
			224 232	5	7			
			228 236	9	7			
			232 236	8	7			
Ots-2	180 184	180 188	180 180	6	7	28	4.86	0.183
			180 184	5	7			
			180 188	5	7			
			184 188	12	7			
iso-Ots-2	205 247	213 227	205 213	7	7	28	0.86	0.836
			205 227	5	7			
			213 247	8	7			
			227 247	8	7			
Ots-3	145 153	145 157	145 145	8	7	28	0.86	0.836
			145 157	7	7			
			145 153	8	7			
			153 157	5	7			
One-13	197 209	197 219	197 197	11	7	28	3.71	0.294
			197 209	7	7			
			197 219	6	7			
			209 219	4	7			
P-53	181 181	173 181	181 181	15	14	28	1.23	0.430
			173 181	13	14			
Oki-1	92 100	96 112	92 96	11	6.75	27	4.26	0.392
			92 112	7	6.75			
			96 100	5	6.75			
			100 112	4	6.75			

nile populations or subpopulations are tested for the presence of full-sibling relationships among all individuals (Table 3*b*). Family structure is especially strong in the RRGV98 sample, which has very high linkage disequilibrium (15 of 21 loci combinations) and a significant excess of heterozygotes (Table 2). More than 40% of pairwise tests for a full-sib relationship in this sample are below the $\alpha = 0.01$ level of significance. The largest identified sibling group contains 28 individuals, the genotypic proportions of which conform to those expected under Mendelian inheritance ratios (Table 4). From the distribution of family sizes within the Green Valley sample and equations and methods described in Hedrick et al. (1995), we estimate the effective number of breeders (N_b) in this tributary to be 14 (Table 5), suggesting that this population is propagated by few adults and is likely undergoing rapid genetic drift.

Similar adjustments to reduce family structure are made to 11 other juvenile samples besides the RRGVY98 sample (Table 3*b*). These adjustments result in a net loss of 134 individuals because of the discarding of full sibs and their replacement by reconstructed parents (261 full sibs removed, 127 parents added).

Within-watershed temporal and spatial variation

We next test for homogeneity among samples within 14 major watersheds for which multiple samples (spatial or temporal) are available (Table 3*c*). Homogeneity is tested by the significance of F_{ST} (significance threshold adjusted for *n* populations) among all samples within each drainage or site, including populations for which adjustments for admixture or family structure were made. Eight pools of homogeneous site populations are formed, including all juvenile populations (except WADY) that comprised heterogeneous subpopulations at their sites prior to adjustments for family structure. Additionally, Russian River hatchery populations are homogeneous, as are different year classes from Lagunitas and Scott creeks and two generations from Olema Creek. Pooling maximizes sample sizes within sites and reduces to 29 the number of populations for analysis of genetic distance among sites, drainages, and ESUs.

Regional variation

A Mantel test among all 29 adjusted populations revealed a highly significant association between genetic and geographic distance ($r = 0.703$, $P = 0.0009$). To visualize genetic diversity, we present two trees depicting genetic distances among samples, one for 32 unadjusted samples grouped by year and watershed (Fig. 2) and one for 29 samples formed after adjustment and homogeneity testing (Fig. 3).

The tree showing genetic distance among 32 unadjusted samples (Fig. 2) has a star-like pattern with few internal nodes having significant bootstrap replication. The tree does support the presence of at least two distinct groupings of populations of coho salmon in the regions sampled. Samples from the Mattole and Eel rivers from the SO/NC ESU are found in a cluster well supported by bootstrap analysis (93% trees). Samples from the Klamath and Trinity rivers, also from the SO/NC ESU, cluster in all of the 1000 trees but are

© 2007 NRC Canada

Table 5. Variance effective size (N_{ev}) for the 1998 Russian River Green Valley coho salmon (*Oncorhynchus kisutch*) population.

Sib group	No. per family	Contribution per parent*
1	4	1.753
2	4	1.753
3	10	4.383
4	6	2.630
5	28	12.273
6	3	1.315
7	4	1.753
8	3	1.315
9	2	0.876
10	2	0.876
11	2	0.876
12	1	0.438
13	1	0.438
14	1	0.438
15	1	0.438
16	1	0.438
	$\bar{k}_m, \bar{k}_f$	2
	$\sigma^2_{k_f}, \sigma^2_{k_m}$†	9.0
$y = m + f\left(\frac{\sigma^2_{k_f}}{\bar{k}_f}\right), x = f + m\left(\frac{\sigma^2_{k_m}}{\bar{k}_m}\right)$‡		2.6
$N_{ev} = \frac{4N_f N_m}{xN_f + yN_m}$		13.9

*Number of offspring contributed by male and female parents of each family, adjusted so that the mean numbers of offspring per parent over all 16 families is 2.0 ($\bar{k}_m = \bar{k}_f = 2$).

†Variance in adjusted number of offspring contributed by male and female parents.

‡Corrections for unequal parental contributions, where m and f are the proportions of male and female progeny at spawning age; here, we assume $m = f = 0.5$.

found on a branch that does not differ significantly from from CCC populations north of San Francisco. Samples from south of San Francisco (SSF) form a second distinct cluster (supported in 97% of trees), but other populations within the CCC ESU are not well differentiated and only several external nodes are supported. Furthermore, several of the juvenile CCC populations have branch lengths exceeding those separating regions.

The tree of the 29 samples formed after adjustments shows two regional groupings within the SO/NC ESU, those from the drainages of the Klamath, Trinity, and Little rivers (83% of trees) and those from Eel and Mattole rivers (recovered in 95% of trees), and SSF populations again cluster in 98% of trees (Fig. 3). Adjusted CCC juvenile populations have shorter branch lengths than unadjusted juvenile populations and are more likely to cluster with populations from the same watershed, producing a greater number of significant nodes among spatially and temporally proximal populations. For example, all adjusted Russian River Green Valley juvenile populations (RRGV98 and RRGV9700) form a significant cluster, whereas unadjusted RRGV97 was not associated with other RRGV populations. The population divergence with four regional groupings is as deep as the divergence when only two ESUs are recognized.

Fig. 2. An unrooted neighbor-joining tree showing chord distances (Cavalli-Sforza and Edwards 1967) among 32 California coho salmon (*Oncorhynchus kisutch*) collections formed by pooling samples within drainages by year class. Bootstrap values greater than 700 out of 1000 are shown; numbers preceding each name correspond to locations in Fig. 1.

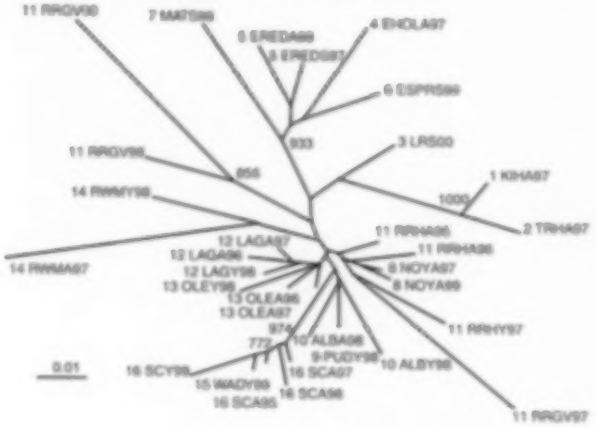

Fig. 3. An unrooted neighbor-joining tree showing chord distances (Cavalli-Sforza and Edwards 1967) among 29 California coho salmon (*Oncorhynchus kisutch*) populations formed after adjustments for admixture, family structure, and pooling of homogenous samples within drainages and sites. Bootstrap values greater than 700 out of 1000 are shown; numbers preceding each name correspond to locations in Fig. 1.

Discussion

Genetic diversity within populations

Numerous studies of Pacific salmon populations over the past 30 years show that genotypic frequencies generally con-

© 2007 NRC Canada

form to those expected under random mating (Utter et al. 1980; Beacham et al. 2003; Ford et al. 2004). Here, we report deviations from single-locus and digenic random mating equilibria in nearly three-quarters of California coho salmon populations sampled (23 of 32). This contrasts with the findings of Bartley et al. (1992) from 15 years prior (1983–1985), in which allozyme genotypes for 27 California coho salmon populations conformed to Hardy–Weinberg proportions and only 6.7% of loci pairs had significant linkage disequilibrium. However, very low levels of protein polymorphism in the Bartley et al. (1992) study significantly limited their power to detect deviations from random mating equilibria. Thus, we are unable to determine whether nonequilibrium conditions were present then and were not detected or whether they are more recent in origin, perhaps associated with reductions in population size over the last five generations. Declines of California coho salmon populations have been precipitous in that time. By 1998, we could not collect juveniles from six of Bartley et al.'s (1992) populations, and at present, four additional populations (37% overall) have declined to such levels that it would be difficult or impossible to collect a sample size of 100 juveniles (S.L. Harris, California Department of Fish and Game, P.O. Box 1690, Willits, CA 95490, personal communication, 2005).

Determining the causes of deviations from random mating equilibria in population samples is important both to our understanding of what shapes local genetic diversity and to an accurate description of genetic diversity at regional and ESU scales. Deviations of genotypic proportions from those expected under random mating can arise at microsatellite DNA markers through a variety of genotyping errors or artifacts. Genotyping errors caused by nonamplifying PCR null alleles would make estimates of F_{IS} more positive because null heterozygotes are scored as homozygotes. Our data, even for *Ots-103*, which deviates from HWE in half of our initial populations, do not show significant deficiency of all heterozygous classes, as might be expected if many nulls were present (Van Oosterhout et al. 2004); indeed, some deviations are caused by excesses rather than deficiencies of heterozygotes. We also do not observe deviations attributable to specific loci or loci interactions, or allele size dependent deficiencies of heterozygotes, which would indicate large allele dropout in competitive PCR reactions. Finally, Mendelian inheritance of all seven markers in a putative full-sib family from Green Valley supports these markers as bona fide genetic loci. Thus, it is unlikely that technical errors or artifacts are sufficient to explain the majority of departures from random mating equilibrium. We therefore turn to two biological causes of these deviations: (*i*) Wahlund effects, created by genetic subdivision of population samples collected in the traditional manner, by year class and watershed; and (*ii*) family structure within samples of juveniles, reflecting small numbers of successful spawners.

Coho salmon have a dominant 3-year age structure, suggesting that in adult collections, Wahlund effect could arise from inadvertent inclusion of genetically differentiated year classes, such as early-returning "jacks". Alternatively, geographic variation, which has been found to be greater than temporal variation (Van Doornik et al. 2002), may account for within-collection heterogeneity (e.g., Klamath hatchery returns). The Wahlund effect in juvenile collections may be the result of spatial differentiation of offspring emerging in different reaches of a stream, as was observed in Chinook salmon (Bentzen et al. 2001). Likewise, outmigrating smolts collected at a single downstream location may represent progeny from multiple subpopulations partially reproductively isolated by spatial separation of small groups of spawning adults. Within equilibrium populations, we do not observe heterogeneity among putative subgroups. For example, samples from Lagunitas and Olema creeks were tested exhaustively for spatial heterogeneity among different river reaches and tributaries and for temporal differences among year and size classes and among sexes; no heterogeneity was detected in any of these tests.

Population differentiation at very small geographic scales has been previously reported for anadromous salmon (Bernatchez et al. 1998; Hendry et al. 2000; Wofford et al. 2005), yet we know of no empirical studies that have further dissected causes of local Wahlund effects (cf. Banks et al. 2000). Here, we use genotype-independent collection data to partition collections on the basis of significant F_{ST}. Significance of departures from HWE genotypic proportions is difficult to test in the resulting subgroups because of decreased sample size and statistical power to detect non-zero LD and, to a lesser degree, F_{IS} (simulation results not shown). However, simulation results indicate that F_{ST} is not sensitive to sample size, so we conclude that biological factors are the most reasonable explanation for the observed departures from random mating.

Departure from random mating equilibria in some juvenile collections appears to stem not from admixture, per se, but from small breeding population size and resulting family structure. As a consequence, juvenile collections may exhibit the "Allendorf–Phelps effect" — many juveniles representing few adult spawners, making differences among populations or population segments appear more significant than they are (Allendorf and Phelps 1981). Whereas Allendorf and Phelps advise sampling only spawners for this reason, we were confronted in this study with very small populations that offered no alternative to juvenile sampling. Thus, to make use of the available samples and information, we attempt to resolve full-sib groups, remove these from the sample, and replace them with the inferred genotypes of their parents. We believe that such adjustments better estimate allelic frequencies in local spawning populations than do the original juveniles samples. A possible bias is introduced by our method if adults that left sampled progeny have substantially different marker allele frequencies than the spawning population as a whole. Because only those parents that have progeny contribute alleles to the next generation, the bias should be negligible.

In juvenile collections, we use a criterion of >3 (19%) significant pairwise LD ($\alpha = 0.05$) or significant F_{IS} to trigger investigation of family structure. Eleven of our initial juvenile collections exceed this threshold value. Other studies use a 10% threshold (Banks et al. 2000; Beacham et al. 2003), dismiss high LD because of multiple testing (Olsen et al. 2003), or find no LD (e.g., Smith et al. 2001). Although we do not adjust for family structure in adult collections, 10 of 17 populations exceed our 19% LD threshold as well. Results from relatedness tests (data not shown) suggest that

© 2007 NRC Canada

adult hatchery populations contain large numbers of full-sib families owing to small effective numbers of breeders, which likely contributes to the observed deviations from random mating expectations.

The increased potential for inbreeding from routine artificial supplementation has been well documented (reviewed in Wang et al. 2002; but see Hedrick et al. 2000). Estimates for populations, such as Russian River Green Valley, further suggest that very few spawners may propagate most wild California coho salmon populations. Supplementation efforts have already been initiated in Green Valley and Scott creeks. In 2000, a program involving a consortium of stakeholder groups and federal and state agencies began using the Green Valley remnant population as a source to reseed extirpated portions of the Russian River. Approximately 300 juveniles collected in-stream per year are raised in captivity to serve as broodstock. Although adult broodstock are genotyped to reduce potential matings between full and half sibs, the consequence of increasing the census size to many thousands of individuals from a stock that in at least one year had 14 estimated breeders is uncertain at best.

Genetic diversity among populations

Bartley et al. (1992), using protein markers, found little concordance between genetic and geographic distances among coastal California populations of coho salmon, although Olin (1984) did find evidence of divergence on a larger scale between Oregon and California stocks. In contrast, we find that genetic distances among coho salmon samples are significantly correlated with geographic distances among populations. After adjustments for admixture and family structure, all populations show high regional fidelity. The major effect of family adjustments is to make populations within and among watersheds of the same region more homogeneous. However, this appears not simply to be the result of our having used regional baseline data to drive selection of mating types. We note that the tree made from adjusted data has three significant nodes within the CCC, where none was found using unadjusted data, and a Mantel test of within-CCC adjusted populations was highly significant ($r = 0.300$, $P = 0.0039$). Furthermore, pairwise F_{ST} of all adjusted populations to the relevant regional baseline population are significant, indicating that use of baseline data for parent reconstruction does not predetermine homogeneity of the adjusted sample.

Finally, concordance of genetic and geographic distances among populations suggests that out-of-basin and out-of-state stocking of hatchery fish have had little impact on the structure of extant California populations. Given the long history of stock transfers within California and between California and other Pacific Northwest states, this finding suggests that stock transfers have not "taken" owing to reduced fitness of salmon introduced via stocking. Two Oregon stocks (Alsea and Klaskanine) have been planted extensively in California watersheds, including the Klamath, Eel, and Russian rivers and Lagunitas and Scott creeks (Weitcamp et al. 1995; L. Weitcamp, Northwest Fisheries Science Center, 2725 Montlake Boulevard East, Seattle, WA 98112–2097, USA, unpublished data). California's Noyo River stock has been repeatedly planted in at least seven of the watersheds sampled in this study (L. Weitcamp, unpublished data). In addition, Klamath River stock, which has been extensively stocked with out-of-basin (and state) coho salmon, maintains more similarity to the geographically proximal Little River coho population than to those of other systems that have received similar plantings. Isolation by distance among California coho salmon populations is inconsistent with recent stocking events and has likely developed over longer time scales.

Other examples of indigenous populations persisting in the face of intensive stocking efforts over long time periods have been reported (e.g., Utter 2000; Nielsen et al. 2001; Spidle et al. 2001). Furthermore, similarly high levels of diversity among small, genetically isolated populations of native coho salmon have been reported recently (Miller et al. 1996; Gharrett et al. 2001; Olsen et al. 2003), though not all studies support a model of isolation by distance. In the Olsen et al. (2003) study, the lack of strong agreement between genetic and geographic distance in some regions (e.g., Kodiak archipelago) may reflect historical colonization events, complex ocean currents, or large spatial distances among populations within regions. Small et al. (1998) provide evidence for the existence of at least three primary components of genetic diversity among British Columbia coho salmon stocks (coastal islands, mainland, and the Thompson drainage). Overall, a cline of decreasing mtDNA diversity is observed from south to north across the Pacific Northwest, indicating that a substantial portion of coho salmon genetic diversity is concentrated in the southerly region (Smith et al. 2001).

Our study implicates population fragmentation, genetic drift, and isolation by distance, owing to very low levels of migration, as the major evolutionary forces shaping genetic diversity within and among extant California coho salmon populations. In reaching these conclusions, we have had to overcome significant challenges, posed by low abundance itself, to sampling and deducing the units of population structure. These challenges are unfortunately likely to arise in other species or regions with similarly declining abundance, and we hope that the methods developed and applied here or improvements upon them will prove useful in such cases. The implications of correctly identifying the units of population structure for conservation can be substantial. In the case of California coho salmon, resolution of smaller population units suggests that they are experiencing rapid genetic drift, inbreeding, and the associated deleterious effects of inbreeding depression. Accordingly, management and rehabilitation of these populations is needed at much smaller scales than current ESU designations.

Acknowledgements

We thank Carolyn Greig for technical assistance in testing and evaluating microsatellite markers, Cheryl Dean for genotyping, and A. I. Pudovkin and W. Eichert for developing the computer applications. We also thank the many dedicated collectors and volunteers who provided samples and insight into the intricacies of the different watersheds. We are especially indebted to Paul Siri, Bob Chamberlain, Mitch Farro, Michael Fawcett, Ken Fox, Scott Harris, David Hines,

© 2007 NRC Canada

Wendy Jones, Dave Manning, Jerry Smith, Dave Streig, David Teel, Harry Vaughn, Jerry Wall, Jim Waldvogel, John West, Bob Will, and the lumber companies for access to their property. We thank Robin Waples whose comments substantially improved this paper. This study was supported by contracts TW 96/97-10 and TW 99/00-110 with the Sonoma County Water Agency.

References

Allendorf, F.W., and Phelps, S.R. 1981. Use of allelic frequencies to describe population structure. Can. J. Fish. Aquat. Sci. **38**: 1507–1514.

Banks, M.A., Blouin, M.S., Baldwin, B.A., Rashbrook, V.K., Fitzgerald, H.A., Blankenship, S.M., and Hedgecock, D. 1999. Isolation and inheritance of novel microsatellites in Chinook salmon (*Oncorhynchus tshawytscha*). J. Hered. **90**: 281–288.

Banks, M.A., Rashbrook, V.K., Calavetta, M.J., Dean, C.A., and Hedgecock, D. 2000. Analysis of microsatellite DNA resolves genetic structure and diversity of chinook salmon (*Oncorhynchus tshawytscha*) in California's Central Valley. Can. J. Fish. Aquat. Sci. **57**: 915–927.

Bartley, D.M., Bentley, B., Olin, P.G., and Gall, G.A.E. 1992. Population genetic structure of coho salmon (*Onchorhynchus kisutch*) in California. Calif. Fish Game, **78**: 88–104.

Beacham, T.D., Supernault, J.K., Wetklo, M., Deagle, B., and Labaree, K., Irvine, J.R., Candy, J.R., Miller, K.M., Nelson, J.R., and Withler, R.E. 2003. The geographic basis for population structure in Fraser River chinook salmon (*Oncorhynchus tshawytscha*). Fish. Bull. **101**(2): 229–242.

Beechie, T.J., Breamer, E., and Wasserman, L. 1994. Estimating coho salmon rearing habitat and smolt production losses in a large river basin, and implications for habitat restoration. N. Am. J. Fish. Manag. **14**: 797–811.

Belkhir, K., Borsa, P., Goudet, J., Chikhi, L., and Bonhomme, F. 1998. GENETIX, logiciel sous Windows™ pour la génétique des populations. Laboratoire Génome et Populations, CNRS UPR 9060, Université de Montpellier II, Montpellier, France.

Bentzen, P., Olsen, J.B., McLean, J.E., Seamons, T.R., and Quinn, T.P. 2001. Kinship analysis of Pacific salmon: insights into mating, homing, and timing of reproduction. J. Hered. **92**: 127–136.

Bernatchez, L., Dempson, B., and Martin, S. 1998. Microsatellite gene diversity analysis in anadromous Arctic char, *Salvelinus alpinus*, from Labrador, Canada. Can. J. Fish. Aquat. Sci. **55**: 1264–1272.

Brown, L.R., Moyle, P.B., and Yoshiyama, R.M. 1994. Historical decline and current status of coho salmon in California. N. Am. J. Fish. Manag. **14**: 237–261.

Carney, B.L., Gray, A.K., and Garrett, A.J. 1994. Mitochondrial DNA restriction site variation within and among five populations of Alaskan coho salmon (*Oncorhynchus kisutch*). Can. J. Fish. Aquat. Sci. **54**: 940–949.

Cavalli-Sforza, L.L., and Edwards, A.W.F. 1967. Phylogenetic analysis: models and estimation procedures. Evolution, **32**: 550–570.

Duchesne, P.and Bernatchez, L. 2002. An analytical investigation of the dynamics of inbreeding in multi-generation supportive breeding. Conserv. Genet. **3**: 47–60.

England, P.R., Osler, G.H., Woodworth, L.M., Montgomery, M.E., Briscoe, D.A., and Frankham, R. 2003. Effects of intense versus diffuse population bottlenecks on microsatellite genetic diversity and evolutionary potential. Conserv. Genet. **4**: 595–604.

Felsenstein, J. 1993. PHYLIP (Phylogeny Inference Package). Version 3.57c. Department of Genetics, University of Washington, Seattle, Wash.

Ford, M.J., Teel, D.J., Van Doornik, D.M., Kuligowski, D.R., and Lawson, P.W. 2004. Genetic population structure of central Oregon Coast coho salmon (*Oncorhynchus kisutch*). Conserv. Genet. **5**: 797–812.

Frankham, R., Ballou, J.D., and Briscoe, D.A. 2002. Introduction to conservation genetics. Cambridge University Press, Cambridge, UK.

Gharrett, A.J., Gray, A.K., and Brykov, V. 2001. Phylogeographic analysis of mitochondrial DNA variation in Alaskan coho salmon, *O. kisutch*. Fish. Bull. **99**: 528–544.

Goodnight, K.F., and Queller, D.C. 1999. Computer software for performing likelihood tests of pedigree relationship using genetic markers. Mol. Ecol. **8**: 1231–1234.

Greig, C., Robertson, J.M., and Banks, M.A. 2002. Rapid PCR-based species tests for threatened sympatric salmonids. Conserv. Genet. **3**: 83–86.

Guo, S.W., and Thompson, E.A. 1992. Performing the exact test of Hardy–Weinberg proportions for multiple alleles. Biometrics, **48**: 361–372.

Hedrick, P.W., Hedgecock, D., and Hamelberg, S. 1995. Effective population size in winter-run Chinook salmon. Conserv. Biol. **9**: 615–624.

Hedrick, P.W., Hedgecock, D., Hamelberg, S., and Croci, S.J. 2000. The impact of supplementation in winter run Chinook salmon on effective population size. J. Hered. **91**(2): 112–116.

Hendry, A.P., Wenburg, J.K., Bentzen, P., Volk, E.C., and Quinn, T.P. 2000. Rapid evolution of reproductive isolation in the wild: evidence from introduced salmon. Science (Washington, D.C.), **290**(5491): 516–518.

Krueger, C.C., and May, B.P. 1991. Ecological and genetic effects of salmonid introductions in North America. Can. J. Fish. Aquat. Sci. **48**: 66–77.

Mantel, N. 1967. The detection of disease clustering and a generalized regression approach. Cancer Res. **27**: 209–220.

Miller, K.M., Whithler, R.E., and Beacham, T.D. 1996. Stock identification of coho salmon (*Oncorhynchus kisutch*) using minisatellite DNA variation. Can. J. Fish. Aquat. Sci. **53**: 181–195.

Nelson, R.J., and Beacham, T.D. 1999. Isolation and cross species amplification of microsatellite loci useful for study of Pacific salmon. Anim. Genet. **30**: 228–229.

Nickelson, T. 2003. The influence of hatchery coho salmon (*Oncorhynchus kisutch*) on the productivity of wild coho salmon populations in Oregon coastal basins. Can. J. Fish. Aquat. Sci. **60**: 1050–1056.

Nickelson, T.E., and Lawson, P.E. 1998. Population viability of coho salmon, *Oncorhynchus kisutch*, in Oregon coastal basins: application of a habitat-based life cycle model. Can. J. Fish. Aquat. Sci. **55**: 2383–2392.

Nielsen, E.E., Hansen, M.M., and Bach, L.A. 2001. Looking for a needle in a haystack: discovery of indigenous Atlantic salmon (*Salmo salar*) in stocked populations. Conserv. Genet. **2**: 219–232.

Olin, P.G. 1984. Genetic variability in hatchery and wild populations of coho salmon *Oncorhynchus kisutch* in Oregon. M.S. thesis, University of California–Davis, Davis, California.

Olsen, J.B., Miller, S.J., Spearman, W.J., and Wenburg, J.K. 2003. Patterns of intra- and inter-population genetic diversity in Alaskan coho salmon: implications for conservation. Conserv. Genet. **4**: 557–569.

© 2007 NRC Canada

Page, R.D.M. 1996. TreeView: an application to display phylogenetic trees on personal computers. Comput. Appl. Biosci. **12**: 357–358.

Park, L.K., Moran, P., and Dightman, D.A. 1996. A Chinook salmon PCR-RFLP marker in the p53 locus. Anim. Genet. **27**: 127–128.

Pess, G.R., Montgomery, D.R., Steel, E.A., Bilby, R.E., Feist, B.E., and Greenberg, H.M. 2002. Landscape characteristics, land use, and coho salmon (*Oncorhynchus kisutch*) abundance, Snohomish River, Wash., U.S.A. Can. J. Fish. Aquat. Sci. **59**: 613–623.

Raymond, M., and Rousset, F. 1995. GENEPOP: Version 3.3. Population genetics software for exact tests and ecumenicism. J. Hered. **86**: 248–249.

Reed, D.H., Lowe, E.H., Briscoe, D.A., and Frankham, R. 2002. Inbreeding and extinction: effects of rate of inbreeding. Conserv. Genet. **4**: 405–410.

Reisenbichler, R.R., and Phelps, R. 1989. Genetic variation in steelhead (*Salmo gairdneri*) from the north coast of Washington. Can. J. Fish. Aquat. Sci. **46**: 66–73.

Saisa, M., Koljonen, M.L., and Tahtinen, J. 2003. Genetic changes in Atlantic salmon stocks since historical times and the effective population size of a long-term captive breeding programme. Conserv. Genet. **4**: 613–627.

Saitou, N., and Nei, M. 1987. The neighbor-joining method: a new method for reconstructing phylogenetic trees. Mol. Biol. Evol. **4**(4): 406–25.

Scribner, K.T., Gust, J.R., and Fields, R.L. 1996. Isolation and characterization of novel salmon microsatellite loci: cross-species amplification and population genetic applications. Can. J. Fish. Aquat. Sci. **53**: 833–841.

Small M.P., Withler, R.E., and Beacham, T.D. 1998. Population structure and stock identification of British Columbia coho salmon, *Oncorhynchus kisutch*, based on microsatellite DNA variation. Fish. Bull. (Washington, D.C.), **96**: 843–858.

Smith, C.T., Koop, B.F., and Nelson, R.J. 1998. Isolation and characterization of coho salmon (*Oncorhynchus kisutch*) microsatellites and their use in other salmonids. Mol. Ecol. **7**: 1614–1616.

Smith, C.T., Nelson, R.J., Wood, C.C., and Koop, B.F. 2001. Glacial biogeography of North American coho salmon (*Oncorhynchus kisutch*). Mol. Ecol. **10**: 2775–2785.

Spidle, A.P., Bane, D., Schill, W., Lubinski, B.A., and King, T.L. 2001. Fine-scale population structure in Atlantic salmon from Maine's Penobscot River drainage. Conserv. Genet. **2**: 11–24.

Utter, F.M. 2000. Patterns of subspecific anthropogenic introgression in two salmonid genera. Rev. Fish Biol. Fish. **10**: 265–279.

Utter, F.M. 2004. Population genetics, conservation and evolution in salmonids and other widely cultured fishes: some perspectives over six decades. Rev. Fish Biol. Fish. **14**: 125–144.

Utter, F.M., Campton, D., and Grant, S., Milner, G., Seeb, J., and Wishard, L. 1980. Population structures of indigenous salmonid species of the Pacific Northwest. *In* Salmonid ecosystems of the Pacific Northwest. *Edited by* W.J. McNeil and D.C. Himsworth. Oregon State University Press and Oregon State University Sea Grant College Program, Corvallis, Oregon. pp. 285–304.

Van Doornik, D.M., Ford, M.J., and Teel, D.J. 2002. Patterns of temporal genetic variation in coho salmon: estimates of the proportion of 2-year-olds in natural and hatchery production. Trans. Am. Fish. Soc. **131**: 1007–1019.

Van Oosterhout, C., Hutchinson, W.F., Wills, D.P.M., and Shipley, P. 2004. MICRO-CHECKER: software for identifying and correcting genotyping errors in microsatellite data. Mol. Ecol. Notes, **4**(3): 535–538.

Wang, S., Hard, J.J., and Utter, F. 2002. Salmonid inbreeding: a review. Rev. Fish Biol. Fish. **11**: 301–319.

Waples, R.S. 1991. Definition of "species" under the Endangered Species Act: application to Pacific Salmon. NOAA Tech. Memo. No. NMFS-F/NWC-19.

Waples, R.S., Gustafson, R.G., Weitkamp, L.A., Myers, J.M., Johnson, O.W., Busby, P.J, Hard, J.J., and Bryant, G.J., Waknitz, F.W., Neely, K., Teel, D., Grant, W.S., Winans, G.A., Phelps, S., Marshall, A., and Baker, B.M. 2001. Characterizing diversity in salmon from the Pacific Northwest. J. Fish Biol. **59**(Suppl. A): 1–41.

Wehrhahn, C.F., and Powell, R. 1987. Electrophoretic variation, regional differences and gene flow in the coho salmon (*Oncorhynchus kisutch*) of southern British Columbia. Can. J. Fish. Aquat. Sci. **44**: 822–831.

Weir, B.S., and Cockerham, C.C. 1984. Estimating *F*-statistics for the analysis of population structure. Evolution, **38**: 1358–1370.

Weitcamp, L.A., Wainwright, T.C., Bryant, G.J., Milner, G.B., Teel, D.J., Koop, R.G., and Waples, R.S. 1995. Status review of coho salmon from Washington, Oregon and California. US Department of Commerce, NOAA Tech. Memo. No. NMFS-NWFSC-24.

Wofford, J.E.B., Gresswell, R.E., and Banks, M.A. 2005. Influence of barriers to movement on within-watershed genetic variation of coastal cutthroat trout. Ecol. Appl. **15**(2): 628–637.

Wright, S. 1931. Evolution in Mendelian populations. Genetics, **16**: 97–159.

© 2007 NRC Canada

Environmental implications of stratification and turbulent mixing in a shallow lake basin

Mark R. Loewen, Josef Daniel Ackerman, and Paul F. Hamblin

Abstract: The extent of stratification and vertical mixing in the water column (7–11 m deep) was investigated over an offshore reef in the western basin of Lake Erie. Measurements reveal that the vertical transport of oxygen and heat is controlled by the complex interaction of several physical mechanisms. Generally, when the wind speed (W) was >7 m·s^{-1} and the air was cooler than the water ($T_{air} < T_w$), the water column was well mixed due to turbulent mixing. However, when $W < 7$ m·s^{-1} (~65% of the summer), turbulence was too weak to overcome the stratification and mix the water column. An analysis of 25 years of meteorological data revealed that a period of 4.5 ± 1.9 days of calm, warm weather ($W < 7$ m·s^{-1} and $T_{air} > T_w$) occurs every year. Results indicate that there is strong probability of hypoxia due to stratification (i.e., when diffusivities < 10^{-6} m^2·s^{-1}) and sediment oxygen demand (i.e., 0.1–1.0 g·m^{-2}·day^{-1}) during these periods. The environmental implications of stratification to water quality and its effects on benthic organisms, such as the burrowing mayfly (*Hexagenia* spp.), require further considerations in large temperate lakes and basins that are sufficiently shallow that there is no permanent seasonal stratification.

Résumé : Nous avons étudié l'importance de la stratification et du brassage vertical dans la colonne d'eau (7–11 m de profondeur) sur un récif du large dans le bassin occidental du lac Érié. Nos mesures indiquent que le transport vertical de l'oxygène et de la chaleur est contrôlé par l'interaction complexe de plusieurs mécanismes physiques. Généralement, lorsque la vitesse du vent (W) est >7 m·s^{-1} et que l'air est plus frais que l'eau ($T_{air} < T_w$), la colonne d'eau est bien brassée à cause de la turbulence. Cependant, lorsque $W < 7$ m·s^{-1} (~65 % de l'été), la turbulence est trop faible pour vaincre la stratification et brasser la colonne d'eau. Une analyse de 25 années de données météorologiques montre qu'une période de 4,5 ± 1,9 jours de chaleur et de calme ($W < 7$ m·s^{-1} et $T_{air} > T_w$) se produit chaque année. Nos résultats indiquent qu'il y a une forte probabilité d'hypoxie à cause de la stratification (par ex., lorsque les diffusions < 10^{-6} m^2·s^{-1}) et de la demande en oxygène des sédiments (par ex., 0,1–1,0 g·m^{-2}·jour^{-1}) durant ces périodes. Les conséquences environnementales de la stratification sur la qualité de l'eau et ses effets sur les organismes benthiques, tels que les éphémères fouisseurs (*Hexagenia* spp.), nécessitent des études supplémentaires dans les grands lacs et bassins qui sont assez peu profonds pour qu'il n'y ait pas de stratification saisonnière.

[Traduit par la Rédaction]

Introduction

Lake Erie is truly an area of transition, with respect to water quality and ecosystem integrity, that has seen many changes in the past century (e.g., Sweeney 1993; Munawar et al. 1999, 2002, and references therein). Agriculture, industrialization, urbanization, and associated pollution led to a significant decline in the water quality of Lake Erie between the 1950s and 1970s due to the influx of phosphorus and other pollutants from agriculture, human waste, and detergents (Fraser 1987; Charlton et al. 1999). A shift from mesotrophic to eutrophic conditions, especially in the relatively shallow western basin of Lake Erie, was observed along with periods of anoxia that impacted benthic organisms (Charlton 1987; Makarewicz and Bertram 1991). Pollution abatement programs and international agreements directed at water treatment and agricultural runoff initiated in the 1970s have led to considerable improvements in water quality in the late 1980s and 1990s (Makarewicz 1993; Schelske and Hodell 1995; Makarewicz et al. 2000). This latter period also corresponds to the period when introduced suspension-feeding zebra mussels (*Dreissena polymorpha*) achieved numerical dominance and may have contributed to the clarification of the lake. Regardless of the cause, pelagic and benthic communities appear to have shifted back toward mesotrophic conditions (Makarewicz 1993; Koonce et al. 1996; Munawar et al. 2002), and indicator organisms such as submerged aquatic plants and burrowing mayflies (e.g., *Hexagenia* spp.) have rebounded to close to historical levels (Knapton and Petrie 1999; Schloesser et al. 2000). There are, however, persistent regions of the offshore benthos in which indicator organisms, such as burrowing mayfly nymphs, have not returned to their former levels perhaps due

Received 31 January 2006. Accepted 29 August 2006. Published on the NRC Research Press Web site at http://cjfas.nrc.ca on 16 January 2007.
J19142

M.R. Loewen.[1] Department of Civil and Environmental Engineering, University of Alberta, Edmonton, AB T6G 2W2, Canada.
J.D. Ackerman. Department of Integrative Biology and Faculty of Environmental Sciences, University of Guelph, Guelph, ON N1G 2W1, Canada.
P.F. Hamblin. National Water Research Institute, Canada Centre for Inland Waters, 867 Lakeshore Road, Burlington, ON L7R 4A6, Canada.

[1]Corresponding author (e-mail: mrloewen@ualberta.ca).

 doi:10.1139/F06-165 © 2007 NRC Canada

to low dissolved oxygen concentrations ($[O_2] < 7$ mg·L^{-1}) (i.e., hypoxia; Winter et al. 1996; Schloesser et al. 2000; Bridgeman et al. 2006).

Lake Erie contains three distinct physiographic basins (western, central, and eastern) with average depths of 10, 25, and 50 m, respectively. Distinct seasonal thermoclines, which are observed in the central and eastern basins, form significant physical barriers separating the surface mixed layer from the deeper water. This stable stratification inhibits diapycnal transfer of momentum, heat, nutrients, phytoplankton, and oxygen, leading to the formation of distinct epilimnion and hypolimnion (Fischer et al. 1979). Conversely, the western basin is often characterized as well mixed (e.g., Schertzer et al. 1987), which suggests that the water column is unstratified and that the vertical transport of oxygen or other quantities is not inhibited by stable stratification. However, field measurements of water temperature in the western basin show that density gradients of sufficient magnitude to inhibit vertical mixing may form diurnally and influence benthic–pelagic coupling (Ackerman et al. 2001). The strength of this vertical mixing will be a function of the magnitude of the density gradients that stabilize the water column (i.e., the strength of the stratification) and the sources of turbulent kinetic energy that mix the water column.

Hypoxia is another consequence of stratification as the downward transport of oxygen from the surface is inhibited in a stratified water column. This situation can be exacerbated by the decomposition of organic matter in the sediments, which creates a sediment oxygen demand (SOD) at the sediment–water interface. Bottom hypoxia also plays an important role in redox-controlled biogeochemical processes at and within aquatic sediments (e.g., Caraco et al. 1993; Rysgaard et al. 1994). If conditions at a given location are such that the water column is stratified for a sufficient duration, SOD will gradually reduce oxygen concentrations in the hypolimnion until local hypoxia occurs (Wetzel 2001). However, if enough turbulent kinetic energy is available to mix the water column, the thermocline will be obliterated and the likelihood of local hypoxia will be reduced greatly.

Wind-generated surface waves, surface gravitational seiches, wind-driven horizontal circulation, convective mixing, and hydraulic flow are all potential sources of turbulent kinetic energy in a shallow lake basin (Fischer et al. 1979). Wind-generated surface waves generate turbulence by breaking, which enhances the vertical transport of heat, mass, and momentum in near-surface waters (Melville 1996) or through the formation of a turbulent wave boundary layer on the bed when the wave height is large or the bed is rough (Dean and Dalrymple 1991). In addition, the currents produced by surface gravitational seiches, wind-driven horizontal circulation, and hydraulic flow may also be a source of turbulent kinetic energy via shear production (i.e., the interaction of the Reynolds stress with the mean shear; Kundu and Cohen 2001). Vertical motions produced by the convective instability of the surface waters subjected to nighttime cooling may also contribute significantly to mixing of the water column (Fischer et al. 1979). An examination of the relative importance of the stabilizing effect of density stratification versus the homogenizing effect of turbulence will provide the environmental setting that determines the water quality in shallow lake basins such as the western basin of Lake Erie. Herein, we report the results of a field experiment that was conducted over an isolated reef in the western basin of Lake Erie in 1994 to examine these issues.

Materials and methods

The experimental site was located on an isolated zebra mussel encrusted shallow rock and sand reef that was completely surrounded by soft, muddy sediments 1 km northwest of North Harbour Island in the western basin of Lake Erie (Fig. 1). The reef is elliptical in shape, with a major axis length of ~500 m and a minor axis length of ~300 m. Water depth ranged from ~8 m at the shallowest point of the reef to a depth of ~11 m over the surrounding soft substrates (see Ackerman et al. (2001) for a discussion of the reef and zebra mussel population).

Four ultrasonic current meters with built-in water temperature sensors (model SACM-3; EG&G, Gaithersburg, Maryland) and a wave and tide recorder (SeaData 365-11; Sea Data Corporation, Newton, Mass.) were moored on the reef from 7 July to 24 August (days of the year 188–235). Three separate data sets were obtained: deployment I, 7 to 19 July (days of the year 188–200); deployment II, 21 July to 3 August (days of the year 202–215); and deployment III, 12 to 23 August (days of the year 224–235). All instruments were calibrated before and after the study by the National Water Research Institute Calibration Laboratory (Canada Centre for Inland Waters, Burlington, Ontario). Meteorological data were obtained from a meteorological buoy installed for the experiment and from an Atmospheric Environment Service (Environment Canada) buoy moored off of Point Pelee (~30 km to the east).

The current meters were moored at depths of 2.2, 3.6, 6.8, and 7.2 m and oriented vertically to measure the horizontal components of the velocity. They were programmed to burst sample the velocity at a rate of 2 Hz for 256 s every hour and to record one 4-min average of the velocity and temperature every 10 min. The wave and tide recorder was moored on the lake bottom and was programmed to record the mean water level once every 10 min. A water quality probe (Hydrolab DataSonde 3; Hach Environmental Sales, Loveland, Colorado) was used to measure vertical profiles of the water temperature, dissolved oxygen, and conductivity on 13 July 1994 (day 194).

The coherence function, which is a quantitative measure of the linear correlation between two random variables (Bendat and Piersol 1986), was used to analyze the time series data. For example, the coherence function, $\gamma^2_{hu}(f)$, between the water level h and a velocity component of the current u is given by

$$(1) \qquad \gamma^2_{hu}(f) = \frac{|G_{hu}(f)|^2}{G_{uu}(f)G_{hh}(f)}$$

where f is the frequency (Hz), G_{hu} is the cross spectrum of the water level and the velocity component, G_{uu} is the autospectrum of the velocity component, and G_{hh} is the autospectrum of the water level (Bendat and Piersol 1986). In this case, the coherence function is a measure of the mean

© 2007 NRC Canada

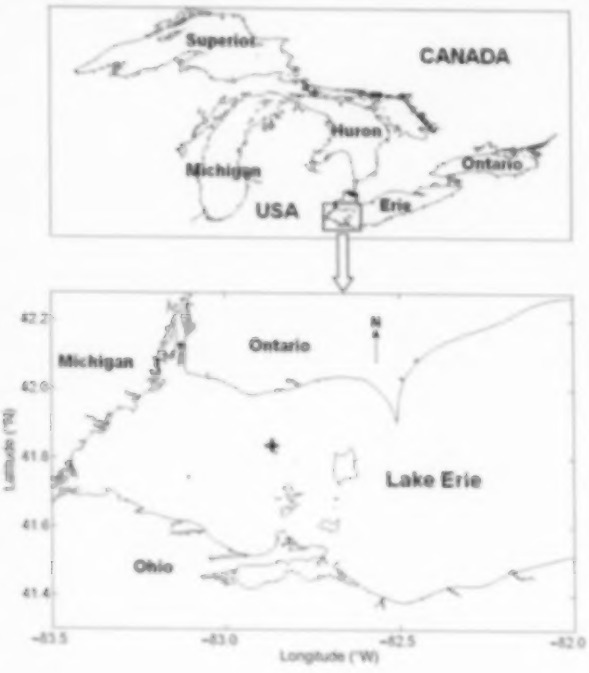

Fig. 1. Map of the western basin of Lake Erie showing the location of the experimental site (plus sign (+); 41.835°N, 82.866°W).

square value of the velocity component that is linearly related to variations in the water level at frequency f.

Additional analyses were undertaken using the densimetric Froude number, F_{rd}, which is a measure of the relative strength of inertial to buoyancy forces and is defined as

$$(2) \qquad F_{rd} = \frac{U}{\sqrt{g\Delta h \frac{\Delta\rho}{\rho_0}}}$$

where U is the magnitude of the velocity, g is the acceleration due to gravity, $\Delta\rho$ is the density difference between two points a vertical distance Δh apart, and ρ_0 is the average water density. F_{rd} is computed using data from the two current meters moored at depths of 2.2 and 3.6 m. The velocity (U) is the average of the velocities at these two depths, Δh is 1.4 m, $\Delta\rho$ is the density difference between these depths, and ρ_0 was assumed to be 1000 kg·m^{-3}. When $F_{rd} < 1$, buoyancy forces are stronger than inertial forces, internal waves continually adjust the density structure, and the water column remains stratified. Alternatively, when $F_{rd} > 1$, inertial forces can overcome buoyancy and the water column remains unstratified (Fischer et al. 1979).

Results

The environmental conditions during July and August 1994 included wind speeds (W) of 5.9 ± 2.8 m·s^{-1} (mean ± standard deviation) at 10 m height, air temperatures (T_{air}) of 22.1 ± 1.9 °C, water temperatures at 2.2 m depth ($T_{2.2}$) of 22.9 ± 0.3 °C, and significant wave heights (H) of 0.31 ± 0.24 m (Table 1). The range in these conditions followed seasonal trends in the case of T_{air} *and* $T_{2.2}$ and more complex patterns in the case of W and H as described below.

There is spatial and temporal information contained in the progressive vector plot of the currents at depths of 2.2 and 7.2 m during deployment III, which demonstrated that the magnitude and direction of the horizontal currents varied significantly with depth (Fig. 2). The net transport was to the east–northeast at approximately 2.8 cm·s^{-1} at 2.2 m and 1.4 cm·s^{-1} at 7.2 m depth (e.g., 5.8 m and 0.8 m above the lakebed, respectively). The average magnitudes of the current at depths of 2.2 and 7.2 m were 4.7 ± 3.0 cm·s^{-1} (maximum = 15.7 cm·s^{-1}) and 3.7 ± 2.1 cm·s^{-1} (maximum = 12.6 cm·s^{-1}), respectively. It is evident that the flow at both depths was influenced to varying degrees by surface gravitational seiches and the mean hydraulic flow from west to east. The seiches produced the loops and sharp curves in the trajectories as the flow oscillated back and forth, and the hydraulic flow advected the water in an east–northeast direction.

A strong diurnal signal was evident in the time series of $T_{2.2}$ throughout deployment I (Fig. 3*a*). During the last half of the deployment, the temperature of the near-surface waters increased gradually. At a depth of 7.2 m, the temperature fluctuated rapidly between 22 and 23 °C for the first 2.5 days (days 188–190.5) and was not well correlated with $T_{2.2}$. For the remaining 10.5 days of deployment I, both the amplitude and the frequency of the temperature fluctuations at 7.2 m depth were considerably lower. The diurnal temperature fluctuations that occurred at a depth of 2.2 m were caused by solar heating of the near-surface waters, and occasionally this signal penetrated to 7.2 m. This was evident in days 193–197 when a diurnal signal was present in the temperature time series at the 7.2 m depth that lagged the time series at 2.2 m by approximately 10 h. For several time periods (e.g., day 191), the temperatures at 2.2 and 7.2 m were essentially equal, indicating that the water column was well mixed.

During deployment III, a diurnal signal occurred sporadically at a depth of 2.2 m, and occasionally on several days, this signal penetrated to depths of 7.2 m (Fig. 3*b*). There were two time periods, each of approximately 2 days in duration (days 225.5–227.5 and days 232.5–234.5) when the temperatures at the two depths were essentially equal. The temperature difference (ΔT) between depths of 2.2 and 7.2 m was found to be 0.43 ± 0.44 °C (maximum = 1.8 °C) and 0.17 ± 0.21 °C (maximum = 0.99 °C) for deployments I and III, respectively. These temperature differences correspond to changes in the density of water ($\Delta\rho$) of approximately 0.09 kg·m^{-3} and 0.04 kg·m^{-3}, respectively. Although these $\Delta\rho$ are very small, it will be shown later that they produce stratification that has significant environmental implications.

The time series of the water temperatures during both deployments indicate that convective mixing events occurred frequently (Figs. 3*a* and 3*b*). These convective mixing events typically occurred during the night as the surface waters cooled because of the colder overlying air. This cooling is evident during every day of deployment I and on days 225, 228–231, and 235 during deployment III. In a number of cases, the convective motions produced by the cooling of the surface waters were strong enough that the water column be-

© 2007 NRC Canada

Table 1. Mean (± standard deviation (SD)), minimum, and maximum values of selected environmental parameters during July–August 1994 in western Lake Erie.

Parameter	Mean ± SD	Minimum	Maximum
Wind speed ($m \cdot s^{-1}$) at 10 m	5.9±2.8	0	15.9
Air temperature (°C)	22.1±1.9	15.7	29.2
Water temperature at 2.2 m (°C)	22.9±0.3	21.7	25.0
Significant wave height (m)	0.31±0.24	0.03	1.0

Fig. 2. A progressive vector plot of the displacement of fluid over deployment III for currents measured at depths of 2.2 m (bold line) and 7.2 m (thin line).

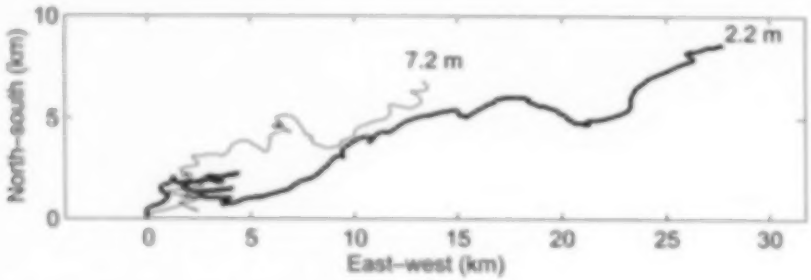

Fig. 3. Time series of the water temperature (T, °C) at depths of 2.2 m (bold line) and 7.2 m (thin line) for (*a*) deployment I and (*b*) deployment III. Time (t) is in days Greenwich mean time (GMT)); local time is GMT minus 4 h.

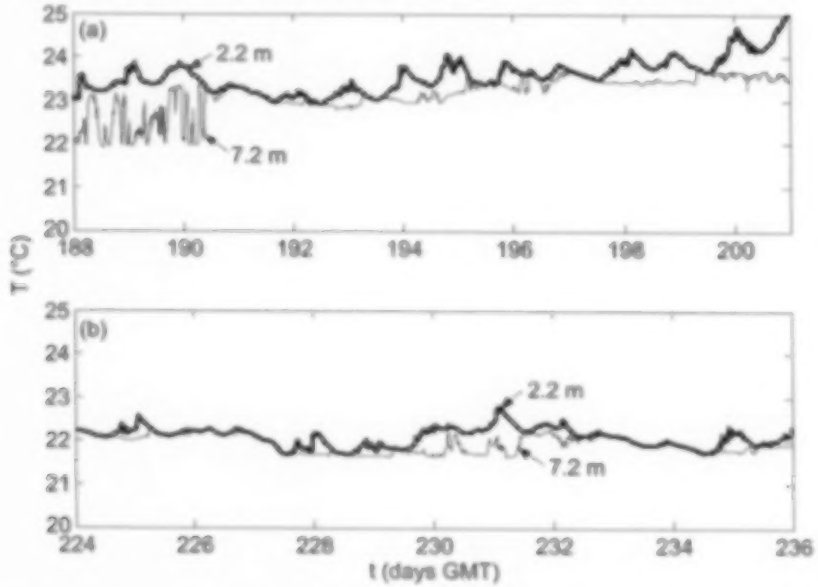

came fully mixed. For example, on days 193 and 228, the water temperature difference between depths of 2.2 and 7.2 m was reduced to approximately zero during the night.

The rapid temperature fluctuations that occurred during days 188–190.5 of deployment I were distinctly different in character from those of the remainder of the time series in that the magnitude and the frequency of the fluctuations were the largest observed (Fig. 3*a*). During this time period, the average wind speed was 5.4 $m \cdot s^{-1}$, the predominant wind direction was to the east, and the directions of the currents at the two depths were within 20° of each other <10% of the time. The currents at the depth of 2.2 m were predominantly to the east, and at the depth of 7.2 m, they were highly variable, with the four most frequently occurring directions being northwest, west, north, and east. Analysis of the current meter and temperature data at the two depths revealed that the large fluctuations in the density difference during this time period were likely caused by the advection of colder water from the central basin along the bottom of the western basin. The fluctuating bottom currents associated with the surface gravitational seiching caused the colder water to advect back and forth over the reef, producing larger fluctuations in the water temperature near the bottom. At approximately 0000 Greenwich mean time (GMT) on day 190,

© 2007 NRC Canada

Fig. 4. Time series of (*a*) wind speed (W, m·s^{-1}), (*c*) water level (h, m), (*e*) the east component of the horizontal current (u, cm·s^{-1}), and (*g*) the north component of the horizontal current (v, cm·s^{-1}) during deployment III. Time (t) is in days Greenwich mean time (GMT); local time is GMT minus 4 h. The corresponding frequency spectra (*b*) G_{WW} (m^2·s^{-2}·cph^{-1}) (*d*) G_{hh} (m^2·cph^{-1}), (*f*) G_{uu} (m^2·s^{-2}·cph^{-1}), and (*h*) G_{vv} (m^2·s^{-2}·cph^{-1}) are the autospectral density functions of W, h, u, and v, respectively, and f is the frequency (in cycles per hour (cph)).

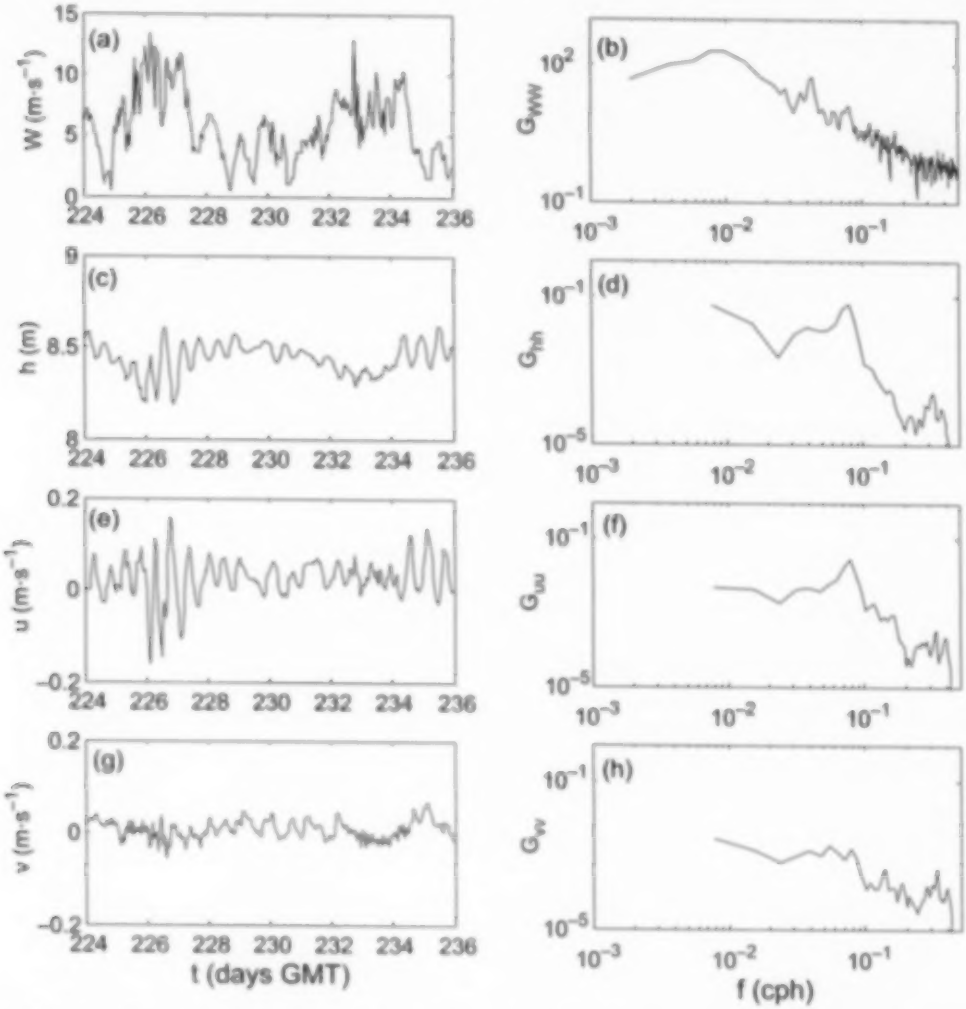

the wind speed increased to ~10 m·s^{-1}, and within a few hours, the vertical mixing had become strong enough to overcome the buoyancy forces and mix the entire water column.

Periods of intense wind activity, in addition to daily fluctuations, were observed in deployment III (Fig. 4*a*). The frequency spectrum of the wind speed, which was computed using a three-month (July–September 1994) time series, had two large amplitude spectral peaks at frequencies of approximately 0.042 and 0.01 cycles per hour (cph) or periods of 1 and 4 days, respectively (Fig. 4*b*). The strong diurnal signal was caused by the cycle of onshore–offshore breezes generated daily as the land surface heats during the daytime and cools at night. The energetic 4-day signal is a result of the dominance of storm events with time scales of approximately 4 days (Hamblin 1987). The time series of water level (Fig. 4*c*) is a narrow-banded signal dominated by fluctuations produced by surface gravitational seiches. There is a strong correlation between the water level and the east component of the current (Figs. 4*c* and 4*e*). The majority of the energy in both time series was centered at a frequency of approximately 0.075 cph, corresponding to a period of 13.3 h (Figs. 4*d* and 4*f*). This is close to the predicted period of the lowest gravitational seiche mode, which is 14 h (Hamblin 1987). The north component of the current (Fig. 4*g*) was not as closely correlated with the water level as the east component, but the spectrum of the north component had a peak at the dominant water level frequency of 0.075 cph, in addition to significant energy at lower frequencies (Fig. 4*h*).

Detailed measurements of the vertical structure of the water column were made using instrument casts taken at 1230 and 1535 h (local time) on 13 July 1994 (day 194; Fig. 5;

© 2007 NRC Canada

Fig. 5. Vertical profiles of (*a*) water temperature (*T*, °C) and (*b*) dissolved oxygen (DO, mg·L^{-1}) sampled 13 July 1994 (day 194) at 1230 (circles) and 1535 (squares) local time.

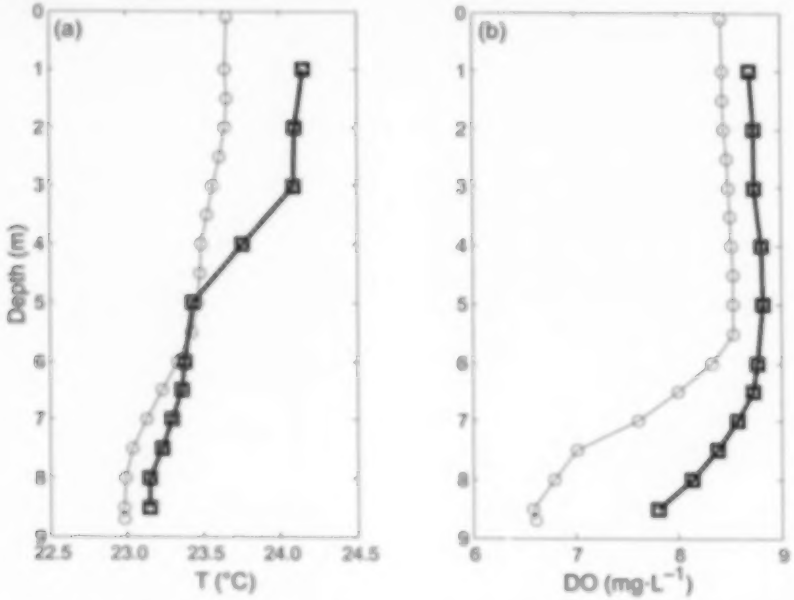

note that local time is GMT – 4 h on other figures). The temperature of the surface water was approximately 0.5 °C warmer due to solar heating at 1535 h (Fig. 5*a*). In addition, the dissolved oxygen concentrations ($[O_2]$) were higher near the surface (Fig. 5*b*), indicating increased photosynthesis during the afternoon. At 1535 h, $[O_2]$ was higher at all depths, which is likely due to photosynthesis and (or) seiche-driven advection of oxygen-rich water over the reef. The $[O_2]$ were lower near the bed at both times, likely as a result of SOD and zebra mussel respiration. Importantly, these data indicate that temperature and chemical stratification may occur daily in the western basin during the summer months. The environmental conditions that produced this stratification on 13 July 1994 were not unusual. The wind speed peaked at 9 m·s^{-1} at 0100 h, decreased to a minimum of 0.5 m·s^{-1} at 0600 h, and then averaged ~4 m·s^{-1} for the remainder of the day. The minimum air temperature of 20 °C occurred at 0900 h and then increased to a maximum value of 24 °C at 1400 h. In comparison with the data in Table 1, the conditions on 13 July 1994 would be characterized as calm and moderately warm but not extreme, as both the air temperature and wind speed were within 1 standard deviation of the mean.

Plots of the time series of the wind speed (W), significant wave height (H), air–water temperature difference ($\Delta T_{am} = \bar{T}_{air} - \bar{T}_{2.2}$), and the water temperature difference between the depths of 2.2 and 7.2 m (ΔT_w; a measure of the degree of water column stratification) provide additional insight into the physical mechanisms that control the vertical transport of heat and momentum (Figs. 6 and 7). During both deployments when $W > 7$ m·s^{-1} (▽ in Figs. 6*d* and 7*d*), H typically exceeded 0.5 m (Figs. 6*b* and 7*b*), and ΔT_w approaches zero (Figs. 6*d* and 7*d*), indicating that the water column was well mixed. The plots also show that sustained $W > 7$ m·s^{-1} were often accompanied by cooler air temperatures (i.e., negative ΔT_{am}), as can be observed on days 225.5–227.5 and 232–234.5 (Fig. 7). In both cases, ΔT_w was approximately equal to zero (Fig. 7*d*), $W > 7$ m·s^{-1} (▽ in Fig. 7*d*), ΔT_{am} was negative, and H approached 1 m (Fig. 7*b*).

The temperature and velocity data from the current meters at depths of 2.2 and 7.2 m were used to evaluate the degree of stratification over the reef. Time series of the density difference demonstrate that although $\Delta\rho$ was small (i.e., <0.4 kg·m^{-3}; Figs. 8*a* and 8*c*), F_{rd} was frequently less than 1.0 (Figs. 8*b* and 8*d*), indicating that buoyancy forces were still significant compared with inertial forces. Moreover, $\Delta\rho$ tended to be very small when $W > 7$ m·s^{-1}, the currents tended to be unidirectional (data not shown), and F_{rd} was often >1 (Figs. 8*b* and 8*d*). Overall, F_{rd} was <1.0 for 76% and 44% of the time during deployments I and III, respectively (equipment failure during deployment II prevented us from obtaining data for this period). It is important to note that because of its shallow depth and the large fetch, seasonal stratification is not observed in the western basin of Lake Erie; however, intermittent stratification was observed during both deployments (Fig. 8).

The data in Figs. 6, 7, and 8 suggest that $W = 7$ m·s^{-1} was a threshold value for mixing (i.e., when $W > 7$ m·s^{-1}, $\Delta\rho \approx 0$). This hypothesis was examined by plotting the median value of F_{rd} versus W (Fig. 9; median values were plotted because the average values become skewed when $F_{rd} \to \infty$ as $\Delta\rho \to 0$; eq. 2), which indicates that $F_{rd} < 1$ when $W < 7$ m·s^{-1} and that $F_{rd} > 1$ when $W > 7$ m·s^{-1}. In other words, at times when $W < 7$ m·s^{-1}, buoyancy forces tended to be stronger than inertial forces, vertical turbulent mixing was weak, and thermal stratification was likely to occur. At $W > 7$ m·s^{-1}, inertia was stronger than buoyancy, vertical turbulent mixing was strong, and the water column tended to be

© 2007 NRC Canada

Fig 6. Time series of (*a*) wind speed (W, m·s^{-1}), (*b*) significant wave height (H, m), (*c*) air–water temperature difference (ΔT_{aw}, °C), and (*d*) water temperature difference between 2.2 and 7.2 m (ΔT_w, °C) for deployment I. Time (t) is in days Greenwich mean time (GMT); local time is GMT minus 4 h.

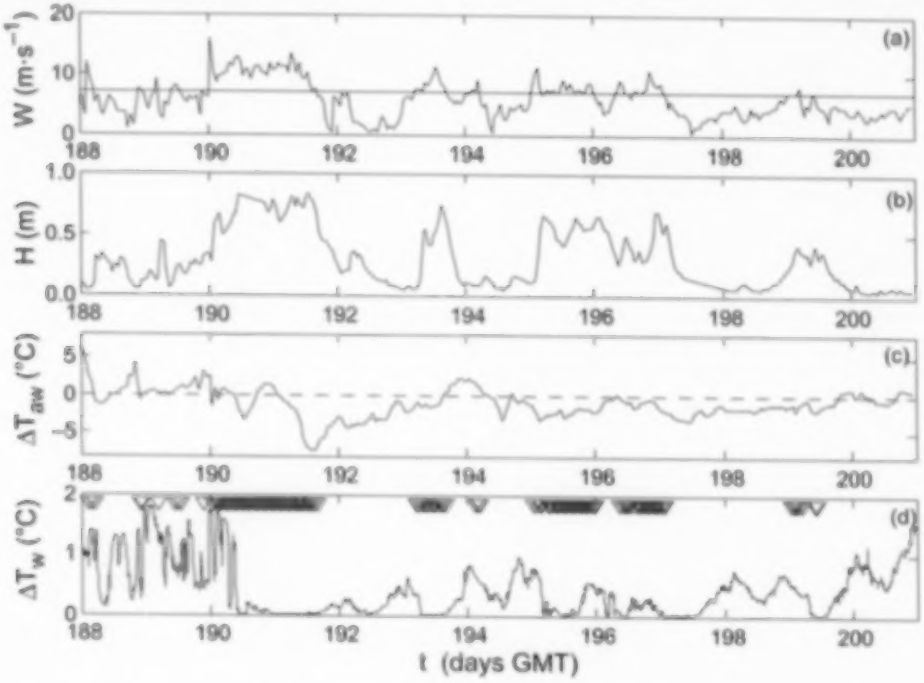

Fig 7. Time series of (*a*) wind speed (W, m·s^{-1}), (*b*) significant wave height (H, m), (*c*) air–water temperature difference (ΔT_{aw}, °C), and (*d*) water temperature difference between 2.2 and 7.2 m (ΔT_w, °C) for deployment III. Time (t) is in days Greenwich mean time (GMT); local time is GMT minus 4 h.

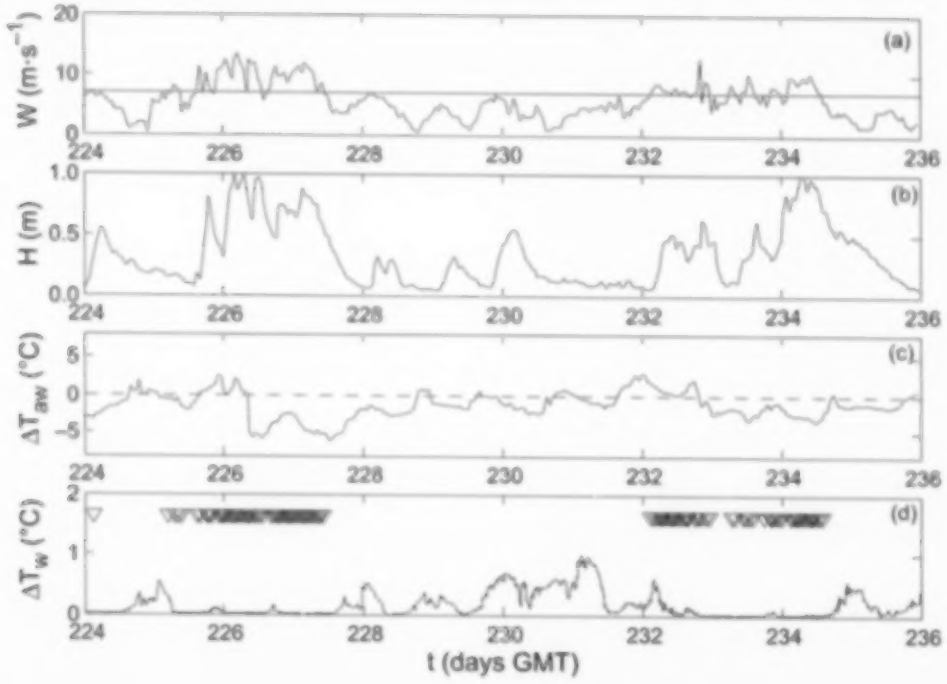

© 2007 NRC Canada

Fig. 8. Time series of (*a* and *c*) density difference between water at depths of 2.2 and 7.2 m ($\Delta\rho$, kg·m^{-3}) and (*b* and *d*) densimetric Froude number (F_{rd}) during deployments (*a* and *b*) I and (*c* and *d*) III. Times when the wind speed exceeded 7 m·s^{-1} are indicated by ▽; convective mixing events are indicated by +. Time (*t*) is in days Greenwich mean time (GMT); local time is GMT minus 4 h.

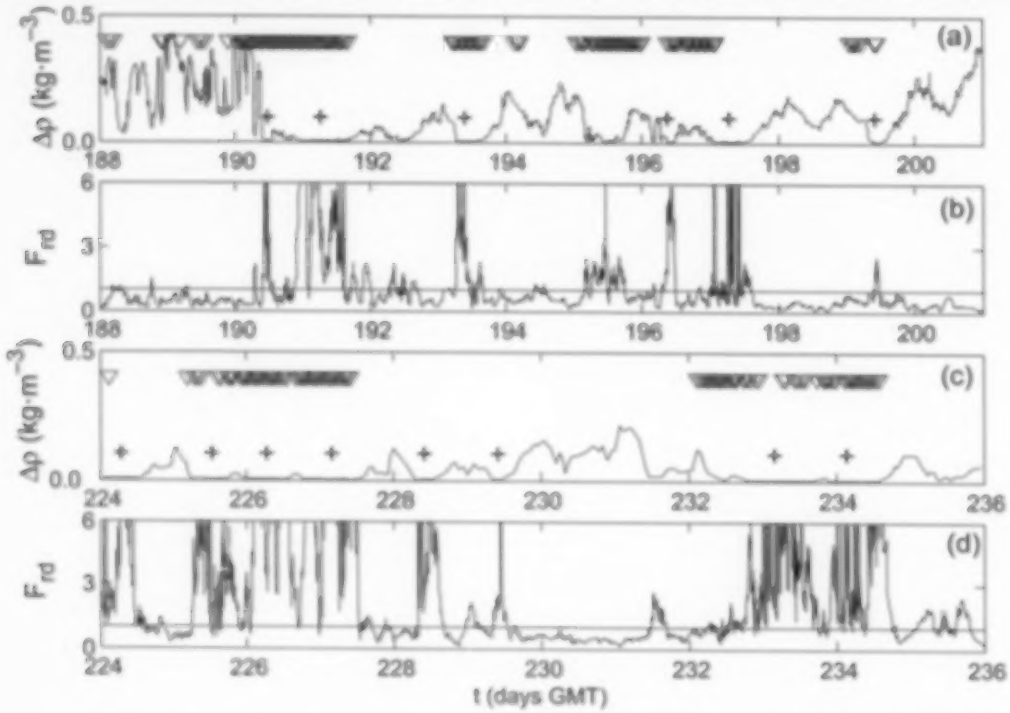

Fig. 9. Median values of the densimetric Froude number (F_{rd}), averaged within 1.0 m·s^{-1} bins, versus wind speed (W, m·s^{-1}). The horizontal line indicates the threshold at which the buoyancy forces are equal to the inertial forces in the water column. The error bars are ± standard error of the median.

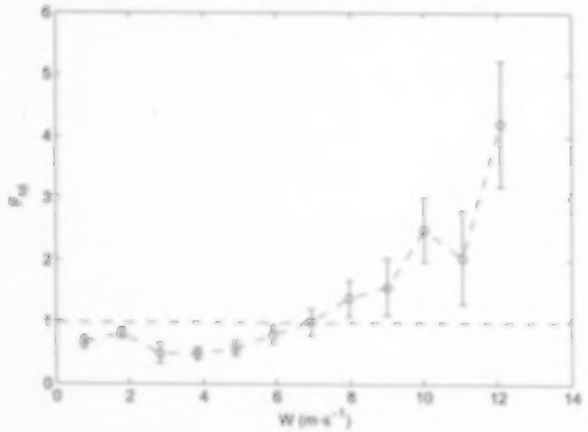

fully mixed or unstratified. It is perhaps surprising that F_{rd} is such a good indicator of water column mixing as it only accounts for the inertia of the current. Mechanisms that also contribute to mixing, e.g., wave breaking and Langmuir circulations, are not directly related to F_{rd}, but like the current, they are also controlled predominantly by the wind. As a result, when W increases, the mixing produced by all of these mechanisms also increases and the magnitude of F_{rd} provides a reasonable measure of the total mechanical mixing. However, it is likely that the relationship between F_{rd} and W depicted in Fig. 9 only applies to western Lake Erie and should not be considered universal.

The coherence function between the water level (h) and the east and north components of the current (u, v) was computed for deployment III (Figs. 10*a* and 10*c*). The coherence between h and u at a depth of 2.2 m was greater than 0.90 for frequencies from 0.05 to 0.17 cph and was equal to 0.98 at the dominant frequency of 0.075 cph (Fig. 10*a*). Conversely, the coherence between the h and v at 2.2 m depth was greater than 0.90 at only two frequencies, 0.29 and 0.42 cph, and was equal to 0.58 at the dominant water level frequency of 0.075 cph (Fig. 10*c*). The percentage of the total variance of the current that was accounted for by fluctuations in h was 73% and 55% for the u and v components, respectively.

Estimates of the multiple coherence between the water level and wind speed and the components of the current at a depth of 2.2 m were computed by assuming that h and W were the two inputs and the current was the output of a two-input single-output linear model (Bendat and Piersol 1986). For both components of the current, the level of coherence increased substantially when variations in W were included (Figs. 10*b* and 10*d*). The percentage of the total variance of the current that was linearly related to fluctuations in both h and W was 90% and 76% for u and v, respectively, at a depth of 2.2 m during deployment III. Surprisingly, the average co-

© 2007 NRC Canada

Fig. 10. (*a*) $\gamma_{uh}^2(f)$, the coherence function between the water level (*h*) and the east component of the horizontal current (*u*); (*c*) $\gamma_{vh}^2(f)$, the coherence function between the water level (*h*) and the north component of the current (*v*); (*b*) $\gamma_{uhW}(f)$, the multiple coherence between *h*, *u*, and wind speed (*W*); and (*d*) $\gamma_{vhW}(f)$, the multiple coherence between *h*, *v*, and *W*. Frequency (*f*) is in cycles per hour (cph).

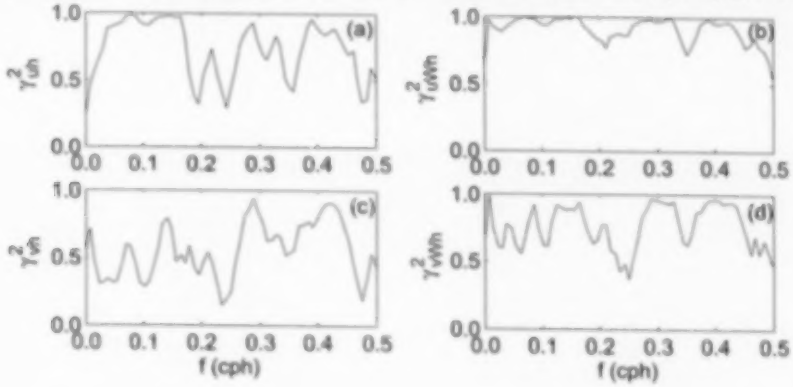

herence values did not vary significantly with depth when the coherence analysis was applied to the time series data for deployments I and III at 2.2 m and 7.2 m. The overall average percentage (i.e., averaged over deployments I and III and depths 2.2. m and 7.2 m) of the total variance of *u* and *v* that was linearly related to *h* fluctuations alone was 63% and 44% for *u* and *v*, respectively. These values increased to 84% and 72%, respectively, when fluctuations in *W* were included (i.e., the multiple coherence was computed). In other words, on average, the addition of *W* as an input explained an additional 21% and 28% of the variance of *u* and *v*, respectively.

Discussion

Vertical mixing

When a water column is stably stratified, vertical mixing will be diminished and there will be a reduction in the magnitude of the vertical turbulent diffusivity, K_z. An estimate of the effect of stratification on the rate of vertical mixing can be obtained from

$$(3) \qquad K_z = K_z(1 + 3.33\mathrm{Ri})^{-3/2} = K_0\beta$$

where K_0 is the value of K_z for neutral stability (i.e., unstratified water column), β is a measure of the strength of stratification, and Ri is the gradient Richardson number (Munk and Anderson 1948; Simpson et al. 2005) given by

$$(4) \qquad \mathrm{Ri} = \frac{-g\dfrac{\partial \rho}{\partial z}}{\rho_0\left(\dfrac{\partial u}{\partial z}\right)^2}$$

where ρ is the density of water, *z* is the vertical coordinate, and *u* is the magnitude of the horizontal velocity (Kundu and Cohen 2001). When Ri equals zero (i.e., ρ is constant), the water column is unstratified and β equals one (i.e., $K_z = K_0$). If the water column is stably stratified, $\partial\rho/\partial z$ will be negative, β will be less than one, and $K_z < K_0$ (i.e., the rate of vertical mixing will be reduced). Experiments have shown that when Ri is greater than ~0.25, buoyancy forces damp the turbulence at a rate greater than the rate at which it is produced by shear production (Kundu and Cohen 2001; Wetzel 2001). For example, if Ri = 1.0, eq. 3 predicts β = 0.11, indicating that in this case vertical turbulent mixing would be severely inhibited. It should be noted that attempts to parameterize vertical mixing in terms of Ri have met with limited success. For example, Simpson et al. (2005) compared measured values of K_z and Ri to an equation proposed by Munk and Anderson (1948) that is similar to eq. 3. They found that although the Munk–Anderson equation followed the general trend of the measurements, there was a considerable amount of unexplained variance in the data. Shih et al. (2005) used direct numerical simulations to show that there is a non-unique mapping between Ri and K_z, and for a given value of Ri, K_z could vary by as much as a factor of four. However, their results clearly showed that on average as Ri decreases, K_z increases (see figure 14*a* in Shih et al. 2005). Therefore, despite its shortcomings, we propose that β could be used as a measure of the strength of vertical mixing in this study (see below).

The current and water temperature at depths of 2.2 and 3.6 m were used to compute Ri and β using eqs. 3 and 4 in order to examine the effect of the stratification on the rate of vertical mixing. These calculations show that K_z was reduced on average by 60% during both deployments at these depths (i.e., β = 0.4). Contours of β are plotted as a function of *W* and ΔT_{ea} using the hourly data from deployments I and III (Fig. 11). In this plot, β = 1 in the upper left corner when *W* was lower and when ΔT_{ea} was positive and large (i.e., low winds and warmer air). The value of $\beta \to 1$ in the lower right corner when *W* was high and ΔT_{ea} was negative and large (i.e., high winds and cold air). This trend in the data is expected because low *W* and air that is warmer than the water provides ideal conditions for water column stratification. Conversely, when *W* is large and the air is colder than the water, vertical mixing will be enhanced by a variety of mechanisms. It should be noted that a similar pattern was observed for the contours of Ri plotted as a function of *W* and ΔT_{ea} (not shown).

Higher *W* leads to more mechanical energy being transferred from the atmosphere to the water column, which produces an increase in the rate of vertical mixing via a number

© 2007 NRC Canada

Fig. 11. Contour plot of β, a measure of the strength of stratification, as a function of the air–water temperature difference (ΔT_{aw}, °C) and wind speed (W, m·s^{-1}).

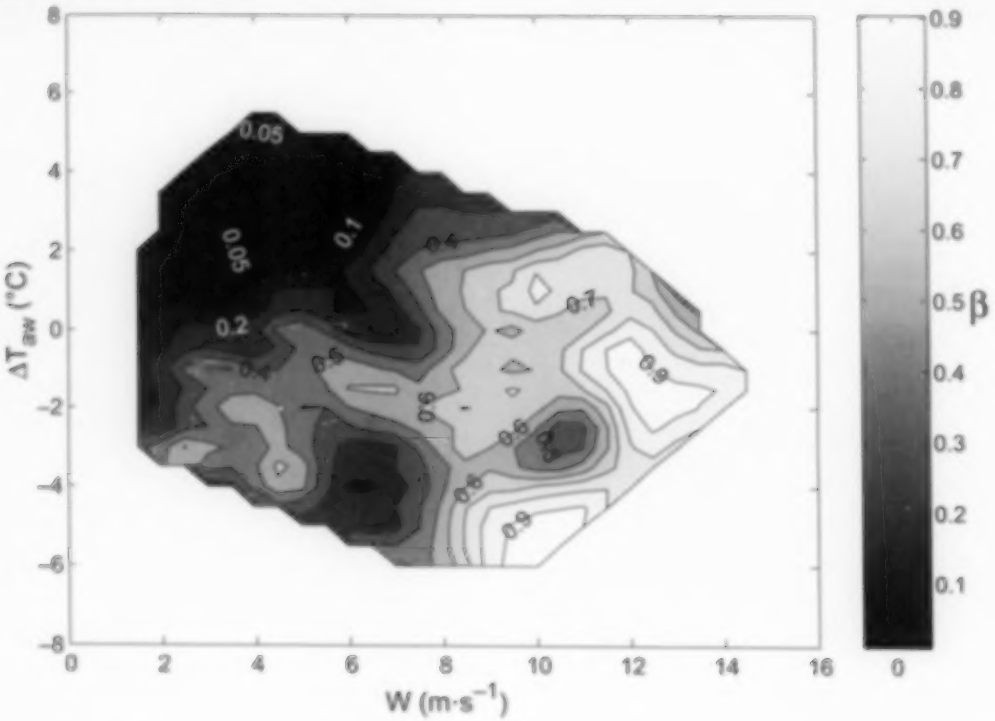

of mechanisms. One mechanism is the production of turbulent kinetic energy by the interaction of the Reynolds stress with the mean shear (i.e., shear production; Kundu and Cohen 2001). Shear production will tend be greatest where the mean velocity gradients are largest in magnitude. In the western basin, shear production will occur in the benthic boundary layer where the currents produced by surface gravitational seiches and the wind-driven circulation generate large velocity gradients and near the water surface where large velocity gradients occur in the wind drift layer. Other mechanisms include the breaking of surface waves and Langmuir circulations (Langmuir 1938; Melville 1996).

Laboratory and field measurements have shown that deep-water wave breaking generates near-surface turbulence and significantly enhances vertical mixing (Melville 1996). At $W = 7$ m·s^{-1} over Lake Erie, deep-water breaking waves (i.e., whitecaps) would be present and their influence on near-surface turbulence would increase at greater wind speeds. For example, empirical equations for whitecap coverage (the fraction of the water surface covered by whitecaps) predict that the whitecap coverage would increase from 0.7% to 4.4% over a range of W from 7 to 12 m·s^{-1} (Monahan 1971). Agrawal et al. (1992) made measurements of near-surface turbulence in Lake Ontario at $W > 8$ m·s^{-1} at a location where the fetch was 1.1 km and the water depth 12 m. They found that rates of dissipation of turbulent kinetic energy were greatly enhanced close to the water surface and attributed these increased levels of dissipation to deep-water wave breaking. Their measurements indicate that in this setting (i.e., water depth ~10 m in a large lake), the vertical mixing is dominated by near-surface processes such as wave breaking rather than processes in the benthic boundary layer. Given that the fetch varied from 15 to 30 km depending on the wind direction and the water depth was ~8 m at our site, we would expect surface wave breaking to have a comparable or greater effect on near-surface turbulence and hence vertical mixing.

When the overlying air is colder than the water, convective instabilities will occur and vertical mixing will be enhanced via buoyant production of turbulence, which is why the values of β tend to be larger in the lower portions of Fig. 11. It is difficult to assess directly the importance of convective mixing relative to the other mechanisms such as wave breaking. However, there is evidence to suggest that convective mixing events initiated by nighttime cooling played some role in mixing the water column. The time series of $\Delta\rho$ between depths of 2.2 and 7.2 m were examined to determine if there were time periods when the water column was well mixed in the absence of high winds. To carry out this analysis, we define a well-mixed water column (as opposed to a completely mixed one, i.e., $\Delta\rho = 0$) to occur when $\Delta\rho < 0.0031$ kg·m^{-3}, which equates to $\Delta T_w \sim 0.02$ °C (e.g., MacIntyre et al. 2002). This very small limit was chosen because it corresponds approximately to the criteria that $F_{rd} > 5$. There were 14 time periods during deployments I and III when the water column was well mixed. These events all occurred between 2330 h and 0830 h (local time, which is GMT – 4 h) when $\Delta T_{aw} \sim -1.6$ °C and $W \sim 7.6$ m·s^{-1}.

© 2007 NRC Canada

which suggests that convective mixing caused by nighttime cooling was at least partially responsible. For six of these events, the average $W < 7$ m·s^{-1}, and for three of these six, $W < 5$ m·s^{-1}, indicating that the water column had become well mixed in the absence of strong winds. Convective mixing would tend to be more important relative to the other mechanisms when W was small, and in fact, it most likely was the dominant mixing mechanism at $W < 5$ m·s^{-1}. Evidence of convective mixing can be found on almost every day of both deployments in that $\Delta\rho$ increased during the day, as heat was transferred from the air to the water, and then decreased during the night when the direction of the heat flux reversed. The magnitude of these oscillations in $\Delta\rho$ varied greatly but the pattern was consistent: convective mixing occurred daily typically during the early morning hours from midnight to 0800. Based on the preceding analysis, we concluded that convective mixing occurred daily (nighttime cooling) and could be an important mixing mechanism at lower wind speeds. At higher wind speeds (i.e., $W >$ 7 m·s^{-1}), the contribution of other mixing mechanisms, particularly wave breaking, becomes more important.

Environmental implications

The distribution and abundance of large-bodied burrowing mayflies of the genus *Hexagenia* have been shown to be sensitive to changes in the water quality of Lake Erie (Krieger et al. 1996; Schloesser et al. 2000; Bridgeman et al. 2006). This is a consequence of their sensitivity to environmental perturbations, especially hypoxia, and as such, they serve as an indicator species for water quality in Lake Erie, as do related genera in Europe (bij de Vaate et al. 1992). *Hexagenia* nymphs are acutely sensitive to hypoxia in that exposure to $[O_2] < \sim 1.0$ mg·L^{-1} for more than 24 h is generally fatal (Winter et al. 1996). In addition, it has been shown that persistent sublethal oxygen stress ($[O_2] < 7$ mg·L^{-1}) and reduced temperature (<20 °C) influence both the size and survival of *Hexagenia* nymphs (Winter et al. 1996). An abrupt reduction in abundance of burrowing mayflies was observed by Britt (1955*a*) following a 2-week period (20 August to 3 September 1953) of warm, calm, and clear weather during which $W < 1.9$ m·s^{-1} ($W_{max} = 5.8$ m·s^{-1}) and the average near-bottom $[O_2] = 2.3$ mg·L^{-1} ($[O_2]_{min} = 0.70$ mg·L^{-1}). The mayfly population recovered quickly from this catastrophic event (Britt 1955*b*), but populations subsequently declined from approximately 1960 until the early 1990s when they began to recolonize the western basin.

Schloesser et al. (2000) have documented the recolonization and recovery of mayflies throughout the nearshore and much of the offshore environments of the western basin of Lake Erie except for two regions: (*i*) a small zone immediately downstream of the Detroit River, and (*ii*) a larger region that extends in a northeasterly direction from West Sister Island to Point Pelee (this region includes the site examined here). They suggest that the absence or low abundance of mayflies in these two regions was caused by high SOD of settled plankton and (or) residual organic carbon in sediments as a result of anthropogenic inputs into these regions before 1980. This explanation is more plausible for the smaller region described above, but in the case of the larger region, we hypothesize that the periodic intrusion of cold low-oxygen water, possibly from the hypolimnion of the central basin, may also be a contributing factor limiting the mayfly populations in this region. More information on this phenomenon is needed to determine its frequency and potential importance.

Conditions that produce more strongly stratified water columns will naturally lead to more severe local hypoxia. The ideal environmental conditions for severe local hypoxia are calm, warm weather and clear skies. During periods of calm weather (i.e., low W), very little kinetic energy is transferred from the atmosphere to the water column and thus the rate of vertical mixing is relatively small. Warmer weather and clear skies will produce warmer surface waters because of increased radiative and conductive heat transfer. Thus, extended periods with low wind speeds, clear skies, and high air temperatures will produce conditions that are most conducive for hypoxia.

Meteorological data sampled at an NOAA buoy (station 45005, 41.68°N, 82.40°W; National Buoy Data Center 2005) were used to investigate the frequency of occurrence of periods of calm, clear weather similar to that described by Britt (1955*a*). This buoy is located 28 km south of Point Pelee at the eastern edge of the western basin in a water depth of 12.6 m, which is the closest buoy to our site (~40 km SE). Data were available for the years 1980 to 2004, typically for the months of April through November. A computer program was written to search this data set for continuous time periods when $W < 7$ m·s^{-1} and $\Delta T_{as} > 0$. The average duration of the longest time period in each year for which these conditions were met was 4.5 days ± 1.9 ($n = 25$). The average W during these periods of calm, warm weather was 3 m·s^{-1}, and the average ΔT_{as} was 2 °C, which corresponds to $\beta \approx 1$ (see Fig. 11). To determine if these time periods could cause severe hypoxia, their durations were compared with the time that it takes for $[O_2]$ to be reduced to zero (i.e., anoxia) by SOD. This would, therefore, be a conservative estimate of the time scale for hypoxia to occur.

An estimate of this time can be obtained using the diffusion equation:

$$(5) \qquad \frac{\partial C}{\partial t} = K_z \frac{\partial^2 C}{\partial z^2}$$

where C is $[O_2]$ (kg·m^{-3}), t is time, and the turbulent diffusivity, K_z, is assumed to be constant. Equation 5 only models concentration variations in the vertical direction, i.e., horizontal variations are ignored. Therefore, one concern when applying eq. 5 to western Lake Erie is that concentration variations caused by advection are not considered. The field data from deployment I indicated that cold water could be advected along the bottom at this site, suggesting that $[O_2]$ could vary in a similar manner to the observed temperature fluctuations. However, these types of signals only appeared on 2 of the 23 days of measurements (i.e., less than 10% of the time), and Bartish (1987) states that these types of intrusions only occur once or twice a year. Therefore, the assumption that advection can be neglected is reasonable. Edwards et al. (2005) compared predictions of zebra mussel algal consumption in western Lake Erie using constant and parabolic turbulent diffusivity and found significant differences between the two models. Nevertheless, because we are

© 2007 NRC Canada

only using eq. 5 to estimate an approximate time scale for hypoxia, the use of a constant value for K_z is reasonable.

We assume that there are no sources of oxygen in the water column and no flux of oxygen from the air to the water. This assumption is reasonable because during calm, warm weather, the rate at which oxygen is transferred across the air–water interface will be small given that the air–water flux of oxygen depends on the magnitude of the wind speed and the concentration difference. During the calm, warm periods, the average wind speed was small (i.e., 3 m·s^{-1}) and our oxygen measurements indicate that the surface waters were typically at or near saturation (e.g., Patterson et al. 1985). The combined effect of these two factors would result in low air–water oxygen fluxes, which supports our assumption. At the same time, the formation of a distinct thermocline will prevent oxygenated surface waters from mixing to any significant depth. It was also assumed that the only sink for oxygen was SOD. The boundary conditions for this problem are zero flux at the water surface and a flux at the bed, q_0, set equal to SOD (g·m^{-2}·s^{-1}). Note that SOD is modelled as a flux across the sediment–water interface when, in fact, the oxygen is being consumed by bacteria, algae, and micro- and macro-fauna located in and on the sediments (Wetzel 2001).

The exact solution to this problem is an infinite series that can be found in Carslaw and Jaeger (1959, see p. 112). The two relevant time scales lead to a simple approximate solution. The first is the diffusive time scale given by

$$\tau_{diff} = h^2/K_z \quad (6)$$

where τ_{diff} is the approximate time that it would take for turbulence to mix a water column of depth h (Koseff et al. 1993). The second relevant time scale is the time scale of SOD defined as

$$\tau_{SOD} = C_0 h/q_0 \quad (7)$$

where τ_{SOD} is the approximate time that it would take for SOD, q_0, to reduce $[O_2]$ from an initial value of C_0 to zero in a well-mixed water column of depth h. Note that τ_{SOD} is analogous to τ_{graze}, the time scale of benthic grazing (Koseff et al. 1993). The ratio of these two time scales can be expressed as

$$\frac{\tau_{sod}}{\tau_{dif}} = \frac{C_0 K_z}{h q_0} \quad (8)$$

or as the ratio of two fluxes,

$$\frac{q_L}{q_0} = \frac{C_0 K_z}{h q_0} \quad (9)$$

where $q_L = C_0 K_z/h$ is a first-order estimate of the vertical turbulent flux. Hypoxia will tend to occur when the time scale of SOD is significantly less that the time scale for diffusion (i.e., $\tau_{SOD} < \tau_{dif}$). At these times, the flux of oxygen into the sediments is significantly greater than the vertical turbulent flux, i.e., $q_0 > q_L$. The simple physical explanation for why hypoxia occurs is that $[O_2]$ in the water adjacent to the lake bed is depleted at a faster rate than the vertical turbulent transport can replenish it from above.

If $\tau_{SOD} < \tau_{dif}$, the time scale for hypoxia to occur is independent of the depth of the water column, h. This occurs when $q_0 > q_L$ because the oxygen near the bed is depleted rapidly and the oxygen concentrations in the upper portion of the water column remain unchanged because the turbulent flux is small. As a result, the water column can be assumed to be infinitely deep, and under these conditions, the time scale for hypoxia, τ_h, is given by

$$\tau_h = \frac{\pi}{4}\left(\frac{C_0^2 K_z}{q_0^2}\right) \quad (10)$$

(c.f., Carslaw and Jaeger 1959, p. 75). τ_h is the approximate time that it would take for $[O_2]$ at the bed to be reduced from C_0 to zero when $q_0 > q_L$. Note that eq. 10 is not valid if $q_0 < q_L$, which is irrelevant because under these circumstances the risk of hypoxia is very low.

In order to use eq. 10, estimates of C_0, K_z, and q_0 are required. C_0 is taken as 8 g·m^{-3} as measured $[O_2]$ at the experimental site typically varied from 7 to 9 g·m^{-3}. Measurements of SOD in Lake Erie range from 0.1 to 1.0 g·m^{-2}·day^{-1} (Boegman et al., Queen's University, Department of Civil Engineering, Kingston, ON K7L 3N6, unpublished data). Estimates of K_z, the depth-averaged turbulent diffusivity for neutral conditions (i.e., unstratified), can be obtained from the following equation:

$$K_z = 0.067 h u^* \quad (11)$$

where u^* is the friction velocity (Fischer et al. 1979), assuming that the mixing of mass and momentum are equivalent (i.e., Reynolds analogy), the turbulent diffusivity varies parabolically, and mixing is caused by bed shear. Ackerman et al. (2001) reported average u^* of 0.4 cm·s^{-1} and 0.65 cm·s^{-1} for deployments I and III, respectively, which are consistent with Edwards et al. (2005) daily averaged values of u^* (0.13 to 1.66 cm·s^{-1}), and u^* between 0.25 and 2.1 cm·s^{-1} reported by Bedford and Abdelrhman (1987) for western Lake Erie. Given these u^* values, eq. 11 predicts $K_z \sim 10^{-3}$–10^{-2} m^2·s^{-1}, which leads to estimates of the turbulent flux, q_L, of 86.4–864 g·m^{-2}·day^{-1} (i.e., » q_0 of 0.1–1.0 g·m^{-2}·day^{-1}). Therefore, when the water column is unstratified (i.e., $K_z = K_0$), $q_L » q_0$, the risk of hypoxia is very small.

During periods of calm, warm weather, however, stratification will reduce the rate of vertical mixing dramatically (see Fig. 11) and increase the risk of severe hypoxia. In other words, the risk of hypoxia will be high when the following two conditions are satisfied: (*i*) τ_{SOD} must be less than τ_{diff}, and (*ii*) the duration of calm, warm weather must approach τ_h (i.e., eq. 10). Given that the longest calm, warm period in each year in western Lake Erie is ~4.5 days (i.e., τ_h = 4.5 days) and that C_0 = 8 g·m^{-3} and q_0 = 0.1–1.0 g·m^{-2}·day^{-1}, eq. 10 indicates that $K_z = 10^{-8}$–10^{-6} m^2·s^{-1}, which corresponds to $\beta < 0.001$ (note that $K_0 = 10^{-3}$–10^{-2} m^2·s^{-1} in an unstratified water column). β was found to be less than 0.001 approximately 5% of the time during deployments I and III, but for never more than a few hours at a time. However, it is logical to assume that during periods of calm, warm weather that extend over more than a few days $\beta < 0.001$ and $K_z < 10^{-6}$ m^2·s^{-1}, which leads to near-bottom hypoxia. It is also evident from eq. 10 that τ_h is sensitive to variations in SOD and C_0 and less sensitive to changes in K_z. It is likely that C_0 will not vary by more than ±50%, and therefore we can assume that it is approximately constant and equal to 8 g·m^{-3}

© 2007 NRC Canada

Fig. 12. Contours of the time scale for hypoxia for $C_0 = 8$ g·m^{-3} (τ_0, days) plotted as a function of the sediment oxygen demand (q_0 (g·m^{-2}·day^{-1}) and the turbulent diffusivity (K_z, m^2·s^{-1}).

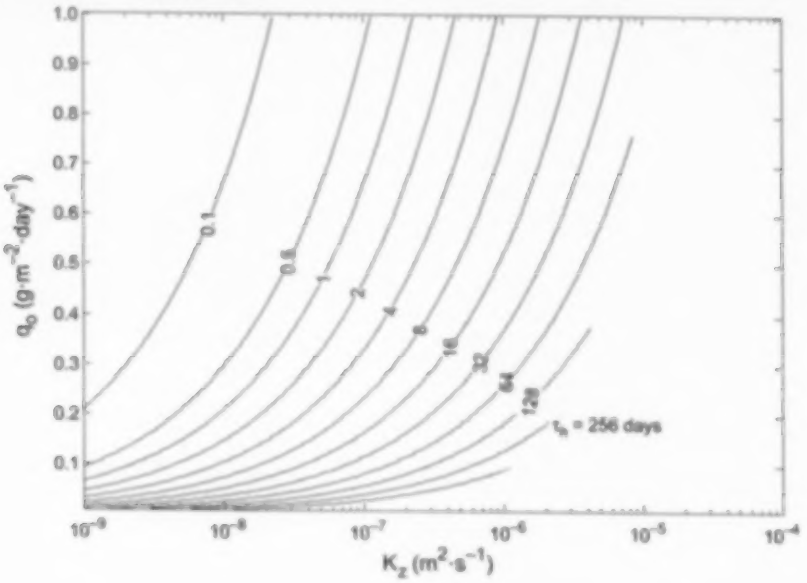

when computing values of τ_0. If $K_z = 10^{-6}$ m^2·s^{-1} and $C_0 = 8$ g·m^{-3}, eq. 10 predicts τ_0 values of 4.3 and 430 days for SOD of 1.0 and 0.1 g·m^{-2}·day^{-1}, respectively. For SOD of 1.0 g·m^{-2}·day^{-1} and $C_0 = 8$ g·m^{-3}, an increase in K_z from 10^{-6} to 10^{-5} m^2·s^{-1} leads to an increase in τ_0 from 4.3 to 43 days. A contour plot of τ_0 predicted using eq. 10 is presented in Fig. 12. Note that the contours end at the point at which $q_t > q_0$. As expected, moving up or to the left in the figure, i.e., increasing q_0 or decreasing K_z, increases the risk of hypoxia. This figure can be used directly to assess the conditions that pose a high risk for hypoxia. For the typical periods of calm, warm weather that are observed yearly in the western basin of Lake Erie, the risk of hypoxia will be very high when conditions along the 4-day contour in Fig. 12 are satisfied. This corresponds to the following combinations of q_0 and K_z: 1.0 g·m^{-2}·day^{-1} and 10^{-6} m^2·s^{-1}; 0.3 g·m^{-2}·day^{-1} and 10^{-7} m^2·s^{-1}; or 0.1 g·m^{-2}·day^{-1} and 10^{-8} m^2·s^{-1}.

The functional form of eq. 10 also provides insight into the spatial scales associated with the risk of hypoxia. Variations in K_z are primarily a function of meteorological conditions, that is, the wind speed and the air–water temperature difference. Conversely, variations in SOD are a function of sediment type and other factors such as infaunal organisms, nutrient levels, and microbial populations. In the offshore regions of the western basin, the depth-averaged values of K_z will not be influenced greatly by changes in topography, and as a result, the spatial variations in K_z will be governed by the scale of the local weather patterns, which are typically greater than 10 km. Conversely, SOD can vary over much smaller spatial scales because the parameters controlling it can vary rapidly over distances as small as ~1 m.

It is also relevant to note that stratification is of importance in linking benthic and pelagic ecosystems, as in the case of the introduced zebra mussel. Specifically, a significant algal concentration boundary layer over the zebra mussel dominated reef (i.e., a reduction in algal concentrations near the bed) described here was observed in the summer of 1994 (Ackerman et al. 2001). This concentration boundary layer was determined to be a consequence of the reduced vertical mixing caused by the diurnal stratification of the water column (Ackerman et al. 2001). The approximate time that it would take a population of zebra mussels to deplete a water column of depth h of phytoplankton is given by $\tau_{graze} = h/\alpha$, where τ_{graze} is the time scale for benthic grazing and α is the areal clearance rate (Koseff et al. 1993). For this reef, τ_{graze} was estimated to be approximately 12 h (Ackerman et al. 2001). During time periods when the risk of hypoxia is high, the diffusive time scale becomes very large, for example, when $K_z = 10^{-6}$ m^2·s^{-1}, $\tau_{diff} = 740$ days. At these times $\tau_{graze} \ll \tau_{diff}$ and a significant algal concentration boundary layer would form, neglecting algal sinking (Edwards et al. 2005). At the experimental site, the algal concentration boundary layer would form ~10 times faster than the oxygen concentration boundary layer because the time scale for benthic grazing is estimated to be ~10 times smaller than the time scale for hypoxia.

In conclusion, we have reported the results from a field experiment conducted in the western basin of Lake Erie to investigate the influence stratification and vertical mixing. The results and conclusions from this study should, for the most part, be applicable to large temperate lakes sufficiently shallow that there is no permanent seasonal stratification. The western basin was found to be well mixed when the wind speed was greater than 7 m·s^{-1}, which occurred approximately one-third of the time in summer, and in the remaining two-thirds of the time, the water column was stratified to varying degrees. Surface wave breaking that occurs when the wind speed exceeds 7 m·s^{-1} is the dominant physical mechanism that leads to increased vertical mixing and the resulting breakdown of stratification. Convective

© 2007 NRC Canada

mixing caused by the nighttime cooling of surface waters was observed daily and also played a role in mixing the water column, particularly at lower wind speeds.

The risk of hypoxia in the western basin was shown to be greatest when the time scale of SOD was significantly less than the time scale for turbulent diffusion (i.e., $\tau_{SOD} < \tau_{diff}$). At these times, the flux of oxygen into the sediments is greater than the vertical turbulent flux. This occurs during extended periods of calm, warm weather, i.e., when the wind speed is less than 7 $m \cdot s^{-1}$ and the atmosphere is warmer than the water. The risk of hypoxia was found to be very sensitive to the magnitude of the SOD as a twofold increase in SOD will effectively quadruple the risk. Meteorological records show that periods of calm, warm weather lasting ~4.5 days typically occur yearly in the western basin. Periods of calm, warm weather of this duration are sufficient to reduce the rate of vertical mixing by as much as three orders of magnitude, creating ideal conditions for hypoxia. Burrowing mayfly (*Hexagenia*) nymphs are particularly sensitive to these episodes of hypoxia. Therefore, it is important that stratification and its effects on benthic organisms be considered in assessments of the environmental conditions in shallow lake basins like the western basin of Lake Erie.

Acknowledgements

The authors thank Chris Rehmann for his helpful comments on the manuscript and acknowledge the Great Lakes University Research Fund (Environment Canada and Natural Sciences and Engineering Research Council of Canada (NSERC)), the University of Toronto, and NSERC for providing funds to undertake this study.

References

Ackerman, J.D., Loewen, M.R., and Hamblin, P.F. 2001. Benthic–pelagic coupling over a zebra mussel reef in western Lake Erie. Limnol. Oceanogr. **46**: 892–904.

Agrawal, Y.C., Terray, E.A., Donelan, M.A., Hwang, P.A., Williams A.J., III, Drennan, W.M., Kahma, K.K., and Kitaigorodskii, S.A. 1992. Enhanced dissipation of kinetic energy beneath surface waves. Nature (London), **359**: 219–220.

Bartish, T. 1987. Review of the exchange processes in Lake Erie. J. Gt. Lakes Res. **13**: 436–453.

Bedford, K.W., and Abdelrhman, M. 1987. Analytical and experimental studies of the benthic boundary layer and their applicability to near-bottom transport in Lake Erie. J. Gt. Lakes Res. **13**: 628–648.

Bendat, J.S., and Piersol, A.G. 1986. Random data. 2nd ed. Wiley Interscience, New York.

bij de Vaate, A., Klink, A., and Oosterbroek, F. 1992. The mayfly, *Ephoron vigio* (Oliver), back in the Dutch parts of the Rivers Rhine and Meuse. Hydrobiol. Bull. **25**: 237–240.

Bridgeman, T.L., Schloesser, D.W., and Krause, A.E. 2006. Recruitment of *Hexagenia* mayfly nymphs in western Lake Erie linked to environmental variability. Ecol. Appl. **16**: 601–611.

Britt, N.W. 1955*a*. Stratification in western Lake Erie in summer of 1953: effects on the *Hexagenia* (Ephemeroptera) population. Ecology, **36**: 239–244.

Britt, N.W. 1955*b*. *Hexagenia* (Ephemeroptera) population recovery in western Lake Erie following the 1953 catastrophe. Ecology, **36**: 520–522.

Caraco, N.F., Coles, J.J., and Likens, G.E. 1993. Sulfate control of phosphorus availability in lakes: a test and re-evaluation of Hasler and Einsele's model. Hydrobiologia, **253**: 275–280.

Carslaw, H.S., and Jaeger, J.C. 1959. Conduction of heat in solids. Oxford University Press, Oxford, UK.

Charlton, M.N. 1987. Lake Erie oxygen revisited. J. Gt. Lakes Res. **13**: 697–708.

Charlton, M.N., Le Sage, R., and Milne, J.E. 1999. Lake Erie in transition: the 1990's. *In* State of Lake Erie (SOLE) — past, present and future. *Edited by* M. Munawar, T. Edsall, and I.F. Munawar. Backhuys Publishers, Leiden. pp. 97–123.

Dean, R.G., and Dalrymple, R.A. 1991. Water wave mechanics for engineers and scientists. World Scientific, River Edge, N.J.

Edwards, W.J., Rehmann, C.R., McDonald, E., and Culver, D.A. 2005. The impact of a benthic filter feeder: limitations imposed by physical transport of algae to the benthos. Can. J. Fish. Aquat. Sci. **62**: 205–214.

Fischer, H.B., List, E.J., Koh, R.C.Y., Imberger, J., and Brooks, N.H. 1979. Mixing in inland and coastal waters. Academic Press, San Diego, California.

Fraser, A.S. 1987. Tributary and point source total phosphorus loading to Lake Erie. J. Gt. Lakes Res. **13**: 659–666.

Hamblin, P.F. 1987. Meteorological forcing and water level fluctuations on Lake Erie. J. Gt. Lakes Res. **13**: 436–453.

Knapton, R.W., and Petrie, S.A. 1999. Changes in distribution and abundance of submerged macrophytes in the inner bay at Long Point, Lake Erie: implications for foraging waterfowl. J. Gt. Lakes Res. **25**: 783–798.

Koonce, J.F., Busch, W.D.N., and Czapla, T. 1996. Restoration of Lake Erie: contribution of water quality and natural resource management. Can. J. Fish. Aquat. Sci. **53**(Suppl. 1): 105–112.

Koseff, J.R., Holen, J.K., Monismith, S.G., and Cloern, J.E. 1993. Coupled effects of vertical mixing and benthic grazing on phytoplankton populations in shallow estuaries. J. Mar. Res. **51**: 843–868.

Krieger, K.A., Schloesser, D.W., Manny, B.A., Trisler, C.E., Heady, S.E., Cibrowski, J.J.H., and Muth, K.M. 1996. Recovery of burrowing mayflies (Ephemeroptera: Ephemeridae; *Hexagenia*) in western Lake Erie. J. Gt. Lakes Res. **22**: 254–263.

Kundu, P.K., and Cohen, I.M. 2001. Fluid mechanics. 2nd ed. Academic Press, San Diego, California.

Langmuir, I. 1938. Surface motion of water induced by wind. Science (Washington, D.C.), **87**(2250): 119–123.

MacIntyre, S., Romero, J.R., and Kling, G.W. 2002. Spatial-temporal variability in surface layer deepening and lateral advection in an embayment of Lake Victoria, East Africa. Limnol. Oceanogr. **47**: 656–671.

Makarewicz, J.C. 1993. Phytoplankton biomass and species composition in Lake Erie, 1970 to 1987. J. Gt. Lakes Res. **19**: 258–274.

Makarewicz, J.C., and Bertram, P. 1991. Evidence for the restoration of the Lake Erie ecosystem. Bioscience, **41**: 216–223.

Makarewicz, J.C., Bertram, P., and Lewis, T.W. 2000. Chemistry of the offshore waters of Lake Erie: pre- and post-*Dreissena* introduction (1983–1993). J. Gt. Lakes Res. **26**: 82–93.

Melville, W.K. 1996. The role of surface-wave breaking in air–sea interaction. Annu. Rev. Fluid Mech. **28**: 279–321.

Monahan, E.C. 1971. Oceanic whitecaps. J. Phys. Oceanogr. **1**: 139–144.

Munawar, M., Edsall, T., and Munawar, I.F. (*Editors*). 1999. State of Lake Erie (SOLE) — past, present and future. Backhuys Publishers, Leiden.

Munawar, M., Munawar, I.F., Dermott, R., Niblock, H., and Carou, S. 2002. Is Lake Erie a resilient ecosystem? Aquat. Ecosyst. Health Manag. **5**: 79–93.

© 2007 NRC Canada

Munk, W., and Anderson, E.R. 1948. Notes on a theory of the thermocline. J. Mar. Res. **7**: 276–295.

National Buoy Data Center. 2005. http://www.ndbc.noaa.gov/, accessed Nov. 2005.

Patterson, J.C., Allason, B.R., and Ivey, G.N. 1985. A dissolved oxygen budget model for Lake Erie in summer. Freshw. Biol. **15**: 683–694.

Rysgaard, S., Risgaard-Petersen, N., Sloth, N.P., Jensen, K., and Nielsen, L.P. 1994. Oxygen regulation of nitrification and denitrification in sediments. Limnol. Oceanogr. **39**: 1643–1652.

Schelske, C.L., and Hodell, D.A. 1995. Using carbon isotopes of bulk sedimentary organic matter to reconstruct the history of nutrient loading and eutrophication in Lake Erie. Limnol. Oceanogr. **40**: 918–929.

Schertzer, W.M., Saylor, J.H., Boyce, F.M., Robertson, D.G., and Rosa, F. 1987. Seasonal thermal cycle of Lake Erie. J. Gt. Lakes Res. **13**: 468–486.

Schloesser, D.W., Krieger, K.A., Cibrowski, J.J.H., and Corkum, L.D. 2000. Recolonization and possible recovery of burrowing mayflies (Ephemeroptera: Ephemeridae; *Hexagenia* spp.) in Lake Erie of the Laurentian Great Lakes. J. Aquat. Ecosyst. Stress Recovery, **8**: 125–141.

Shih, L.H., Koseff, J.R., Ivey, G.N., and Ferziger, J.H. 2005. Parameterization of turbulent fluxes and scales using homogeneous sheared stably stratified turbulence simulations. J. Fluid Mech. **52**: 193–214.

Simpson, J.H., Williams, E., Brasseur, L.H., and Brubaker, J.M. 2005. The impact of tidal straining on the cycle of turbulence in a partially stratified estuary. J. Continental Shelf Res. **25**: 51–64.

Sweeney, R.A. 1993. "Dead" Sea of North America — Lake Erie in the 1960s and '70s. J. Gt. Lakes Res. **19**: 198–199.

Wetzel, R.G. 2001. Limnology. 3rd ed. Academic Press, San Diego, California.

Winter, A., Cibrowski, J.J.H., and Reynoldson, T.B. 1996. Effects of chronic hypoxia and reduced temperature on survival and growth of burrowing mayflies, *Hexagenia limbata* (Ephemeroptera: Emphemeridae). Can. J. Fish. Aquat. Sci. **53**: 1565–1571.

© 2007 NRC Canada

Controls on phytoplankton physiology in Lake Ontario during the late summer: evidence from new fluorescence methods

Katharine L. Pemberton, Ralph E.H. Smith, Greg M. Silsbe, Todd Howell, and Susan B. Watson

Abstract: Fast repetition rate fluorescence (FRRF) and spectral fluorescence, together with measures of nutrients and pigments, were used to characterize the composition and photosynthetic physiology of Lake Ontario phytoplankton in late summer and relate them to environmental conditions. Two stations demonstrated effects from relatively heavy anthropogenic disturbance and showed that the response of phytoplankton physiology to different impacts is highly variable. Other stations were more similar in phytoplankton composition, and in situ fluorescence yields (F_q'/F_m') in the lower surface mixed layer suggested good physiological condition (0.45–0.50). Nutrient ratios and mean irradiance indicated a general state of light saturation and slight phosphorus (P) deficiency, but physiological variations among stations were unrelated to measures of P deficiency. Fluorescence yields often decreased when surface layer samples were held in the dark, consistent with an induction of chlororespiration and prior exposure to supersaturating levels of irradiance. Comparative estimates of photosynthesis by FRRF and ^{14}C revealed disparities suggestive of substantial differences between in situ and incubation methods, while spectral fluorescence appeared to underestimate cyanobacterial abundance. FRRF parameters, particularly F_q'/F_m', were effective in identifying higher-impact stations and showed promise as an efficient means of characterizing variations in phytoplankton condition that may underlie phenomena such as taste and odour production.

Résumé : La fluorescence à haute fréquence de répétition (FRRF) et la fluorescence spectrale, combinées à des dosages des nutriments et des pigments, nous ont servi à caractériser la physiologie de la photosynthèse et la composition du phytoplancton du lac Ontario en fin d'été et de les relier aux conditions du milieu. Deux des stations montrent les effets d'une perturbation anthropique relativement forte et indiquent que la réaction de la physiologie du phytoplancton aux divers impacts est très variable. D'autres stations ont des compositions phytoplanctoniques plus semblables et les rendements in situ de la fluorescence (F_q'/F_m') dans la surface inférieure de la couche de mélange indiquent que les conditions physiologiques sont bonnes (0,45–0,50). Les rapports de nutriments et l'irradiation moyenne montrent une situation générale de saturation lumineuse et une faible carence de le phosphore (P), mais les variations physiologiques entre les stations ne sont pas reliées aux mesures de carence de P. Les rendements de fluorescence décroissent souvent lorsque les échantillons de la couche superficielle sont gardés à l'obscurité, ce qui est compatible avec une induction de la chlororespiration et une exposition préalable à des niveaux de sursaturation d'irradiation. Une comparaison des estimations de la photosynthèse par les méthodes FRRF et ^{14}C montre des disparités qui indiquent des différences importants entre la méthode in situ et l'incubation, alors que la fluorescence spectrale semble sous-estimer l'abondance des cyanobactéries. Les paramètres FRRF, particulièrement F_q'/F_m', servent à identifier de manière efficace les stations à plus fort impact et montrent un potentiel comme moyens valables de caractériser les variations de la condition du phytoplancton qui peuvent sous-tendre des phénomènes tels que la production de goûts et d'odeurs.

[Traduit par la Rédaction]

Introduction

Many parts of the Laurentian Great Lakes, including Lake Ontario, experienced pronounced cultural eutrophication in the mid-20th century, followed by a return to lower nutrient conditions as controls on phosphorus (P) loading became effective in the 1970s and 1980s (Schelske 1991). By the late 1980s, open lake primary production in Lake Ontario was

Received 23 January 2006. Accepted 3 September 2006. Published on the NRC Research Press Web site at http://cjfas.nrc.ca on 17 January 2007.
J19126

K.L. Pemberton, R.E.H. Smith,[1] and G.M. Silsbe. Department of Biology, University of Waterloo, Waterloo, ON N2L 3G1, Canada.
T. Howell. Environmental Monitoring and Reporting Branch, Ontario Ministry of the Environment, 125 Resources Road, Toronto, ON M9P 3V6, Canada.
S.B. Watson. National Water Research Institute, 867 Lakeshore Road, Burlington, ON L7R 4A6, Canada.

[1]Corresponding author (e-mail: rsmith@uwaterloo.ca).

 doi:10.1139/F06-166 © 2007 NRC Canada

Fig. 1. Position of stations in Lake Ontario. Inset map shows location within the Great Lakes region.

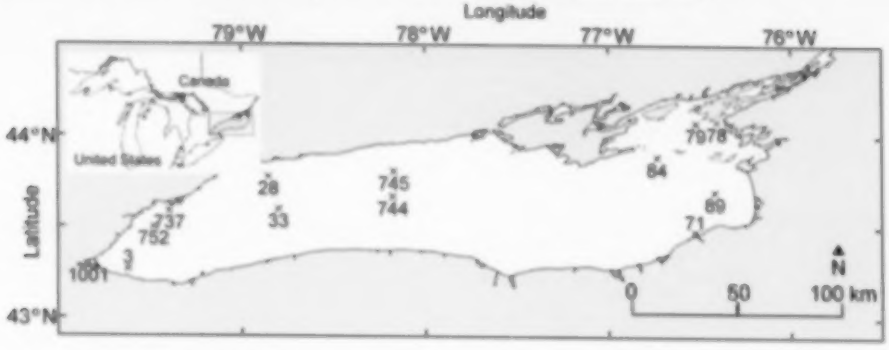

estimated to have decreased by about 30% of the value measured near the peak of eutrophication in 1972 (Millard et al. 1996*a*), and phytoplankton revealed symptoms of P deficiency for much of the summer (Millard et al. 1996*b*). Lake Ontario has also been perturbed by the extensive exotic species invasions and introductions that have affected most of the Great Lakes (Mills et al. 1993). Among these, the dreissenid mussels (*Dreissena polymorpha* and *Dreissena bugensis*) have been associated with particularly notable effects on phytoplankton and P, although the implications for patterns of phytoplankton abundance and primary production on the whole-lake scale are uncertain (Bailey et al. 1999). In recent years, drinking water supplies from Lake Ontario have experienced major taste and odour problems in the late summer (e.g., Watson 2004), and the nuisance alga *Cladophora* sp. has become problematic (T. Howell, unpublished data) even though the major water quality variables are mostly in the desired range established by the Great Lakes Water Quality Agreement.

Continued and even increased observation of phytoplankton composition, condition, and productivity is an important part of understanding the continued changes in the lake and managing their implications for amenity value and ecological integrity. However, such work has traditionally been labour intensive and expensive, particularly in large systems such as Lake Ontario. There has been no published study of primary production in the open lake since the early 1990s (Millard et al. 1996*a*), while surveys of phytoplankton composition are conducted infrequently and with limited spatial resolution (Barbiero and Tuchman 2001*a*). Recently commercialized instruments use fluorescence emission from chlorophyll *a* to enable relatively rapid, in situ estimates of phytoplankton condition, productivity, and composition and may help meet the need for more efficient methods of quantifying primary production processes in large lakes. Fast repetition rate fluorescence (FRRF) measures the fluorescence induction and quenching parameters of chlorophyll *a* in photosystem II (Kolber and Falkowski 1993) and has been used recently to estimate physiological condition and productivity of phytoplankton in the ocean (e.g., Suggett et al. 2001; Moore et al. 2003; Smyth et al. 2004; see Fast repetition rate and spectral fluorescence measurements, Materials and methods). The fluoroprobe derives estimates of the abundance of major phytoplankton pigment groups (chromophytes, cryptophytes, cyanophytes, and chlorophytes) from the excitation spectrum of chlorophyll *a* fluorescence (Beutler et al. 2002) and has been used to track cyanobacterial blooms in lakes (Leboulanger et al. 2002; Ghadouani and Smith 2005). The fluoroprobe was designed specifically for freshwater phytoplankton, but the FRRF has been used almost exclusively in marine systems. Neither instrument has been widely used in lakes as yet, so information on their performance, and comparisons with alternate methods (Kaiblinger et al. 2005), are still limited.

During the late summer and early fall, mixing depths and the balance between light and nutrient limitation undergo major changes in Lake Ontario (Millard et al. 1996*b*). Different regions of the lake undergo these seasonal changes at different rates and times (Millard et al. 1996*a*, 1996*b*). Urban and agricultural development vary widely around the shores of the lake. Discharges from major tributaries and urbanized embayments, in conjunction with prevailing lake circulation patterns and a pervasive population of dreissenid mussels, contribute to the variability in environmental conditions. Phytoplankton abundance, composition, physiological condition, and productivity may therefore vary substantially across the lake and contribute to the variable incidence of taste and odour problems (Rao et al. 2003; Watson 2004). One of our goals was to employ the newer fluorescence technologies to characterize this variability and seek evidence for the environmental factors producing the variation. We also wished to exploit the capabilities of the fluorescence-based instruments to improve our knowledge of phytoplankton variability in the vertical dimension, which can be appreciable (Barbiero and Tuchman 2001*b*). Finally, we assessed the ability of the FRRF to provide rapid, in situ estimates of phytoplankton productivity, with comparison against a widely used carbon-14 (^{14}C) method.

Materials and methods

Study design and water chemistry

A 5-day survey of Lake Ontario was carried out aboard the CCGS *Limnos* from 30 August to 3 September 2004. Measurements were made at 13 stations (Fig. 1) to look for evidence of horizontal variability in physiological state and the relationship between such variability and light and nutrient availability. Vertical profiles of temperature, FRRF parameters, and major pigment groups were made at the same stations. Stations were selected to represent the range of

© 2007 NRC Canada

Table 1. Definitions of terms used in the text.

Term	Definition
F_0 or F'	Minimal fluorescence obtained when all reaction centres are open in dark-adapted samples or under ambient light, respectively (arbitrary units)
F_m or F_m'	Maximum fluorescence obtained when all reaction centres are closed in dark-adapted samples or under ambient light, respectively (arbitrary units)
F_v or F_q'	Variable fluorescence in dark-adapted samples (i.e., $F_m - F_0$) or under ambient light (i.e., $F_m' - F'$), respectively (arbitrary units)
F_v/F_m	Maximum quantum efficiency of photochemistry of dark-adapted samples (dimensionless)
F_q'/F_m'	Maximum quantum efficiency of photochemistry of samples under ambient light (dimensionless)
σ_{PSII} or σ_{PSII}'	Effective absorption cross section in dark-adapted samples or under ambient light, respectively ($Å^2$·quanta^{-1}; 1 Å = 0.1 nm)
N_{PSII}	Number of PSII reaction centres per mole chlorophyll *a* (mol RCII·(mol Chl *a*)$^{-1}$)
PQ	Photosynthetic quotient (mol O_2·(mol CO_2)$^{-1}$)
PAR	Photosynthetically active radiation (μmol photons·m^{-2}·s^{-1})
Chl *a*	Chlorophyll *a* concentration (mg·m^{-3})
$\bar{a}^*$	Mean absorption cross section per unit of chlorophyll *a* (m^2·mg Chl *a*$^{-1}$)
α^B	Initial slope of photosynthesis vs. irradiance curve normalized to chlorophyll *a* (mg C·(mg Chl *a*)$^{-1}$·h^{-1}·(μmol photons·m^{-2}·s^{-1})$^{-1}$)
$PP_{z,t}$	Primary production at depth *z* and time *t* (mg C·m^{-3}·h^{-1})

conditions encountered over the lake and included two nearshore sites impacted by anthropogenic disturbance: Station 1001 is in the highly enriched Hamilton Harbour, while station 71 is near the mouth of the Oswego River. In addition, stations 79 and 78 were in the relatively shallow eastern end of the lake, where different physical conditions prevail and dreissenid mussel impacts on the plankton may have been stronger than in most of the lake (Mills et al. 2003).

K_{PAR} was calculated empirically as the coefficient of the regression of the natural log of photosynthetically active radiation (PAR) against depth. PAR was measured using a Chelsea Technologies HB071 PAR irradiance meter (Chelsea Technologies Group, Surrey, UK) attached to the FRRF, and the K_{PAR} value used was the average for the surface mixed layer. The depth of the surface mixed layer was defined as the shallowest depth at which the temperature gradient was at least 1 °C·m^{-1} and temperatures were at least 1 °C lower than at surface. Mean irradiance (light climate) in the surface mixed layer (SML), relative to surface, was then calculated (Hiriart et al. 2002) to characterize differences in availability of sunlight due to variations of mixing depth and water transparency among stations. Surface incident PAR was not monitored but skies were clear or nearly clear throughout, and the climatic mean incident irradiance for these latitudes and dates would average 805 μmol photons·m^{-2}·s^{-1} at noon, or 23.9 mol photons·m^{-2}·day^{-1}.

Concentrations of dissolved nitrate and nitrite (NO_3 + NO_2), ammonium (NH_3), and soluble reactive phosphorus (SRP) were measured at the National Laboratory for Environmental Techniques (National Water Research Institute, Environment Canada, Burlington, Ontario). Particulate carbon (C), nitrogen (N), and phosphorus (P) concentrations were measured using the methods of Stainton et al. (1977). Briefly, 500 mL aliquots of water were filtered through precombusted glass fibre filters (pore size of 0.8 μm) and the filters frozen at –20 °C for later analysis. C and N concentrations were measured in an elemental analyser after the filters had been exposed to HCl for 24 h to remove inorganic C. P concentration was measured spectrophotometrically. Blank values (measured on clean filters) were subtracted from all sample values. Chlorophyll *a* (Chl *a*) concentration was assessed fluorometrically after extraction in 90% acetone (Holm-Hansen et al. 1965). Phytoplankton absorption spectra were measured in a Cary 100 dual beam spectrophotometer. Measurements were made before and after depigmentation with NaClO, and values from blanks (clean filters, dampened using filtered lake water) were subtracted from sample values. Values at 750 nm were subtracted from blank corrected sample values, and beta correction (for scattering within the filter) was carried out using the equations of Tassan and Ferrari (1998). Ratios of phytoplankton absorption at different wavelengths were used to estimate pigment group ratios. The ratio of absorption at 674 nm (a674) to a443 was used as an indicator of the ratio of Chl *a* to carotenoid pigments (Chl *a*/Carot), and a674/a490 was used as an indicator of the Chl *a*/total pigment ratio (Chl *a*/TPig) (see Aiken et al. 2004 for explanation of wavelength choice). The mean Chl *a* specific absorption coefficient ($\bar{a}^*$) was calculated by normalizing wavelength-specific absorption to Chl *a* and taking the average of values between 400 and 700 nm. Unless otherwise noted, parameter values measured from water samples collected at 2 m depth were considered to be representative of the surface mixed layer.

Fast repetition rate and spectral fluorescence measurements

A FAST^{tracka} (Chelsea Technologies Group) FRRF with dual light and dark chambers was used to measure vertical profiles of active fluorescence. Maximal and minimal fluorescence, F_m and F_0, respectively (see Table 1 for definitions of all terms), were measured on dark-adapted samples using a gradient of pump flashes of increasing intensity to gradually close all reaction centres by the controlled reduction of the primary acceptor, Q_A. The dark chamber of the FRRF has a flush time of 0.2–1.0 s, which is sufficient to inhibit

© 2007 NRC Canada

photochemistry but not nonphotochemical quenching. The ratio of F_v/F_m (where $F_v = F_m - F_0$) measures the maximum quantum efficiency of photosystem II (PSII) (Kolber and Falkowski 1993). For the purpose of the FRRF work, when F_v/F_m is equal to 0.65, it is assumed that 100% of PSII reaction centres are functional (Kolber and Falkowski 1993). Variability in F_v/F_m is associated with the physiological state of the phytoplankton (Olaizola et al. 1996) and has been linked to nutrient availability in some waters (e.g., Falkowski et al. 1991; Geider et al. 1993; Olson et al. 2000). Measurements of variable fluorescence made under ambient light indicate the effective quantum efficiency of PSII. Under ambient light, F'_m and F' are the maximal and minimal fluorescence values, respectively, and variable fluorescence is referred to as F'_q/F'_m (where $F'_q = F'_m - F'$). The effective absorption cross section, σ_{PSII}, is the effective size of the light-absorbing target in $Å^2$·quanta^{-1} (1 Å = 0.1 nm) (Falkowski and Raven 1997). It is related not only to the number of molecules that make up the light-harvesting antennae but also to the efficiency of energy transfer from these molecules to a reaction centre. σ_{PSII} has been shown to be sensitive to nutrient concentration (Kolber et al. 1998) and light (Vassiliev et al. 1994; Moore et al. 2003). When measured under ambient light, σ_{PSII} is denoted σ'_{PSII}.

The FRRF was deployed where possible over the sunward side of the deck to avoid ship shadow, and the system profiled slowly at less than 0.1 m·s^{-1}. An acquisition sequence of 100 saturation flashes, 20 relaxation flashes, and 10 ms sleep time between acquisitions was used. The flash duration was set to either 4 or 8 (instrument units) and the AUTOgain function was used. During the quality control procedure, data were deleted where the instrument gain setting was greater than 16, where depth was less than 0, where PAR was less than 0, and where σ_{PSII} was greater than 750×10^{-20} $Å^2$·quanta^{-1}. The in situ data were aggregated over fixed 1 m depth intervals. For comparison with the in situ values, measurements were also made on samples from 2 m and dark-adapted in the lab for at least 1 h before measurement. For these dark-adapted measurements, the instrument gain was manipulated to ensure clear saturation curves were obtained.

For comparison with data from ^{14}C incubations, estimates of the spectrally dependent σ_{PSII} were corrected to correspond to the in situ spectrum using the measured absorption spectra, measured surface irradiance, the wavelength-specific attenuation coefficient spectra from the literature (Jerome et al. 1983), and the approach of Babin et al. (1996). The light-limited rate of photosynthesis, α^B, was estimated from FRRF parameters using eq. 1, adapted from Moore et al. (2003).

$$(1) \qquad \alpha^B = 1.21 \times 10^{-4} \cdot \sigma'_{PSII(z,t)} \cdot \left[\frac{\max\left(\frac{F'_q}{F'_m}\right)}{0.65} \right]$$

where the factor 1.21×10^{-4} accounts for the conversion of units from mol C·(g Chl a)$^{-1}$·mol quanta^{-1}·m^{-2} to mg C·(mg Chl a)$^{-1}$·h^{-1}·(μmol quanta·m^{-2}·s^{-1})$^{-1}$, the requirement of eight electrons to evolve one molecule of oxygen (O_2) and a photosynthetic quotient (PQ) value of 1.2. The maximum value of F'_q/F'_m was chosen to avoid using a value that was quenched by high light. The rate of primary production, at the time of sampling, was estimated for every depth using eq. 2, taken from Smyth et al. (2004).

$$(2) \qquad PP_{(z,t)} = 1.87 \times 10^{-4} \cdot \frac{F'_q}{F'_m}(z,t) \cdot \sigma'_{PSII(z,t)} \times PAR_{(z,t)} \cdot [\text{Chl } a]$$

where $PP_{(z,t)}$ is primary production in mg C·m^{-2}·h^{-1}. $PAR_{(z,t)}$ was calculated using the measured value for $PAR_{(0,t)}$ and K_{PAR}. The constant is based on the assumption that four electrons are passed to the reaction centres of PSII per O_2 evolved and that there are 500 Chl a molecules per reaction centre of PSII (i.e., N_{PSII} = 1/500). It also includes the following conversions: 12 g C·mol C^{-1}, 892 g Chl a·mol^{-1}, 3600 s·h^{-1}, 6.02×10^{23} molecules·mol^{-1}, and 10^{20} photon·m^{-2}. The Chl a concentration measured at 2 m was used for the whole SML. $PP_{(z,t)}$ values were integrated over depth to get estimates for the entire SML.

Spectral fluorescence measurements used a Fluoroprobe (Beutler et al. 2002) deployed with the FRRF as part of the same instrument package. Instrument offsets were calibrated against deionized water, and the algal "fingerprints" already incorporated in the instrument's software by the manufacturer were used without modification. A similar mode of operation in Lake Erie produced Chl a estimates that agreed well with independent measurements and algal composition estimates that were broadly consistent with prior knowledge of phytoplankton communities in the lake (Ghadouani and Smith 2005).

Carbon assimilation and statistical methods

For incubations with ^{14}C, whole water samples were filtered through Nitex mesh (200 μm pore size) to remove large zooplankton. The screened sample (80 mL) was inoculated with ^{14}C sodium bicarbonate (ICN Biomedicals, Irvine, California; 2 mCi·mL^{-1} (1 Ci = 37 Gbq)) and dispensed into 20 mL borosilicate glass scintillation vials in 5 mL aliquots. For each experiment, a time zero sample was acidified with 100 μL of 6 mol·L^{-1} HCl, allowed to degas for 24 h, and subsequently fixed with 15 mL of Ecolume scintillation cocktail (ICN Pharmaceuticals, Costa Mesa, California). Duplicate total activity (100 μL) samples were taken to verify the specific activity and fixed with ethanolamine. Nine vials were placed into a light gradient incubator modelled after Lewis and Smith (1983) and equipped with a 300 W Quartzline lamp (General Electric Co., Cleveland, Ohio) that provided different light intensities from 0 to 1400 μmol photons·m^{-2}·s^{-1}. At the end of the incubation (1 h), 100 μL of 6 mol·L^{-1} HCl was added to each scintillation vial to drive off any unincorporated ^{14}C, and samples were allowed to degas and were chemically fixed as above. The activity of all samples was determined by liquid scintillation counting (model 1209 Rackbeta, LKB Wallac, Turku, Finland) using external standards for quench correction and converted to photosynthetic carbon assimilation rates using the dissolved inorganic carbon concentration of each water sample as determined by Gran titration (Wetzel and Likens 1991). The

© 2007 NRC Canada

Fig. 2. Vertical profiles of chlorophyll *a* (Chl *a*; broken line) and temperature (circles) at stations 1001 (*a*), 33 (*b*), 744 (*c*), 71 (*d*), 78 (*e*), and 84 (*f*). The thick line indicates maximum depth.

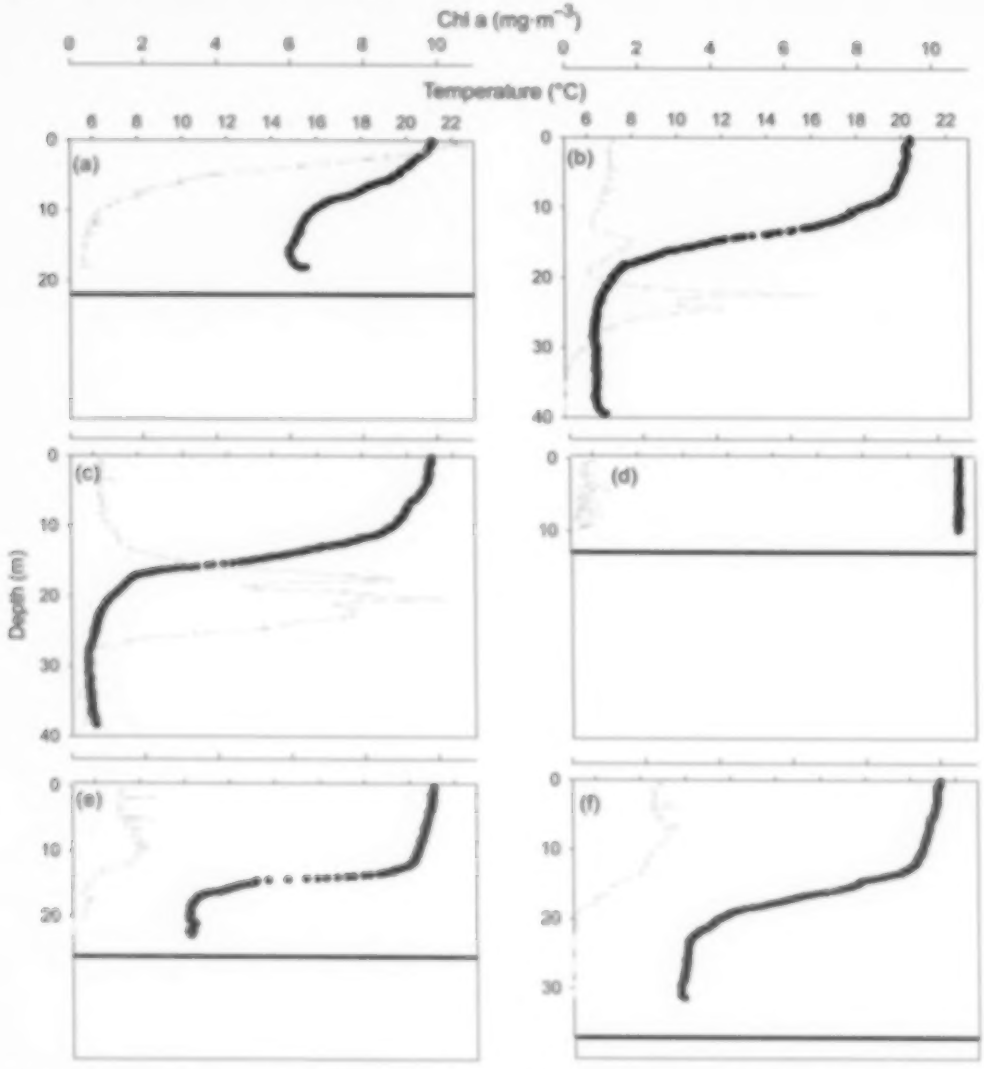

photosynthetic light response was fitted by the model PSPARMS (Fee 1990) to derive α^B and P_m^B, the maximum rate of photosynthesis measured under experimental conditions. The rate of in situ primary production was estimated for the hour of sampling using the derived parameters and the same equation, this time parameterised with depth-specific PAR at 1 m intervals, derived as described above.

Given the potential sampling error associated with our variables, the relationships between different parameters were initially evaluated manually using type II regressions (geometric mean). However, for ease of calculation and to assess the significance of the relationships, type I regression statistics and the significance of relationships were calculated in MINITAB (Minitab, Inc., State College, Pennsylvania) and are the values quoted in the text. Principle components analysis (PCA) was carried out in PRIMER, a software package for the analysis of multivariate ecological data (Clarke and Gorley 2001), to determine how the stations were grouped according to both particulate nutrient concentrations and FRRF parameter values. Data were log-transformed and normalized before correlation-based PCA. The analysis was first carried out using concentrations of particulate C, N, and P as the variables and was then repeated, this time using F_q'/F_m' and σ_{PSII}' as the variables.

Results

Vertical structure of the water column and phytoplankton

Six stations were selected to represent the range of vertical structures observed over the lake. Surface temperature was similar at all stations except station 71, which experienced an effect from the Oswego River and was ~1 °C warmer than the others (Fig. 2). The Oswego River plume

© 2007 NRC Canada

Fig. 3. Vertical profiles of phytoplankton groups as indicated by Fluoroprobe measurements at stations 1001 (*a*), 33 (*b*), 744 (*c*), 71 (*d*), 78 (*e*), and 84 (*f*): greens (squares), cyanobacteria (triangles), chromophytes (inverted triangles), and cryptophytes (crosses). The thick line indicates maximum depth.

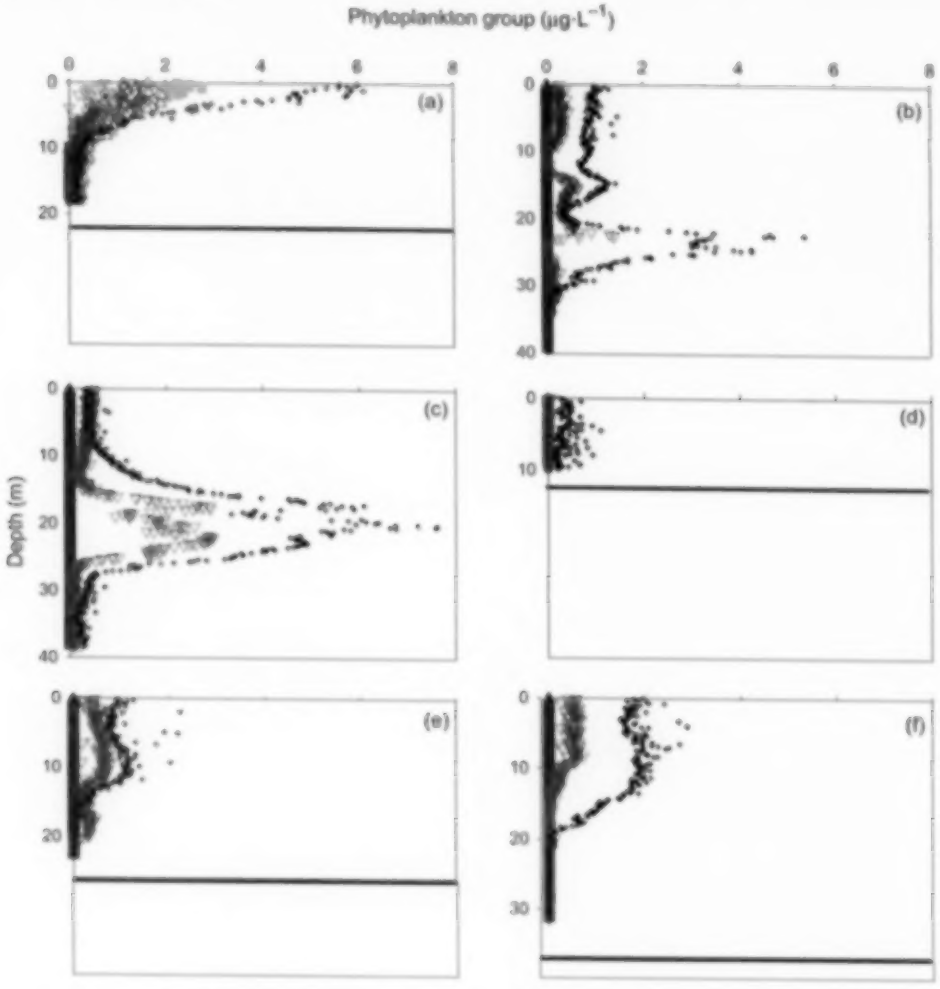

Table 2. Biomass (fresh weight) and percent composition of major phytoplankton groups at open lake stations, with percent composition from spectral fluorescence analysis (Fluoroprobe) indicated in parentheses.

	Station 33, 2 m		Station 33, 20.5 m		Station 84, 2 m	
Group	μg·L⁻¹	%	μg·L⁻¹	%	μg·L⁻¹	%
Cyanophytes	5.4	24 (0)	43.1	33 (0)	162.9	31 (0)
Chlorophytes	1.9	8 (0)	8.1	6 (0)	97.9	20 (0)
Cryptophytes	7.6	33 (66)	33.0	25 (70)	61.8	13 (74)
Chrysophytes	7.4	32	8.5	6	98.4	20
Haptophytes	0.6	2	1.0	1	0	0
Diatoms	0	0	16.5	13	2.2	1
Dinoflagellates	0	0	20.2	1315	72.5	15
All chromophytes	8.0	35 (34)	46.2	35 (30)	173.1	36 (26)

(71) station was not thermally stratified, and the Hamilton Harbour station (1001) had a relatively small thermal gradient. The two midlake stations (33 and 744) showed clear stratification, and both had distinct thermoclines between 10 and 20 m (~12 °C change in both cases). At station 33, chlorophyll peaks occurred at 16 and 25 m. At Station 744, the

© 2007 NRC Canada

Fig. 4. Vertical profiles of F'_q/F'_m from the light (dotted line) and dark chambers (solid line) at stations 1001 (*a*), 33 (*b*), 744 (*c*), 71 (*d*), 78 (*e*), and 84 (*f*) (data binned at 1 m intervals). The thick line indicates maximum depth.

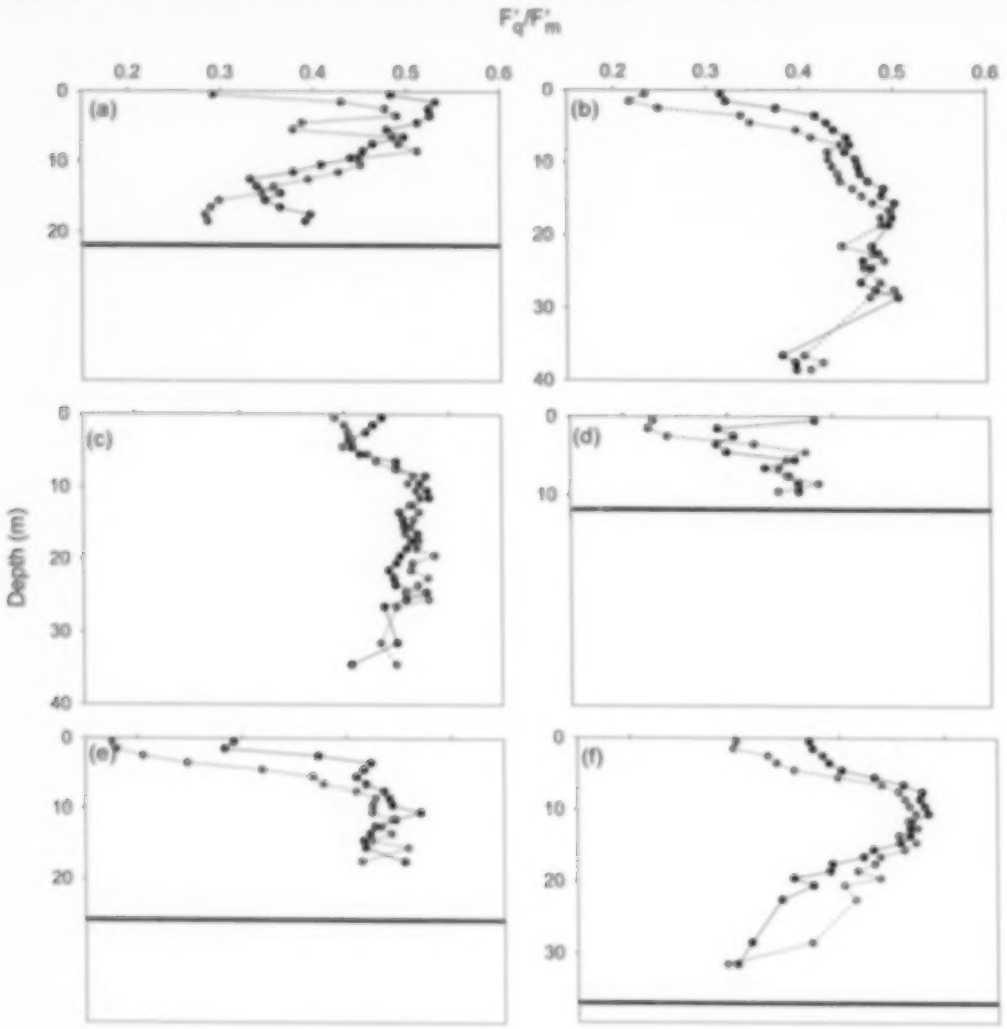

chlorophyll peak was wider and centred around 21 m. Both stations at the east of the lake, 78 and 84, had thermoclines around 15 m, below which the water was ~10 °C cooler and Chl *a* concentrations were lower than in the SML.

Fluorescence measurements indicated that cryptophytes dominated at all stations and chromophytes were also present at high levels at most stations (Fig. 3). Only station 1001 contained cyanophytes and green algae in measurable concentrations, and although cryptophytes dominated at the surface, below 10 m all four algal groups had similar concentrations. At station 71, only cryptophytes were present in measurable concentrations. At stations 33 and 744, chromophytes and cryptophyes had very similar distribution profiles, with large peaks below the thermocline, but cryptophytes were always dominant. At stations 78 and 84, cryptophyte concentrations were much higher than chromophyte concentrations in the surface layer but dropped to very low levels below the thermocline, and at station 78, chromophytes were the dominant group in the hypolimnion.

Limited comparisons against phytoplankton biomass and composition by microscopic analysis (Table 2) showed disagreements with the spectral fluorescence results. A major presence of chromophytes (which were mainly dinoflagellates and chrysophyte flagellates in shallow samples but also diatoms in the deep sample) was confirmed by the microscopic analysis. In contrast with the fluorescence results, however, picocyanobacteria were important in all three samples together with large colonial forms (specifically *Anabaena flos-aquae*) at station 84 and fine filamentous forms in the deep sample. Cryptophytes were much less dominant than indicated by fluorescence, and there was a major contribution from large colonial chlorophytes at station 84 that did not appear in the fluorescence results. Nonquantitative examination of samples from six additional

© 2007 NRC Canada

Fig. 5. Vertical profiles of σ'_{PSII} from the light (dotted line) and dark chambers (solid line) at stations 1001 (*a*), 33 (*b*), 744 (*c*), 71 (*d*), 78 (*e*), and 84 (*f*) (data binned at 1 m intervals). 1 Å = 0.1 nm. The thick line indicates maximum depth.

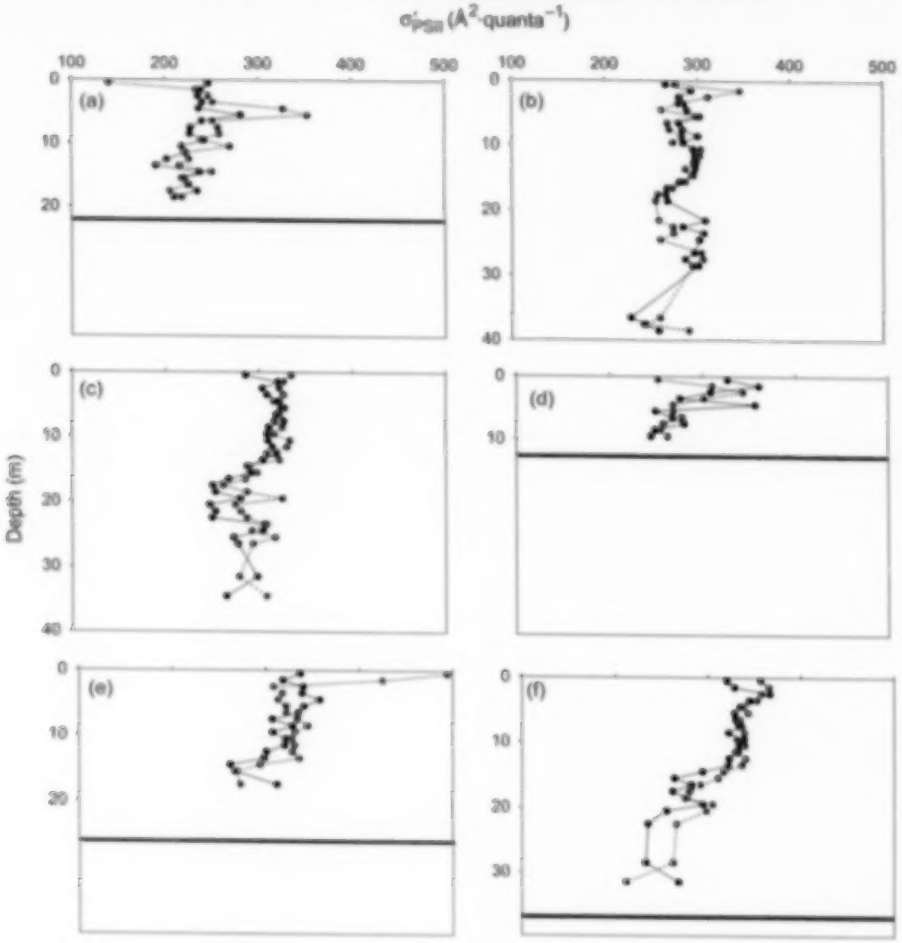

Table 3. Values of physical and chemical parameters in the surface mixed layer.

Station	Total depth (m)	Mixed layer depth (m)	K_{PAR} (m^{-1})	Mean PAR (% of surface)	$NO_3 + NO_2$ ($\mu g \cdot L^{-1}$)	NH_3 ($\mu g \cdot L^{-1}$)	SRP ($\mu g \cdot L^{-1}$)
1001	22	2.5	0.540	55	ND	ND	ND
3	25	5	0.233	59	272	37	1.8
752	70	7	0.212	53	257	27	1.0
737	26	11	0.278	31	250	9	0.9
33	138	13	0.304	42	257	10	1.8
28	61	13	0.299	35	241	8	1.2
745	67	13	0.283	27	220	12	1.2
744	146	8	0.305	37	241	10	0.9
71	13	WM	0.306	31	240	13	1.7
89	82	18	0.193	29	230	8	1.2
79	22	10	0.325	30	242	9	0.9
78	26	16	0.196	42	235	0	6.9
84	37	14	0.377	29	233	17	5.9
Mean±SD			0.296±0.091	38±11	243±14	13±10	2.1±2.0

Note: SRP, soluble reactive phosphorus; WM, well-mixed; ND, no data.

© 2007 NRC Canada

Table 4. Values of biological parameters in the surface mixed layer.

			Particulate nutrients (μg·L^{-1})							
Station	Time of cast	PAR at 0 m	Chl *a*	C	N	P	C/P	N/P	C/N	C/Chl *a*
1001	1109	315	20.27	1160	198	18	166	24	7	4.8
3	1337	223	4.90	487	75	8	157	21	8	8.3
752	1646	408	2.61	418	67	9	120	16	7	13.3
737	1926	339	3.15	574	94	7	212	30	7	15.2
33	0922	159	2.84	415	63	7	153	20	8	12.2
28	1149	1804	2.36	490	73	5	253	32	8	17.3
745	1717	63	2.17	450	63	10	116	14	8	17.3
744	1903	19	1.68	408	60	6	176	22	8	20.2
71	0917	93	1.20	244	45	12	53	8	6	17.0
89	1250	158	1.98	416	61	9	119	15	8	17.5
79	1802	51	1.59	413	63	6	178	23	8	21.6
78	1547	162	1.69	360	55	6	155	20	8	17.7
84	1804	116	2.31	581	85	5	300	38	8	20.9
Mean±SD			3.75±5.05	494±218	77±38	8±4	166±63	22±8	8±1	15.6±4.9

Note: Stations in bold were not P deficient according to the guidelines of Guildford and Hecky (2000). FRRF (fast repetition rate fluorescence) pigments; TPig, total pigments.

*Units for light-limited rate of photosynthesis (α^B) are mg C·(mg Chl *a*)$^{-1}$·h^{-1}·(μmol photons·m^{-2}·s^{-1})$^{-1}$.

†Units for the maximum rate of photosynthesis measured under experimental conditions (P^B_m) are mg C·(mg Chl *a*)$^{-1}$·h^{-1}.

stations (S. Watson, unpublished data) confirmed that cryptophytes and chromophytes were among the dominant groups, as indicated by fluorescence, but also showed that cyanobacteria were widely important and underreported by fluorescence.

FRRF profiles revealed strong near-surface quenching of F'_q/F'_m at all stations (Fig. 4). In all cases, surface values were higher in the dark chamber (D) than in the light chamber (L), but the difference largely disappeared at or above the bottom of the SML. The highest profile values of F'_q/F'_m were measured at station 1001 (max F'_q/F'_m, D = 0.53; max F'_q/F'_m, L = 0.51) and the lowest at station 71 (max F'_q/F'_m, D = 0.38; max F'_q/F'_m, L = 0.39). At station 1001, L and D values were similar in the midwater column but diverged below 15 m, with lower values in L chamber. This was not reflected in any patterns in the physical or community structure data. F'_q/F'_m values at some of the other stations (e.g., 744, 78) were fairly uniform below the quenched zone, while at others (e.g., 33, 84) they decreased, but features clearly associated with the main thermocline or deep chlorophyll maxima were not obvious. σ_{PSII} was more uniform than F'_q/F'_m through the photic zone at most stations, and values were relatively similar between the stations (Fig. 5). Although σ_{PSII} was quite uniform with depth at some stations (e.g., 33), it did decrease below the SML at others (e.g., 84). There was a slight decrease in σ_{PSII} within the thermocline at stations 33 and 744, but there were no other clear similarities between σ_{PSII} and either the physical structure or deep chlorophyll maxima.

Horizontal variations of phytoplankton and environmental variables

Stations were selected to represent the range of conditions encountered over the lake and included two nearshore sites impacted by anthropogenic disturbance: Station 1001 is in the highly enriched Hamilton Harbour, while station 71 is near the mouth of the anthropogenically impacted Oswego River. Light attenuation (K_{PAR}) was highest at station 1001 (0.540 m^{-1}) and lowest at station 89 (0.193 m^{-1}). The concentration of nitrate in the mixed layer did not vary much over the lake (average = 243 ± 13 μg·L^{-1}). SRP was particularly high at stations 78 and 84 and was lowest at stations 737, 744, and 79. Station 1001, in Hamilton Harbour, had the highest values of many of the biological parameters considered (Chl *a*, C, N, K_{PAR}, Chl *a*/Carot, Chl *a*/TPig, F_m, and F'_q/F'_m), and station 71, near the Oswego River, had many of the lowest values (Tables 3, 4). The concentration of Chl *a* in the SML ranged considerably from 1.19 (station 71) to 20.01 mg·m^{-3} (station 1001). However, the concentration at station 1001 was exceptionally high and the next highest value was 4.9 mg·m^{-3}. The ratio of C to N ranged from 6.40 to 8.32; C to P from 52 to 287, and N to P from 8 to 36, indicating slight or moderate P limitation in the SML at most stations by the criteria of Guildford and Hecky (2000). In some cases (stations 3, 33, and 744), P was limiting relative to C but not to N, reflecting low levels of both N and P in the seston. The Chl *a*/Carot ratio ranged from 0.45 to 0.66 (coefficient of variation (CV) = 12), with the highest and lowest values at stations 1001 and 71, respectively. The Chl *a*/TPig ratio ranged from 0.65 to 1.08 (CV = 14), with the highest value at station 1001 and the lowest at stations 79 and 71.

The strong vertical variations of F'_q/F'_m complicated comparisons among stations. However, while values in the upper part of the SML and the F_v/F_m measured on dark-adapted samples revealed considerable between-station variation, measurements near the base of the SML were less variable and were mostly in the 0.4–0.5 range (Table 3). Unusually, values of F_v/F_m measured on dark-adapted samples were often lower than F'_q/F'_m measured in situ. Neither F'_q/F'_m nor F_v/F_m showed any relationship to indices of nutrient status (C/P, C/N, N/P), dissolved nutrient concentrations, C/Chl *a* ratios, $\bar{a}^*$, or light climate. Both C/Chl *a* and $\bar{a}^*$ were negatively correlated to light climate (Fig. 6), such that brighter

© 2007 NRC Canada

Light absorption			FRRF (in situ, base SML)			^{14}C
$\bar{a}^*$ (m^{-2}·(mg Chl a)$^{-1}$)	Chl a/Carot	Chl a/TPig	F_v/F_m	σ'_{PSII} (Å·photon^{-1})	α^{B*}	$P_m^{B\dagger}$
0.008	0.66	1.08	0.49	251	0.015	0.026
0.011	0.57	0.85	0.43	273	0.014	0.009
0.019	0.47	0.78	0.43	258	0.013	0.026
0.019	0.49	0.79	0.47	303	ND	ND
ND	ND	ND	0.44	299	0.016	0.008
0.017	0.60	0.88	0.44	291	0.015	0.017
0.030	0.51	0.78	0.46	299	0.016	0.016
0.017	0.52	0.72	0.47	325	0.017	0.023
0.024	0.45	0.66	0.35	262	0.011	0.018
0.021	0.53	0.77	0.46	251	0.015	0.043
0.024	0.45	0.65	0.41	273	0.013	0.013
0.019	0.52	0.75	0.46	316	0.017	0.023
0.022	0.48	0.75	0.46	336	0.018	0.058
0.019±0.006	0.52±0.06	0.79±0.11	0.44±0.04	287±28	0.015±0.002	0.023±0.014

parameters are for the lower surface mixed layer (SML) except for F_v/F_m, which was measured on dark-adapted samples from 2 m. Carot, carotenoid

Fig. 6. Regression plots of C/Chl a ratio and $\bar{a}^*$ against light climate and C/N ratio.

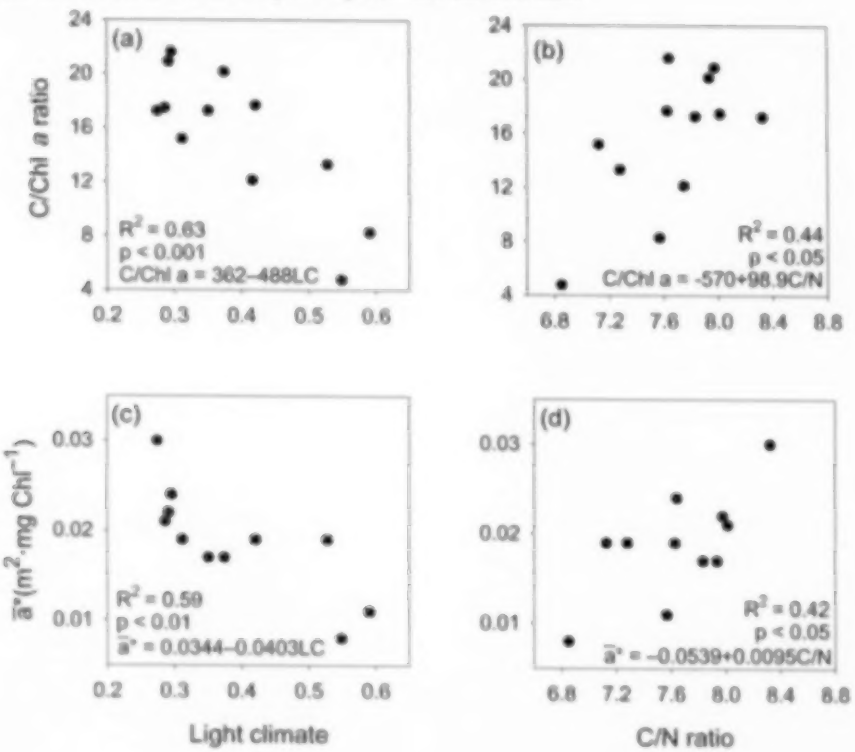

light environments were associated with higher pigment contents and lower optical cross sections, although this was only significant if data from station 71 were removed (C/Chl a regressed against light climate: R^2 = 0.63, p < 0.001, C/Chl a = 362–488 × light climate, df = 11; $\bar{a}^*$ regressed against light climate: R^2 = 0.59, p < 0.01, $\bar{a}^*$ = 0.0344–0.0403 × light climate, df = 10). C/Chl a and $\bar{a}^*$ were also positively related to the C/N ratio (station 71 excepted) (C/Chl a regressed against C/N: R^2 = 0.38, p < 0.05, C/Chl a = –570 + 98.9C/N, df = 11; $\bar{a}^*$ regressed

© 2007 NRC Canada

Fig. 7. Principle components analysis (PCA) of stations based on (*a*) particulate C, N, and P concentrations and (*b*) F_q'/F_m' and σ_{PSII}' data.

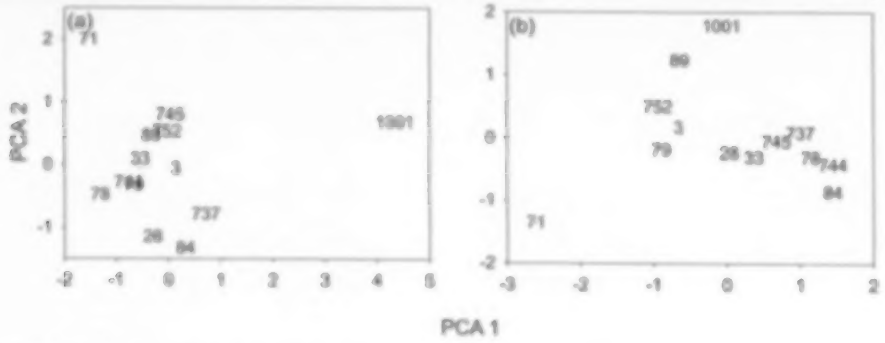

Fig. 8. Estimates of α^B (triangles) and primary production (circles) from the fast repetition rate fluorescence (FRRF) method plotted against those from the ^{14}C method.

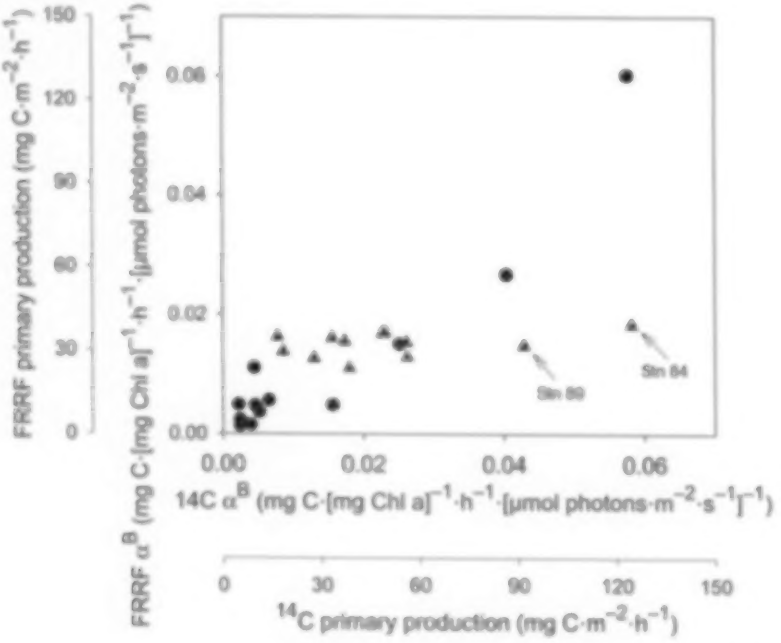
FRRF primary production (mg C·m⁻²·h⁻¹)
FRRF α^B (mg C·[mg Chl a]⁻¹·h⁻¹·[µmol photons·m⁻²·s⁻¹]⁻¹)
14C α^B (mg C·[mg Chl a]⁻¹·h⁻¹·[µmol photons·m⁻²·s⁻¹]⁻¹)
14C primary production (mg C·m⁻²·h⁻¹)
Stn 89
Stn 84

against C/N: R^2 = 0.42, $p < 0.05$, $\bar{a}^* = -0.0539 + 0.0095C/N$, df = 10) but not to C/P or SRP. σ_{PSII}', which may be expected to reflect longer-term photoadaptive responses as well as nutrient status influences, showed no clear relationship to C/Chl *a*, $\bar{a}^*$, or the light climate of the SML. σ_{PSII}' also failed to show significant general relationships with dissolved nutrients or indices of nutrient status, although the two most impacted stations (1001, 71) had the two lowest values for both C/N and σ_{PSII}' (Table 3). There was a clear correlation between σ_{PSII}' values and the number of hours from solar noon (data not shown, Pearson's correlation of significance, r = 0.738, $p < 0.01$, calculated in MINITAB).

PCA on the nutrient status indicators (particulate nutrient data) grouped most of the stations in one cluster but clearly separated the two higher impact stations (71, 1001) and placed station 84 at the furthest distance from them (Fig. 7). The photosynthetic physiology, as reflected by the in situ FRRF parameters, resulted in similar separations and groupings by PCA, although the separation was not as clear for station 1001. The first axis of the nutrient PCA (PC1) accounted for 73% of the variance, and for this axis, C and N were roughly equally weighted but the influence of P was slightly lower (eigenvectors: C = 0.644, N = 0.663, and P = 0.381). The second axis was largely dominated by P concentration and accounted for the remaining 27% of the variance (eigenvectors: C = –0.332, N = 0.207, and P = 0.921). The first and second axes of the FRRF PCA accounted for 66% and 34%, respectively, of the total variance, and both were roughly equally loaded by F_q'/F_m' and σ_{PSII}'.

Comparison of primary production estimates from FRRF and ^{14}C

Estimates of photosynthetic parameters derived from FRRF data (values taken from light chamber data at the base of the SML) were compared with estimates from incubations with

© 2007 NRC Canada

^{14}C (Fig. 8). Estimates of α^B from the FRRF showed less variability than those from ^{14}C, and the two measures were not significantly correlated. In most cases, values from ^{14}C were higher than those from the FRRF, although this pattern was strongly influenced by two data points (stations 84 and 89) with high ^{14}C values. With those two stations removed, the two measures were still not significantly correlated, but they were in similar range (0.011–0.018 from the FRRF compared with 0.008–0.026 mg C·(mg Chl a)$^{-1}$·h^{-1}·(μmol photons·m^{-2}·s^{-1})$^{-1}$ from incubations with ^{14}C). Estimates of areal production rates by the two techniques were significantly correlated (Fig. 8).

Discussion

In this study, a range of optical and chemical approaches was used to investigate the controls on phytoplankton in Lake Ontario at a time of year when taste and odour events are considerable but extremely variable, which may reflect both physical transport processes and variability in phytoplankton composition and condition (Rao et al. 2003; Watson 2004). The principal taste and odour compound, MIB (methylisoborneol), was present at 1.5 to 2 times the olfactory detection threshold at most stations during this study (S.B. Watson, unpublished data) and will be the subject of detailed analysis to be published later, using additional data from other years (including full taxonomic analysis of the phytoplankton). The purpose here was to assess the variability and environmental control of phytoplankton physiology that might be considered in the ongoing study of the taste and odour phenomenon. Substantial variations in nutrient and biological variables were observed. The FRRF measurements also revealed variations in photosynthetic efficiency and physiological condition, especially in the vertical dimension. Between-station variations were more limited, except at the two most impacted stations. FRRF showed promise in its ability to discriminate the more highly impacted stations, but it and the spectral fluorescence method still require careful evaluation.

One major aspiration for FRRF and related fluorescence methods is to provide primary productivity estimates with less effort and uncertainty than traditional incubation methods, but the fluorescence approach does rely on assumptions about a number of aspects of phytoplankton physiology, such as the size of the photosynthetic unit (N_{PSII}) and the ratio of photosynthesis to respiration (PQ). PQ and N_{PSII} are variable but are assigned constant assumed values in the FRRF calculations. Respiration and the loss of electrons due to the Mehler reaction (Kana 1992) are not accounted for at all. Uncertainties associated with ^{14}C incubations include artefacts of enclosure, exposure to artificially constant irradiance, and tracer recycling (Williams 1993). For estimates from the FRRF and ^{14}C techniques to agree, every photosynthetically generated electron would have to be used for the production of reductant, all the reductant would have to be used for C fixation, none of the newly fixed C could be respired during the incubation, and the community must function identically in situ and in vitro. Obviously, this is never the case.

As previously observed with marine phytoplankton (Moore et al. 2003; Smyth et al. 2004), estimates of α^B from the FRRF were less variable than those from ^{14}C. Commonly, the FRRF values are slightly higher than ^{14}C values (Suggett et al. 2001; Smyth et al. 2004), but the reverse was usually true here, even when FRRF measurements were corrected for background fluorescence and the correlation between methods was poor. Variable degrees of photoacclimation and (or) use of reductant for purposes other than C fixation during the ^{14}C incubation could contribute to the greater variability of the ^{14}C estimates. The physiology of the phytoplankton in this freshwater lake may also have differed substantially from the marine phytoplankton for which the average parameter values used in the FRRF calculations were derived. The value of N_{PSII} is a particular point of uncertainty, so we estimated it using the equation of Suggett et al. (2004) and our measured values of σ_{PSII} and $\bar{a}^*$. The resulting estimates for N_{PSII} were generally lower than the conventional value used in the equation and actually worsened the disagreement between methods. With the data at hand, we cannot identify the sources of disagreement and fully reconcile the two methods. However, the estimates of α^B were at least in a similar range, with the notable exception of stations 89 and 84.

The large disagreements between methods at stations 89 and 94 were near the limits of what might normally be explicable based on the foregoing considerations and may indicate that production rates at those stations truly were different in situ than in vitro. Incubation methods are commonly suspected to bias production estimates downwards rather than upwards (e.g., Williams 1993), but we may have observed the opposite. One mechanism that might produce such a result is inorganic C limitation. The protocols for ^{14}C and alkalinity measurements both abolish any undersaturation of CO_2 that might constrain photosynthesis in situ and, unfortunately, prevent us from estimating the in situ CO_2 concentrations. However, calcite precipitation, associated with diminished CO_2 concentrations, is common during summer in Lake Ontario (Hodell et al. 1998), and CO_2 can limit photosynthesis in other alkaline, hardwater lakes (Hein 1997). Widespread but highly variable undersaturation of CO_2 has recently been observed in the chemically similar Lake Erie, where CO_2 enrichments at some stations also stimulated photosynthesis (M. Squires, Department of Biology, University of Waterloo, Waterloo, ON N2L 3G1, personal communication). If this explanation is correct, then the FRRF was giving the more accurate estimate of photosynthesis in Lake Ontario.

The similarity of areal production rate estimates from the two techniques, by contrast, may seem encouraging, but these estimates depend heavily on the common variables of Chl a concentration, incident irradiance, and K_{PAR}. Both measures did indicate a wide range of areal productivity of the SML among stations, showing that the variations in biology and chemistry were accompanied by variations in productivity as well. Given the assumptions of the FRRF equations and the possible artefacts associated with ^{14}C incubations, we cannot be sure which values are more realistic. Where physiological variability is of interest, the need to make assumptions and use average parameter values risks disguising real differences between stations. The values of F_q'/F_m' and σ_{PSII} in themselves are much more sensitive and realistic indicators of the variability in phytoplankton physiology.

© 2007 NRC Canada

The physiological status of Lake Ontario phytoplankton in 1998–1999 was assessed by Millard et al. (1996*b*), who showed that the severity of P deficiency was minimal (low or none) when the mean daylight irradiance in the SML was less than 1 mmol photons·m^{-2}·min^{-1} and was always moderate to extreme when mean irradiance was greater than 5 mmol photons·m^{-2}·min^{-1}. They inferred that a mean irradiance of 5 mmol photons·m^{-2}·min^{-1} marked the onset of light saturation. In this study, mean irradiance for the SML ranged from 12.2 to 26.3 mmol photons·m^{-2}·min^{-1} among stations or, with a definition of mixing depth more similar to Millard et al. (1996*a*), from 9.6 to 17.2 mmol photons·m^{-2}·min^{-1}. We would therefore expect the phytoplankton to be light saturated and P deficient, and the nutrient ratios at most stations suggested that they were indeed slightly P deficient. Based on the late summer observations in 1988 and 1989, we might have expected signs of more severe deficiency. Our nutrient ratios may be less sensitive than the physiological index used by Millard et al. (1996*a*) because they are more affected by the presence of heterotrophic and detrital particulate matter. Alternatively, there may have been a real change in phytoplankton physiology consequent to food web changes, such as the major reduction in alewife biomass since the late 1980s. The altered pelagic food web may have allowed increases in zooplankton abundance, more efficient P regeneration in the SML, and a moderation of physiological P deficiency (Mills et al. 2003), although the available data on zooplankton do not present an unambiguous case for such changes (Johansson 2003). Nonetheless, the FRRF fluorescence parameters suggested, like the nutrient stoichiometry, a relatively good physiological condition at most stations.

F_q'/F_m' values were often lower near the surface, but this appeared to reflect surface quenching and adaptation to irradiance more than a depression by nutrient deficiency. The rapid recovery of F_q'/F_m' to higher values with increasing depth in the SML was not consistent with a condition of strong nutrient deficiency throughout the SML. In addition, the variable fluorescence ratios were uncorrelated with measures of nutrient concentrations and particle stoichiometry whether measured at 2 m, deeper in the SML, or on dark-adapted samples. The values of F_q'/F_m' observed in the lower part of the SML, although lower than the theoretical optimum value of 0.65 (Kolber and Falkowski 1993; Kolber et al. 1998), were in a range of 0.4–0.5 associated with a good physiological condition in freshwater algae (Beardall et al. 2001). Relatively high F_q/F_m (0.35–0.5) were measured in the dark chamber even at 2 m, even though the chamber would only partially remove the strong surface quenching effect. The response of variable fluorescence ratios, as measured by FRRF, to P deficiency in freshwater phytoplankton has not been extensively studied, but a freshwater diatom forced into P deficiency in laboratory culture displayed much lower ratios (less than 0.2; R.E.H. Smith, unpublished data) than those observed in Lake Ontario.

Although fluorescence parameters were not significantly correlated to nutrients or to light climate, we did observe that C/N was positively correlated to C/Chl *a* and $\bar{a}^*$. Such correlations are consistent with the expected effect of N supply on pigment content and thus the optical cross section (Falkowski and Kolber 1995), albeit surprising in this supposedly P-limited lake. However, C/N was not significantly related to σ_{PSII}', F_q'/F_m', or the Chl *a*/Carot and Chl *a*/TPig ratios, even though we would expect such correlations if N status was really driving the variations in pigment content and optical cross section. C/Chl *a* and $\bar{a}^*$ were significantly correlated with variations of light climate among stations, which might be expected, but the direction of the correlation was such that brighter light environments were associated with higher pigment contents and lower optical cross sections. This is counter to the pattern normally expected because of photoacclimation (Falkowski and Raven 1997). F_q'/F_m' and σ_{PSII}' were weakly or not at all related to $\bar{a}^*$, C/Chl *a*, or light climate but did show diel variability, as has been reported in other studies (eg Moore et al. 2003). Collectively, these results were not consistent with normal photoacclimation responses or a true controlling role for N and suggested that some correlated variable produced the changes in pigment content and optical cross section.

Mean irradiance in the SML indicated that PAR should have been saturating at all stations, while attenuation coefficients for ultraviolet radiation (UVR) wavelengths (data not shown) averaged less than 70% of those reported for Lake Ontario in summer of 2000 (Smith et al. 2004), indicating that UVR penetration would be relatively high. Under the clear sky conditions of the expedition and based on work in the neighbouring Lake Erie, we would expect UVR-dependent photoinhibition to have been significant (e.g., Hiriart-Baer and Smith 2005), and the near-surface quenching of F_q'/F_m' was consistent with such effects. Moderate exposures to UVR, and particularly the longer-wavelength UVA waveband, have been shown to stimulate higher cell N content (Sobrino et al. 2004) and higher Chl *a* contents (Nilawati et al. 1997; Montero et al. 2002; Yu et al. 2005) in a variety of microalgae. The correlations observed here among light climate, C/Chl *a*, $\bar{a}^*$, and C/N ratios, so hard to understand in terms of acclimation to varying amounts of limiting irradiance or nutrients, may therefore be a response to varying amounts of stressful UVR. Recovery of photosynthetic processes from such stress is typically rapid (e.g., Hiriart-Baer and Smith 2005) and would lead to the good level of photosynthetic efficiency manifested here in the lower SML under most scenarios of mixing strength. If photoinhibition in the upper part of the SML has increased since the late 1980s because of stratospheric ozone depletion and increased water clarity in Lake Ontario (Mills et al. 2003), it may have helped to constrain phytoplankton P demand and moderate the physiological symptoms of P deficiency relative to those observed by Millard et al. (1996*a*).

Supraoptimal irradiance in the SML may also explain why dark-adapted F_v/F_m values were commonly less than F_q'/F_m' in situ. This pattern is unprecedented in fieldwork with FRRF (including surveys in other parts of Lakes Ontario and Erie; K.L. Pemberton, unpublished data) but is consistent with effects of chlororespiration. Chlororespiration regulates photosynthesis by controlling the flow of electrons to PSI (Peltier and Cournac 2002) and can be induced by exposure to excess irradiance. It occurs via the oxygen-dependent cyclic flow of electrons within PSII, which leads to reduction of the electron transfer chain (Bennoun 2001). Chlororespiration creates an energy gradient across the thylakoid membrane, which leads to nonphotochemical quenching of

© 2007 NRC Canada

fluorescence and a decrease in F_v/F_m because of a reduction in F_m and an increase in F_0 (Lavaud et al. 2002). If chlororespiration did indeed cause the low F_v/F_m values in the dark-adapted samples, the difference between in situ and dark-adapted values of F_v/F_m should be stronger in phytoplankton exposed to higher irradiance. We did in fact observe a significant correlation with variations of light climate among stations ($p < 0.05$ when station 1001 was removed).

In among-station comparisons, the two higher-impact stations (1001 and 71) differed from all the others but in different ways. The high values of many of the physiological parameters at station 1001, with its very high nutrient loading, indicated a healthy phytoplankton community and light rather than nutrient limitation. The station had the highest observed K_{PAR} value and unusually high Chl *a*/Carot and Chl *a*/TPig ratios, and the divergence of light and dark F_q'/F_m' profiles with depth, particularly the higher values in the light chamber, are likely to reflect light limitation. Conversely, at station 71, photosynthetic efficiency was very low, the Chl *a*/other pigments and C/P ratios were low, and N/P ratios were high. The low Chl *a*/Carot and Chl *a*/TPig ratios measured at station 71 further support the idea that phytoplankton were unhealthy compared with those at other sites (Heath et al. 1990).

In this study, only the cryptophyte group of phytoplankton was detected by spectral fluorescence at station 71. This group includes any species containing Chl *a* and chlorophyll *c* and in which phycoerythrin is the dominant phycobillin pigment (Beutler et al. 2002). The FRRF is inaccurate at measuring the photosynthetic efficiency of some phycocyanin-containing phytoplankton but is thought to be reliable for species containing phycoerythrin (Raateoja et al. 2004), so the low F_q'/F_m' values measured at this station are likely to be real rather than artefacts of the FRRF excitation wavelengths. In a previous study carried out at a similar time of year to this one, Makarewicz (1997) noted that the Oswego River contains contaminants deriving from domestic, agricultural, and industrial sources and found evidence of impacts on the phytoplankton community in the river mouth, independent evidence that this region of the lake is subject to stresses. It is possible that the anthropogenic influences at our nearby station 71 were associated with shifts in community structure that while undetected by spectral fluorescence, helped drive the observed changes in physiology.

In the three samples available here for quantitative comparison against microscopic analyses, it seems likely that the fluorometer mistook the abundant phycoerythrin-rich picocyanobacteria for cryptophytes. Such confusion between different phycobilin-containing phytoplankton has been identified as a source of error in other pigment-related approaches to plankton analysis (Vincent et al. 2004), and it was apparent in this study that fluorescence also failed to quantify larger, filamentous cyanobacteria and some large colonial chlorophytes. Large colonial forms can be a challenge to microscopic as well as pigment-based analysis, and we do not yet have enough quantitative data on the phytoplankton taxonomic or pigment composition to make a full analysis of these discrepancies. Fluoresence analysis can be adjusted to improve discrimination between related pigment groups (e.g., Leboulanger et al. 2002), and our results show that the method will need careful calibration and verification to reliably discriminate different phycobilin-containing groups.

Our interpretations about the mechanisms controlling phytoplankton in Lake Ontario in late summer are necessarily somewhat conjectural but are readily testable with further work. In terms of better understanding of taste and odour events, two important considerations would be the strong vertical structure of the populations at many stations, which could affect their transport to water intake facilities (cf. Rao et al. 2003), and the evidence that varying levels of supra-optimal irradiance could play an important role in variable chemical composition, physiology, and possibly odour compound production (cf. Watson 2004). By contrast, variations in P deficiency did not seem to be an important influence on spatial variations of phytoplankton composition or condition. The ability of FRRF parameters to distinguish high-impact stations suggests the method can provide a practical means of detecting and characterizing environmental impacts and controls in lakes.

Acknowledgements

Financial support was from grants to R.E.H.S. by Natural Sciences and Engineering Research Council of Canada (NSERC) and the Ontario Ministry of the Environment. Officers and crew of CCGS *Limnos* provided invaluable professional help, and Environment Canada financed ship time and technical assistance on board. We thank S. Malkin and A. Pemberton for generous help in field logistics.

References

Aiken, J., Fishwick, J., Moore, G., and Pemberton, K. 2004. The annual cycle of phytoplankton photosynthetic quantum efficiency, pigment composition and optical properties in the western English Channel. J. Mar. Biol. Assoc. U.K. **84**: 1–13.

Babin, M., Morel, A., Claustre, H., Bricaud, A., Kolber, Z., and Falkowski, P.B. 1996. Nitrogen- and irradiance-dependent variations of the maximum quantum yield of carbon fixation in eutrophic, mesotrophic and oligotrophic marine systems. Deep-Sea Res. I. **43**: 1241–1272.

Bailey, R.C., Grapentine, L., Stewart, T.J., Schaner, T., Chase, M.E., Mitchell, J.S., and Coulas, R.A. 1999. Dreissenidae in Lake Ontario: impact assessment at the whole lake and Bay of Quinte spatial scales. J. Gt. Lakes Res. **25**: 482–49

Barbiero, R.P., and Tuchman, M.L. 2001*a*. Results from the US EPA's biological open water surveillance program of the Laurentian Great Lakes: I. Introduction and phytoplankton results. J. Gt. Lakes Res. **27**: 134–154.

Barbiero, R.P., and Tuchman, M.L. 2001*b*. Results from the US EPA's biological open water surveillance program of the Laurentian Great Lakes: II. Deep chlorophyll maxima. J. Gt. Lakes Res. **27**: 155–166.

Beardall, J., Berman, T., Heraud, P., Kadiri, M.O., Light, B.R., Patterson, G., Roberts, S., Sulzberger, B., Sahan, E., Uehlinger, U., and Wood, B. 2001. A comparison of methods for detection of phosphate limitation in microalgae. Aquat. Sci. **63**: 107–121.

Bennoun, P. 2001. Chlororespiration and the process of carotenoid biosynthesis. Biochim. Biophys. Acta, **1506**: 133–142.

Beutler, M., Wiltshire, K.H., Meyer, B., Moldaenke, C., Luring, C., Meyerhofer, M., Hansen, U.-P., and Dau, H. 2002. A fluorometric method for the differentiation of algal populations *in vivo* and *in situ*. Photosynth. Res. **72**: 39–53.

© 2007 NRC Canada

Clarke, K.R., and Gorley, R.N. 2001. PRIMER v5. User manual/tutorial. PRIMER-E, Plymouth, UK.

Falkowski, P.G., and Kolber, Z. 1995. Variations in chlorophyll fluorescence yields in phytoplankton in the world oceans. Aus. J. Plant Physiol. **22**(2): 341–355.

Falkowski, P.G., and Raven, J.A. 1997. Aquatic photosynthesis. Blackwell Science, Malden, Mass., USA.

Falkowski, P.G., Ziemann, D., Kolber, Z., and Bienfang, P.K. 1991. Role of eddy pumping in enhancing primary production in the ocean. Nature (London), **352**: 55–58.

Fee, E.J. 1990. Computer programs for calculating *in situ* phytoplankton photosynthesis. Central and Arctic Region, Department of Fisheries and Oceans, Ottawa, Ont. Tech. Rep. No. 1740.

Geisler, R.J., Greene, R.M., Kolber, Z., Macintyre, H.L., and Falkowski, P.G. 1993. Fluorescence assessment of the maximum quantum efficiency of photosynthesis in the western North Atlantic. Deep-Sea Res. Part I Oceanogr. Res. Pap. **40**: 1205–1224.

Ghadouani, A., and Smith, R.E.H. 2005. Phytoplankton distribution in Lake Erie as assessed by a new *in situ* spectrofluorometric technique. J. Gt. Lakes Res. **31**: 154–167.

Guildford, S.J., and Hecky, R.E. 2000. Total nitrogen, total phosphorus, and nutrient limitation in lakes and oceans: Is there a common relationship? Limnol. Oceanogr. **45**(6): 1213–1223.

Heath, M.R., Richardson, K., and Kiorboe, T. 1990. Optical assessment of phytoplankton nutrient depletion. J. Plankton Res. **12**: 381–396.

Hein, M. 1997. Inorganic carbon limitation of photosynthesis in lake phytoplankton. Freshw. Biol. **37**: 545–552.

Hiriart, V.P., Greenberg, B.M., Guildford, S.J., and Smith, R.E.H. 2002. Effects of ultraviolet radiation on rates and size distribution of primary production by Lake Erie phytoplankton. Can. J. Fish. Aquat. Sci. **59**: 317–328.

Hiriart-Baer, V.P., and Smith, R.E.H. 2005. The effect of ultraviolet radiation on freshwater planktonic primary production: the role of recovery and mixing processes. Limnol. Oceanogr. **50**(5): 1352–1361.

Hodell, D.A., Schelske, C.L., Fahnenstiel, G.L., and Robbins, L.L. 1998. Biologically induced calcite and its isotopic composition in Lake Ontario. Limnol. Oceanogr. **43**: 187–199.

Holm-Hansen, O., Lorenzen, C.J., Holmes, R.W., and Strickland, J.D.H. 1965. Fluorometric determination of chlorophyll. J. Conseil. Explor. Mer, **30**(1): 3–15.

Jerome, J.H., Bukata, R.P., and Bruton, J.E. 1983. Spectral attenuation and irradiance in the Laurentian Great Lakes. J. Gt. Lakes Res. **9**(1): 60–68.

Johansson, O.E. 2003. A history of changes in zooplankton community structure and function in Lake Ontario: responses to sholelake remediation and exotic invasions. *In* State of Lake Ontario, past present and future. *Edited by* M. Munawar. Ecovision World Monograph Series, Goodward Books, New Delhi. pp. 221–256.

Kaiblinger, C., Teubner, K., and Dokulil, M.T. 2005. Comparative assessment of phytoplankton photosynthesis using conventional ^{14}C-determination and Fast Repetition Rate Fluorometry in freshwaters. Verh. Int. Verein. Limnol. **29**: 245–256.

Kana, T.M. 1992. Relationship between photosynthetic oxygen cycling and carbon assimilation in *Synechococcus* WH7803 (Cyanophyta). J. Phycol. **28**: 304–308.

Kolber, Z., and Falkowski, P.G. 1993. Use of active fluorescence to estimate phytoplankton photosynthesis *in situ*. Limnol. Oceanogr. **38**: 1646–1665.

Kolber, Z.S., Prasil, O., and Falkowski, P.G. 1998. Measurements of variable chlorophyll fluorescence using fast repetition rate techniques: defining methodology and experimental protocols. Biochim. Biophys. Acta, **1367**(1–3): 88–106.

Lavaud, J., van Gorkom, H.J., and Etienne, A.-L. 2002. Photosystem II electron transfer cycle and chlororespiration in planktonic diatoms. Photosynth. Res. **74**: 51–59.

Leboulanger, C., Dorigo, U., Jacquet, S., Le Berre, B., Paolini, G., and Humbert, J.-F. 2002. Application of a submersible spectrofluorometer for rapid monitoring of freshwater cyanobacterial blooms: a case study. Aquat. Microb. Ecol. **30**: 83–89.

Lewis, M.R., and Smith, J.C. 1983. A small-volume, short-incubation time method for the measurement of photosynthesis as a function of incident irradiance. Mar. Ecol. Prog. Ser. **13**: 99–102.

Makarewicz, J.C. 1997. Phytoplankton composition, abundance, and distribution: nearshore Lake Ontario and Oswego Harbour. J. Gt. Lakes Res. **13**(1): 56–64.

Millard, E.S., Myles, D.D., Johannsson, O.E., and Ralph, K.M.1996*a*. Phytoplankton photosynthesis at two index stations in Lake Ontario 1987–1992: assessment of the long-term response to phosphorus control. Can. J. Fish. Aquat. Sci. **53**: 1092–1111.

Millard, E.S., Myles, D.D., Johannsson, O.E., and Ralph, K.M. 1996*b*. Phosphorus demand of Lake Ontario phytoplankton at two index stations: light vs. phosphorus limitation to growth. Can. J. Fish. Aquat. Sci. **53**: 1112–1124.

Mills, E.L., Leach, J.H., Carlton, J.T., and Secor, C.L. 1993. Exotic species in the Great Lakes: a history of biotic crises and anthropogenic introductions. J. Gt. Lakes Res. **19**: 1–54.

Mills, E.L., Casselman, J.M., Dermott, R., Fitzsimons, J.D., Gal, G., Holeck, K.T., Hoyle, J.A., Johannsson, O.E., Lantry, B.F., Makarewicz, J.C., Millard, E.S., Munawar, I.F., Munawar, M., O'Gorman, R., Owens, R.W., Rudstam, L.G., Schaner, T., and Stewart, T.J. 2003. Lake Ontario: food web dynamics in a changing ecosystem (1970–2000). Can. J. Fish. Aquat. Sci. **60**: 471–490.

Montero, O., Klisch, M., Hader, D.P., and Lubian, L.M. 2002. Comparative sensitivity of seven marine microalgae to cumulative exposure to ultraviolet-B radiation with daily increasing doses. Bot. Mar. **45**: 305–315.

Moore, C.M., Suggett, D.J., Holligan, P.M., Sharples, J., Abraham, E.R., Lucas, M.I., Rippeth, T.P., Fisher, N.R., Simpson, J.H., and Hydes, D.J. 2003. Physical controls on phytoplankton physiology and production at a shelf sea front: an FRRF-based field study. Mar. Ecol. Prog. Ser. **259**: 29–45.

Nilawati, J., Greenberg, B.M., and Smith, R.E.H. 1997. Influence of ultraviolet radiation on growth and photosynthesis of two cold ocean diatoms. J. Phycol. **33**: 215–224.

Olaizola, M., Geider, R.J., Harrison, W.G., Graziano, L.M., Ferrari, G.M., and Schlittenhardt, P.M. 1996. Synoptic study of variations in the fluorescence-based maximum quantum efficiency of photosynthesis across the North Atlantic Ocean. Limnol. Oceanogr. **41**: 755–765.

Olson, R.J., Sosik, H.M., Chekalyuk, A.M., and Shalapyonok, A. 2000. Effects of iron enrichment on phytoplankton in the Southern Ocean during late summer: active fluorescence and flow cytometric analyses. Deep-Sea Res. Part II Top. Stud. Oceanogr. **47**: 3181–3200.

Peltier, G., and Cournac, L. 2002. Chlororespiration. Annu. Rev. Plant. Biol. **52**: 523–550.

Raateoja, M., Seppala, J., and Kuosa, H. 2004. Bio-optical modelling of primary production in the SW Finnish coastal zone, Baltic Sea: fast repetition rate fluorometry in Case 2 waters. Mar. Ecol. Prog. Ser. **267**: 9–26.

Rao, R.R., Skafel, M.G., Howell, T., and Murthy, R.C. 2003. Physical processes controlling taste and odour episodes in Lake Ontario drinking water. J. Gt. Lakes Res. **29**: 70–87.

© 2007 NRC Canada

Schelske, C.L. 1991. Historical nutrient enrichment of Lake Ontario: paleolimnological evidence. Can. J. Fish. Aquat. Sci. **48**: 1529–1538.

Smith, R.E.H., Allen, C.D., and Charlton, M.N. 2004. Dissolved organic matter and ultraviolet radiation penetration in the Laurentian Great Lakes and tributary waters. J. Gt. Lakes Res. **30**: 367–380.

Smyth, T.J., Pemberton, K.L., Aiken, J., and Geider, R.J. 2004. A methodology to determine primary production and phytoplankton photosynthetic parameters from Fast Repetition Rate Fluorometry. J. Plankton Res. **26**: 1337–1350.

Sobrino, C., Montero, O., and Lubian, L.M. 2004. UV-B radiation increases cell permeability and damages nitrogen incorporation mechanisms in *Nannochloropsis gaditana*. Aquat. Sci. **66**: 421–429.

Stainton, M.P., Capel, M.J., and Armstrong, F.A.J. 1977. The chemical analysis of freshwater. 2nd ed. Can. Fish. Mar. Serv. Misc. Spec. Publ. 25.

Suggett, D.J., Kraay, G., Holligan, P.M., Davey, M., Aiken, J., and Geider, R.J. 2001. Assessment of photosynthesis in a spring cyanobacterial bloom using a fast repetition rate fluorometer. Limnol. Oceanogr. **46**: 802–810.

Suggett, D.J., MacIntyre, H.L., and Geider, R.J. 2004. Evaluation of biophysical and optical determinations of light absorption by photosystem II in phytoplankton. Limnol. Oceanogr. Methods, **2**: 316–332.

Tassan, S., and Ferrari, G.M. 1998. Measurement of light absorption by aquatic particles retained on filters: determination of the optical pathlength amplification by the 'transmittance-reflectance' method. J. Plankton Res. **20**: 1699–1709.

Vassiliev, I.R., Prasil, O., Wyman, K.D., Kolber, Z., Hanson, A.K., Prentice, J.E., and Falkowski, P.G. 1994. Inhibition of PS-II photochemistry by PAR and UV-radiation in natural phytoplankton communities. Photosynth. Res. **42**: 51–64.

Vincent, R., Qina, X., McKay, R.M., Miner b, M., Czajkowskic, K., Savinod, J., and Bridgeman, T. 2004. Phycocyanin detection from LANDSAT TM data for mapping cyanobacterial blooms in Lake Erie. Remote Sens. Environ. **89**: 381–392.

Watson, S.B. 2004. Aquatic taste and odour: a primary signal of drinking water integrity. J. Toxicol. Environ. Health A, **67**: 1779–1795.

Williams, P.J.leB. 1993. Chemical and tracer methods of measuring plankton production. ICES Mar. Sci. Symp. **197**: 20–36.

Wetzel, R.G., and Likens, G.E. 1991. Limnological analyses. Springer, New York.

Yu, J., Tang, X.X., Zhang, P.Y., Tian, J.Y., and Dong, S.L. 2005. Physiological and ultrastructural changes of *Chlorella* sp. induced by UV-B radiation. Prog. Nat. Sci. **15**: 678–683.

© 2007 NRC Canada

Distinguishing trophic variation from seasonal and size-based isotopic ($\delta^{15}N$) variation of zooplankton

Blake Matthews and Asit Mazumder

Abstract: We measured the $\delta^{15}N$ of particulate organic matter (POM), *Daphnia pulex* (D), *Holopedium gibberum* (H), *Leptodiaptomus tyrelli* (LT), *Epischura nevadensis* (E), and *Chaoborus trivittatus* (C) over an annual cycle in Council Lake, a pristine, oligotrophic, fishless lake. Annual averages of the $\delta^{15}N$ of plankton (C, LT, E > D, H > POM) matched expected differences in trophic position, but seasonal patterns differed among species. During midsummer, the $\delta^{15}N$ of D, H, and LT increased above the $\delta^{15}N$ of E and C, despite little temporal or spatial variation in the $\delta^{15}N$ of POM (<41 μm). Larger size fractions of POM (41–200 μm) helped explain some of the temporal variability of zooplankton $\delta^{15}N$. Body size of zooplankton was correlated with $\delta^{15}N$ for D, C, and E, which could indicate size-based, trophic-level variation; selective feeding; or physiological differences in ^{15}N enrichment. We propose that detailed time series of $\delta^{15}N$ for multiple zooplankton species can help determine the seasonal variability of trophic structure in zooplankton assemblages.

Résumé : Nous avons mesuré les $\delta^{15}N$ de la matière organique particulaire (POM), de *Daphnia pulex* (D), d'*Holopedium gibberum* (H), de *Leptodiaptomus tyrelli* (LT), d'*Epischura nevadensis* (E) et de *Chaoborus trivittatus* (C) durant un cycle annuel au lac Council, un lac oligotrophe non perturbé et sans poissons. Les valeurs moyennes annuelles de $\delta^{15}N$ du plancton (C, LT, E > D, H > POM) correspondent aux différences attendues, compte tenu des positions trophiques, mais les patrons saisonniers varient d'une espèce à l'autre. Durant la mi-été, les $\delta^{15}N$ de D, H et LT dépassent les $\delta^{15}N$ de E et C, malgré le peu de variation temporelle ou spatiale du $\delta^{15}N$ de POM (<41 μm). Les fractions de plus grande taille de POM (41–200 μm) aident à expliquer une partie de la variabilité temporelle du $\delta^{15}N$ du plancton. Il y a une corrélation entre la taille corporelle du zooplancton et le $\delta^{15}N$ chez D, C et E, ce qui pourrait indiquer une variation du niveau trophique, une alimentation sélective ou des différences physiologiques dans l'enrichissement en $\delta^{15}N$ en fonction de la taille. Nous croyons que des séries chronologiques détaillées de $\delta^{15}N$ pour plusieurs espèces du zooplancton pourraient aider à déterminer la variabilité saisonnière de la structure trophique des peuplements de zooplancton.

[Traduit par la Rédaction]

Introduction

The trophic position of freshwater zooplankton varies among taxa, seasons, and different sizes (or life stages) of the same species (Moore et al. 1994; Sanders et al. 1996; Brandl 2005). Such trophic variation within zooplankton assemblages may arise from spatial and seasonal variation in the importance of algal and microbial food chains in pelagic food webs (Porter 1996). Depending on the species, calanoid and cyclopoid copepods can forage on algae, protists, rotifers, and small cladocerans (Sanders et al. 1996; Brandl 2005). Compared with the more herbivorous cladocerans, calanoids feed more readily on larger prey from the microbial food chain (Porter 1996; Burns and Schallenberg 2001), which could lead to a higher trophic position (sensu Vander Zanden and Rasmussen 1996) of copepods compared with cladocerans (Matthews and Mazumder 2003; Karlsson et al. 2004). Intraspecific, trophic-level variation is also common in many zooplankton species (Moore et al. 1994; Brandl 2005). During their ontogeny, many invertebrate predators, such as *Leptodora*, *Chaoborus*, *Bythotrephes*, and *Mysis*, increase the average size and trophic position of prey in their diet (Moore et al. 1994; Branstrator 1998; Abrusan 2003). Naupliar stages of calanoid and cyclopoid copepods are mainly herbivorous, but can mature into herbivores, detritivores, omnivores, or predators (Chow-Fraser and Wong 1986; Hansen and Santer 1995; Brandl 2005).

Stable isotope analysis (using $\delta^{15}N$) is an intriguing way to reveal the complexities of inter- and intra-specific variation in the trophic position of zooplankton (Kling et al.

Received 21 March 2006. Accepted 18 November 2006. Published on the NRC Research Press Web site at http://cjfas.nrc.ca on 13 January 2007.
J19238

B. Matthews. Department of Zoology, The University of British Columbia, 2370-6270 University Boulevard, Vancouver, BC V6T 1Z4, Canada.
A. Mazumder. Natural Sciences and Engineering Research Council of Canada (NSERC) – Industry Research Chair (IRC) Program on Environmental Management of Drinking Water, Department of Biology, University of Victoria, P.O. Box 3020 STN CSC, Victoria, BC V8N 3N5, Canada.

[1]Corresponding author (e-mail: matthews@zoology.ubc.ca).

 doi:10.1139/F06-168 © 2007 NRC Canada

1992; Matthews and Mazumder 2003; Karlsson et al. 2004). In particular, measuring the seasonal and size-based variation of zooplankton $\delta^{15}N$ may help detect seasonal changes in the trophic structure of plankton communities. Several studies have documented large seasonal variation in the $\delta^{15}N$ of individual zooplankton taxa (Graham 1997; Leggett et al. 2000; Matthews and Mazumder 2005). The $\delta^{15}N$ of *Daphnia* can change by >10‰ over a summer (Matthews and Mazumder 2005), even though differences in $\delta^{15}N$ between a consumer and its resource (trophic enrichment) are typically <3‰ (McCutchan et al. 2003; Vanderklift and Ponsard 2003). Most of the within-taxon temporal variation in the $\delta^{15}N$ of zooplankton is unrelated to trophic-level variation and can be explained by the large, seasonal, isotopic variability of primary producers (Leggett et al. 2000; Lehmann et al. 2004). The difference in $\delta^{15}N$ between zooplankton taxa (Δ_{Z1-Z2}) more likely reflects trophic-level differences (Kling et al. 1992; Matthews and Mazumder 2003; Karlsson et al. 2004). However, there is considerable uncertainty about the $\delta^{15}N$ of primary consumers (Vuorio et al. 2006) and about species-specific differences in ^{15}N enrichment (McCutchan et al. 2003; Vanderklift and Ponsard 2003). Nonetheless, seasonal variation in Δ_{Z1-Z2} could help reveal the dynamics of trophic structure in zooplankton assemblages, but no studies have reported detailed enough time series to explicitly test this hypothesis (Karlsson et al. 2004; Matthews and Mazumder 2005; Perga and Gerdeaux 2005).

Intraspecific variation in $\delta^{15}N$ is often correlated with consumer size (Fry et al. 1999; Genner et al. 2003), but few studies have explored such size-based isotopic variation in plankton (but see Branstrator et al. 2000, 2003). Several zooplankton taxa might exhibit positive relationships between body size and trophic position, based on ontogenetic changes in their diet (Branstrator 1998; Brandl 2005). Therefore, testing for relationships between zooplankton body size and $\delta^{15}N$ might reveal size-based diet variation within species. For example, as *Chaoborus* increases its body size, it may switch from feeding on small cladocerans (low $\delta^{15}N$) to larger copepods (high $\delta^{15}N$). Ultimately, using $\delta^{15}N$ to detect size-based, trophic-level variation of consumers depends on the relationship among $\delta^{15}N$, size, and the trophic position of prey. This is an ongoing challenge because relationships between size and $\delta^{15}N$ can also result from shifts in habitat use (Genner et al. 2003), temporal variation of food sources (Matthews and Mazumder 2005), or size-based variation in a consumer's trophic enrichment of ^{15}N (Overman and Parrish 2001; Trueman et al. 2005).

In this paper, we examine whether the seasonal patterns of zooplankton $\delta^{15}N$ reflect our expectations about trophic-level variation of different instars, sizes, and taxa of zooplankton. We sampled a pristine, fishless, oligotrophic lake (Council Lake) and measured the $\delta^{15}N$ of several common zooplankton species that have well-known dietary preferences, including *Daphnia pulex*, *Holopedium gibberum*, *Leptodiaptomus tyrelli*, *Epischura nevadensis*, and *Chaoborus trivittatus*. These species can all potentially feed on multiple trophic levels (i.e., can all be omnivorous), but they vary in their propensity and ability to do so. Over their lifetime, *D. pulex* and *H. gibberum* tend to be more herbivorous than *L. tyrelli*, *E. nevadensis*, or *C. trivittatus*; however, the actual diet of a zooplankton species will depend on the composition of the available resources (Anderson 1967; Folt and Byron 1989; Fedorenko and Swift 1972). Given the zooplankton assemblage in Council Lake (only a few species each with well-studied feeding behaviors), we expected covariation in the $\delta^{15}N$ of zooplankton over the season (as seen in Perga and Gerdeaux 2005). In addition, we tested for relationships between zooplankton body size and $\delta^{15}N$. We expected a positive relationship between body size and $\delta^{15}N$ for *C. trivittatus*, *E. nevadensis*, and *L. tyrelli*, but did not expect the same relationship for either *D. pulex* or *H. gibberum*.

Table 1. Limnological characteristics of Council Lake for the period May to August 2002.

Parameter	Mean (SE)
Surface area (ha)	17
Max depth (m)	17
Secchi depth (m)	7.8
TP ($\mu g \cdot L^{-1}$)	5.7
TN ($\mu g \cdot L^{-1}$)	77.0
DOC ($\mu g \cdot L^{-1}$)	2200
Chl *a* (<41 μm) ($\mu g \cdot L^{-1}$)	
E	0.50 (0.27)
M	0.69 (0.30)
H	0.89 (0.41)
Chl *a* (>0.7 μm) ($\mu g \cdot L^{-1}$)	
E	0.54 (0.16)
M	0.85 (0.37)
H	1.78 (0.48)

Note: Total phosphorus (TP), total nitrogen (TN), and dissolved organic carbon (DOC) are seasonal averages. Chlorophyll *a* < 41 μm was measured in the epilimnion (E), metalimnion (M), and hypolimnion (H) at the same depths as particulate organic matter (POM) < 41 μm. The standard errors (SE) are based on the number of sampling dates for each average.

Materials and methods

We studied the zooplankton community structure in Council Lake, which is situated on Vancouver Island (48°31′N, 123°41′W), in British Columbia, Canada. Council Lake is a warm, monomictic, oligotrophic lake that rarely freezes over. Detailed limnological data collection in Council Lake began in 2001, and we have compiled data for the summer of 2002 (May to September) from an ongoing research program investigating the water quality of lakes and reservoirs in Victoria, British Columbia (Table 1). Details about the limnological sampling procedures and sample analysis for these data are available elsewhere (Davies et al. 2004).

We sampled zooplankton and particulate organic matter (POM) <41 μm in Council Lake 28 times between 14 February 2002 and 17 March 2003. During lake stratification (May to November), we collected samples every 2 weeks, except in July when we sampled every 3–4 days. We collected daytime samples of zooplankton from the deepest site in the lake using a 50 cm diameter Wisconsin net (64 μm mesh) by vertical tows through the entire water column and horizontal tows through the epilimnion. Samples were

© 2007 NRC Canada

Table 2. Isotopic summary of main food web compartments.

	Mean $\delta^{15}N$ (SE)	25th and 75th percentiles	*n*
Chaoborus trivittatus	5.1 (0.1)	4.5, 5.6	28
Epischura nevadensis	4.9 (0.2)	4.4, 5.2	10
Leptodiaptomus tyrelli	5.2 (0.3)	4.7, 6.0	15
Holopedium gibberum	2.9 (0.4)	1.9, 3.2	18
Daphnia pulex	2.4 (0.3)	1.7, 2.9	28
D. pulex (>1.8 mm)	2.9 (0.3)	2.0, 3.8	22
D. pulex (<1.8 mm)	1.8 (0.3)	1.4, 2.4	25
POM (<41 μm)	1.2 (0.2)	0.2, 1.5	27
E	0.8 (0.2)	0.2, 1.5	17
M	0.7 (0.2)	−0.1, 1.1	17
H	0.8 (0.2)	0.4, 1.3	17

Note: Averages of the zooplankton are for all measurements made during the entire sampling period 14 February 2002 to 17 March 2003. Particulate organic matter (POM) measurements in the epilimnion (E), metalimnion (M), and hypolimnion (H) are from sampling dates during the stratified period (5 May to 20 October).

frozen within 4 h and later sorted into five taxonomic groups (Table 2): *D. pulex*, *H. gibberum*, *L. tyrelli*, *E. nevadensis*, and *C. trivittatus*. Zooplankton individuals were hand-picked with fine-tip tweezers (Excelta) to reduce contamination from other planktonic material.

Prior to isotopic analysis, we measured the body size of all zooplankton individuals and the head length of *C. trivittatus* using a dissecting microscope, a digital camera, and zooplankton counting software (Z-Count). We separated larval instars of *C. trivittatus* on the basis of head length (Fedorenko and Swift 1972). For each cladoceran sample, we selected individuals of varying sizes, but for copepods we tended to exclude the smaller size classes (annual range of average size: *L. tyrelli*, 0.88 to 1.64 mm, $n = 15$; *E. nevadensis*, 1.14–2.19 mm, $n = 10$). *Chaoborus trivittatus* instars II and III only appeared in our samples from the middle of June to the end of July, whereas instar IV larvae were present all year.

In the spring of 2002, we used a Niskin bottle to collect lake water from three depths (2, 8, 16 m). Starting in May 2002, and for the rest of the study, we sampled six depths (~2, 6, 8, 10, 12, 14 m), except in July when we sampled nine depths (1, 3, 5, 7, 8, 9, 12, 14, 16 m). We chose these depths so that during the stratified period we could sample two to three discrete depths in the epilimnion, metalimnion, and hypolimnion. For each sample of POM < 41 μm, we filtered at least 1 L of lake water through a 41 μm Nitex mesh and onto precombusted (550 °C for 1 h) 25 mm GFC filters (Whatman).

Starting in July, we observed a bloom of *Synura lapponica* (a 100–250 μm colonial algae) that was restricted to the hypolimnion (Goldstein et al. 2005). In response, for seven dates in July we filtered >4 L for POM 41–200 μm (POM_{41-200}) from three depths (3, 9, and 14 m) and picked out clumps of POM from our zooplankton net samples that had large aggregations of *S. lapponica* (POM_{SL}), but that also included microzooplankton. We dried the POM filters overnight at 60 °C and packaged them in tin cups for isotopic analysis. We also analyzed chlorophyll *a* for replicate POM_{41} filters by extracting them in 95% ethanol at 4 °C overnight and analyzing the extracts on a spectrophotometer (Ultraspec® 2000, Amersham) using a 10 cm quartz cell (as in Davies et al. 2004). All stable isotope samples were analyzed on a Finnegan Delta Plus Advantage stable isotope ratio mass spectrometer at the Water and Watershed Research Laboratory at the University of Victoria. We included a powdered *Daphnia* internal standard ($\delta^{15}N = 1.7‰$) and found that its standard error was <0.2‰ for each run and among all runs. We used the percent carbon and nitrogen of POM to calculate particulate organic carbon concentrations and molar C/N ratios.

We used SYSTAT v. 10.2 (SYSTAT Software Inc., Point Richmond, California) for all our statistical analysis. Residuals from all analyses of variance (ANOVAs) and linear regressions were normally distributed, and Levene's tests indicated homogeneity of variance among groups. We used Pearson's *r* to test for relationships between variables, and in one case we used a nonparametric Spearman's rank correlation.

Results

Variation in the $\delta^{15}N$ of zooplankton

Over the entire sampling season, the average $\delta^{15}N$ of *E. nevadensis* and *C. trivittatus* was about 2.4‰ higher than that of *D. pulex* and *H. gibberum* (Table 2). The seasonal average $\delta^{15}N$ of *L. tyrelli* was within 0.5‰ of *E. nevadensis* and *C. trivittatus*, but the difference depended on the time of year (Fig. 1). During July and August, the $\delta^{15}N$ of *D. pulex* and *H. gibberum* increased and surpassed the $\delta^{15}N$ of *E. nevadensis* and *C. trivittatus*. The $\delta^{15}N$ of *L. tyrelli* was similar to *E. nevadensis* and *C. trivittatus* during the unstratified period, but then reached a maximum at the end of July concurrently with the maximum $\delta^{15}N$ of *D. pulex* and *H. gibberum* (Figs. 1, 2).

Isotopic differences among zooplankton taxa depended primarily on the time of year (Fig. 1) and, for some taxa, secondarily on zooplankton body size (Figs. 3, 4, 5). The range of *D. pulex* $\delta^{15}N$ was 10.9‰ over the entire sampling period, and *D. pulex* body size accounted for 25% of this seasonal variability ($F_{[1,91]} = 31.4$, $r^2 = 0.25$, $p < 0.001$; Fig. 3*a*). Using nonparametric rank correlation (samples ranked for each sampling day), we found that larger *D. pulex* had a higher $\delta^{15}N$ than smaller *D. pulex* (Fig. 3*b*; Spearman's rank correlation: $r_S = 0.786$, $p < 0.001$). Isotopic differences between large (>1.8 mm) and medium-sized (<1.8 mm) *D. pulex* (categorized post hoc based on Fig. 4*a*) depended on the time of year (Fig. 4*b*). Only large *D. pulex* ever exceeded 5‰ (Fig. 4*b*) and on average were 1.1‰ (SD = 0.9, $n = 19$) higher than medium-sized *D. pulex*. Body size and $\delta^{15}N$ were uncorrelated in *H. gibberum* ($r = 0.01$, $p = 0.42$) over a narrow size range (0.8 to 1.2 mm), though the amplitude of variation in $\delta^{15}N$ of *H. gibberum* was similar to that of *D. pulex* (Fig. 1*b*).

In July and August, when instars II, III, and IV of *C. trivittatus* were all present in the water column, we found that $\delta^{15}N$ of *C. trivittatus* increased by about 0.5‰·mm^{-1} of head length (Fig. 5). The slope of this positive relationship was not significantly different between months (analysis of

© 2007 NRC Canada

Fig. 1. (*a* and *b*) Temporal variability of plankton $\delta^{15}N$ in Council Lake in 2002 to 2003. Error bars are ±1 SE, based on between one and five replicates per day. The period of thermal stratification is shown with broken vertical lines.

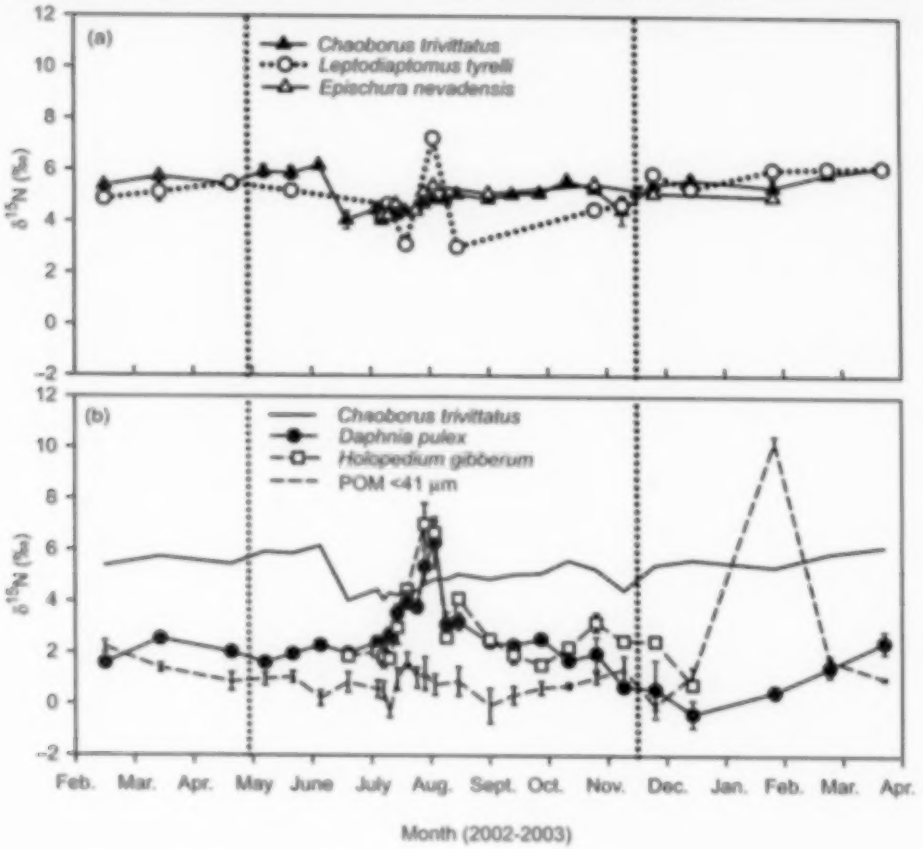

covariance, ANCOVA: $F_{[1,59]} = 0.004$, $p = 0.81$), but the intercept was slightly higher in August. The sharp drop in the $\delta^{15}N$ of *C. trivittatus* in the middle of June can partially be explained by the appearance of instar II and III larvae in our samples that had a lower $\delta^{15}N$. However, the $\delta^{15}N$ of instar IV larvae also declined by ~1‰ in June and then increased over the summer.

Seasonal variation in body size and $\delta^{15}N$ was positively correlated in *E. nevadensis* ($r = 0.55$, $p = 0.042$) but not significantly correlated in *L. tyrelli* ($r = 0.23$, $p = 0.33$). The maximum size of *L. tyrelli* (1.64 mm) coincided with its maximum $\delta^{15}N$ (7.3‰), but 2 weeks later a similar sized sample (1.56 mm) had a $\delta^{15}N$ of 3.0‰. In the current study, we only have a limited seasonal range of copepod body sizes, so we do not discuss potential ontogenetic trophic variation in these two copepod taxa.

Temporal change in the composition of POM

The range in the $\delta^{15}N$ of POM < 41 μm (POM_{41}) was 12.5‰ over the entire study period (Fig. 2; Table 2). Excluding 20 January 2003, the total range of $\delta^{15}N$ for POM_{41} was 6.0‰ (minimum = –1.5‰, maximum = 4.5‰). The average range in the $\delta^{15}N$ of POM_{41} over the entire water column was 2.3‰ (SE = 0.27, $n = 27$). During the stratified period (May to October), the average POM_{41} $\delta^{15}N$ was not significantly different among strata (Table 2; ANOVA, $F_{[2,48]} = 0.06$, $p = 0.95$). During July and August, when the $\delta^{15}N$ of *D. pulex*, *H. gibberum*, and *L. tyrelli* reached their maxima, the $\delta^{15}N$ of POM_{41} did not increase substantially. As a result, the average isotopic difference between *D. pulex* and POM_{41} ($\Delta_{D\text{-}POM41}$) was 3.1‰ during July and August (range: 2.2‰–5.6‰) and only 1.4‰ (range: 0.6‰–2.1‰) for the rest of stratification. The $\delta^{15}N$ of larger size fractions of POM (POM_{41-200} and POM_{SL}) increased rapidly prior to the peak $\delta^{15}N$ of *D. pulex*, *H. gibberum*, and *L. tyrelli* (Fig. 2*b*). The $\delta^{15}N$ of POM_{41-200} peaked on 17 July just prior to the peak $\delta^{15}N$ for *H. gibberum* (26 July) and *D. pulex* (31 July), whereas the $\delta^{15}N$ of POM_{SL} fraction increased to a 31 July maximum that was higher than that of either *D. pulex* or *H. gibberum*. We cannot explain the large isotopic excursion of POM_{41} on 20 January 2003. Lehmann et al. (2004) also found a high $\delta^{15}N$ for POM in the winter and attributed it to algal uptake of recycled nitrogen.

The C/N of POM_{41} was highest during thermal stratification and reached its two highest values on the 12th and 17th of July. On these two days, the average carbon concentration (PC) of POM in the water column (0.17 mg C·L^{-1})

© 2007 NRC Canada

Fig. 2. (*a*) Temporal variability of average water column chlorophyll *a* (Chl *a*), particulate organic carbon (PC), and C/N ratio for particulate organic matter (POM) < 41 μm from Fig. 1. The right axis shows both the concentration of PC (in mg C·L^{-1}) and one-sixth of the actual Chl *a* concentration (in μg·L^{-1}). The seasonal average of Chl *a* in Council Lake for this period is 0.65 μg·L^{-1}. (*b*) Comparison of *Daphnia pulex* δ^{15}N with the δ^{15}N of other plankton size fractions (see text) and a fraction dominated by *Synura lapponica* (POM_{SL}).

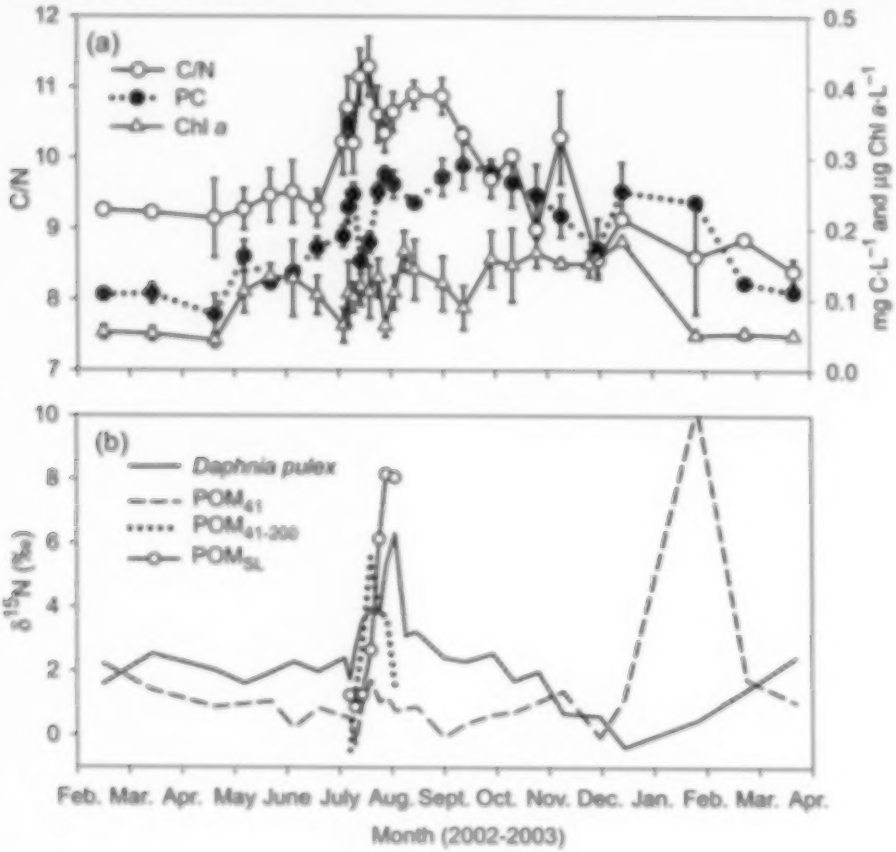

was ~30% lower than during the rest of stratification (Fig. 2*a*). This week of low PC (low food quantity) with a high C/N (low food quality) occurred a week before the maximum δ^{15}N of *D. pulex*. However, Chl *a* (indicator of algal biomass) was not unusually low during this time period. The Chl *a* of POM_{41} was typically <1 μg·L^{-1} and was lowest in the spring and at the beginning of July and August (Fig. 2*a*).

Vertical variation in the composition of POM

Previous zooplankton sampling in Council Lake (2001) revealed that *D. pulex* feed in the hypolimnion during the day and night in July (Matthews and Mazumder 2006). Therefore, in July 2002 we increased our sampling frequency and depth resolution of POM to test for potential effects of feeding depth on the δ^{15}N of zooplankton. We found that the δ^{15}N of POM_{41} did not increase with depth and that the C/N was highest in the metalimnion and lowest in the hypolimnion (Fig. 6). Size-fractionated Chl *a* revealed that algal abundance was highest in the hypolimnion, particularly in larger size fractions. The average δ^{15}N of POM_{41-200} in July was 2.6‰ (~2‰ higher than POM_{41}) and did not vary among strata (ANOVA: $F_{[2,19]} = 2.59$, $p = 0.10$).

Discussion

Studies that make repeated seasonal measurements of δ^{15}N for multiple taxa are rare in the literature, despite their potential for elucidating the dynamics of food web structure (Grey et al. 2001; Matthews and Mazumder 2005; Mooney and Tillberg 2005). A major challenge with this approach is to distinguish trophic-level variation from isotopic variation (δ^{15}N). In eutrophic lakes, the δ^{15}N of POM can change by >10‰ over the summer because of the biogeochemical cycling of nitrogen or because of changes in the δ^{15}N of the lake's nitrogen source (Lehmann et al. 2004; Leavitt et al. 2006). In the current study, we found large seasonal variation in the δ^{15}N of zooplankton despite little seasonal variation in the δ^{15}N of POM. More importantly, we found that the differences in δ^{15}N between zooplankton taxa strongly depended on the time of year and that the δ^{15}N of the more herbivorous zooplankton surpassed the δ^{15}N of the more carnivorous zooplankton. We

© 2007 NRC Canada

Fig. 3. (*a*) Relationship between average *Daphnia pulex* body size and $\delta^{15}N$ for all samples picked in Council Lake over the entire study period. Each sample is a composite of >20 individuals. The solid circles are during thermal stratification of the lake, and the open circles are samples from the rest of the year. (*b*) Relationship between *D. pulex* size rank and the $\delta^{15}N$ rank for each sampling day with two or more samples (maximum seven). We have applied a random jitter to reduce overlapping points. Spearman's rank correlation is positive significant (r_S = 0.786, $p < 0.001$).

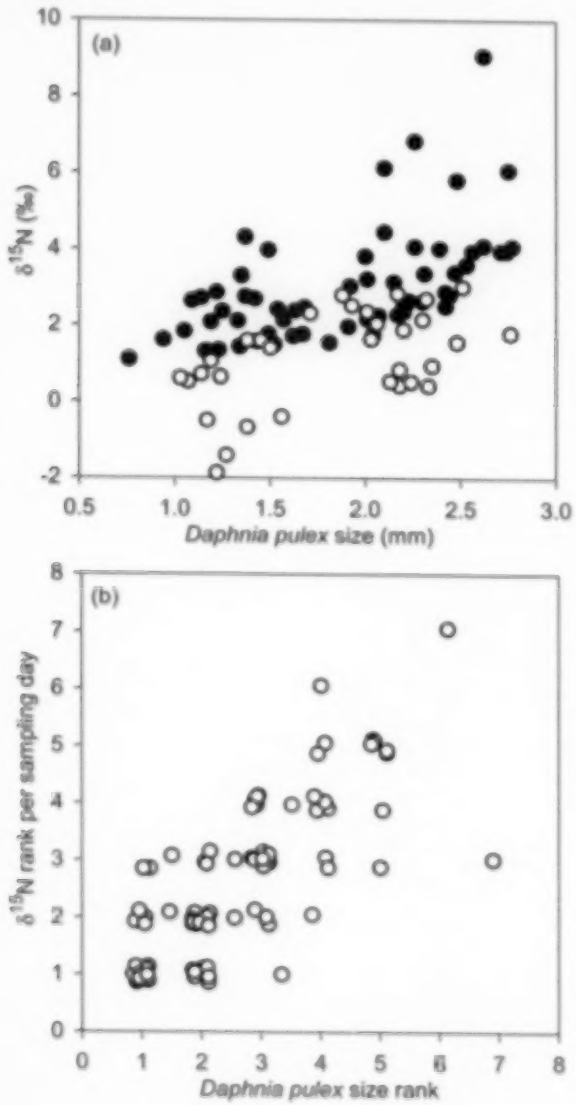

also found positive relationships between body size and $\delta^{15}N$ for both *D. pulex* and *C. trivittatus*. We conclude that both seasonal and size-based variation in the $\delta^{15}N$ of consumers should be considered when using $\delta^{15}N$ to detect trophic-level variation in natural communities. We believe this conclusion is generally applicable to studies of trophic-level variation of consumers in diverse ecosystems.

Fig. 4. (*a*) Average body size of *Daphnia pulex* individuals (n = 30 to >100 per sample) for each sampling event (n = 1 to 5 samples per day). In both panels, solid circles are large *D. pulex* (>1.8 mm), and open circles are medium-sized *D. pulex* (<1.8 mm). (*b*) $\delta^{15}N$ of each sample in panel (*a*) over the sampling season.

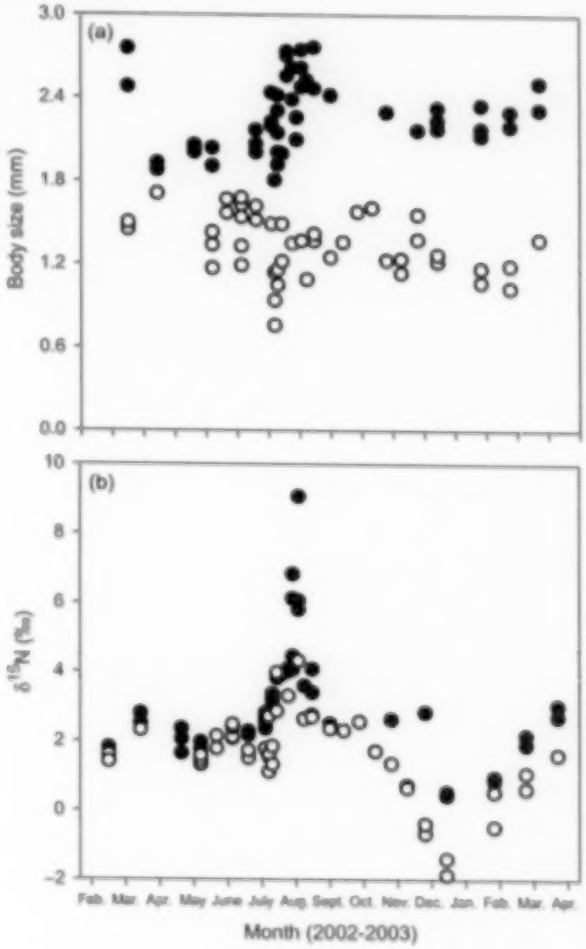

Seasonal variation of $\delta^{15}N$

Ecological studies are increasingly using time series of $\delta^{15}N$ to detect omnivory in complex food webs (Lancaster et al. 2005; Mooney and Tillberg 2005). Our study has revealed additional complexities involved in detecting trophic-level variation using $\delta^{15}N$. The $\delta^{15}N$ of the more herbivorous zooplankton (*D. pulex*, *H. gibberum*) rapidly increased and surpassed the $\delta^{15}N$ of the more predacious zooplankton (*E. nevadensis*, *C. trivittatus*), despite little variation in the $\delta^{15}N$ of presumed basal food sources (POM_{41}). O'Reilly et al. (2002) argued that abrupt variation in the $\delta^{15}N$ at the base of a food chain can lead to a distortion in the isotopic representation of food web inter-

© 2007 NRC Canada

Fig. 5. Relationship between head length and $\delta^{15}N$ for *Chaoborus trivittatus* in July (open triangles) and August (solid triangles) in Council Lake. Vertical broken lines denote instar separation following Fedorenko and Swift (1972). Each data point is a composite of multiple individuals. The regression equation for July is $\delta^{15}N = 3.8$ (standard error, SE = 0.12) + 0.54 (SE = 0.10)·length ($F_{[1,41]} = 28.48$, $p < 0.001$, $r^2 = 0.41$), and for August is $\delta^{15}N = 4.2$ (SE = 0.16) + 0.59 (SE = 0.13)·length ($F_{[1,16]} = 26.6$, $p < 0.001$, $r^2 = 0.53$).

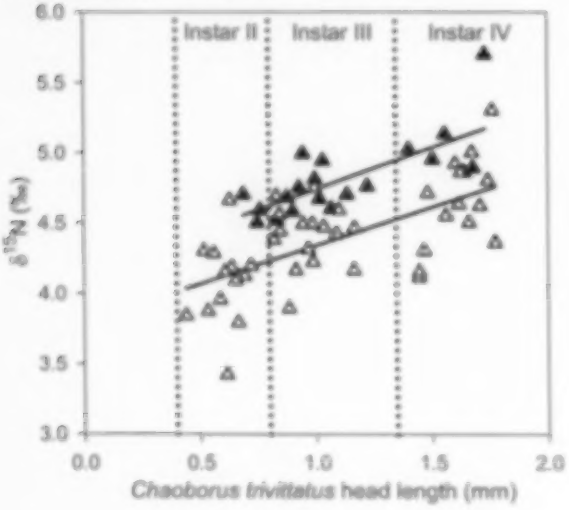

actions. This is unlikely the case in Council Lake, because the $\delta^{15}N$ of POM_{41}, which is a grazable size fraction for herbivorous zooplankton, did not increase rapidly prior to the peak $\delta^{15}N$ of zooplankton.

It is difficult to explain why the $\delta^{15}N$ of *D. pulex* and *H. gibberum* increased rapidly during midsummer in Council Lake. Larger size fractions of plankton (POM_{41-200} and POM_{SL}) also increased rapidly in early July and peaked just prior to the maximum $\delta^{15}N$ of large *D. pulex*. We visually confirmed, by looking at fecal pellets, that copepods can ingest colonies of *S. lapponica* (which makes up POM_{SL}), but we found no evidence of *S. lapponica* in the gut of large *D. pulex*. However, the $\delta^{13}C$ of both POM_{41-200} and POM_{SL} are similar to large *D. pulex* in Council Lake, suggesting that large *D. pulex* either directly consume these large size fractions or rely on a similar carbon source (Matthews 2006). The maximum particle size ingested by cladocerans increases with body size (Burns 1968), and it is possible that large *D. pulex* (>1.8 mm) can graze particles >41 µm. We are less certain that the high $\delta^{15}N$ of POM_{41-200} and POM_{SL} can explain the seasonal patterns of *H. gibberum* $\delta^{15}N$, because *H. gibberum* tend to graze a smaller size range of particles, particularly in oligotrophic lakes (Cyr 1998). Supporting this conclusion, the $\delta^{13}C$ of *H. gibberum* is more similar to the $\delta^{13}C$ of POM_{41} above the hypolimnion (Matthews and Mazumder 2006). Instead, we suspect that the $\delta^{15}N$ of POM_{41} masks the food source that *H. gibberum* assimilates. POM is a heterogeneous mixture of algae, detritus, and heterotrophs and may mask the $\delta^{15}N$ of any food source that makes up a small fraction of the total POM nitrogen (Vuorio et al. 2006). It is possible that small algae within POM_{41} follow a similar $\delta^{15}N$ pattern as larger algae in POM_{41-200}, provided they rely on the same source of dissolved inorganic nitrogen, and similarly discriminate against ^{15}N during uptake (but see Needoba et al. 2003). We believe that a combination of selective feeding by zooplankton within POM_{41} and direct feeding on larger size classes of POM can explain the large increase in $\delta^{15}N$ of *D. pulex*, *H. gibberum*, and *L. tyrelli* during midsummer in Council Lake.

The vertical distribution of zooplankton food sources did not help resolve seasonal patterns of zooplankton $\delta^{15}N$ in Council Lake. Algal biomass and food quality (indicated by C/N) were both highest in the hypolimnion (>10 m). In a separate study, we found that zooplankton species in Council Lake differentially exploited deepwater algal resources (Matthews and Mazumder 2006). This led to divergent seasonal patterns in the $\delta^{13}C$ of *D. pulex* and *H. gibberum* that were associated with differences in feeding depth (Matthews and Mazumder 2006). Large *D. pulex* were rarely observed above the hypolimnion, and medium-sized *D. pulex* and *H. gibberum* were common in the epi- and meta-liminion. This vertical habitat segregation of zooplankton cannot directly explain the different seasonal $\delta^{15}N$ patterns among taxa, because there was little spatial variation with depth in the $\delta^{15}N$ of POM_{41} and POM_{41-200}.

Size-based intrapopulation variation of $\delta^{15}N$

It is a common difficulty to determine whether size-based variation of a consumer's $\delta^{15}N$ reflects trophic-level variation (Fry et al. 1999; Genner et al. 2003) or just size-based variation in the $\delta^{15}N$ of food sources that have the same trophic position. Our results from Council Lake provide some of the first evidence (see also Branstrator et al. 2003) that $\delta^{15}N$ can increase with body size in both a herbivore (*D. pulex*) and a predator (*C. trivittatus*). The positive relationship for *D. pulex* could occur if large individuals prey more on heterotrophs that have a higher $\delta^{15}N$ than algae. However, we are uncertain if the size-based variation in the $\delta^{15}N$ of POM is related to trophic-level differences among *D. pulex* diet items, so we cannot confirm that larger *D. pulex* are at a higher trophic position. In Council Lake, the situation is complicated by *S. lapponica*, which dominates the POM_{41-200} size fraction. Little is known about the ecology of *S. lapponica*, but it is a large colonial algae (100–250 µm) and may be mixotrophic (Pipes and Leedale 1992), which could explain its high $\delta^{15}N$ relative to POM_{41}. We can only speculate about a possible influence of mixotrophy on the $\delta^{15}N$ of zooplankton in Council Lake.

The positive relationship between $\delta^{15}N$ and body size of *C. trivittatus* is consistent with life history omnivory (sensu Branstrator et al. 2000), but we cannot exclude alternate hypotheses. *Chaoborus* is a size-selective predator whose gape width increases throughout its ontogeny, potentially leading to the positive relationship between *C. trivittatus* body size and $\delta^{15}N$. To attribute this relationship to trophic-level variation, we have to confirm that size-based variation in $\delta^{15}N$ of prey items also reflects trophic-level variation. If *C. trivittatus* switches from small cladocerans to copepods, then Fig. 5 could indicate trophic-level variation. Alternatively, the $\delta^{15}N$ of *C. trivittatus* may increase with body size because of a diet switch from small to large *D. pulex*. We

© 2007 NRC Canada

Fig. 6. Depth profiles of chlorophyll *a* (Chl *a*), particulate carbon (PC), molar C/N ratio, and δ^{15}N for particulate organic matter (POM) < 41 μm in July. Error bars are all ±1 SE based on seven sampling dates in July. The temperature profile was taken on 12 July 2002 at the deepest site in Council Lake. Solid circles show samples taken from water filtered through a 41 μm mesh, whereas open circles are unfiltered.

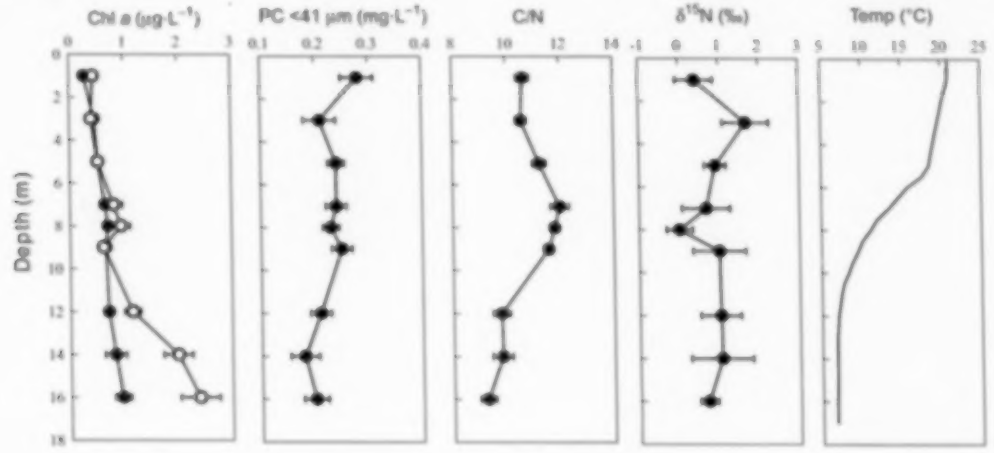

cannot confirm size-based trophic-level variation in *C. trivittatus* (life history omnivory), because we could not confirm that the positive relationship between *D. pulex* body size and δ^{15}N reflects trophic-level differences. Species of *Chaoborus* are known to exhibit life history omnivory (Moore et al. 1994), and perhaps combining size-based isotopic analysis with gut content analysis would help quantify the trophic position of different larval instars (Fedorenko and Swift 1972).

Uncertainties in zooplankton trophic enrichment of ^{15}N

Uncertainties in trophic enrichment (i.e., the difference in δ^{15}N between consumers and their diet: Δ_N) currently challenge all our attempts at using δ^{15}N to detect seasonal differences in trophic position. Temporal variation in Δ_N of zooplankton relative to POM_{41} may partially explain the decoupling of δ^{15}N between zooplankton and POM_{41}.

The quantity, quality, and identity of zooplankton food are seasonally variable in Council Lake and may affect the Δ_N of herbivores (Spence and Rosenheim 2005). Adams and Sterner (2000) found that the δ^{15}N of *Daphnia magna* increased by ~2.5‰ concurrently with an increase in the C/N of an algal food source from 7.3 to 24.8. The C/N of POM in Council Lake only increased by ~1.4 following thermal stratification. Nonetheless, we found a positive relationship between the C/N of POM and the difference in δ^{15}N between *D. pulex* and POM < 41 μm for all sampling dates ($\Delta_{D\text{-}POM41}$ = −15.4 + 1.7(C/N), $p < 0.01$) and for all dates excluding 20 January 2003 ($\Delta_{D\text{-}POM41}$ = −8.6 + 1.03(C/N), $p < 0.01$). This result is consistent with the direction but not the magnitude of Adams and Sterner's (2000) experimental result that the Δ_N of *D. magna* increases with increasing food source C/N. However, we found no significant relationship between POM C/N and the difference in δ^{15}N between *H. gibberum* and POM_{41} ($\Delta_{H\text{-}POM41}$ = −5.1 + 0.7(C/N), $p = 0.17$). Given the rapid increase in the δ^{15}N of the large POM size fractions and the uncertainty about the zooplankton assimilation of POM_{41}, we believe it is unlikely that a 4‰ increase in the δ^{15}N of *D. pulex* and *H. gibberum* is solely a result of an increase in the C/N of POM_{41}. Future studies would benefit from more detailed analysis of the composition of POM and from experiments that determine the sources of variation in zooplankton ^{15}N enrichment.

Positive relationships between a consumer's size (or age) and δ^{15}N may result from size-based variation in trophic enrichment (Δ_N), but the current research is inconclusive. Some studies suggest that Δ_N increases with organism age (Overman and Parrish 2001), whereas others have found no correlation between age and Δ_N (Minagawa and Wada 1984; Hobson and Clark 1992). Size-based variation in the nitrogen balance of *Daphnia* could lead to relationships between *Daphnia* size and δ^{15}N. For example, larger *Daphnia* may have a higher trophic enrichment than smaller *Daphnia* if ingestion rate increases with body size and digestion efficiency decreases with body size (Power et al. 2003). Alternatively, if larger *Daphnia* are more susceptible to starvation then the δ^{15}N of *Daphnia* could increase with size (Adams and Sterner 2000). We believe this is unlikely in Council Lake because the summertime peak of *D. pulex* δ^{15}N coincided with a peak lipid content of large *D. pulex* (Matthews 2006). There are several physiological mechanisms that could lead to size-based variation in δ^{15}N, but no studies have attempted to resolve these issues for *Daphnia* or any other zooplankton taxa.

Distinguishing trophic-level variation from isotopic variation

It is a general challenge for stable isotope studies to determine the source of temporal variation in the δ^{15}N of consumers and determine if it is related to trophic-level variation. A promising new approach involves coupling information about the rates of nitrogen flux among food web compartments with seasonal changes in the δ^{15}N of food web compartments (Rastetter et al. 2005). In our study, we can draw conclusions by comparing the relative seasonal patterns of each zooplankton species. The δ^{15}N of *L. tyrrelli* generally

© 2007 NRC Canada

tracked the $\delta^{15}N$ of *C. trivittatus*, except for a few weeks in July and August when it followed the $\delta^{15}N$ of *D. pulex* and *H. gibberum*. This suggests that *L. tyrelli* switched its feeding behavior during this time period to more closely match the food sources of *D. pulex* and *H. gibberum*. This is consistent with a previous study that found the diet of *L. tyrelli* depended on the availability of food sources (Anderson 1967). The $\delta^{15}N$ of *E. nevadensis* was always within 0.5‰ of *C. trivittatus*, which is consistent with *E. nevadensis*'s more predatory style of feeding (Folt and Byron 1989).

Aquatic food webs consist of algal and microbial food chains that are intertwined (Porter 1996). Multiple pathways of nitrogen flow through a food web (i.e., multiple food chains) could explain the divergent seasonal $\delta^{15}N$ patterns of zooplankton in Council Lake. The $\delta^{15}N$ of a zooplankton species gives an indication of the temporal integration of the nitrogen cycle leading up to that species in the food chain (Robinson 2001). If a zooplankton community consists of a simple food chain, we would expect covarying seasonal patterns of $\delta^{15}N$ among taxa (with some time lags). In accordance with this expectation, Perga and Gerdeaux (2005) found seasonally correlated patterns of zooplankton $\delta^{15}N$ in Lake Geneva. Lake Geneva has many of the same zooplankton groupings (*Leptodora*, *Bythotrephes*, copepods, and *Daphnia*) as in Council Lake (*Chaoborus*, copepods, *Daphnia*), but in Council Lake, the divergent $\delta^{15}N$ patterns suggest a different food web organization. Therefore, we speculate that Council Lake has multiple food chains (i.e., algal and microbial) and that zooplankton species differentially rely on alternate pathways of nitrogen transfer from basal resources. This is consistent with the observation that the zooplankton species in Council Lake differentially rely on allochthonous carbon (Matthews and Mazumder 2006). We propose that time series of $\delta^{15}N$ for multiple consumer taxa may help detect alternate nitrogen pathways through complex food webs.

Acknowledgements

We thank K. Young, J. Samodien, and M. Stojkovic for help with sorting and preparing zooplankton for stable isotopes and N. Bock, I. Patchett, M. Schwarzfeld, C. Peet, and A. Miskelly for help in the field. R. Hesslein, P. Leavitt, M. Perga, J.M. Davies, K. Young, and P. Ramsay provided helpful comments and editorial corrections. We especially thank S. Mazumder for her work on the manuscript. This research has been supported by an NSERC – Canada Graduate Scholarship to B.M. and an NSERC–IRC grant and industrial support (Capital Regional District Water Department, Greater Vancouver Water Department) to A.M.

References

Abrusan, G. 2003. Morphological variation of the predatory cladoceran *Leptodora kindtii* in relation to prey characteristics. Oecologia, **134**: 278–283.

Adams, T.S., and Sterner, R.W. 2000. The effect of dietary nitrogen content on the trophic level ^{15}N enrichment. Limnol. Oceanogr. **45**: 601–607.

Anderson, R. 1967. Diaptomid copepods from two mountain ponds in Alberta. Can. J. Zool. **45**: 1043–1047.

Brandl, Z. 2005. Freshwater copepods and rotifers: predators and their prey. Hydrobiologia, **546**: 475–489.

Branstrator, D.K. 1998. Predicting diet composition from body length in the zooplankton predator *Leptodora kindtii*. Limnol. Oceanogr. **43**: 530–535.

Branstrator, D.K., Cabana, G., Mazumder, A., and Rasmussen, J.B. 2000. Measuring life history omnivory in the opposssum shrimp, *Mysis relicta*, with stable nitrogen isotopes. Limnol. Oceanogr. **45**: 463–467.

Branstrator, D.K., Mwebaza-Ndawula, J.P., and Montoya, J.P. 2003. Resource–consumer relationships in Lake Victoria, East Africa. Hydrobiologia, **493**: 27–34.

Burns, C.W. 1968. The relationship between body size of filter feeding Cladocera and the maximum size of particle ingested. Limnol. Oceanogr. **13**: 675–678.

Burns, C.W., and Schallenberg, M. 2001. Calanoid copepods versus cladocerans: consumer effects on protozoa in lakes of different trophic status. Limnol. Oceanogr. **46**: 1558–1565.

Chow-Fraser, P., and Wong, C. 1986. Dietary change during development in the freshwater calanoid copepod *Epischura lacustris* Forbes. Can. J. Fish. Aquat. Sci. **43**: 938–944.

Cyr, H. 1998. Cladoceran- and copepod-dominated zooplankton communities graze at similar rates in low-productivity lakes. Can. J. Fish. Aquat. Sci. **55**: 414–422.

Davies, J.M., Nowlin, W.H., and Mazumder, A. 2004. Temporal changes in nitrogen and phosphorus codeficiency of plankton in lakes of coastal and interior British Columbia. Can. J. Fish. Aquat. Sci. **61**: 1538–1551.

Fedorenko, A.Y., and Swift, M.C. 1972. Comparative biology of *Chaoborus americanus* and *Chaoborus trivittatus* in Eunice Lake, British Columbia. Limnol. Oceanogr. **17**: 721–730.

Folt, C., and Byron, E.R. 1989. A comparison of the effects of prey and non-prey neighbors on foraging rates of *Epischura nevadensis* (Copepoda, Calanoida). Freshw. Biol. **21**: 283–293.

Fry, B., Memford, P.L., Tam, F., Fox, D.D., Warren, G.L., Havens, K.E., and Steinman, A.D. 1999. Trophic position and individual feeding histories of fish from Lake Okeechobee, Florida. Can. J. Fish. Aquat. Sci. **56**: 590–600.

Genner, M.J., Hawkins, S.J., and Turner, G.F. 2003. Isotopic change throughout the life history of a Lake Malawi cichlid fish. J. Fish Biol. **62**: 907–917.

Goldstein, M., McLachlan, J., and Moore, J. 2005. Morphology and reproduction of *Synura lapponica* (Synurophyceae). Phycologia, **44**: 566–571.

Graham, M.D. 1997. Omnivory and selective feeding by zooplankton along a lake production gradient: complementary ^{15}N isotope and gut pigment analyses. M.Sc. thesis, University of Regina, Sask.

Grey, J., Jones, R.I., and Sleep, D. 2001. Seasonal changes in the importance of the source of organic matter to the diet of zooplankton in Loch Ness, as indicated by stable isotope analysis. Limnol. Oceanogr. **46**: 505–513.

Hansen, A.M., and Santer, B. 1995. The influence of food resources on the development, survival and reproduction of the two cyclopoid copepods: *Cyclops vicinus* and *Mesocyclops leuckarti*. J. Plankton Res. **17**: 631–646.

Hobson, K.A., and Clark, R.G. 1992. Assessing avian diets using stable isotopes. 2. Factors influencing diet–tissue fractionation. Condor, **94**: 189–197.

Karlsson, J., Jonsson, A., Meili, M., and Jansson, M. 2004. $\delta^{15}N$ of zooplankton species in subarctic lakes in northern Sweden: effects of diet and trophic fractionation. Freshw. Biol. **49**: 526–534.

Kling, G.W., Fry, B., and O'Brien, W.J. 1992. Stable isotopes and planktonic trophic structure in arctic lakes. Ecology, **73**: 561–566.

© 2007 NRC Canada

Lancaster, J., Bradley, D.C., Hogan, A., and Waldron, S. 2005. Intraguild omnivory in predatory stream insects. J. Anim. Ecol. **74**: 619–629.

Leavitt, P.R., Brock, C.S., Ebel, C., and Patoine A. 2006. Landscape-scale effects of urban nitrogen on a chain of freshwater lakes in central North America. Limnol. Oceanogr. **51**: 2262–2277.

Leggett, M.F., Johannsson, O., Hesslein, R., Dixon, D.G., Taylor, W.D., and Servos, M.R. 2000. Influence of inorganic nitrogen cycling on the Lake Ontario biota. Can. J. Fish. Aquat. Sci. **57**: 1489–1496.

Lehmann, M.F., Bernasconi, S.M., McKenzie, J.A., Barbieri, A., Simona, M., and Veronesi, M. 2004. Seasonal variation of the $\delta^{13}C$ and $\delta^{15}N$ of particulate and dissolved carbon and nitrogen in Lake Lugano: constraints on biogeochemical cycling in a eutrophic lake. Limnol. Oceanogr. **49**: 415–429.

Matthews, B. 2006. Food web ecology of zooplankton communities in lakes. Ph.D. thesis, University of Victoria, B.C.

Matthews, B., and Mazumder, A. 2003. Compositional and interlake variability of zooplankton affect baseline stable isotope signatures. Limnol. Oceanogr. **48**: 1977–1987.

Matthews, B., and Mazumder, A. 2005. Consequences of large temporal variability of zooplankton $\delta^{15}N$ for estimates of fish trophic position and variation. Limnol. Oceanogr. **50**: 1404–1414.

Matthews, B., and Mazumder, A. 2006. Habitat specialization and the exploitation of allochthonous carbon by zooplankton. Ecology, **87**: 2800–2812.

McCutchan, J.H., Lewis, W.M., Kendall, C., and McGrath, C.C. 2003. Variation in trophic shift for stable isotopes ratios of carbon, nitrogen, and sulfur. Oikos, **102**: 378–390.

Minagawa, M., and Wada, E. 1984. Stepwise enrichment of ^{15}N along food chains: further evidence and the relation between ^{15}N and animal age. Geochim. Cosmochim. Acta, **48**: 1135–1140.

Mooney, K.A., and Tillberg, C.V. 2005. Temporal and spatial variation of ant omnivory in pine forests. Ecology, **86**: 1225–1235.

Moore, M., Yan, N., and Pawson, T. 1994. Omnivory of the larval phantom midge (*Chaoborus* spp.) and its potential significance for freshwater planktonic food webs. Can. J. Zool. **72**: 2055–2065.

Needoba, J.A., Waser, N.A., Harrison, P.J., and Calvert, S.E. 2003. Nitrogen isotope fractionation in 12 species of marine phytoplankton during growth on nitrate. Mar. Ecol. Prog. Ser. **255**: 81–91.

O'Reilly, C.M., Hecky, R.E., Cohen, A.S., and Plisnier, P.D. 2002. Interpreting stable isotopes in food webs: recognizing the role of time averaging at different trophic levels. Limnol. Oceanogr. **47**: 306–309.

Overman, N., and Parrish, D. 2001. Stable isotope composition of walleye: ^{15}N accumulation with age and area-specific differences in $\delta^{13}C$. Can. J. Fish. Aquat. Sci. **58**: 1253–1260.

Perga, M., and Gerdeaux, D. 2005. 'Are fish what they eat' all year round? Oecologia, **144**: 598–606.

Pipes, L.D., and Leedale, G.F. 1992. Scale formation in *Tessellaria volvocina* (Synurophyceae). Br. Phycol. J. **27**: 11–19.

Porter, K. 1996. Integrating the microbial loop and the classic grazer food chain into a realistic planktonic food web. *In* Food webs: integration of patterns and dynamics. *Edited by* G. Polis and K.O. Winemiller. Chapman and Hall, New York. pp. 51–59.

Power, M.E., Guiguer, K.R.R.A, and Barton, D.R. 2003. Effects of temperature on isotopic enrichment in *Daphnia magna*: implications for aquatic food-web studies. Rapid Commun. Mass Spectrom. **17**: 1619–1625.

Rastetter, E.B., Kwiatkowski, B.L., and McKane, R.B. 2005. A stable isotope simulator that can be coupled to existing mass balance models. Ecol. Appl. **15**: 1772–1782.

Robinson, D. 2001. $\delta^{15}N$ as an indicator of the nitrogen cycle. Trends. Ecol. Evol. **16**: 153–162.

Sanders, R.W., Williamson, C.E., Stutzman, P.L., Moeller, R.E., Goulden, C.E., and Aoki-Goldsmith, R. 1996. Reproductive success of 'herbivorous' zooplankton fed algal and non-algal food resources. Limnol. Oceanogr. **41**: 1295–1305.

Spence, K.O., and Rosenheim, J.A. 2005. Isotopic enrichment in herbivorous insects: a comparative field based study of variation. Oecologia, **146**: 89–97.

Trueman, C.N., McGill, R.A.R, and Guyard, P.H. 2005. The effect of growth rate on tissue-diet isotopic spacing in rapidly growing animals. An experimental study with Atlantic salmon (*Salmo salar*). Rapid Commun Mass Spectrom. **19**: 3239–3247.

Vanderklift, M., and Ponsard, S. 2003. Sources of variation in consumer-diet $\delta^{15}N$ enrichment: a meta-analysis. Oecologia, **136**: 169–182.

Vander Zanden, M.J., and Rasmussen, J.B. 1996. A trophic position model of pelagic food webs: impacts on contaminant bioaccumulation in lake trout. Ecol. Monogr. **66**: 451–477.

Vuorio, K., Meili, M., and Sarvala, J. 2006. Taxon specific variation in the stable isotopic signatures ($\delta^{13}C$ and $\delta^{15}N$) of lake phytoplankton. Freshw. Biol. **51**: 807–822.

© 2007 NRC Canada

The role of seasonally altering photoperiod in regulating physiology in Atlantic cod (*Gadus morhua*). Part I. Sexual maturation

Andrew Davie, Mark J.R. Porter, Niall R. Bromage, and Herve Migaud

Abstract: While the Atlantic cod (*Gadus morhua*) displays clear seasonality in its reproductive cycle, the exact photic signal that entrains this rhythm is yet undefined. This present work developed a model to describe the photic regulation of reproduction in the species in comparison with other commercially important temperate teleosts. This was achieved through the strategic masking of the natural photoperiod cycle during the first 2 years of life with the application of continuous illumination. The results demonstrated that it is the falling autumnal photoperiod signal after the summer solstice, more specifically after October, that is responsible for recruiting individuals to enter the sexual maturation cycle. Furthermore, in all treatments where this signal was masked through the application of continuous illumination, there was no significant reproductive activity and growth was improved by up to 60% at 27 months posthatch. This information is of particular value to the developing cod aquaculture industry in which the management of reproduction using artificial photoperiod manipulation will be of vital economic importance.

Résumé : Bien que la morue Atlantique (*Gadus morhua*) soit caractérisée par un cycle de reproduction très saisonnier, le signal lumineux à l'origine de ce rythme n'a pas encore été déterminé. Notre étude a permis de développer un modèle de régulation du cycle de reproduction par la lumière chez cette espèce en comparaison avec d'autres espèces de téléostéens commercialement importantes en région tempérée. Pour cela, le cycle naturel de la photopériode a été masqué par l'application de périodes d'éclairement continu de façon stratégique durant les 2 premières années de vie. Les résultats de notre étude démontrent l'importance de la diminution de la durée du jour en automne après le solstice d'été, et plus précisément après le mois d'octobre, pour entraîner les individus dans le cycle de la maturation sexuelle. De plus, dans tous les régimes où ce signal a été masqué par l'application de périodes d'éclairement, aucun signe de développement sexuel n'a été observé chez les populations et leur croissance mesurée après 27 mois après l'éclosion a augmenté jusqu'à 60 %. Ces résultats sont tout particulièrement importants pour l'industrie en émergence de la pisciculture de la morue dans laquelle l'utilisation de régimes photopériodiques afin de contrôler la reproduction est d'importance économique vitale.

Introduction

Atlantic cod (*Gadus morhua*) is one of the most economically important teleost species in the northern Atlantic region both for its fisheries value and more recently for its recognized aquaculture potential. However, one of the most significant hurdles inhibiting the potential productivity of the aquaculture industry is loss of growth and product quality owing to early puberty under culture conditions (Hansen et al. 2001; Davie et al. 2003; Hemre et al. 2004). Furthermore, broadcast spawning in production cages represents a significant environmental concern because of the potential for genetic pollution of local wild stocks. Such early maturation is a problem common to many other cultured teleost species and as such, a number of management strategies exist, which can allow the farmer to inhibit, prevent, or avoid maturation during commercial ongrowing. These include photoperiod manipulation (Bromage et al. 2001), monosex production (Donaldson and Hunter 1982), or sterilization through ploidy manipulation (Cotter et al. 2000; Benfey 2001). To date, in Atlantic cod, two main experimental approaches (dietary–nutritional restriction (Karlsen et al. 1995) and photoperiod manipulation (Hansen et al. 2001; Davie et al. 2003)) have been examined to regulate sexual maturation during ongrowing. The use of artificial photoperiod manipulation (e.g., continuous illumination (LL)) is increasingly becoming standard operating practice within the aquaculture industry for a number of species such as Atlantic salmon (*Salmo*

Received 21 March 2006. Accepted 29 September 2006. Published on the NRC Research Press Web site at http://cjfas.nrc.ca on 19 January 2007.
J19234

A. Davie,[1] M.J.R. Porter,[2] N.R. Bromage,[3] and H. Migaud. Institute of Aquaculture, University of Stirling, Stirling, Scotland, FK9 4LA, UK.

[1]Corresponding author (e-mail: andrew.davie@stir.ac.uk).
[2]Present address: Ridely Aquafeed, P.O. Box 187, Deception Bay, Queensland, 4508, Australia.
[3]Deceased.

 doi:10.1139/F06-169 © 2007 NRC Canada

salar) (Porter et al. 1999; Endal et al. 2000) or European sea bass (*Dicentrarchus labrax*) (Begtashi et al. 2004). Because of this general acceptance, the cod farming sector views the use of photoperiod management as the most favourable methodology to employ.

To date, all photoperiod designs to regulate maturation in Atlantic cod have focused on applying LL on, or after, the summer solstice prior to maturation at 2 years of age (Dahle et al. 2000; Hansen et al. 2001; Davie et al. 2003). While these tank-based trials reported the prevention of spawning at 2 years of age, evidence suggested the presence of underlying endogenous maturation rhythms. This is evident from maturing males (gonadosomatic index elevated to 6% in 9% of population reared under LL) observed by Hansen et al. (2001) and a suppression of growth in conjunction with observed gonadal development and regression in Davie (2005) and Davie et al. (2003). Such observations are in accordance with results obtained in cod maintained under artificial illumination in open cage systems both in the United Kingdom (A. Davie, C. Blair, N. Bromage, and H. Migaud, unpublished data) and in Norway (Taranger et al. 2006) where spawning was not prevented; rather, it was delayed by 3–5 months. This demands that the potential entrainment of sexual maturation by photoperiod rhythms before the summer solstice prior to spawning should be further investigated.

Photoperiod regulation of physiological processes like reproduction are explained using a gating theory in which a proximate photic signal is used as a rate-limiting step that individuals of a suitable energetic condition can proceed through to initiate sexual maturation (Bromage et al. 2001). These individuals will then spawn at a later date, the timing of which is regulated by ultimate cues, the principal of which is temperature. Duston and Saunders (1992) have characterized the photoperiod windows that regulate sexual maturation as well as smolting in Atlantic salmon. In cod, however, such a proximate photic window has not yet been defined.

This present study was designed to further our understanding of photoperiod regulation of sexual maturation and somatic growth in Atlantic cod. To this end, the work had two principal aims: the first was to explore the significance of seasonally altering photoperiod in regulating puberty through targeted masking of the seasonal cycle by application of LL at key stages throughout the first 2 years of rearing. The second aim (reported more extensively in Davie et al. 2007) was to examine thereafter the interaction between photoperiod exposure, somatic growth, and sexual maturation. While answering fundamental questions concerning the environmental regulation of key physiological traits in Atlantic cod, this work is also of great commercial value by assisting the aquaculture sector in developing species-specific management strategies that will improve productivity and reduce negative environmental impacts.

Materials and methods

Fish stocks and rearing conditions

On 26 September 2001, 630 six-month-old immature Atlantic cod juveniles (Machrihanish Marine Farms, Machrihanish, UK) previously reared under natural photoperiod and temperature regimes at the Machrihanish Marine Environmental Research Laboratory (55°44′N, 5°44′W) were individually tagged with a passive integrated transponder tag (Avid Plc, Uckfield, UK). Fish were stocked into 7 m^3 indoor, lightproof tanks at the Machrihanish Marine Environmental Research Laboratory. Tanks were supplied with seawater filtered to 60 µm at a flow rate of ~50 $L \cdot min^{-1}$ and drained to waste. Throughout the experimental period, water temperature ranged from 5 to 15 °C (Fig. 1) and salinity ranged between 29‰ and 34‰. Fish were held within a stocking density range of 10–30 $kg \cdot m^{-3}$. Artificial light was provided by two 9 W fluorescent bulbs (Osram Dulux S G23 energy saver, Osram, St Helens, UK) located centrally under the tank cover ~0.5 m above the water surface. Light intensity at the water surface was 0.32 $W \cdot m^{-2}$ (1.705 $\mu mol \cdot m^{-2} \cdot s^{-1}$ or 105 lx) when illuminated and 0 $W \cdot m^{-2}$ in the dark phase (irradiance measured using NPL calibrated light meters supplied by Skye Instruments Ltd., Powys, UK). During the experimental period, the fish were fed to satiation four times per day, 7 days a week with a commercial dry pellet (Cod DANA-EX; DANA Feed A/S, Horsens, Denmark).

Experimental design

All individuals were randomly assigned to one of eight photoperiod treatments (Fig. 1; Table 1). Unequal numbers (n = 50–110) were assigned to populations to optimize the experimental setup owing to the restricted animal numbers and tank facilities available. Photoperiod treatments in tanks were held constant (simulated natural photoperiod or LL) with experimental populations being transferred between tanks as the experimental photoperiod regime dictated. The number of treatment tanks used (Table 2) was regulated by fish number and size with the stocking density ranges being the limiting factors. Where more than one treatment tank (i.e., simulated natural photoperiod or LL) was required, individuals for each photoperiod group were evenly assigned between the tanks. Every 3 months, tank biomass was recalculated following the complete population sampling (described below) and tank depth was adjusted by standpipe height to balance and return stocking densities to a common basal level in accordance with the predetermined range. On 8 July 2003, all experimental treatments were terminated.

Data sampling and analysis

From 1 October 2001 onwards, a 3-monthly sampling schedule was undertaken. At each sample time, following anaesthesia (1:10000 concentration of 2-phenoxyethanol; Sigma-Aldrich Co. Ltd., Poole, UK), individuals were measured for whole-body weight (±0.1 g) and total length (±1 mm). Specific growth rate (SGR) and thermal growth coefficient (TGC) were calculated using the respective formulae $SGR = (e^g - 1) \times 100$, where $g = [\ln(W_2) - \ln(W_1)] \times (t_2 - t_1)^{-1}$, and $TGC = \{[(W_2)^{1/3} - (W_1)^{1/3}] \times 1000\} \times (\text{degree-days})^{-1}$, where W_2 and W_1 are the weight at time t_2 and t_1, respectively. Maturation status for each individual was visually assessed at each time point with individuals being designated mature when gametes were released on inspection. Additional checks for maturation status were also made on 24 February 2003 and 28 May 2003 in all populations.

As part of the 3-monthly sampling schedule, 10 individuals were preselected at random from each different photo-

© 2007 NRC Canada

Fig. 1. Summary of experimental photoperiod treatments 1–8 (black line) in relation to ambient temperature (grey line). Horizontal bars represent periods when mature males (black) and females (grey) releasing gametes were observed for the respective treatments. The percentage of the total population being recorded as spawning (% maturation) is listed.

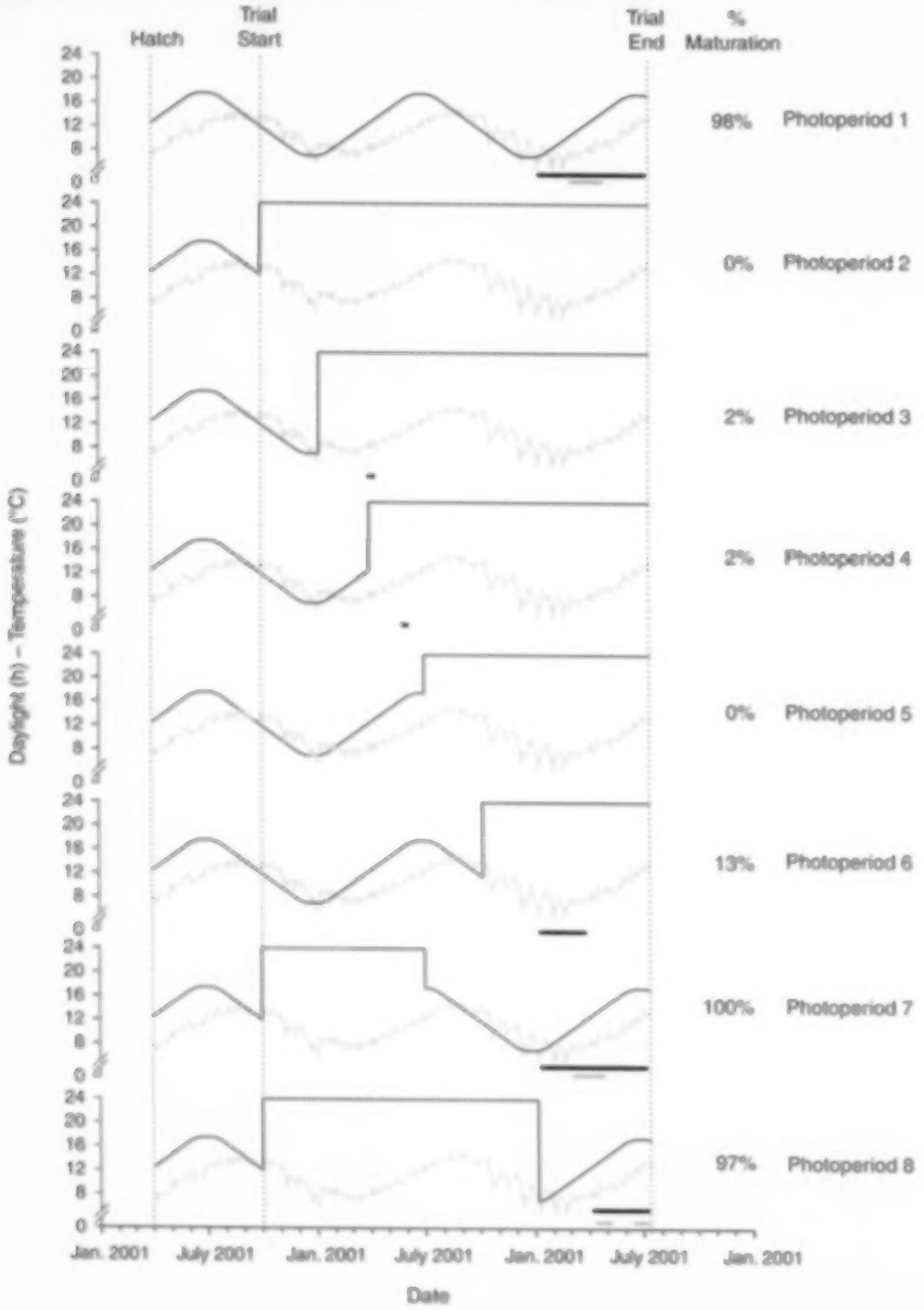

© 2007 NRC Canada

Table 1. Experimental groups listing the number of individuals at setup and a description of the respective photoperiod treatment.

Photoperiod treatment	No. of individuals	Description
1	110	Simulated natural photoperiod (SNP)
2	100	SNP until 1 October 2001 (6 MPH) and then continuous illumination (LL)
3	90	SNP until 1 January 2002 (9 MPH) and then LL
4	80	SNP until 1 April 2002 (12 MPH) and then LL
5	70	SNP until 1 July 2002 (15 MPH) and then LL
6	60	SNP until 1 October 2002 (18 MPH) and then LL
7	70	SNP until 1 October 2001 (6 MPH), then LL until 1 July 2002 (15 MPH), and then SNP
8	50	SNP until 1 October 2001 (6 MPH), then LL until 1 January 2003 (21 MPH), and then SNP

Note: MPH, months posthatch.

Table 2. Summary of the number of tanks used and their allocation to the photoperiod treatments in association with the presence of experimental populations.

Date	SNP photoperiod		LL photoperiod	
	Treatment groups	No. of tanks	Treatment groups	No. of tanks
Oct. 2001 – Jan. 2002	1, 3, 4, 5, 6	1	2, 7, 8	1
Jan. 2002 – Apr. 2002	1, 4, 5, 6	1	2, 3, 7, 8	1
Apr. 2002 – July 2002	1, 5, 6	1	2, 3, 4, 7, 8	2
July 2002 – Oct. 2002	1, 6, 7	1	2, 3, 4, 5, 8	3
Oct. 2002 – Jan. 2003	1, 7	2	2, 3, 4, 5, 6, 8	4
Jan. 2003 – July 2003	1, 7, 8	2	2, 3, 4, 5, 6	4

Note: SNP, simulated natural photoperiod; LL, continuous illumination.

period treatment. Once identified, these individuals were sacrificed (Table 3) (note: sampling error caused this number to vary between 4 and 11 individuals and the sex ratio was variable because of the random selection process). Following morphometric measurements, a blood sample was withdrawn into heparinized syringes and the plasma, separated by centrifugation at 1200*g* for 15 min at 4 °C, was stored at –70 °C prior to later analysis. Plasma levels of testosterone and estradiol-17β were measured using a direct radioimmunoassay according to Duston and Bromage (1987). Testosterone and estradiol standards (Sigma-Aldrich Co. Ltd.) stored in absolute ethanol at –20 °C at a concentration of 94 and 75 pg·mL^{-1}, respectively, were used to check the reproducibility of measurements. The intraassay coefficient of variation was 7.7% (n = 4) and 10.6% (n = 4), respectively, and the interassay coefficient of variation was 14.4% (n = 80) and 10.9% (n = 8), respectively, for testosterone and eastrdiol-17β. Plasma total calcium concentrations (indirect measurement of vitellogenin) were measured by atomic absorbtion spectrophotometry according to Elliot et al. (1984).

Gonads were removed and weighed to 0.01 g. The gonadosomatic index (GSI) was calculated using GSI = (gonad weight/whole-body weight) × 100. Thereafter, gonads were preserved in 10% buffered formalin for histological analysis. Gonad samples from July 2003 (three males and three females from each photoperiod treatment) were dehydrated and embedded in wax. Sections were cut at 5 µm, stained using Mayers haematoxylin and eosin Y, and examined under a light microscope to determine developmental stages. Ovarian sections were classified according to Tomkiewicz et al. (2003) and testis sections according to Dahle et al. (2003). Furthermore, the diameters of 100 randomly chosen oocytes (longest diameter through the nucleus) were measured for each female using digital image processing software (Image-Pro Plus™; Media Cybernetics, Silver Spring, Maryland).

At times when populations experienced common photoperiod histories, terminal samples were taken from one population and the subsequent data assigned to all relevant treatments within the respective time point (e.g., April 2002 data for photoperiods 1, 4, 5, and 6 are from the same 10 individuals). This was necessary because of the restricted availability of experimental animals. At the end of the experiment, in July 2003, there remained a core group of 32–43 individuals per photoperiod treatment. These were sacrificed and dissected to record the sex of the individuals.

Statistical analysis

The data were analysed using MINITAB® release 14.13 (Minitab Ltd., Coventry, UK). Hormone levels, GSI data, and oocyte diameters were analysed using a general linear model (Zar 1999). Normality and homogeneity of variance were improved where necessary by either log or reciprocal transformations. GSI data were first subjected to arcsine transformation. A significance level of $p < 0.05$ was set with all significant interactions being analysed with a Tukey post hoc test. Maturation and mortality rates (described as a percentage) were analysed using analysis of proportions where 95% confidence limits were calculated for the respective proportions (Fowler and Cohen 1987). When the upper and lower confidence limits of the respective proportions were not found to overlap, the proportions were considered to be statistically different at the 5% level ($p = 0.05$). In all cases, the data are presented as mean ± SE of the mean.

© 2007 NRC Canada

Table 3. Numbers of individual males (M) and females (F) terminally sampled at each sample time for each photoperiod treatment (1–8).

	January 2002		April 2002		July 2002		October 2002		January 2003		April 2003		July 2003	
Photoperiod treatment	M	F	M	F	M	F	M	F	M	F	M	F	M	F
1	5	4	6	4	7	3	3	6	3	1	2	7	5	5
2	6	4	4	6	7	3	5	5	6	4	5	5	3	5
3	5	4	5	4	5	5	5	5	7	1	6	4	4	6
4	5	4	6	4	3	5	4	6	4	5	6	3	6	4
5	5	4	6	4	7	3	5	5	3	7	6	4	6	4
6	5	4	6	4	7	3	3	6	1	6	8	2	5	5
7	6	4	4	6	7	3	5	5	6	4	3	7	5	3
8	6	4	4	6	7	3	5	5	6	4	4	6	8	3

Results

Sex ratios and mortality

The overall population sex ratio (males to females) was 1:1.19; the range within the treatment groups was 1:0.94 to 1:1.58. Throughout the trial period, the overall mortality rate was 5%. The range within the photoperiod groups was 1.4%–8.3%; however, there was no significant difference between treatments.

Spawning and gonadal development

In the spring–summer of 2002 (up to 14 months posthatch (MPH)), there were only two observed sexually mature individuals (males). The first individual, sacrificed during a terminal sampling in April (12 MPH), was a male from photoperiod 3 with a GSI of 1.9%. The second individual, a male from photoperiod 4, was observed to be releasing milt during a routine monthly inspection on 10 June 2002 (14 MPH). As this was not a scheduled sampling, the entire population was not inspected. The next complete sample performed 1 month later on 9 July 2002 revealed no individuals releasing gametes in any treatment.

In the second year of the trial, mature individuals were observed in four of the photoperiod treatments. These were in treatments 1, 6, 7, and 8 (Figs. 1 and 2). For both photoperiods 1 and 7, the spawning season lasted from January through to July 2003 (21–27 MPH) with a peak in activity in April 2004 (24 MPH) (98% of both populations releasing gametes on inspection). While all individuals in photoperiod 7 ($n = 39$) were recorded as releasing gametes by the trial's end (27 MPH), in photoperiod 1 ($n = 43$), a single female (2% of the population) was not. In both treatments, males were spermiating from January to July 2003; however, females were only observed to be ovulating from the end of February (22 MPH) through to April (24 MPH). In the population reared under photoperiod 6, the spawning season lasted from January through to April 2003 (21–24 MPH). Only five spermiating males, representing 13% of the population ($n = 40$), were recorded as releasing gametes throughout the trial. The peak of activity was in January (21 MPH); thereafter, one male (3% of the population) continued to release milt until April (24 MPH). Under photoperiod treatment 8, the spawning season lasted from April to July 2003 (24–27 MPH). Individuals of both sexes were observed to be mature in April (23% of the total population) with the peak in spawning activity being observed in July 2003 when 80% of the population were releasing gametes on inspection. Overall, however, 97% of the total population (population $n = 35$) were recorded as releasing gametes by the end of the trial, while a single female (3%) was not.

There were no significant differences in mean gonad weights between treatments up to October 2002 (18 MPH) (Fig. 3) with GSI levels remaining below 0.4% for males and 0.8% for females (with the exception of a single male under photoperiod 3 in April 2002 with a GSI of 1.9%). In January 2003 (21 MPH), gonad weight was significantly higher in photoperiods 1 (males: females 3.9%:5.1%) and 7 (males:females 5.1%:6.9%) than in all other treatments with the exception of a single male in photoperiod 6 (GSI = 3%). The female GSI in photoperiod 6 doubled from a basal level of ~0.6% to 1.2% ($n = 9$) owing to a single female with a GSI of 4.6%. The remaining individuals had a mean GSI of 0.6% ($n = 8$). In all other treatments, GSI levels remained below 0.3% for males and 1.5% for males. In April 2003 (24 MPH), GSI values peaked for treatments 1 (males:females 10.1%:12.2%) and 7 (males:females 10.7%:9.7%), which coincided with the peak in spawning activity. Such sizes were significantly larger than all other treatments except those under photoperiod 7, which had risen to 6.5% and 2.7% in the males and females, respectively. By July 2003 (27 MPH), GSI levels in photoperiods 1 and 7 had fallen to be comparable with those of treatments 2–6 (males:females <0.4%:<1.5%), while gonad weights continued to rise in photoperiod 8 (males:females 8.7%:9.9%) in relation to the increase in spawning activity.

Plasma testosterone, estradiol-17β, and calcium

Mean plasma testosterone levels in males ranged between a minimum of 0.31 ng·mL^{-1} and a maximum of 10.5 ng·mL^{-1} (Fig. 4*a*). Males under treatments 2–5 maintained levels ≤2 ng·mL^{-1} throughout the course of the experiment. In photoperiods 1 and 7, up to July 2002 (15 MPH), testosterone levels remained at basal levels below 2 ng·mL^{-1} after which levels increased, and from January to April 2003 (21–24 MPH), mean plasma concentrations were ≥7 ng·mL^{-1} before returning to basal levels in July 2003. Fish under photoperiod 8 displayed a similar profile with the peak values (10.5 ± 2.1 ng·mL^{-1}, $n = 3$) delayed to July 2003 (27 MPH). While under photoperiod 6, with the exception of an apparent rise in testosterone in October 2002 (15 MPH, 2.6 ± 0.5 ng·mL^{-1}, $n = 3$) as was observed under photoperiods 1 and 7 at this time, mean plasma concentrations remained below 2 ng·mL^{-1} during the course of the experiment.

© 2007 NRC Canada

Fig. 2. Percentage of males and females within the total population releasing gametes while maintained under photoperiods 1, 6, 7, and 8 in the 2003 spawning season (n = 33–43). Different letters denote significant differences between overall treatments.

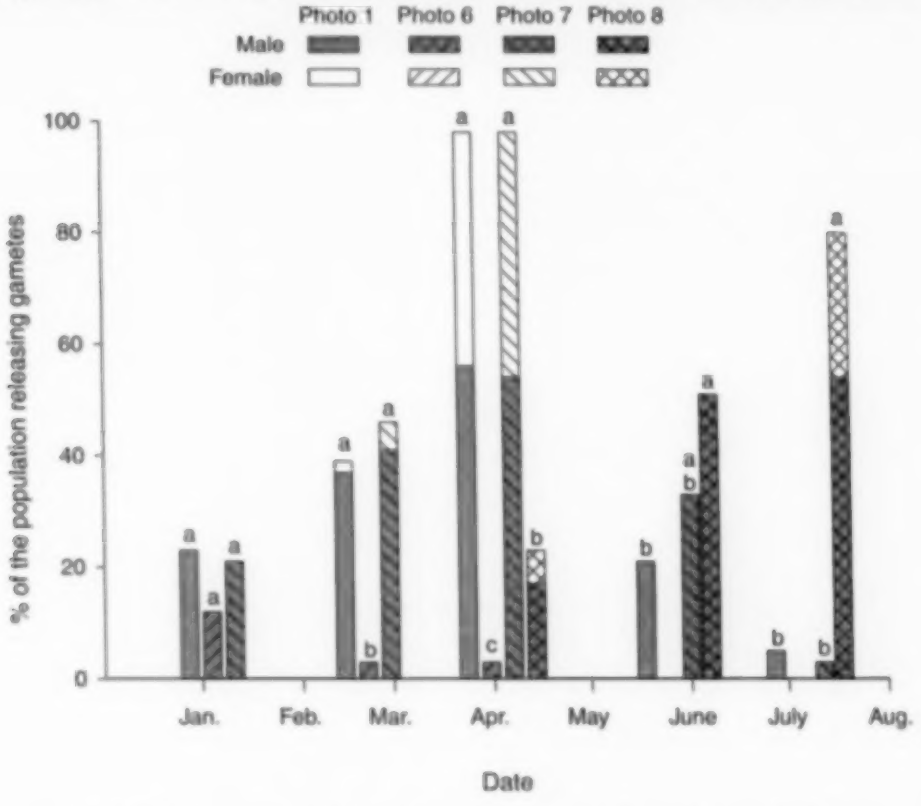

Mean plasma estradiol-17β concentrations in females ranged between a minimum of 1.2 ng·mL^{-1} and a maximum of 13.1 ng·mL^{-1} (Fig. 4*b*). Profiles were comparable with those observed for testosterone in males. Mean plasma concentrations remained below 4 ng·mL^{-1} throughout the course of the experiment in all treatments with the exception of the January and April 2003 (21 and 24 MPH) samples for photoperiods 1 and 7 as well as the July 2003 sample for photoperiod 8, at which times the plasma concentrations (>8 ng·mL^{-1}) were significantly higher than in all other treatments.

As with estradiol-17β, calcium concentrations in females from photoperiods 2–6 maintained a constant basal level of ~140–170 mg·dL^{-1} throughout the trial (Fig. 4*c*). Levels in photoperiods 1 and 7 rose significantly in January 2003 (21 MPH) to ≥200 mg·dL^{-1} and thereafter declined to return to basal levels in July 2003 (27 MPH). As for photoperiod 8, calcium levels rose above the basal levels after January 2003 (21 MPH) to reach a peak of >200 mg·dL^{-1} in April 2003 (24 MPH), which was maintained to the trial's end.

Gonad histology

At the trial's end (27 MPH) in photoperiods 1, 7, and 8, male testes contained large areas of spermatozoa with no earlier germ cell stages apparent (Figs. 5*a* and 5*e*). Testis samples from treatments 2–6 were dominated by the earlier developmental stages of spermatogonia and spermatocytes; however, in all samples examined, there were limited pockets of spermatozoa observed (Fig. 5*c*).

The females in both treatments 1 and 7 were classified as spent (stage VIII), as they possessed a clear mix of primary growth oocytes (diameter = 128 ± 3 and 109 ± 4 µm, respectively) in between postovulatory follicles and atretic (vitellogenic) oocytes (Fig. 5*b*). Under photoperiod 8, the ovarian samples displayed oocytes in various stages of vitellogenesis including those about to enter final oocyte maturation and hence were classified as spawning (stage V) individuals (Fig. 5*f*). Mean oocyte diameter was significantly larger than for all other treatments at 385 ± 14 µm. In the remaining treatments (photoperiods 2–6) (Fig. 5*d*), all females were classified as immature (stage II), with the ovaries containing only previtellogenic oocytes with a mean oocyte diameter <128 µm in all treatments.

Growth performance

There was no significant difference in mean individual size (i.e., weight and length) within the study populations at the start of the experiment (33.2 ± 0.3 g, 146 ± 0.4 mm). Overall growth performance (SGRw, SGRl, and TGC) from 6 to 21 MPH was significantly lower in populations that matured, i.e., those under photoperiods 1, 7, and 8, than in those that did not (Table 4). This differential growth performance was reflected in the final weight and length (Table 4) where populations under photoperiods 2–6 were significantly

© 2007 NRC Canada

Fig. 3. Mean gonadosomatic index ± SE of the mean for (*a*) males (n = 1–9) and (*b*) females (n = 1–7) for individuals maintained under photoperiod treatments 1–8. Horizontal bars denote periods when spermiating males or spawning females were present. Where significant differences existed within a given date, homogeneous subsets are enclosed within an ellipse.

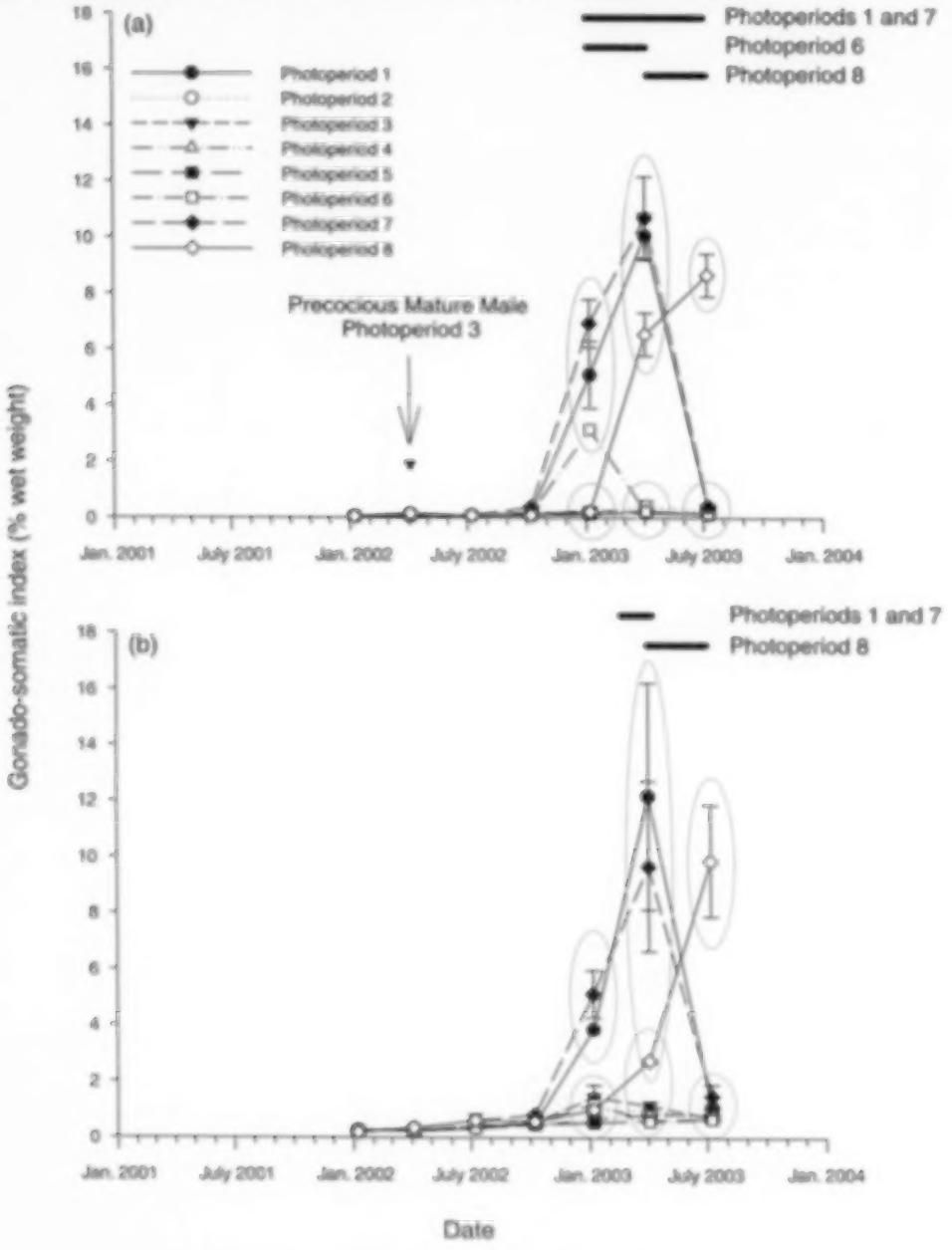

larger than those under photoperiods 1 and 7, while those under photoperiods 3–5 were significantly larger than those under photoperiod 8.

Discussion

While Norberg et al. (2004) demonstrated that photoperiod acts as an important "zeitgeiber" for the timing of spawning in Atlantic cod, definitions of the entraining photoperiod signals have not been forthcoming. This study demonstrated that transition to LL at or before 15 MPH (or in other words the summer solstice prior to first maturation) held individuals in an immature state. Hence, it can be concluded that a descending photoperiod on or after this date (15 MPH) will recruit individuals to begin the maturation cycle. With the exception of two precocious males observed

© 2007 NRC Canada

Fig. 4. Mean plasma (*a*) testosterone concentration in males (n = 1–9) and (*b*) estradiol-17β concentration and (*c*) calcium concentration in females (n = 1–7) maintained under photoperiod treatments 1–8. Horizontal bars denote periods when spermiating or spawning individuals were present. Where significant differences existed on a given date, homogeneous subsets are enclosed within an ellipse.

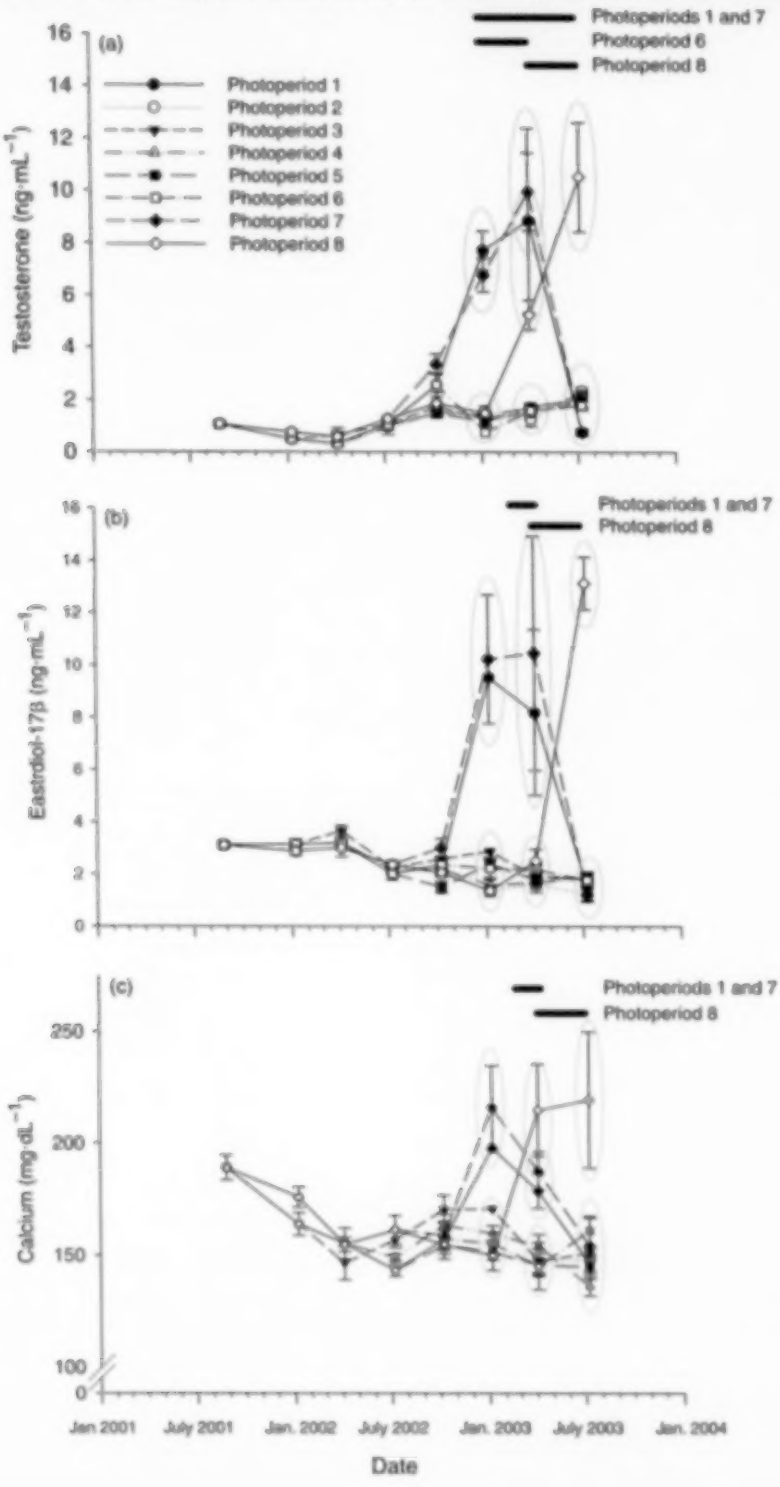

© 2007 NRC Canada

Fig. 5. Photomicrographs of sections (5 µm thick) of Atlantic cod (*Gadus morhua*) gonads taken in July 2003 (27 MPH, trial end) from (*a*) a male and (*b*) a female maintained under photoperiod 1 typical of the morphology observed under photoperiods 1 and 7, (*c*) a male and (*d*) a female maintained under photoperiod 2 typical of the morphology observed under photoperiods 2–6, and (*e*) a male and (*f*) a female maintained under photoperiod 8. Scale bar divisions = 25 µm in Figs. 5*a*, 5*c*, and 5*e* and 100 µm in Figs. 5*b*, 5*d*, and 5*f*.

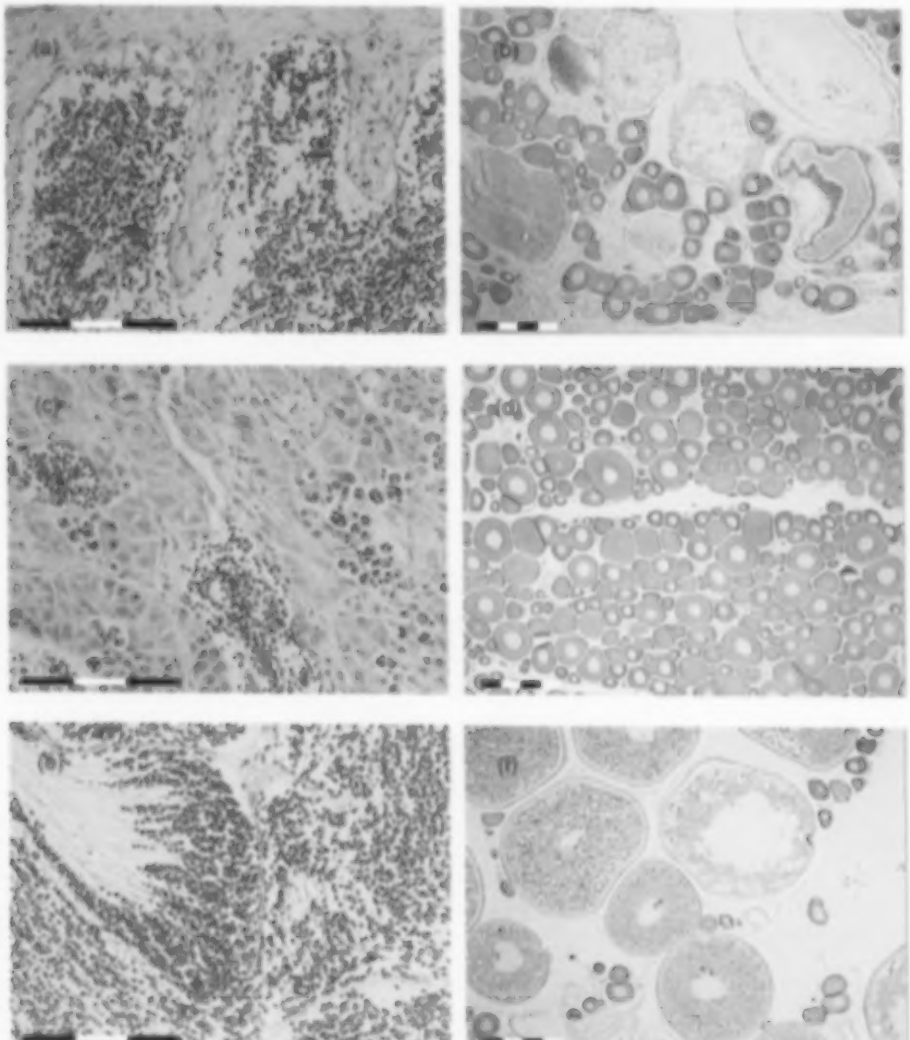

in spring 2002, the main spawning event occurred in the second year between January and July 2003 (i.e., 21–27 MPH) when mature individuals were observed in treatments 1, 6, 7, and 8 only. With the exception of photoperiod 6, all of the photoperiod treatments recorded close to 100% maturation commitment. For treatments 1, 6, and 7, spawning activity was first observed in January 2003 (21 MPH), while it was delayed until April 2003 (24 MPH) in those individuals exposed to photoperiod 8. Of these spawning profiles, only the populations reared under photoperiods 1 and 7 were comparable (timing and rate of commitment) with the natural spawning season for cod in the eastern Atlantic Ocean (Hislop 1984; Kjesbu 1994; Cardinale and Modin 1999) and with the timing of the ambient photoperiod reared populations reported in numerous laboratory-based studies (Dahle et al. 2003; Davie et al. 2003; Norberg et al. 2004). With regard to photoperiod 8, despite the initial 3-month delay, the relative time frame of the spawning profile was comparable with that of the natural populations. The GSI data accurately reflected what was observed in the spawning activity and are comparable with those reported by Hansen et al. (2001) and Kristoffersen et al. (2004). The gonads represent <1% of the round weight of an immature individual (<0.5% in males); however, as an individual enters maturation, the GSI increases to reach a peak of ~12%, at which point it is the largest paired organ. With regard to the plasma testosterone,

© 2007 NRC Canada

Table 4. Population mean weight (g) and length (mm) at trial's end (27 months posthatch (MPH)) and individual growth rate assessments (SGRw, weight-specific growth rate (%·day^{-1}); SGRl, length-specific growth rate (%·day^{-1}); TGC, thermal growth coefficient) from 6 to 27 MPH.

Photoperiod treatment	*n*	Weight	Length	SGRw	SGRl	TGC
1	43	1522±60c	483±5c	0.59±0.01b	0.19±0.002c	1.25±0.020c
2	37	2154±115ab	527±8ab	0.64±0.01a	0.20±0.002b	1.43±0.034ab
3	41	2387±128a	547±8a	0.65±0.01a	0.20±0.002ab	1.50±0.035a
4	32	2533±145a	563±9a	0.66±0.01a	0.20±0.002ab	1.53±0.039a
5	34	2504±125a	561±8a	0.67±0.01a	0.21±0.002a	1.54±0.036a
6	39	2209±112ab	530±7ab	0.65±0.01a	0.20±0.002ab	1.49±0.030a
7	39	1587±57c	486±5c	0.59±0.01b	0.18±0.002c	1.25±0.021c
8	35	1726±65bc	498±7bc	0.61±0.01b	0.19±0.003c	1.31±0.020bc

Note: Letters denote significant difference between photoperiods (analysis of variance).

estradiol-17β, and calcium concentrations recorded, only treatments 1, 7, and 8 recorded any significant elevations in plasma concentrations. The peaks reached >8 ng·mL^{-1} for plasma testosterone (males) and estradiol-17β (females) and >200 mg·dL^{-1} for plasma calcium (females), and are comparable with levels previously recorded for mature cod (Norberg et al. 2004). The large individual variation in mean levels observed is an artefact of the low sample size confounded by the fact that maturing individuals will be at different stages of development (Kjesbu et al. 1996) at the time of sampling. The lack of elevation in GSI and sex steroids levels in treatments 2–5 throughout the study confirmed that no significant gonadal development occurred in these populations (Dahle et al. 2003; Tomkiewicz et al. 2003). The final confirmation of gametogenic activity came from the histological examination of gonadal sections taken at the studies' end at 27 MPH. The females from photoperiods 1 and 7 displayed clear evidence of recently completed spawning, evident from the postovulatory follicles and atretic oocytes in conjunction with predominately primary growth oocytes, which would be recruited in later maturation cycles. The males of both treatments still contained spermatozoa within clear empty lobular regions with little evidence, in the sections screened, of early germ cell stages. Such characteristics have been referred to by Dahle et al. (2003) as being indicative of "stage IV" spent testes. As for photoperiod 8, the individuals in question were recorded as releasing eggs or milt on inspection, which was reflected in the histological analysis in both sexes (e.g., highest recorded mean oocyte diameter 385 ± 14 µm). While it is acknowledged that oocyte measurements were not corrected for the possible impact of the fixing and sectioning process (i.e., oocyte shrinkage: see Kjesbu 1994; Svasand et al. 1996; Dahle et al. 2003), it is felt that the measurements still provided valuable quantification of relative oocyte development.

The apparent developmental differences observed in gonadal histology between the sexes in treatments 2–6 are of great interest. While all ovarian sections revealed only primary growth oocytes suggesting no gonadal development, the testes samples consistently demonstrated germ cells at varying stages of development with clusters of later stages including spermatozoa in all individuals. Morrison (1990) has described such morphology in wild cod testes as spent–resting and hence being indicative of previous spawning activity. With the exception of a limited number of spermiating males in photoperiod 6 (13% of the population; note: individuals were not included in this histological study), in all other treatments, the remaining reproductive parameters investigated suggested no sexual maturation activity. It is acknowledged, however, that the limited sampling schedule may have excluded such a possible detection. Interestingly, Kristoffersen et al. (2004) similarly noted evidence of limited spermatogenesis in male cod maintained on LL photoperiods, comparable with photoperiod 5 in this present work, which had been held in either enclosed or semi-open tank systems. The same authors reported that this was in association with "an increase in germ cell death (apoptosis)" suggestive of regression in testicular development. This apparent developmental difference between sexes under photoperiods 2–6 requires further investigation to determine whether the apparent male gametogenesis is a significant phenomenon. The demonstration that it appears in all immature photoperiod treatments (photoperiods 2–5) is at least suggestive that it is not linked to any specifically timed photoperiodic event and therefore may be under some other entraining signal common to all treatments, for example, temperature (Bromage et al. 2001). Importantly, however, the present data suggest that histological classification of such a condition as "spent–resting" as proposed by Morrison (1990) should be assigned with care, as wrongly assigned individuals could lead to an overestimation of past spawning activity.

In the present study, the exposure to LL from October 2003 (18 MPH), as in photoperiod 6 (i.e., following a reduction in daylength from 17.5 to 11.5 h over 3 months), led to the recruitment of only a limited percentage of male individuals (13%) to mature. Interestingly, both Hansen et al. (2001) and Davie (2005) have shown that application of LL 3 months later still, at ~21 MPH, in line with the winter solstice, actually advances maturation by ~1 month. Hence, it can be suggested that with regard to reproduction, within this window of 3 months, the role of long-day photoperiods reverses from an inhibitory to a stimulatory photoperiodic signal. This is indicative of a phase–response curve for an endogenous clock controlled rhythm in maturation (Randall et al. 1998; Bromage et al. 2001). The endogenous control of reproduction is reliant on a gating theory in which "win-

© 2007 NRC Canada

Fig. 6. Model indicating the proposed role of seasonally changing photoperiod in recruiting individuals into sexual maturation (decision period) and subsequently regulating the final stages of the process (completion) in relation to natural spawning seasons (open boxes) in Atlantic cod (AC), Atlantic salmon (AS), and Atlantic halibut (AH). Modified from Duston and Saunders (1992).

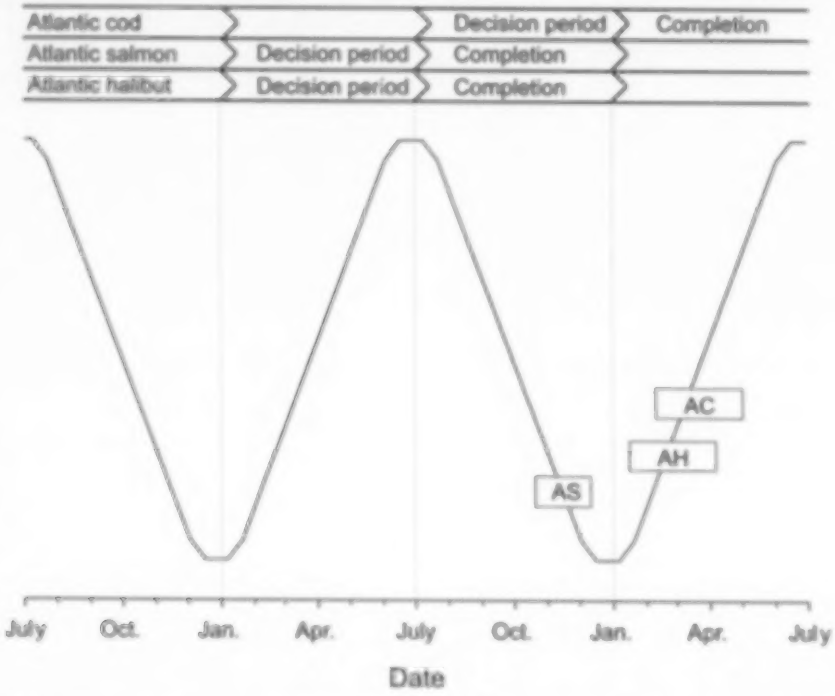

dows of opportunity" (Bromage et al. 2001) regulate when an individual can initiate a physiological process like maturation. This window corresponds to a specific entraining photoperiod signal in conjunction with a permissive physiological state. In this present case, to maintain the analogy, the window would be opened by a descending photoperiod (autumnal period in ambient conditions), and in the case of the population maintained under photoperiod 6, the application of LL from October 2002 closed this window before most of the individuals had attained a suitable physiological status or had perceived that the window was open in the first place. Of interest is the fact that these mature individuals under photoperiod 6 were exclusively male, which prior to the opening of the window could be characterized as having a larger size and better condition (increased Fulton's condition factor) than those nonmaturing fish (data not presented). This is in accordance with the theories that elevated physiological condition allows earlier commitment to maturation (Bromage et al. 2001) and that males frequently mature earlier than females (Karlsen et al. 1995; Imsland et al. 1997). Of great future importance would be the definitions of the physiological conditions in cod that act as the permissive rate limiter in this process.

The characterization of the photoperiodic entrainment of maturation in cod is of great interest, as the results are not in accordance with the definitions in photoperiod regulation of maturation in other northern latitude teleosts such as rainbow trout (*Oncorhynchus mykiss*), Atlantic salmon, and Atlantic halibut (*Hippoglossus hippoglossus*) (Fig. 6). In the Atlantic halibut, another marine batch-spawning teleost found in comparable latitudes as Atlantic cod (Jakupsstovu and Haug 1988; Neilson et al. 1993), it has been demonstrated that long days enhanced the recruitment of maturing males (Norberg et al. 2001). Furthermore, following exposure to LL, the return to an ambient photoperiod at the summer solstice prior to maturation resulted in the maximum reduction in maturation commitment. These results suggest that in halibut, an increasing daylength or long-day photoperiod is the window-opening signal, as proposed for flatfish in general by Bromage et al. (2001), while a descending photoperiod is the window closing. As with Atlantic halibut, in salmonid species including rainbow trout (Bromage and Duston 1986) and Atlantic salmon (Duston and Saunders 1992), a rising photoperiod or application of long daylengths recruits individuals into and advances the time course of reproduction. Such findings are out of phase with what is observed in cod and may be a reflection of a shorter-term maturation cycle in cod compared with these other species. Overall, these findings add further credence to the theory that the "gate open" position can vary between species (Imsland et al. 2003).

Anecdotal reports from aquaculture industry representatives suggested that mortality rates could increase during spawning seasons (C. Blair, Lakeland Marine Farm Ltd., Argyll, Scotland, personal communication). In the present study, there was no significant impact of any treatment on mortality rates, nor was there any increase in mortality rates in association with maturation in the populations that did pass through this process. Increased mortality during spawning has been previously reported in wild stocks (Dutil and

© 2007 NRC Canada

Lambert 2000; Dutil et al. 2003), which is linked to lack of energy reserves and feed availability over the winter period immediately prior to maturation. The lack of such specific mortalities in the present work is most likely a reflection of the ad libitum feeding conditions and good husbandry practices, ensuring that energy levels never descended to life-threatening levels.

The significant improvement in growth performance observed between mature and immature populations between 42% and 66% increase in mean weight over the simulated natural photoperiod is comparable with similar earlier studies (Hansen et al. 2001; Davie et al. 2003). This weight loss is principally due to a significant reduction in somatic growth during the spawning season in those populations that matured. Interestingly in the immature populations, there is no apparent correlation between length of exposure to LL and growth–final size, suggesting that there is no long-term stimulation of somatic growth by LL in Atlantic cod (for further discussion of growth performance and impact of LL exposure on cod, see Davie et al. 2007).

Although the majority of data discussed so far relate to maturation in the second year of this study, it should be acknowledged that there were isolated incidences of male maturation recorded in the first year (photoperiods 2 and 4 at 12 and 14 MPH, respectively; one single male in each case). Along with the present study, maturation at such an age in cod has been observed in cultured stocks in Norway (Ø. Karlsen, Institute of Marine Research, N-5817 Bergen, Norway, personal communication) as well as in limited proportions of individuals of a similar size and age in North Sea surveys (Cook et al. 1999). While the quantification of maturation in year 1 was not an aim of the present study, the identification of these individuals highlights a possible future concern for the aquaculture sector. Such precocious maturation has been reported in a limited number of other commercially significant teleost species including masu salmon (*Oncorhynchus masou*) (Amano et al. 1999, 2000), Atlantic salmon (Jones and King 1952; Saunders et al. 1982; Fleming 1996), Chinook salmon (*Oncorhynchus tshawytscha*) (Unwin and Glova 1997; Shearer and Swanson 2000), and sea bass (Rodriguez et al. 2001; Zanuy et al. 2001) and can cause significant financial losses. It remains to be seen whether precocious maturation will become an issue within cod farming. However, as the environmental entrainment of reproduction will be consistent across the year-classes, remediation of any impacts using similar husbandry techniques (i.e., photoperiod manipulation) should be possible as long it is applied within an appropriate time frame.

In conclusion, these results clarify the importance of seasonally altering photoperiod for the entrainment of puberty in Atlantic cod. Photoperiod management of reproduction in cultured stocks utilizing LL will be an important management technique to improve aquaculture efficiency. As extended exposure to LL appeared to offer no further significant growth benefit (Davie et al. 2007), LL should be applied from the summer solstice prior to maturation. Although these results clearly showed the efficiency of such photoperiod regimes to arrest sexual maturation in tank systems, failure of such regimes in commercial ongrowing facilities are currently reported within the cod industry (Taranger et al. 2006). This failure is now believed to be due to the reduced efficacy of the available metal halide lighting systems to illuminate a cage environment appropriately. Future work should thus focus on not only the characterization of light perception in Atlantic cod but also on the species' behavioural dynamics in relation to submerged lighting to aid the development of appropriate lighting systems.

Acknowledgments

The authors thank Dr. Derek Robertson for his support in instigating the experiment and the staff of Machrihanish Marine Environmental Research Laboratory for its daily management. Fish were provided by Machrihanish Marine Farms Ltd. and financial support was provided by a Natural Environment Research Council award (NER/S/A/2000/03640) and the British Marine Finfish Association.

References

Amano, M., Ikuta, K., Kitamura, S., and Aida, K. 1999. Effects of photoperiod on salmon GnRH mRNA levels in brain of castrated underyearling precocious male masu salmon. Gen. Comp. Endocrinol. **115**: 70–75.

Amano, M., Iigo, M., Ikuta, K., Kitamura, S., Yamada, H., and Yamamori, K. 2000. Roles of melatonin in gonadal maturation of underyearling precocious male masu salmon. Gen. Comp. Endocrinol. **120**: 190–197.

Begtashi, I., Rodríguez, L., Moles, G., Zanuy, S., and Carrillo, M. 2004. Long-term exposure to continuous light inhibits precocity in juvenile male European sea bass (*Dicentrarchus labrax*, L.). I. Morphological aspects. Aquaculture, **241**: 539–559.

Benfey, T.J. 2001. Use of sterile triploid Atlantic salmon (*Salmo salar* L.) for aquaculture in New Brunswick, Canada. ICES J. Mar. Sci. **58**: 525–529.

Bromage, N., and Duston, J. 1986. The control of spawning in the rainbow trout (*Salmo gardneri* Richardson) using photoperiod techniques. Inst. Freshw. Res. Drottningholm Rep. **63**: 26–35.

Bromage, N., Porter, M., and Randall, C. 2001. The environmental regulation of maturation in farmed finfish, with special reference to the role of photoperiod and melatonin. Aquaculture, **197**: 63–98.

Cardinale, M., and Modin, J. 1999. Changes in size-at-maturity of Baltic cod (*Gadus morhua*) during a period of large variations in stock size and environmental conditions. Fish. Res. **41**: 285–295.

Cook, R.M., Kunzlik, P.A., Hislop, J.R.G., and Poulding, D. 1999. Models of growth and maturity for North Sea cod. J. Northwest Atl. Fish. Sci. **25**: 91–99.

Cotter, D., O'Donovan, V., O'Maoiléidigh, N., Rogan, G., Roche, N., and Wilkins, N.P. 2000. An evaluation of the use of triploid Atlantic salmon (*Salmo salar* L.) in minimising the impact of escaped farmed salmon on wild populations. Aquaculture, **186**: 61–75.

Dahle, R., Taranger, G.L., and Norberg, B. 2000. Sexual maturation and growth of Atlantic cod *Gadus morhua* reared at different light intensities. *In* Proceedings of the 6th International Symposium on the Reproductive Physiology of Fish, Bergen, Norway, 4–9 July 1999. *Edited by* B. Norberg, O.S. Kjesbu, G.L. Taranger, E. Andersson, and S.O. Stefansson. John Greig AS, Bergen. p. 336.

Dahle, R., Taranger, G.L., Karlsen, O., Kjesbu, O.S., and Norberg, B. 2003. Gonadal development and associated changes in liver size and sexual steroids during the reproductive cycle of captive male and female Atlantic cod (*Gadus morhua* L.). Comp. Biochem. Physiol. A, **136**: 641–653.

© 2007 NRC Canada

Davie, A. 2005. Effects of photoperiod manipulation on growth and reproduction in Atlantic cod (*Gadus morhua* L.). Ph.D. thesis, Institute of Aquaculture, University of Stirling, Stirling, UK.

Davie, A., Porter, M.J.R., and Bromage, N.R. 2003. Photoperiod manipulation of maturation and growth of Atlantic cod (*Gadus morhua*). Fish Physiol. Biochem. **28**: 399–400.

Davie, A., Porter, M.J.R., Bromage, N.R., and Migaud, H. 2007. The role of seasonally altering photoperiod in regulating physiology in Atlantic cod (*Gadus morhua*). Part II. Somatic growth. Can. J. Fish. Aquat. Sci. **64**: 98–112.

Donaldson, E.M., and Hunter, G.A. 1982. Sex control in fish with particular references to salmonids. Can. J. Fish. Aquat. Sci. **39**: 99–110.

Duston, J., and Bromage, N.R. 1987. Constant photoperiod regimes and the entrainment of the annual cycle of reproduction in the female rainbow trout (*Salmo gairdneri*). Gen. Comp. Endocrinol. **65**: 373–384.

Duston, J., and Saunders, R.L. 1992. Effects of 6-, 12-, and 18-month photoperiod cycles on smolting and sexual maturation in juvenile Atlantic salmon (*Salmo salar*). Can. J. Fish. Aquat. Sci. **49**: 2273–2280.

Dutil, J.D., and Lambert, Y. 2000. Natural mortality from poor condition in Atlantic cod (*Gadus morhua*). Can. J. Fish. Aquat. Sci. **57**: 826–836.

Dutil, J.D., Lambert, Y., and Chabot, D. 2003. Winter and spring changes in condition factor and energy reserves of wild cod compared with changes observed during food-deprivation in the laboratory. ICES J. Mar. Sci. **60**: 780–786.

Elliot, J.A.K., Bromage, N., and Springate, J. 1984. Endocrine and ovarian changes in three strains of rainbow trout subjected to both constant and seasonally changing photoperiods. *In* Proceedings of the International Symposium on Salmonid Reproduction, Seattle, Washington, 31 October – 2 November 1984. *Edited by* R.N. Iwamoto and S. Sower. Washington Sea Grant Program, Seattle. pp. 36–37.

Endal, H.P., Taranger, G.L., Stefansson, S.O., and Hansen, T. 2000. Effects of continuous additional light on growth and sexual maturity in Atlantic salmon, *Salmo salar*, reared in sea cages. Aquaculture, **191**: 337–349.

Fleming, I.A. 1996. Reproductive strategies of Atlantic salmon: ecology and evolution. Rev. Fish Biol. Fish. **6**: 379–416.

Fowler, J., and Cohen, L. 1987. Statistics for ornithologists. Guide 22. British Trust for Ornithology, Hertfordshire, UK.

Hansen, T., Karlsen, O., Taranger, G.L., Hemre, G.-I., Holm, J.C., and Kjesbu, O.S. 2001. Growth, gonadal development and spawning time of Atlantic cod (*Gadus morhua*) reared under different photoperiods. Aquaculture, **203**: 51–67.

Hemre, G.I., Karlsen, O., Eckhoff, K., Tveit, K., Mangor-Jensen, A., and Rosenlund, G. 2004. Effect of season, light regime and diet on muscle composition and selected quality parameters in farmed Atlantic cod, *Gadus morhua* L. Aquacult. Res. **35**: 683–697.

Hislop, J.R.G. 1984. A comparison of the reproductive tactics and strategies of cod, haddock, whiting and Norway pout in the North Sea. *In* Fish reproduction: strategies and tactics. *Edited by* G.W. Potts and R.J. Wootton. Academic Press, London, UK. pp. 311–329.

Imsland, A.K., Folkvord, A., Jonsdottir, O.D.B., and Stefansson, S.O. 1997. Effects of exposure to extended photoperiods during the first winter on long-term growth and age at first maturity in turbot, *Scopthalmus maximus*. Aquaculture, **159**: 125–141.

Imsland, A.K., Dragsnes, M., and Stefansson, S.O. 2003. Exposure to continuous light inhibits maturation in turbot (*Scopthalmus maximus*). Aquaculture, **219**: 911–919.

Jakupstovu, S.H.I., and Haug, T. 1988. Growth, sexual maturation and spawning season of Atlantic halibut, *Hippoglossus hippoglossus*, in Faroese waters. Fish. Res. **6**: 201–215.

Jones, J.W., and King, G.M. 1952. Spawning of the male salmon parr (*Salmo salar* Linn. Juv.). Nature (London), **169**: 882.

Karlsen, O., Holm, J.C., and Kjesbu, O.S. 1995. Effects of periodic starvation on reproductive investment in first-time spawning Atlantic cod *Gadus morhua*. Aquaculture, **133**: 159–170.

Kjesbu, O.S. 1994. Time of start of spawning in Atlantic cod, *Gadus morhua*, females in relation to vitellogenic oocyte diameter, temperature, fish length and condition. J. Fish Biol. **45**: 719–735.

Kjesbu, O.S., Kryvi, H., and Norberg, B. 1996. Oocyte size and structure in relation to blood plasma steroid hormones in individually monitored spawning Atlantic cod. J. Fish Biol. **49**: 1197–1215.

Kristoffersen, C., Karlsen, O., Schultz, R.W., Andersson, E., Torsvik, A., Stefansson, S., and Taranger, G.L. 2004. Can use of additional light in outdoor tanks delay puberty in farmed male Atlantic cod (*Gadus morhua*). *In* Proceedings of the ICES Symposium on Gadoid Mariculture: Development and Future Challenges, Bergen, Norway, 13–16 June 2004. *Edited by* O.S. Kjesbu, G.L. Taranger, and E.A. Trippel. Institute of Marine Research, Bergen. p. 69.

Morrison, C.M. 1990. Histology of the Atlantic cod, *Gadus morhua*: an atlas. Part three. Reproductive tract. Can. Spec. Publ. Fish. Aquat. Sci. No. 110.

Neilson, J.D., Kearney, J.F., Perley, P., and Sampson, H. 1993. Reproductive biology of Atlantic halibut, *Hippoglossus hippoglossus*, in Canadian waters. Can. J. Fish. Aquat. Sci. **50**: 551–563.

Norberg, B., Weltzien, F.A., Karlsen, O., and Holm, J.C. 2001. Effects of photoperiod on sexual maturation and somatic growth in male Atlantic halibut (*Hippoglossus hippoglossus* L.). Comp. Biochem. Physiol. B, **129**: 357–365.

Norberg, B., Brown, C.L., Halldorsson, O., Stensland, K., and Bjornsson, B.T. 2004. Photoperiod regulates the timing of sexual maturation, spawning, sex steroid and thyroid hormone profiles in the Atlantic cod (*Gadus morhua*). Aquaculture, **229**: 451–467.

Porter, M.J.R., Duncan, N.J., Mitchell, D., and Bromage, N.R. 1999. The use of cage lighting to reduce plasma melatonin in Atlantic salmon *Salmo salar* and its effects on the inhibition of grilsing. Aquaculture, **176**: 237–244.

Randall, C.F., Bromage, N., Duston, J., and Symes, J. 1998. Photoperiod induced phase–phase shifts of the endogenous clock controlling reproduction in rainbow trout: a circannual phase–response curve. J. Reprod. Fertil. **112**: 399–405.

Rodriguez, L., Zanuy, S., and Carillo, M. 2001. Influence of daylength on the age at first maturity and somatic growth in male sea bass (*Dicentrarchus labrax* L.). Aquaculture, **196**: 159–175.

Saunders, R.L., Henderson, E.B., and Glebe, B.D. 1982. Precocious sexual maturation and smoltification in male Atlantic salmon (*Salmo salar*). Aquaculture, **28**: 211–229.

Shearer, K.D., and Swanson, P. 2000. The effect of whole body lipid on early sexual maturation of 1+ age male chinook salmon (*Oncorhynchus tshawytscha*). Aquaculture, **190**: 343–367.

Svasand, T., Jorstad, K.E., Ottera, H., and Kjesbu, O.S. 1996. Differences in growth performance between arcto-Norwegian and Norwegian coastal cod reared under identical conditions. J. Fish Biol. **49**: 108–119.

Taranger, G.L., Aardal, L., Hansen, T., and Kjesbu, O.S. 2006. Continuous light delays sexual maturation and increases growth of Atlantic cod (*Gadus morhua* L.) in sea cages. ICES J. Mar. Sci. **63**: 365–375.

© 2007 NRC Canada

Tomkiewicz, J., Tybjerg, L., and Jespersen, A. 2003. Micro- and macroscopic characteristics to stage gonadal maturation in female Baltic cod. J. Fish Biol. **62**: 253–275.

Unwin, M.J., and Glova, G.J. 1997. Changes in life history parameters in a naturally spawning population of chinook salmon (*Oncorhynchus tshawytscha*) associated with releases of hatchery-reared fish. Can. J. Fish. Aquat. Sci. **54**: 1235–1245.

Zanuy, S., Carillo, M., Felip, A., Rodriguez, L., Blazquez, M., Ramos, J., and Piferrer, F. 2001. Genetic, hormonal and environmental approaches for the control of reproduction in the European sea bass (*Dicentrarchus labrax* L.). Aquaculture, **202**: 187–203.

Zar, J.H. 1999. Biostatistical analysis. 4th ed. Prentice Hall, Upper Saddle River, N.J.

© 2007 NRC Canada

The role of seasonally altering photoperiod in regulating physiology in Atlantic cod (*Gadus morhua*). Part II. Somatic growth

Andrew Davie, Mark J.R. Porter, Niall R. Bromage, and Herve Migaud

Abstract: Research to date has not clearly defined the role of photoperiod in regulating somatic growth in Atlantic cod (*Gadus morhua*). The present study followed individual growth performance, plasma insulin-like growth factor-I, and relative liver size in response to a range of experimental photoperiod treatments where populations were transferred from an ambient photoperiod regime to continuous illumination at strategic times during the first 2 years of life. While this work demonstrated that application of continuous illumination could directly stimulate somatic growth, this growth stimulation is transitory with no accumulative effect of prolonged exposure to continuous illumination. Importantly, it was apparent that the photic inhibition of maturation realized a far more significant growth stimulation, and in populations where this occurred, sexually dimorphic growth patterns became apparent. Plasma insulin-like growth factor-I displays a seasonal rhythm correlated with ambient temperature under natural photic conditions and in certain circumstances could be used as an accurate predictor of growth rate. Overall, this work further refines the guidelines on photoperiod management during commercial ongrowing of the species to help realize the maximum economic potential of cod aquaculture.

Résumé : Les travaux de recherche menés jusqu'a ce jour n'ont pas permis de définir clairement le rôle joué par la photopériode dans la régulation de la croissance somatique chez la morue Atlantique (*Gadus morhua*). Durant notre étude, nous avons fait un suivi individuel des performances de croissance, analysé les teneurs plasmatiques en facteur 1 de croissance de type insulinique et mesuré l'indice hépato-somatique en réponse à une variété de traitements expérimentaux photopériodiques consistant à transférer des populations de morue, à des temps précis, d'un régime de photopériode naturelle vers un éclairement continu durant leurs 2 premières années de vie. Notre étude a démontré que, même si des périodes de lumière continue peuvent stimuler directement la croissance somatique chez la morue, cette stimulation n'est que transitoire et n'augmente pas proportionnellement à la durée d'exposition à l'éclairement continu. Il est important de noter que l'inhibition du cycle de reproduction par le régime de lumière permet une stimulation de la croissance bien plus importante. De plus, chez ces populations restées immatures, on observe un dimorphisme sexuel de croissance. Il existe un rythme saisonnier des teneurs plasmatiques en facteur 1 de croissance de type insulinique corrélé à la fois aux variations de la température de l'eau en conditions naturelles d'éclairement et, dans certains cas, aux taux de croissance des poissons. D'une façon globale, nos travaux ont permis de déterminer avec plus de précision les régimes photopériodiques à appliquer pendant la phase de grossissement par l'industrie de la pisciculture de la morue pour améliorer le rendement.

Introduction

Commercial exploitation of gadoid species like Atlantic cod (*Gadus morhua*) has been a long-standing tradition in the North Atlantic. This whitefish trade is a staple and important dietary component across the world. In the face of such demand, harvesting of wild stocks has now reduced the once plentiful stocks to the lowest recorded levels worldwide with much of the commercial fishing now strictly regulated to maintain the existing spawning stock biomass. Owing to such conditions, cod aquaculture is now a commercial reality. A major production bottleneck, however, is that of maturation prior to the attainment of the preferred harvest weight (≥3 kg). Early maturation is a production hurdle common to many commercially important marine teleost species, e.g., Atlantic salmon (*Salmo salar*) (Porter et al. 1999), European sea bass (*Dicentrarchus labrax*) (Begtashi et al. 2004), and Atlantic halibut (*Hippoglossus hippoglossus*) (Norberg et al.

Received 21 March 2006. Accepted 29 September 2006. Published on the NRC Research Press Web site at http://cjfas.nrc.ca on 18 January 2007.
J19235

A. Davie,[1] M.J.R. Porter,[2] N.R. Bromage,[3] and H. Migaud. Institute of Aquaculture, University of Stirling, Stirling, Scotland, FK9 4LA, UK.

[1]Corresponding author (e-mail: andrew.davie@stir.ac.uk).
[2]Present address: Ridely Aquafeed, P.O. Box 187, Deception Bay, Queensland, 4508, Australia.
[3]Deceased.

 doi:10.1139/F06-170 © 2007 NRC Canada

Table 1. Experimental groups listing the number of individuals at setup and a description of the respective photoperiod treatment.

Photoperiod treatment	No. of individuals	Description
1	110	Simulated natural photoperiod (SNP)
2	100	SNP until 1 October 2001 (6 MPH) and then continuous illumination (LL)
3	90	SNP until 1 January 2002 (9 MPH) and then LL
4	80	SNP until 1 April 2002 (12 MPH) and then LL
5	70	SNP until 1 July 2002 (15 MPH) and then LL
6	60	SNP until 1 October 2002 (18 MPH) and then LL
7	70	SNP until 1 October 2001 (6 MPH), then LL until 1 July 2002 (15 MPH), and then SNP
8	50	SNP until 1 October 2001 (6 MPH), then LL until 1 January 2003 (21 MPH), and then SNP

Note: MPH, months posthatch.

2001). This leads to a reduction in growth potential along with possible changes in flesh quality, which results in an extended culture cycle (Hansen et al. 2001; Davie et al. 2003; Hemre et al. 2004).

Recent work has demonstrated in cod that the successful prevention of spawning in enclosed tank-based trials (Hansen et al. 2001; Davie et al. 2003), through the timely application of photoperiod manipulation, can realize a significant growth benefit (e.g., over 40% in Davie et al. 2003). However, the exact nature of this growth benefit (growth stimulation by extended light exposure versus redirection of energy reserves from gonadic to somatic growth) is not clear as yet. Neither Hansen et al. (2001) nor Davie et al. (2003) recorded any apparent somatic growth promotion in continuous illumination (LL) treated groups in the 6 months prior to sexual maturation. However, Folkvord and Ottera (1993), Hall (2000), and Imsland et al. (2005) all reported improved growth performance in juvenile Atlantic cod under relatively short-term exposures to long-day or LL photoperiods. From the reviews on photoperiod and growth in teleosts by Boeuf and Le Bail (1999) and Boeuf and Falcon (2001), it is apparent that cod is not the only species that has an uncertain growth response to light. There are two proposed modes by which photoperiod may be regulating somatic growth in teleosts, firstly through the entrainment of endogenous growth rhythms (Duncan et al. 1999; Oppedal et al. 1999; Endal et al. 2000) or secondly through direct photostimulation of the growth axis and eventually muscle fibre recruitment (Johnston et al. 2003). It is therefore of great interest in cod to decipher the links between photoperiod treatment and its impact on sexual maturation and somatic growth. A common problem, however, is that previous work (e.g., Dahle et al. 2000; Karlsen et al. 2000; Davie et al. 2003) has included individuals that passed through sexual maturity while only round wet weight was considered. As such, the concomitant fluctuations in associated tissues (i.e., gonads and liver) during maturation (Eliassen and Vahl 1982*a*; Schwalme and Chouinard 1999; Yaragina and Marshall 2000) were not taken into account in the assessment of growth. Studies of somatic growth should therefore take into consideration these components to quantify the true underlying somatic growth response.

One of the most compelling arguments for light stimulating somatic growth is the demonstration of improved feed conversion efficiencies, which is only achievable through direct stimulation of the somatic growth axis (Boeuf and Le Bail 1999). Somatic growth in fish is regulated by a number of hormones along the growth axis including growth hormone (GH) and insulin-like growth factor-I (IGF-I), which are likely to be key mediators of potential growth effects. IGF-I in particular has recently been demonstrated to act as an accurate predictor of growth potential (Dyer et al. 2004*a*, 2004*b*) and hence can be used to demonstrate direct photic stimulation of the somatic growth axis (Taylor et al. 2005). However, plasma IGF-I and its relationship with photoperiod regulation have yet to be characterized for Atlantic cod.

In this present study, the impact of long-term photoperiod treatments applied from the juvenile stage through to a potential harvest size allowed for the first time in Atlantic cod the examination of light-induced growth effects to further decipher the complex interaction of photoperiod, somatic growth, and sexual maturation.

Materials and methods

Fish rearing conditions and experimental design

On 26 September 2001, 630 six-month-old immature Atlantic cod juveniles (Machrihanish Marine Farms, Machrihanish, UK), previously reared under natural photoperiod and temperature regimes at the Machrihanish Marine Environmental Research Laboratory (55°44′N, 5°44′W), were individually tagged with a passive integrated transponder tag (Avid Plc, Uckfield, UK) and stocked into indoor, light-proof tanks at the Machrihanish Marine Environmental Research Laboratory. All individuals were randomly assigned to one of eight photoperiod treatments (Table 1; Fig. 1). Unequal numbers (n = 50–110) were assigned to populations to optimize the experimental setup owing to the restricted animal numbers and tank facilities available. On 8 July 2003, all experimental treatments were terminated. Throughout the experimental period, water temperature ranged from 5 to 15 °C (Fig. 1) and salinity ranged between 29‰ and 34‰. For a fuller description of rearing conditions and the experimental design, see Davie et al. (2007).

Data sampling and analysis

From 1 October 2001 onwards, a 3-monthly sampling schedule was undertaken. At each sample time, following anaesthesia (1:10 000 concentration of 2-phenoxyethanol; Sigma-Aldrich Co. Ltd., Poole, UK), individuals were measured for whole-body weight (±0.1 g) and total length (±1 mm). Specific growth rate (SGR) (Houde and Schekter 1981) and thermal growth coefficient (TGC)

© 2007 NRC Canada

Fig. 1. Summary of photoperiod treatments (black line) in relation to water temperature (grey line). Horizontal bars of photoperiods 2–8 represent the 24-h period of illumination; vertical bars represent transfer from or to simulated natural photoperiod illumination.

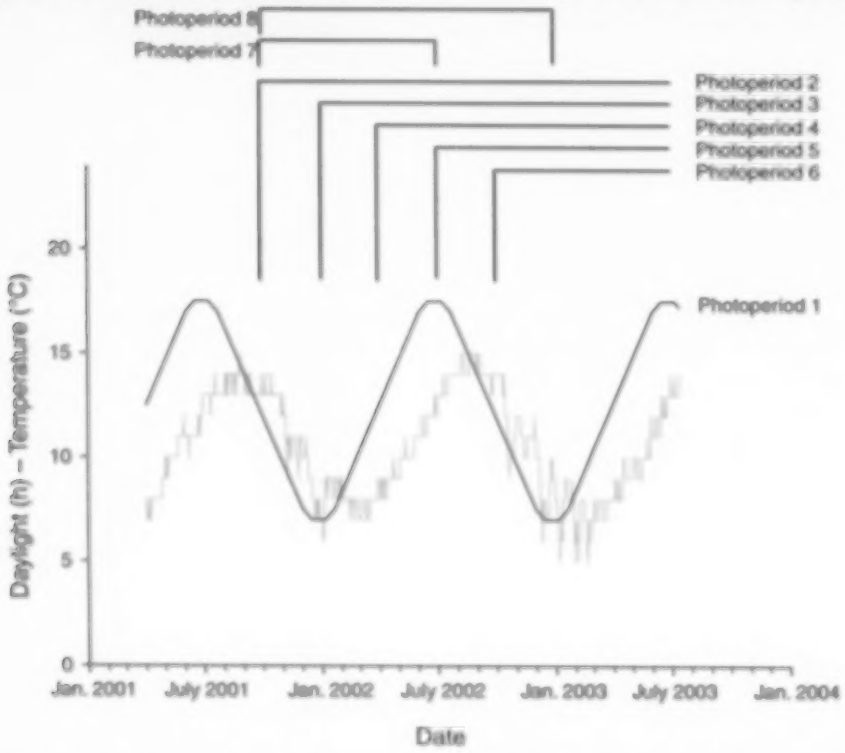

(Iwama and Tautz 1981) were calculated using the respective formulae SGR = $(e^g - 1) \times 100$, where $g = [\ln(W_2) - \ln(W_1)] \times (t_2 - t_1)^{-1}$, and TGC = $\{[(W_2)^{1/3} - (W_1)^{1/3}] \times 1000\} \times (\text{degree-days})^{-1}$, where W_2 and W_1 are the weight at time t_2 and t_1, respectively. Individual condition was calculated using Fulton's condition factor (K) using the formula $K = 100 \times (W \times TL^{-3})$, where W is whole-body weight and TL is total length. Fulton's condition factor was deemed an appropriate condition index to use with this data set, as a scatterplot of all individual weights versus lengths for the total trial ($n = 2401$, size range = 16.5–4239 g and 115–642 mm) had a regression coefficient of 3 with an adjusted r^2 of 0.99 ($p < 0.01$) (Bolger and Connolly 1981).

Maturation status for each individual was visually assessed at each time point with individuals being designated mature when gametes were released on inspection. Additional checks for maturation status were also made on 24 February 2003 and 28 May 2003 in all populations.

As part of the 3-monthly sampling schedule, from each different photoperiod treatment, 10 individuals were preselected at random. Once identified, these individuals were sacrificed (note: sampling error caused this number to vary between 4 and 11 individuals and the sex ratio was variable because of the random selection process). Following morphometric measurements, a blood sample was withdrawn into heparinized syringes and the plasma, separated by centrifugation at 1200*g* for 15 min at 4 °C, was stored at –70 °C prior to later analysis. Plasma IGF-1 was measured in duplicate using a commercially available radioimmunoassay kit (Dyer et al. 2004*b*). Prior to adoption of the technique, serial dilutions of pooled Atlantic cod plasma were used to check if the cod plasma and standards were immunologically comparable (Fig. 2). Both the standard and cod plasma curves were parallel with no statistically significant difference in the slopes (analysis of variance). Quality control line standards (provided by the manufacturer) with a content of ~50 ng·mL^{-1} were used to check the reproducibility of measurements both within and between assays. The intra-assay coefficient of variation was 6.5% ($n = 2$) and the interassay coefficient of variation was 18.4% ($n = 16$). Livers were removed and weighed (±0.1 g), with the relative weight expressed as the hepatosomatic index (HSI) using the formula HSI = (liver weight × body weight^{-1}) × 100. At times when populations experienced common photoperiod histories, terminal samples were taken from one population and the subsequent data assigned to all relevant treatments within the respective time point (e.g., April 2002 data for photoperiods 1, 4, 5, and 6 are from the same 10 individuals). This was necessary because of the restricted availability of experimental animals. At the end of the experiment in July 2003, there remained a core group of 32–43 individuals per photoperiod treatment. These were sacrificed and dissected to record the sex of the individuals.

Flesh samples for proximate compositional analysis taken in line with the first ray of the dorsal fin above the lateral line were taken from individuals ($n = 8$–10) from each treatment in July 2003. Samples were dried to a constant mass at

© 2007 NRC Canada

Fig. 2. Parallelism of the inhibition curves obtained from the insulin-like growth factor-I (IGF-I) standard (circles) and a serial dilution of cod plasma (squares). Each point represents the mean of duplicate measurements. The *x* axis denotes the natural logarithm of the IGF-I content in the standards.

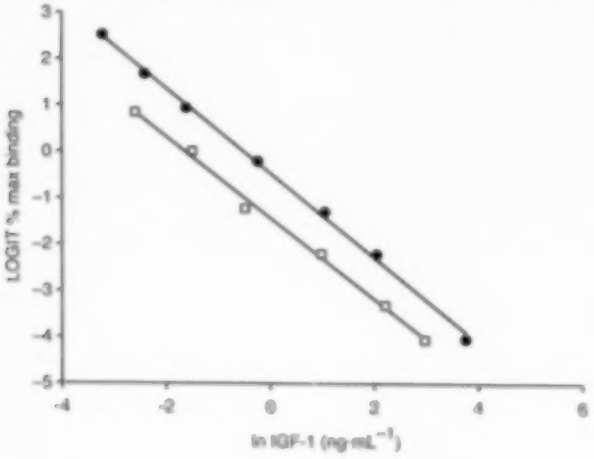

100 °C for ~24 h to calculate moisture content and then homogenized. Each sample was then assessed (in triplicate) for lipid content using the Soxhlet extraction method using petroleum ether to extract the lipid content (Fisher Scientific UK, Manchester, UK). Protein content was measured (in triplicate) using the Kjeldahl analysis technique (Association of Official Analytical Chemists 1990).

Statistical analysis

The data were analysed using MINITAB® release 14.13 (Minitab Ltd., Coventry, UK). Growth parameters, HSI, IGF-I levels, and flesh proximate compositions were analysed using a general linear model (Zar 1999). Normality and homogeneity of variance were improved where necessary by either log or reciprocal transformations. Parameters expressed as a proportion were first subjected to arcsine transformation. A significance level of $p < 0.05$ was set with all significant interactions being analysed with a Tukey post hoc test. There was no significant effect of sex on weight, plasma IGF-I, and HSI data; hence, the data presented are of the mixed sex population. Correlations between plasma IGF-I and growth performances (i.e., SGR and TGC) and temperature as well as between flesh proximate constituents were analysed using the Pearson product moment method (Zar 1999). In all cases, data are presented as mean ± SE of the mean.

Results

Growth and condition

There was no significant difference in mean individual size (i.e., weight and length) within the study populations at the start of the experiment (population mean = 33.2 ± 0.3 g and 146 ± 0.4 mm). Populations under photoperiods 2–6 all significantly increased in weight between each sample point throughout the trial length (Fig. 3), while those under photoperiods 1 and 7 significantly increased in weight except between January and April 2003 (21–24 months posthatch (MPH)) when weight remained constant at ~1200 and 1400 g, respectively, which coincided with the start of spawning activity (for a fuller description of sexual maturation within populations, see Davie et al. 2007). Equally, the population under photoperiod 8, which had a 3-month delay in spawning activity (April–July 2003), did not significantly increase in weight after April 2003 (24 MPH). At the trial's end (27 MPH), there was an apparent trend that immature populations (photoperiods 2–6) were significantly heavier than mature populations (photoperiods 1, 7, and 8) (Table 2; Fig. 3). It was also evident that at the trial's end, there was a tendency for the immature populations (photoperiods 2–6) to be displaying sexually dimorphic growth patterns with female mean weight being between 11% and 25% heavier than the males' weight (Table 2). Such a trend was not apparent in the mature populations (photoperiods 1, 7, and 8) where female mean weight was ±4% of male mean weight.

Mean SGR ranged between 1.48 ± 0.02 and 0.00 ± 0.02%·day^{-1} with a general trend for SGR to decline as size increased. SGR was significantly elevated following transfer to LL under photoperiods 2–5, 7, and 8 (Fig. 4), resulting in the mean weight being significantly heavier than photoperiod 1 fish (simulated natural photoperiod (SNP) control) when measured 3 months post-transfer to LL in treatment 3–5, 7, and 8 (Fig. 3). Such a growth stimulation was less pronounced under photoperiods 2 and 6, resulting in the population mean weight not being significantly heavier than those in photoperiod 1 until 6 months following transfer to LL. Following this growth boost, SGRw in the LL-treated populations returned to a rate comparable with that of the SNP treatment, which meant that once heavier than the SNP population, photoperiods 3–6 and 8 all remained significantly heavier for the remainder of the trial. Photoperiod 7 fish were significantly heavier at all times except on the last sampling in July 2003 (27 MPH) when there was no significant difference compared with the SNP population owing to a reduced SGR between 24 and 27 MPH in relation to spawning activity. Photoperiod 2 fish were not significantly different from the SNP population between July 2002 and January 2003 (15–21 MPH) (dates inclusive). However, following this period, the population was again significantly heavier.

Condition factor increased in all treatments starting at around 1.00 and ending at between 1.30 and 1.45 (Fig. 5). Photoperiod 1 steadily increased in condition over the first 9 months of the trial from October 2001 to July 2002 (6–15 MPH) following which condition remained comparable (1.26–1.33) except for a transient peak in January 2003 (21 MPH) when condition rose to 1.39 ± 0.02, which coincided with the onset of spawning activity (i.e., peak in recorded gonadosomatic index; see Davie et al. 2007). In comparison, photoperiods 3–8 all showed a significant rise in condition in the 3 months following transfer to LL. In photoperiod 2, this rise, although apparent, was not significant over that in photoperiod 1 until 6 months after transfer to LL. In photoperiods 3–6, this elevated level (<1.3) was then maintained for the remainder of the trial and displayed no apparent further variation. In photoperiod 7, while condition was significantly elevated following transfer to LL, it mirrored the changes in condition observed in photoperiod 1

© 2007 NRC Canada

Fig. 3. Mean individual wet weight ± SE of the mean for individuals (n = 32–43) maintained under photoperiod 1 versus (*a*) photoperiod 2, (*b*) photoperiod 3, (*c*) photoperiod 4, (*d*) photoperiod 5, (*e*) photoperiod 6, (*f*) photoperiod 7, (*g*) photoperiod 8, and (*h*) all treatments. In panels *a*–*g*, photoperiod treatments are shown as grey lines, photoperiod 1 is a broken line, and photoperiods 2–8 are solid lines. Horizontal bars denote the spawning season for the respective photoperiods. An asterisk in panels *a*–*g* denotes significant differences between the experimental treatment and photoperiod 1 at a specified time point.

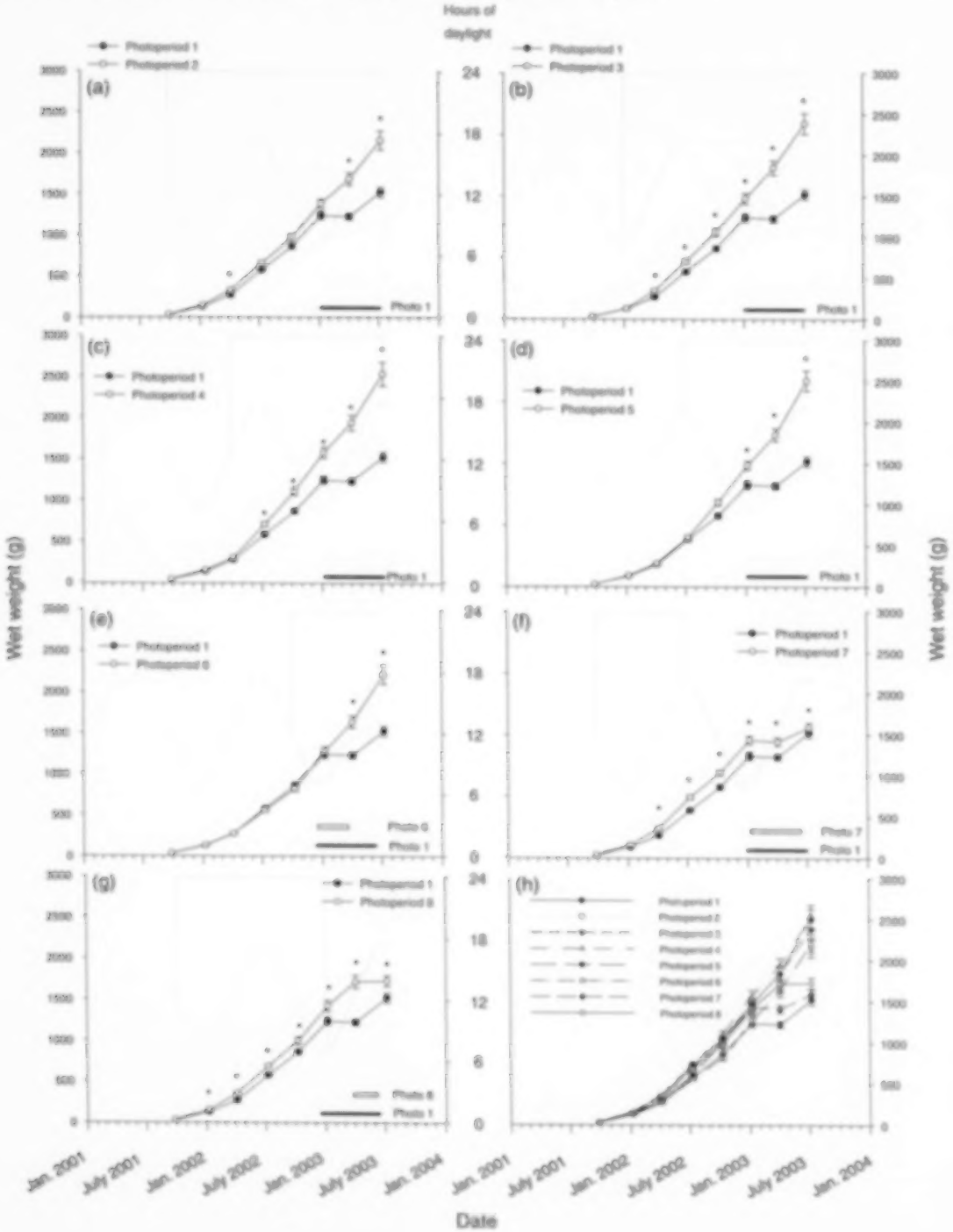

© 2007 NRC Canada

Table 2. Summary of population structure at the trial's end (July 2003) describing sex ratio and individual numbers, final weight, and relative % difference in mean weight between males (M) and females (F) per photoperiod treatment.

Photoperiod treatment	*n* (M:F)	Weight ± SE of the mean (g)	Male mean weight expressed as a % of female mean weight
1	24:19	1522±60d	104
2	14:23	2154±115b	89
3	26:15	2387±128ab	81
4	18:14	2533±145a	89
5	18:16	2504±125a	83
6	23:16	2209±112ab	75
7	21:18	1587±57cd	96
8	22:13	1726±65c	99

Note: Letters denote significant difference between photoperiod treatments.

including a transitory peak (1.49 ± 0.02) in January 2003 (21 MPH), which coincided with the start of spawning activity in both treatments. Only in July 2003 (27 MPH) following spawning did the condition return to a level comparable with that of photoperiod 1. In photoperiod 8, there was a general trend for increased condition from the trial start to a peak of 1.47 ± 0.03 in April 2003 (6–21 MPH). Thereafter, in conjunction with the onset of spawning activity, condition showed a significant decline (1.39 ± 0.04) to end the trial comparable with photoperiod 1.

IGF-I

The total plasma IGF-I was in the range of 5–32 ng·mL^{-1} (Fig. 6). Over the course of the entire study, plasma IGF-I levels in only the SNP-reared population (photoperiod 1) displayed a significant curvilinear relationship with water temperature (IGF-I = (17.66 – 2.88) × temperature + 0.2 × temperature^2; $r^2 = 0.41$, $p < 0.001$, df = 67). The transfer of populations under photoperiods 2–4 and 6–8 from SNP to LL induced, within 3–6 months, an apparent (although not significant at the $p < 0.05$ level) elevation in IGF-I levels. Significant differences in plasma levels between photoperiod treatments became evident only in the months of April and July 2003 (24 and 27 MPH). In both months, the lowest IGF-I levels were recorded in the spawning populations (i.e., photoperiods 1 and 7 in April 2003 and photoperiod 8 in July 2003).

While individual growth rates measured as TGC versus plasma IGF-I levels were significantly correlated within all growth periods (except between 15 and 18 MPH), these relationships were generally very weak (r^2 ranged between 0.08 and 0.28, data not presented). However, in the periods between 21–24 and 24–27 MPH (January–July 2003), when a great divergence in population growth performance was present, there were strong positive correlations between group mean plasma IGF-I and group mean growth rate (SGRw, SGRl, and TGC) (Table 3; Fig. 7). Demonstration of similar correlations in earlier growth periods was confounded by the small population numbers (n = <6) along with low variation in growth performance.

HSI

Population mean HSI levels ranged from 3% to 10% (Fig. 8). Significant differences in HSI were only recorded in the months of April and July 2003 (24 and 27 MPH, respectively). In April, the HSI of treatments 2–6 and 8 was comparable, while that of treatments 1 and 7 fell to below 5%, which, although lower than that of the remaining treatments, was only significantly lower than that of treatments 3, 5, 6, and 8. In July 2003, photoperiod 8 showed a significant decline in HSI from 7.8% ± 0.4% to 3.4% ± 0.4%, which was significantly lower than that of treatments 3–6. Meanwhile, photoperiods 1 and 7 exhibited a moderate increase in HSI (to ~5.6%) to be statistically comparable with treatments 2–6.

Flesh proximate composition

The proximate composition (total protein, lipid, and moisture content) of the flesh was measured in the individuals taken from the July 2003 sample (27 MPH). The muscle of cod was very lean (mean composition: 77% moisture, 20.9% protein, and 0.16% lipid) (Table 4). Overall, moisture content could be described with the model moisture content = (101.45 – 1.135) × protein content – 2.287 × lipid content ($r^2 = 0.963$, $p < 0.0001$, $n = 74$). Flesh proximate composition was significantly affected by the physiological status of the individuals (Table 4). This could be summarized as follows. Fish under photoperiod 8 (spawning at time of measurement) had significantly higher moisture levels than treatments 3–6 (immature) and lower protein levels than treatments 2–6 (immature). Similarly, photoperiod 1 (postspawning) had significantly higher moisture content than photoperiods 5 and 6 (immature) and lower protein content than photoperiods 3, 5, and 6 (immature). Finally, photoperiod 7 (postspawning) had significantly higher moisture content and hence lower protein content than photoperiod 6 (immature). While a similar trend with maturation status and lipid content was apparent, there was no statistical difference between treatments.

Discussion

The interrelationship between photoperiod, sexual maturation, and somatic growth in cod is unclear, with results to date being somewhat ambiguous (Hall 1988; Hansen et al. 2001; Imsland et al. 2005). The present study examined for the first time in Atlantic cod the impact of long-term exposure to LL (up to 22 months in photoperiod regime 2) on somatic growth in maturing as well as nonmaturing cohorts. Results clearly showed that in photoperiod regimes 2–5, growth rate was elevated over a period of 3–6 months fol-

© 2007 NRC Canada

Fig. 4. Box plots of specific growth rate of weight for photoperiods 1–8 between (*a*) October 2001 and January 2002, (*b*) January and April 2002, (*c*) April and July 2002, (*d*) July and October 2002, (*e*) October 2002 and January 2003, (*f*) January and April 2003, and (*g*) April and July 2003. The box represents the 25th and 75th percentiles and whiskers denote the 5th and 95th percentile ranges. The median and mean are shown as a solid line and a broken line, respectively, where different (n = 32–43). Arrows indicate transfer of the population from a simulated natural photoperiod to a continuous illumination photoperiod at the start of the growth period. Different letters denote significant differences between treatments.

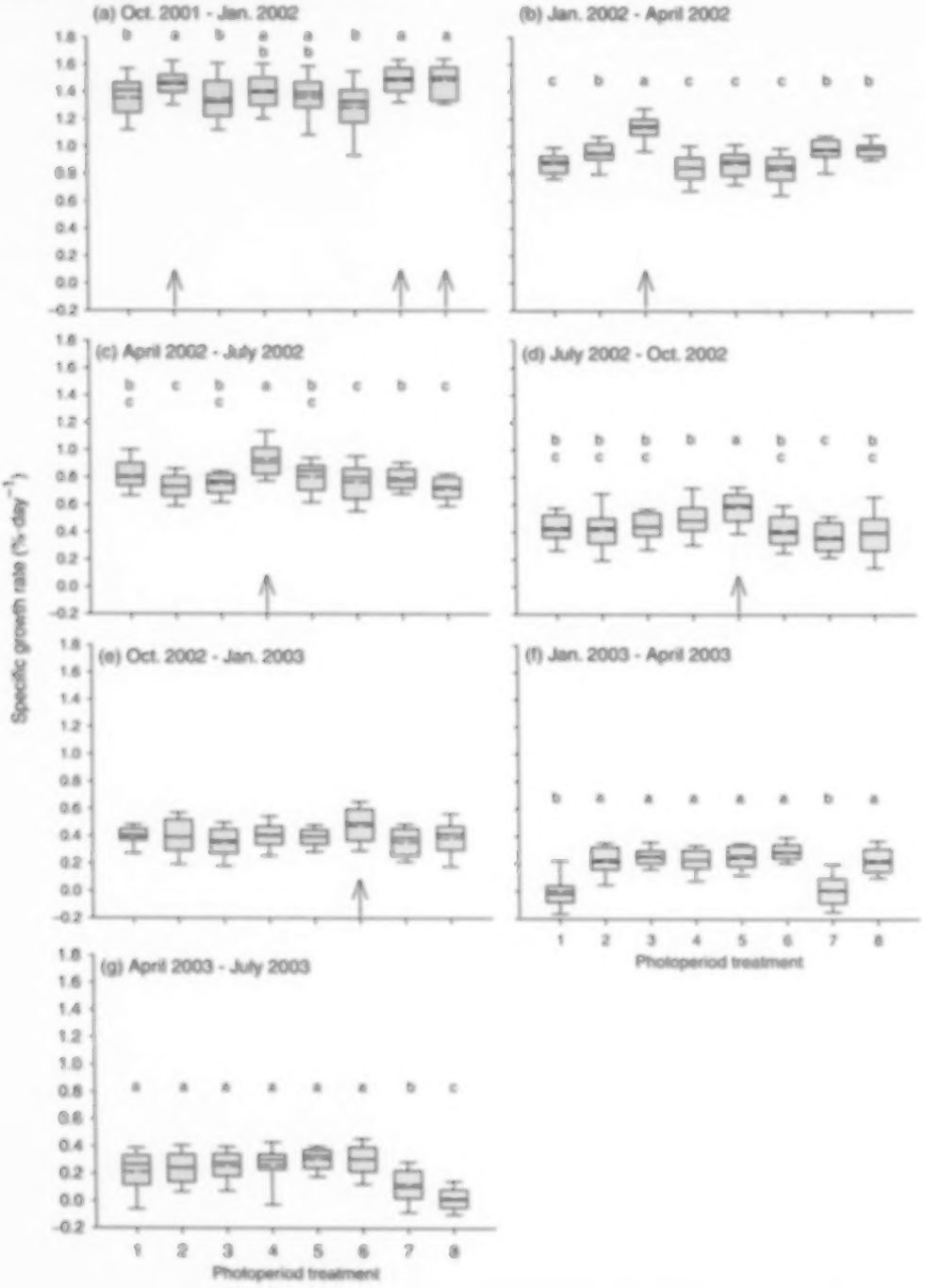
(a) Oct. 2001 - Jan. 2002
(b) Jan. 2002 - April 2002
(c) April 2002 - July 2002
(d) July 2002 - Oct. 2002
(e) Oct. 2002 - Jan. 2003
(f) Jan. 2003 - April 2003
(g) April 2003 - July 2003
Specific growth rate (% · day⁻¹)
Photoperiod treatment

© 2007 NRC Canada

Fig. 5. Mean Fulton's condition factor ± SE of the mean of individuals (n = 32–43) maintained under photoperiod 1 versus (*a*) photoperiod 2, (*b*) photoperiod 3, (*c*) photoperiod 4, (*d*) photoperiod 5, (*e*) photoperiod 6, (*f*) photoperiod 7, (*g*) photoperiod 8, and (*h*) all treatments. In panels *a*–*g*, photoperiod treatments are shown as grey lines, photoperiod 1 is a broken line, and photoperiods 2–8 are solid lines. Horizontal bars denote the spawning season for the respective photoperiods. An asterisk in panels *a*–*g* denotes significant differences between the experimental treatment and photoperiod 1 at a specified time point.

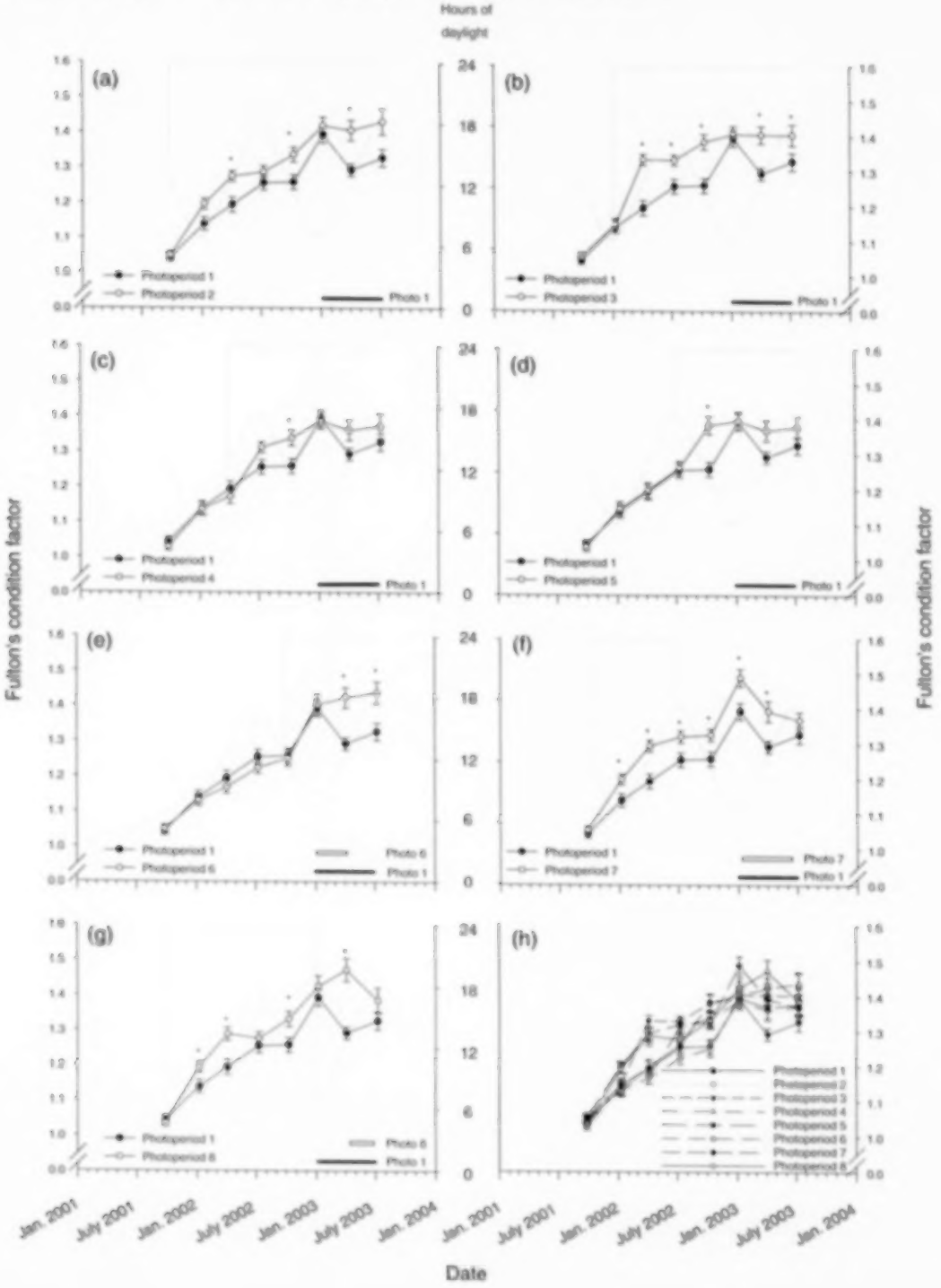

© 2007 NRC Canada

Fig. 6. Mean plasma insulin-like growth factor-I (IGF-I) ± SE of the mean for individuals (n = 4–10) maintained under photoperiod 1 versus (*a*) photoperiod 2, (*b*) photoperiod 3, (*c*) photoperiod 4, (*d*) photoperiod 5, (*e*) photoperiod 6, (*f*) photoperiod 7, (*g*) photoperiod 8, and (*h*) all treatments. In panels *a*–*g*, photoperiod treatments are shown as grey lines, photoperiod 1 is a broken line, and photoperiods 2–8 are solid lines. Horizontal bars denote the spawning season for the respective photoperiods. An asterisk in panels *a*–*g* denotes significant differences between the experimental treatment and photoperiod 1 at each time point, while in panel *h*, letters denote significant differences between treatments.

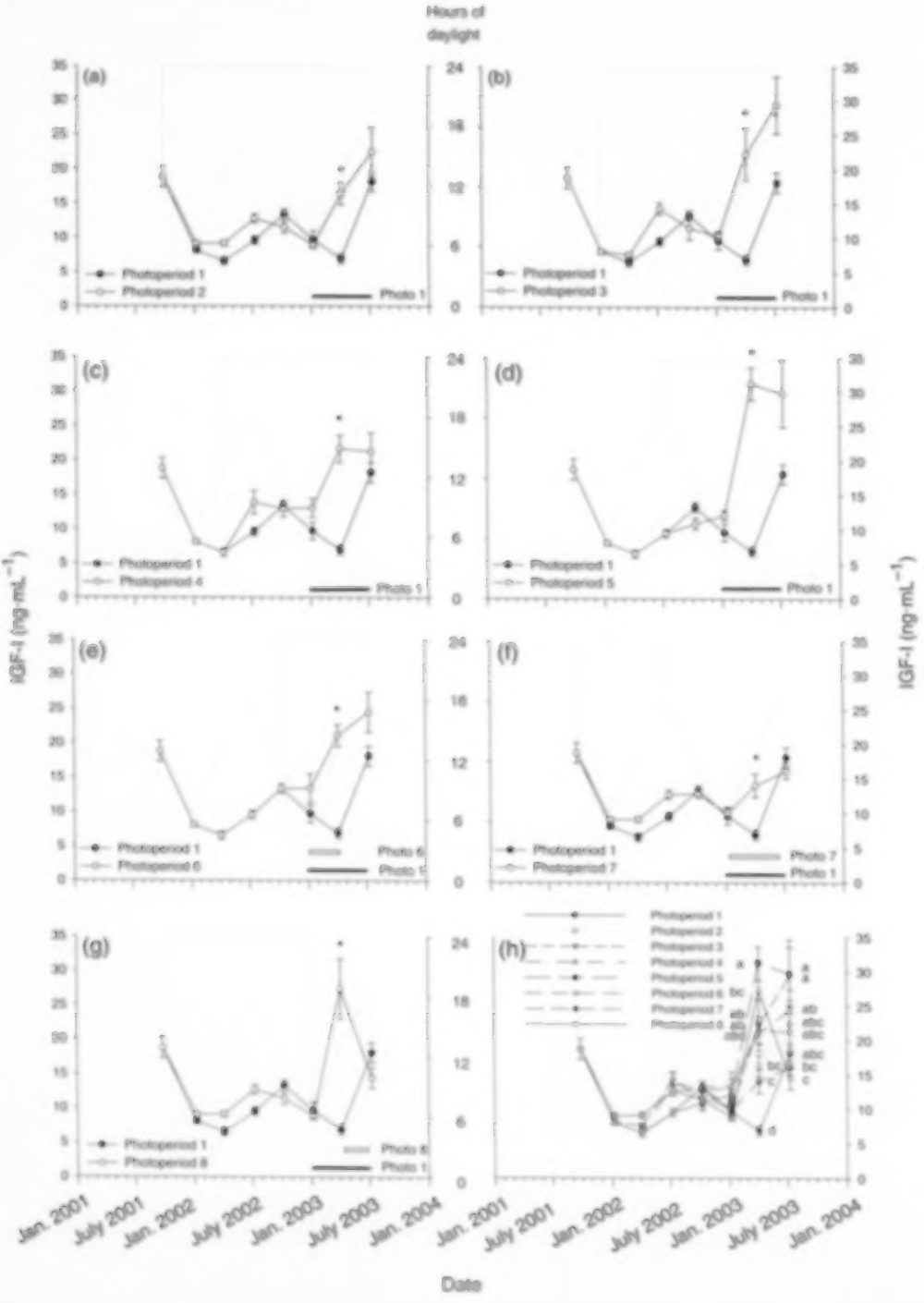

© 2007 NRC Canada

Table 3. Regression relationships between population mean plasma insulin-like growth factor-I (IGF-I) levels measured at the end of the growth period and population mean growth rates (SGRw, weight-specific growth rate; SGRl, length-specific growth rate; TGC, thermal growth coefficient) recorded over the 3-month growth period.

Growth rate	Pearson's correlation coefficient	F	p	r^2	Gradient	Intercept
January–April 2002						
SGRw	0.743	7.40	0.035	0.552	0.015	–0.135
SGRl	0.770	8.73	0.026	0.593	0.003	0.001
TGC	0.755	7.97	0.032	0.571	0.082	–0.748
April–July 2003						
SGRw	0.853	16.06	0.007	0.728	0.017	–0.156
SGRl	0.931	38.80	0.001	0.866	0.005	–0.037
TGC	0.879	20.33	0.004	0.772	0.075	–0.780

lowing LL exposure. These findings are in accordance with those of Hall (1988), Folkvord and Ottera (1993), and Imsland et al. (2005), all of whom investigated the effect of short-term photoperiod treatment in immature cod. However, the present results further demonstrated that such a growth enhancement was not maintained thereafter and that out with this 3- to 6-month window, growth rates were comparable in all treatments, including LL versus SNP treatments. As a result of this, at the trial's end, fish under photoperiod regimes 3–5 were of a comparable size, while those under photoperiod treatment 2 (longest exposure to LL) were significantly smaller than those under photoperiod regimes 4 and 5 (shortest exposure to LL). Endal et al. (2000) tested comparable photoperiod treatments in Atlantic salmon and reported both larger mean weights and increased maturation rates (8%–37%) with increasing exposure to LL, a reflection of the species-specific nature of photoperiodic regulation of physiology in teleosts. However, population mean growth data were presented without any distinction between mature and immature cohorts, thus limiting any possible comparison. Equally, Norberg et al. (2001) reported elevated growth rates in male Atlantic halibut following transfer from SNP to LL at ~14, 20, and 26 MPH, all of which ended the trial at ~40 MPH with comparable final weights as well as resulting in 100% maturation. However, females under the same treatments that remained immature throughout displayed significantly improved growth in those populations reared under LL photoperiods (B. Norberg, Institute of Marine Research, N-5817 Bergen, Norway, personal communication).

The growth benefit following continuous light exposure is commonly ascribed to the shifting of endogenous growth rhythms (Duncan et al. 1999; Oppedal et al. 1999; Endal et al. 2000). Nevertheless, in this present study, it appears that the transfer to LL from SNP caused instead a temporary direct stimulation of somatic growth. Following this enhancement, growth rates were maintained at a similar rate compared with other LL and SNP treatments. Furthermore, the transfer of photoperiod treatment 7 to SNP at 15 MPH, following 9 months of LL exposure, did not suppress growth rate in the subsequent 3 months; instead, it remained comparable with that of both photoperiod 2 (LL) and the ambient photoperiod control (SNP). This lack of influence on growth in the present study further suggests that no endogenous growth rhythms were present. Both Bromage et al. (1993) and Endal et al. (2000) have reported that a reduction in photoperiod length is a stronger zeitgeber of endogenous circadian rhythms than a rising photoperiod. It is thus proposed that at least in the case of Atlantic cod, light is stimulating the somatic growth axis directly. This is made evident from the fact that in all cases, transfer to LL caused a significant rise in condition factor, and once elevated, it was generally then unchanging in the immature populations. Increased condition implies an increase in weight with respect to length. At the same time, gonadosomatic index (Davie et al. 2007) and HSI, the relative size of the two principal seasonally fluctuating organs in cod (Eliassen and Vahl 1982*a*; Schwalme and Chouinard 1999), did not increase in response to LL treatment unlike in the mature populations where comparable condition increases were concurrent with elevated gonadosomatic index levels. This suggests that the relative carcass weight for a given length or ultimately muscle mass has increased in response to LL exposure. Johnston et al. (2003) have demonstrated that the growth enhancement under LL treatment over the winter in postsmolt salmon is due to increased muscle fibre recruitment. Such a mechanism might also be at work in the present trial, although this requires further investigation.

As the trial progressed, it became apparent that growth in the immature populations was showing sexually dimorphic tendencies with, in all cases, females being larger than males at the end of the trial. Male weight as a percentage of female size was in the range 75%–89%, which is comparable with the summary data presented by Imsland et al. (1997). Calvo (1989) reported that five members of the Merlucciidae family (members of the Gadiformes) exhibit a sexual growth dimorphism and suggested that females were recruiting muscle fibres for a longer period than males, thus resulting in a greater muscle mass and hence larger size. It is possible that the LL manipulation of somatic growth acting through muscle fibre recruitment (Johnston et al. 2003) may be responsible for the currently observed phenomenon. If proven, this may provide a compelling argument for the creation of all-female populations in preference to mixed sex for future commercial cod ongrowing.

IGF-I was chosen in this study as a target hormone to monitor endocrine activity within the growth axis because of its key regulatory role in nutrient uptake, protein synthesis,

© 2007 NRC Canada

Fig. 7. Relationship between mean plasma insulin-like growth factor-I (IGF-I) and weight-specific growth rate for fish maintained under photoperiods 1–8 between (*a*) January and April 2003 and (*b*) April and July 2003. The weight-specific growth rate calculated between sampling points is in comparison with IGF-I levels measured at the end of the growth period (e.g., January–April 2003 weight-specific growth rate versus April 2003 IGF-I) (n = 8–11 per treatment). Regression statistics: (*a*) $y = 0.015x - 0.135$ ($r^2 = 0.55$, $p = 0.035$); (*b*) $y = 0.017x - 0.156$ ($r^2 = 0.73$, $p = 0.07$).

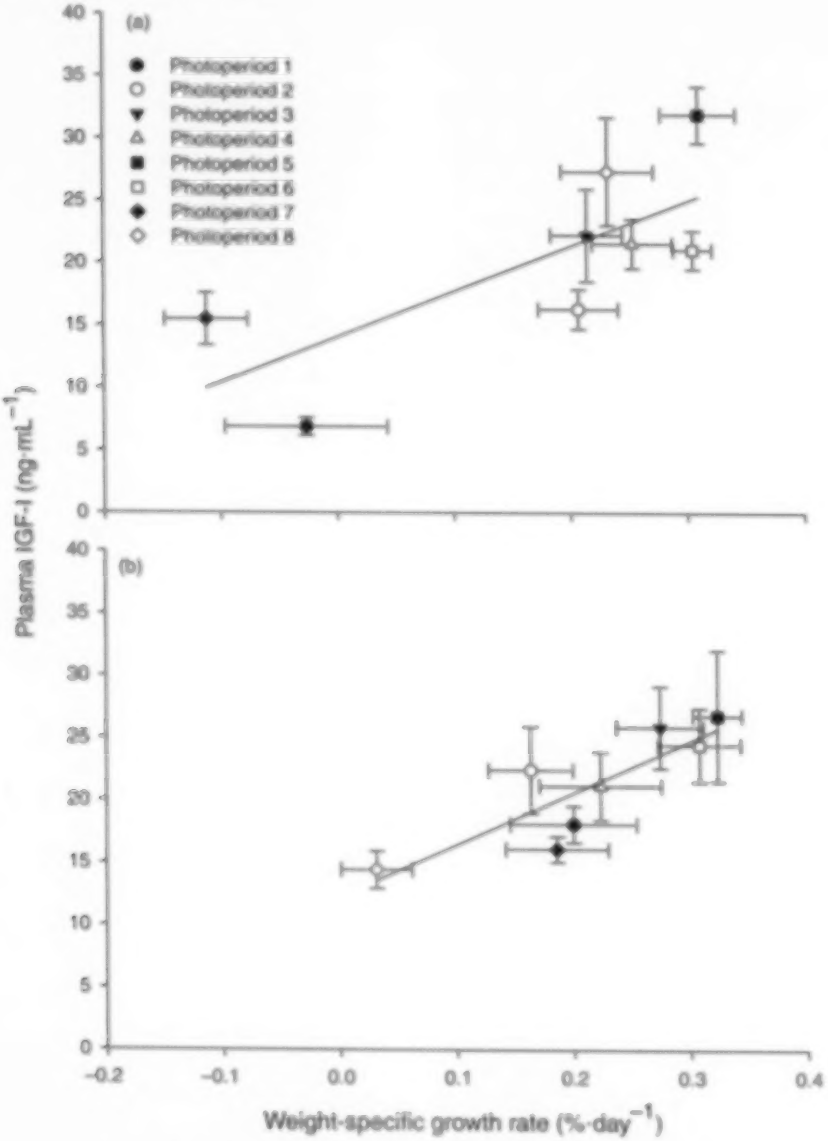

and cell division (Duan 1997), which has led to the general acceptance that IGF-I measurement can act as an accurate predictor of growth potential (Dyer et al. 2004*a*). To date and to the authors' knowledge, no published data of plasma IGF-I in Atlantic cod are available; the levels herein reported (5–35 ng·mL^{-1}) are comparable with those quoted for a wide range of other teleost species including Atlantic halibut (Weltzien et al. 2003), Atlantic salmon, southern bluefin tuna (*Thunnus maccoyii*), black bream (*Acanthopargus butcherii*), and silver perch (*Bidyanus bidyanus*) (Dyer et al. 2004*b*), rainbow trout (*Oncorhynchus mykiss*) (Taylor et al. 2005), Chinook salmon (*Oncorhynchus tshawytscha*) (Beckman et al. 2001), coho salmon (*Oncorhynchus kisutch*) (Larsen et al. 2001), barramundi (*Lates calcarifer*) (Nankervis et al. 2000), and channel catfish (*Ictalurus punctatus*) (Silverstein et al. 2000). In the present study, mean plasma IGF-I levels under ambient photothermal conditions exhibited a circannual pattern that positively correlates with the ambient water temperature. Weltzien et al. (2003) recorded no such seasonal association in halibut, while McCormick et al. (2000) and Taylor et al. (2005) both recorded a significant relationship between temperature and IGF-I levels in

© 2007 NRC Canada

Fig. 8. Mean hepatosomatic index ± SE of the mean for individuals (n = 4–11) maintained under photoperiod treatments 1–8. Letters denote significant differences between treatments at a given time point.

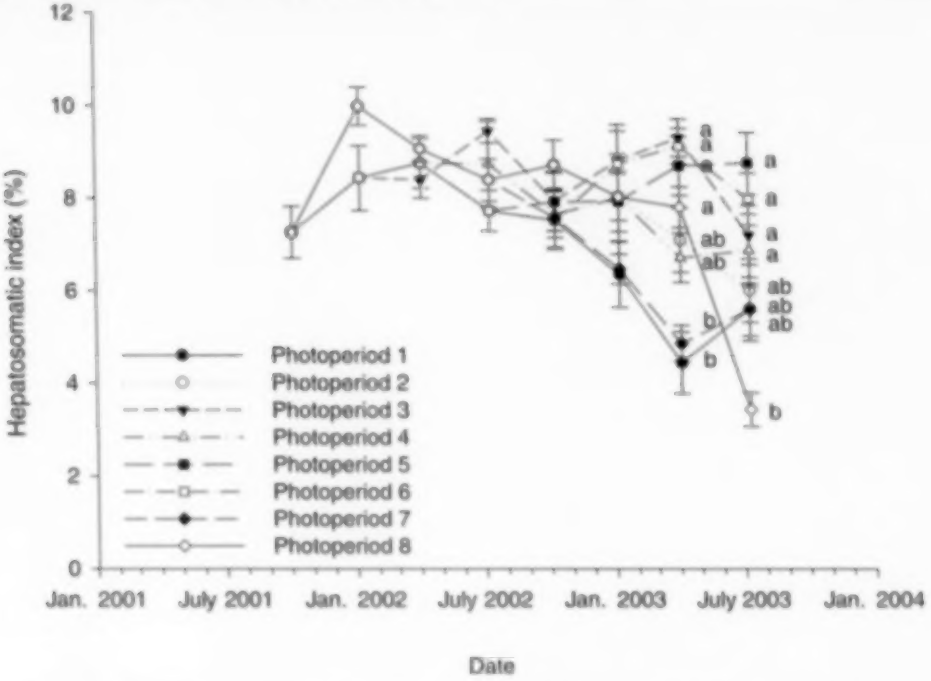

Table 4. Proximate composition of muscle (g·100 g^{-1}) of individuals (n = 8–10) maintained under photoperiods 1–8 in July 2003 (27 months posthatch (MPH)).

Photoperiod treatment	n	Moisture	Dry matter	Protein	Lipid
1	9	78.2±0.4ab	21.8±0.4cd	20.1±0.3cd	0.15±0.02
2	8	77.4±0.2abcd	22.6±0.2abcd	21.0±0.2abc	0.15±0.02
3	9	76.7±0.4bcd	23.3±0.4abc	21.5±0.3ab	0.17±0.01
4	10	77.3±0.4bcd	22.7±0.4abc	21.0±0.3abc	0.17±0.01
5	10	76.4±0.3cd	23.6±0.3ab	21.7±0.2ab	0.17±0.01
6	10	76.1±0.3d	23.9±0.3a	22.0±0.2a	0.17±0.01
7	8	77.9±0.5abc	22.1±0.5bcd	20.5±0.4bcd	0.14±0.02
8	10	78.9±0.4a	21.1±0.4d	19.6±0.4d	0.12±0.02

Note: Letters denote significant difference between photoperiod treatments.

salmonids. However, the subsequent application of artificial (LL) photoperiods in the current study influenced IGF-I levels to disassociate this seasonal rhythm. This appears to be due to two principal phenomena. Firstly, there was an apparent, although not significant, increase in IGF-I levels with respect to the ambient treatment following LL exposure. Among its range of actions, IGF-I has been shown to stimulate both the rate of proliferation and the rate of differentiation of muscle cells (Castillo et al. 2004; Oksbjerg et al. 2004), potentially adding further credence to the suggestion that LL was directly stimulating muscle growth in immature fish. Secondly, at 24 and 27 MPH (April and July 2003), IGF-I levels were significantly different between groups, and most notably, IGF-I levels of LL-treated populations showed significant elevations in comparison with comparable dates in year 1 (12 MPH and 15 MPH). These differences predominately reflect those seen in growth rate, as maturing populations at this time (i.e., treatments 1, 7, and 8) exhibited significantly reduced growth, which is reflected in the fall in IGF-I levels. The difference in levels observed between year 1 and year 2 in LL-treated populations may have been a size-related effect with the suppression in growth due to maturation in populations under treatments 1, 7, and 8 inhibiting such an elevation in these treatments.

Correlations between IGF-I and growth have been reported in many previous studies (e.g., Mingarro et al. 2002; Beckman et al. 2004*a*; Dyer et al. 2004*a*), leading to the proposal that monitoring of IGF-I can be used as a rapid assessment of growth response under various experimental conditions (Dyer et al. 2004*a*, 2004*b*). However, in the present study, individual growth rate correlations were generally very weak (r^2 range between 0.08 and 0.25, data not presented); fur-

© 2007 NRC Canada

thermore, owing to the small relative sample size (n = 10 or less) per photoperiod treatment, it was not possible to compare individual growth rate versus IGF-I relationships at the population level. It must be acknowledged that the strength of these relationships could have been weakened by both the sampling regime and the experimental thermal conditions, as it has been proposed that plasma IGF-I levels would reflect shorter-term growth activity (Dyer et al. 2004*a*), and fluctuating rearing temperatures (decreasing especially) have been shown to reduce the efficacy of IGF-I as a growth predictor (Beckman et al. 2004*b*). Nevertheless, strong significant growth rate correlations were observed at the trial's end when a large divergence in growth rate was manifested by the spawning activity. Therefore, there is clearly potential to utilize IGF-I as a growth predictor in the species, and importantly, these results suggest a possible route by which photoperiod manipulation may be influencing somatic growth, which demands further examination.

The liver is the principal energy reserve in cod (Holdway and Beamish 1984) and, as such, HSI is a valuable tool to describe fluctuations in this energy resource (Lambert and Dutil 1997). No differences in HSI levels between the sexes were recorded, as was noted by Lloret and Ratz (2000) in stocks off Greenland. However, Karlsen et al. (1995) did report temporal differences in HSI between the sexes, which led the authors to conclude that male gadoids prepare for spawning earlier than in females. The lack of such detection in the present trial may be a reflection of the restricted sample time frame and (or) numbers analysed. However, the fact that the majority of individuals included in the study of Karlsen et al. (1995) had experienced a period of starvation may have increased their dependence on endogenous energy reserves, which in turn could have induced the observed phenomenon. Within the present work, the only significant difference noted was the temporary decline in HSI in populations 1, 7, and 8 that coincided with the peak in spawning activity in these treatments (Davie et al. 2007), as was reported by Eliassen and Vahl (1982*a*) and Hansen et al. (2001). The lack of detectable fluctuations in the other populations suggests, once again, the lack of maturation commitment under these photoperiod treatments.

Fluctuations in muscle proximate composition, as a potential indicator of flesh quality, were also examined at the end of the trial. Owing to the significant inverse relationship between water content versus protein and lipid content in cod muscle, the photoperiod treatments 1, 7, and 8, in which the populations matured, exhibited a tendency towards higher water content and consequently lower protein and lipid content than the immature treatments 2–6. The range recorded in this present trial (78.9%–76.1% moisture content versus 19.6%–22% protein content from photoperiod 8 (mature) versus photoperiod 6 (immature), respectively) is comparable with that noted in other studies examining fluctuations in muscle proximate composition over seasonal cycles in cod (Love 1970; Eliassen and Vahl 1982*b*; Hemre et al. 2004). While it is recognized that these variations are low, the present association with reproduction is in accordance with Love (1970) and Hemre et al. (2004). In further support, Hemre et al. (2002), who studied whole-body proximate content instead of muscle alone, observed a significant decline in whole-body protein content and a reciprocal rise in moisture content in relation to spawning in cod, which the authors believed was a reflection of the requirement for protein in oocyte development. While it is apparent that this protein loss in the muscle can be prevented through the inhibition of maturation, such variations may not be considered to be commercially significant, although the impact on other flesh quality parameters such as texture or gaping incidence was not investigated in this trial.

While the results of this study provide evidence for direct stimulation of somatic growth by photoperiod manipulation, it is important to place such gains in context with the growth benefit realized in association with prevention of sexual maturation. Until 21 MPH, the difference in mean weight between immature and mature populations was <25%; however, at the trial's end (27 MPH), there was an improvement of over 60% in weight in the immature populations in comparison with the ambient mature population. Such gains are comparable with those reported in the previous works of Hansen et al. (2001) and Davie et al. (2003). Hence, with regard to the commercial significance of this work, it must be concluded that the most important factor in growth improvement in farmed cod is the prevention of maturation. Overall, the work presented in this paper aimed to further optimize industrial guidelines for photoperiod management during ongrowing. In the commercial application of photoperiod regimes, there must be a balance between cost and benefit where, in the simplest sense, cost can be measured as time of light application, while benefit is marked as firstly preventing maturation and secondly through further enhancement of somatic growth. The present work shows that to prevent maturation, LL should be applied from the summer solstice prior to likely maturation (15 MPH in the present case), which serves to mask the opening of the window of opportunity (Davie et al. 2007). Earlier application of LL photoperiods realized no further significant growth gain, which therefore defines the summer solstice photoperiod as the optimum timing of application to prevent maturation and realize maximum growth potential in farmed Atlantic cod. The reported failure of such manipulations in open cage systems (Taranger et al. 2006) is suggestive of inappropriate lighting systems being deployed. Future research should therefore focus on the perception of light by the species to refine the lighting systems that are subsequently employed.

Acknowledgements

The authors thank Dr. Derek Robertson for his support in instigating the experiment and the staff of the Machrihanish Marine Environmental Research Laboratory for its daily management. Fish were provided by Machrihanish Marine Farms Ltd., and financial support was provided by a Natural Environment Research Council award (NER/S/A/2000/03640) and the British Marine Finfish Association.

References

Association of Official Analytical Chemists. 1990. Official methods of analysis. 15th ed. Association of Official Analytical Chemists, Arlington, Va.

Beckman, B.R., Shearer, K.D., Cooper, K.A., and Dickhoff, W.W. 2001. Relationship of insulin-like growth factor-1 and insulin to

© 2007 NRC Canada

size and adiposity of under-yearling chinook salmon. Comp. Biochem. Physiol. A, **129**: 585–593.

Beckman, B.R., Shimizu, M., Gadberry, B.A., and Cooper, K.A. 2004*a*. Response of the somatotropic axis of juvenile coho salmon to alterations in plane of nutrition with an analysis of the relationships among growth rate and circualting IGF-1 and 41 kDa IGFBP. Gen. Comp. Endocrinol. **135**: 334–344.

Beckman, B.R., Shimizu, M., Gadberry, B.A., Parkins, P.J., and Cooper, K.A. 2004*b*. The effect of temperature change on the relations among plasma IGF-I, 41-kDa IGFBP, and growth rate in postsmolt coho salmon. Aquaculture, **241**: 601–619.

Begtashi, I., Rodriguez, L., Moles, G., Zanuy, S., and Carrillo, M. 2004. Long-term exposure to continuous light inhibits precocity in juvenile male European sea bass (*Dicentrarchus labrax*, L.). I. Morphological aspects. Aquaculture, **241**: 539–559.

Boeuf, G., and Falcon, J. 2001. Photoperiod and growth in fish. Vie Milieu, **51**, 547–266.

Boeuf, G., and Le Bail, P.Y. 1999. Does light have an influence on fish growth? Aquaculture, **177**: 129–152.

Bolger, T., and Connolly, P.L. 1981. The selection of suitable indices for the measurement and analysis of fish condition. J. Fish Biol. **34**: 171–182.

Bromage, N., Randall, C., Duston, J., Thrush, M., and Jones, J. 1993. Environmental control of reproduction in salmonids. *In* Recent advances in aquaculture IV. *Edited by* J. Muir and R.J. Roberts. Blackwell, Oxford, UK. pp. 55–66.

Calvo, J. 1989. Sexual differences in the increase of white muscle fibres in Argentine hake, *Merluccius hubbsi*, from the San Matais Gulf (Argentina). J. Fish Biol. **35**: 207–214.

Castillo, J., Codina, M., Martinez, M.L., Navarro, I., and Gutinez, J. 2004. Metabolic and mitogenic effects of IGF-1 and insulin on muscle cells of rainbow trout. Am. J. Physiol. **286**: R935–R941.

Dahle, R., Taranger, G.L., and Norberg, B. 2000. Sexual maturation and growth of Atlantic cod *Gadus morhua* reared at different light intensities. *In* Proceedings of the 6th International Symposium on the Reproductive Physiology of Fish, Bergen, Norway, 4–9 July 1999. *Edited by* B. Norberg, O.S. Kjesbu, G.L. Taranger, E. Andersson, and S.O. Stefansson. John Greig AS, Bergen. p. 336.

Davie, A., Porter, M.J.R., and Bromage, N.R. 2003. Photoperiod manipulation of maturation and growth of Atlantic cod (*Gadus morhua*). Fish Physiol. Biochem. **28**: 399–400.

Davie, A., Porter, M.J.R., Bromage, N.R., and Migaud, H. 2007. The role of seasonally altering photoperiod in regulating physiology in Atlantic cod (*Gadus morhua*). Part I. Sexual maturation. Can. J. Fish. Aquat. Sci. **64**: 84–97.

Duan, C. 1997. The Insulin-like growth factor system and its biological actions in fish. Am. Zool. **37**: 491–503.

Duncan, N., Mitchell, D., and Bromage, N. 1999. Post-smolt growth and maturation of out-of-season 0+ Atlantic salmon *Salmo salar* reared under different photoperiods. Aquaculture, **177**: 61–71.

Dyer, A.R., Barlow, C.G., Bransden, M.P., Carter, C.G., Glencross, B.D., Richardson, N., Thomas, P.M., Williams, K.C., and Carragher, J.F. 2004*a*. Correlation of plasma IGF-1 concentrations and growth rate in aquacultured finfish: a tool for assessing the potential of new diets. Aquaculture, **236**: 583–592.

Dyer, A.R., Upton, Z., Stone, D., Thomas, P.M., Soode, K.L., Higgs, N., Quinn, K., and Carragher, J.F. 2004*b*. Development and validation of a radioimmunoassay for fish insulin-like growth factor 1 (IGF-1)and the effect of aquaculture related stressors on circualting IGF-1 levels. Gen. Comp. Endocrinol. **135**: 268–275.

Eliassen, J.E., and Vahl, O. 1982*a*. Seasonal variations in biochemical composition and energy content of liver, gonad and muscle of mature and immature cod, *Gadus morhua*, from Balsfjorden, northern Norway. J. Fish Biol. **20**: 707–716.

Eliassen, J.E., and Vahl, O. 1982*b*. Seasonal variations in the gonad size and the protein and water content of Cod, *Gadus morhua*, muscle from northern Norway. J. Fish Biol. **20**: 527–533.

Endal, H.P., Taranger, G.L., Stefansson, S.O., and Hansen, T. 2000. Effects of continuous addiational light on growth and sexual maturity in Atlantic salmon, *Salmo salar*, reared in sea cages. Aquaculture, **191**: 337–349.

Folkvord, A., and Ottera, H. 1993. Effects of initial size distribution, daylength, and feeding frequency on growth, survival and cannibalism in juvenile Atlantic cod (*Gadus morhua* L.). Aquaculture, **114**: 243–260.

Hall, S.J. 1988. The effects of reversal of seasonal changes in photoperiod on the growth and food consumption of cod *Gadus morhua*. J. Fish Biol. **32**: 783–792.

Hall, S.J. 2000. The biological consequence of photoperiod manipulation in Atlantic cod, *Gadus morhua*. M.Sc. thesis, Institute of Aquaculture, University of Stirling, Stirling, UK.

Hansen, T., Karlsen, O., Taranger, G.L., Hemre, G.-I., Holm, J.C., and Kjesbu, O.S. 2001. Growth, gonadal development and spawning time of Atlantic cod (*Gadus morhua*) reared under different photoperiods. Aquaculture, **203**: 51–67.

Hemre, G.I., Taranger, G.L., and Hansen, T. 2002. Gonadal development influences nutrient utilisation in cod (*Gadus morhua*). Aquaculture, **214**: 201–209.

Hemre, G.I., Karlsen, O., Eckhoff, K., Tveit, K., Mangor-Jensen, A., and Rosenlund, G. 2004. Effect of season, light regime and diet on muscle composition and selected quality parameters in farmed Atlantic cod, *Gadus morhua* L. Aquacult. Res. **35**: 683–697.

Holdway, D.A., and Beamish, F.W.H. 1984. Specific growth rate and proximate body composition of Atlantic cod (*Gadus morhua*). J. Exp. Mar. Biol. **81**: 147–170.

Houde, E.D., and Schekter, R.C. 1981. Growth rates, rations and cohort consumption of marine fish larvae in relation to prey concentrations. Rapp. P.-v. Réun. Cons. Int. Explor. Mer, **178**: 441–453.

Imsland, A.K., Folkvord, A., Grung, G.L., Stefansson, S.O., and Taranger, G.L. 1997. Sexual dimorphism in growth and maturation of turbot *Scopthalmus maximus* (Ratinesque 1810). Aquacult. Res. **28**: 101–114.

Imsland, A.K., Foss, A., Folkvord, A., Stefansson, S.O., and Jonassen, T.M. 2005. Genotypic response to photoperiod treatment in Atlantic cod (*Gadus morhua*). Aquaculture, **250**: 525–532.

Iwama, G.K., and Tautz, A. 1981. A simple growth model for salmonids in hatcheries. Can. J. Fish. Aquat. Sci. **38**: 649–656.

Johnston, I.A., Manthri, S., Smart, A., Campbell, P., Nickell, D., and Alderson, R. 2003. Plasticity of muscle fibre number in seawater stages of Atlantic salmon in response to photoperiod manipulation. J. Exp. Biol. **206**: 3425–3435.

Karlsen, O., Holm, J.C., and Kjesbu, O.S. 1995. Effects of periodic starvation on reproductive investment in first-time spawning Atlantic cod *Gadus morhua*. Aquaculture, **133**: 159–170.

Karlsen, O., Taranger, G.L., Dahle, R., and Norberg, B. 2000. Effects of exercise and continuous light on early sexual maturation in farmed Atlantic cod *Gadus morhua*. *In* Proceedings of the 6th International Symposium on the Reproductive Physiology of Fish, Bergen, Norway, 4–9 July 1999. *Edited by* B. Norberg, O.S. Kjesbu, G.L. Taranger, E. Andersson, and S.O. Stefansson. John Greig AS, Bergen. pp. 328–330.

Lambert, Y., and Dutil, J.D. 1997. Can simple condition indices be used to monitor and quantify seasonal changes in the energy reserves of Atlantic cod (*Gadus morhua*). Can. J. Fish. Aquat. Sci. **54**: 104–112.

© 2007 NRC Canada

Larsen, D.A., Beckman, B.R., and Dickhoff, W.W. 2001. The effect of low temperature and fasting during the winter on metabolic stores and endocrine physiology (insulin, insulin-like growth factor-I and thyroxine) of coho salmon, *Oncorhynchus kisutch*. Gen. Comp. Endocrinol. **123**: 308–323.

Lloret, J., and Rätz, H.J. 2000. Condition of cod (*Gadus morhua*) off Greenland during 1982–1998. Fish. Res. **48**: 79–86.

Love, R.M. 1970. The chemical biology of fishes. Academic Press, London and New York.

McCormick, S.D., Moriyama, S., and Bjornsson, B.T. 2000. Low temperature limits photoperiod control of smolting in Atlantic salmon through endocrine mechanisms. Am. J. Physiol. Regul. Integr. Comp. Physiol. **278**: R1352–R1361.

Mingarro, M., de Celis, S.V.R., Astola, A., Pendon, C., Valdivia, M.M., and Perez-Sanchez, J. 2002. Endocrine mediators of seasonal growth in gilthead sea bream (*Sparus aurata*): the growth hormone and somatolactin paradigm. Gen. Comp. Endocrinol. **128**: 102–111.

Nankervis, L., Matthews, S.J., and Appleford, P. 2000. Effect of dietary non-protein energy source on growth, nutrient retention and circulating insulin-like growth factor 1 and triiodothyronine levels in juvenile barramundi, *Lates calcarifer*. Aquaculture, **191**: 323–335.

Norberg, B., Weltzien, F.A., Karlsen, O., and Holm, J.C. 2001. Effects of photoperiod on sexual maturation and somatic growth in male Atlantic halibut (*Hippoglossus hippoglossus* L.). Comp. Biochem. Physiol. B, **129**: 357–365.

Oksbjerg, N., Gondret, F., and Vestergaard, M. 2004. Basic principles of muscle development and growth in meat-producing mammals as affected by the insulin-like growth factor (IGF) system. Domest. Anim. Endocrinol. **27**: 219–240.

Oppedal, F., Taranger, G.L., Juell, J.E., and Hansen, T. 1999. Growth, osmoregulation and sexual maturation of underyearling Atlantic salmon smolt *Salmo salar* L. exposed to different intensities of continuous light in sea cages. Aquacult. Res. **30**: 491–499.

Porter, M.J.R., Duncan, N.J., Mitchell, D., and Bromage, N.R. 1999. The use of cage lighting to reduce plasma melatonin in Atlantic salmon *Salmo salar* and its effects on the inhibition of grilsing. Aquaculture, **176**: 237–244.

Schwalme, K., and Chouinard, G.A. 1999. Seasonal dynamics in feeding, organ weights, and reproductive maturation of Atlantic cod (*Gadus morhua*) in the southern Gulf of St. Lawrence. ICES J. Mar. Sci. **56**: 303–319.

Silverstein, J.T., Wolters, W.R., Shimizu, M., and Dickhoff, W.W. 2000. Bovine growth hormone treatment of channel catfish: strain and temperature effects on growth, plasma IGF-1 levels, feed intake and efficiency and body composition. Aquaculture, **190**: 77–88.

Taranger, G.L., Aardal, L., Hansen, T., and Kjesbu, O.S. 2006. Continuous light delays sexual maturation and increases growth of Atlantic cod (*Gadus morhua* L.) in sea cages. ICES J. Mar. Sci. **63**: 365–375.

Taylor, J.F., Migaud, H., Porter, M.J.R., and Bromage, N.R. 2005. Photoperiod influences growth rate and plasma insulin-like growth factor-I levels in juvenile rainbow trout, *Oncorhynchus mykiss*. Gen. Comp. Endocrinol. **142**: 169–185.

Weltzien, F.A., Karlsen, O., and Norberg, B. 2003. Growth patterns and plasma levels of testosterone, 11-ketotestosterone, and IGF-1 in male Atlantic halibut (*Hippoglossus hippoglossus*) from juvenile stages throughout sexual development. Fish Physiol. Biochem. **28**: 227–228.

Yaragina, N.A., and Marshall, C.T. 2000. Trophic influences on interannual and seasonal variation in the liver condition index of Northeast Arctic cod (*Gadus morhua*). ICES J. Mar. Sci. **57**: 42–55.

Zar, J.H. 1999. Biostatistical analysis. 4th ed. Prentice Hall, Upper Saddle River, N.J.

© 2007 NRC Canada

The demography of recovery of an overexploited bull trout, *Salvelinus confluentus*, population

Fiona D. Johnston, John R. Post, Craig J. Mushens, Jim D. Stelfox, Andrew J. Paul, and Brian Lajeunesse

Abstract: An exploited bull trout, *Salvelinus confluentus*, population experienced a 28-fold increase in adult density during a 10-year period from a minimum of 60 individuals. This demonstrates the extent to which this population was overharvested. Its ability to respond in fewer than two generations to the implementation of zero-harvest regulations suggests this population was growth-overfished not recruitment-overfished. Examination of stock–recruitment relationships of various life stages indicates that recovery of this population was regulated by the density-dependent survival of juveniles in the rearing creek. This compensatory response occurred between egg deposition and age-1 and regulated the number of fish recruiting into the adult population. A second population bottleneck became apparent later in the recovery process when density-dependent survival of the adult population resulted in its approach to an asymptote, highlighting the necessity of long-term data sets for examining these compensatory responses. Results from this study demonstrate the importance of understanding the influence of individual life stages on the ability of overexploited populations such as threatened bull trout to recover and for their future management.

Résumé : Une population exploitée d'ombles à tête plate, *Salvelinus confluentus*, a connu une augmentation de densité de l'ordre de 28 fois des adultes durant une période de 10 ans à partir d'un minimum de 60 individus. Cela démontre le degré de surexploitation de la population. Sa capacité de réagir en moins de deux générations à la mise en application d'un règlement d'interdiction absolue des récoltes laisse croire que la population était surexploitée quant à la croissance, mais non quant au recrutement. L'examen des relations stock–recrutement des divers stades du cycle biologique indique que la récupération de cette espèce est contrôlée par la survie dépendante de la densité des jeunes dans le cours d'eau d'élevage. Cette réaction compensatoire se produit entre la ponte des oeufs et l'âge 1 et contrôle le nombre de poissons qui entrent dans la population adulte. Il se produit un second goulot d'étranglement plus tard dans le processus de récupération lorsque la survie dépendante de la densité de la population adulte a pour effet de lui faire atteindre une asymptote; cela illustre la nécessité d'obtenir des séries de données à long terme pour étudier ce type de réponse compensatoire. Les résultats de notre étude démontrent l'importance de comprendre l'influence des divers stades du cycle sur la capacité de récupération d'une population surexploitée, telle que celle de l'omble à tête plate, une espèce menacée; ils sont aussi importants pour sa gestion future.

[Traduit par la Rédaction]

Introduction

By the end of the 20th century, many marine and freshwater fish populations were severely overharvested (Pauly et al. 2002; Post et al. 2002; Hilborn et al. 2003). This leads us to question whether these populations will be able to recover from their depressed levels of abundance and what factors will influence their recovery. Theory suggests that the reduction in competition and cannibalism at low densities allows populations to recover from low levels through compensatory density dependence, where increased juvenile survival compensates for decreased egg production (Frank and Brickman 2000; Walters and Kitchell 2001; Milner et al. 2003). However, at these low population densities, depensatory processes or Allee effects, which result in decreased survival or further reduced fecundity at low densities, may result in population collapse even after harvest mortality is removed (Frank and Brickman 2000; Walters and Kitchell 2001). Abiotic factors also affect population abundance (Armstrong et al. 2003; Milner et al. 2003). Fisheries biologists need to understand the influence of compensatory, depensatory, and density-independent processes on

Received 12 March 2006. Accepted 29 September 2006. Published on the NRC Research Press Web site at http://cjfas.nrc.ca on 20 January 2007.
J19222

F.D. Johnston,[1] J.R. Post, C.J. Mushens, and A.J. Paul. Department of Biological Sciences, University of Calgary, Calgary, AB T2N 1N4, Canada.
J.D. Stelfox. Alberta Sustainable Resource Development, 2nd Floor Provincial Building, 213 – 1 Street West, Cochrane, AB T4C 1B4, Canada.
B. Lajeunesse. Alberta Sustainable Resource Development, 2nd Floor Provincial Building, 800 Railway Avenue, Canmore, AB T1W 1P1, Canada.

[1]Corresponding author (e-mail: fdjohnst@ucalgary.ca).

 doi:10.1139/F06-172 © 2007 NRC Canada

Fig. 1. Lower Kananaskis Lake and Smith-Dorrien Creek study area in the East Slopes of the Rocky Mountains in southwestern Alberta, Canada. The location of the fish counting fence and traps in 1991 and in all other years is indicated. The sections of the creek where redds were counted are shown with roman numerals.

population abundance to predict the ability of populations to recover and to manage them appropriately in the future.

The degree to which density-dependent and density-independent processes contribute to the regulation of populations not dominated by harvest has long been debated (Sinclair 1989; Berryman et al. 2002; Milner et al. 2003). Some studies that dismiss density dependence as a regulating process may have done so because they were too short in duration or incorporated an insufficient range in density to detect it (Begon et al. 1996; Shea and Mangel 2001; Milner et al. 2003). In addition, for species that have complex life histories and numerous life stages, density dependence may only act upon one life stage for a short period of time (Milner et al. 2003). However, during periods prior to and after this stage, the population is influenced by density-independent processes (Elliott 1994; Jonsson et al. 1998; Milner et al. 2003). If studies do not incorporate the appropriate life stage or period of development, conclusions about the influence of density dependence may differ (Prout and McChesney 1985; Whalen et al. 2000). In general, density-dependent regulation in taxa such as fish and insects with high reproductive rates occurs primarily in the early juvenile stage, whereas taxa with intermediate or lower reproductive rates are often regulated at later juvenile stages (i.e., birds and small mammals) or by changes in fecundity (i.e., large mammals) (Sinclair 1989).

While many fish populations are dominated by harvest, the imposition of harvest restrictions provides an opportunity to assess the natural processes regulating populations as they recover from overexploitation and the life stages at which they occur. The bull trout (*Salvelinus confluentus*) population in Lower Kananaskis Lake, Alberta, provides a unique opportunity to examine the processes of population regulation over a broad range of densities, as a species with complex life history recovers from heavy overexploitation. In general, many bull trout populations have declined in abundance and distribution in the last century because of overexploitation and habitat deterioration (see articles within Mackay et al. 1997; Rieman et al. 1997; Post and Johnston 2002). Bull trout are currently listed as a threatened under the Endangered Species Act in the coterminous United States (US Fish and Wildlife Service 2006) and are considered sensitive in Alberta, Canada (Alberta Sustainable Resource Development 2001). The bull trout population in Lower Kananaskis Lake is no exception and was in decline from 1947 until 1992, primarily because of overfishing (Stelfox 1997). This species is highly vulnerable to angling because of their opportunistic feeding behaviour and because they attain a catchable size several years prior to maturity (Paul et al. 2000, 2003; Post and Johnston 2002). By 1992, the spawning population was depressed to 60 spawning adults, at which time fishing regulations were changed to zero harvest.

We monitored numerous life stages over a 12-year period to study the demography of recovery of this severely overexploited population and to identify processes of population regulation. The objectives of this study were (*i*) to assess what the demographic response of this population was to the reduction in harvest mortality from angling and (*ii*) to determine what life stage(s) limit population growth. By understanding the processes that influence bull trout population dynamics, better management strategies may lead to the conservation of this species.

Materials and methods

Study area

Lower Kananaskis Lake is a 646 ha reservoir located in Peter Lougheed Provincial Park, Alberta, Canada, at 1667 m above sea level (Fig. 1). Prior to the dam's construction in 1955, Lower Kananaskis Lake supported self-sustaining populations of native bull trout and westslope cutthroat trout (*Oncorhynchus clarkii lewisi*) (Stelfox 1997). The dam isolated these fish populations and destroyed potential spawning habitat, leaving Smith-Dorrien Creek as the only suitable spawning habitat for the native bull trout population in Lower Kananaskis Lake (Fig. 1) (Stelfox and Egan 1995). Smith-Dorrien Creek is 18 km long, but because of impassable beaver dams only the lower 13 km are accessible to bull trout spawners. The stream drains 108 km^2 and has an average gradient from the first impassable beaver dam to the lake of 13 $m \cdot km^{-1}$. Average stream width ranges from about 7 m near the first dam to 13 m near the mouth. Stream discharge near the mouth ranges from >7 $m^3 \cdot s^{-1}$ in spring (late May to early July) to <1 $m^3 \cdot s^{-1}$ in autumn (late September to October) (Mushens 2003).

Prior to 1 April 1992, anglers were allowed a harvest of two bull trout per day (five bull trout prior to 1984) of a minimum size of 40 cm (no size limit prior to 1987), which allowed for the harvest of fish not yet sexually mature. In response to the declining numbers of bull trout, angling regulations for Lower Kananaskis Lake were changed on 1 April 1992. The new regulations introduced a full closure of Smith-Dorrien Creek and the northwest bay of Lower Kananaskis Lake to angling to protect staging and spawning bull trout. In addition, a bait ban and catch-and-release regulations for bull trout were imposed on the rest of Lower Kananaskis Lake.

Life history

The bull trout in Lower Kananaskis Lake spend most of their adult life in the reservoir and migrate up Smith-Dorrien Creek to spawn in the fall. The adfluvial bull trout begin their spawning migration between August and September and remain in the stream anywhere from a week to more than a month, returning downstream between September and early November (Mushens 2003; Johnston 2005). During the spawning event, the females build redds. Fry hatch the following spring and rear in the creek for 1–4 years before moving downstream to the reservoir, remaining there for an additional 3–5 years before attaining sexual maturity (Johnston 2005). Bull trout in Lower Kananaskis Lake reach

© 2007 NRC Canada

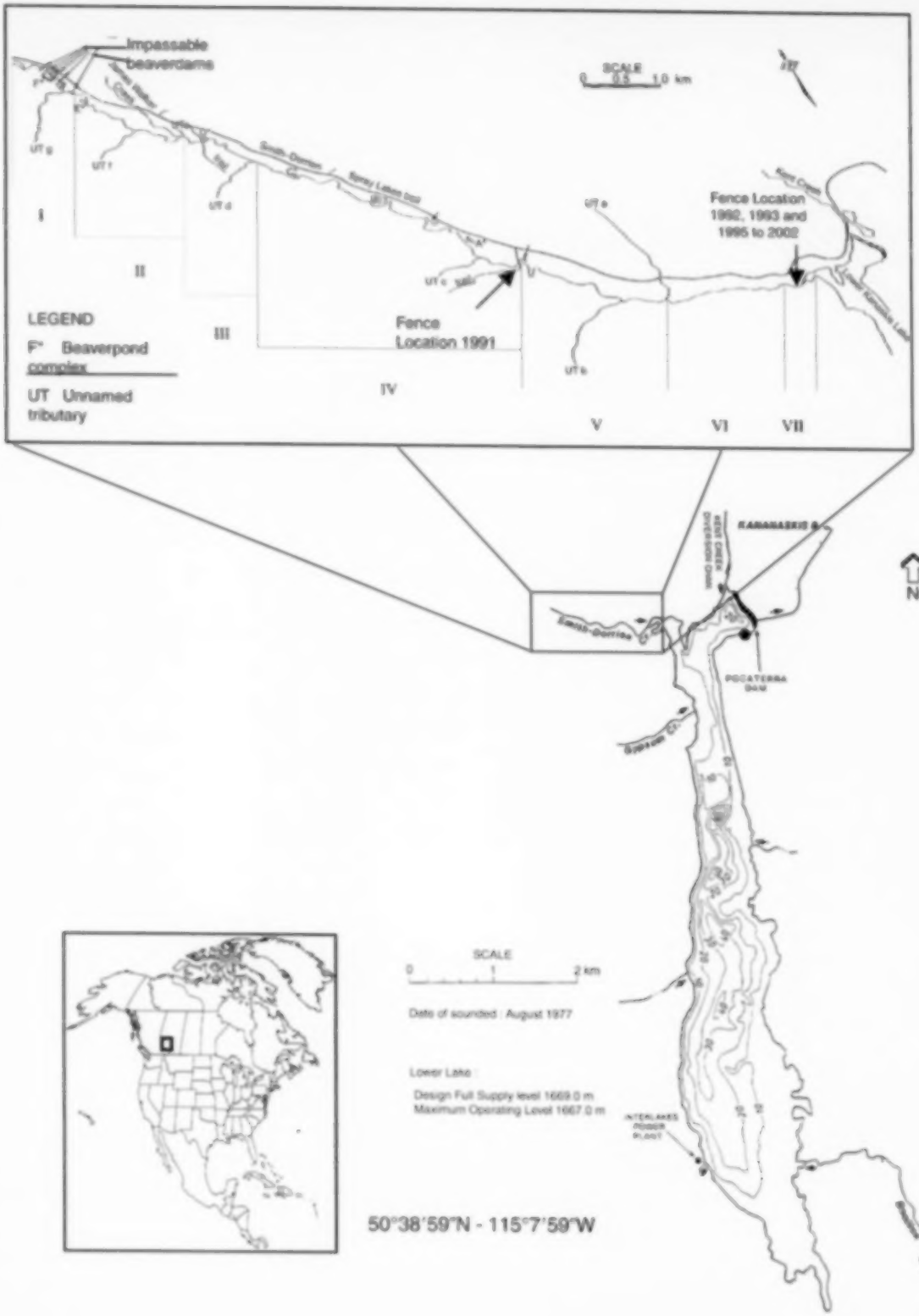

© 2007 NRC Canada

maturity at approximately 7 years of age (range 6–9) and are iteroparous (Johnston 2005). However, individuals may not spawn in sequential years (Johnston 2005), henceforth referred to as nonrepetitive spawning.

Field methods

The abundance of three different life stages were monitored during this study: adult spawners, juveniles in the stream, and redds. The spawning population was enumerated in Smith-Dorrien Creek during their migration. A fish fence that funnelled fish into either an upstream- or downstream-oriented trap was installed at the mouth of Smith-Dorrien Creek at the beginning of each spawning season from 1992 to 2002, excluding 1994 when the fence was not installed (Johnston 2005). The fence was generally in place from early to mid-August until mid- to late October to encompass the majority of the spawning migration, making it likely that a fish was caught moving in at least one direction of their migration. Design of the fence, traps, and trapping procedure are described fully in Johnston (2005). The fence was also installed in 1991. However, it was installed at a different site, 5.2 km upstream of the mouth of Smith-Dorrien Creek (Fig. 1). Only the downstream trap was installed in 2001.

Electrofishing was used to assess the relative abundance of juveniles in Smith-Dorrien Creek from 1995 to 2003. Electrofishing was carried out in August to early September when flow rates were suitably low, with the exception of 1995 when it was done in late July. A Smith Root Model 12-B battery-powered backpack electroshocker was used with a pulse frequency of 30 Hz, 4 ms^{-1}, and an output voltage of 600 V. The same 500 m index reach was electrofished using a standard three-pass removal–depletion technique, except in 1995 when 600 m was electrofished. The index reach represents moderate quality rearing habitat and was chosen for its accessibility to electrofishing crews. We assume that juvenile abundance in this section of the stream represents the relative abundance of juveniles over the entire creek. Two sections of Smith-Dorrien Creek, ~1 km in length, were also electrofished in 1991 using the three-pass removal–depletion technique (Stelfox and Egan 1995); however, these areas were not within the section of the stream electrofished from 1995 onward.

Bull trout captured in either the traps or electrofishing were weighed (to the nearest 1 g for adults and 0.1 or 0.01 g for juveniles), fork length (FL) was measured (to the nearest mm), and where possible sex and state of maturity was determined. In most years, all bull trout >400 mm were tagged with individually coded Floy® tags and VI Alpha visual implant tags and had their adipose fin removed to identify them as previously captured individuals. Fish were anaesthetized prior to tagging using either clove oil or tricaine methanesulfonate (MS-222). Replicate marking of individual fish aided in their future identification in the event of tag loss. In most years, fish <400 mm were given individually coded passive integrated transponder (PIT) tags and were given adipose and 1/3 dorsal fin clips. Electrofished juveniles were PIT-tagged and given an upper caudal fin clip. Trapped fish were released above or below the trap in relation to their original direction of travel and after consideration of their reproductive state (i.e., ripe or spent). Electrofished juveniles were released within the index reach where they were captured.

Redds were counted in Smith-Dorrien Creek throughout each spawning season, from 1990 to 2002. The upper sections of the creek, which were the primary spawning areas (sections I and II in Fig. 1), were examined twice during the spawning season, and redds were counted and marked. At the end of October, redds in the entire 13 km of Smith-Dorrien Creek were counted to obtain a complete census. The same protocol for identifying redds was used in all years. These counts were incomplete in 1990, 1994, and 2002 when lower sections of the creek (Fig. 1, sections V to VII) were not censused. However, these sites were used very little for spawning throughout the study period.

Abundance estimates

Using data collected from trapping, electrofishing, and redd counts, abundance was estimated for first-time spawners, total spawners, total adults, population-level fecundity (i.e., total egg number), juveniles by age class, and redds. Individuals caught in the trap each year are assumed to represent a complete census of the spawning population (except in 2001 when trapping was incomplete). We had to estimate the number of spawners in 2001 from those caught moving in the downstream direction only because we were unable to install the upstream trap. However, we believe that some fish were able to escape over an upstream-directed incline plane (designed to allow for only upstream fish passage) during periods of ice buildup. We estimated this loss rate by trapping and releasing 113 marked upstream migrants and counting the number of these that were subsequently caught returning downstream. The entire 13 km of stream was electrofished at the end of October to confirm these fish had not remained upstream after the trap removal. Of the 113 released upstream, 83 were subsequently recaptured moving downstream. Therefore, our best estimate of spawner abundance in 2001 is the number of downstream migrants multiplied by the ratio 113/83.

Abundance of first-time spawners was the census of sexually mature fish caught in the trap for the first time. Exceptions to this were in 1991, 1992, and to a lesser extent in 1993 because these fish may have spawned prior to the commencement of the study and then, because of nonrepetitive spawning, not returned for a few intervening years. Therefore, these cohorts were excluded from analyses of first-time spawners. By 1995, all nonrepetitive spawners from the period prior to 1991 were likely to have returned. However, the 1995 estimate includes first-time spawners from 1994 when the trap was not installed. The 2001 estimate of first-time spawners was adjusted for fish loss over the incline plane as detailed above, and the 2002 count was negatively adjusted to account for this estimated number of 2001 first-time spawners that were missed in 2001 and returned to spawn in 2002.

The annual abundance of adults alive in the system was estimated by tracking individuals interannually using the timing of their last known capture (i.e., an individual must be alive between first tagging and last capture). As a result, the adult abundance estimate is sensitive to the number of additional years of information available after the year being estimated. The more additional years of information avail-

© 2007 NRC Canada

Table 1. The proportion of estimated adult abundance (mean, minimum, and maximum) that was known after the spawning event (represented by zero additional years of data) and 1 to 3 additional years of information.

Additional years of information			
0	1	2	3
0.863 (0.706–0.925)	0.987 (0.977–0.998)	0.996 (0.990–0.999)	0.999 (0.997–1.000)

Table 2. The recruitment models fit to several life-stage intervals to examine density-dependent recruitment and survival of bull trout, *Salvelinus confluentus*.

Model description	Model	Parameter definition
Linear: density independent	$R = pS$	R = abundance of recruits in the resulting life stage; p = proportion of the cohort surviving to recruit; S = abundance of initial life stage (i.e., egg abundance)
Beverton–Holt: compensating density dependent	$R = (kS)/(h + S)$	k = maximum number of recruits produced; h = cohort size required to produce half of the maximum number of recruits
Ricker: overcompensating density dependent	$R = aSe^{-bS}$	a = recruits per unit stock at low stock levels; b = rate of decrease in recruits per unit stock as stock size increases

Note: Models are as described in Haddon (2001).

able, the more accurate the estimate of adult abundance, since the probability of recapturing nonrepetitive spawners increases with subsequent years. This time-series bias was addressed by calculating how much information was gained from each additional year of data. Nonrepetitive spawners were found to miss a maximum of 4 years in a row between spawning events. However, of all known nonrepetitive spawners during the period 1995–1999, 93.5% of these fish only missed 1 year of spawning before they returned to spawn again, 4.3% missed 2 years, 1.7% missed 3 years, and 0.4% missed 4 years. Therefore, one additional year of information was substantial but the value of each additional year after the first declined rapidly. Table 1 presents the proportion of the estimated actual population that was known after each additional year of information was added. The mean (from 1995 to 1999) was used to estimate the adult population size, with the minimum and maximum used to present uncertainty associated with the time-series bias.

In addition to estimating the total adult population size based on assumptions about time-series bias and nonrepetitive spawning, a discrete logistic population growth model was fit to the census data for 1991–1993 and 1995–2000 to obtain estimates for 2001, 2002 and the carrying capacity of the system:

$$(1) \qquad N_{t+1} = N_t + rN_t\left(1 - \frac{N_t}{K}\right)$$

where N_{t+1} is the population size one time step in the future, N_t is the current population size, r is the discrete growth factor or maximum intrinsic rate of increase, and K is the asymptotic size of the otherwise referred to carrying capacity (Gotelli 1998). The discrete logistic population growth model was fit to the data using maximum likelihood analysis with the assumption of normally distributed residuals, and likelihood profiles were used to calculate 95% confidence intervals (CIs) around the parameter estimates (Hood 2004).

Population-level fecundity, measured as total egg deposition, was estimated from measured FLs of spawning females captured at the trap and a FL minus individual fecundity (E; eggs per female) relationship established for Lower Kananaskis Lake (Johnston 2005).

$$(2) \qquad E = 1.72 \times 10^{-3} \times (\mathrm{FL}^{2.31})$$

$$(N = 26, r^2 = 0.78, p < 0.0001)$$

The estimate of population-level fecundity was adjusted for any ripe female mortalities that were found, for any females that returned downstream without spawning, or for females that were stripped for hatchery purposes (this occurred in 1999 and 2002).

Abundance of each age class of juveniles in the index reach of Smith-Dorrien Creek was determined by length–frequency analysis. Normally distributed age classes were fit to length–frequency distributions using maximum likelihood estimation of a multinomial distribution (Haddon 2001). Individual fish were assigned an age based on a conditional probability function as outlined in Paul et al. (2000). Precision was assessed by comparing ages determined by this technique and ages obtained from otoliths or fin rays of incidental mortalities. Paired sample t tests in SAS® were used to determine if results from the two aging techniques differed significantly ($p < 0.05$) (SAS Institute Inc. 2001).

Analysis of density-dependent survival

Three different intracohort recruitment models were fit to data on interannual cohort abundance using maximum likelihood methods. The three models are linear, compensating density dependence, and overcompensating density dependence (Table 2). Residuals were assumed to be log-normally distributed to allow for occasional large recruitment events, such as might occur under optimal environmental conditions (Hilborn and Walters 1992; Haddon 2001). All models run through the origin making the assumption that there was no recruitment without stock, a reasonable assumption because of the absence of immigration or emigration in the system (Hilborn and Walters 1992). Likelihood profiles were used to calculate 95% CIs around parameter estimates (Hood 2004). The small-sample-corrected Akaike information criterion (AIC_c) (Burnham and Anderson 1998) was used to

© 2007 NRC Canada

determine the most parsimonious model of the three candidates.

Recruitment models (Table 2) were fit to several life-stage intervals. Recruitment from the egg stage into the adult population was analysed. Maturity was assumed to occur at age 7 for this analysis. Survival of juveniles was then examined over shorter time steps (egg to age-1, age-1 to age-2, and age-2 to age-3) to determine the life stage where density dependence occurred.

To determine the potential influence of abiotic factors on juvenile recruitment in Smith-Dorrien Creek, mean daily autumn discharge (10 August – 10 October) and mean daily water temperature in August were also included in the survival models. These were the abiotic factors for which we had consistent measurements from 1996 to 2002. Both temperature and discharge have been considered to influence the survival of juvenile salmonids either because they occur during sensitive life stages (Jensen and Johnsen 1999) or because they alter habitat selection and resulting competitive interactions (Zorn and Seelbach 1995; Armstrong et al. 2003). High summer temperatures have also been found to decrease juvenile bull trout growth and survival (Selong et al. 2001), and high velocities may alter the efficiency of food capture, therefore affecting growth in salmonids (Armstrong et al. 2003). Using methods outlined in Hilborn and Walters (1992) and maximum likelihood estimation, environmental variables were added individually to the best-fit stock–recruitment model to determine if they improved the fit of the recruitment model. We tested these models with and without a 1-year time lag in environmental conditions. A 1-year time lag examined the influence on survival from environmental conditions in the year previous to capture (the last full growing season). The analysis that did not incorporate a time lag examined the influence on survival from environmental conditions experienced during the census year. Owing to availability of temperature and discharge data (1996–2002) and the time lag, these analyses were performed on two different subsets of the juvenile abundance data used to fit the survival models (1996–2002 for same year comparisons and 1997–2003 for one year lag). As a result, likelihood values are not directly comparable.

Survival of adult cohorts upon reaching maturity was also examined by fitting survival models. This represents intracohort effects and was done for survival from age-7 to age-8 and age-8 to age-9. However, data from 2001 was removed because of the uncertainty of these estimates. In addition, intercohort density-dependent survival to maturity was analyzed by logistic regression in SAS® using the Logit link function in PROC GENMOD (SAS Institute Inc. 2001). The survival of adults over a 1-year period as a function of total adult density was examined using this method for the periods 1992–1993, 1995–1996, 1996–1997, 1997–1998, 1998–1999, and 1999–2000, as they represent the periods when adults were no longer vulnerable to angler harvest and there was minimal time-series bias (discussed above and in Table 1). In addition, the proportion of first-time spawners that survived to their second year of maturity was examined as a function of total adult density. This analysis was done to determine if the observation of density dependence in adult survival was simply a function of senescence in a population that was allowed to age once released from harvest mortality.

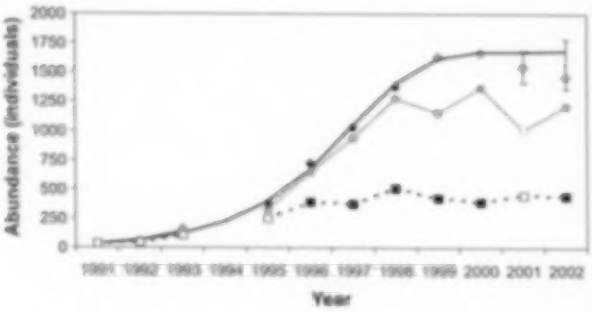

Fig. 2. Abundance of the adult population (solid diamonds), all spawning (grey circles and line), and first-time spawning (solid squares and broken line) bull trout, *Salvelinus confluentus*, in Lower Kananaskis Lake during the study period (1991–1993 and 1995–2002). The solid black line indicates predictions from the logistic population growth curve of adult population abundance. Open symbols from 1999 to 2002 indicate values that have been corrected for the bias associated with their occurrence near the end of the study and in 2001 for an incomplete census. The error bars indicate estimated minimum and maximum values calculated from bias corrections related to spawner return rates. Open symbols of first-time spawners prior to 1996 indicate cohorts that may have been overestimated because information on when these fish first spawned is limited to the years studied. However, the reduction of these estimates would only strengthen the recovery relationship.

Results

Population abundance

Since 1992, the abundance of spawners, adults, and first-time spawners has increased (Fig. 2). The number of spawners experienced a >20-fold increase during the study period, fluctuating around an asymptote after 1998. The adult population in Lower Kananaskis Lake increased by almost 28-fold from 60 individuals in 1992 to over 1650 individuals by the year 2000, where it also appears to have reached an asymptote. Maximum likelihood analysis of the discrete logistic model fit suggests that the carrying capacity of the adult population is 1680 (95% CI 1635–1729) individuals. The intrinsic rate of increase is estimated to be 0.91 year^{-1} (95% CI 0.89–0.93). Similar to the adult population, the number of adult recruits (first-time spawners) entering the adult population also increased initially but reached an asymptote of ~440 (Fig. 2). However, the asymptote was reached ~3 years earlier for first-time spawners than it was by the total population and occurred when spawner abundance was still rapidly increasing.

Population-level fecundity increased initially and then approached an asymptote in 1998 (Fig. 3). However, juvenile and first-time spawner abundance did not follow a similar trend. Four cohort groups within the recovery process can be delineated (Fig. 3). Group A represents cohorts that were

© 2007 NRC Canada

Fig. 3. Life stage abundance of bull trout, *Salvelinus confluentus*, in Smith-Dorrien Creek and Lower Kananaskis Lake by year. The solid lines track individual cohorts through time and divide the figure into cohort groups that represent different stages of population recovery (identified by the letters A–D). The panels are as follows from bottom to top: (*e*) population-level fecundity, (*d*) age-1 relative abundance, (*c*) age-2 relative abundance, (*b*) age-3 relative abundance, and (*a*) first-time spawner abundance. The number of years exposed to legal harvest is indicated by the numbers above the bars in (*a*). Abundance estimates of age-1, age-2, and age-3 juveniles (*b*–*d*) are relative because these values were obtained from a 500 m index reach that was electrofished annually. The only assessment of juveniles in Smith-Dorrien Creek before 1995 was done in 1991 in two nonindex sections of Smith-Dorrien Creek (shaded columns indicate the minimum relative abundance of the two surveys, and the error bars indicate the maximum relative abundance). The hatched bars represent years when first-time spawner abundance is uncertain, because information on when these fish first spawned is limited by the years studied.

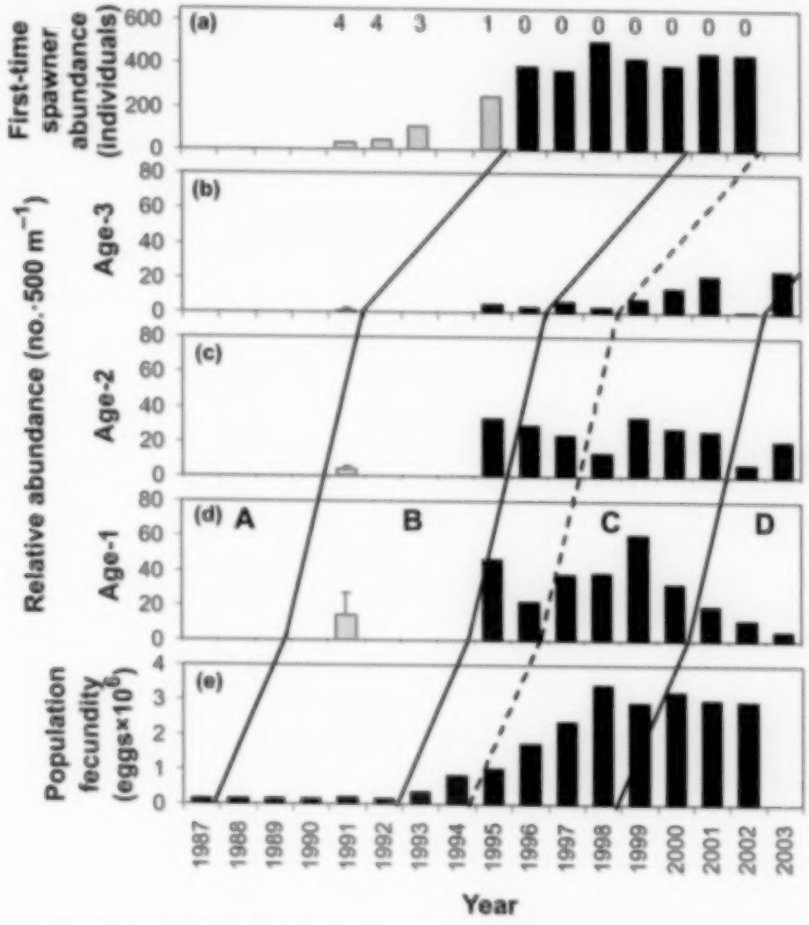

present in Lower Kananaskis Lake and therefore vulnerable to angling harvest as juveniles prior to the regulation changes in 1992. An increasing trend in the abundance of first-time spawners was observed for these cohorts and corresponds with a reduction in the number of years that these fish would have been vulnerable to harvest under the pre-1992 regulations. For example, some of the first-time spawners in 1995 would have been in the reservoir for 1 year prior to the regulation changes and may have experienced some angling mortality as a result, whereas recruits in 1993 would likely have been vulnerable for up to 3 years after migrating into Lower Kananaskis Lake.

Low population-level fecundity due to adult harvest from pre-1992 angling regulations occurred for cohorts represented by group B (Fig. 3). However, despite low fecundity, recruitment into the adult cohort is high and relatively constant during this period. Group C represents cohorts produced when egg abundance began to increase as the spawning population grew. Cohorts, up to the dashed line, may be tracked to adult recruitment. Although there are only 2 years of data during the growth phase, population-level fecundity increased 5-fold; however, a corresponding increase in the number of adult recruits was not observed. Nor does the relative abundance of the age-1 and age-2 cohorts show a corresponding increase despite the 20-fold increase in population-level fecundity experienced by this group. Additional electrofishing data from nonindex sections of the stream in 1991 suggests that age-1 abundance was either

© 2007 NRC Canada

Table 3. Stock–recruitment model fits to data for population-level fecundity and recruitment of first-time spawning bull trout, *Salvelinus confluentus*, and for intervening life stages using maximum likelihood (negative log-likelihood (–LL)) and AIC_c values.

		Model (no. of parameters)		
Life stage		Density independent (1)	Beverton–Holt (2)	Ricker (2)
Egg–recruit	*N*	8	8	8
	–LL	6.62	–2.07	–1.23
	AIC_c	15.90	2.26	3.94
	ΔAIC_c	13.64	0	1.68
Egg – age-1	*N*	9	9	9
	–LL	14.47	9.52	8.57
	AIC_c	31.50	25.04	23.15
	ΔAIC_c	8.35	1.89	0
Age-1 – age-2	*N*	8	8	8
	–LL	6.05	4.66	4.85
	AIC_c	14.78	15.72	16.10
	ΔAIC_c	0	0.95	1.33
Age-2 – age-3	*N*	8	8	8
	–LL	14.37	12.83	12.84
	AIC_c	31.40	32.06	32.07
	ΔAIC_c	0	0.66	0.67

Note: The most parsimonious models are assigned ΔAIC_c value of zero. The models tested include a density-independent model (linear), a compensating survival model (Beverton–Holt), and an overcompensating survival model (Ricker).

somewhat lower or did not differ substantially for cohorts of group B compared with group C. The abundance of age-3 individuals showed a slight increase or a similar trend for group C. Group D represents cohorts produced when population-level fecundity was high and relatively constant. Age-1 relative abundance during this period either declined or remained relatively constant.

Agreement between the ages assigned using length–frequency analysis versus the aging of boney structures of the fish was 89.3% for juveniles ($N = 131$) and 93.3% for adult mortalities that had been previously captured as juveniles in the stream ($N = 30$). Ages were not found to significantly differ between the two aging techniques for either juveniles or adults ($t_{[130]} = 1.07$, $\alpha = 0.05$, $p = 0.2868$; and $t_{[29]} = 0$, $\alpha = 0.05$, $p = 1.00$, respectively). This suggests that the age designation based on length gives a reasonable estimate of the age structure of the juveniles captured by electrofishing.

Redd abundance was directly related to the number of females that spawned ($N = 10$, $r^2 = 0.95$, $p < 0.001$). This relationship was not found to differ significantly from a 1:1 relationship (i.e., slope = 1, intercept = 0) ($N = 10$, $r^2 = 0.001$, $p = 0.937$), suggesting that the redd–female abundance relationship remained constant throughout the 20-fold increase in spawner population size.

Density-dependent survival

Survival of bull trout from the egg stage to age-at-maturity was found to be density dependent (Table 3). The compensatory Beverton–Holt model was found to be most parsimonious with a >5-fold range in survival across the observed range of abundance and a predicted asymptote of 466 fish (95% CI 307–763) (Figs. 4*a* and 4*e*). The ΔAIC_c for the overcompensating Ricker model was less than two, therefore it could not be rejected (Table 3). However, the difference in AIC_c values between the density-dependent models and the density-independent model was >8 (Table 3), suggesting that some form of density dependence did influence survival from the egg stage to age-at-maturity.

Survival of juveniles was examined by age class to identify when density-dependent regulation occurred. It should be noted that juvenile abundance estimates indicate relative abundance, not a measure of absolute abundance, and older age classes may be influenced by migration (Mushens 2003). Survival rates are the result of both mortality and emigration. Survival from the egg stage to age-1 was found to be density dependent (Table 3). The Ricker model was the most parsimonious; however, based on AIC_c values, the Beverton–Holt model could not be rejected. The density-independent model was rejected (Table 3). Linear regression results of the linear form of the Ricker relationship support this result ($N = 9$, $F_{[1,7]} = 18.92$, $\alpha = 0.05$, $p = 0.003$, $r^2 = 0.73$). This model also appears to be consistent with data collected on juvenile abundance in nonindex reaches in 1991 (Figs. 4*b* and 4*f*). Results suggest that the relative proportion of eggs surviving to age-1 appears to be decreasing at a decelerating rate (Fig. 4*f*).

The pattern differed for survival from age-1 to age-2 and from age-2 to age-3 (Figs. 4*c*, 4*d*, 4*g*, and 4*h*). The density-independent model was found to be the most parsimonious model (Table 3), a result that was strengthened when the 2003 data point was removed from the data set (ΔAIC_c density-independent model = 0, Beverton–Holt model = 3.88, Ricker = 3.85 for survival from age-1 to age-2; ΔAIC_c density-independent model = 0, Beverton–Holt model = 3.78, Ricker = 3.97 for survival from age-2 to age-3). Electrofishing uses cumulative measures of fish removed to estimate actual population size (Hilborn and Walters 1992).

© 2007 NRC Canada

Fig. 4. (*a–d*) Stock and recruitment relationships among bull trout, *Salvelinus confluentus*, life history stages. The lines are predictions from the best-fit models, and the points represent the empirical data. (*e–h*) Density-dependent survival calculated from the data and model fits (*a–d*). The open diamonds in panels *a* and *e* indicate values from 1995, a cohort that was potentially vulnerable to angler harvest as juveniles and also includes fish that matured in 1994 when the trap was not in place. However, a reduction in the estimate of first-time spawners in 1995 would only strengthen this relationship. The open diamonds in panels *b* and *f* indicate the abundance of juvenile bull trout electrofished in 1991 in two nonindex sections of Smith-Dorrien Creek. The 1991 data were not utilized to fit the stock–recruitment models. The open diamonds in panels *c*, *d*, *g*, and *h* represent 2003 when the juvenile population did not deplete over three passes.

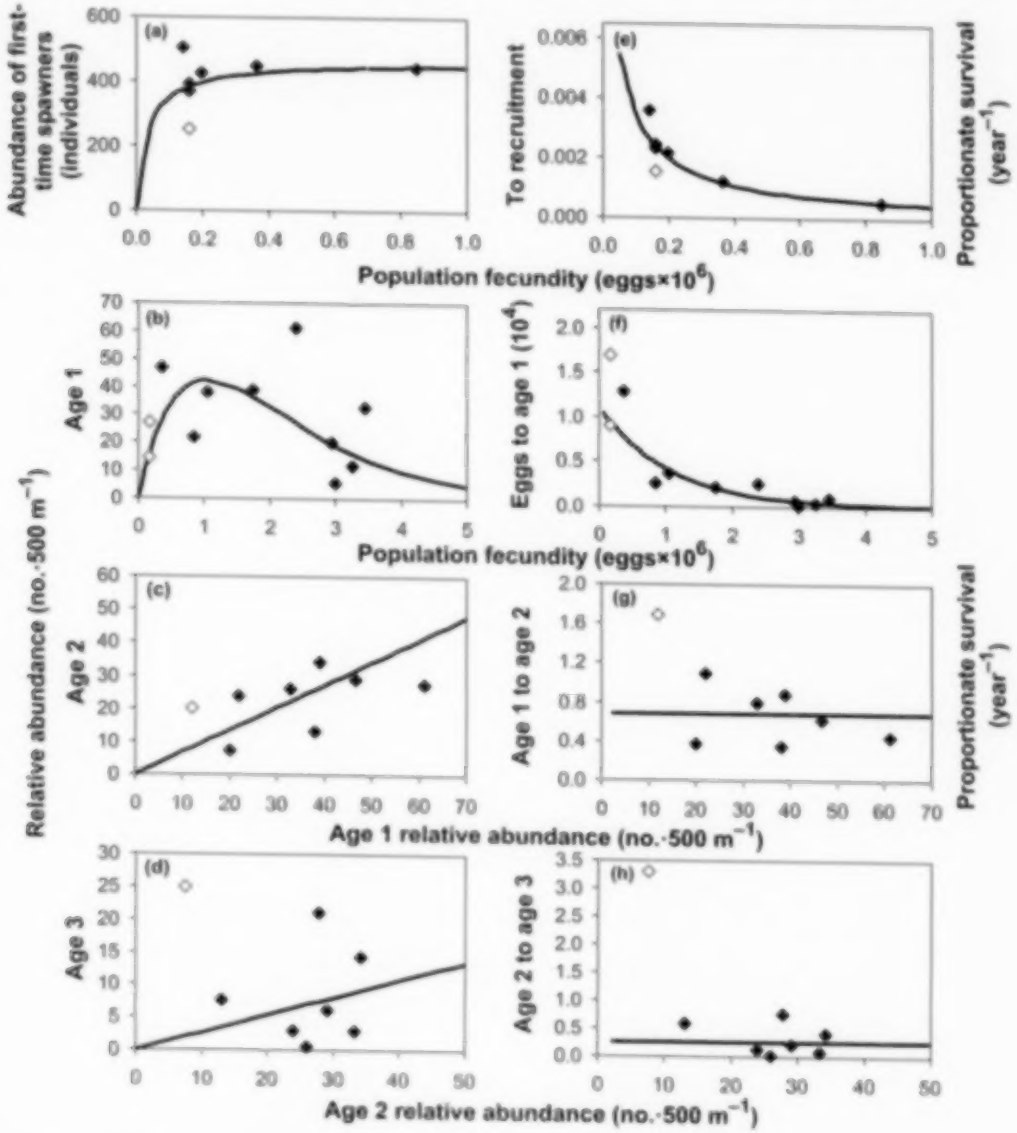

This was a successful technique, except in 2003 when the population did not deplete over the three passes. The finding that recruitment was not density dependent was further supported by linear regression analyses of both age-1 to age-2 and age-2 to age-3 survival, in which the linearized Ricker curve was not significant either with or without 2003 data included ($N = 8$, $F_{[1,6]} = 2.10$, $\alpha = 0.05$, $p = 0.197$, $r^2 = 0.26$ for age-1 to age-2 survival; $N = 8$, $F_{[1,6]} = 2.80$, $\alpha = 0.05$, $p = 0.145$, $r^2 = 0.32$ for age-2 to age-3 survival). Therefore, survival of juveniles was found to be influenced by density dependence during the egg stage to age-1, but not during older juvenile stages. There was a 1.6 $m^3 \cdot s^{-1}$ range in mean daily autumn discharge and a 2.1 °C range in mean August temperature over the 7- to 8-year period recorded (Fig. 5). Adding mean autumn stream discharge or mean August water temperature with or without a time lag did not improve

© 2007 NRC Canada

Fig. 5. Mean autumn discharge and mean August temperature over the study period. Mean autumn discharge is the mean daily discharge from 10 August to 10 October (solid squares and line). Mean August temperature is the mean daily water temperature in the month of August (shaded diamonds and line).

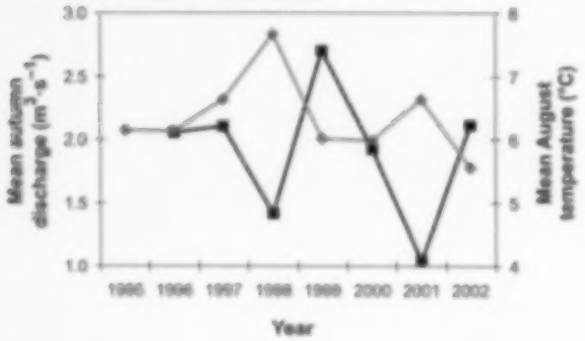

the fit of the density-dependent or density-independent recruitment models (Table 4).

Survival of adult bull trout in Lower Kananaskis Lake was negatively density dependent, with lower survival of males than females (N = 5204, χ^2_1 = 53.16, α = 0.05, $p < 0.0001$) (Fig. 6*a*). We cannot, a priori, reject the hypothesis that this observation is due to an aging population in which annual survival declines with age. Therefore, we also assessed the survival rate of adults within their first year after spawning, which shows the same pattern of density dependence (N = 1942, χ^2_1 = 53.46, α = 0.05, $p < 0.0001$) (Fig. 6*b*), suggesting that the process is density, not age dependent.

Discussion

The bull trout population in Lower Kananaskis Lake was monitored over a 12-year period to assess the rate of recovery and the demographic processes involved following elimination of legal harvest. The low competitive environment produced from overexploitation should encourage the rebuilding of a population because of compensatory effects (Walters and Kitchell 2001). However, some severely overharvested fish populations have shown a poor ability to rebuild after harvest closures (Hutchings 2000). Recruitment overfishing may deplete spawner abundance below sustainable levels, leading to population collapse (Myers and Barrowman 1996), and depensatory processes and Allee effects may prevent population recovery (Shelton and Healy 1999; Frank and Brickman 2000). However, not all populations or species are equally vulnerable to these processes (Post et al. 2002). We found no evidence of depensatory processes operating in the Lower Kananaskis Lake bull trout population, despite being suppressed to <5% of the unfished equilibrium density. The abundance of adult bull trout began to increase as soon as regulations were changed and grew to an unfished equilibrium population in fewer than two generations. This suggests that the population was growth overfished, not recruitment overfished. The population still had sufficient numbers of sexually mature fish to produce enough recruits to replace those removed by mortality (Haddon 2001). The lack of evidence for depensatory effects is consistent with results from a study by Myers et al. (1995), in which they found only 3 out of 128 fish populations examined displayed significant depensation. However, it could be that the Lower Kananaskis Lake bull trout population was not depressed sufficiently to exceed the threshold required to observe depensatory effects (Myers et al. 1995; Shelton and Healy 1999; Post et al. 2002). The ability for this population to rebuild begs the following questions: how close to the threshold of collapse was this population pushed and what are the demographic and genetic implications of this?

We were able to examine the demographics of the recovery process by incorporating predictions from the stock–recruitment models with empirical data to track cohort groups over time and through their various life stages. We will use Fig. 7 to clearly illustrate this (labelling corresponds with the same groups presented in Fig. 3). Owing to their use of two distinct habitats during their complex ontogeny, population bottlenecks may occur at a variety of bull trout life stages. These include the following: the egg stage, where spawning habitat could be limiting; the juvenile stage, where rearing habitat may be limiting; and the adult stage, where adult habitat may be limiting. Assessment of the recruitment and survival across life stages demonstrated that both density-dependent and density-independent processes were important in regulating the population.

Early in the recovery process, exposure of juvenile and adult cohorts to harvest mortality was the dominant factor limiting adult abundance. The increase in number of fish maturing when juveniles were exposed to shorter periods of angling harvest under the pre-1992 regulations provide support for this hypothesis (Group A, Fig. 7). Similarly, a rapid increase in adult and spawner abundance occurred once mature cohorts were released from harvest mortality (Group C, Fig. 7). It is not surprising that angler harvest is likely what limited the adult population abundance, when it is estimated that 70% of the fish legally harvested in the winter of 1991–1992 were sexually immature and that 50% of the adult population was harvested during the same period (Stelfox 1997). In contrast, the annual mortality rate for the adult population dropped to 5% during the 1992–1993 period (0% for first-time spawners) once regulation changes were implemented. Long-lived and late-maturing species are often unable to support high levels of mortality (Hilborn et al. 2003), and harvesting fish prior to maturity substantially increases the probability of population collapse (Myers and Mertz 1998). However, compensation primarily during the early life stages prevented collapse from occurring. Despite low levels of egg production because of adult exposure to harvest mortality, maximum numbers of first-time spawners were produced (Group B, Fig. 7). First-time spawner cohorts were no longer directly limited by harvest and, as a result, were characterized by relatively constant recruitment near the asymptote predicted by the Beverton–Holt model.

Density-dependent survival during the earliest of the juvenile stages, between eggs and age-1, was found to regulate recruitment into the adult population throughout the recovery process. This is clearly demonstrated by Group C (Fig. 7), where no corresponding increase in age-1 abundance occurs despite an over 20-fold increase in egg abundance that occurred when adults were released from harvest pressure. Our observations are consistent with others studies that concluded that density-dependent survival occurred at

© 2007 NRC Canada

Table 4. The relationship between juvenile bull trout, *Salvelinus confluentus*, survival and environmental factors in the year of sampling and the year prior to sampling.

		Stock–recruitment model + environmental factor					
		Only stock–recruitment		Mean fall discharge		Mean August temperature	
Life stage		No lag	Lag	No lag	Lag	No lag	Lag
Egg – age-1	*N*	7	7	7	7	7	7
	–LL	6.83	4.07	6.77	3.51	5.26	3.94
	AIC_c	20.65	15.13	27.54	21.02	24.52	21.89
	ΔAIC_c	0	0	6.88	5.89	3.87	6.75
Age-1 – age-2	*N*	6	6	6	6	6	6
	–LL	5.75	3.71	5.71	3.48	5.38	3.69
	AIC_c	14.30	10.22	18.43	13.97	17.75	14.37
	ΔAIC_c	0	0	4.13	3.75	3.46	4.16
Age-2 – age-3	*N*	6	6	6	6	6	6
	–LL	9.79	7.10	8.82	7.09	9.78	6.68
	AIC_c	22.57	17.19	25.65	22.18	27.55	21.36
	ΔAIC_c	0	0	3.08	4.99	4.98	4.17

Note: Mean autumn discharge is the mean daily discharge from 10 August to 10 October. Mean August temperature is the mean daily water temperature in August. Environmental variables were added individually to the best-fit stock–recruitment model (i.e., Ricker for egg to age-1 and the density-independent (linear) model for age-1 to age-2 and for age-2 to age-3). Negative log-likelihood (–LL) values were calculated independently for a 1-year time lag and no lag. These analyses are not directly comparable, as they required the use of different data sets.

Fig. 6. Density-dependent survival, by gender, of (*a*) all adult bull trout, *Salvelinus confluentus*, and (*b*) adult bull trout in their first year of maturity in Lower Kananaskis Lake. Panel *a* describes the survival of all adults over the annual periods 1992–1993 and from 1995–1996 to 1999–2000 ($N = 5204$). Panel *b* describes the survival for first-time spawners only, including the annual periods from 1995–1996 to 1999–2000 ($N = 1942$). The solid squares represent male survival and the shaded diamonds female survival. The black and shaded lines indicate the predicated survival for males and females, respectively, from logistic regression analyses.

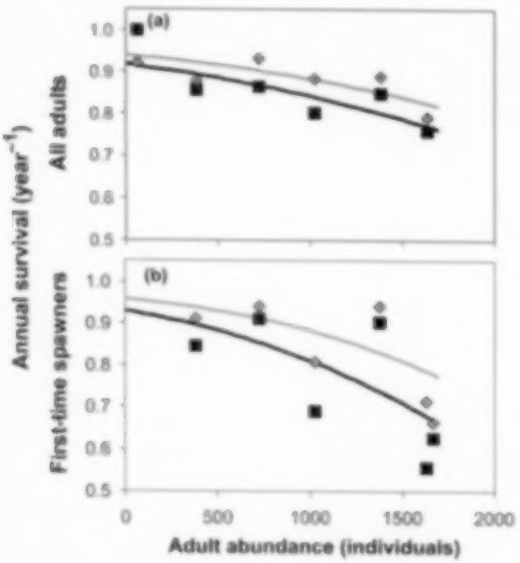

the early juvenile stage followed by constant survival at later stages (Sinclair 1989 and references therein; Elliott 1994; Einum and Fleming 2000); this demonstrates the need for long-term studies to understand the relationship between juvenile and adult numbers (Shea and Mangel 2001). We were unable to determine on a finer temporal scale when these compensatory processes occurred (i.e., the egg-laying stage, the incubation stage, or the emergence and early rearing stages). However, it has been proposed that density-dependent population bottlenecks usually occur when there is some type of niche shift or developmental shift, such as fry emergence or sexual maturity (Elliott 1994). For example, Einum and Fleming (2000) found that the majority of mortality of brown trout (*Salmo trutta*) fry occurred in the first 4 months after emergence. When examined more closely, developmental or niche shifts often provide insight into the mechanisms that give rise to density-dependent regulation. These mechanisms were not examined explicitly in this study; however, it is worthwhile to discuss possible reasons for the dynamics observed, as it provides avenues for understanding and future research.

The mechanisms behind density dependence can be varying and complex, linking behaviour, growth, and resource allocation. Armstrong et al. (2003) provides a good review of a variety of factors that may affect salmonids and how these factors might interact. Competition for spawning habitat is one possible mechanism regulating age-1 abundance. However, redd abundance was not found to differ significantly from the number of females that spawned, suggesting spawning habitat availability was likely not limiting the growth of this population. Although redd superimposition was observed in the latter years of the study (Johnston 2005), if females were experiencing increased competition for redd sites at higher spawner density, these effects would not have been seen in adult recruitment until after the study was finished. However, no assumption can be made about the quality of the habitat that redds were found in, nor the success of broods from these different habitats. The failure of all broods other than those located in prime spawning habitat could be a mechanism behind the density-dependent

© 2007 NRC Canada

Fig. 7. Empirical estimates and model predictions for population-level fecundity (solid squares and broken line), the relative abundance of age-1 fish (solid triangles and solid line), and the abundance of first-time spawners (shaded circles and shaded line) in relation to the year their cohort was produced. Therefore, cohorts may be followed vertically rather than diagonally, as was seen in Fig. 3. The solid vertical lines track individual cohorts through time and divide the figure into cohort groups representing different stages of population recovery (identified by letters A–D). The data points indicate empirical data, while the lines in sections without data points represent predictions from the stock–recruitment models, or in the case of population-level fecundity, a conservative estimate. The open squares represent years when the number of females spawning (hence egg abundance) was estimated because of incomplete surveys. The open circles indicate that first-time spawner abundance may be overestimated because of the inclusion of fish that spawned in 1994 (cohort 1987) or fish that spawned prior to the commencement of the study and then displayed nonrepetitive spawning. However, the reduction of these estimates would only strengthen the recovery relationship. The open triangles indicate the abundance of age-1 bull trout, *Salvelinus confluentus*, electrofished in 1991 in two nonindex sections of Smith-Dorrien Creek.

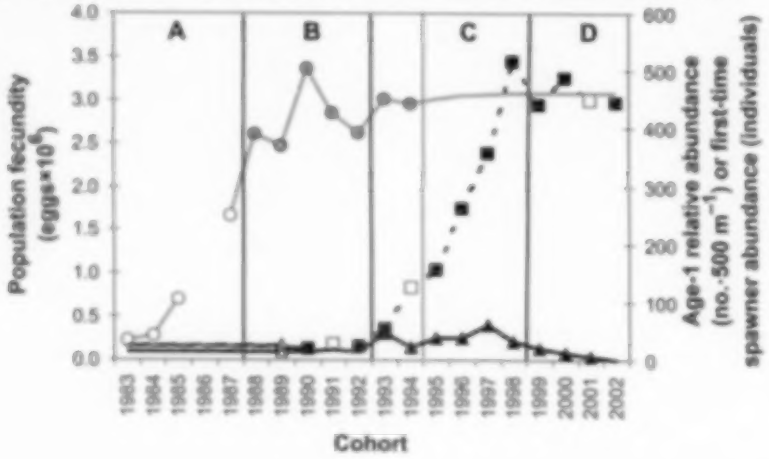

survival from the egg stage to age-1 observed in this system. This was not examined explicitly during this study; however, the course gravels required for spawning and incubation (Post and Johnston 2002) were observed in abundance within the creek, and age-1 abundance did not change even when female abundance was extremely low, suggesting that spawning habitat availability was unlikely the mechanism driving the observed density dependence.

Intraspecific competition of juveniles for habitat or resources is another mechanism that may regulate the number of fish a stream can support, either through exploitative and (or) interference competition (Thurow 1997; Harwood et al. 2002). Many stream-dwelling salmonids show aggressive behaviour and establish territorial hierarchies that may be important in limiting fish density during some periods (Elliott 1990; Nakano et al. 1998; Milner et al. 2003). When territories are filled and density increases, fish may migrate in search of more suitable habitat. Elliott (1994) found that juvenile brown trout in search of territories migrated downstream during a "critical period" (30–70 days after emergence), after which time fish had either died or located an appropriate territory. The length of this critical period increased as density increased because of the number of fish seeking territories (Elliott 1990). Competition for suitable habitat is not an unrealistic mechanism for the regulation in age-1 abundance that we see in this system and could explain the maximum density associated with the stock–recruitment curve. Work by Mushens (2003) on this system indicates that juveniles display a high fidelity to their daytime refuges and suggests that once fish have found suitable habitat they become much more sedentary in their behaviour. It is further suggested that the availability of daytime refuge habitat may be a key limiting factor for juvenile abundance in this system (Mushens 2003). Paul et al. (2000) also found that there was little emigration of age-1 bull trout at low densities in Eunice Creek, and Nakano et al. (1998) found that competitive interactions were important in population regulation, with bull trout establishing territorial hierarchies even in the presence of other species. However, this type of competition may only predominate under the appropriate conditions (Elliott and Hurley 1998). Abiotic factors such as extreme flow rates may also affect abundance (Zorn and Seelbach 1995; Jensen and Johnsen 1999; Selong et al. 2001), although environmental conditions did not improve the explanatory power of recruitment models in this study. However, this could be due to the lack of extreme changes in the abiotic factors measured or the appropriateness of the factors available.

The importance of competition and territoriality is somewhat complicated when it is examined on both the intra- and inter-cohort levels. Paul et al. (2000) found that age-1 and age-2 survival was negatively correlated with effective density, a measure which provides an index of total consumption, indicating that these cohorts interact exploitatively (Post et al. 1999). It has been suggested that these inter-cohort processes should lead to cycling in age-class abundance (Paul et al. 2000), but we see no evidence of this in the time series of relative cohort strengths of three co-occurring cohorts of juvenile bull trout in Smith-Dorrien Creek.

© 2007 NRC Canada

Predation, or the risk of predation, is another mechanism that is suggested to be important in structuring populations (Elliott 1994; Tonn et al. 1994; Biro et al. 2003). Biro et al. (2003) found that the increased mortality at high densities of age-0+ rainbow trout was linked to increased activity and use of environments where individuals were more vulnerable to predation. Tonn et al. (1994) found that survival of age-0+ crucian carp (*Carassius carassius*) to be negatively related to the abundance of older fish and attributed this either to starvation-induced mortality from competition or to cannibalism. Cannibalism is one of the hypothesized mechanisms producing the reduction in recruitment at high stock densities, as seen in the Ricker model, which best described the survival from egg to age-1 bull trout in this population. Cannibalism does occur in this system. It has been directly observed, and four adults were found that had PIT tags in their systems that had been injected into juveniles (Mushens 2003; Johnston 2005). However, it is unclear if the pressure from cannibalism is sufficient to regulate age-1 abundance in the stream, especially as it is restricted to the spawning season when juveniles and adults overlap spatially in the spawning stream.

In the final stage of population recovery, density-dependent survival of adults is apparent. Proportionate survival from age-1 through the juvenile years produces a constant input of adult recruits (Group D, Fig. 7), which in the absence of angling harvest produces an adult population of ~1680 individuals. This suggests that with an annual recruitment estimate of first-time spawners of 440–465 individuals, the equilibrium adult bull trout annual natural mortality rate is ~26%–28%. The mortality was found not to be solely the responsibility of senescence, since survival of new recruits to their second year of maturity also declined as abundance increased. This suggests that intercohort competition among adults is also important in limiting abundance in this population. In this last stage, it appears that both the creek and lake habitats have reached saturation.

A 28-fold increase in the adult population of bull trout in fewer than two generations in response to elimination of harvest clearly demonstrates the extent of overharvest this population experienced. This rapid demographic response in a relatively long-lived and late to mature species demonstrates that the population was growth overfished not recruitment overfished. However, given that only 17 females spawned in 1991, it is hypothesized that this population was approaching the threshold of recruitment overfishing. This study also clearly demonstrates the life history stages that are regulated through density dependence and highlights the importance of having a data series of sufficient length that incorporates the appropriate stage structure of the population to examine these processes. Compensatory density dependence that occurs between the egg and age-1 stages limits the production of recruits into the spawning population. In addition, compensation in adult survival rates produces a second regulatory stage that results in an apparent carrying capacity of adults in the lake. Intervening life stages show no evidence of regulation. In concert, the density-dependent processes occurring at these two life stages provide demographic compensation for low population size. But clearly the ability of the recreational fishery to overcome these natural compensatory processes, and to severely overharvest populations, is pervasive (Hutchings 2000; Post et al. 2002).

Acknowledgements

We acknowledge financial support from Challenge Grants in Biodiversity, TransAlta Utilities, Alberta Conservation Association, and the Natural Sciences and Engineering Research Council of Canada. We also thank the staff and administration of Kananaskis Country and Peter Lougheed Provincial Park for their support throughout the study and all the field assistants and volunteers that participated in this study. Finally, we thank the Alberta Conservation Association and Alberta Sustainable Resource Development for their assistance over the years.

References

Alberta Sustainable Resource Development. 2001. The general status of Alberta wild species 2000. Alberta Sustainable Resource Development, Fish and Wildlife Service, Edmonton, Alta.

Armstrong, J.D., Kemp, P.S., Kennedy, G.J.A., Ladle, M., and Milner, N.J. 2003. Habitat requirements of Atlantic salmon and brown trout in rivers and streams. Fish. Res. **62**(2): 143–170.

Begon, M., Harper, J.L., and Townsend, C.R. 1996. Ecology: individuals, populations and communities. 3rd ed. Blackwell Scientific Publications, Oxford, UK.

Berryman, A.A., Lima Arce, M., and Hawkins, B.A. 2002. Population regulation, emergent properties, and a requiem for density dependence. Oikos, **99**(3): 600–606.

Biro, P.A., Post, J.R., and Parkinson, E.A. 2003. Population consequences of a predator-induced habitat shift by trout in whole-lake experiments. Ecology, **84**(3): 691–700.

Burnham, K.P., and Anderson, D.R. 1998. Model selection and inference: a practical information–theoretic approach. Springer-Verlag New York Inc., New York.

Einum, S., and Fleming, I.A. 2000. Selection against late emergence and small offspring in Atlantic salmon (*Salmo salar*). Evolution, **54**(2): 628–639.

Elliott, J.M. 1990. Mechanisms responsible for population regulation in young migratory trout, *Salmo trutta*. III. The role of territorial behaviour. J. Anim. Ecol. **59**(3): 803–818.

Elliott, J.M. 1994. Quantitative ecology of the brown trout. Oxford University Press, Oxford, UK.

Elliott, J.M., and Hurley, M.A. 1998. Population regulation in adult, but not juvenile, resident trout (*Salmo trutta*) in a Lake District stream. J. Anim. Ecol. **67**(2): 280–286.

Frank, K.T., and Brickman, D. 2000. Allee effects and compensatory population dynamics within a stock complex. Can. J. Fish. Aquat. Sci. **57**(3): 513–517.

Gotelli, N.J. 1998. A primer of ecology. 2nd ed. Sinauer Associates Inc., Sunderland, Mass., USA.

Haddon, M. 2001. Modelling and quantitative methods in fisheries. Chapman & Hall/CRC, Boca Raton, Fla., USA.

Harwood, A.J., Metcalfe, N.B., Griffiths, S.W., and Armstrong, J.C. 2002. Intra- and inter-specific competition for winter concealment habitat in juvenile salmonids. Can. J. Fish. Aquat. Sci. **59**(9): 1515–1523.

Hilborn, R., and Walters, C.J. 1992. Quantitative fisheries stock assessment: choice, dynamics, and uncertainty. Chapman & Hall, London, UK.

© 2007 NRC Canada

Hilborn, R., Branch, T.A., Ernst, B., Magnusson, A., Minte-Vera, C.V., Scheuerell, M.D., and Valero, J.L. 2003. State of the world's fisheries. Annu. Rev. Environ. Resour. **28**: 359–399.

Hood, G.M. 2004. PopTools. Version 2.6.2. Available from http://www.cse.csiro.au/poptools [accessed 12 January 2004].

Hutchings, J.A. 2000. Collapse and recovery of marine fishes. Nature (London), **406**(6798): 882–885.

Jensen, A.J., and Johnsen, B.O. 1999. The functional relationship between peak spring floods and survival and growth of juvenile Atlantic salmon (*Salmo salar*) and brown trout (*Salmo trutta*). Funct. Ecol. **13**(6): 778–785.

Johnston, F.D. 2005. Demographic and life-history responses of an over-exploited bull trout (*Salvelinus confluentus*) population to zero harvest regulations. M.Sc. thesis, Department of Biological Sciences, University of Calgary, Alta.

Jonsson, N., Jonsson, B., and Hansen, L.P. 1998. The relative role of density-dependent and density-independent survival in the life cycle of Atlantic salmon *Salmo salar*. J. Anim. Ecol. **67**(5): 751–762.

Mackay, W.C., Brewin, M.K., and Monita, M. (*Editors*). 1997. Friends of the Bull Trout Conference Proceedings. Bull Trout Task Force (Alberta), c/o Trout Unlimited Canada, Calgary, Alta.

Milner, N.J., Elliott, J.M., Armstrong, J.D., Gardiner, R., Welton, J.S., and Ladle, M. 2003. The natural control of salmon and trout populations in streams. Fish. Res. **62**(2): 111–125.

Mushens, C.J. 2003. Migration, diel movement and habitat use of juvenile bull trout (*Salvelinus confluentus*). M.Sc. thesis, Department of Biological Sciences, University of Calgary, Alta.

Myers, R.A., and Barrowman, N.J. 1996. Is fish recruitment related to spawner abundance? Fish. Bull. **94**(4): 707–724.

Myers, R.A., and Mertz, G. 1998. The limits of exploitation: a precautionary approach. Ecol. Appl. **8**(Suppl. 1): S165–S169.

Myers, R.A., Barrowman, N.J., Hutchings, J.A., and Rosenberg, A.A. 1995. Population dynamics of exploited fish stocks at low population levels. Science (Washington, D.C.), **269**(5227): 1106–1108.

Nakano, S., Kitano, S., Nakai, K., and Fausch, K.D. 1998. Competitive interactions for foraging microhabitat among introduced brook charr, *Salvelinus fontinalis*, and native bull charr, *S. confluentus*, and westslope cutthroat trout, *Oncorhynchus clarki lewisi*, in a Montana stream. Environ. Biol. Fishes, **52**(1–3): 345–355.

Paul, A.J., Post, J.R., Sterling, G.L., and Hunt, C. 2000. Density-dependent intercohort interactions and recruitment dynamics: models and a bull trout (*Salvelinus confluentus*) time series. Can. J. Fish. Aquat. Sci. **57**(6): 1220–1231.

Paul, A.J., Post, J.R., and Stelfox, J.D. 2003. Can anglers influence the abundance of native and nonnative salmonids in a stream from the Canadian Rocky Mountains? N. Am. J. Fish. Manag. **23**(1): 109–119.

Pauly, D., Christensen, V., Guénette, S., Pitcher, T.J., Sumaila, U.R., Walters, C.J., Watson, R., and Zeller, D. 2002. Towards sustainability in world fisheries. Nature (London), **418**: 689–695.

Post, J.R., and Johnston, F.D. 2002. Status of bull trout (*Salvelinus confluentus*) in Alberta. Alberta Sustainable Resource Development, Fish and Wildlife Division, and Alberta Conservation Association, Edmonton, Alta. Wildl. Status Rep. No. 39.

Post, J.R., Parkinson, E.A., and Johnston, N.T. 1999. Density-dependent processes in structured fish populations: interaction strengths in whole-lake experiments. Ecol. Monogr. **69**(2): 155–175.

Post, J.R., Sullivan, M., Cox, S., Lester, N.P., Walters, C.J., Parkinson, E.A., Paul, A.J., Jackson, L., and Shuter, B.J. 2002. Canada's recreational fisheries: the invisible collapse? Fisheries, **27**(1): 6–17.

Prout, T., and McChesney, F. 1985. Competition among immatures affects their adult fertility: population dynamics. Am. Nat. **126**(4): 521–558.

Rieman, B.E., Lee, D.C., and Thurow, R.F. 1997. Distribution, status, and likely future trends within the Columbia River and Klamath River basins. N. Am. J. Fish. Manag. **17**: 1111–1125.

SAS Institute Inc. 2001. Version 8.2. SAS Institute Inc., Cary, N.C.

Selong, J.H., McMahon, T.E., Zale, A.V., and Barrows, F.T. 2001. Effect of temperature on growth and survival of bull trout, with application of an improved method for determining thermal tolerance in fishes. Trans. Am. Fish. Soc. **130**(6): 1026–1037.

Shea, K., and Mangel, M. 2001. Detection of population trends in threatened coho salmon (*Oncorhynchus kisutch*). Can. J. Fish. Aquat. Sci. **58**(2): 375–385.

Shelton, P.A., and Healey, B.P. 1999. Should depensation be dismissed as a possible explanation for the lack of recovery of the northern cod (*Gadus morhua*) stock? Can. J. Fish. Aquat. Sci. **56**(9): 1521–1524.

Sinclair, A.R.E. 1989. Population regulation in animals. *In* Ecological Concepts: the Contribution of Ecology to an Understanding of the Natural World. The 29th Symposium of the British Ecological Society, 12–13 April 1988, London. *Edited by* J.M. Cherrett. Blackwell Scientific Publications, Oxford, UK. pp. 197–241.

Stelfox, J.D. 1997. Seasonal movements, growth, survival and population status of the adfluvial bull trout population in Lower Kananaskis Lake, Alberta. *In* Friends of the Bull Trout Conference Proceedings. *Edited by* W.C. Mackay, M.K. Brewin, and M. Monita. Bull Trout Task Force (Alberta), c/o Trout Unlimited Canada, Calgary, Alta. pp. 309–316.

Stelfox, J.D., and Egan, K.L. 1995. Bull trout investigations in the Smith-Dorrien Creek/Lower Kananaskis Lake system. Report prepared by Fisheries Management Division, Alberta Environmental Protection and by Golder Associates Limited, Calgary, Alta.

Thurow, R.F. 1997. Habitat utilization and diel behavior of juvenile bull trout (*Salvelinus confluentus*) at the onset of winter. Ecol. Freshw. Fish **6** (1): 1–7.

Tonn, W.M., Holopainen, I.J., and Paszkowski, C.A. 1994. Density-dependent effects and the regulations of crucian carp populations in single-species ponds. Ecology, **75**(3): 824–834.

US Fish and Wildlife Service. 2006. Species information: threatened and endangered animals and plants. Washington D.C. 20240. Available from: http://ecos.fws.gov/species_profile/servlet/gov.doi.species_profile.servlets.SpeciesProfile?spcode = E065 [accessed 9 August 2006].

Walters, C., and Kitchell, J.F. 2001. Cultivation/depensation effects on juvenile survival and recruitment: implications for the theory of fishing. Can. J. Fish. Aquat. Sci. **58**(1): 39–50.

Whalen, K.G., Parrish, D.L., Mather, M.E., and McMenemy, J.R. 2000. Cross-tributary analysis of parr to smolt recruitment of Atlantic salmon (*Salmo salar*). Can. J. Fish. Aquat. Sci. **57**(8): 1607–1616.

Zorn, T.G., and Seelbach, P.W. 1995. The relation between habitat availability and the short-term carrying capacity of a stream reach for smallmouth bass. N. Am. J. Fish. Manag. **15**(4) 773–783.

© 2007 NRC Canada

Morphological and swimming stamina differences between Yellowstone cutthroat trout (*Oncorhynchus clarkii bouvieri*), rainbow trout (*Oncorhynchus mykiss*), and their hybrids

Steven M. Seiler and Ernest R. Keeley

Abstract: We hypothesized that body shape differences between Yellowstone cutthroat trout (*Oncorhynchus clarkii bouvieri*), rainbow trout (*Oncorhynchus mykiss*), and their hybrids may influence swimming ability and thus play an important role in the invasion of nonnative rainbow trout and hybrid trout into native cutthroat trout populations. We reared Yellowstone cutthroat trout, rainbow trout, and reciprocal hybrid crosses in a common environment and conducted sustained swimming trials in order to test for genetically based morphological and swimming stamina differences. Linear and geometric morphometric analyses identified differences in body shape, with cutthroat trout having slender bodies and small caudal peduncles and rainbow trout having deep bodies and long caudal peduncles. Hybrid crosses were morphologically intermediate to the parental genotypes, with a considerable maternal effect. Consistent with morphological differences, cutthroat trout had the lowest sustained swimming velocity and rainbow trout had the highest sustained swimming velocity. Sustained swimming ability of hybrid genotypes was not different from that of rainbow trout. Our results suggest that introduced rainbow trout and cutthroat–rainbow trout hybrids potentially outcompete native Yellowstone cutthroat trout through higher sustained swimming ability.

Résumé : Nous avons émis l'hypothèse selon laquelle les différences de forme du corps entre la truite fardée de Yellowstone (*Oncorhynchus clarkii bouvieri*), la truite arc-en-ciel (*Oncorhynchus mykiss*) et leurs hybrides peuvent affecter la capacité de nage et ainsi jouer une rôle dans l'envahissement des populations indigènes de truites fardées par les truites arc-en-ciel non indigènes et les truites hybrides. Nous avons élevé des truites fardées de Yellowstone, des truites arc-en-ciel et de truites issues de croisements hybrides réciproques dans un environnement commun et nous avons mené des tests de nage soutenue afin de vérifier l'existence des différences d'origine génétique dans la morphologie et dans la vigueur de nage. Des analyses morphométriques linéaires et géométriques mettent en évidence des différences dans la forme du corps: les truites fardées possèdent un corps élancé et un pédoncule caudal réduit, alors que les truites arc-en-ciel ont un corps profond et un long pédoncule caudal. Les truites des croisements hybrides ont une morphologie intermédiaire par rapport aux génotypes des parents avec un effet maternel marqué. En accord avec les différences morphologiques, les truites fardées ont la vitesse de nage soutenue la plus faible et les truites arc-en-ciel la vitesse de nage soutenue la plus élevée. La capacité de nage soutenue des génotypes hybrides ne diffère pas de celle des truites arc-en-ciel. Nos résultats indiquent que les truites arc-en-ciel introduites et les hybrides des truites fardées et arc-en-ciel peuvent potentiellement gagner la compétition avec les truites fardées indigènes à cause de leur capacité supérieure de nage soutenue.

[Traduit par la Rédaction]

Introduction

Nonnative species are commonly thought to cause declines and extinction of native species through predation, competition, or habitat alteration; however, a more severe impact may occur by hybridization with native species (Rhymer and Simberloff 1996; Sakai et al. 2001). Intraspecific hybridization, occurring between distinct populations, is thought to have played an important role in evolution of many plant taxa (Stebbins 1959) and some vertebrates (Dowling and DeMarais 1993). In contrast, hybridization between species is often highly detrimental to native populations when closely related nonnative species are introduced into native species ranges and form interspecific hybrids (Rhymer and Simberloff 1996). When hybrid offspring are sterile, genetic resources are wasted and small native populations may lose significant portions of important recruitment classes. When hybrids are fertile, reproduction between first generation hybrids and parental or advanced crosses of hybrids is termed introgression (Anderson 1949).

Received 13 February 2006. Accepted 7 December 2006. Published on the NRC Research Press Web site at http://cjfas.nrc.ca on 30 January 2007.
J19172

S.M. Seiler[1] and E.R. Keeley. Department of Biological Sciences, Box 8007, Idaho State University, Pocatello, ID 83209, USA.

[1]Corresponding author (e-mail: seilstev@isu.edu).

 doi:10.1139/F06-175 © 2007 NRC Canada

Introgression of alleles from nonindigenous species has caused rapid genomic extinction in many populations of birds, mammals, and fish (Rhymer and Simberloff 1996; Sakai et al. 2001).

In salmonid fishes, competition and hybridization with introduced species has been implicated in the demise of many native populations (Behnke 1992). In western North America, many cutthroat trout (*Oncorhynchus clarkii* spp.) populations are under pressure from introduced rainbow trout (*Oncorhynchus mykiss*; Hitt et al. 2003; Weigel et al. 2003; Rubidge and Taylor 2004). Because of ecological similarities and a recent common ancestry, rainbow and cutthroat trout are thought to compete for food and space when in sympatry (Griffith 1988) and they produce fertile offspring when they interbreed (Krueger and May 1991). Although rainbow trout are also native to western North America, spatial and temporal isolating mechanisms prevented most hybridization with cutthroat trout where their native ranges overlap (Trotter 1989). In areas where geological barriers prevented rainbow trout from moving into interior watersheds, cutthroat trout populations existed in isolation for at least 10 000 years (McPhail and Lindsey 1986; Behnke 1992). However, because of widespread propagation and introduction of rainbow trout across all of North America, rainbow trout now have reproducing populations in areas where cutthroat trout were the only native trout. Competition and hybridization with rainbow trout are recognized as key reasons for the decline of inland cutthroat trout populations (Young 1995).

Historically, Yellowstone cutthroat trout (*Oncorhynchus clarkii bouvieri*) were the only trout species within the upper Snake River drainage in Wyoming, Idaho, Utah, and Nevada and the Yellowstone River drainage in Wyoming and Montana (Fig. 1; Varley and Gresswell 1988; Behnke 1992). Rainbow trout were stocked to supplement a sport fishery in many of these drainages, and over the past 20 years, increasing numbers of rainbow trout and hybrid trout have raised concerns regarding the persistence of native Yellowstone cutthroat trout populations (Schrader and Gamblin 1996; Jaeger et al. 2000). Unlike most inland cutthroat trout, native rainbow trout populations are often sympatric with other indigenous salmonids that compete for food and space with them (Quinn 2005). Such co-existing populations of stream-dwelling salmonids are thought to co-occur because of habitat partitioning between species (Hartman 1965). Because native cutthroat trout often decline or disappear when rainbow trout are introduced (Jaeger et al. 2000; Hitt et al. 2003; Weigel et al. 2003), it is likely that cutthroat trout lack the competitive abilities that evolved in salmonids experiencing similar co-occurring competitors.

For invasive species to become established and proliferate when introduced into new habitats, they must possess characteristics that allow them to out-compete ecologically similar native species. Swimming ability is an important correlate of fitness in fishes (Taylor and Foote 1991; Hawkins and Quinn 1996) and may play an important role in the spread of rainbow trout genes into Yellowstone cutthroat trout populations. Because body shape is strongly related to swimming ability in fishes (Lindsey 1978; Webb 1984), differences in body shape and therefore swimming ability may influence the decline in native fish species by introduced species and

Fig. 1. Historic distribution of Yellowstone cutthroat trout (*Oncorhynchus clarkii bouvieri*, dark shading) and rainbow trout (*Oncorhynchus mykiss*, light shading) in western North America.

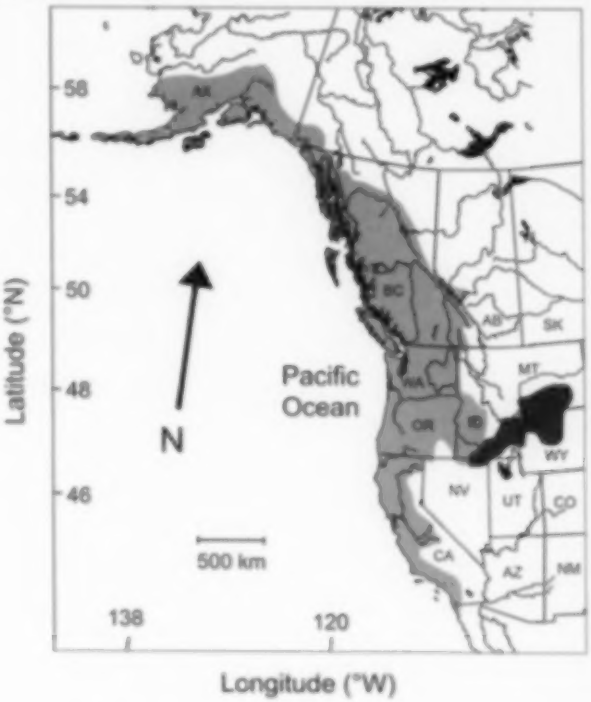

their hybrids. In stream ecosystems, salmonids feed primarily on drifting aquatic invertebrates by swimming to hold position in the current. The most profitable foraging areas are found where the supply of invertebrates is high relative to the cost of maintaining position in the current (Hughes and Dill 1990). Because the abundance of drifting invertebrates is thought to be positively related to the velocity of water, individuals with the ability to sustain swimming at higher velocities may benefit by foraging and gaining energy more efficiently than those with weaker abilities.

To test for inherent differences in swimming stamina and morphology between native and invasive salmonid fishes, we raised Yellowstone cutthroat trout, rainbow trout, and their reciprocal hybrids in a common garden experiment. First, we conducted swimming stamina trials to determine whether differences in sustained swimming ability exist between parental and hybrid trout. Secondly, we examined whether differences in body shape distinguishing parental and hybrid genotypes were related to any differences in sustained swimming ability. Given the decline of previously allopatric cutthroat trout after the introduction of nonnative rainbow trout, we predicted that Yellowstone cutthroat trout would have lower swimming stamina than rainbow trout and their hybrids. Although few studies have directly compared individual morphology and swimming performance in fishes (but see Boily and Magnan 2002; Ojanguren and Brana 2003), salmonid fish from higher velocity streams tend to have larger paired fins and deeper bodies than those from slower streams or standing water (Swain and Holtby 1989; Keeley

© 2007 NRC Canada

et al. 2005). Hence, if cutthroat trout are poorer competitors because of morphologically linked differences in swimming ability, we expect them to have shorter paired fins and shallower bodies than rainbow or hybrid trout.

Materials and methods

Collection and rearing of experimental animals

On 23 April 2004, we collected Yellowstone cutthroat trout and rainbow trout gametes to create experimental populations. Cutthroat trout eggs and sperm were collected from Henry's Lake, located near Island Park, Idaho. Each spring, the Henry's Lake hatchery collects gametes from wild cutthroat trout as they prepare to spawn. Rainbow trout eggs and sperm were collected from the Hayspur Hatchery, Hayspur, Idaho, from a captive population of rainbow trout. All gametes were placed in coolers with ice and transported to Idaho State University.

To create cohorts of juvenile fish to be used in our experiment, we divided the clutches from each female in half. To minimize the possibility of using an infertile male, we then combined sperm from two conspecific males and used half to fertilize a conspecific egg lot and half to fertilize a heterospecific egg lot. This process created experimental cohorts of cutthroat trout, maternal cutthroat hybrid (cutthroat trout eggs crossed with rainbow trout sperm), maternal rainbow hybrid (rainbow trout eggs crossed with cutthroat trout sperm), and rainbow trout. We created four replicate cohorts of each genotype (16 total populations). Within each replicate, hybrid offspring were maternal or paternal half-siblings to the pure parental crosses.

Each cohort was incubated in an upwelling incubator supplied with water from a common reservoir. A slow input of dechlorinated city water (~2.5 L·min^{-1}) maintained water temperature at 12.5 °C (±0.5 °C) and ensured high water quality. Overflow from incubators was collected in a common drain, filtered, and pumped back to the reservoir. The temperature of the freshwater supply slowly increased during the third and fourth week of incubation and development, reaching a maximum temperature of 13.5 °C. On 24 May 2004, a water chilling unit was added to the common reservoir, which maintained water temperature at 12.5 °C (±0.5 °C) for the remainder of experiment. We removed dead eggs daily and did not detect a qualitative difference in mortality between genotypes. After hatching and development to the exogenously feeding stage, up to 100 trout from each cross were transferred to rearing channels.

The rearing system consisted of four channels constructed out of plywood lined with fiberglass and coated with nontoxic aquaculture paint. Each channel was divided into four compartments by screens to create a total of 16 rearing compartments measuring 109 cm long × 36 cm wide. Water was supplied from the common reservoir to each channel (~3 L·min^{-1}). Channel depth was maintained at 24 cm by a standpipe drain. Outflow from all channels was pooled, filtered, and pumped back to the header reservoir. Although we did not expect position within channels to influence development in a population, we accounted for any potential position effect by assigning each replicate cohort of a genotype to one of the 16 compartments such that each genotype appeared only once in each channel and in every possible position across the array of channels. Over the first month of feeding, trout were fed hatchery feed three times a day until satiation and twice daily thereafter (Biodry 1000, Bio-Oregon Inc., Warrenton, Oregon). Uneaten food and waste were removed several times a week. Water quality remained high throughout rearing; periodic tests never detected build-up of nitrogenous wastes.

Swimming stamina

As an estimate of swimming performance, we measured sustained swimming ability using a Blazka-type swimming chamber (Brett 1964). The swim chamber consisted of a clear acrylic tube (30 cm long × 9 cm diameter) contained within a larger tube (47 cm long × 24 cm diameter). An impeller powered by a variable-speed ½ HP DC motor cycled water through the central chamber. Each test fish was contained within the swim chamber by 1 cm × 1 cm screening on its ends. To ensure laminar flow through the swim chamber, we attached an 8 cm long plastic grid with 2 cm × 2 cm openings to the upstream end of the central chamber. During all trials, water pumped into the chamber from the rearing system reservoir maintained temperature at 12.5 °C (±0.5 °C) and near saturation with oxygen.

On the day before trials, one trout from each of the four genotypes was haphazardly selected from a randomly chosen stream channel. Each trout was measured (fork length, ±1 mm), placed into a holding tube, and returned to its rearing channel. Holding tubes were sections of polyvinyl chloride (PVC) pipe matching the dimensions of the swim tunnel. Isolation allowed the trout to acclimate to a confinement similar to the swim chamber and assured that no test fish ate for 24 h before the swim trial. On the following day, trout were individually tested for sustained swimming velocity.

Sustained swimming velocity trials were conducted between 24 November 2004 and 23 December 2004. We did not expect differences in body size to influence absolute sustained swimming velocity across the size range of fish tested in this study (range for each genotype: 78–98 mm fork length). However, to account for size differences, we corrected the absolute water velocity (cm·s^{-1}) that each fish encountered to body lengths per second (bl·s^{-1}). Trials were initiated by placing individual trout in the swim tunnel for 5 min without flow, followed by 30 min at 4 bl·s^{-1}. After this acclimation period, velocity was increased by 0.5 bl·s^{-1} every 10 min until the test fish could not maintain its position in the chamber and became pinned against the back screen. A mild electrical stimulus (1 volt, ½ amp) was used to encourage fish resting on the back screen to continue swimming. When a test fish became pinned against the back screen and could not be stimulated to swim any longer, the time elapsed from the last velocity increase was recorded, flow was turned off, and the fish was removed from the chamber. Each trout was euthanized, placed on its right side with fins extended, photographed for morphometric comparisons, and preserved in 10% formalin.

We compared swimming velocity among genotypes using analysis of variance (ANOVA). The response variable, critical swimming velocity (U_{crit}, bl·s^{-1}) was calculated by the following formula:

$$U_{crit} = V + V_i(T_i / T_i)$$

© 2007 NRC Canada

Fig. 2. (*a*) Locations for 15 landmarks identified on each trout photograph. Broken lines indicate the head depth (2–15), body depth 1 (3–11), body depth 2 (4–11), caudal depth 1 (5–10), caudal depth 2 (6–8), caudal length 1 (5–7), caudal length 2 (7–9), pelvic fin (11–12), and pectoral fin (13–14). These nine measurements are used in the linear morphometric analysis. (*b*) Landmarks used in the geometric analysis of body shape.

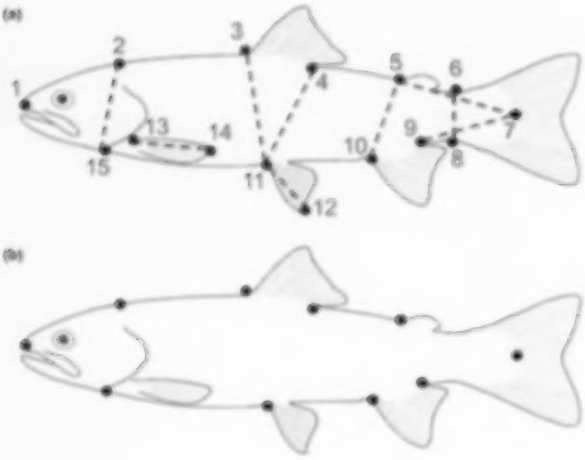

where V is the highest velocity at which a fish swam for the entire time increment (bl·s^{-1}), V_i is the velocity increment (0.5 bl·s^{-1}), T_f is the time elapsed between the final velocity increase and fatigue (min), and T_i is the time between velocity increases (10 min). Because the cross-sectional area of the largest fish was <5% of the cross-sectional area of the tunnel, we did not consider solid blocking effects that sometimes occur when fish of a given size swim in relatively small chambers (Bell and Terhune 1970). When we found significant differences in mean U_{crit} values, we identified which genotypes differed using Tukey's test ($\alpha = 0.05$).

Morphological comparisons

To compare body morphology between genotypes, 15 landmarks (Fig. 2*a*) were digitized onto the photograph of each trout using tpsDig (Rohlf 2005*a*). A scale bar included in each photograph allowed landmark locations (x and y coordinates) to be translated into linear measurements using the Pythagorean theorem. Nine measurements were chosen to compare linear morphological characters of body depth, caudal depth, caudal length, and paired fin length (Fig. 2*a*). To correct for size-related differences across individuals, we regressed each morphological characteristic against fork length. All measurements were $\log_{10}$-transformed to ensure that we met the assumption of homogeneity of variance, and we visually examined the residuals from all analyses by plotting them against body size to ensure that we met this assumption. Because of the large number of pairwise comparisons of slopes, we could not assume that the slope describing the relationship between each morphological trait and body size was equal across all genotypes. We used separate within-group slopes (groups = genotypes) to adjust each trait to a common body size based on the method of Thorpe (1976).

Fig. 3. Mean sustained swimming velocity (body lengths per second (bl·s^{-1}); +1 standard error) of trout genotypes. Means sharing the line do not differ significantly (Tukey's test, $\alpha = 0.05$). Acronyms: CT, cutthroat trout (*Oncorhynchus clarkii bouvieri*); MCH, maternal cutthroat hybrid; MRH, maternal rainbow hybrid; RBT, rainbow trout (*Oncorhynchus mykiss*).

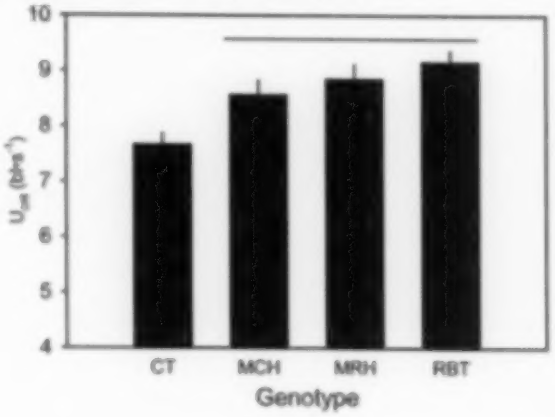

In addition to the linear morphometric technique, we also compared body shape using geometric morphometrics (cf. Zelditch et al. 2004). For this analysis, we used a subset of 10 landmarks, which were spread across the body of each trout at easily identifiable, stationary points (Fig. 2*b*). Geometric morphometric techniques quantify the spatial covariation of each landmark relative to all other landmarks and allow visualization of shape through thin plate spline diagrams. The landmark locations from each trout were used to create geometric shape variables (partial warp scores and uniform shape components) using tpsRelw (Rohlf 2005*b*).

We used multivariate analysis of variance (MANOVA) of the nine size-adjusted linear characters to assess body shape differences among genotypes, followed by ANOVAs to compare how individual traits differed across genotypes. When differences were detected on individual traits, we used post-hoc Tukey's tests to identify which genotypes differed. We conducted a separate MANOVA to assess whether the genotypes differed based on the geometric shape variables.

To summarize shape differences across the linear measurements and across the geometric shape variables, we used principal component analyses (PCA). By using size-adjusted linear characters in the PCA, principal axes represent variation in the relative size of linear characters (Keeley et al. 2005). PCA on geometric shape variables, commonly called a relative warps analysis (Rohlf 1993), allowed us to summarize differences in body shape and graphically examine implied morphological changes along principal axes using tpsRelw (Rohlf 2005*b*). We used ANOVA to compare differences in mean factor scores among genotypes for the linear and geometric analyses, and we used Tukey's tests to examine differences in mean factor scores for pairwise comparisons. For both PCAs, we examined principal axes with eigenvalues greater than 1 (Quinn and Keough 2002); however, we only considered axes which differentiated at least

© 2007 NRC Canada

Fig. 4. Comparisons of mean size-adjusted linear measurements (+1 standard error) for (*a*) head depth, (*b*) body depth 1, (*c*) body depth 2, (*d*) caudal depth 1, (*e*) caudal depth 2, (*f*) caudal length 1, (*g*) caudal length 2, (*h*) pelvic fin length, and (*i*) pectoral fin length. For each measurement, means that do not share letters are significantly different (Tukey's test, $p < 0.05$). Acronyms: CT, cutthroat trout (*Oncorhynchus clarkii bouvieri*); MCH, maternal cutthroat hybrid; MRH, maternal rainbow hybrid; RBT, rainbow trout (*Oncorhynchus mykiss*). All measurements are based on $\log_{10}$-transformed data.

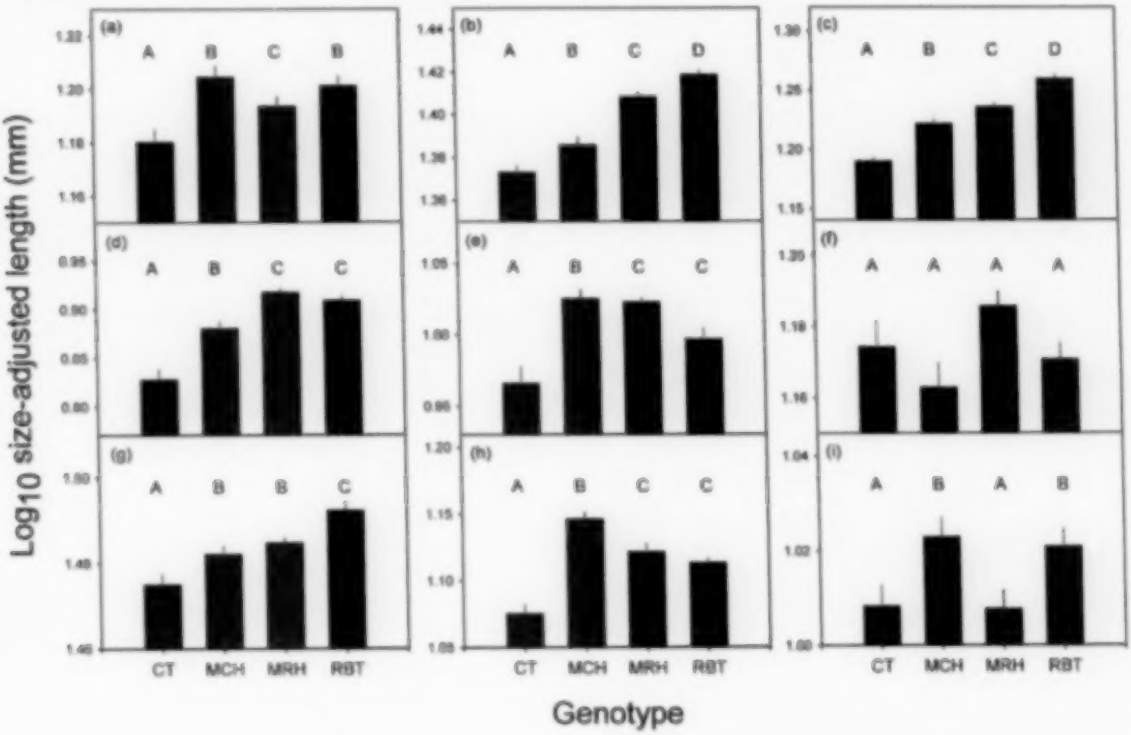

one genotype in further analyses. Finally, we tested whether morphological scores from PCA of linear characters and geometric shape variables were related to swimming ability by regressing U_{crit} scores from each trout on its corresponding factor score from the first principal axis.

Results

Swimming stamina

We completed 25 swimming trials with 25 fish from each genotype for a total of 100 trials. The average (±1 standard error, SE) number of swimming increments was 8.16 (0.43) for Yellowstone cutthroat trout, 9.84 (0.51) for maternal cutthroat hybrids, 10.40 (0.56) for maternal rainbow hybrid, and 11.08 (0.41) for rainbow trout. When we compared sustained swimming stamina, we found a significant difference in sustained swimming velocity across the four genotypes (ANOVA, $F_{[3,96]} = 7.05$, $P < 0.001$; Fig. 3). Tukey's test revealed that cutthroat trout had lower mean U_{crit} than all other genotypes. Although both hybrid groups had mean U_{crit} scores intermediate to those of cutthroat trout and rainbow trout, we found no differences between either hybrid group and rainbow trout (Fig. 3). As expected, U_{crit} was not correlated with fork length across genotypes (each genotype, $F_{[1,24]} \leq 1.16$, $P \geq 0.2$), lending support to our assumption that the body length – water velocity correction removed any effect of size on absolute swimming velocity.

Morphological comparisons

Based on our morphological analysis of linear measurements, we found a significant difference among genotypes (MANOVA, Wilk's $\lambda = 0.0657$, $F_{[27,257.65]} = 14.70$, $P < 0.0001$). When we compared each size-adjusted linear character across the four classes of trout, we found that cutthroat trout had the shallowest distance on all five measures of depth (Figs. 4*a*–4*e*). We did not find any differences in caudal length 1 (Fig. 4*f*); however, cutthroat trout had the shortest caudal length 2 measurements (Fig. 4*g*). This apparent discrepancy can be explained by increased body depth found in rainbow and hybrid trout, which leads to longer distance between landmarks 7 and 9 than between landmarks 5 and 7 (Fig. 2). Cutthroat trout had the shortest pelvic fins (Fig. 3*h*) and shortest pectoral fins, which were similar to maternal rainbow hybrids (Fig. 3*i*).

When we summarized the variation in linear measurements using PCA, we found that all four genotypes were separated based on three principal axes (Fig. 5). The first three principal axes had eigenvalues greater than 1, explaining 66.4% of the total variation (Table 1). None of these axes was correlated with body length (for all correlations, $r^2 \leq$

© 2007 NRC Canada

Fig. 5. Mean principal component scores (±1 standard error) from a PCA of nine size-adjusted measurements for (*a*) principal component (PC) 1 versus PC 2 and (*b*) PC 1 versus PC 3. On each axis, means that share brackets do not differ significantly (Tukey's test, $\alpha = 0.05$). Symbols: ●, cutthroat trout (*Oncorhynchus clarkii bouvieri*); ■, maternal cutthroat hybrid; □, maternal rainbow hybrid; ○, rainbow trout (*Oncorhynchus mykiss*).

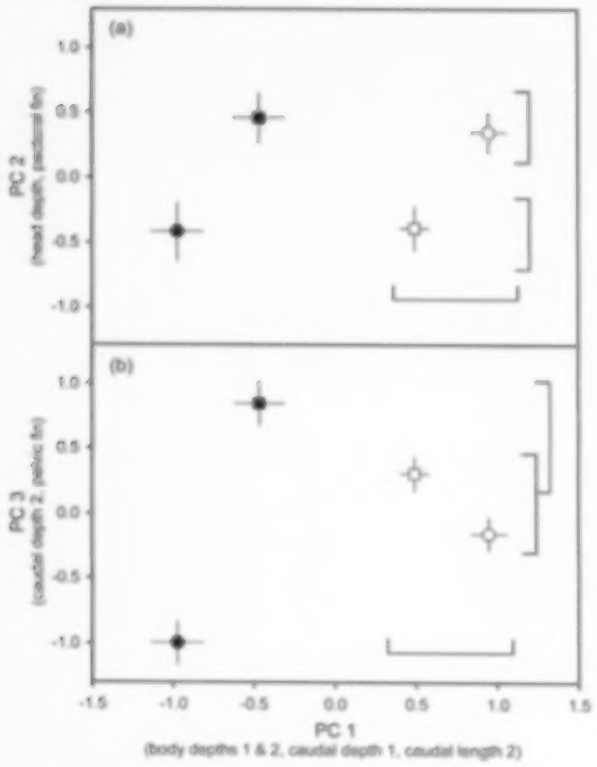

0.0008, $P \geq 0.78$), verifying that the size-correction method effectively removed any effect of size across the test fish.

Principal component (PC) 1 summarized variation in body depths 1 and 2, caudal depth 1, and caudal length 2 (Table 1) and was the most effective at distinguishing differences in size-adjusted linear measurements among genotypes (ANOVA, $F_{[3,99]} = 77.95$, $P < 0.0001$; Fig. 5*a*). Based on PC 1, cutthroat trout had shallow bodies and short caudal peduncles, whereas rainbow trout had deep bodies with longer caudal peduncles. Hybrid genotypes were intermediate, with maternal cutthroat hybrids more similar to cutthroat trout and maternal rainbow hybrids more similar to rainbow trout. PC 2 summarized variation in head depth and pectoral fin length (Table 1) and identified differences between the genotypes with a paternal effect (ANOVA, $F_{[3,99]} = 9.20$, $P < 0.0001$; Fig. 5*a*); cutthroat trout and maternal rainbow hybrid trout had shallower head depth and shorter pectoral fins than maternal cutthroat hybrids and rainbow trout. PC 3 summarized variation in caudal depth 2 and pelvic fin length (Table 1) and identified differences among genotypes (ANOVA, $F_{[3,99]} = 12.29$, $P < 0.0001$). Based on PC 3, cutthroat trout had shallower caudal peduncles and shorter pelvic fins than the other genotypes (Fig. 5*b*).

The morphometric analysis with geometric shape variables provided results similar to those from the size-adjusted linear measurements. A MANOVA of the partial warp scores detected significant differences among genotypes (Wilk's $\lambda = 0.0441$, $F_{[45,244.38]} = 10.10$, $P < 0.0001$). Principal component scores from axis 1 and 2 from the PCA of the geometric shape variables summarized 35.4% of the variation in landmark locations. Across both axes, we found a significant effect of genotype (PC 1, $F_{[3,99]} = 37.59$, $P < 0.0001$; PC 2, $F_{[3,99]} = 9.66$, $P < 0.0001$). When we graphically interpreted the implied shape changes for these axes, we found that PC 1 describes similar shape changes as PC 1 from the analysis of linear characters. Increasing scores on the first axis describe a deepening of the fish across the entire body (Fig. 6). Based on PC 1, cutthroat trout had the shallowest bodies, rainbow trout had the deepest bodies, and hybrid genotypes had intermediate body depth (Fig. 6). PC 2 describes a slight elongation of the head owing to a shift in landmarks 1, 2, and 15 (Fig. 6). Based on PC 2, cutthroat trout had more elongated heads than the other genotypes (Fig. 6).

Swimming performance in relation to morphology

When we combined swimming performance and body shape from individual fish, we found that body shape explained a significant proportion of the variation in critical swimming velocity. We found a positive relationship between U_{crit} scores and PC 1 from the linear measurements ($F_{[1,99]} = 11.11$, $P = 0.001$; Fig. 7*a*) and PC 1 from the geometric shape variables ($F_{[1,99]} = 7.69$, $P = 0.007$; Fig. 7*b*). Higher sustained swimming velocities are related to the combination of deeper bodies, larger fins, and larger caudal peduncles found in rainbow trout and hybrid trout.

Discussion

Our study provides evidence for differences in maximum sustained swimming speed and morphology between Yellowstone cutthroat trout, rainbow trout, and their hybrids. Although rainbow and cutthroat trout have similar body plans, our data show that rainbow trout have deeper bodies and larger paired fins than cutthroat trout. Morphological differences in salmonid fishes are often related to swimming and feeding ecology (McLaughlin and Grant 1994; Keeley et al. 2005), and sustained swimming ability is often measured as a correlate of fitness because it influences several components of fitness, including habitat use and the ability to undergo extensive migrations (Brett 1964; Taylor and McPhail 1985*a*; Taylor and Foote 1991). We found that individuals with the highest swimming stamina were those with the deepest bodies and largest fins. Hence, even subtle differences in morphology appear to provide an advantage in sustained swimming ability to rainbow trout and hybrid trout.

Although co-occurring species sometimes hybridize, intermediate morphological or behavioral characteristics often put hybrid individuals at a competitive disadvantage (Arnold 1997). Such selective disadvantages are thought to be a primary mechanism in preventing introgression between species. In contrast, natural isolating mechanisms may not be present when one species is moved outside of its native range and can interbreed with an indigenous species. If hy-

© 2007 NRC Canada

Table 1. Loading coefficients from a principal component analysis with varimax rotation of size-adjusted linear measurements of experimentally reared genotypes.

	Rotated component loadings				
Morphological character	Landmarks	PC 1	PC 2	PC 3	
Head depth	2–15	0.178	0.774	0.125	
Body depth 1	3–11	0.894	–0.110	0.174	
Body depth 2	4–11	0.787	0.164	0.364	
Caudal depth 1	5–10	0.734	0.098	0.376	
Caudal depth 2	6–8	0.324	0.088	0.632	
Caudal length 1	5–7	0.399	–0.359	–0.342	
Caudal length 2	7–9	0.833	0.161	–0.026	
Pelvic fin length	11–12	0.106	–0.008	0.809	
Pectoral fin length	13–14	0.011	0.843	–0.051	
Eigenvalue		3.4	1.5	1.0	Total
Variation (%)		38.2	16.7	11.4	66.4

Fig. 6. Mean principal component scores (±1 standard error) from a principal component analysis (PCA) of geometric shape variables. Thin-plate spline deformation grids show shape changes implied by low and high scores on each axis. On each axis, means that share brackets do not differ significantly (Tukey's test, α = 0.05). Symbols: ●, cutthroat trout (*Oncorhynchus clarkii bouvieri*); ■, maternal cutthroat hybrid; □, maternal rainbow hybrid; ○, rainbow trout (*Oncorhynchus mykiss*).

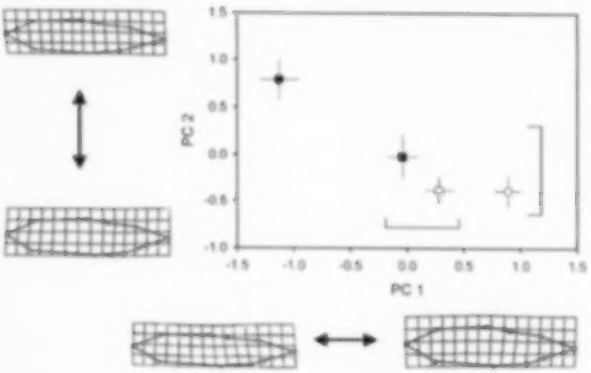

Fig. 7. (*a*) The relationship between sustained swimming velocity and body shape as defined by PC 1 from the principal component analysis (PCA) of nine linear measurements. The equation of the line is U_{crit} (body lengths per second (bl·s^{-1})) = 8.566 + 0.408 × PC 1, r^2 = 0.11, p = 0.001. (*b*) The relationship between sustained swimming velocity and body shape as defined by PC 1 from the PCA of geometric shape variables. The equation of the line is U_{crit} (bl·s^{-1}) = 8.566 + 0.364 × PC 1, r^2 = 0.08, p = 0.003. Symbols: ●, cutthroat trout (*Oncorhynchus clarkii bouvieri*); ■, maternal cutthroat hybrid; □, maternal rainbow hybrid; ○, rainbow trout (*Oncorhynchus mykiss*). Symbols above the *x* axis indicate the mean PC 1 score (±1 standard error) for each genotype.

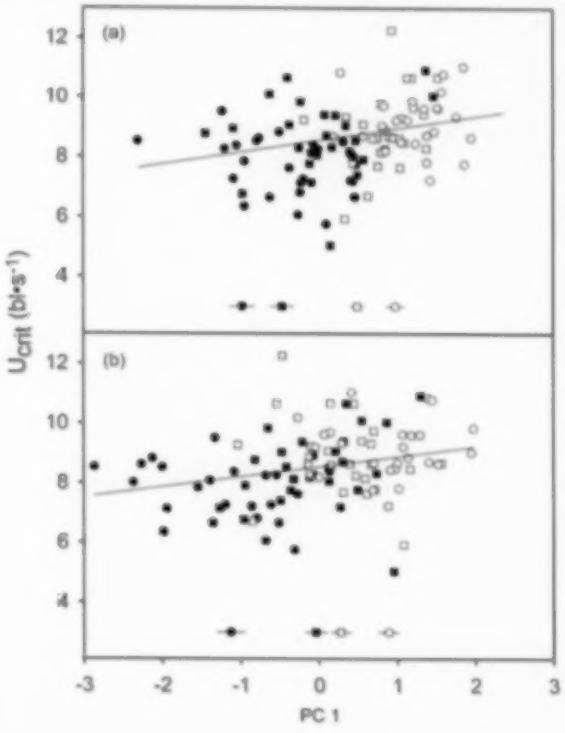

brid individuals possess greater competitive abilities than one of the parental forms, it is likely that hybrids will not be at a selective disadvantage. Our study supports this contention: first generation hybrids had intermediate morphological characteristics and demonstrated swimming abilities that were higher than cutthroat trout. Therefore, unless strong selection occurs against cutthroat–rainbow hybrids at another component of their life cycle, they are likely to be important competitors with native cutthroat trout. Past studies of hybridization between rainbow trout and coastal cutthroat trout indicate similar shape differences and swimming performance (Hawkins and Quinn 1996), as well as no reduced survivorship of hybrid individuals from fertilization to exogenous feeding (Hawkins and Foote 1998). Hence, higher swimming ability of introduced rainbow trout and cutthroat–rainbow hybrids may be especially detrimental to inland cutthroat trout species and is consistent with the pattern of rapid replacement of cutthroat trout populations by rainbow

© 2007 NRC Canada

trout and hybrid swarms (Jaeger et al. 2000; Hitt et al. 2003; Weigel et al. 2003).

In addition to the pattern between morphology and sustained swimming performance that we report, other factors may play an important role in rainbow–cutthroat trout interactions. For example, in salmonid fishes, burst swimming speed is thought to be important for predator evasion (Taylor and McPhail 1985*b*), and the impact of propagation and rearing of salmonids in hatcheries may affect interactions between cutthroat trout and rainbow trout by promoting increased growth rates, elevated aggression, and decreased swimming ability (see review by Weber and Fausch 2003). Increased size and behavioral differences may confer a competitive advantage to hatchery-influenced rainbow trout. Across many salmonid species, larger fish have a competitive advantage in territorial competition (Grant 1990; Rhodes and Quinn 1998), with relative mass differences as small as 5% predicting the outcome of territorial competition (Abbott et al. 1985). Similarly, more aggressive trout tend to defend larger feeding territories and obtain more food by displacing conspecifics from profitable foraging locations (Grant 1990). The evidence for decreased swimming ability by hatchery-influenced salmonids provides evidence that our results may be a conservative estimate of the sustained swimming differences between Yellowstone cutthroat trout, rainbow trout, and their hybrids. Given that most, if not all, rainbow trout present within native inland cutthroat trout waterways were reared in hatcheries or are wild descendants from hatchery stocks, future studies should address how growth rate, relative size, and behavioral differences influence competitive interactions between native cutthroat trout, introduced rainbow trout, and their hybrids.

Our study provides an example in which an introduced species and hybrids between the introduced species and a native species have superior performance over the native species in an ecologically important characteristic. Few other studies of animal populations have examined the mechanisms by which introduced species and their hybrids may compete with and spread into native populations. One notable example is Rosenfield et al. (2004), who show that hybrids between Pecos pupfish (*Cyprinodon pecosensis*) and the nonnative sheepshead minnow (*Cyprinodon variegatus*) have higher swimming stamina than both parental species. Our study is unique in that it makes an additional finding: subtle differences in morphology can influence swimming performance and potentially the competitive abilities of individuals.

The spread of rainbow trout into watersheds with native cutthroat trout represents a conspicuous case of freshwater homogenization (see review by Rahel 2002) and provides an excellent case study for invasive species ecology. The native distributions of cutthroat and rainbow trout are well documented (McPhail and Lindsey 1986; Young 1995); therefore, patterns of cutthroat trout displacement can be investigated in watersheds with different histories of rainbow trout introduction and across environmental factors (cf. Hitt et al. 2003; Weigel et al. 2003). Furthermore, hybridization between native cutthroat trout and introduced rainbow trout presents a special opportunity to study a type of ecological invasion thought to have severe implications for native populations. Further studies on this system could lead to stronger protection of native cutthroat trout populations and develop a better ecological understanding of invasive species.

Acknowledgements

This study was supported in part by NSF grants (DEB-0212445 and 0211818) awarded to ERK and Margaret Ptacek. Additional funding for the trout rearing system came from NSF EPSCoR, a NSF Dissertation Improvement grant (DEB-0508915) awarded to SMS, as well as Idaho State University through awards from the Department of Biological Sciences and the Graduate Student Research and Scholarship Committee (F01-111). Experimental crosses were made possible with help from the Idaho Department of Fish and Game. In particular, we thank Tom Frew, Damon Keen, Brad Dredge, John Mitchell, Jarrett Page, and Dan Baker. Rearing system construction, fish care, and valuable input to this project were provided by Meredith Seiler, Margaret Ptacek, Ken Rodnick, Ralph Chapman, Marjorie Matocq, Janet Loxterman, Adam Keeley, Laurie Fielder, Chad Shouse, Chris Leeseberg, Kelly Gunnell, Ryan McManamay, Trevor Knight, and Michael Sheehy. Two anonymous reviewers provided helpful comments on an earlier draft. Animal care and experimental procedures were approved the Idaho State University Animal Welfare Committee (Protocol No. 0502532).

References

Abbott, J.C., Dunbrack, R.L., and Orr, C.D. 1985. The interaction of size and experience in dominance relationships of juvenile steelhead trout (*Salmo gairdneri*). Behaviour, **92**: 241–253.

Anderson, E. 1949. Introgressive hybridization. John Wiley & Sons, New York.

Arnold, M.L. 1997. Natural hybridization and evolution. Oxford University Press, Oxford, UK.

Behnke, R.J. 1992. Native trout of western North America. American Fisheries Society, Bethesda, Md.

Bell, W.H., and Terhune, L.D.B. 1970. Water tunnel design for fisheries research. Fish. Res. Board Can. Tech. Rep. No. 195. pp. 1–69.

Boily, P., and Magnan, P. 2002. Relationship between individual variation in morphological characters and swimming costs in brook charr (*Salvelinus fontinalis*) and yellow perch (*Perca flavuscens*). J. Exp. Biol. **205**: 1031–1036.

Brett, J.R. 1964. The respiratory metabolism and swimming performance of young sockeye salmon. J. Fish. Res. Board Can. **21**: 1183–1226.

Dowling, T.E., and DeMarais, B.D. 1993. Evolutionary significance of introgressive hybridization in cyprinid fishes. Nature (London), **362**: 444–446.

Grant, J.W.A. 1990. Aggressiveness and the foraging behaviour of young-of-the-year brook charr (*Salvelinus fontinalis*). Can. J. Fish. Aquat. Sci. **47**: 915–920.

Griffith, J.S. 1988. Review of competition between cutthroat trout and other salmonids. *In* Status and management of interior stocks of cutthroat trout. *Edited by* R.E. Gresswell. Am. Fish. Soc. Symp. **4**: 134–140.

Hartman, G.F. 1965. The role of behavior in the ecology and interaction of underyearling coho salmon (*Oncorhynchus kisutch*) and steelhead trout (*Salmo gairdneri*). J. Fish. Res. Board Can. **22**: 1035–1081.

Hawkins, D.K., and Foote, C.J. 1998. Early survival and development of coastal cutthroat trout (*Oncorhynchus clarki clarki*),

© 2007 NRC Canada

steelhead (*Oncorhynchus mykiss*), and reciprocal hybrids. Can. J. Fish. Aquat. Sci. **55**: 2097–2104

Hawkins, D.K., and Quinn, T.P. 1996. Critical swimming velocity and associated morphology of juvenile coastal cutthroat trout (*Oncorhynchus clarki clarki*), steelhead trout (*Oncorhynchus mykiss*), and their hybrids. Can. J. Fish. Aquat. Sci. **53**: 1487–1496.

Hitt, N.P., Frissell, C.A., Muhlfeld, C.C., and Allendorf, F.W. 2003. Spread of hybridization between native westslope cutthroat trout, *Oncorhynchus clarki lewisi*, and nonnative rainbow trout, *Oncorhynchus mykiss*. Can. J. Fish. Aquat. Sci. **60**: 1440–1451.

Hughes, N.F., and Dill, L.M. 1990. Position choice by drift-feeding salmonids: model and test for Artic grayling (*Thymallus arcticus*) in subartic mountain streams, interior Alaska. Can. J. Fish. Aquat. Sci. **47**: 2039–2048.

Jaeger, M.W., Van Kirk, R.W., and Kellogg, T. 2000. Distribution and status of Yellowstone cutthroat trout in the Henry's Fork watershed. Intermt. J. Sci. **6**: 197–216.

Keeley, E.R., Parkinson, E.A., and Taylor, E.B. 2005. Ecotypic differentiation of native rainbow trout (*Oncorhynchus mykiss*) populations from British Columbia. Can. J. Fish. Aquat. Sci. **62**: 1523–1539.

Krueger, C.C., and May, B. 1991. Ecological and genetic effects of salmonid introductions in North America. Can. J. Fish. Aquat. Sci. **48**(Suppl. 1): 66–77.

Lindsey, C.C. 1978. Form, function, and locomotory habits in fish. *In* Fish physiology. Vol. II. *Edited by* W.S. Hoar and D.J. Randall. Academic Press, New York. pp. 1–100.

McLaughlin, R.L., and Grant, J.W.A. 1994. Morphological and behavioral differences among recently-emerged brook charr, *Salvelinus fontinalis*, foraging in slow- vs. fast-running water. Environ. Biol. Fishes, **39**: 289–300.

McPhail, J.D., and Lindsey, C.C. 1986. Zoogeography of the freshwater fishes of Cascadia (the Columbia system and rivers north to the Stikine). *In* The zoogeography of North American freshwater fishes. *Edited by* C.H. Hocutt and E.O. Wiley. John Wiley and Sons, New York. pp. 615–637.

Ojanguren, A.F., and Brana, F. 2003. Effects of size and morphology on swimming performance in juvenile brown trout (*Salmo trutta* L.). Ecol. Freshw. Fish. **12**: 241–246.

Quinn, G.P., and Keough, M.J. 2002. Experimental design and data analysis for biologists. Cambridge University Press, Cambridge, UK.

Quinn, T.P. 2005. The behavior and ecology of Pacific salmon and trout. University of Washington Press, Seattle, Wash.

Rahel, F.J. 2002. Homogenization of freshwater faunas. Annu. Rev. Ecol. Syst. **33**: 219–315.

Rhodes, J.S., and Quinn, T.P. 1998. Factors affecting the outcome of territorial contests between hatchery and naturally reared coho salmon parr in the laboratory. J. Fish Biol. **53**: 1220–1230.

Rhymer, J.M., and Simberloff, D. 1996. Extinction by hybridization and introgression. Annu. Rev. Ecol. Syst. **27**: 83–109.

Rohlf, F.J. 1993. Relative warp analysis and an example of its application to mosquito wings. *In* Geometrical morphometrics. *Edited by* L.F. Marcus, E. Bello, and A. Garcia-Valdecasas. Monografias Museo Nacional de Ciencias Naturales, Madrid, Spain. pp. 131–159.

Rohlf, F.J. 2005*a*. tpsDig, digitize landmarks and outlines. Version 2.04. Department of Ecology and Evolution, State University of New York at Stony Brook, New York.

Rohlf, F.J. 2005*b*. tpsRelw, relative warps analysis. Version 1.42. Department of Ecology and Evolution, State University of New York at Stony Brook, New York.

Rosenfield, J.A., Nolasco, S., Lindauer, S., Sandoval, C., and Kodric-Brown, A. 2004. The role of hybrid vigor in the replacement of Pecos pupfish by its hybrids with sheepshead minnow. Conserv. Biol. **18**: 1589–1598.

Rubidge, E.M., and Taylor, E.B. 2004. Hybrid zone structure and the potential role of selection in hybridizing populations of native westslope cutthroat trout (*Oncorhynchus clarki lewisi*) and introduced rainbow trout (*O. mykiss*). Mol. Ecol. **13**: 3735–3749.

Sakai, A.K., Allendorf, F.W., Holt, J.S., Lodge, D.M., Molofsky, J., With, K.A., Baughman, S., Cabin, R.J., Cohen, J.E., Ellstrand, N.C., McCauley, D.E., O'Neil, P., Parker, I.M., Thompson, J.N., and Weller, S.G. 2001. The population biology of invasive species. Annu. Rev. Ecol. Syst. **32**: 305–332.

Schrader, W.C., and Gamblin, M. 1996. Region 6 rivers and streams investigation, South Fork Snake River. Idaho Department of Fish and Game, Federal Aid in Sport Fisheries Restoration, Regional Fisheries Management Investigation, Job Performance Report Program F-TIR-16, Boise, Idaho.

Stebbins, G.L. 1959. The role of hybridization in evolution. Proc. Am. Philos. Soc. **103**: 231–251.

Swain, D.P., and Holtby, L.B. 1989. Differences in morphology and behavior between juvenile coho salmon (*Oncorhynchus kisutch*) rearing in a lake and in its tributary stream. Can. J. Fish. Aquat. Sci. **46**: 1406–1414.

Taylor, E.B., and Foote, C.J. 1991. Critical swimming velocity of juvenile sockeye salmon and kokanee, the anadromous and non-anadromous forms of *Oncorhynchus nerka* (Walbaum). J. Fish Biol. **38**: 407–419.

Taylor, E.B., and McPhail, J.D. 1985*a*. Variation in body morphology among British Columbia populations of coho salmon, *Oncorhynchus kisutch*. Can. J. Fish. Aquat. Sci. **42**: 2020–2028.

Taylor, E.B., and McPhail, J.D. 1985*b*. Burst swimming and size-related predation of newly emerged Coho salmon, *Oncorhynchus kisutch*. Trans. Am. Fish. Soc. **114**: 546–551.

Thorpe, R.S. 1976. Biometric analysis of geometric variation and racial affinities. Biol. Rev. **51**: 105–108.

Trotter, P.C. 1989. Coastal cutthroat trout: a life history compendium. Trans. Am. Fish. Soc. **118**: 463–473.

Varley, J.D., and Gresswell, R.E. 1988. Ecology, status, and management of the Yellowstone cutthroat trout. *In* Status and management of interior stocks of cutthroat trout. *Edited by* R.E. Gresswell. Am. Fish. Soc. Symp. **4**: 13–24.

Webb, P.W. 1984. Body form, locomotion, and foraging in aquatic vertebrates. Am. Zool. **24**: 107–120.

Weber, E.D., and Fausch, K.D. 2003. Interactions between hatchery and wild salmonids in streams: differences in biology and evidence for competition. Can. J. Fish. Aquat. Sci. **60**: 1018–1036.

Weigel, D.E., Peterson, J.T., and Spruell, P. 2003. Introgressive hybridization between native cutthroat trout and introduced rainbow trout. Ecol. Appl. **13**: 38–50.

Young, M.K. 1995. Conservation assessment for inland cutthroat trout. US For. Serv. Gen. Tech. Rep. No. RM-256.

Zelditch, M.L., Swiderski, D.L., Sheets, H.D., and Fink, W.L. 2004. Geometric morphometrics for biologists. Elsevier Academic Press, San Diego, Calif.

© 2007 NRC Canada

Modelling feeding, growth, and habitat selection in larval Atlantic cod (*Gadus morhua*): observations and model predictions in a macrocosm environment

Trond Kristiansen, Øyvind Fiksen, and Arild Folkvord

Abstract: Individual-based models (IBMs) integrate behavioural, physiological, and developmental features and differences among individuals. Building on previous process-based models, we developed an IBM of larval Atlantic cod (*Gadus morhua*) that included foraging, size-, temperature-, and food-limited growth, and environmental factors such as prey-field, turbulence, and light. Direct comparison between larval fish IBMs and experimental studies is lacking. Using data from a macrocosm study on growth and feeding of larval cod, we forced the model with observed temperature and prey-field and compared model predictions with observed distribution, diet, size-at-age, and specific growth rates. We explored implications of habitat selection rules on predicted growth rates. We analyze the sensitivity of model predictions by the Latin Hypercube Sampling method and individual parameter perturbation. Food limitation prevented larvae from growing at their physiological maximum, especially in the period 5–17 days post hatch (DPH). Active habitat selection had the potential to enhance larval growth rates. The model predicted temperature-limited growth rates for first-feeding larvae (5–20 DPH) when prey density is >5 nauplii·L^{-1}. After age 20 DPH, maximum modelled growth required a diet of copepodites. Simulated growth rates were close to observed values except for the period just after the start of exogenous feeding when prey density was low.

Résumé : Les modèles centrés sur l'individu (IBMs) intègrent les caractéristiques du comportement, de la physiologie et du développement, ainsi que les différences entre les individus. Nous servant de modèles antérieurs basés sur les processus, nous bâtissons un IBM pour les larves de morue franche (*Gadus morhua*) qui inclut la recherche de nourriture, la croissance limitée par la température et l'alimentation, de même que des facteurs du milieu, tels que l'univers des proies, la turbulence et la lumière. Il n'existe pas de comparaisons directes entre les IBM de larves de poissons et les études expérimentales. À l'aide de données provenant d'une étude de la croissance et de l'alimentation de larves de morue en macrocosme, nous avons forcé le modèle avec les températures et les communautés de proies observées; nous avons ensuite comparé les prédictions du modèle à la répartition, au régime alimentaire, à la taille en fonction de l'âge et aux taux spécifiques de croissance observés. Nous avons exploré les conséquences des règles de sélection de l'habitat sur les taux de croissance prédits. Nous analysons la sensibilité des prédictions du modèle par la méthode d'échantillonnage par hypercubes latins et par la perturbation des paramètres individuels. La pénurie de nourriture empêche les larves de croître à leur taux physiologique maximal, particulièrement dans la période des jours 5–17 après l'éclosion (DPH). Une sélection active de l'habitat peut potentiellement améliorer les taux de croissance des larves. Le modèle prédit des taux de croissance limités par la température chez les larves qui se nourrissent pour la première fois (5–20 DPH), lorsque la densité des proies est >5 nauplius·L^{-1}. À l'âge de 20 DPH, la croissance maximale prédite par le modèle exige un régime composé de copépodites. Les taux de croissance simulés sef rapprochent des valeurs observées à l'exception de la période qui suit immédiatement le début de l'alimentation exogène à un moment où la densité des proies est basse.

[Traduit par la Rédaction]

Introduction

Individual-based models (IBMs) are an important tool that can integrate from individual-level properties of environmental exposure, behaviour, and physiology to population-level characteristics of larval fish growth, survival, and spatial distribution (Grimm and Railsback 2005). Presently, there are many attempts to develop coupled biophysical models where IBMs of larval fish are embedded in general circulation models (Werner et al. 2001; Hinrichsen et al.

Received 24 March 2006. Accepted 9 October 2006. Published on the NRC Research Press Web site at http://cjfas.nrc.ca on 30 January 2007.
J19240

T. Kristiansen,[1] Ø. Fiksen, and A. Folkvord. Department of Biology, University of Bergen, P.O. Box 7800, N-5020 Bergen, Norway.

[1]Corresponding author (e-mail: trond.kristiansen@bio.uib.no).

 doi:10.1139/F06-176 © 2007 NRC Canada

Fig. 1. (*a*) Temperature distribution (°C) and (*b*) average prey abundance (μg·L^{-1}) during the macrocosm experiment and observed (*c*) day and (*d*) night distribution (%·m^{-1}) of larval Atlantic cod (*Gadus morhua*).

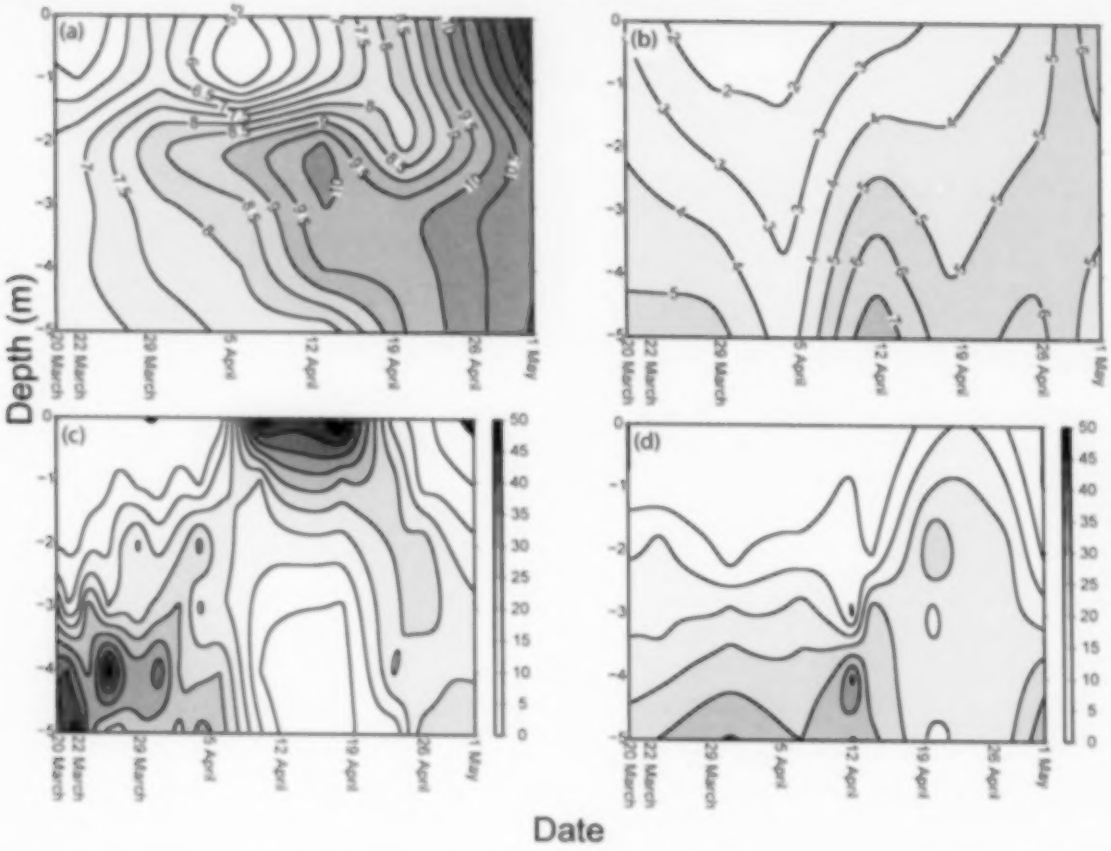

Table 1. Length (lp_i), width (dp_i), and dry weight (wp_i) for the 13 various zooplankton categories (i) available as prey in the pond.

	R	NI	NII	NIII	NIV	NV	NVI	CI	CII	CIII	CIV	H	M
lp_i (mm)	0.10	0.22	0.27	0.40	0.48	0.55	0.61	0.79	1.08	1.38	1.80	0.30	0.60
dp_i (mm)	0.10	0.10	0.10	0.10	0.15	0.18	0.20	0.22	0.25	0.31	0.40	0.10	0.30
wp_i (μg)	0.16	0.33	0.49	1.0	1.51	2.09	2.76	4.18	13.24	23.13	63.64	0.30	1.00

Note: R, rotifer; N, nauplius; C, copepodite; H, harpactacoid; M, miscellaneous. Sizes taken from Lough et al. (2005). Image area of prey (A_p, mm^2) is estimated as $lp \times dp \times 0.75$ (elongate prey).

2002; Lough et al. 2005). However, direct comparisons between model predictions and the observed growth patterns or feeding habits of larvae in natural or seminatural environments are rare. Therefore, direct comparisons between model predictions and observations of larval fish feeding, growth, and spatial distribution are warranted. Such efforts may strengthen our confidence in predictions from large-scale, physical–biological-coupled models. Controlled environments in macrocosms or landlocked fjords provide a balance between the realism of a natural habitat and the tractability of the laboratory (Folkvord et al. 1994). Information on the environmental conditions and larval properties from such studies can be used as forcing data to drive IBMs.

In the pelagic realm, vertical environmental gradients are typically much stronger than horizontal gradients. Therefore, when implementing IBMs into circulation models, accurate representation of the vertical distribution is important for predicting the exposure of larvae to environmental factors. Also, the horizontal dispersal of larvae often depends on their vertical positioning (Vikebø et al. 2005). However, little information exists on criteria for habitat selection of larval Atlantic cod (*Gadus morhua*). This is particularly so for larvae facing trade-offs between food availability, temperature, advection, and predation risk. Here, we present a mechanistic model of foraging and growth of cod larvae. The feeding processes are adopted from Fiksen and MacKenzie (2002), while our formulation of assimilation and transformation of energy from prey to larval tissue and growth is new. It incorporates the empirical models developed by Finn et al. (2002) and Folkvord (2005). Explicit

© 2007 NRC Canada

simulations of the macrocosm experiment by Folkvord et al. (1994) allow for direct comparison between model predictions and observed properties of the larvae in a monitored, nearly predator-free environment. We compare modelled and observed growth and diet of larvae for the first 42 days of their life. In addition, we explore the effects of habitat selection by the larvae on realized growth rates in the pond.

Biological background: the macrocosm experiment

This model effort uses observed temperature and prey density from a macrocosm experiment (Folkvord et al. 1994) as forcing. Observations of larval growth and weight at dates are compared with model predictions. Below, we provide a brief summary of the Folkvord et al. (1994) experiment.

Sampling

In spring 1983, larval Atlantic cod were released in five cohorts separated by 10-day intervals into the 5.5 m deep naturally enclosed 63 000 m^3 Hyltropollen (Folkvord et al. 1994). Fish larvae were 5 days post hatch (DPH) at the day of release and still at the yolk-sac stage. A total of 40 000 larvae samples were collected between 20 March and 3 May 1983, and 4354 larvae were individually measured. The environment was monitored by weekly measurements of temperature (Fig. 1*a*) and zooplankton biomass (Fig. 1*b*) at 1 m intervals from the surface to the bottom (Folkvord et al. 1994). Observations of zooplankton and temperature are available to day 42 (47 DPH) of the experiment.

The environment

An average turbulent dissipation rate was estimated using the mean wind field obtained from the Meteorological Institute in Norway for a nearby station (Flesland) and the empirical relationship between wind and turbulence from Mackenzie and Leggett (1993). Both temperature and zooplankton concentrations showed strong vertical and temporal variation (Fig. 1). Initially, strong vertical gradients characterized the hydrography after a cold weather period with patches of ice at the surface. By mid-April, most of the gradients had eroded and the water column was mixed (Fig. 1*a*).

Prey

In late March, total zooplankton biomass was very low at the surface but increased towards the bottom (Fig. 1). As time passed, the zooplankton became distributed homogenously in the water column. Prey types available in the pond were nauplii and copepodite stages of *Calanus finmarchicus*, rotifers, and harpacticoids. Rotifers were an important prey item for first-feeding larvae (Folkvord et al. 1994). A peak in abundance of rotifers occurred in the beginning of April (33·L^{-1} at the surface). Total prey density rarely exceeded 10·L^{-1} with an average close to 6·L^{-1} (Folkvord et al. 1994). Mean, standard deviation, minimum, and maximum values for the period 20 March – 1 May were 1.0 ± 5.0·L^{-1} (0.0–33·L^{-1}) for rotifers, 2.1 ± 1.7·L^{-1} (0.1–8.3·L^{-1}) for nauplii, 0.6 ± 0.4·L^{-1} (0.1–1.9·L^{-1}) for copepodites, 0.5 ± 1.0·L^{-1} (0.0 ± 5.8·L^{-1}) for harpacticoids, and 1.7 ± 2.2·L^{-1} (0.3 ± 13.6·L^{-1}) for miscellaneous species.

The sampling only separated between nauplii and copepodites. To obtain smaller incremental steps between size-classes of prey, we divided the *C. finmarchicus* data into developmental stages NI–NVI for nauplii and CI–CIV for copepods (Table 1). We assumed an exponential decrease in numbers between stages, where prey concentrations and prey size spectra correspond to estimated densities of nauplii and copepodites (Table 1).

Fig. 2. Flow chart of the individual-based model (IBM) where submodels are open boxes and state variables are shaded boxes. Each hourly calculations start with estimation of encounter, approach, capture, and ingestion for 13 prey types and sizes. Ingested biomass is stored in the stomach variable and determines together with ambient temperature the corresponding growth. The model has a spatial and temporal resolution of 1 m. Larval drawing by Tamara L. Clark, Woods Hole, Massachusetts.

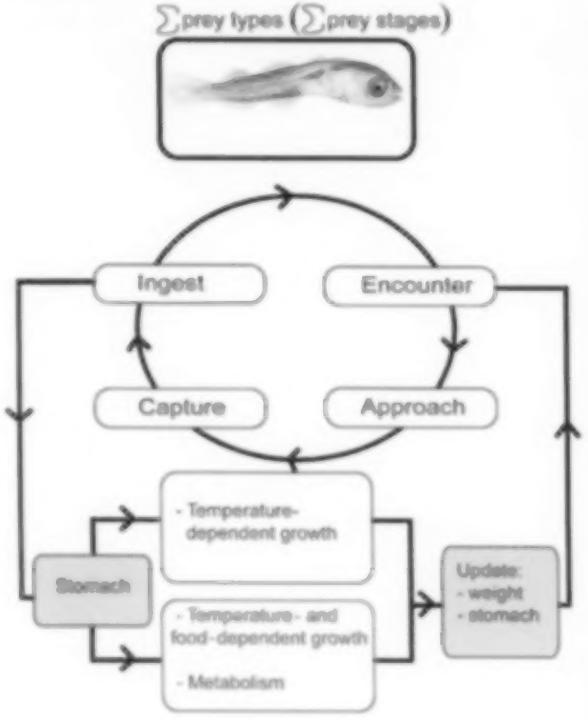

Model description

The model description follows the outline recommended by Grimm and Railsback (2005) (PSPC + 3).

Purpose

This IBM simulates the early life history of larval cod based on environmental factors and underlying processes that we believe are important. Each process is formulated and parameterized from laboratory experiments conducted on larval cod (Fiksen and MacKenzie 2002). The combination of these processes describes mechanistically how larval

© 2007 NRC Canada

Table 2. Variables and parameters from the IBM.

Symbol	Description	Units	Value
SGR[a]	Specific growth rate	%·day^{-1}	Eq. 2
R^b	Respiration rate	µg	Eq. 1
s	Stomach size	µg µg^{-1}·individual^{-1}	Eq. 5
wp_i	Weight of prey of type i	µg	Table 1
lp_i	Length of prey type i	mm	Table 1
dp_i	Width of prey type i	mm	Table 1
e^c	Encounter rate	Prey·s^{-1}	$e = \frac{2}{3}\pi fr^3 + \pi r^2 Nf\lambda\sqrt{w^2 + 2\omega^2}$
f^c	Pause frequency	s^{-1}	0.43
N	Prey density	mm^3	
r^d	Distance of perception	mm	$r^2 \exp(cr) = E' C A_p \frac{E_b}{E_b + K_e}$
u	Prey swimming speed	mm·s^{-1}	$100 \times lp_i$
ω^e	Turbulent velocity	mm·s^{-1}	$\omega = \sqrt{3.615(\varepsilon r)^{0.667}}$
λ^c	Pause duration	s	2.0
E'^a	Eye sensitivity of larva	Dimensionless	$E' = \frac{SL^2}{C \times 0.1 \times 0.2 \times 0.75}$
C^d	Prey inherent contrast	Dimensionless	0.4
A_p^f	Image of elongate prey	mm^2	$lp \times dp \times 0.75$
K_e^d	Larva half-saturation parameter	µmol·m^{-2}·s^{-1}	1.0
E_b^d	Light	µmol·m^{-2}·s^{-1}	$E_b(z,h) = E_0(h)\exp(-zk)$
A^h	Assimilation efficiency	Dimensionless	0.75
c	Beam attenuation coefficient	m^{-1}	$3k$
ε^e	Turbulent dissipation rate	kg·m^{-2}·s^{-3}	$\varepsilon = 5.82 \times 10^{-9} W^3$
W	Windspeed	m·s^{-1}	3.0
k	Attenuation coefficient	m^{-1}	0.18

[a]Folkvord (2005).
[b]Finn et al. (2002).
[c]MacKenzie and Kiørboe (1995).
[d]Aksnes and Utne (1997).
[e]MacKenzie and Leggett (1993).
[f]Fiksen and Folkvord (1999).
[g]Fiksen and MacKenzie (2002).
[h]Kiørboe (1989).

cod encounter, capture, and ingest food and use the energy for growth. The main purpose is to evaluate model performance in a well-studied seminatural situation.

Structure

We simulated growth for a period of 5–47 DPH for 160 individual cod larvae in a closed macrocosm with no predators assuming no mortality and no interactions among individual larvae. Behavioural responses to changes in the environment were restricted to vertical movements with a spatial resolution of 1 m and a temporal resolution of 1 h.

Processes

Submodels govern the interaction between environmental forcing (temperature, turbulence, and zooplankton density) and the dynamic state variables weight, stomach content, and length. These states are updated once every hour (Fig. 2). A key element is the mechanistic foraging submodel combined with a stomach as a state variable. Ingested mass or energy results from the successful completion of sequential processes: encounter, approach, and capture (Fiksen and MacKenzie 2002). The foraging processes are iterated for all prey types and size categories (Fig. 2). Holling's (1966) disc equation ensures that the total time spent handling prey reduces available search time. Stomach fullness and body mass determine whether growth is only temperature dependent or also food limited.

Concepts

An important and difficult topic for larval fish modelling is the behavioural positioning of the larvae in environmental gradients. We expect strong selection pressures on habitat selection in larval fish, since the pelagic environment is typically characterized by strong vertical gradients of variables related to growth (temperature, prey concentrations, light, and turbulence), predation risk (distribution and search efficiency of predators), and the probability of being advected out of favourable areas (Werner et al. 1993; Vikebø et al. 2005). Here, we explore the consequences of four different vertical behavioural rules: (*i*) larvae move along the depth of

© 2007 NRC Canada

Fig. 3. Growth rates (left panels) for three fish sizes, (*a*) 0.1, (*b*) 1.0, and (*c*) 100 mg, experiencing a range of ingestion rates (0–0.6 $g \cdot g^{-1} \cdot day^{-1}$) and temperatures (4–16 °C). Also shown are larval and juvenile (0.01–100 mg) growth rates assuming three fixed ingestion rates (*d*) 0.8, (*e*) 0.3, and (*f*) 0.0 $g \cdot g^{-1} \cdot day^{-1}$ for different temperatures (4–16 °C).

observed larval maximum abundances (ObsD), (*ii*) larvae follow the depth of highest temperature (HighT), (*iii*) larvae move along the depth with highest prey biomass (HighP), and (*iv*) larvae find the depth that yields the highest growth rate (HighG). We also included a simulation of larvae without active selection, i.e., larvae that move randomly up or down the water column. Our null hypothesis was that individuals with a strategy would grow faster than individuals moving randomly in the water column. To test this, we recorded average weight-at-age and depth distribution of 100 individuals for 32 days with random vertical positioning. All larvae were initialized with a start weight of 58 µg.

Initialization

We used observed data on each of four dates (26 and 31 March and 6 and 10 April) to describe the initial population weight distribution. For each date (11, 16, 22, and 26 DPH), we drew 160 (maximum number of larvae sampled at 16 DPH) individual weights randomly from the observations to yield averages of 58 ± 9, 112 ± 22, 234 ± 48, and 410 ± 87 µg, respectively. Using the four start dates and 160 individuals, simulations were repeated for the four rules. This resulted in 2560 individual realizations.

The simulation initiated on 10 April was run until 47 DPH and was compared with final observations from the pond on day 49, the final day of the Folkvord et al. (1994) experiment. This provides us with as many direct comparisons between predictions and observations as possible and also allows for identifying under which environmental conditions the model failed.

Input

Observed (Folkvord et al. 1994) prey density and turbulence were input to the foraging processes and temperature for the growth processes. We modelled light as a function of date, time of day, and latitude.

Submodels

The IBM was written as an object-oriented Fortran 90 code, which allows for tracking properties for every individual. Following is a detailed description of the various submodels.

Larval feeding processes

Prey encounter rate, pursuit success, and capture success determine larval feeding success. We applied the detailed and mechanistic model by Fiksen and MacKenzie (2002) based on earlier developments (MacKenzie and Kiørboe 1995; Aksnes and Utne 1997; Caparroy et al. 2000). This model predicts (*i*) prey encounter rates as a function of prey characteristics, larval size, ambient light, turbulence, and prey density and the probability that (*ii*) prey detect the approaching larvae and escape (Psa), (*iii*) prey are advected out of the larva's perception range owing to turbulence (Psp), and (*iv*) prey are successfully captured and ingested (Pca). Prey ingestion is limited by stomach capacity, while the prey items that compose the diet are estimated from all prey items captured within the last time step. Predictions from this model generated larval prey size selectivity in agreement with observations by Munk (1997). Key variables and parameter values are defined in Table 2. Visual foragers depend on light. Light conditions E_0 vary with time of day h and depth z and are a function of the surface light E_0 and the diffuse light attenuation k (Table 2). Surface light is calculated according to time of day, latitude (60°N), and day of the year (here, 20 March – 2 May 1983).

Respiration rates

Routine respiration rate of larval cod was thoroughly estimated by Finn et al. (2002). Routine respiration R (µg·individual^{-1}·h^{-1}) varies with dry-weight body mass w (mg) and temperature T (°C) as

$$(1) \qquad R = 2.38 \times 10^{-7} w^{0.9} \exp(0.0.88T)$$

Respiration rates were measured in light and darkness (Finn et al. 2002). Higher values occurred in light than in darkness, indicating that the values from darkness were closer to resting respiration. In the present model, we have applied the averaged value for R. The metabolism is elevated by a factor of 2.0 (Lough et al. 2005) when light conditions are suitable for foraging (visual range ≥1.0 mm) and the larvae are active.

Size- and temperature-limited growth rate

If the larvae ingest more food than they can process and assimilate, then size- and temperature-dependent physiological processes will limit their growth. We applied the model derived from extensive laboratory rearing experiments on coastal cod by Otterlei et al. (1999) and Folkvord (2005) to find larval specific growth rates (SGR, %·day^{-1}) under such conditions:

$$(2) \qquad \mathrm{SGR}(w, T) = a - b\ln(w) - c\ln(w)^2 + d\ln(w)^3$$

where SGR is the specific growth rate in percentage per day, expressed as a function of temperature (T) and dry mass (w, mg), and $a = 1.08 + 1.79T$, $b = 0.074T$, $c = 0.0965T$, and $d = 0.0112T$ (Folkvord 2005). The SGR can be expressed as specific growth rate g per time step (dt, day^{-1}), $g = \ln[(\mathrm{SGR}/100) + 1)/\mathrm{dt}]$.

Larval state variables and food-limited growth

Larvae are characterized by the state variables body mass (w, dry weight) and stomach fullness (s). The maximum energy content of the stomach (s) is set to 6.0% of the total weight, which corresponds to observations of stomach content and size of cod larvae on Georges Bank (E. Broughton, National Marine Fisheries Service, NOAA, Northeast Fisheries Science Center, Woods Hole, MA 02543, USA, personal communication) and to the upper limit of ingested material used by Lough et al. (2005). The amount of food in the stomach and the growth potential of the larvae determine

© 2007 NRC Canada

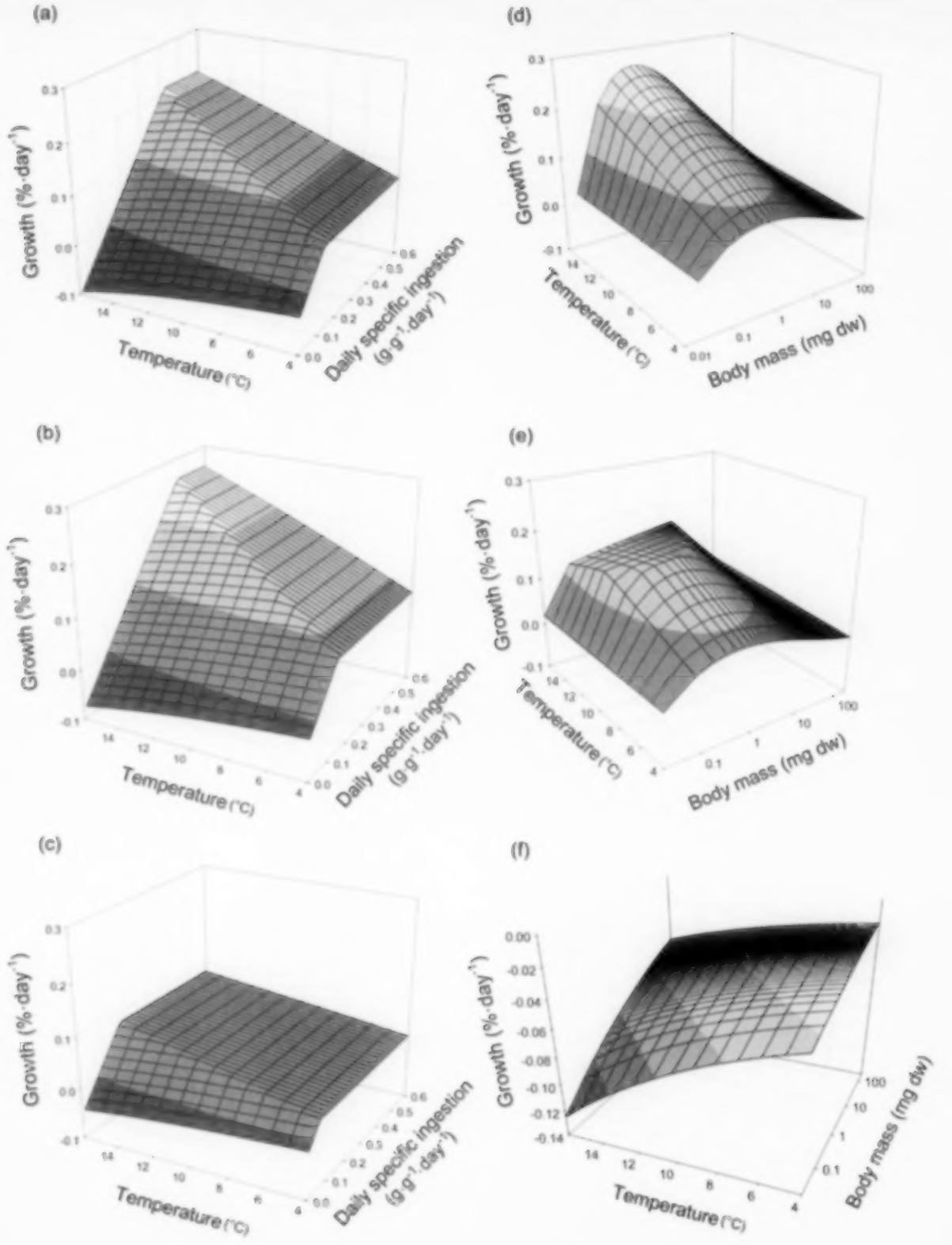

© 2007 NRC Canada

Table 3. Variables and parameters examined in the sensitivity analysis, divided into internal and external variables, and further grouped into submodel level.

		r^2			10% increase individual parameter perturbation (% increase in weight from base after 48 h)	
Parameter–variable	Mean value (min.–max.)	5 mm	11 mm	Submodel	5 mm	11 mm
External						
Temperature (°C)	7.0 (6.5–7.5)	0.05	0.98	Environment	0.4	1.6
Prey density (L^{-1})	2.5 (0.5–4.5)	0.88	0.02		0.4	0.05
Surface wind	3.0 (1.0–5.0)	0.00	0.00		0.1	0.01
Surface light ($\mu mol \cdot m^{-2} \cdot s^{-1}$)	250 (200–300)	0.00	0.00		0.0	0.0
Beam attenuation coefficient (m^{-1})	0.18 (0.1–0.3)	0.00	0.00		–0.3	0.0
Attenuation coefficient (m^{-1})	0.54 (0.33–0.89)	0.00	0.00		–0.1	0.0
Sum		0.94	1.00			
Internal						
Initial perception (mm^2)	0.015 (0.014–0.016)	0.00	0.01	Mechanistic foraging	–0.5	–0.06
Attack speed ($m \cdot s^{-1}$)	10 (8–12)	0.34	0.08		2.9	0.02
Escape speed ($m \cdot s^{-1}$)	100 (80–120)	0.32	0.08		–0.1	–0.07
Mean jump angle (rad)	$\pi/6$ (0.3–0.7)	0.12	0.01		–0.3	0.0
Half-saturation parameter	1.0 (0.001–5)	0.00	0.00		–0.2	0.0
Activity (dimensionless)	2.0 (1.5–2.5)	0.00	0.00	Bioenergetic	1.4	0.0
Respiration exponent (dimensionless)	0.9 (0.85–0.95)	0.00	0.01		1.4	0.0
Gut size (% dry weight)	0.06 (0.05–0.07)	0.03	0.24		0.45	0.5
Assimilation (dimensionless)	0.75 (0.6–0.9)	0.00	0.01		3.1	0.0
Sum		0.81	0.45			

Note: Mean values of the parameter distribution are shown together with the range (min.–max.). The influence (r^2) from each parameter on the simulated weight (after 48 h) is given for two larval sizes (5 and 11 mm). By increasing the parameter value by 10%, the corresponding increase in weight (% increase from base run) is given in the individual parameter perturbation columns for two sizes of larval cod.

whether growth is maximal (size and temperature limited) or food limited.

The mass (or energy) D required to sustain maximal growth within each time step is given by

$$D = dt(gw + R)/A \quad (3)$$

Here, A is the assimilation efficiency equal to 0.75, correcting for energy losses through feces and specific dynamic action (Kiørboe 1989). The stomach then acts as a reactor and dynamic storage where mass is withdrawn depending on potential growth. The stomach fullness is a function of previous state s_t, digested material D, and ingestion i:

$$s_{t+1} = s_t - D + i \quad (4)$$

The change in body mass dw within each time-step is then given by

$$\frac{dw}{dt} = \begin{cases} gw & \text{if } D \le s_t \\ sA - R & \text{if } D > s_t \end{cases} \quad (5)$$

This is where growth becomes either food or temperature limited. If stomach content s_t can supply the matter and energy required D ($D = s_t$), then growth proceeds at maximum rate. Otherwise, if $D > s_t$, then what is in the stomach is processed and turned into body mass. The predicted growth rates of larval cod under various temperatures, body mass, and prey ingestion rates are presented in Fig. 3. This approach integrates solid laboratory studies on larval cod growth and metabolism and a simple, but reasonable, representation of mass and energy flow through the larvae. The model predicts that growth drops linearly with food availability below a threshold that depends on both temperature and larval weight (Fig. 3*c*). It captures the general view that food requirements are higher when growth rates are high and acts as an interpolation between the food-satiated growth pattern observed by Folkvord (2005) and the starving case of Finn et al. (2002) (Fig. 3*b*).

Sensitivity analysis

Trust in model predictions is gained through validation and testing of the IBM. Comparison between simulation results and observations may increase confidence in the hypotheses formalized in the model, depending on its ability to match observed patterns. Also, the importance of submodels in a complex model can be analyzed through sensitivity analyses. If small changes in parameter values generate large responses, the model is sensitive to the parameter.

Sensitivity analysis of the IBM was performed using a Monte Carlo simulation where parameter values are randomly selected from a distribution. We implemented this method using Latin Hypercube Sampling (Rose 1987; Rose et al. 1991*b*) and used it to determine the contribution of parameter variation to prediction error (Bartell et al. 1986). First, we assigned a specific distribution for all parameters

© 2007 NRC Canada

Table 4. Density of *Calanus finmarchicus* (nauplii and copepodites) in the water column as experienced by a larva according to vertical behavioural rule and age.

Simulation period (DPH)		Mean density (no.·L^{-1} ± SD (min.–max.))			
		ObsD	HighT	HighP	HighG
5–22	Total prey density	2.4±0.8 (1.0–4.0)	2.7±0.9 (0.9–4.4)	4.8±2.2 (1.2–10.0)	3.5±2.0 (0.9–10.0)
	Available for larva	1.2±0.6 (1.3–2.9)	1.3±0.5 (0.4–2.6)	2.8±1.7 (0.4–6)	1.9±1.2 (0.7–5.7)
22–47	Total prey density	2.4±0.7 (1.4–4.0)	2.7±1.0 (0.9–4.4)	6.1±1.8 (4.0–10.0)	2.7±0.9 (0.9–4.3)
	Available for larva	2.1±0.7 (1.0–3.7)	2.1±0.8 (0.9–3.8)	5.4±1.6 (3.3–9.0)	2.1±0.8 (0.9–3.8)

Note: The simulation period for the first 17 days post hatch (DPH) and that for the last 25 DPH are separated, as the size of the larvae in the time windows differs significantly and thereby the number of available prey types for ingestion. Only *C. finmarchicus* is considered, as this is the dominant prey item found in gut analysis (Folkvord et al. 1994) both in observations and in simulations. ObsD, depth where maximum abundances of larvae were observed during assessment; HighT, depth of highest temperature; HighP, depth with highest prey biomass; HighG, depth that yields the highest growth rate.

Fig. 4. (*a* and *b*) Specific growth rates and (*c* and *d*) specific ingestion rates for a larva of fixed size, (*a* and *c*) 5 and (*b* and *d*) 8 mm, experiencing the same environmental and biological conditions. Values are calculated at fixed depths of 1 m resolution.

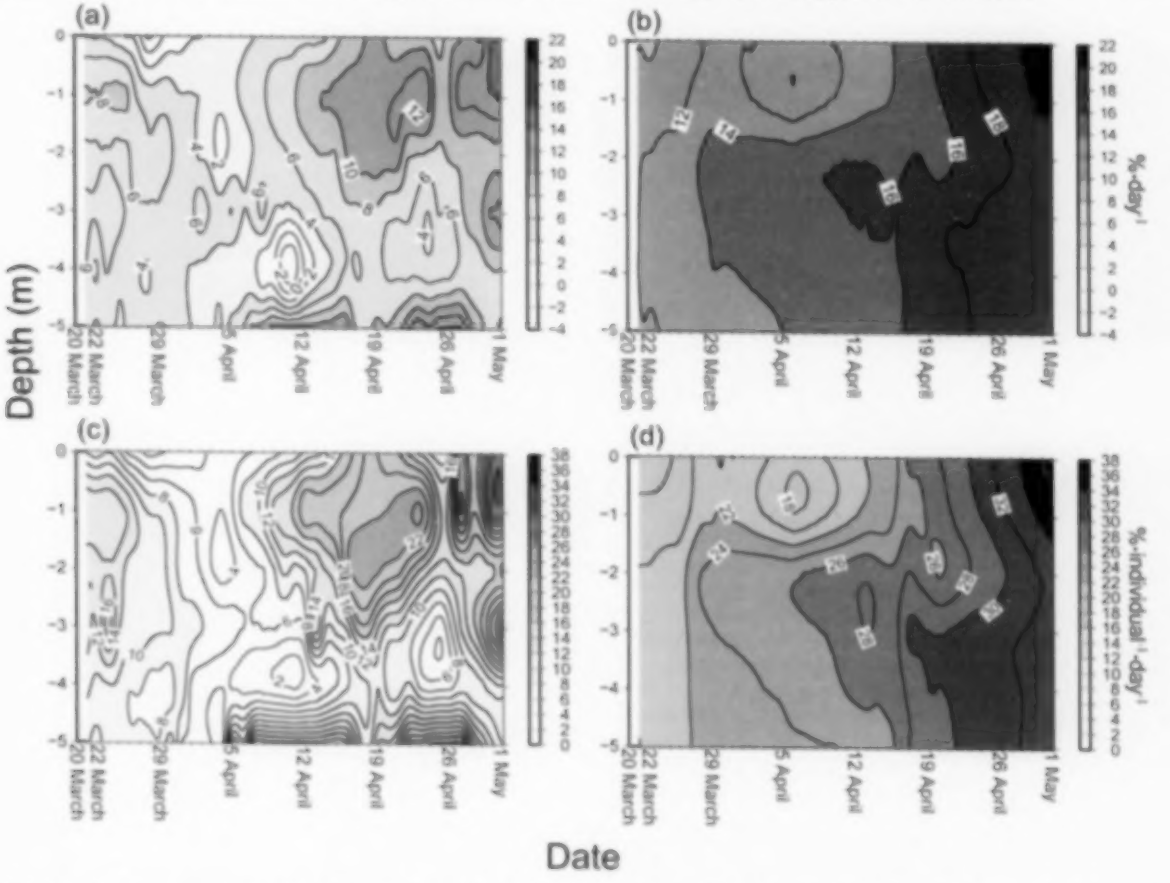

included in the error analysis. The nominal value for each parameter defines the mean value of the distribution. We then drew values randomly from the distributions to create a set of parameter values in each model realization.

A typical approach to sensitivity analysis in IBMs is the individual parameter perturbation method where each variable–parameter in the model is varied ±10% or ±20% between simulations. Model results (weight in this case), with and without this change, determine the impact of the change in variable value. Although this method leaves us with an indication of the sensitivity of that particular variable, the results can be biased if different processes behave in a nonlinear fashion and interaction exists between variables (Gardner and O'Neill 1981). We included the individual parameter perturbation approach as a companion to the error analysis.

The Monte Carlo error analysis combined with the Latin Hypercube Sampling approach has been used by several au-

© 2007 NRC Canada

Fig. 5. Simulated state variables (mean) for 10 larvae (35.4 ± 5.6 µg) over 42 days using vertical positioning rule HighG (depth that yields the highest growth rate). (*a*) Dry weight, (*b*) specific growth rate (SGR), and (*c*) stomach fullness (% of maximum (6% dry weight)) (averaged over 24 h) increase when the prey density in the pond is increased by 1 or 2 nauplii·L^{-1}. The potential temperature-dependent (food-unlimited) growth is marked with circles (Folkvord equation). Excluding the mechanistic submodel from the individual-based model (IBM) and assuming that prey is captured if lp/SL < 0.08 is marked "gape limited".

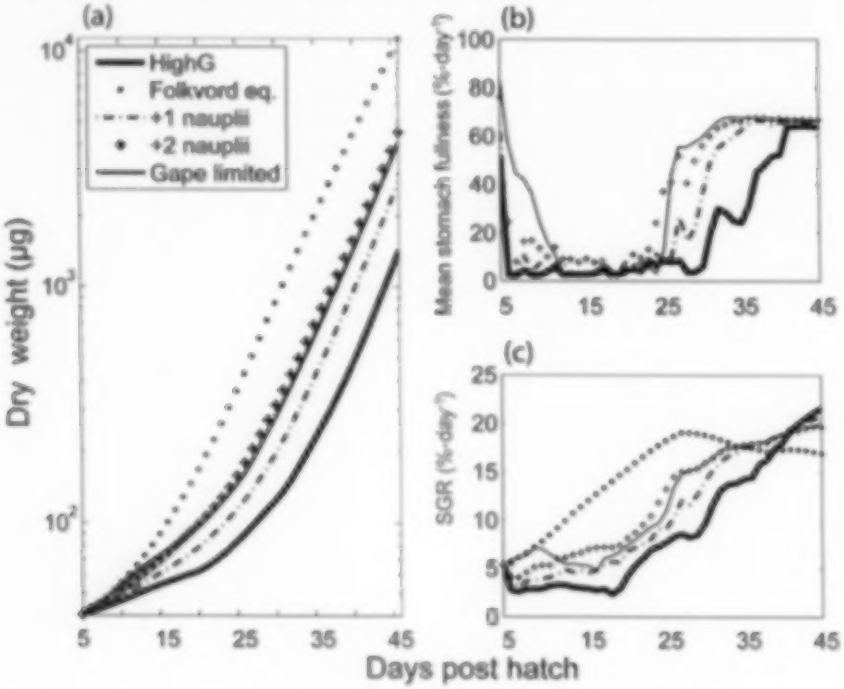

thors (Rose et al. 1991*a*; Letcher et al. 1996; Megrey and Hinckley 2001). In general, these studies found the methods to provide similar results for linear models. We applied the error analysis to the IBM model in two steps by varying (*i*) six of the external (environmental) variables and (*ii*) 10 of the internal variables.

We assumed a normal distribution of both internal and external parameters by defining a mean, minimum, and maximum value of each parameter (Table 3). Each parameter distribution was sampled 300 times. During sensitivity analysis of the internal parameters, the environmental variables are not kept constant but vary according to observations. Internal and external parameter analysis resulted in two data sets of size 300 times 11 and 7 (parameters and simulated larval weight), respectively. These data sets were further analysed statistically by simple correlation analysis (Pearson). Correlation between parameters and model results determines the individual contribution from each parameter to model variance. We repeated the analysis for two sizes of larval cod (5 and 11 mm).

Results

Sensitivity analysis

The Monte Carlo sensitivity analysis revealed interesting properties of the model. In particular, growth rates were sensitive to variance in certain variables, which differed for large and small larvae (Table 3). For small larvae (5 mm), prey density strongly influences growth. The range of prey density varied between 0.8 and 10 nauplii·L^{-1} depending on choice of vertical rule. Estimated prey concentration within edible size range depended on larval size and vertical rule (Table 4), with very low values for age 5–22 DPH larvae (0.4–6 nauplii·L^{-1}). For small larvae, the prey size category available for capture is limited to rotifers and small nauplii (NI-NIII) (Table 1). The sensitivity of the internal parameters revealed that small changes in prey escape speed and larval attack speed can increase or decrease the range of possible prey items (Table 3). In a food-limited situation, this is critical to maintain high growth rates. Larger larvae (11 mm) are unaffected by variation in prey density, as long as the values exceed 2–3 nauplii·L^{-1} (Table 4), and variance in growth is explained almost solely by the changes in temperature (r^2 = 0.98) (Table 3). This situation also explains why parameters related to foraging efficiency are sensitive for small but not for larger larvae. Similarly, gut size is important for larger larvae, since maintaining growth during night is occasionally dependent on stomach capacity.

Variation in surface light, beam attenuation, and extinction coefficient does not influence the result at all, mainly because light conditions limit foraging only at sunset and at night. The pond is shallow so that light is not the important limiting factor; this has been shown to be so in models of cod in marine environments (Lough et al. 2005).

© 2007 NRC Canada

Fig. 6. Simulated state variables (mean) for 10 larvae (35.4 ± 5.6 µg) over 42 days using vertical positioning rule HighG. (*a*) Dry weight, (*b*) specific ingestion rate (before assimilation), and (*c*) specific growth rate increase gradually as prey concentration is raised from 1 to 10 nauplii·L^{-1}. The potential temperature-dependent (food-unlimited) growth is marked with circles (Folkvord equation).

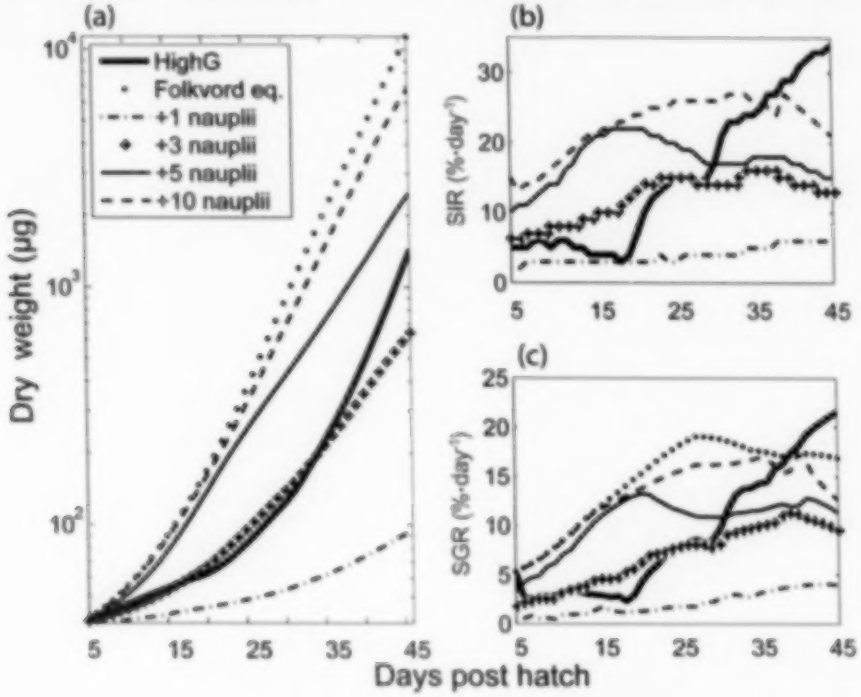

Comparison between simulation runs with a 10% increase in parameter values (individual parameter perturbation method) produces low impact on the simulated weight over 48 h. The growth difference was generally lower than 1%, with the exception of the attack speed of the larvae and the prey escape speed for small larvae.

Vertical behaviour and growth rates

Behavioural conduct in a spatial environment affects the potential growth rates for small larvae, even in a pond of only 5 m depth. Modelled growth and ingestion rates for a 5 mm larva vary considerably between depths (Figs. 4*a* and 4*c*). One of the rules applied for habitat selection is related to growth (HighG), and therefore, modelled habitat selection becomes dependent on stomach fullness, temperature, and prey density (Figs. 5 and 6). Larvae adapting to rule HighG achieve the highest growth rates. Larvae of size 5 mm are mechanistically restricted to forage on rotifers and copepod nauplii compared with 8 mm larvae that are capable of capturing copepodites. This results in large depth-dependent differences in growth rates for the two sizes of larval cod (Fig. 4) that experience the same habitat. Growth rates are mainly temperature dependent for 8 mm larvae, while growth of a 5 mm larva depends on the correct choice of habitat. Given the relatively low prey concentrations found in the pond (Table 4), a small increase in nauplii (1–2·L^{-1}) increases the growth rates considerably for small larvae, especially at the onset of feeding (Fig. 5). The minimum prey density necessary to obtain purely temperature-dependent growth rates was analyzed by increasing the prey concentration of nauplii (NI) in the macrocosm from 1 to 10·L^{-1} (Fig. 6). A prey density of >10 nauplii·L^{-1} enables small larvae (5 mm) to encounter and capture enough prey to sustain the energetic demands of temperature-dependent growth (Fig. 6), although at 25 DPH, growth is food limited, and the larva needs to switch to or include copepodites in the diet to sustain optimal growth rates. Otherwise, the larva is eventually limited by the encounter rate and ceases to capture enough prey. To determine the effect of the mechanistic submodel, we modelled growth where foraging is gape limited and where upper prey length to predator length ratio is a maximum of 8%. Corresponding growth increases equal to an increase in prey density of 2 nauplii·L^{-1} (Fig. 5).

Average observed growth rates for the population aged 5–25 DPH were 12.7%·day^{-1} (Folkvord et al. 1994), while simulated growth rates depended on the choice of vertical behavioural rule, 9.1%, 10.5%, 10.7%, and 11.2%·day^{-1} for ObsD, HighT, HighP, and HighG, respectively (Fig. 7). Simulated growth rates for larval age 5–22 DPH were lower than observed, but the difference diminished after 22 DPH as the simulated larvae increased in size and grew close to observations (Figs. 7 and 8).

Diet

Gut analysis of larval cod revealed a diet consisting of rotifers and nauplii for the first 20 DPH (Folkvord et al. 1994) and then switched to a diet composed mainly of copepodites (90% of the energy and 20% of the prey items in the stom-

© 2007 NRC Canada

Fig. 7. Simulated growth rates for 160 individual larvae. Model runs are initialized with the observed (Folkvord et al. 1994) weight distribution at 11, 16, 22, and 26 days post hatch (DPH) (arrows) using four vertical positioning rules, (*a*) ObsD (depth where maximum abundances of larvae were observed during assessment), (*b*) HighT (depth of highest temperature), (*c*) HighP (depth with highest prey biomass), and (*d*) HighG (depth that yields the highest growth rate). Temperature-limited growth rate is estimated using the average weight distribution for each day (line) and defines the upper physiological restricted growth rate for the given environment.

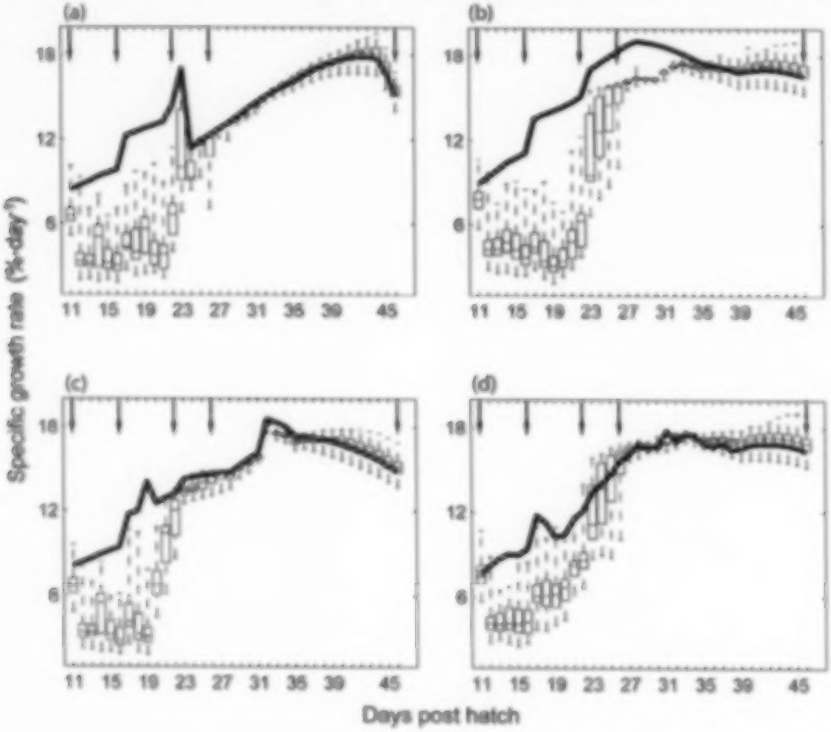

ach) (Fig. 9, top left panel). Nauplii are the most abundant prey in the pond, which is also reflected in simulated gut contents (Fig. 9). After day 20, the larger larval size opens up for a wider range of prey items and the importance of copepodites increases (Fig. 9).

Rules compared with random walk

Weight-at-age varied for larvae following different rules, and all rules perform better than a random movement strategy (Fig. 10*a*). Larvae moving according to rules HighP and HighG did best. The vertical movement during 32 days for a larva following rule HighG varies considerably over time (Fig. 10*b*). The frequent vertical repositioning is related to stomach dynamics: which habitat has maximum growth rates depends on stomach fullness, temperature, and prey abundance (Fig. 10*c*). The vertical position of the larva follows the depth where prey abundance satiates maximum growth at the highest possible temperature (Figs. 10*c*, 1*a*, and 1*b*). The average depth for the random walk converges towards an average of 2.5 m.

Discussion

Sensitivity analysis suggests that small changes in parameters or variables do not create large differences in simulation results. This reassures us that the model is robust within the parameter space, possibly with the exception of the prey jump speed and the cod attack speed for small larva. The IBM uses the ratio between larva attack speed and prey escape speed (1/10), as discussed by Fiksen and MacKenzie (2002) in the calculation of the capture success. A larval attack speed of 10 standard lengths·s^{-1} and a prey escape speed of 100 prey lengths·s^{-1} are based on intermediate values from experiments (for details, see Fiksen and Mackenzie 2002). An increased ratio results in an increased capture success (restricted by the gape limitation of the larva) and vice versa. However, the selected ratio simulates a prey preference size of 5% of larval body length (Fiksen and MacKenzie 2002) and agrees well with observations by Munk (1997). This indicates that the chosen velocity values are sensible, although an improved version of this IBM would gain realism by including differences between prey species, e.g., contrast of prey to the background and difference in escape speed between species.

Smaller larvae are sensitive to changes in prey density, which is not surprising, as 2–4 nauplii·L^{-1} seems to be the minimum values needed for larvae to sustain metabolism. Model results predict that larvae are able to grow at 2%–5%·day^{-1} at quite low prey density (2 nauplii·L^{-1}), although growth after 25 DPH at this prey density is severely limited.

© 2007 NRC Canada

Fig. 8. Simulated growth rates (%·day^{-1}) for 160 individual larvae. Model runs are initialized with the observed (Folkvord et al. 1994) weight distribution at 11, 16, 22, and 26 days post hatch (DPH) (boxes) using four vertical positioning rules, (*a*) HighG (depth that yields the highest growth rate), (*b*) ObsD (depth where maximum abundances of larvae were observed during assessment), (*c*) HighT (depth of highest temperature), and (*d*) HighP (depth with highest prey biomass).

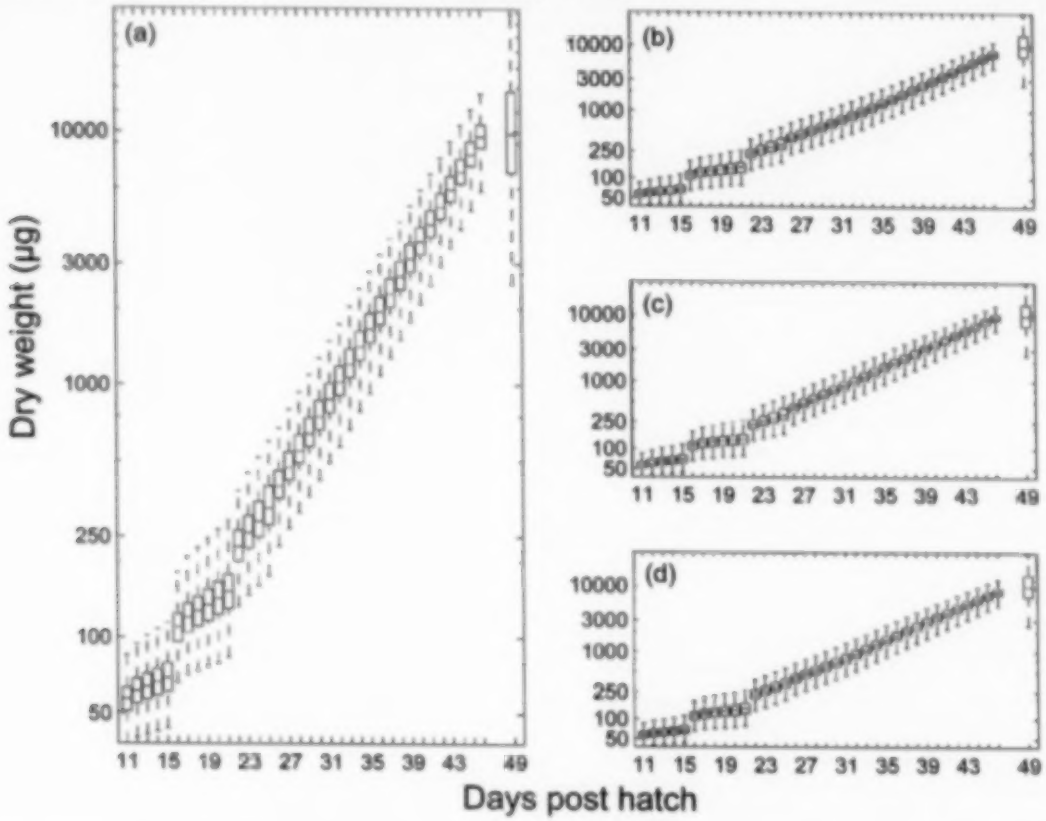

When we increased the prey density to 10 nauplii·L^{-1}, the larvae achieved high growth rates for the first 25 DPH (500 µg). As the body size of the larva reaches 1000 µg, it seems that optimal growth is only viable to sustain if the diet includes copepodites.

Light did not limit foraging in the pond, except for a short period at night (2200–0200), although food-limited growth through this period is avoided if the larva keeps a full stomach.

Early life history (growth and survival) of larval cod is determined from the larva's interaction with physical and biological properties, such as turbulence (Sundby et al. 1994; MacKenzie and Kiørboe 1995, 2000), light (Aksnes and Giske 1993; Aksnes and Utne 1997; Fiksen et al. 1998), temperature (Otterlei et al. 1999; Sundby 2000; Folkvord 2005), ocean transport (Werner et al. 1993; Vikebø et al. 2005), prey abundance (Cushing 1990; Beaugrand et al. 2003), and predators. Larval cod may be able to utilize its environment by adaptive vertical positioning. Model simulations indicate that active vertical behaviour in the pond does influence growth rates and is especially important for the first 5–25 DPH of feeding. This is not necessarily true in general but is of importance in our model setup where food abundance is limited and spatially distributed. Simulations indicate a 2% difference in daily specific growth rate between rules for a pond of only 5 m depth. The simple rules may not be very applicable to natural conditions but indicate the potential gain of being flexible and actively seeking patches of prey to optimize its growth rate, particularly when stomach fullness is decreasing. We have used weight and growth rate as fitness a measure for comparison between rules. This was a natural choice, as mortality was not included in the model and the experimental habitat was predator free, although Folkvord et al. (1994) did observe an increased size-selective cannibalism as the experiment evolved. We are currently exploring the use of more sophisticated behavioural rules in situations with multiple trade-offs between growth, predation risk, drift trajectories, and dispersal (Fiksen et al., in press).

In natural environments, the larva has to consider the trade-off between foraging and risk from predators. In the nearly predator-free pond, Folkvord et al. (1994) observed that larvae aggregated along the bottom for the first week after release, before gradually dispersing throughout the water column. The dispersal corresponded to a period of low prey concentration and probably the end of yolk sac utilization.

© 2007 NRC Canada

Fig. 9. (*a*) Observed (Folkvord et al. 1994) and simulated energy content in the stomach according to choice of vertical positioning rule (*b*) ObsD (depth where maximum abundances of larvae were observed during assessment), (*c*) HighT (depth of highest temperature), (*d*) HighP (depth with highest prey biomass), and (*e*) HighG (depth that yields the highest growth rate). Prey categories are confined to rotifers, *Calanus finmarchicus* nauplii and copepodites, miscellaneous, and harpactacoids. The energetic contribution from these five prey categories was estimated using the conversion between prey weight and energy content from Blom et al. (1991).

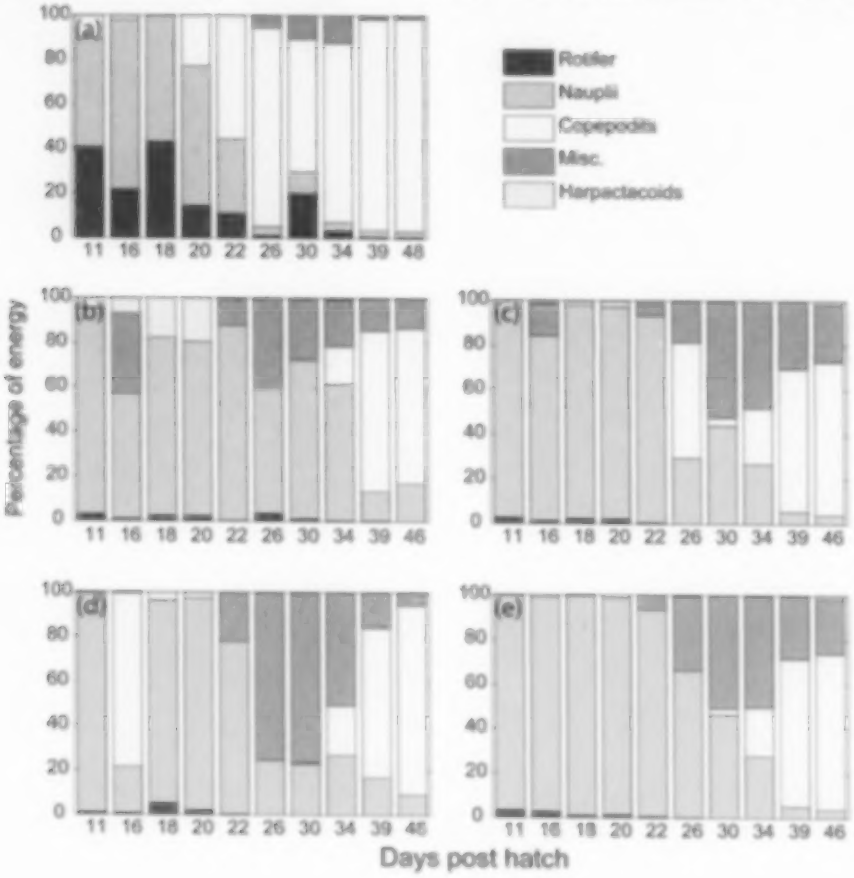

Larval cod that are able to maximize growth (HighG) avoid areas of low prey density. They also tend to find the depths where prey densities are able to sustain high growth rates at depths of high temperature. Small larvae are therefore able to grow fast, but their energy storage is low. It is also evident from the model results that even simple rules outperform random vertical behaviour. For the larvae to obtain growth rates comparable with what Folkvord et al. (1994) observed, it would therefore be tempting to say that the larvae would need some form of strategy. Information on to what extent larval cod are able to optimize the water column in this fashion and to migrate vertically is limited. Grønkjær and Wieland (1997) observed vertical distribution of small larvae (4–5 mm) in the Baltic Sea. The Baltic Sea is characterized by low-density surface water, making the eggs neutrally buoyant below the halocline (>45 m). Larval cod are visual feeders, and food and light at the depth of hatching are limited, causing the larvae to swim upward, closer to the surface, to forage. This behaviour is observed from the onset of first feeding (2–5 DPH) and indicates the ability of small larvae to be able to adequately assess the environment. Larval behaviour is probably connected to environmental gradients, especially the gradient of light in a water column. Light is essential for detecting prey but also for larval exposure to predators. As the larvae grow in size, they develop a diel vertical migration pattern based on the trade-offs between feeding and the risk to predation (Lough and Potter 1993). Larval cod on Georges Bank, larger than 9 mm, seem to follow a diurnal cycle, moving into the surface layer (upper 20 m) at night and into deeper water (35 m) during the day (Lough and Potter 1993; Lough et al. 1996). This vertical behaviour is probably initiated when larvae reach 6–8 mm (Lough and Potter 1993).

Folkvord et al. (1994) observed that larvae fed mainly on rotifers and nauplii (80% of the stomach content) for the first 20 DPH and then switched to a diet of larger copepodites, contributing up to 90% of the energy and 20% of the prey number in the stomach at 48 DPH. Both simula-

© 2007 NRC Canada

Fig. 10. (*a*) Average simulated weight for 10 individuals that follow the rules ObsD (depth where maximum abundances of larvae were observed during assessment), HighT (depth of highest temperature), HighP (depth with highest prey biomass), and HighG (depth that yields the highest growth rate) compared with the average weight of 100 individuals that move randomly (Ran) and (*b*) depth position and (*c*) specific stomach content for a 32-day period of an individual that optimize the growth rate (HighG) (6 h running mean).

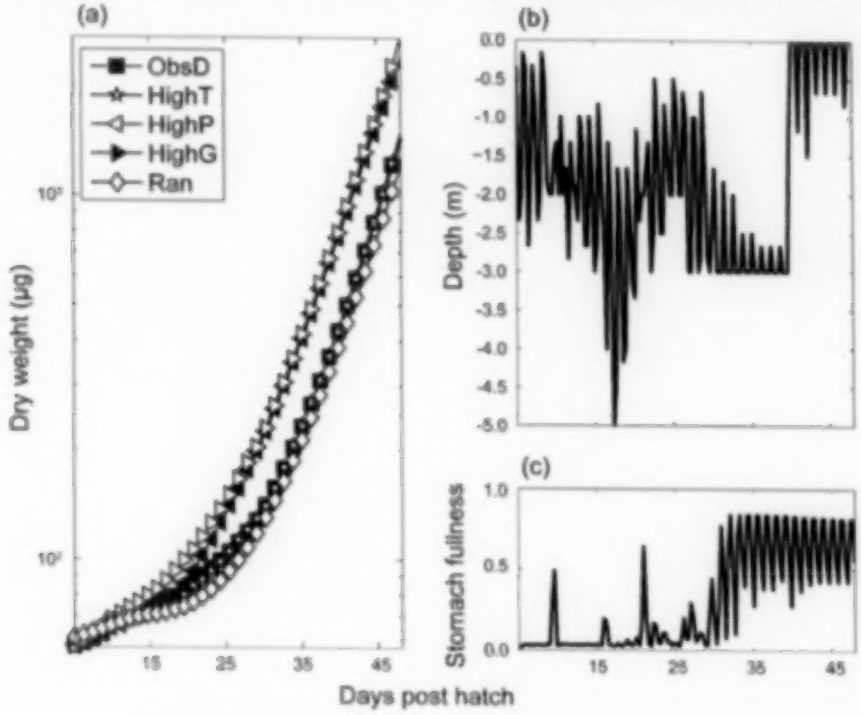

tions and observations indicate that nauplii are the main prey species for smaller larvae. A striking difference between observations and simulations is the high numbers of rotifers found in the gut analysis. This bias between observations and simulations could stem from underestimated sampling of rotifers, perhaps caused by patchy distribution of rotifers not captured by the sampling routines. Also, alternative prey such as ciliates may have been present in the pond but not detected in the sampling. Alternatively, the encounter rate with small prey is severely underestimated in the model, but it is difficult, then, to point out exactly which element of the feeding model is biased. Rotifers could also be detected at larger distance and encountered more frequently than anticipated owing to their movement pattern.

After day 20, the simulated larvae are able to capture and digest larger copepodites, but the level of copepodites in the stomach is lower in simulations compared with observations. Abundance of copepodites in the pond could have been higher than sampling data reveal, or perhaps larvae in the pond actively select larger prey.

The foraging model is biased towards the prey with the highest encounter rate, given that the size of the prey is feasible to capture for the larva. Larvae in natural conditions are often size selective and favour larger prey (McLaren and Avendano 1995; Munk 1995, 1997) if food is plentiful. Here, the mechanistic model merely includes passive selection resulting from the physical and biological characteristics between the prey and the predator, some of which include functions of size.

An energy source for the larvae at the onset of exogenous feeding was phytoplankton. Dinoflagellates in combination with rotifers were observed by Theilacker and McMaster (1971) to provide anchovy larvae with enough energy to grow at a physiological optimal rate. Fossum and Ellertsen (1994) observed the dominance of phytoplankton in gut analysis of larval cod in Lofoten (Norway) for the first 2–3 days after the start of feeding. Folkvord et al. (1994) observed "green guts" in the stomach analysis, indicating active foraging on phytoplankton. This extra energy source could be vital for survival during the critical first days after hatching, as simulations with the observed zooplankton field were too low to provide the necessary amount of prey of the correct size range for the larvae to grow at a rate comparable with observations. It seems that the ability of larvae to utilize potential energy of, e.g., protozoans (von Herbing and Gallager 2000) and phytoplankton (Pedersen et al. 1989; van der Meeren 1993; Lough and Mountain 1996), in food-limited areas may be crucial for first-feeding cod larvae.

Simulated and observed growth rates differ considerably for the first 17 days (22 DPH). One obvious error concerning this comparison is that the IBM does not account for size-dependent mortality. It is probable that size-dependent mortality removed the smallest individuals in the pond, especially regarding the low prey availability. The overall mortal-

© 2007 NRC Canada

ity to metamorphosis (12 mm) was very low (60%), but most effective during the first 2 weeks of the experiment (Folkvord et al. 1994). From the starvation control experiment, Folkvord et al. (1994) found that 90% of the total mortality occurred between day 15 and day 20. Differences between model results and observations are partly explained by the combination of an extra energy source in phytoplankton and size-dependent mortality. After 22 DPH, there is a strong resemblance to the model and experimental data, suggesting that the model is capable of simulating larval growth, given the correct input data.

In conclusion, the use of IBMs as tools for bringing knowledge and processes at an individual level to the population level is becoming increasingly popular (Grimm and Railsback 2005). IBMs as a reliable laboratory can help us understand how population patterns emerge from individual traits, how physical characteristics affect behavior of pelagic fish, and possibly the impact of climatic variability on individuals and populations. It is also a way to bridge experimental studies with modelling to generate understanding of patterns at a larger scale. However, to obtain reliable patterns, we need to develop IBMs that have been tested and used with data from natural conditions. Our model does not provide results with a perfect fit to observations but provides some hypotheses on the interaction between processes and the relative importance of processes. It also identifies where the model fails, although it is difficult to point exactly to particular processes. Possibly, the sampling procedure could also be the reason for some of the discrepancies. We also realize that there are likely to be substantial differences between natural environments and the macrocosm used here. This type of systematic use of IBMs can also give feedback to future experimental work.

Even in a pond of only 5 m depth, the light, prey, and temperature gradients are strong, and this research has pinpointed how larval vertical behaviour influence realized growth rates. Modelling efforts today often strive to explain both large- and small-scale processes combined by using coupled IBMs and three-dimensional physical models. The type of behaviour that the larvae inhibit in these model setups colours the simulated larval drift, distribution, and growth, and it is therefore important to consider implementing sound vertical behavior, e.g., as a function of larval condition (stomach fullness, larval size) and light (Fiksen et al., in press). The failure to do so could severely influence model results and conclusions.

Acknowledgements

This work was financed by the Norwegian Research Council (project No. 155930/700) and is part of the ECOBE (NORWAY-GLOBEC) project. The authors thank J. Titelman for comments on early versions of the manuscript and K.A. Rose for help with the Latin Hypercube Sampling method.

References

Aksnes, D.L., and Giske, J. 1993. A theoretical-model of aquatic visual feeding. Ecol. Model. **67**: 233–250.

Aksnes, D.L., and Utne, A.C.W. 1997. A revised model of visual range in fish. Sarsia, **82**: 137–147.

Bartell, S.M., Breck, J.E., Gardner, R.H., and Brenkert, A.L. 1986. Individual parameter perturbation and error analysis of fish bioenergetics models. Can. J. Fish. Aquat. Sci. **43**: 160–168.

Beaugrand, G., Brander, K.M., Lindley, J.A., Souissi, S., and Reid, P.C. 2003. Plankton effect on cod recruitment in the North Sea. Nature (London), **426**: 661–664.

Blom, G., Otterå, H., Svåsand, T., Kristiansen, T.S., and Serigstad, B. 1991. The relationship between feeding conditions and production of cod fry (*Gadus morhua* L.) in a semi-enclosed marine ecosystem in western Norway, illustrated by use of a consumption model. ICES Mar. Sci. Symp. **192**: 176–189.

Caparroy, P., Thygesen, U.H., and Visser, A.W. 2000. Modelling the attack success of planktonic predators: patterns and mechanisms of prey size selectivity. J. Plankton Res. **22**: 1871–1900.

Cushing, D.H. 1990. Plankton production and year-class strength in fish populations — an update of the match/mismatch hypothesis. Adv. Mar. Biol. **26**: 249–293.

Fiksen, Ø., and Folkvord, A. 1999. Modelling growth and ingestion processes in herring *Clupea harengus* larvae. Mar. Ecol. Prog. Ser. **184**: 273–289.

Fiksen, Ø., and MacKenzie, B.R. 2002. Process-based models of feeding and prey selection in larval fish. Mar. Ecol. Prog. Ser. **243**: 151–164.

Fiksen, Ø., Utne, A.C.W., Aksnes, D.L., Eiane, K., Helvik, J.V., and Sundby, S. 1998. Modelling the influence of light, turbulence and ontogeny on ingestion rates in larval cod and herring. Fish. Oceanogr. **7**: 355–363.

Fiksen, Ø., Jørgensen, C., Kristiansen, T., Vikebø, F., and Huse, G. In press. Linking behavioural ecology and oceanography: larval behaviour determines growth, mortality, and dispersal. Mar. Ecol. Prog. Ser.

Finn, N., Rønnestad, I., van der Meeren, T., and Fyhn, H.J. 2002. Fuel and metabolic scaling during the early life stages of Atlantic cod *Gadus morhua*. Mar. Ecol. Prog. Ser. **243**: 217–234.

Folkvord, A. 2005. Comparison of size-at-age of larval Atlantic cod (*Gadus morhua*) from different populations based on size- and temperature-dependent growth models. Can. J. Fish. Aquat. Sci. **62**: 1037–1052.

Folkvord, A., Oiestad, V., and Kvenseth, P.G. 1994. Growth-patterns of 3 cohorts of Atlantic cod larvae (*Gadus morhua* L.) studied in a macrocosm. ICES J. Mar. Sci. **51**: 325–336.

Fossum, P., and Ellertsen, E. 1994. Gut content analysis of first-feeding cod larvae (*Gadus morhua* L.) sampled at Lofoten, Norway, 1979–1986. ICES Mar. Sci. Symp. **198**: 430–437.

Gardner, R.H., and O'Neill, R.V. 1981. A comparison of sensitivity analysis and error analysis based on a stream ecosystem model. Ecol. Model. **12**: 173–190.

Grimm, V., and Railsback, S.F. 2005. Individual based modeling and ecology. 1st ed. Princeton University Press, Princeton, N.J.

Grønkjær, P., and Wieland, K. 1997. Ontogenetic and environmental effects on vertical distribution of cod larvae in the Bornholm Basin, Baltic Sea. Mar. Ecol. Prog. Ser. **154**: 91–105.

Hinrichsen, H.-H., Möllmann, C., Voss, R., Köster, F.W., and Kornilovs, G. 2002. Biophysical modeling of larval Baltic cod (*Gadus morhua*) growth and survival. Can. J. Fish. Aquat. Sci. **59**: 1858–1873.

Holling, C.S. 1966. The functional response of invertebrate predators to prey density. Mem. Entomol. Soc. Can. **48**: 1–86.

Kiørboe, T. 1989. Growth in fish: are they particularly efficient? Rapp. P.-v. Réun. Cons. Int. Explor. Mer, **191**: 383–389.

Letcher, B.H., Rice, J.A., Crowder, L.B., and Rose, K.A. 1996. Variability in survival of larval fish: disentangling components

© 2007 NRC Canada

with a generalized individual-based model. Can. J. Fish. Aquat. Sci. **53**: 787–801.

Lough, R.G., and Mountain, D.G. 1996. Effect of small-scale turbulence on feeding rates of larval cod and haddock in stratified water on Georges Bank. Deep-Sea Res. Part II. Top. Stud. Oceanogr. **43**: 1745–1772.

Lough, R.G., and Potter, D.C. 1993. Vertical distribution patterns and diel migrations of larval and juvenile haddock *Melanogrammus aeglefinus* and Atlantic cod *Gadus morhua* on Georges Bank. Fish. Bull. **91**: 281–303.

Lough, R.G., Caldarone, E.M., Rotunno, T.K., Broughton, E.A., Burns, B.R., and Buckley, L.J. 1996. Vertical distribution of cod and haddock eggs and larvae, feeding and condition in stratified and mixed waters on southern Georges Bank, May 1992. Deep-Sea Res. Part II. Top. Stud. Oceanogr. **43**: 1875–1904.

Lough, R.G., Buckley, L.J., Werner, F.E., Quinlan, J.A., and Edwards, K.P. 2005. A general biophysical model of larval cod (*Gadus morhua*) growth applied to populations on Georges Bank. Fish. Oceanogr. **14**: 241–262.

MacKenzie, B.R., and Kiørboe, T. 1995. Encounter rates and swimming behavior of pause–travel and cruise larval fish predators in calm and turbulent laboratory environments. Limnol. Oceanogr. **40**: 1278–1289.

MacKenzie, B.R., and Kiørboe, T. 2000. Larval fish feeding and turbulence: a case for the downside. Limnol. Oceanogr. **45**: 1–10.

MacKenzie, B.R., and Leggett, W.C. 1993. Wind-based models for estimating the dissipation rates of turbulent energy in aquatic environments — empirical comparisons. Mar. Ecol. Prog. Ser. **94**: 207–216.

McLaren, I.A., and Avendano, P. 1995. Prey field and diet of larval cod on Western Bank, Scotian Shelf. Can. J. Fish. Aquat. Sci. **52**: 448–463.

Megrey, B., and Hinckley, S. 2001. Effect of turbulence on feeding of larval fish: a sensitivity analysis using an individual-based model. ICES J. Mar. Sci. **58**: 1015–1029.

Munk, P. 1995. Foraging behaviour of larval cod (*Gadus morhua*) influenced by prey density and hunger. Mar. Biol. **122**: 205–212.

Munk, P. 1997. Prey size spectra and prey availability of larval and small juvenile cod. J. Fish Biol. **51**(Suppl. A): 340–351.

Otterlei, E., Nyhammer, G., Folkvord, A., and Stefansson, S.O. 1999. Temperature- and size-dependent growth of larval and early juvenile Atlantic cod (*Gadus morhua*): a comparative study of Norwegian coastal cod and northeast Arctic cod. Can. J. Fish. Aquat. Sci. **56**: 2099–2111.

Pedersen, T., Eliassen, J.E., Eilertsen, H.C., Tande, K.S., and Olsen, R.E. 1989. Feeding, growth, lipid composition, and survival of larval cod (*Gadus morhua* L.) in relation to environmental conditions in an enclosure at 70° in northern Norway. Rapp. P.-v. Réun. Cons. Int. Explor. Mer, **191**: 409–420.

Rose, K.A. 1987. Sensitivity analysis in ecological simulation models. *In* Systems and control encyclopedia: theory, technology, applications. *Edited by* M.G. Singh. Oxford Press, Toronto, Ont. pp. 4230–4235.

Rose, K.A., Brenkert, A.L., Cook, R.B., and Gardner, R.H. 1991*a*. Systematic comparison of ILWAS, MAGIC, and ETD watershed acidification models 2. Monte Carlo analysis under regional variability. Water Resour. Res. **27**: 2591–2603.

Rose, K.A., Smith, E.P., Gardner, R.H., Brenkert, A.L., and Bartell, S.M. 1991*b*. Parameter sensitivities, Monte-Carlo filtering, and model forecasting under uncertainty. J. Forecasting, **10**: 117–133.

Sundby, S. 2000. Recruitment of Atlantic cod stocks in relation to temperature and advection of copepod populations. Sarsia, **85**: 277–298.

Sundby, S., Ellertsen, B., and Fossum, P. 1994. Encounter rates between first-feeding cod larvae and their prey during moderate to strong turbulent mixing. ICES Mar. Sci. Symp. **198**: 293–405.

Theilacker, G.H., and McMaster, M.F. 1971. Mass culture of the rotifer *Brachionus plicatilis* and its evaluation as a food for larval anchovies. Mar. Biol. **10**: 183–188.

van der Meeren, T. 1993. Feeding ecology, nutrition, and growth in young cod (*Gadus morhua* L.) larvae. Dr. Sci., University of Bergen, Bergen, Norway.

Vikebø, F., Sundby, S., Ådlandsvik, B., and Fiksen, Ø. 2005. The combined effect of transport and temperature on distribution and growth of larvae and pelagic juveniles of Arcto-Norwegian cod. ICES J. Mar. Sci. **62**: 1375–1386.

von Herbing, I.H., and Gallager, S.M. 2000. Foraging behavior in early Atlantic cod larvae (*Gadus morhua*) feeding on a protozoan (*Balanion* sp.) and a copepod nauplius (*Pseudodiaptomus* sp.). Mar. Biol. **136**: 591–602.

Werner, F.E., Page, F.H., Lynch, D.R., Loder, J.W., Lough, R.G., Perry, R.I., Greenberg, D.A., and Sinclair, M.M. 1993. Influences of mean advection and simple behavior on the distribution of cod and haddock early life stages on Georges Bank. Fish. Oceanogr. **2**: 43–64.

Werner, F.E., MacKenzie, B.R., Perry, R.I., Lough, R.G., Naimie, C.E., Blanton, B.O., and Quinlan, J.A. 2001. Larval trophodynamics, turbulence, and drift on Georges Bank: a sensitivity analysis of cod and haddock. Sci. Mar. **65**: 99–115.

© 2007 NRC Canada

Unsupervised Bayesian reconstruction of individual life histories from otolith signatures: case study of Sr:Ca transects of European eel (*Anguilla anguilla*) otoliths

Ronan Fablet, Françoise Daverat, and Hélène De Pontual

Abstract: The reconstruction of individual life histories from chemical otolith measures is stated as an unsupervised signal-processing issue embedded in a Bayesian framework. This computational methodology was applied to a set of 192 European eel (*Anguilla anguilla*) otoliths. It provided a robust and unsupervised analysis of the individual chronologies of habitat use (either river, estuary, or coastal) from Sr:Ca measures acquired along an otolith growth axis. Links between Sr:Ca values and habitat, age, and season and the likelihood of the transitions from one habitat type to another were modelled. Major movement characteristics such as age at transition between habitats and time spent in each habitat were estimated. As a straightforward output, an unsupervised classification of habitat use patterns showed great variability. Using a hidden Markov model, 37 patterns of habitat use were found, with 20 different patterns accounting for 90% of the sample. In accordance with literature, residence behaviour was observed (28% of the eels). However, about 72% changed habitat once or several times, mainly before age 4. The potential application of this method to any other measures taken along an otolith growth axis to reconstruct individual chronologies gives a new insight in life history tactics analysis.

Résumé : Nous considérons ici la reconstitution des histoires de vies d'après des mesures chimiques d'otolithes comme un problème de traitement d'un signal non supervisé dans un cadre bayésien. Cette méthode numérique a été appliquée à un jeu de 192 données d'otolithes d'anguilles (*Anguilla anguilla*). Une analyse robuste et non supervisée des chronologies d'utilisation des habitats (soit de rivière, d'estuaire ou de milieu côtier) a été obtenue à partir des mesures Sr:Ca acquises le long d'un axe de croissance de l'otolithe. Les liens entre les valeurs Sr:Ca, les habitats, l'âge, la saison et les probabilités de transition d'un habitat à un autre ont été modélisés. Des caractéristiques importantes, telles que l'âge à la transition entre habitats et le temps passé dans un habita, ont été estimées. En résultat immédiat, une classification non supervisée des patrons d'utilisation d'habitat montre une grande variabilité. En utilisant un modèle de Markov caché, 37 patrons d'utilisation d'habitat ont été trouvés 20 représentant 90 % de l'échantillon. En accord avec la littérature, un comportement résident a été observé chez 28 % des anguilles. Cependant, 72 % des anguilles ont changé d'habitat une ou plusieurs fois, surtout avant l'âge de 4 ans. L'application potentielle de cette méthode à d'autres types de mesure prises sur un axe de croissance d'un otolithe pour reconstituer des chronologies individuelles ouvre une perspective nouvelle pour l'analyse des tactiques d'histoire de vie.

Introduction

The recent bloom of ecology studies using otolith microchemistry emphasises the remarkable potential of the otolith for investigating fish life history traits. The use of otolith chemistry to trace migration pathways is premised on a significant correlation between the elemental composition of otoliths and physicochemical properties of the ambient environment (Thorrold et al. 1997; Campana 1999; Martin and Thorrold 2005). Hence, sequential elemental measures acquired along an otolith growth axis are thought to record environmental information along the fish life span (Elsdon and Gillanders 2003). River basin origin are inferred from strontium isotope ratios (Thorrold and Shuttleworth 2000; Milton and Chenery 2003), whereas salinity level has been inferred from strontium to calcium ratios (Sr:Ca) (Tzeng et al. 1994). With more than 200 research articles published, Sr:Ca is the most popular microchemistry application to fish ecology, where it is used as a tool to track movements across water masses of different salinities for at least 20 fish species. To date, more than 28 published studies rely on the analysis of Sr:Ca for the characterization of life histories of

Received 9 January 2006. Accepted 12 August 2006. Published on the NRC Research Press Web site at http://cjfas.nrc.ca on 30 January 2007.
J19093

R. Fablet[1] **and H. De Pontual.** Ifremer/LASAA, BP 70, 29280 Plouzane, France.
F. Daverat. Cemagref, 50 Avenue de Verdun, 33612 Cestas, France.

[1]Corresponding author (e-mail: rfablet@ifremer.fr).

 doi:10.1139/F06-173 © 2007 NRC Canada

eel species (*Anguilla* spp.). Data acquisition of otolith chemistry remains technically demanding, time consuming, and costly. Hence, the challenge has first been a matter of data acquisition rather than a matter of data interpretation. So far, the interpretation of transects of otolith chemical signatures generally relies on a visual evaluation of each signal. Whenever formalised, the treatment of sequential Sr:Ca measures of eel otoliths data consists of the calculation of the mean values for each individual eel (Tsukamoto and Arai 2001; Tzeng et al. 2002). For instance, Tzeng et al. (2002) classified eel life histories from the number of years assigned to a specific water mass according to the mean value of Sr:Ca measures. This is questionable, as each Sr:Ca otolith measure is a specific indicator of a water mass, so that the mean of two different water masses has no ecological meaning. Also, the temporal dimension of the data is lost. In other studies, individual Sr:Ca values, plotted against age-class graphs, are assigned to a water mass according to their level (Morrison et al. 2003). Because of the nonlinearity of the otolith growth pattern, this is not satisfactory either; the otolith growth pattern during the first years of the fish's life has a finer spatial resolution than that of the last years. As a consequence, evenly spaced Sr:Ca transects result in an inequal number of measurements for each year of the fish's life. In addition, the classification of individual migratory behaviours relied on a priori classes, which may not account for the actual diversity observed in the processed data set (Tzeng et al. 2002; Daverat and Tomas 2006). For instance, in Daverat and Tomas (2006), the visual interpretation of Sr:Ca signals is carried out to classify 270 eels according to six a priori categories of movement patterns. Although time consuming, such a scheme also appears rather subjective.

This overview of previous work emphasizes the need for an unsupervised and well-founded computational method dedicated to the analysis of otolith signatures in terms of environmental information (here the habitat visited by the fish). Such a contribution is expected to account for the temporal nature of the signatures sampled along otolith transects. It is also intended to provide robust and objective (as opposed to expert subjectivity) tools to perform a quantitative analysis of statistically meaningful data sets (typically, several hundred samples). These issues can be regarded as inverse problems within the scope of signal processing. Multidisciplinary studies have already applied signal-processing techniques to process fish otolith data for ageing purposes (Troadec et al. 2000; Fablet 2006) or other issues such as stock discrimination (Campana and Casselman 1993) or fish individual status (Cardinale et al. 2004). From a signal-processing perspective, each Sr:Ca measure is associated with a hidden state variable standing for an environmental parameter (in our case, a habitat type), and the temporal nature of the sequence of Sr:Ca measures can be restored from the otolith growth pattern. Formally, the reconstruction of the individual patterns of habitat use is stated as the Bayesian reconstruction of the temporal sequence of the hidden state variables given the observed sequence of Sr:Ca signatures. The proposed scheme mainly relies on Gaussian mixture models (GMM) and hidden Markov models (HMM). All these developments are implemented under Matlab 7 using Netlab (Nabney 2001) and CRF (Murphy 2004) toolboxes. This method is applied to the analysis of individual habitat use histories for a data set of 192 eel otolith Sr:Ca transects. The generalisation of such a method for the treatment of sequential measures acquired along an otolith growth axis is further discussed.

Materials and methods

Data sets

An eel ecology study (Daverat et al. 2005) led to the acquisition of 192 individual eel Sr:Ca series. The fish samples were collected in the Gironde River basin (southwest France) in three main habitats (water masses). Sixty-three (33%), 115 (60%), and 14 (7%) eels were collected in freshwater, estuary, and coastal habitats, respectively.

The aim of this study is to characterize the habitat use patterns of eels from the Gironde River basin during their continental growing phase as a yellow eel. Sr:Ca transects are used to track the eel movements across freshwater, brackish, and marine habitats. Hence, only the part of the otolith corresponding to the continental life of the eel is retained (from glass eel mark to the edge). The acquisition method is described in Daverat et al. (2005) and consists of electron microprobe measures of Sr and Ca concentrations in 8 µm diameter spots evenly spaced every 20 µm along the longest growth axis of the otolith from the glass eel mark to the edge. Along this transect of Sr:Ca measures, the position of each annual age mark is recorded as a distance from the glass eel mark.

Calibration over time of Sr:Ca series

The interpretation of the macrostructures, so-called "rings", laid annually (Berg 1985) and observed on the otoliths along the longest growth axis, provides an estimation of individual growth patterns. The elver mark is set as the origin of the time axis. Only the interval between the elver mark and the edge is taken into account, as the ecological issue is the continental habitat use pattern of the eel after the glass eel stage until the time of capture. Annual rings are used as time references to map Sr:Ca series acquired with respect to the distance to the elver mark to time series using a linear interpolation. The time series are interpolated at a monthly precision (i.e., a time sampling rate of 1/12). In the following, we will refer to this time axis as the age axis, as it refers to the time spent from the elver mark.

The actual temporal resolution of the Sr:Ca series depends on both the sampling resolution of the electron microprobe and, of course, the otolith growth rate. In a previous experiment (Daverat et al. 2005), a mean otolith growth rate of 20 µm·month^{-1} was found for young individuals, so that about 12 Sr:Ca measures are usually sampled for the earlier growth years, whereas from the year 6 onward, fewer measures (down to three or four) may be available because of slower growth. Therefore, the results issued from the analysis of interpolated Sr:Ca time series need to be cautiously analyzed in terms of temporal precision, especially for the last years of life of the older individuals.

Eels have a strong territorial behaviour, as stressed by tagging–recapture and telemetry experiments (Helfman and Bozeman 1983; Aoyama and Sasai 2002). Therefore, because of the temporal resolution associated with otolith

© 2007 NRC Canada

Sr:Ca signatures permits investigating eel movements within the Gironde watershed at a relevant time scale.

Determination of the habitat-related Sr:Ca model

Following Daverat et al. (2005), Sr:Ca measures are regarded as proxies for habitat type for eels of the Gironde River watershed. Three habitat categories are considered according to salinity: river, estuarine, and marine. We do not aim to reconstruct the salinity from the Sr:Ca measure but rather discriminate habitat types The variations of Sr:Ca measures due to interhabitat characteristics, including salinity, are much greater than those due to intrahabitat characteristics (e.g., spatiotemporal variations of the salinity within a given habitat type) or interindividual variability (e.g., individual growth rate) as validated by the ex situ experiment conducted in Daverat et al. (2005) for eels from the Gironde River watershed.

We further model the distribution of Sr:Ca signatures for each habitat type as a Gaussian distribution parameterized by a mean model and a standard deviation. Different models could be chosen. In this study, two different cases are investigated. The first one is a constant model parameterized by a mean value. To test for the influence of seasonality and age on the incorporation of strontium, a linear model with two explanatory variables is also considered. Formally, let us denote by $g(\cdot|\Theta_H,\sigma_H)$ the Gaussian distribution of Sr:Ca measures for habitat type H, parameterized by the mean model Θ_H and the standard deviation σ_H. Using a constant model $\Theta_H = m_H$, $g(\cdot|m_H,\sigma_H)$ is computed for a Sr:Ca measure y as

$$g(y|m_H,\sigma_H) = \frac{1}{\sqrt{2\pi\sigma_H^2}} \exp\left(-\frac{(y-m_H)^2}{2\sigma_H^2}\right)$$

Considering a linear model, model Θ_H is parameterized by the mean value m_H, the effects of age λ_A and season λ_S. For a Sr:Ca measure y at age a and hydrological season s (normalized average monthly flow), the associated likelihood $g(y|a,s,\Theta_H,\sigma_H)$ for habitat type H is given by

$$g(y|a,s,\Theta_H,\sigma_H) = \frac{1}{\sqrt{2\pi\sigma_H^2}} \times \exp\left(-\frac{(y-m_H-\lambda_A a-\lambda_S s)^2}{2\sigma_H^2}\right)$$

The constant model is a particular case of the linear model with $\lambda_A = \lambda_S = 0$; hence, in the rest of this paper, we will only detail the developments for the latter.

The first step consists of determining the associated model parameters (Θ_H,σ_H) for each habitat type H. One should note that no labelled data are available to perform this estimation, only a mixed set of Sr:Ca measures $\{y_t\}$ associated with unknown habitat types (within the three considered). The estimation of the parameters of the habitat models $\{\pi_H, \Theta_H,\sigma_H\}_{H\in\{R,E,M\}}$ is then an unsupervised issue and can be solved for using a mixture model (Bishop 1995). (Unsupervised problems are defined as having no labelled data available, whereas in supervised problems, labelled data are provided, i.e., in our case, Sr:Ca data for which the assignment to an habitat type would be known.) For the latter, model parameter estimation directly resorts to model fitting for the independent subsets of data formed by the labelled data associated with each class. In contrast, the unsupervised estimation of model parameters requires analyzing the considered set of unlabelled data as a whole (Bishop 1995).

To this end, given the Sr:Ca measures $\{y_t\}$ relative to explanatory variables $\{a_t,s_t\}$, the whole distribution of $\{y_t\}$ is modelled as a GMM issued from the superimposition of the three Gaussian habitat models:

$$p(y_t|a_t,s_t,\{\pi_H,\Theta_H,\sigma_H\}_{H\in\{R,E,M\}}) = \sum_{H\in\{R,E,M\}} \pi_H\, g(y_t|a_t,s_t,\Theta_H,\sigma_H)$$

where R, E, and M represent the labels relative to the three habitat types river, estuarine, and marine, respectively. π_R, π_E, and π_M are the prior probabilities or mixing proportions of the three habitat types. Given a set of unlabelled data $\{y_t\}$ and the associated explanatory variables $\{a_t,s_t\}$, we aim to estimate the parameters of the mixture model $\{\pi_H,\Theta_H,\sigma_H\}_{H\in\{R,E,M\}}$ such that $p(y|a,s,\{\pi_H,\Theta_H,\sigma_H\}_{H\in\{R,E,M\}})$ best fits the distribution of the data set $\{y_t\}$ according to the maximum likelihood (ML) (Bishop 1995). This model estimation is carried out using the expectation maximization (EM) algorithm (Bishop 1995). The computations involved in this iterative procedure are detailed in Appendix A.

The estimated mixture parameters are assigned to each habitat type by sorting the mean values of the Gaussian modes. We rely on the statement that the lower the salinity of the habitat, the lower the mean Sr:Ca measure (Fig. 1).

The goodness of the fits of the constant and the linear models for each mode is compared with Akaike's information criterion (AIC) method (Awad 1996), and the influence of age and season on the Sr:Ca signature is tested according to correlation statistics between the model prediction and the data (McCullagh and Nelder 1989). The comparison of the contributions of each group of predictors permits us to evaluate the relative importance of habitat, season, and age (Silber et al. 1995). These statistical tests are performed with R software (R Development Core Team 2005).

Estimation of individual habitat use from Sr:Ca series

Our goal is to analyze the individual patterns of habitat use from the series of Sr:Ca measures as illustrated (Fig. 2). This issue is stated as the estimation of the temporal sequence of habitat types (x_t) corresponding to a given observed series of Sr:Ca measures (y_t), where x_t is a label R, E, or M, for each time t.

Formally, this labelling issue is embedded within a Bayesian framework. The term labelling comes from the signal-processing terminology (Rabiner 1989). It refers to the process of determining the sequence of labels (in our case, the sequence of habitat types) associated with a given sequence of observations (in our case, the Sr:Ca signatures). More precisely, it is regarded as the search for the best sequence $(\hat{x}_0,\ldots,\hat{x}_T)$, according to the maximum a posteriori (MAP) criterion (Rabiner 1989), over all possible habitat sequences. The MAP criterion maximizes the posterior likelihood of the habitat sequence (x_t) given an observed series of Sr:Ca measures (y_t), i.e.,

$$(1) \qquad (\hat{x}_0,\ldots,\hat{x}_T) = \arg \max_{(x_0,\ldots,x_T)} p(x_0,\ldots,x_T|y_0,\ldots,y_T)$$

© 2007 NRC Canada

Fig. 1. Distribution of Sr:Ca values (solid line) and the three modes (dashed line, dotted line, bold solid line) of the fitted Gaussian mixture model.

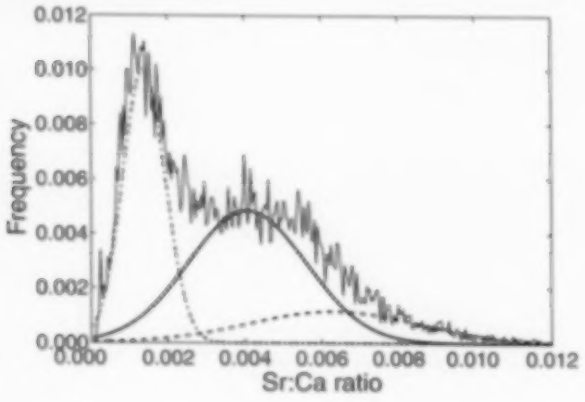

Within a Bayesian framework, posterior likelihood $p(x_0,\ldots,x_T|y_0,\ldots,y_T)$ is rewritten according to Bayes's rule (Bishop 1995) and, solving for eq. 1, is equivalent to

$$(\hat{x}_0,\ldots,\hat{x}_T) = \arg \max_{(x_0,\ldots,x_T)} p(y_0,\ldots,y_T|x_0,\ldots,x_T) \times p(x_0,\ldots,x_T)$$

where $p(y_0,\ldots,y_T|x_0,\ldots,x_T)$ is generally referred to as the data-driven term, which evaluates the likelihood of a sequence of observations given a sequence of labels, and $p(x_0,\ldots,x_T)$ is the prior specifying some a priori knowledge on the characteristics of the sequence of labels. One might note here that the proposed Bayesian method defines a prior (or hyperprior) on the temporal dynamics of the hidden variables (i.e., in our case, habitat type variables) and noton the distribution of the parameters of the observation models (in our case, the habitat-related Sr:Ca models). Though not considered here, the combination of both types of priors could be investigated.

We first specify the data-driven term $p(y_0,\ldots,y_T|x_0,\ldots,x_T)$. As Sr:Ca measures ($y_t$) primarily depend on state variables (x_t), it can be assumed that y_t are conditionally independent of x_t. Hence, data-driven likelihood $p(y_0,\ldots,y_T|x_0,\ldots,x_T)$ is factorized as the product of likelihoods $\prod_t p(y_t|x_t)$. Likelihood $p(y_t|x_t)$ specifies the distribution of the Sr:Ca measures for each habitat type. This information is conveyed by the estimated GMM $\{\pi_H,\Theta_H,\sigma_H\}_{H\in\{\text{R.E.M}\}}$ and $p(y_t|x_t)$ is given by $g(y_t|a_t, s_t, \Theta_{x_t}, \sigma_{x_t})$.

As far as prior $p(x_0,\ldots,x_T)$ is concerned, two solutions are investigated. First, assuming that state variables (x_t) are statistically independent, eq. 1 reduces for each time t to

$$(2)\qquad \hat{x}_t = \arg \max_{H\in\{\text{R.E.M}\}} p(y_t|x_t = H)p(x_t = H)$$

The prior term reduces to the a priori likelihood of each habitat type and is specified by the mixing proportions $\{\pi_H\}_{H\in\{\text{R.E.M}\}}$ of the estimated GMM. Equation 2 then becomes

$$\hat{x}_t = \arg \max_{H\in\{\text{R.E.M}\}} \pi_H g(y_t|a_t, s_t, \Theta_{H_t}, \sigma_{H_t})$$

Given that this likelihood only depends on the Sr:Ca signature and model parameters $\{\pi_H,\Theta_H,\sigma_H\}_{H\in\{\text{R.E.M}\}}$, this labelling equation can be interpreted as a threshold-based procedure for which Sr:Ca – habitat equations, derived from model parameters $\{\pi_H,\Theta_H,\sigma_H\}_{H\in\{\text{R.E.M}\}}$, take into account the mean Sr:Ca model, the associated standard deviation, and the mixing proportion of each habitat type. Whereas Sr:Ca – habitat equations exploited in previous work (Elsdon and Gillanders 2003) are generally set a priori, the GMM is a method for determining such equations from an unlabelled data set.

This first model is rather simplistic, however, and does not explicitly model fish movements among habitat types. To account for these temporal dynamics, first-order Gaussian HMMs (Rabiner 1989) are used. These models were initially developed and exploited for speech analysis. As illustrated (Fig. 3), they rely on the actual modelling of the temporal dynamics of the state variables (x_t) using a first-order Markov chain. Given the sequence of state variables $(x_0, x_1,\ldots, x_{t-1})$ from time 0 to time $t-1$, a first-order Markov chain is such that state variable x_t at time t only depends on x_{t-1}. In other words, this model only keeps the memory of its last state to jump to the next one. Formally, this leads to the property that $p(x_t|x_{t-1},\ldots, x_1, x_0) = p(x_t|x_{t-1})$ and implies that the first-order Markov chain is fully characterized by its transition matrix Γ: $p(x_t = H_1|x_{t-1} = H_2) = \Gamma(H_1,H_2)$. This transition matrix specifies the likelihood that the fish switches to habitat type H_1 at time t given that it is in habitat type H_2 at time $t-1$. By definition, the sum over each column of Γ equals one. A graphical representation of the transition matrix is provided (Fig. 3). Let us stress that some transitions may be forbidden, that is, pairs of habitats for which $\Gamma(H_1,H_2) = 0$ (for instance, the transition from A to C in Fig. 3*b*). However, this does not prevent reaching one state from another by going through other states, if there is a sequence involving several transitions with a non-null likelihood. As illustrated for an abstract example (Fig. 4), although direct transitions from A to C are impossible, paths from A to C going through B are possible. Such features are expected in our case, as it seems unrealistic that fish can switch directly from the river to the marine area without going through the estuarine area.

As far as computational aspects are concerned, we first need to specify the parameters of the Markovian prior (i.e., transition matrix Γ). Here, no prior knowledge is available to set a priori these parameter values. They are estimated from the considered data set according to the ML criterion. This comes to search for transition matrix $\hat{\Gamma}$ associated with the maximum likelihood for the whole set of samples

$$\hat{\Gamma} = \arg \max_{\Gamma} \prod_i p(y_0^i,\ldots,y_T^i|\Gamma)$$

This maximization issue is solved for using the expectation–maximization algorithm. We let the reader refer to Rabiner (1989) for a detailed description of this estimation procedure and only review its main characteristics here. The following two steps are iterated until convergence. Given the current estimate Γ^q of the transition matrix, the expectation step computes the posterior likelihoods:

$$\xi^i_{H_1,H_2}(t) = p(x_t^i = H_2, x_{t-1}^i = H_1|y_0^i,\ldots,y_T^i,\Gamma^q)$$

$$\gamma^i_{H_1}(t) = p(x_t^i = H_1|y_0^i,\ldots,y_T^i,\Gamma^q)$$

© 2007 NRC Canada

Fig. 2. Principle of the reconstruction of the time habitat sequence from the acquired Sr:Ca measures spatially sampled along a growth axis of the otolith: it relies on the assumption that the habitat type influences the chemical composition of the otolith such that the individual temporal sequence of habitat types can be reconstructed from otolith chemical signatures sampled along a reference growth axis.

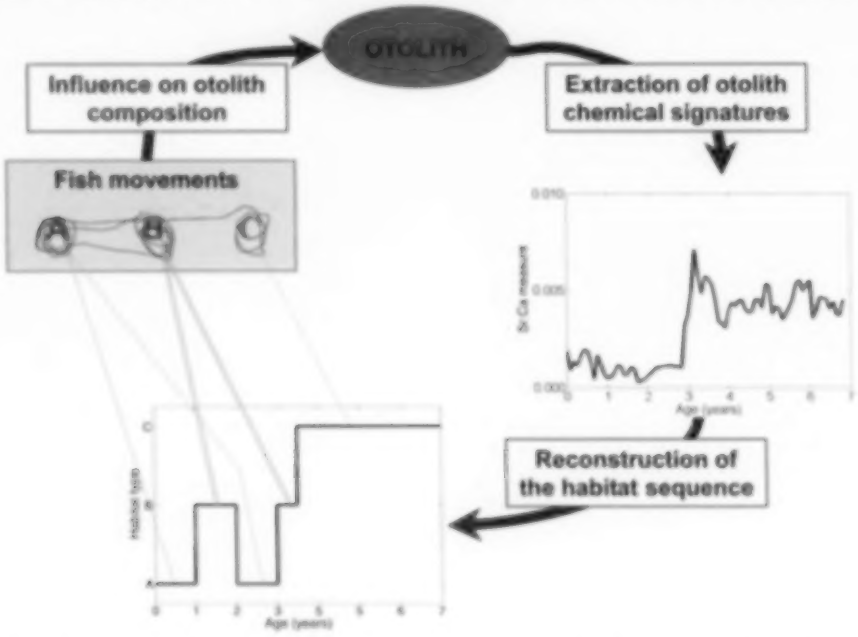

The maximization step updates the transition matrix Γ^{q+1} from these posterior likelihoods as their average over the whole data set:

$$\Gamma(H_1, H_2) = \frac{\sum_{i=1}^{N}\sum_{t=0}^{T}\xi_{H_1,H_2}(t)}{\sum_{i=1}^{N}\sum_{t=0}^{T}\gamma_{H_1}(t)}$$

One might stress that the analysis of the estimated transition matrix provides the mean for evaluating the relevance of the HMM, compared with the GMM, for the considered data set. As the latter reduces the temporal prior $p(x_t|x_{t-1})$ to a static prior $p(x_t)$, it can be viewed as a constrained HMM for which the transition matrix verifies $\Gamma(H_1,H_2) = \Gamma(H_1)$. For a given data set, the estimated transition matrix Γ of the HMM can then be compared with the transition matrix Γ' associated with the GMM (i.e., $\Gamma(H_1,H_2) = \pi_{H_2}$), and it can be determined whether or not it is worth considering the generic HMM rather than the GMM.

Given the estimated HMM parameters, the reconstruction of the optimal habitat sequence $(\hat{x}_0,\ldots,\hat{x}_T)$ according to the MAP criterion comes to solve for

$$(\hat{x}_0,\ldots,\hat{x}_T) = \arg\max_{(x_0,\ldots,x_T)} \prod_{t=0}^{T} p(y_t|x_t) \times \prod_{t=1}^{T} p(x_t|x_{t-1})p(x_0)$$

This maximization can not be solved for analytically. However, the Viterbi algorithm (Rabiner 1989) guarantees to retrieve the best state sequence using an efficient forward–backward procedure. We let the reader refer to Rabiner (1989) for a complete description of the Viterbi algorithm andonly review its main steps here, which involve computations similar to the forward procedure of the EM scheme described above for the estimation of the transition matrix. More precisely, it first computes recursively (from time 0 to time T) for any habitat type H the likelihood, denoted by $\delta_H(t)$, of the most likely habitat sequence leading to habitat H at time t:

$$\delta_H(t) = \max_{(x_0,\ldots,x_{t-1})} p(y_0,\ldots,y_t,x_0,\ldots,x_{t-1},x_t = H|\Phi,\Gamma)$$

At the last step of the forward procedure (i.e., at time T), the habitat label maximizing $\delta_H(T)$ provides the optimal habitat type $\hat{x}_T$. A backward procedure then reconstructs recursively the optimal habitat sequence $(\hat{x}_0,\ldots,\hat{x}_T)$ by retrieving the state H_1 at time $t-1$, which leads to the reconstructed state $\hat{x}_t$ at time t with the maximum likelihood. Contrary to the GMM, this labelling procedure cannot be interpreted as a thresholding technique based on Sr:Ca – habitat equations. The observed sequence of Sr:Ca signatures is interpreted as a whole, not as a sequence of independent variables. Depending on temporal context, similar Sr:Ca values might then be assigned to different habitat types; meanwhile the reconstructed habitat sequence is guaranteed to be the most likely given the observed Sr:Ca sequence.

Analysis of habitat sequences

Given the set of the individual habitat sequences, a quantitative analysis of fish movements is carried out. More precisely, the movement pattern is defined as the sequence of the successive habitats visited by the fish. This sequence

© 2007 NRC Canada

Fig. 3. Graphical representation of the hidden Markov model (HMM). (*a*) Graphical representation of the conditional dependencies involved in the HMM. The horizontal arrows indicate the conditional dependencies $x_t|x_{t-1}$ modeling the temporal dynamics of the hidden state, and the vertical arrows indicate the conditional dependencies $y_t|x_t$ modeling the likelihood of measure y_t given state x_t. This graphical representation emphasizes that observations (y_t) are independent conditionally to hidden states (x_t), and that x_t is assumed independent on $(x_0,\ldots,x_{t-2})$ given x_{t-1}. (*b*) Illustration of the characteristics of the transition matrix that specifies the temporal dynamics of the state variable for a HMM with four hidden states A, B, C, and D. The transition matrix specifying the likelihoods $p(x_t|x_{t-1})$ is graphically represented as arrows linking two states with an associated likelihood. For instance, the transition from A to B, associated with likelihood $p(x_t = B|x_{t-1} = A)$ set to 0.3, is visualized by the arrow from A to B. Note that the likelihood to leave one state, i.e., the sum of all the likelihoods of the transitions issued from one state, is one. Some transitions may be forbidden, i.e., associated with a null probability, for instance, transitions from B to A. A particular case of transitions is the one corresponding to staying in the current state (for instance, transitions A to A or C to C).

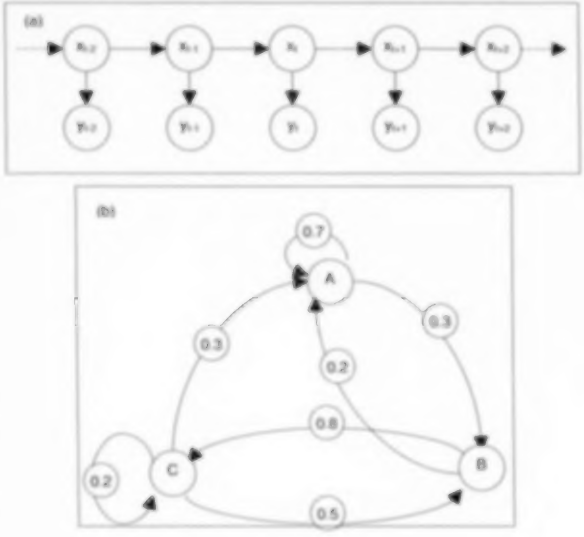

takes into account both the quality and the order of the visited habitats, for instance, the movement pattern issued from habitat sequence RRRREEEERRRRR is RER. For a given otolith set, the set of all of the associated movement patterns can be determined, as well as the corresponding relative frequencies. This procedure then leads to an automated categorization of the observed movement patterns. Contrary to previous work relying on the definition of a priori movement patterns (typically, resident behaviour, as well as migrations from one habitat type to another) (Secor 1999; Daverat and Tomas 2006), this procedure delivers an unsupervised classification of the individual movement patterns and permits investigation of the actual variability of the individual fish behaviours with a finer characterization and not ignoring unexpected behaviours. An analysis based on macrocategories, resulting from the grouping of certain movement patterns (for instance, those involving one or several movements between two habitat types), can also be used to deliver a more synthetic view of the relative occurrences of the different categories of movement patterns.

Fig. 4. Comparison of the habitat sequence reconstructed using the Gaussian mixture model (GMM) and the hidden Markov model (HMM) for a given Sr:Ca series: (*a*) GMM-based reconstruction, (*b*) HMM-based reconstruction. In each plot, the Sr:Ca signal (solid line) and the estimated habitat sequence (broken line) are reported as a function of fish age (in years).

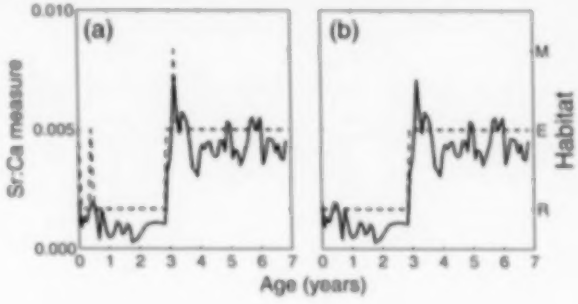

Because the habitat sequences are calibrated over time, a variety of measures can also be defined to characterize individual life traits. We focus on the analysis of the time at which the transitions from one habitat to another occurs and of the time spent in a given habitat between the two transitions. For a given type of transition from habitat type H_1 to habitat type H_2 (i.e., within the set of transitions {R to E, R to M, E to M, E to R, M to R, M to E}), the whole set of habitat sequences $\{(x_t^i)_{t\in\{0,\ldots,T_i\}}\}_{i\in\{1,\ldots,N\}}$ is analyzed to extract the set of all transitions from H_1 to H_2. These transitions are characterized by their transition times $\{t_{H_1H_2}^n\}$ and the times spent in H_2 $\{D_{H_1H_2}^n\}$. The statistical distributions of these quantities are then computed using a nonparametric technique, as they are clearly multimodal. More precisely, given a scale parameter μ and a set of quantities $\{w^n\}$, the likelihood $p(w)$ is computed as

$$p(w) = \frac{1}{Z}\sum_n \exp(-\mu(w - w^n)^2)$$

where Z is the normalization factor. The computation of the statistics of transition times $\{t_{H_1H_2}^n\}$ is performed in terms of age, month, and age group at which the transitions occur. Scale parameter μ is set to one for quantities given as monthly values and age groups and to $1/10^2$ for quantities given as ages.

Results

Comparison between constant and linear models

The linear model accounting for habitat, age, and season effects (AIC value of 45 167) outperforms the model only accounting for habitat effect (AIC value of 46 465). Habitat, age, and hydrological season (river flow) factors all have a significant influence on Sr:Ca values for each habitat ($p < 0.001$) (Table 1).

The comparison of the relative contribution of the habitat factor to the contribution of both age and season factors reveals that habitat contributes more to the variation of Sr:Ca values than age and season, with a ratio of effect standard

© 2007 NRC Canada

deviations of 4.58 (95% confidence interval (CI) 4.38–4.79) (Silber et al. 1995). Because the effect of age and season is significant in terms p statistics, we report the results of the analysis of the individual chronologies of habitat use with respect to the linear model.

Table 1. Analysis of variance (ANOVA) table for the linear model.

Factor	Likehood ratio χ^2	df	$Pr(>\chi^2)$
Habitat	43 744	2	$<2.2\times10^{-16}$
Season	31	1	2.397×10^{-8}
Age	1 984	15	$<2.2\times10^{-16}$

Individual chronologies of habitat use

A comparison of the habitat sequences issued from the GMM and the HMM is illustrated (Fig. 5). As the GMM does not account for time coherence, the associated habitat sequences are less smooth and involve numerous short transitions. As stressed above, the GMM can be regarded as a constrained HMM for which the transition matrix verifies $\Gamma(H_1,H_2) = \Gamma(H_1)$. The transition matrix of the GMM can not approximate the one estimated for the HMM (Table 2). The latter refers to the temporal dynamics $p(x_t|x_{t-1})$ observed over the whole eel data set. It stresses that the prior likelihood of leaving a given habitat type is clearly different for each habitat type. In all cases, the resident behaviour has the highest likelihood. Whereas the likelihoods of the transitions from the estuary to the river and the marine area are roughly in the same order of magnitude, direct transitions from the river to the marine area, and vice versa, are highly unlikely (about 10 times less likely than the transitions from the river and the marine area to the estuary).

The GMM can not handle these temporal dynamics and, hence, is then less relevant than the HMM for the considered data set. An important output of this result is that the observed very short transitions observed in the GMM-based habitat sequences are highly unlikely given the overall transition statistics over the whole data set. These elements lead us to consider the HMM method as the reference method to further characterize life traits from the estimated habitat sequences. Eels sampled in the Gironde River watershed display a wide repertoire of habitat use patterns, such as lifelong residences in the same habitat, as defined in the model (river, estuary, marine area) or as single or multiple shifts among habitats (Fig. 6). From these examples, it should be stressed that the considered model is not a simple thresholding technique. The temporal Sr:Ca signal is analyzed as a whole to determine the optimal MAP habitat sequence. Because the HMM labelling results from an optimal (according to the MAP criterion) trade-off between the temporal prior and the data-driven term, similar Sr:Ca values might be associated with different habitat types.

Analysis and classification of movement patterns

From the overall analysis of the reduced habitat sequences, the different classes of movement patterns associated with the considered data set are automatically determined. Given the temporal resolution associated with the spatial sampling of Sr:Ca signatures, movement patterns are analyzed up to age 6. Also, only fish older than 4 years are analyzed, which guarantees that movement patterns can actually be compared and relevantly characterized in terms of relative frequencies. Using the HMM, 37 patterns are represented (Fig. 6). Although only the first 20 patterns account for more than 80% of the samples, the first five patterns occur with a frequency greater than 5%. Among the first four patterns, three correspond to resident behaviour. The GMM-based approach leads to 88 different patterns, within which only the first five account for more than 3% of the samples. A more synthetic view of the diversity of the movement patterns according to 10 classes is also reported (Fig. 7). This classification results from the grouping of movement patterns involving one or several transitions between two habitat types. More precisely, 10 macrocategories are formed. They comprise three classes associated with the resident behaviour in the river (R), the estuary (E), and the marine area (M), four classes corresponding to one or several movements from the river to the estuary (ER), from the estuary to the river (RE), from the estuary to the marine area (EM), and from the marine area to the estuary (ME), and two classes (REM and MER) associated with movements from the river to the estuary (respectively, from the marine area to the estuary) followed by movements from the estuary to the marine area (respectively, from the estuary to the river). The last class refers to the remaining movement patterns, all of them involving a stay in each of the three habitat types. The comparison of the GMM- and HMM-based categorizations indicates that the main differences occur for the relative frequencies evaluated for the resident behaviours (10% vs 28%) and the class "others" (21% vs 3%), which is mainly due to the presence of very short transitions in the GMM-based sequences. In particular, the resident behaviour in the estuary is only assigned to 0.6% of the samples by the GMM. This does not seem consistent with the results retrieved for the two other resident behaviours (6.5% and 3.5% of the samples classified as residents in the river and the marine area, respectively) and previous work (Tsukamoto and Arai 2001; Daverat et al. 2004, 2005). For other macrocategories, especially those involving one or several movements between two habitat types, similar results are reported for the two methods. Movement patterns between two habitat types involve about 54% of the samples. Most of these movement patterns involve movements between the river and the estuary (38% for the GMM-based scheme and 35% for the HMM-based method), whereas patterns involving movements between the estuary and the marine area account for 16% and 18% of the samples, respectively.

Focusing on the HMM-based categorization, resident behaviours account for only 28% of the samples, and 72% of the movement patterns involve at least one movement. Residents in the marine habitat account for 6.5% of the sample, which is quite consistent with the 7% of fish collected in the marine area. Although 33% of the samples have been collected in the river, only 14.3% of the samples are labelled as residents in the river habitat. Similarly, the reported categorization leads to 7.8% of residents in the estuary area, whereas our sample is composed of 60% of fish collected in the estuary. For migration behaviours, patterns involving only one migration, as well as patterns involving several migrations between two types of habitats, are encountered, but only be-

© 2007 NRC Canada

Fig. 5. Examples of estimated habitat sequences for four individual eels using the hidden Markov model (HMM) based reconstruction: (*a*) example of residency in the river ; (*b*) example of residency in the estuary ; (*c*) example of residency in the marine area ; (*d*, *e*, *f*) examples of multiple movements between the river, the estuary, and (or) the marine area. In each subplot, the Sr:Ca signal (solid line) and the estimated habitat sequence (broken line) are reported as a function of fish age (in years).

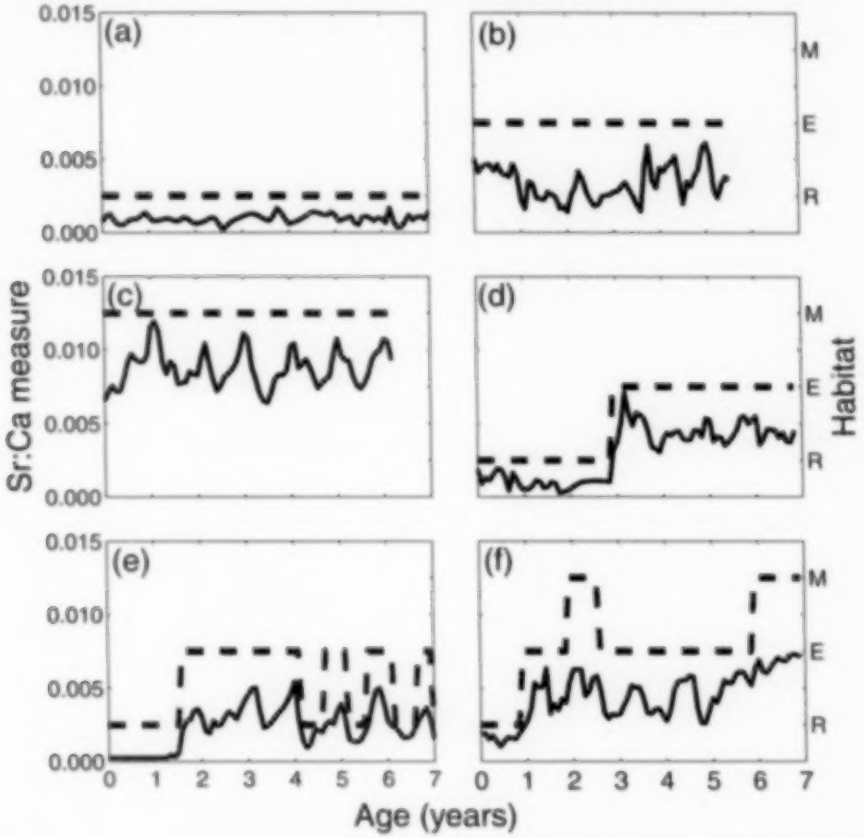

Table 2. Comparison of the transition statistics associated with the Gaussian mixture model (GMM) and the hidden Markov model (HMM).

Transitions from	Method	River	Estuary	Marine area
River	GMM	0.295	0.52	0.185
	HMM	0.903	0.096	0.001
Estuary	GMM	0.29	0.52	0.18
	HMM	0.063	0.905	0.032
Marine area	GMM	0.29	0.52	0.18
	HMM	0.009	0.274	0.717

Note: This table reports the values of the transition likelihood $p(x_t = H_i | x_{t-1} = H_j) = \Gamma(H_i, H_j)$ estimated for the considered data set. The GMM can be viewed as a constrained HMM such that $\Gamma(H_i, H_j) = \Gamma(H_i)$. The table should be read as follows: each row reports the transition likelihood from the associated habitat type.

tween the river and the estuary or the estuary and marine area. Noticeably, up to five successive migrations between the river and the estuary can be observed for the same individual before age 6. Fewer samples involve migrations among the three habitats. However, about 9% of the samples are associated with patterns including a first migration from the river to the estuary and then one or several movements between the estuary and the marine area. Conversely, very few individuals (below 2%) move from the marine area to the river after a stay in the estuary. Interestingly, the characteristics of the movement patterns seem to be different depending on the early phase of the habitat sequence. More precisely, 32% of the fish having an initial phase (according to the elver mark) in the river remain in the river, whereas 47% shift once or several times between the river and the estuary. The remaining 20% spend their last phase between the estuary and the marine area. For fish having an initial phase in the estuary, 23% remain in the estuary, 46% and 29% shift one or several times, respectively, to the river and to the marine area. Among all fish having an initial phase in the marine area, 29% remain in the marine area, 41% shift one or several times between the marine area and the estuary, and 28% move initially to the estuary (with possible returns to the marine area) and later to the river (with possible returns to the estuary).

Analysis of the transitions between habitats

As previously noted, only the first 6 years of life of the fish are considered for the rest of the analysis of the transi-

© 2007 NRC Canada

Fig. 6. Unsupervised analysis of the movement patterns: frequencies of the movement patterns extracted from the estimated habitat sequences using the hidden Markov model (HMM) framework. Each habitat sequence is represented by the sequence of the habitat types visited by the fish, e.g., a habitat sequence EEEEEERRRRRRRR would be represented by the movement pattern ER. The relative frequencies (%) of all the movement patterns present in the processed data set are reported in decreasing order.

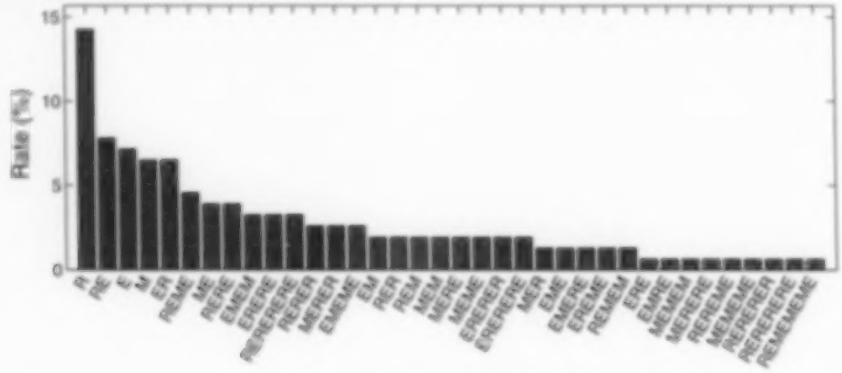
Rate (%)
15
10
5
0
R
RE
E
M
ER
REME
ME
RERE
EMEM
ERERERE

Fig. 7. Categorization of the movement patterns into 10 macrocategories (*a*) issued from the Gaussian mixture model (GMM) method and (*b*) issued from the hidden Markov model (HMM) method. The 10 macrocategories are as follows: three residency behaviours (in the river (R), estuary (E), and marine area (M)); four patterns (RE, ER, EM, and ME) corresponding to one or several movements between two areas; two patterns (REM and MER) involving one or several movements between two areas (i.e., movements from the river to the estuary (RE) or from the marine area to the estuary (ME)) followed by one or several movements between two other areas (i.e., movements from the estuary to the river (ER) or from the estuary to the marine area (EM)). The last class, denoted as "others", contains the remaining movement patterns, which all correspond to movement patterns between the three different areas. We depict the relative frequencies of the considered classes of movement patterns for the processed otolith data set.

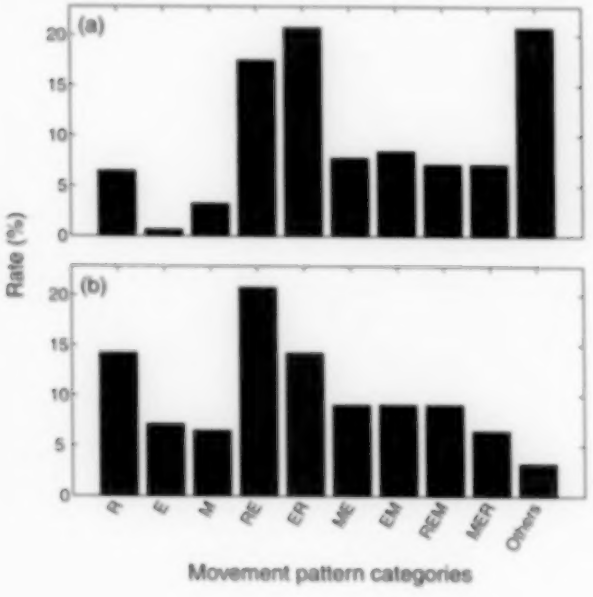

Gironde River watershed at different seasons has shown that slight seasonal fluctuations can be observed without affecting the discrimination of marine, estuarine, and riverine habitats. This is confirmed by the proposed unsupervised method. Growth rate is also known to have an effect on the Sr:Ca. In this study, only the yearly growth rates are available such that its relative effect can not be directly analyzed. Results reported in Daverat et al. (2005) for eels from the same area indicate that this effect is very weak compared with the strong relationship between habitat type and Sr:Ca value, a result validated for eels and other species using coupled experimental and field validations (Kraus and Secor 2004; Elsdon and Gillanders 2005). The effect of the growth rate on Sr:Ca might have led to misclassifications of very slow-growing eels as higher-salinity migrants (and vice versa). However, given the high salinity contrast among the three considered habitats, such situations should seldom occur.

Further applications of this model could take into account other types of effects, e.g., physiological parameters, feeding conditions, or temperature (Campana 1999; Campana et al. 2000). In addition, other kinds of parametric models (polynomial, log-normal, exponential, etc.) could also be straightforwardly used. Multiproxy approaches using multidimensional structural and (or) chemical otolith signatures may also be investigated within this framework with a view to retrieving a more precise estimation of the environments or the states experienced thought the fish's life. The combination of Sr:Ca with oxygen isotope ratios as a proxy of water temperature (Nelson et al. 1989) may, for instance, provide a more precise estimation of the temporal resolution of the measures in the example developed here.

Reconstruction of habitat use chronologies

The proposed method turned out to be particularly well adapted to the analysis of large data sets. The processed data set consists of 192 individual Sr:Ca series containing 70 points of Sr:Ca measures on average. Hence, a total of 14 649 Sr:Ca measures are analysed as 14 649 events representing a habitat use. Th proposed approach is computationally efficient, as only a few minutes are required to process the whole sample set, including both the estimation of the habitat Sr:Ca GMM and the reconstruction of all of the individual patterns of habitat use. Compared with previous work, the key feature of this quantitative framework is that a nonsubjective interpretation of individual Sr:Ca series in terms of habitat use is provided from an unsupervised analysis.

In the investigation of individual habitat use chronologies from chemical otolith signatures, the key assumption is that the temporal resolution associated with the sampling of these signatures on the otolith is a relevant scale for the analysis of fish movement. In our case, the sampled Sr:Ca measures lead to an approximately monthly resolution (for the first 6 years after the glass eel mark). Hence, movements at a finer submonthly scale can not be investigated. It should be stressed that this assumption underlies not only the present study, but also all previous work dedicated to the analysis of eel behaviour from otolith Sr:Ca. It is motivated by previous results (Helfman and Bozeman 1983; Aoyama and Sasai 2002; Cairns et al. 2004) showing that eels have a strong territorial behaviour. Exploiting the HMM framework, the estimated transition statistics indicate that short (i.e., 1 or 2 months) transitions from one habitat type to another are highly unlikely. Reconstructed habitat sequences then depict a strong temporal coherence. These results justify, from a statistical point of view, the choice of the HMM, as well as the assumption that eel movements among habitat types occur at a temporal resolution greater than 1 month, which can be analyzed from otolith chemical signatures.

The absence of known labelled data (i.e., fish for which at least partial habitat use chronologies would be known) prevents the performance of some direct validation of the proposed framework. It should be stressed that this issue is not specific to this work. It can also be noted for most previous work dedicated to the reconstruction of individual life traits from the analysis of otolith signatures (Elsdon and Gillanders 2003). Controlled experiments have been carried out to analyze and validate the combined effects of environment and ontogeny on chemical otolith features (Elsdon and Gillanders 2003; Daverat et al. 2005). Such experiments can be used to calibrate Sr:Ca – habitat equations. These equa-

© 2007 NRC Canada

Fig. 8. Analysis of transition features for the processed otolith data set: (*a*–*b*) relative frequencies (in log scale) of the instantaneous transitions from the estuarine state to one of the three states (namely, riverine (dotted lines), estuarine (solid lines), marine (broken lines)) as a function of (*a*) age or (*b*) season; (*c*) distribution of ages at transition from the river (R) to the estuary (E); (*d*) distribution of the duration of the stay in the riverine (R) state prior to the transition to the estuary (E); (*e*) distribution of ages at transition from the estuary (E) to the river (R; solid line) and the marine area (M; broken line); (*f*) distribution of the duration of the stay in the estuarine (E) state prior to the transition to the river (R; solid line) and the marine area (M; broken line).

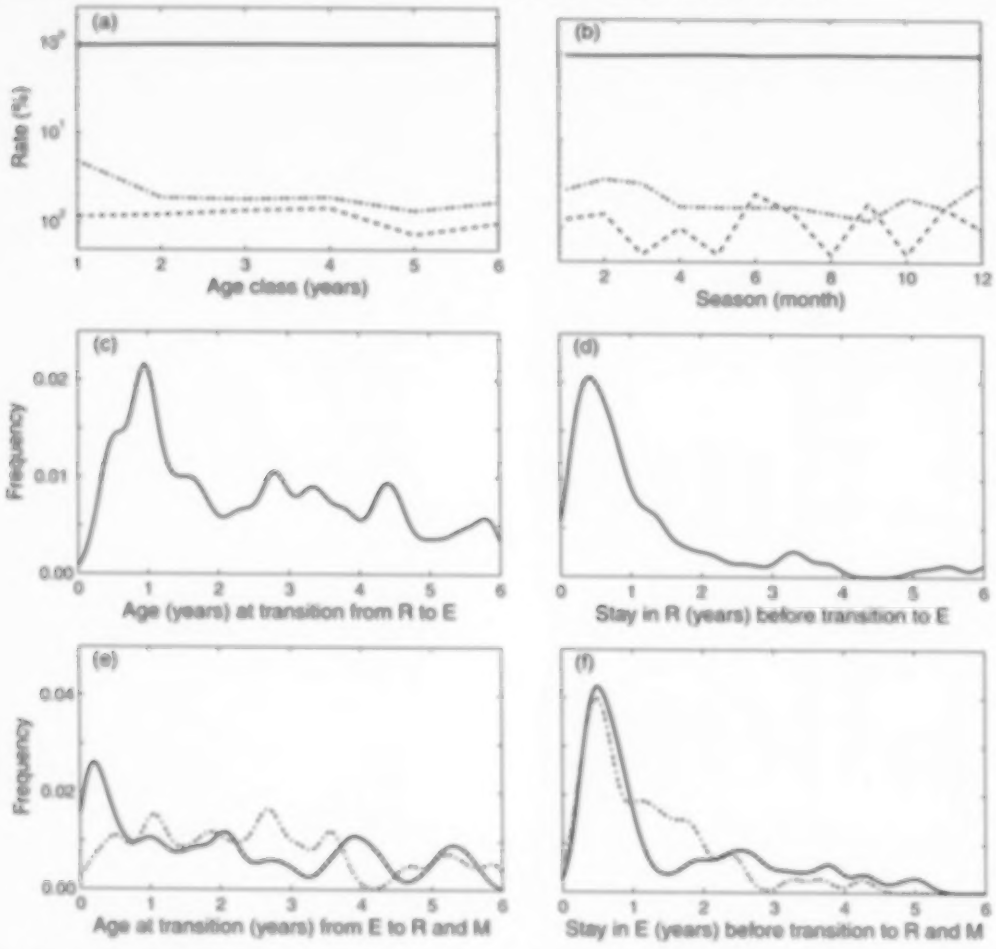

tions cannot necessarily be extended to samples from the wild, especially regarding model uncertainty (e.g., the standard deviation in Gaussian models). More importantly, such experiments do not permit the assessment of the temporal dynamics of the habitat sequence. As illustrated by the reported results, habitat sequences depict a strong temporal correlation and can not be modelled as sequences of independent variables. The HMM can be viewed as a means for combining the characterization of Sr:Ca – habitat relationship to a dynamic prior (i.e., the transition matrix) fitted to the considered data set. Though no direct validation can be reported for the individual HMM-based reconstructions of the habitat sequences, the HMM is valid from a statistical point of view in its ability to characterize and reconstruct the transitions of eels among habitat types in the Gironde River watershed.

From a methodological point of view, the proposed probabilistic models could obviously take into account other types of discrete parameters, i.e., physiological, but they might also be extended to continuous state variables (e.g., temperature). Recent developments in the field of conditional random fields (Lafferty et al. 2001) might also be investigated to take into account more complex time dynamics or continuous state sequences.

Unsupervised extraction and analysis of movement patterns

A major contribution of the proposed Bayesian framework lies in the nonsubjective, unsupervised, and thus exhaustive categorization of individual movement patterns. Thirty-seven different patterns of habitat use, with 20 patterns accounting for more than 80% of the sample, are identified within the processed sample set using the HMM scheme. Owing to the weaker temporal coherence of the GMM-based habitat sequences, the unsupervised categorization of these GMM-based sequences lead to 88 movement patterns, with only

© 2007 NRC Canada

five accounting for more than 3% of the samples. Considering macrocategories resulting from the grouping of movement patterns involving one or several migrations between two habitat types, it is shown that the results issued from GMM and HMM schemes mainly differ in the estimation of the relative frequencies of the resident behaviours (respectively, 10% and 28% of the samples). In particular, resident behaviours in the estuary account for 7.6% according to the HMM method and only 0.6% according to the GMM method. The latter result is not consistent with previous work (Tsukamoto and Arai 2001; Daverat et al. 2004, 2005) and reinforces the preference given to the HMM scheme.

Treatment of the same data set is performed according to a supervised classification in a previous study (Daverat and Tomas 2006). This categorization, based on only six classes, fails in precisely describing the repertoire of behaviour of the eels. Those six classes are defined a priori from the visual inspection of all the plots of the individual Sr:Ca series and from results for other populations found in the literature, which are not very robust. Previous work relies mainly on such supervised classification for testing a priori hypotheses on patterns of habitat use. In most cases, some individual patterns do not fit these a priori hypotheses (Tsukamoto and Arai 2001; Tzeng et al. 2002; Kotake et al. 2005) and are then withdrawn from the analysis. In contrast, the robust and unsupervised categorization of movement patterns greatly improves the investigation of unknown populations thanks to the direct determination of the diversity of the patterns of habitat use and the associated proportions.

The diversity of habitat use chronologies reported here is consistent with habitat use patterns found for *Anguilla anguilla* in the Baltic Sea (Tzeng et al. 1997; Limburg et al. 2003), as well as those of other temperate eel species such as *A. japonica* (Tsukamoto and Arai 2001; Tzeng et al. 2002), *A. rostrata* (Jessop et al. 2002; Morrison et al. 2003; Cairns et al. 2004), and *A. australis* and *A. dieffenbachii* (Arai et al. 2004). The present work confirms the existence of resident eels behaviours of their capture site (about 28%). As suggested by "transients" (Tsukamoto and Arai 2001) or "nomads" (Daverat et al. 2004, 2005), a significant number of eels (more than 72%) is reported to change habitats once or more. Interestingly, most of the fish (53%) involve habitat shifts between only two habitat types (namely, between the river and the estuary and between the estuary and the marine area). Chronologies with multiple transitions between the river and the estuary found for some eels collected in the estuary might be interpreted as an absence of movement under the seasonal fluctuations of river flows into the estuary. Though the estimated habitat-related models account for these seasonal fluctuations and Sr:Ca distributions are well discriminated whatever the season, the GMM-based reconstruction may be affected by these fluctuations. In the HMM-based reconstruction, the temporal prior estimated by the HMM imposes a strong temporal coherence. Consequently, the reconstruction of such mislabelled HMM-based habitat sequences is unlikely, so that the hypothesis of patterns with multiple or seasonal movements is confirmed by the present study.

As a by-product of the proposed approach, statistical descriptors of the fish movements between habitats, such as the distribution of the transition time from one habitat to another or the distribution of time spent in a given habitat after a transition, are evaluated for the considered data set. This results in a significant gain in analysis time and power compared with previous methods that require the information from each Sr:Ca series to be retrieved individually. The analysis of the transitions reveals that movements between two different habitats are not as frequent as residence in the same habitat throughout the fish's life. The same result is reported for studies using mark–recapture techniques (Jellyman et al. 1996; Morrison and Secor 2003) and telemetry (Parker 1995), which show that most yellow eels tend to adopt a resident behaviour. Transitions are rare temporal events throughout the fish's life, which makes them difficult to observe directly. In this study, the frequency of transitions between two different habitats decreases as the age of the eel increase. Similar results are known for *A. japonica* (Tzeng et al. 2002) and *A. rostrata* (Morrison et al. 2003), as well as *A. anguilla* (Daverat and Tomas 2006). It is also revealed that most eels spent less than 1 year in one habitat before changing again.

The unsupervised categorization framework enlarges the scope of possible analysis in terms of fish ecology. Further developments of the analysis of eel habitat use could consist of comparing individual parameters (size at age, age at maturity) of the different habitat use patterns. Such analysis could also focus on a specific stage of the fish (age or size class). More generally, it provides a powerful tool for assessing the relative efficiency of individual tactics in terms of fitness. At a broader scale, the proposed approach demonstrates the actual interest in using advanced processing techniques to fully exploit the rich potential of individual biological archives, such as fish otoliths, to characterize individual life traits. A wide range of applications for the analysis of individual life traits might be stated as such a Bayesian reconstruction of the time series of a state sequence from a set of chemical and structural measures.

Acknowledgement

We thank the anonymous referees for helpful comments on an earlier version of the manuscript.

References

Arai, T., Kotake, A., Lokman, P.M., Miller, M.J., and Tsukamoto, K. 2004. Evidence of different habitat use by New Zealand freshwater eels *Anguilla australis* and *A. dieffenbachii*, as revealed by otolith microchemistry. Mar. Ecol. Prog. Ser. **266**: 213–225.

Awad, A.M. 1996. Properties of the Akaike information criterion. Microelectron. Reliab. **36**: 457–464.

Aoyama, J., and Sasai, S. 2002. A preliminary study of the movements of yellow and silver eels, *Anguilla japonica*, in the estuary of the Fukui River, Japan, as revealed by acoustic tracking. Hydrobiologia, **470**: 31–36.

Berg, R. 1985. Age determination of eels, *Anguilla anguilla* (L.): comparison of field data with otolith ring patterns. J. Fish Biol. **26**: 537–554.

Bishop, C. 1995. Neural networks for pattern recognition. Oxford University Press, Oxford, UK.

Cairns, D.K., Shiao, J.C., Iizuka, Y., Tzeng, W.N., and MacPherson, C.D. 2004. Movement patterns of American eels in an impounded

© 2007 NRC Canada

watercourse, as indicated by otolith microchemistry. N. Am. J. Fish. Manag. **24**: 452–458.

Campana, S.E. 1999. Chemistry and composition of fish otoliths: pathways, mechanisms and applications. Mar. Ecol. Prog. Ser. **188**: 263–297.

Campana, S.E., and Casselman, J.M. 1993. Stock discrimination using otolith shape analysis. Can. J. Fish. Aquat. Sci. **50**: 1062–1083.

Campana, S.E., Chouinard, G.A., Hanson, J.M., Frechet, A., and Brattey, J. 2000. Otolith elemental fingerprints as biological tracers of fish stocks. Fish. Res. **46**: 343–357.

Cardinale, M., Doering-Arjes, P., Kastowsky, M., and Mosegaard, H. 2004. Effects of sex, stock, and environment on the shape of known-age Atlantic cod (*Gadus morhua*) otoliths. Can. J. Fish. Aquat. Sci. **61**: 158–167.

Daverat, F., and Tomas, J. 2006. Tactics and demographic attributes of the European eel (*Anguilla anguilla*): the case study of the Gironde watershed (Southwest France). Mar. Ecol. Prog. Ser. **307**: 247–257.

Daverat, F., Elie, P., and Lahaye, M. 2004. Microchemistry contribution to a first approach to the diversity of life histories of eels from the lower part of the Gironde Garonne Dordogne watershed. Cybium, **28**: 83–90.

Daverat, F., Tomas, J., Lahaye, M., Palmer, M., and Elie, P. 2005. Tracking continental habitat shifts of eels using otolith Sr/Ca ratios: validation and application to the coastal, estuarine and riverine eels of the Gironde–Garonne–Dordogne watershed. Mar. Freshw. Res. **56**: 619–627.

Elsdon, T.S., and Gillanders, B.M. 2003 Reconstructing migratory patterns of fish based on environmental influences on otolith chemistry. Rev. Fish Biol. Fish. **13**: 219–235

Elsdon, T.S., and Gillanders, B.M. 2005. Consistency of patterns between laboratory experiments and field-collected fish in otolith chemistry: an example and applications for salinity reconstructions. Mar. Freshw. Res. **56**: 609–617.

Fablet, R. 2006. Semi-local extraction of ring structures in images of biological hard tissues: application to the Bayesian interpretation of fish otoliths for age and growth estimation. Can. J. Fish. Aquat. Sci. **63**(6): 141–1428.

Helfman, G.S., and Bozeman, E.L. 1983. Ultrasonic telemetry of American eel in a tidal creek. Trans. Am. Fish. Soc. **112**: 105–110.

Jellyman, D.J., Glova, G.J., and Todd, P.R. 1996. Movements of shortfinned eels, Anguilla australis, in Lake Ellesmere, New Zealand: results from mark–recapture studies and sonic tracking. N.Z. J. Mar. Freshw. Res. **30**: 371–381.

Jessop, B.M., Shiao, J.-C., Iizuka, Y., and Tzeng, W.-N. 2002. Migratory behaviour and habitat use by American eels *Anguilla rostrata* as revealed by otolith microchemistry. Mar. Ecol. Prog. Ser. **233**: 217–229.

Kawakami, Y., Mochioka, N., Morishita, K., Tajima, T., Nakagawa, H., Toh, H., and Nakazono, A. 1998. Factors influencing otolith strontium/calcium ratios in *Anguilla japonica* elvers. Environ. Biol. Fishes, **52**: 299–303.

Kotake, A., Okamura, A., Yamada, Y., Utoh, T., Arai, T., Miller, M.J., Oka, H., and Tsukamoto, K. 2005. Seasonal variation in the migratory history of the Japanese eel *Anguilla japonica* in Mikawa Bay, Japan. Mar. Ecol. Prog. Ser. **293**: 213–225.

Kraus, R.T., and Secor, D.H. 2003. Response of otolith Sr:Ca to a manipulated environment in young American eels. Am. Fish. Soc. Symp. **33**: 79–85.

Kraus, R.T., and Secor, D.H. 2004. Incorporation of strontium into otoliths of an estuarine fish. J. Exp. Mar. Biol. Ecol. **302**: 85–106.

Lafferty, J., McCallum, A., and Pereira, F. 2001. Conditional random fields: probabilistic models for segmenting and labeling sequence data. In Proceedings of the 18th International Conference on Machine Learning (ICML'2001), 28 June – 1 July 2001, Williamstown, Mass. *Edited by* C.E. Brodley and A.P. Danyluk. Morgan Kaufmann Publishers Inc., San Francisco.

Limburg, K.E., Svedang, H., Elfman, M., and Kristiansson, P. 2003. Do stocked freshwater eels migrate? Evidence from the Baltic suggests "yes". *In* Biology, management and protection of catadromous eels. Am. Fish. Soc. Symp. **33**: 275–284.

Martin, G.B., and Thorrold, S.R. 2005. Temperature and salinity effects on magnesium, manganese, and barium incorporation in otoliths of larval and early juvenile spot *Leiostomus xanthurus*. Mar. Ecol. Prog. Ser. **293**: 223–232.

McCullagh, P., and Nelder, J.A. 1989. Generalized linear models. Chapman and Hall, London.

Milton, D.A., and Chenery, S.R. 2003. Movement patterns of the tropical shad hilsa (*Tenualosa ilisha*) infered from transects of $^{87}Sr/^{86}Sr$ isotope ratios in their otoliths. Can. J. Fish. Aquat. Sci. **60**: 1376–1385.

Morrison, W.E., and Secor, D.H. 2003. Demographic attributes of yellow-phase American eels (*Anguilla rostrata*) in the Hudson River estuary. Can. J. Fish. Aquat. Sci. **60**: 1487–1501.

Morrison, W.E., Secor, D.H., and Piccoli, P.M. 2003. Estuarine habitat use by Hudson River American eels as determined by otolith strontium:calcium ratios. *In* Biology, management and protection of catadromous eels. Am. Fish. Soc. Symp. **33**: 87–100.

Mounaix, B., and Fontenelle, G. 1994. Anguilles estuariennes et fluviales: apports de l'otolithométrie. Bull. Fr. Peche Piscic. **335**: 67–80.

Murphy, K. 2004. Conditional random field (CRF) toolbox for Matlab [online]. Available from www.cs.ubc.ca/~murphyk/Software/CRF/crf.html [updated 23 May 2006].

Nabney, I. 2001. Netlab: algorithms for pattern recognition. Springer-Verlag, New York.

Nelson, C.S., Northcote, T.G., and Hendy, C.H. 1989. Potential use of oxygen and carbon isotopic composition of otoliths to identify migratory and non-migratory stocks of the New Zealand common smelt: a pilot study. N.Z. J. Mar. Freshw. Res. **23**: 337–344.

Parker, S.J. 1995. Homing ability and home range of yellow phase American eels in a tidally dominated estuary. J. Mar. Biol. Assoc. U.K. **75**: 127–140.

Rabiner, L.R. 1989. Tutorial on hidden Markov models and selected applications in speech recognition. Proc. IEEE, **77**: 257–286.

R Development Core Team. 2005. R: a language and environment for statistical computing. R Foundation for Statistical Computing, Vienna, Austria.

Secor, D.H. 1999. Specifying divergent migrations in the concept of stock: the contingent hypothesis. Fish. Res. **43**: 13–34.

Silber, J.H., Rosenbaum, P.R., and Ross, R.N. 1995. Comparing the contribution of groups of predictors: which outcomes vary with hospital rather than patient characteristics? J. Am. Statist. Assoc. **90**: 7–18.

Thorrold, S.R., and Shuttleworth, S. 2000. In situ analysis of trace elements and isotope ratios in fish otoliths using laser ablation sector field inductively coupled plasma mass spectrometry. Can. J. Fish. Aquat. Sci. **57**: 1232–1242.

Thorrold, S.R., Jones, C.M., and Campana, S.E. 1997. Response of otolith microchemistry to environmental variations experienced by larval and juvenile Atlantic croaker (*Micropogonias undulatus*). Limnol. Oceanogr. **42**: 102–111.

Troadec, H., Benzinou, A., Rodin, V., and Le Bihan, J. 2000. Use of deformable template for two-dimensional growth ring detection of otoliths by digital image processing: application to plaice (*Pleuronectes platessa*) otoliths. Fish. Res. **46**: 155–163.

© 2007 NRC Canada

Tsukamoto, K., and Arai, T. 2001. Facultative catadromy of the eel *Anguilla japonica* between freshwater and seawater habitats. Mar. Ecol. Prog. Ser. **220**: 265–276.

Tzeng, W.N., Wu, H.F., and Wickstrom, H. 1994. Scanning electron microscopic analysis of annulus microstructure in otolith of European eel, *Anguilla anguilla*. J. Fish Biol. **45**: 479–492.

Tzeng, W.N., Severin, K.P., and Wickstrom, H. 1997. Use of otolith microchemistry to investigate the environmental history of European eel *Anguilla anguilla*. Mar. Ecol. Prog. Ser. **149**: 73–81.

Tzeng, W.N., Shiao, J.C., and Iizuka, Y. 2002. Use of otolith Sr:Ca ratios to study the riverine migratory behaviors of Japanese eel *Anguilla japonica*. Mar. Ecol. Prog. Ser. **245**: 213–221.

Appendix A

EM parameter estimation for Gaussian mixture models

The estimation of the parameters of the Gaussian mixture models is carried out according to the maximum likelihood (ML) criterion. It resorts to the following maximization issue:

$$\{\hat{\pi}_H, \hat{\Theta}_H, \hat{\sigma}_H\}_{H\in\{\text{R.E.M}\}} = \arg \max_{\{\pi_H, \Theta_H, \sigma_H\}_{H\in\{\text{R.E.M}\}}} \times \prod_i p(y_i|a_i, s_i, \{\pi_H, \Theta_H, \sigma_H\}_{H\in\{\text{R.E.M}\}})$$

To solve for this maximization issue, we use the expectation–maximization (EM) algorithm (Bishop 1995). Let us denote by x_i the variable stating that the ith sample is issued from habitat x_i. The EM algorithm iterates two steps until convergence. At iteration k, the E step computes the posterior likelihood $p(x_i|y_i, a_i, s_i, \{\pi_H^k, \Theta_H^k, \sigma_H^k\}_{H\in\{\text{R.E.M}\}})$ of assigning x_i to habitat H given the observed measure y_i and the current estimate of the mixture parameters $\{\pi_H^k, \Theta_H^k, \sigma_H^k\}_{H\in\{\text{R.E.M}\}}$:

$$p(x_i = H_1|y_i, a_i, s_i, \{\pi_H^k, \Theta_H^k, \sigma_H^k\}_{H\in\{\text{R.E.M}\}}) = \frac{\pi_{H_1}^k p(y_i|a_i, s_i, \Theta_{H_1}^k, \sigma_{H_1}^k)}{\sum_{H_2\in\{\text{R.E.M}\}} \pi_{H_2}^k p(y_i|a_i, s_i, \Theta_{H_2}^k, \sigma_{H_2}^k)}$$

Given the posterior probabilities, the M step aims at updating model parameters $\{\pi_H^{k+1}, \Theta_H^{k+1}, \sigma_H^{k+1}\}_{H\in\{\text{R.E.M}\}}$. To simplify the notations, let us denote by τ_{iH} the posterior $p(x_i|y_i, a_i, s_i, \{\pi_H^k, \Theta_H^k, \sigma_H^k\}_{H\in\{\text{R.E.M}\}})$. The new priors $\{\pi_H^{k+1}\}_{H\in\{\text{R.E.M}\}}$ are updated as

$$\pi_H^{k+1} = \frac{1}{N}\sum_i \tau_{iH}$$

The new model parameters $\Theta_H^{k+1} = (m_H, \lambda_H, \mu_H)$ are estimated as the solution of the following weighted least-square problem, where the weights are give by posterior likelihoods τ_{iH}:

$$\Theta_H^{k+1} = \arg\min_{\Theta}\left[\sum_i \tau_{iH}(y_i - Z_i^t\Theta)^2\right]$$

where $\mathbf{Z}_i$ is the vector defined by $[1, a_i, s_i]$. This weighted linear regression leads to

$$\Theta_H^{k+1} = \left[\sum_i \tau_{iH} Z_i^t Z_i\right]^{-1} \sum_i \tau_{iH} y_i Z_i$$

Then, the updated standard deviations $\{\sigma_H^{k+1}\}_{H\in\{\text{R.E.M}\}}$ are computed from the weighted average of the squared residual error $r_{iH} = y_i - Z_i^t\Theta_H^{k+1}$ with respect to the prediction issued from the current model estimate:

$$\sigma_H^{k+1} = \sqrt{\frac{1}{N}\sum_i \tau_{iH} r_{iH}^2}$$

© 2007 NRC Canada

Acoustic data collected during and between bottom trawl stations: consistency and common trends

Nicolas Bez, David Reid, Suzanna Neville, Yves Vérin, Vidar Hjellvik, and Hans D. Gerritsen

Abstract: Acoustic data are often collected during bottom trawl surveys. Their use can potentially improve the precision and accuracy of fish abundance estimates if acoustic data collected between trawl stations are consistent with those collected during trawling operations. This question is addressed here through the analysis of 20 bottom trawl surveys (three survey areas and five different survey series) with coincident acoustic measurements during and between trawl stations. Firstly, on-station and underway acoustic data were compared using statistics computed globally over each survey (average vertical profiles, global indices of collocations, and spatial structures) for various combinations of depth layers. Secondly, we focussed on underway acoustic data recorded in the vicinity of stations, distinguishing between data recorded before and after the tows. On-station and underway acoustic data were highly consistent, and no systematic perturbation of the acoustic sign due to the presence of the gear a few hundred metres behind the vessel was observed.

Résumé : On récolte souvent des données acoustiques durant les inventaires faits au chalut de fond. Leur utilisation peut potentiellement améliorer la précision et la justesse des estimations d'abondance des poissons, si les données acoustiques récoltées entre les stations de chalutage sont compatibles avec celles récoltées durant les opérations de pêche. Nous examinons la question en analysant 20 inventaires faits au chalut de fond (trois zones d'inventaire et cinq séries différentes d'inventaires) pour lesquels il existe des mesures acoustiques coïncidentes obtenues dans et entre les stations de chalutage. Nous avons d'abord comparé les données acoustiques obtenues en route et dans les stations à l'aide de statistiques calculées globalement pour chaque inventaire (profils verticaux moyens, indices globaux de collocation et structures spatiales) selon diverses combinaisons de couches de profondeur. Ensuite, nous nous sommes intéressés aux données acoustiques obtenues en route près des stations, en distinguant entre les données enregistrées avant et après le chalutage. Il existe un excellent accord entre les données acoustiques obtenues dans les stations et celles enregistrées en route; on n'observe pas de perturbation systématique du signal acoustique due à la présence des engins de pêche à quelques centaines de mètres derrière le navire.

[Traduit par la Rédaction]

Introduction

Bottom trawl surveys are one of the main survey methods used in the assessment of demersal fish stocks around the world (Gunderson 1993). It has recently become possible to carry out combined acoustic and bottom trawl surveys (e.g., in the Barents Sea, Aglen and Nakken 1997; Korsbrekke et al. 2001) or to collect acoustic and trawl

Received 28 July 2006. Accepted 12 August 2006. Published on the NRC Research Press Web site at http://cjfas.nrc.ca on 30 January 2007.
J19448

N. Bez.[1,2] Ecole des Mines, Géostatistique, F-77305 Fontainebleau, France.
D. Reid. Fisheries Research Services – Marine Laboratory Aberdeen (FRS–MLA), P.O. Box 101, Victoria Road, Torry, Aberdeen, AB11 9DB, United Kingdom.
S. Neville. Centre for Environment, Fisheries, and Aquaculture Science (CEFAS), Lowestoft Laboratory, Pakefield Road, Lowestoft, Suffolk, NR33 OHT, United Kingdom.
Y. Vérin. Institut Français de Recherche pour l'Exploitation de la Mer (IFREMER), 150 Quai Gambetta, 62 321 Boulogne sur Mer, France.
V. Hjellvik. Institute of Marine Research (IMR), P.O. Box 1870 N-5024, Bergen, Norway.
H.D. Gerritsen.[3] Queen's University Belfast – Department of Agriculture and Rural Development, Northern Ireland (QUB–DARDNI), Newforge Lane, Belfast, BT9 5PX, Northern Ireland, United Kingdom.

[1]Corresponding author (e-mail: nicolas.bez@ird.fr).
[2]Present address: Institut de recherche pour le développement (IRD), Rue Jean Monnet, BP171, 34203 Sète, France.
[3]Present address: Marine Institute, Rinville, Oranmore, Galway, Ireland.

 doi:10.1139/F06-174 © 2007 NRC Canada

Fig. 1. Study areas (*a*) and sampling schemes for (*b*) the International Bottom Trawl Surveys (IBTS), (*c*) the Northern Irish Bottom Trawl Surveys (NIBTS), and (*d*) the combined acoustic and bottom trawl surveys for Atlantic cod (*Gadus morhua*) and haddock (*Melanogrammus aeglefinus*) in the Barents Sea. Solid squares represent stations. Crosses represent between-station recordings. They appear as lines when the density of between stations observations is large.

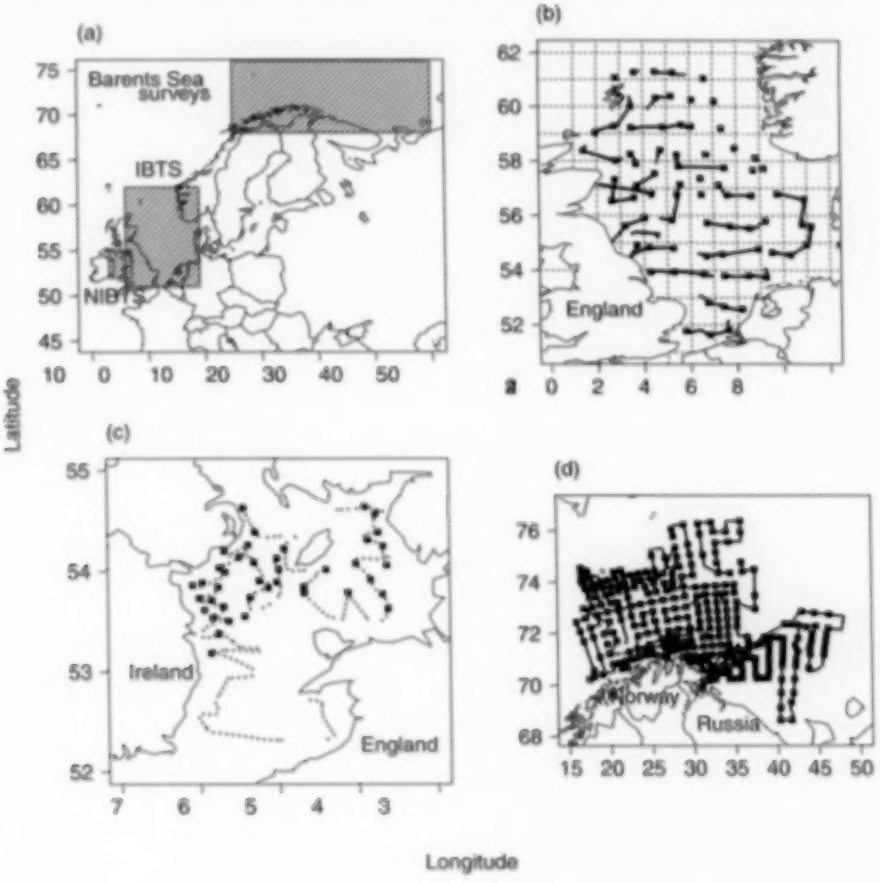

data while carrying out a bottom trawl survey (Cachera et al. 1999; Krieger et al. 2001). In some cases, such as Atlantic cod (*Gadus morhua*) in the Barents Sea (Korsbrekke et al. 2001), the acoustic data are used to generate a secondary abundance index from the survey in addition to a trawl catch-rate index. Acoustic observations can also be used to gain additional information on fish availability and distribution away from the trawl station to improve the precision and accuracy of the trawl-based estimate. These two approaches were the basis for the EU-funded (Framework Programme 5) project CATEFA (Combining Acoustic and Trawl data for Estimating Fish Abundance).

Two hypotheses need to be confirmed to allow this combination of acoustic and trawl survey data. The first is that the fishing gear and the acoustic devices are measuring the same thing. If true, it would become possible to derive a relationship between trawl catch and acoustic observations (Krieger et al. 2001; Hjellvik et al. 2003). The second is that acoustic data collected away from the trawl stations are consistent with that collected during the trawling operations. The present paper deals with the second hypothesis.

There is considerable evidence that fish engage in avoidance behaviour to the trawl–vessel combination (Godø et al. 1999; Michalsen 1999; Handegard et al. 2003). Vessel speed is generally low during trawling (e.g., around 3 knots; 1 knot = 1.852 km·h^{-1}), and a large and noisy net is being towed. Away from the trawl stations, the survey vessel moves much faster (usually over 10 knots) and without a net. The evidence is mixed as to whether fish also engage in avoidance behaviour under this scenario (Fréon and Misund 1999; Fernandes et al. 2000; Mitson and Knudsen 2003). Different avoidance reactions, and hence availability to the echosounder, could have a major impact on what is seen on the echogram. To use the acoustic data between trawl stations for the purpose of improving trawl survey estimates or for combining the data, we must be sure that the echosounder is seeing the same component of a population during trawling as it does while running between stations. This study uses data from a number of different trawl sur-

© 2007 NRC Canada

Table 1. Main characteristics of the various surveys used in the analyses.

Area	Source survey series	Year	Month	No. of stations	Mean towed distance (n.mi.)*	Original ESDU (n.mi.)*	No. of between-station data (after regularization)	Height used to split vertical profiles (m)	Depth range (m)	GIC bottom layers	GIC midwater layers
Barents Sea	IMR	1997	Feb.–Mar.	176	1.50	1	5209	40	143–699	0.98	0.95
	IMR	1998	Feb.	198	1.53	1	5135	40	63–720	0.9	0.85
	IMR	1999	Jan.–Feb.	223	1.49	1	5567	40	104–480	0.99	0.97
	IMR	2000	Jan.–Feb.	302	1.42	1	7680	40	58–550	0.98	0.99
	IMR	2001	Jan.–Mar.	300	1.49	1	7666	40	55–487	0.97	0.96
	IMR	2002	Jan.–Mar.	287	1.44	1	7383	40	63–542	0.98	0.98
North Sea	FRS	2000	Jan.–Feb.	44	1.8	0.5	468	10	45–150	0.6	1
	FRS	2002	Jan.–Feb.	46	2.01	0.5	351	10	48–144	0.89	0.74
	FRS	2003	Jan.–Feb.	47	1.98	0.5	430	10	49–150	0.9	0.98
	CEFAS	2000	Aug.–Sept.	71	1.98	0.5	1038	10	24–178	0.99	0.99
	CEFAS	2001	Aug.–Sept.	70	2.01	0.5	883	10	24–211	0.99	0.84
	CEFAS	2002	Feb.	23	1.98	0.5	1140	10	24–84	0.93	0.97
	IFREMER	2002	Feb.	77	1.83	0.1	440	10	9–88	0.9	0.95
	IFREMER	2003	Feb.	82	1.89	0.1	722	10	14–90	0.93	0.75
Irish Sea	DARDNI	1997	Oct.	13	3.00	0.5	84	10	25–103	0.98	0.91
	DARDNI	2000	Mar.	37	2.90	0.5	110	10	26–106	0.99	0.95
	DARDNI	2001	Oct.	34	2.70	0.5	236	10	23–90	0.94	0.99
	DARDNI	2002	Mar.	41	2.85	0.5	173	10	24–102	0.93	0.98

Note: ESDU, elementary sampling distance unit; GIC, global index of collocation; IMR, Institute of Marine Research; FRS, Fisheries Research Services; CEFAS, Centre for Environment, Fisheries, and Aquaculture Science; IFREMER, Institut Français de Recherche pour l'Exploitation de la Mer; DARDNI, Department of Agriculture and Rural Development, Northern Ireland.

*1 n.mi. = 1.852 km.

© 2007 NRC Canada

Fig. 2. Bottom-referenced depth layers used for the acoustic integration. The first 10 layers from the bottom have a height of 1 m; the following layers are 10 m in height. Midwater and bottom layers used for the analysis are represented for the Barents Sea surveys (right) and the North Sea or Irish Sea surveys (left).

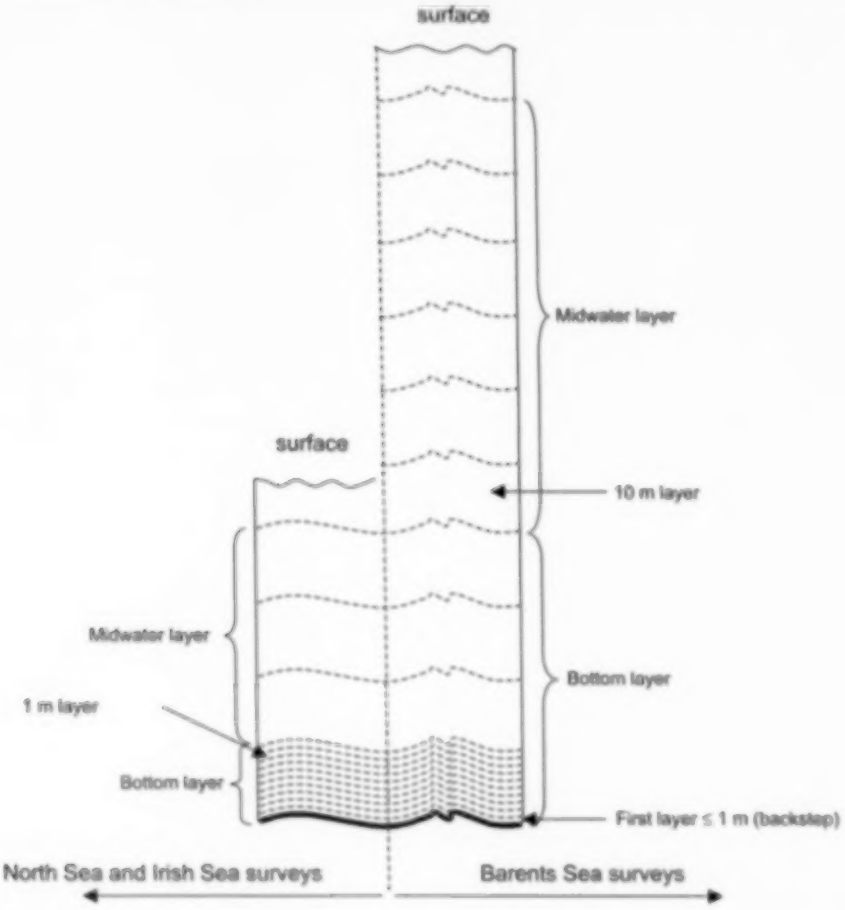

veys in the North, Irish, and Barents seas (Fig. 1*a*). It examines the relationship between on-station and between-station acoustic data at both the local level (i.e., immediately adjacent to the trawl station) and more globally for each survey.

Materials and methods

Surveys and data preparation

Bottom trawl data with coincident acoustic measurements from three survey areas and five different survey series were used in this analysis (Table 1).

The International Council for the Exploration of the Sea (ICES) coordinates the International Bottom Trawl Surveys (IBTS) in the North Sea. These surveys follow a random design, stratified by an ICES rectangle (Fig. 1*b*). Trawl and acoustic data are only collected during daylight hours. The surveys used in this study were those carried out by the Centre for Environment Fisheries and Aquaculture Science (CEFAS), Lowestoft (2000, 2001, and 2002); the Fisheries Research Services (FRS), Aberdeen (1999, 2000, and 2002); and the Institut Français de Recherche pour l'Exploitation de la Mer (IFREMER), Boulogne (2002 and 2003). Each survey comprises between 60 and 80 stations. The North Sea data had the most skewed distributions, with many low values and a few extremely high values. In the case of the French data, 65% of the total backscattering energy on-station was concentrated in 3% of the stations.

The Northern Irish Bottom Trawl Surveys (NIBTS) in the Irish Sea are mostly small (35 to 45 stations) and follow a random sampling design stratified by depth and substrate (Fig. 1*c*). Depth varied between 23 and 102 m. Four surveys carried out by DARDNI (Department of Agriculture and Rural Development, Northern Ireland), Belfast, were available: autumn 1997, spring 2000, autumn 2001, and spring 2002. These surveys tend to encounter much more pelagic fish like Atlantic herring (*Clupea harengus*) and sprat (*Sprattus sprattus*) than in the North Sea or Barents Sea surveys.

The combined acoustic and bottom trawl surveys for Atlantic cod and haddock (*Melanogrammus aeglefinus*) in the Barents Sea are conducted by the Institute of Marine Research (IMR), Bergen. Sampling follows a regular grid with

© 2007 NRC Canada

Fig. 3. Vertical profiles of acoustic backscattering, Barents Sea survey (1997–2002). Representation is shown of the 25% and 75% quantiles of nautical area scattering coefficient (NASC) values per layer for on-station data (broken lines) and between-station data (solid lines). The *x* axis is the mean NASC value (in $m^2 \cdot n.mi.^{-2}$; 1 n.mi. = 1.852 km) per layer. The *y* axis is the height of each layer relative to the detected bottom (in metres). The numbers of samples taken on-station and between-stations are denoted by N^a and N^b, respectively.

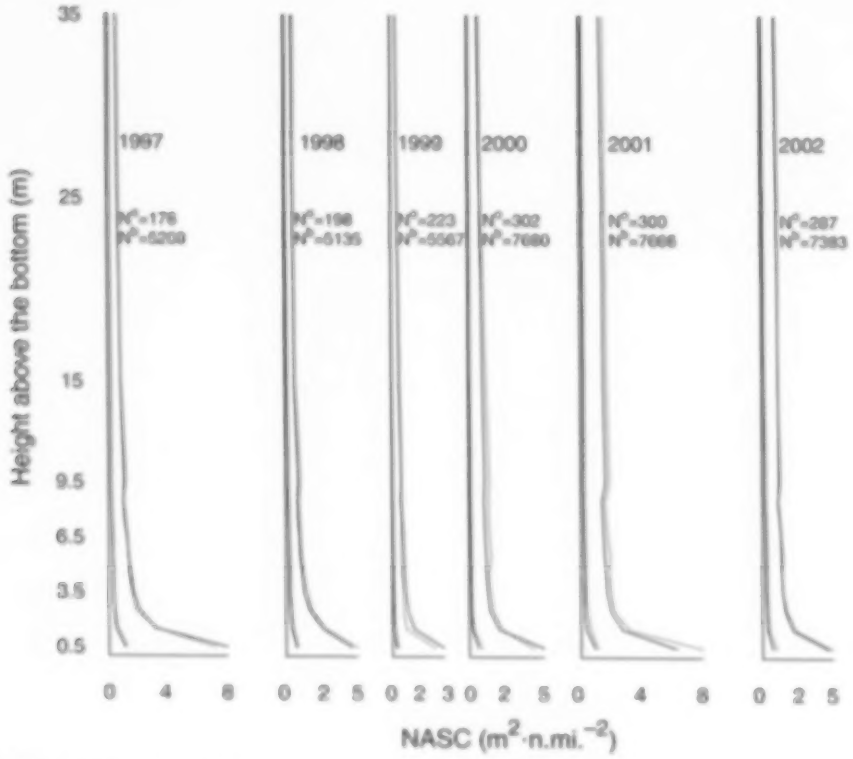

a haul every 20 n.mi. (1 n.mi. = 1.852 km) (Fig. 1*d*). The number of hauls varied between 200 and 300. Surveys were available from 1997 to 2002.

Simrad EK500 scientific echosounders were used for all surveys, with at least a 38 kHz split-beam transducer. The echosounder angle was 7°, and its pulse duration was 1 ms. For this frequency, the efficiency of the TVG is 580 m (Diner and Marchand 1995). Since the maximum depth encountered in the different surveys used in this study was between 23 (Irish Sea) and 540 m (Barents Sea), the propagation loss was not a problem. The acoustic backscattering energies were converted to nautical area scattering coefficient (NASC, MacLennan et al. 2002) and expressed in $m^2 \cdot n.mi^{-2}$. The integration threshold was set at –70 dB. NASC values were available from trawl stations and between trawl stations. For the on-station NASC, integration was carried out for the whole trawling period. In general, the tow length was fixed within each survey series. NASC values between trawl stations were available at fixed elementary sampling distance units (ESDU), which differed by survey series: 0.1 n.mi. for IFREMER data, 1 n.mi. for IMR data, and 0.5 n.mi. for the rest of the data sets (Table 1).

Because the ESDUs were smaller than the average tow lengths, between-station NASC values were pooled (regularized) to produce ESDU values as close to the average tow lengths as possible for each survey series: 3 n.mi in the Irish Sea, 1 n.mi. in the Barents Sea, and 2 n.mi in the North Sea.

NASC values for each ESDU and trawl station were subdivided into a series of bottom-referenced layers (Fig. 2): ten 1 m layers sequentially from the seabed followed by several 10 m layers. The accuracy of the sounder-detected bottom was verified and corrected where needed. This was achieved using manual or semiautomated procedures in the analysis of the acoustic data. In the latter case, the layer closest to the bottom included a backstep to avoid integrating the seabed. The size of the backstep varied between 10 and 40 cm, depending on the survey series and weather conditions. Acoustic data preparation was carried out using SIMRAD BI500 (SIMRAD, Horten, Norway) for the Norwegian data, Movies Plus (IFREMER, Brest, France) for the French data, and SonarData EchoView 3.1 (SonarData, Hobart, Australia) for all of the other data.

Acoustic signals of obvious and well-defined pelagic fish schools were excluded from the analysis.

Notations

The superscripts indicate whether a parameter refers to on-station (^{a}) or between-station (^{b}) data. For instance, the numbers of samples taken on-station and between-stations are denoted by N^a and N^b, respectively. Equations are only

© 2007 NRC Canada

Fig. 4. Vertical profiles of acoustic backscattering, International Bottom Trawl Surveys (IBTS): (*a*) Fisheries Research Services (FRS), (*b*) Centre for Environment, Fisheries, and Aquaculture Science (CEFAS), and (*c*) Institut Français de Recherche pour l'Exploitation de la Mer (IFREMER). Representation is shown of the 25% and 75% quantiles of nautical area scattering coefficient (NASC) values per layer for on-station data (broken lines) and between-station data (solid lines). The *x* axis is the mean NASC value (in m^2·n.mi.$^{-2}$; 1 n.mi. = 1.852 km) per layer. The *y* axis is the height of each layer relative to the detected bottom (in metres). The numbers of samples taken on-station and between-stations are denoted by N^o and N^b, respectively.

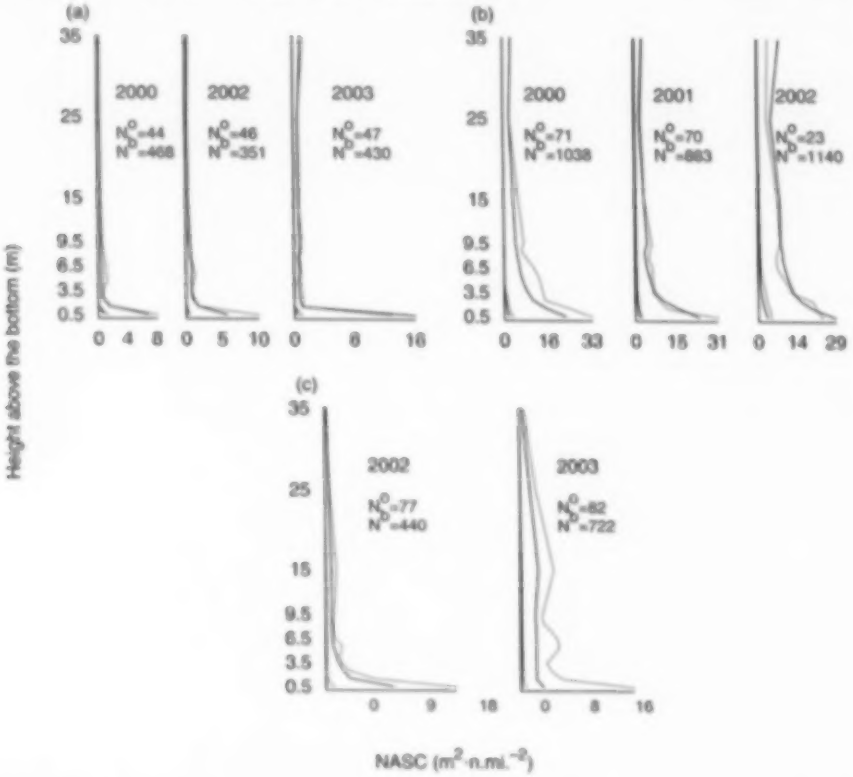

given for the on-station data. They are interchangable with between-station data by changing the superscripts.

The NASC values observed at sample i in layer k are denoted $s_A^o(i, k)$, $i \in [1, N^o]$. The longitude and latitude (x_i, y_i) are expressed in decimal degrees. The number and the thickness of the depth layers are denoted by k and t_k as follows:

(1) $t_1 = 1$ m if no backstep (manual bottom correction)

$0.6 \text{ m} \le t_1 \le 0.9$ m

if backstep (semiautomatic bottom correction)

$t_k = 1$ m for $k = 2, \ldots, 10$

$t_k = 10$ m for $k \ge 11$

Volumetric scattering coefficients, s_V, are expressed in m^{-1} and are obtained by

$$(2) \qquad s_V^o(i, k) = \frac{s_A^o(i, k)}{t_k}$$

Layers were also integrated and grouped into a bottom and a midwater layer. In the North Sea and Irish Sea, the bottom layer was defined as the bottom 10 m and the midwater layer was between 10 and 40 m off the bottom (Fig. 2). Because of the high average depth in the Barents Sea area and the large vertical opening of the trawl, the first 40 m were regarded as the bottom layer and the midwater layer was between 40 and 100 m above the bottom:

$$(3) \qquad s_A^o(i, 0\text{–}40) = \sum_{k=1}^{13} s_A^o(i, k)$$

and

$$s_A^o(i, 40\text{–}100) = \sum_{k=14}^{19} s_A^o(i, k)$$

The sum over all the layers is denoted by $s_A^o(i)$.

Global statistics

Vertical profiles

We computed the average vertical profiles for both on-station and between-station NASCs for each survey according to

© 2007 NRC Canada

Fig. 5. Vertical profiles of acoustic backscattering, Northern Irish Bottom Trawl Surveys (NIBTS) without pelagic data. Representation is shown of the 25% and 75% quantiles of nautical area scattering coefficient (NASC) values per layer for on-station data (broken lines) and between-station data (solid lines). The *x* axis is the mean NASC value (in m^2·n.mi.$^{-2}$; 1 n.mi. = 1.852 km) per layer. The *y* axis is the height of each layer relative to the detected bottom (in metres). The numbers of samples taken on-station and between-stations are denoted by N^o and N^b, respectively.

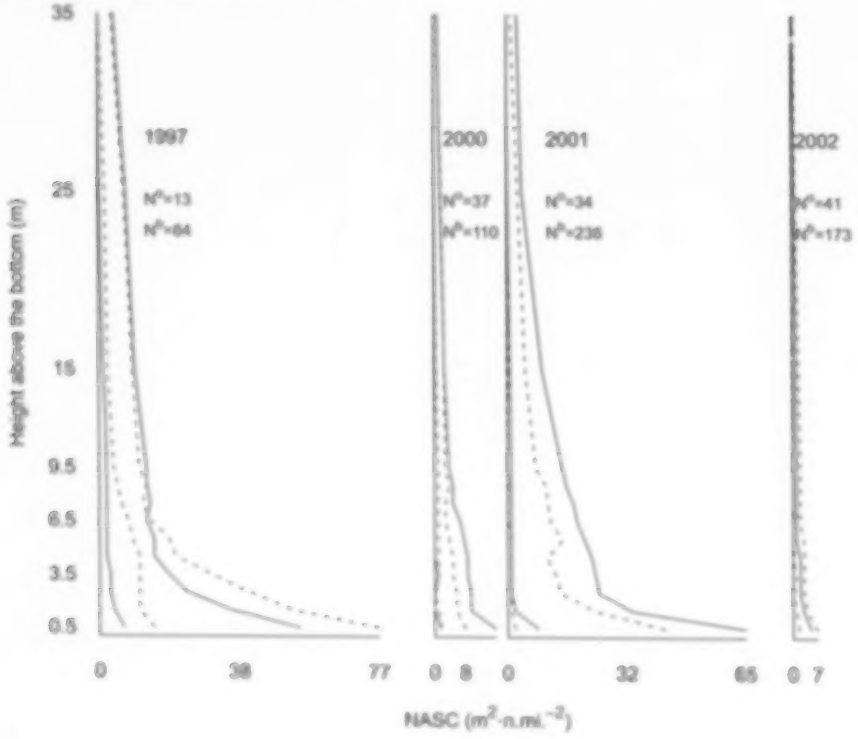

$$s_V^o(\hat{k}) = \frac{\sum_{i=1}^{N^o} s_V^o(i,\hat{k})}{N^o} \quad (4)$$

This allows for a visual comparison of vertical fish distributions seen on-station and between stations.

Horizontal structures

Global index of collocation

The match between the two spatial distributions was evaluated using a global index of collocation (GIC; Bez and Rivoirard 2000). This index is based on the centre of mass and inertia of each spatial distribution. The centre of mass, for example, of the on-station bottom layers in a given area (CoM^o_{0-40}) was computed as

$$CoM^o_{0-40} = \left(\frac{\sum_{i=1}^{N^o} s_A^o(i,0-40)x_i}{\sum_{i=1}^{N^o} s_A^o(i,0-40)} , \frac{\sum_{i=1}^{N^o} s_A^o(i,0-40)y_i}{\sum_{i=1}^{N^o} s_A^o(i,0-40)} \right) \quad (5)$$

with equal weight given to each sample. The CoM is a vector of coordinates giving the mean location of the population in terms of longitude and latitude. The inertia

$$I^o_{0-40} = \frac{\sum_{i=1}^{N^o} s_A^o(i,0-40)[(x_i - CoM^o_{0-40})^2 + (y_i - CoM^o_{0-40})^2]}{\sum_{i=1}^{N^o} s_A^o(i,0-40)} \quad (6)$$

is expressed in surface units (typically square nautical miles) and quantifies the spatial dispersal of the population. The GIC is given by

$$GIC_{0-40} = 1 - \frac{(CoM^o_{0-40} - CoM^b_{0-40})^2}{(CoM^o_{0-40} - CoM^b_{0-40})^2 + I^o_{0-40} + I^b_{0-40}} \quad (7)$$

It measures the spatial overlap between the on-station and between-station populations and ranges from 1 for complete spatial overlap between the two populations to 0 when the two are distinct. Numerically, it decreases quickly with decreasing spatial overlap. This index is analogous to an analysis of variance type of criteria, as it compares the mean (square) distance between the centroids of the two populations and the mean (square) distance between two individuals taken at random and independently from any of the two populations (Bez 2007).

© 2007 NRC Canada

Variograms

Spatial structures of the vertically integrated NASC values were compared in more detail using variography (e.g., Rivoirard et al. 2000). Because the goal was to compare the spatial structures and not to estimate biomass, the NASC values were transformed as follows:

$$(8) \qquad \log[1 + s_A^*(i)]$$

While this nonlinear transformation modifies the spatial structure, it does not preclude comparisons of spatial structures from being made. Zero values remain zero after the transformation, but differences between large data values are reduced.

Because the sample sizes of the two sets were significantly different (a few dozen for on-station data and a few hundred for between-station), we did not expect the variances to be equal (especially when dealing with skewed data). We therefore compared normalized variograms (i.e., variograms divided by the empirical variance of input data). In two instances, a poor match was observed between the variograms of on-station and between-station data. The impact of extreme values was then investigated by excluding some of the largest data. Normalized variograms were averaged by surveys series, resulting in one variogram per survey series.

Local statistics: before, during, and after trawl

To test for the existence of changes in the acoustic signal due to fish response to trawl gear, we compared records made during trawling with those made just before and after trawling. The objective was to test the null hypothesis (H_0) that on-station and nearby between-station NASC values were similar and, more precisely, as similar as two consecutive between-station NASC values that lie outside the stations' areas of influence.

A window of the same order of magnitude of the tow durations was chosen to select between-station data located nearby each trawl station (1 n.mi. for Barents Sea surveys, 2 n.mi. for North Sea surveys, and 3 n.mi. for Irish Sea surveys). This window was considered to be small enough to provide local statistics but large enough to include a sufficient number of observations.

Bottom and midwater layers were summarized by two statistics: a biomass criteria (i.e., the NASC values integrated over the depth layers) and a measure of vertical distribution (i.e., the altitude of the CoM of the acoustic energy). The H_0 to be tested was that these two criteria were equal on average for observations made before, during, and after trawling for both the bottom and midwater layers.

Comparisons of observations recorded before, during, and after the tows were sensitive to possible mixture of a trawl effect and a distance effect. The objective of the test was thus to disentangle how much the observed differences originated from the distance between the observations and from trawl effects, respectively. When the spatial distribution of fish is such that any two proximate values are naturally similar (strong spatial structure of the study variable), observations made before, during, and after a trawl station must be very similar in order for H_0 not to be rejected. On the other hand, if the spatial structure is weak, the average difference between two proximate values is naturally relatively large, and H_0 cannot be rejected, even for a relatively large discrepancy among observations made before, during, and after trawling. Tests were thus evaluated with regards to the similarity of 1000 randomly selected pairs of successive between-station observations sufficiently far away from trawl stations to preclude a trawl effect. For each survey, the following three differences were thus considered: during – before; during – after; and random1 – random2 (the first two being positive when the observations recorded during trawling operations were larger). These differences were considered relative to the mean values of the integrated NASC values and of the altitude of the CoM of the acoustic energy; both parameters were pooled by survey series. Empirical cumulative density functions (cdf) were thus built for each survey series and for bottom and midwater layers separately.

Finally, a paired Student test, robust to departure from normality, was used to test if mean differences were equal to zero. Given H_0, a large p value indicates a high likelihood that observed differences are consistent with a zero mean.

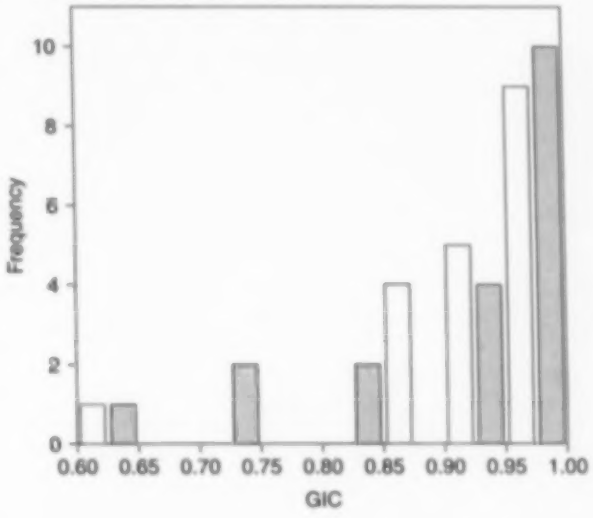

Fig. 6. Histogram of global indices of collocation (GIC values) between on-station and between-station spatial distributions of nautical area scattering coefficient (NASC) values, all surveys combined. Distinction between bottom layers (open bars: i.e., $GIC_{0\text{–}40}$ for the Barents Sea surveys and $GIC_{0\text{–}10}$ for the others) and midwater layers (shaded bars: i.e., $GIC_{40\text{–}100}$ for the Barents Sea surveys and $GIC_{10\text{–}40}$ for the others).

Time of day considerations

With the exception of the Barents Sea surveys, all surveys were performed during daylight and no impact of the time of the day was expected. In the Barents Sea, however, there is ample evidence that vertical zonation of gadoid fish can vary throughout the day or year (Hjellvik et al. 2002). In the present analysis, this would not be expected to have a major impact. For the pooled analyses, we have combined data for all times of day, and equal compensation is expected for both on-station and between-station data, as these are homogeneously distributed in time. For the before–during–after studies, each haul is matched to adjacent between-station data taken at the same time, thus reducing the impact of diel

© 2007 NRC Canada

Fig. 7. Variograms of log-transformed nautical area scattering coefficient (NASC), showing the average of normalized variograms per series of surveys. (*a*) Barents Sea surveys 1997–2002. International Bottom Trawl Surveys (IBTS): (*b*) Fisheries Research Services (FRS), (*c*) Centre for Environment, Fisheries, and Aquaculture Science (CEFAS) and (*d*) Institut Français de Recherche pour l'Exploitation de la Mer (IFREMER). (*e*) Northern Irish Bottom Trawl Surveys (NIBTS). Solid lines indicate between-station variograms; broken lines indicate on-station variograms. Computations considered omnidirectional distances. Distance lags are the elementary sampling distance unit (ESDU) for between-station NASC and the interstation distance for the on-station NASC. The quantile of active data is indicated (98% means that the most extreme 2% of the data was removed).

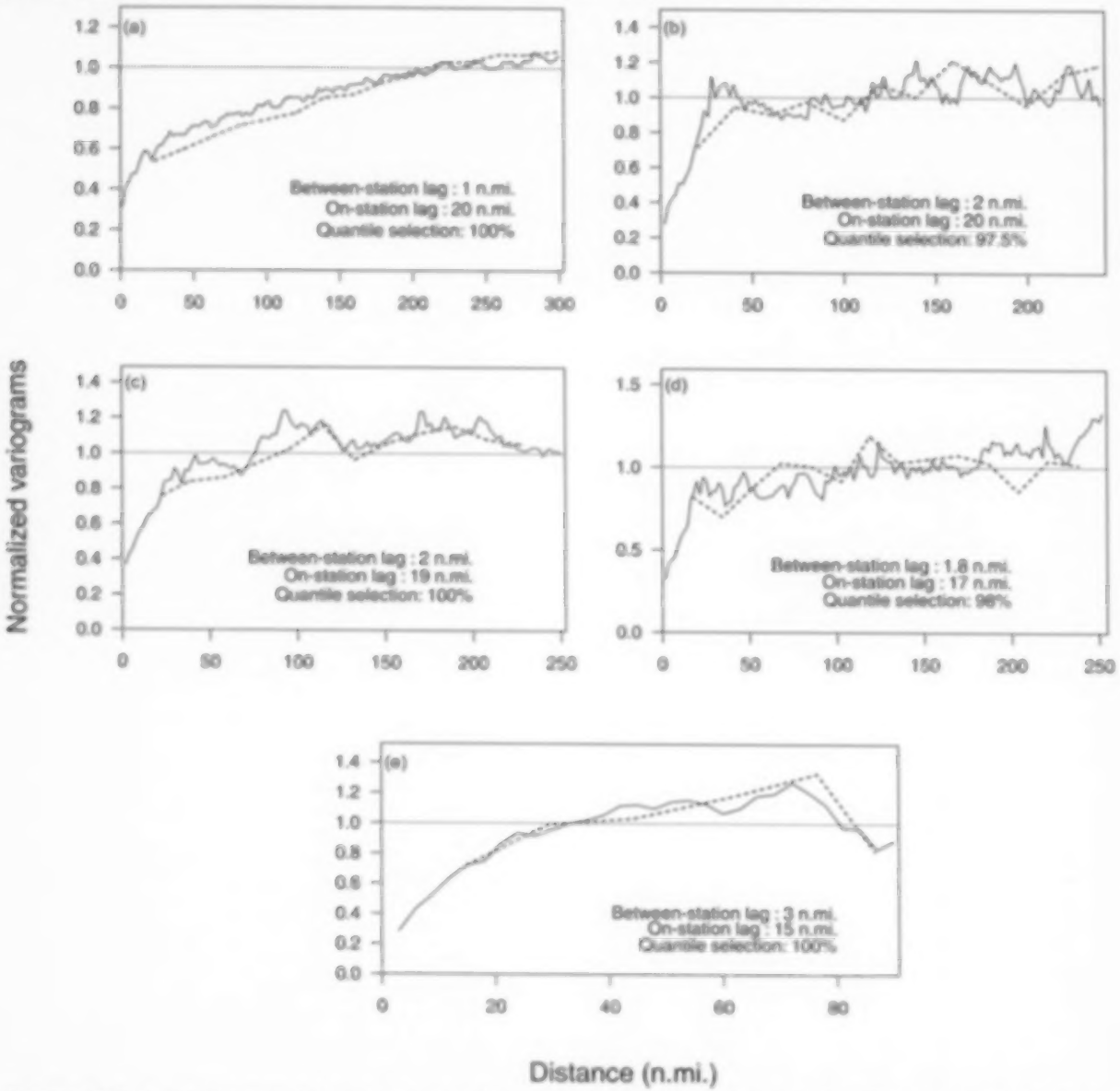

changes. Finally, surveys were taken at the same time of year (Table 1), thus reducing seasonal effects.

Coordinates transformations

To compute true distances between samples, coordinates were transformed to an orthogonal system. A gnomonic projection with a centre at 72°00′N, 30°00′E was used for the Barents Sea data. A transformation based on the cosine of the mean latitude of the coordinates was applied to the North Sea and the Irish Sea data separately.

Results

Vertical profiles

There is a clear and consistent trend in the vertical acoustic profiles across surveys and survey series (Figs. 3,

© 2007 NRC Canada

Fig. 8. Difference between the vertically integrated nautical area scattering coefficient (NASC) observed before, during, and after trawling (▽, (during – before) and (during – after)) and for two randomly selected successive between-station observations (□). The mean difference is indicated by the symbols and cumulative distribution of the differences is indicated by the lines. Each panel represents the pooled data for each survey series (see Table 1 for definitions). The *x* axis represents relative differences of NASC in m^2-n.mi.$^{-2}$ (1 n.mi. = 1.852 km). The y axis represents the empirical cumulative density function. Distinction is made between midwater layers (*a*) and bottom layers (*b*). *p* values of the Student tests are indicated; solid symbols represent values smaller than 0.1.

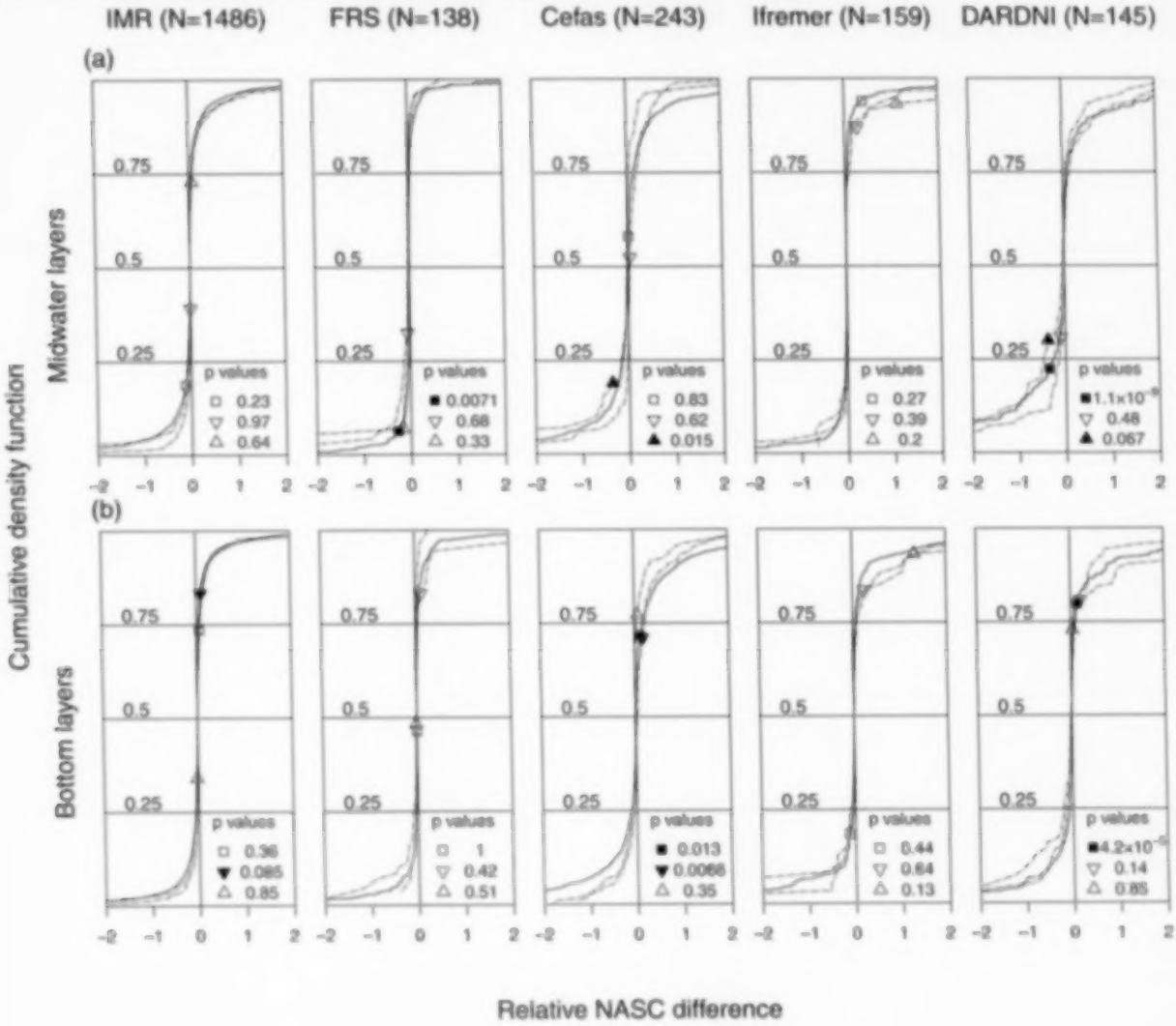

4, and 5). In general, the mean NASC value is highest in the depth layer closest to the bottom and decreases approximately exponentially over the next 5–9 m. Above this, the mean NASC is either relatively constant or decreases steadily both for on-station and between-station data. For the Irish Sea (Fig. 5) where a lot of the backscatter can be attributed to fish schools, the above-mentioned trend only appears after dense (pelagic) school echo traces have been excluded from the analyses. If these are retained, they result in a more bell-shaped vertical profile, with the maximum energy a few metres above the bottom. The match between on-station and between-station vertical profiles is nearly perfect for both represented quantiles for the Barents Sea case where the number of stations is large (Fig. 3), but less evident as the number of samples decreases (e.g., Irish Sea; Fig. 5). However, there is no general pattern of on-station or between-station profiles being systematically larger than the other. Similarly, the year-to-year differences in the vertical profiles are consistently reflected in both the on-station and between-station data, regardless of the number of samples.

Global Index of Collocation

The GIC values were greater than 0.9 in 75% of the surveys, suggesting a strong overall correspondance in the spatial distributions of NASC values between on-station

© 2007 NRC Canada

Fig. 9. Difference between the altitude of the centre of mass of the nautical area scattering coefficient (NASC) values observed before, during, and after trawling (▽, (during – before) and (during – after)) and for two randomly selected, successive, between-station observations (□).The mean difference is indicated by the symbols, and cumulative distribution of the differences is indicated by the lines. Each panel represents the pooled data for each survey series (see Table 1 for definitions). The *x* axis represents relative differences of NASC in m^2·n.mi.$^{-2}$ (1 n.mi. = 1.852 km). The *y* axis represents the empirical cumulative density function. Distinction is made between midwater layers (*a*) and bottom layers (*b*). *p* values of the Student tests are indicated; solid symbols represent values smaller than 0.1.

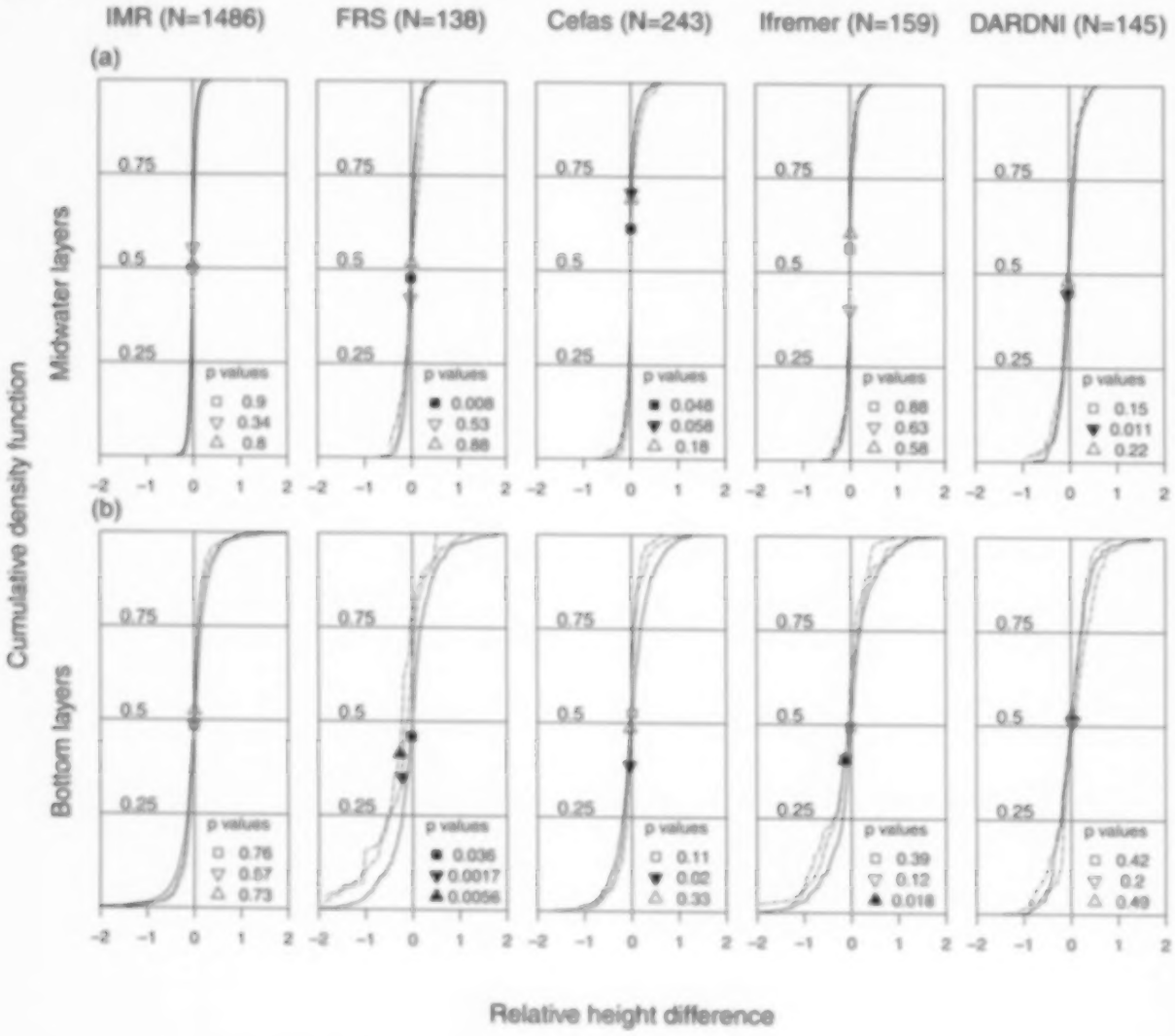

and between-station data (Fig. 6). The GIC was considerably lower (around 0.6) in only two cases where centres of mass of each distribution was far apart each other compared with the respective dispersion of each population (inertia).

No systematic difference in the GIC values was observed between the bottom and midwater layers. The midwater GIC values were generally smaller than those of the bottom layers (average GIC values of 0.91 and 0.93, respectively), but the difference was not statistically significant (Student's *t* test, *p* value = 0.57).

Variograms

The match between the log-transformed variograms for on-station and between-station data was very good for the Barents Sea surveys (Fig. 7*a*). For the other survey series (Figs. 7*b*–7*e*), a reasonable match was observed. However, in two cases (IBTS from FRS and IFREMER), this was only obtained after 2.5% and 2%, respectively, of the most extreme values were removed. The between-station data allowed resolution of the small-scale spatial structures that are inaccessible with the on-station data alone. This would lead to geostatistical models compounded of a nugget effect that

© 2007 NRC Canada

explains ~40% of the total variability (regardless of survey series) and of a component with an autocorrelation limit distance of 200 n.mi for the Barents Sea surveys and approximately 50 n.mi for the others.

Correlation before–during–after trawl

Integrated NASC for midwater layers and for bottom layers

All the cumulative histograms of the relative differences were symetrical with a narrow mode around zero (Fig. 8), indicating that in half of the cases NASC values were larger during trawling than before and after. Empirical cdf were visually highly consistent for a given survey series; the differences between them being larger between than within-survey series. The empirical cdf between the quantiles 25% and 75% were highly consistent. Differences were observed in the distributions' tails only. There was no evidence of the relative differences (during – before) and (during – after) having a systematically higher or lower spread than those obtained for randomly selected data. For bottom layers and for all surveys (Fig. 8*b*), NASC integrations were on average higher during the tow than before or after. However, these means were not significantly different from 0 in most cases (two p values out of ten below 0.1). Interestingly, the differences between randomly selected off-station data showed the same symetrical and skewed distributions and were considered equal to 0 for all but two cases as well. The picture was somewhat different for the midwater layers, where the NASC values were alternatively smaller and larger during trawling than before or after. This, however, was rarely statistically significant (two p values out of ten below 0.1). Here again, the average differences between randomly selected off-station data were considered not equal to 0 for two cases.

Differences in altitudes of the CoM for midwater layers and for bottom layers

Differences in altitudes of the CoM from NASC values showed weaker tails and weaker modes than the integrated NASC values did resulting in similar medians and means (Fig. 9). For the bottom layers (Fig. 2), the majority of the observed differences were less than 1 m. In only one case (FRS) did the differences (during – before) and (during – after) show empirical distributions shifted towards lower values compared with that of the reference situation. Despite the fact that the mean of the latter was significantly different from zero, this was the sole case where we observed a reduction of the mean heigh of the acoustic energy associated with trawling activities. None of the other cases indicated an impact of trawl presence: average differences were alternatively positive or negative, the proportion of p values smaller than 0.1 was similar for cases with the trawl and without, and the differences between empirical cdf were larger between survey series than within. Interestingly, the (during – before) and (during – after) trawling differences observed in the Barents Sea surveys were more concentrated around zero than the differences observed where no trawl was in the water; variations in vertical distributions were thus smoothed when the trawl was present.

Fig. 10. Global indices of collocation (GIC) for simulated situations. Fish distributions are considered to be isotropic and have a Gaussian distribution with fish density being set to zero for densities below the 5% quantile. Two types of fish populations are concerned (patchy (Population 1) or spread (Population 2)). Several possible distances between the centres of mass are concerned.

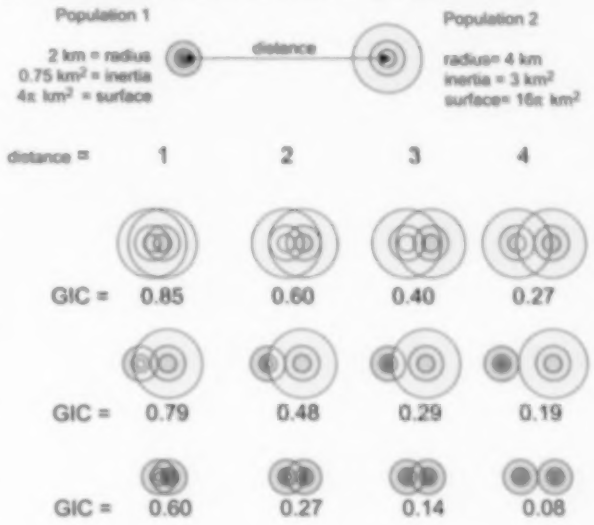

Discussion

With the final goal to combine acoustic and catch data, which was not considered in this study, we examined the hypothesis that acoustic data collected away from the trawl stations were consistent with those collected during the trawling operations. Rather than examine one survey with a particular format, we chose to study a series of different surveys ranging from the Barents Sea to the North Sea and Irish Sea to attempt to identify broad trends in this type of data. The major differences between the data sets were the numbers of data points available on-station and the proportion of stations connected with acoustic transects. The Barents Sea surveys included between 200 and 300 trawl stations per survey, whereas in the North and Irish seas surveys included between 13 and 80 stations. IBTS data were only taken in daylight hours, with the last station of the day and the first one of the following day not being connected by acoustic transects. As a consequence, relationships between on-station and between-station observations are likely to be more apparent for the Barents Sea than for any of the other surveys.

The first type of analysis was a straightforward global comparison using all the available data for the pooled NASCs by layers for the on-station and between-station data. The general pattern was broadly consistent across all the surveys. The bulk of the acoustic energy was found in the deepest layers in the water column; the backscattering energy reduces exponentially as the range from the seabed increases and then stabilizes somewhere between 5 and 10 m off the bottom. More importantly, the pattern is similar for both on-station and between-station data. Where differences occurred, they were not systematic, as on-station integrated

© 2007 NRC Canada

Fig. 11. Scale representation of the observation protocol. North Sea and Irish Sea survey protocols are not distinguished.

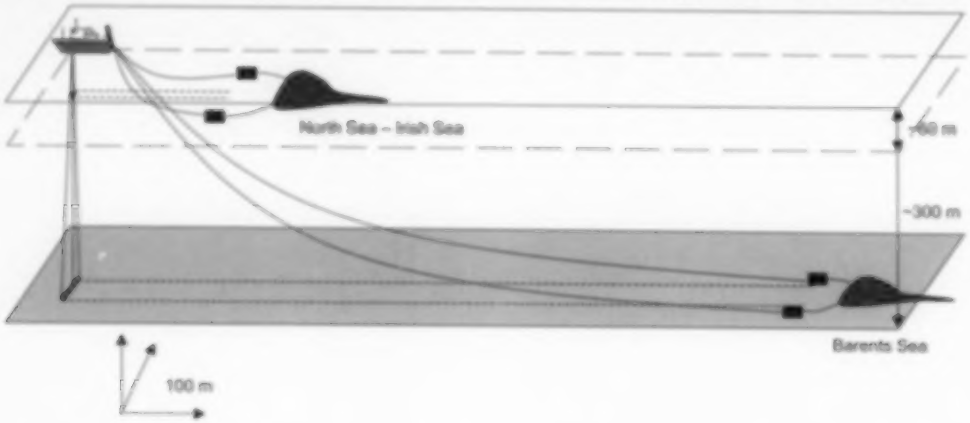

values could be both greater or less than between-station data. Furthermore, where deviations from the general pattern occurred in a particular survey, they were seen in both on-station and between-station data.

The GIC values confirmed the subjective appraisal of the vertical profiles. To help interpretations, GIC values were computed for simulated fish distributions (isotropic Gaussian fish density with fish density being set to zero for densities below the 5% quantile). From this simulation, it was concluded that a GIC between 0.6 and 0.8 could be considered as a low value, and a threshold of 0.8 might be adopted as a minimum value for a good match (Fig. 10). For the bottom layers, only 1 survey out of 20 showed a poor match, and this had low station numbers (N^o = 46). Slightly poorer results were obtained for the midwater layers, with 3 out of the 20 surveys having low GIC values. NASC values were generally much lower in the midwater layers and also much more variable, so this outcome is not surprising.

The variograms allowed a more detailed study of the spatial structures associated with the on-station and between-station data. For the Barents Sea data, the relatively high number of stations allowed the generation of good quality variograms for on-station and between-station data. These variograms were highly similar. For the other surveys, the variograms were less well-behaved, reflecting the smaller number of samples relative to the sampling area and the large skewness of the data. However, they were also similar, provided that some extreme values were removed in two cases. Variograms were considered relative to their variances; we only compared their shapes. The variance of the between-station data was often larger than the variance of the on-station data because the chances of encountering rare extreme fish concentrations is higher with several thousand samples than with a few dozen or a few hundred samples (Bouleau and Bez 2005). Still, the strong similarity in the shapes of the variograms would allow using the spatial structures depicted by the between-station data (rescaled to the on-station data variance) to obtain a variogram model usable for the purpose of quantitative estimation. It is worth reiterating here that the variograms were computed with log-transformed data. This nonlinear transformation induces bias, and the variograms obtained here cannot be directly used for estimation purposes. Both the log-transformation and the selection of a certain quantile (97.5% or 98%) of the data aim to reduce the impact of the extreme data. This is not at odds with the fact that most of the total abundance is explained by a very small proportion of data. As a matter of fact, it is usually agreed that fish data behave like lognormal variables. When simulating a lognormal variable, the likelihood of getting an extreme value increases with the number of samples. Therefore, we could not have expected on-station data to sample the tails of the distributions with the same accuracy as the between-station data, the latter being much more numerous than the former. In addition, the impact of few extreme values on empirical variograms is known to be large and not meaningful for the comparative exercise we did in this study. In other words, what made between-station variograms different from the on-station variograms was only the occurrence of extreme rare data. The bulk of the observations had spatial distributions that matched well.

The final step in the analysis was to examine the relationship between on-station and between-station data in the areas close to each haul. For this comparison, we only used the most adjacent between-station data to each haul. However, given the survey protocol, a small but non-zero distance existed between observations made before, during, or after trawling. To disentangle how much of the observed differences originated from the distance between the observations and from a possible trawl effect, we bootstrapped between-station data to serve as a reference situation for the comparisons. We found that both before and during trawling data and during and after trawling data were, with one exception, not more different than two successive, randomly selected between-station data (the distributions of their differences are strongly similar). The statistical approach is designed so that under H_0, 10% of the p values are below 0.1. In this study, 25% (10 out of 40) of the p values obtained when testing on station data with adjacent ones were smaller than 0.1 (six times for the (during – before) differences and four times for the (during – after) differences). Contrary to expectation, this proportion was 35% (7 out of 20) for the so-called reference situations provided by the bootstrapped between-station data. The null hypothesis that the average difference in biomass or in height of the CoM for observa-

© 2007 NRC Canada

tion made before, during, or after trawling was thus acceptable.

Most critically for the purposes of this analysis, the inference supported by all the results is that we see similar energy values on-station and between stations, suggesting that we were observing the same fish assemblages in the two situations. However, there is some evidence in the literature of fish reaction to research vessels during trawling (e.g., Godø et al. 1999; Handegard et al. 2003). Reactions can be both vertical, as in diving, or horizontal, as in moving out of or towards the path of the trawl. We shall distinguish between gear- and vessel-induced reactions. In the Barents Sea for instance, Handegard et al. (2003) showed that the fish present in the first 40 m above the seabed exhibit a slight diving reaction to the vessel passing and a marked horizontal reaction to the warp. Given the mean depths of the study areas, the distances between the acoustic beam beneath the vessel and the trawl ranged from 100–200 m for Irish Sea and North Sea to more than 500 m for the Barents Sea (Fig. 11). It is likely, though, that if the gear does not perturb the fish distribution long in advance (long with regards to the above-mentioned distances), onboard-mounted echosounders can only reveal vessel perturbations. In such a case, the only expected perturbation comes from the vessel that is running both between-station and on-station; the two situations are therefore comparable.

We shall also distinguish reactions that lower fish acoustic densities from reactions that increase them. Fish diving would tend to increase fish biomass in the metres above the seabed. It would also tend to increase tilt angle and hence reduce target strength (MacLennan et al. 1987; Kloser and Horne 2003; McQuinn and Winger 2003). Fish may also move into the acoustic dead zone (Ona and Mitson 1996; Lawson and Rose 1999) and be inaccessible to the echosounder. In the present study, the statistically nonsignificant but systematic stability or increase of NASC value in the bottom layers during trawling is associated neither to a corresponding systematic decrease of NASC values in the midwater layers nor to a change in height of the mean energy in any of the bottom or midwater layers. This suggests that none of the above-mentioned gear-avoidance behaviours are operating in the study situations and that the area of influence of gear perturbations is, on average, less than the trawl-to-vessel distances. This does not suggest that trawl perturbations do not exist, but rather that they cannot be observed with onboard-mounted echosounders. In particular, gear perturbations were considered to explain the lack of correlations observed between the acoustic signal and catch data or to explain why the highest correlations between acoustic and trawl catches were obtained after acoustic data were integrated over a greater depth than that of the headline height of the trawl (Bouleau et al. 2003; Hjellvik et al. 2003).

In conclusion, the acoustic data collected between trawl stations were consistent with the acoustic data collected on stations. Overall, there was good agreement between the two data sets, while there were some exceptions in some individual survey series. Poor matches could be explained by the sparseness and the skewness of the corresponding data. The Barents Sea case shows what can be achieved for bottom layers with a more substantial data set, where in all cases the on-station and between-station data were consistent for all indicators and methods. In this case, the correlation between catch data and on-station acoustics data is high, making it possible to use between-station acoustics to enhance the quality of trawl survey abundance indices.

Acknowledgements

This study is part of the EU-funded project CATEFA No. Q5RS-2001-02038 (Combining Acoustic and Trawl data for Estimating Fish Abundance). Authors are also grateful to one of the reviewers who made precise suggestions of modifications to the text.

References

Aglen, A., and Nakken, O. 1997. Improving time series of abundance indices applying new knowledge. Fish. Res. **30**: 17–26.

Bez, N. 2007. Spatial statistics for assessing and describing marine resources: the transitive geostatistical approach and the statistics per individual. Journal de la Société Française de Statistique. In press.

Bez, N., and Rivoirard, J. 2000. Indices of collocation between populations. *In* Report of a workshop on the use of Continuous Underway Fish Egg Sampler (CUFES) for mapping spawning habitat of pelagic fish. *Edited by* D.M. Checkley, J.R. Hunter, L. Motos, and C.D. van der Lingen. GLOBEC Rep. **14**. pp. 1–65.

Bouleau, M., and Bez, N. 2005. Using a Markov-type model to combine trawl and acoustic data in fish surveys. *In* Geostatistics for environmental applications. *Edited by* P. Renard, H. Demougeot-Renard, and R. Froidevaux. Springer, Berlin. pp. 111–123.

Bouleau, M., Bez, N., Hjellvik, V., Godø, O.R., Reid, D., Beare, D., Greig, T., Amstrong, M., Gerritsen, H., Mackinson, S., Neville, S., van der Kooij, J., Vérin, Y., and Massé, J. 2003. Differences between near bottom biomass spatial structure observed in the Irish Sea, the North Sea and the Barents Sea in recent years. ICES CM 2003/Q:17.

Cachera, S., Massé, J., and Vérin, Y. 1999. How the use of acoustics during bottom trawl surveys may provide more accurate abundance indices: an application to IBTS surveys carried out in the southern North Sea. ICES-CM-1999/J:12.

Diner, N., and Marchand, P. 1995. Acoustique et pêche maritimes. Ed IFREMER, Plouzané.

Fernandes, P.G., Brierley, A.S., Simmonds, E.J., Millard, N.W., McPhail, S.D., Armstrong, F., Stevenson, P., and Squires, M. 2000. Fish do not avoid survey vessels. Nature (London), **404**: 35–36.

Fréon, P., and Misund, A.A. 1999. Dynamic of pelagic fish distribution and behaviour: effects on fisheries and stock assessment. Fishing News Books, Oxford, UK.

Godø, O.R., Somerton, D., and Totland, A. 1999. Fish behaviour during sampling as observed from free floating buoys: application for bottom trawl survey assessment. ICES-CM-1999/J:10.

Gunderson, D.R. 1993. Surveys of fisheries resources. John Wiley and Sons, New York.

Handegard, N.O., Michalsen, K., and Tjøstheim, D. 2003. Avoidance behaviour in cod (*Gadus morhua*) to a bottom trawling vessel. Aquat. Living Resour. **16**: 265–270.

Hjellvik, V., Godø, O.R., and Tjøstheim, D. 2002. Diurnal variation in bottom trawl survey catches: does it pay to adjust? Can. J. Fish. Aquat. Sci. **59**: 33–48.

Hjellvik, V., Michalsen, K., Aglen, A., and Nakken, O. 2003. An attempt at estimating the effective fishing height of the bottom

© 2007 NRC Canada

trawl using acoustic survey recordings. ICES J. Mar. Sci. **60**: 967–979.

Kloser, R.J., and Horne, J.K. 2003. Characterizing uncertainty in target strength measurements of a deep water fish: orange roughy (*Hoplostethus atlanticus*). ICES J. Mar. Sci. **60**: 516–523.

Korsbrekke, K., Mehl, S., Nakken, O., and Pennington, M. 2001. A survey based assessment of the north east arctic cod stock. ICES J. Mar. Sci. **58**: 763–769.

Krieger, K., Heifetz, J., and Ito, D. 2001. Rockfish assessed acoustically and compared to bottom trawl catch rates. Alaska Fish. Res. Bull. **8**: 71–77.

Lawson, G.L., and Rose, G.A. 1999. The importance of detectability to acoustic surveys of semi-demersal fish. ICES J. Mar. Sci. **56**: 370–380.

MacLennan, D.N., Magurran, A.E., Pitcher, T.J., and Hollingworth, C.E. 1987. Behavioural determinants of fish target strength. Rapp. P.-V. Réun. CIEM, **189**: 245–253.

MacLennan, D.N., Fernandes, P.G., and Dalen, J. 2002. A consistent approach to definitions and symbols in fisheries acoustics. ICES J. Mar. Sci. **59**: 365–369.

McQuinn, I.H., and Winger, P.D. 2003. Tilt angle and target strength: target tracking of Atlantic cod (*Gadus morhua*) during trawling. ICES J. Mar. Sci. **60**: 575–583.

Michalsen, K. 1999. Distribution of gadoids in the Barents Sea: impact on survey results. Ph.D. thesis, University of Bergen, Norway.

Mitson, R.B., and Knudsen, H.P. 2003. Causes and effects of underwater noise on fish abundance estimation. Aquat. Living Resour. **16**: 255–263.

Ona, E., and Mitson, R.B. 1996. Acoustic sampling and signal processing near the seabed: the deadzone revisited. ICES J. Mar. Sci. **53**: 677–690.

Rivoirard, J., Simmonds, J., Foote, K., Fernandes, P., and Bez, N. 2000. Geostatistics for estimating fish abundance. Blackwell Science Ltd., Oxford.

© 2007 NRC Canada

Instructions to Authors

Canadian Journal of Fisheries and Aquatic Sciences

Scope of the Journal and guidelines for papers

The Journal welcomes manuscripts reporting significant new knowledge and understanding of fisheries and aquatic sciences. Manuscripts may concern cells, organisms, populations, communities, ecosystems, or processes that affect aquatic systems. They may cover a range of disciplines including biology and ecology of marine and freshwater organisms, limnology, oceanography, physiology, toxicology, genetics, economics, disease, and management. Manuscripts are selected for publication according to the extent and significance of new knowledge or ideas presented. Preference will be given to manuscripts that emphasize understanding of observed phenomena and interpretation of experimental results.

We encourage papers that lead from clearly stated purpose or rationale, and from testable hypotheses, concepts, or questions, to identifiable conclusions or syntheses. Such papers may amplify, modify, question, or redirect accumulated knowledge embodied in contemporary perceptions of a particular state of aquatic sciences. **Rationale for the study and interpretation of the results should be set in a broad disciplinary or interdisciplinary context.** Methodological and modeling papers should include applications and provide verification of enhanced performance.

We continue to discourage papers that are essentially descriptive, except in emerging disciplines; have only site-specific or local applications (a certain year, place, taxon, chemical compound, etc.); confirm only previously established principles; or apply standard techniques without breaking new methodological ground. Studies that are clearly preliminary or fragmentary, or whose relevance to broader issues is not demonstrated, and interpretations solely of an unsupported speculative nature will not be entertained.

Manuscripts submitted should be as comprehensive as possible; if a single paper can not be produced, then closely related papers should be cross-referenced and submitted together.

Types of papers

The Journal considers the following types of contributions:

Articles — Studies of broad scope that are original contributions to science.

Perspectives — Syntheses, critical reviews, and reevaluations of current concepts and paradigms.

Discussions — Comment and Reply on subjects recently published in the Journal.

Rapid communications — New concepts, methodology, and topical or controversial subjects.

Guidelines for these contribution types are available from the Editorial Office's Web site (uoguelph.ca/~cjfas/).

Language

Papers must be clearly and concisely written in **good English or French**. Authors whose native language is not English or French should consult someone fluent in English or French prior to submission of the manuscript. Good writing improves the speed and effectiveness of review and publication.

Abstracts should be submitted in the language of the paper. They will be translated into the other official language by the Journal translator. However, authors able to submit abstracts in both fluent English and French are encouraged to do so.

Page charges

There are **no page charges** for publication in the *Canadian Journal of Fisheries and Aquatic Sciences*.

Purpose of these instructions

To **facilitate publication**, authors must check symbols, abbreviations, and technical terms for accuracy, consistency, and readability. NRC Research Press maintains the right to preserve the technical quality of the Journal. Authors are requested to refer to a recent issue of the Journal for details of layout, especially for tables and reference lists. **Manuscripts and illustrations must meet the requirements outlined below; otherwise, publication may be delayed**.

To submit

New manuscripts

Manuscripts can be submitted by either the Web or e-mail (cjfas@uoguelph.ca). Web submission via OSPREY (Online Submission and Peer Review) is encouraged.

Via the Web

Authors may submit manuscripts at the OSPREY Online Submission and Peer Review site (pubs.nrc-cnrc.gc.ca/cjfas/osprey). OSPREY is best viewed in Netscape 7.0 or higher or Internet Explorer 6.0 or higher. During registration, authors choose a username/password. The security of manuscripts is protected by the username/password system. Authors may register at any time on the site, but should register only once. Those individuals who have submitted to or reviewed for the Journal in the past will have an existing profile in OSPREY and may access it by entering their e-mail address in the "Forgot Your Password" field on the Web site.

For technical support at any point during submission, contact Louis Lafleur (613-998-9432; louis.lafleur@nrc-cnrc.gc.ca) from 8:00 am to 4:00 pm EST.

A user manual with full instructions is available on the Web site.

Authors must submit at least a cover letter and manuscript; tables and figures may be included in the manuscript file, or may be uploaded separately. OSPREY accepts files in most

© 2007 NRC Canada

common text and graphics formats (see complete list of formats on the Web site).

Research Press is not currently accepting MS Word 12 documents (.docx extension). Please note that saving .docx documents to other formats (i.e., .doc, .rtf, or .txt) will likely lead to changes to or losses in formatting or other data. Authors saving .docx manuscripts to other formats are requested to check their manuscripts carefully before submission for any losses or other errors.

When first submitting a manuscript for peer review, low-resolution versions of figures should be uploaded to limit file size. When submitting, authors should be working at a computer where all of the relevant files for their paper are available. Submission of a typical manuscript requires about 10 minutes, but upload time depends on the speed of the Internet connection.

All correspondence about manuscripts submitted through OSPREY will be sent to the person listed as the corresponding author during submission. Correspondence is by e-mail.

Revised manuscripts

For revisions, the corresponding author will be contacted by e-mail and asked to submit a revision.

Accepted manuscripts

The author will be contacted to advise him or her of acceptance and asked to provide the final accepted manuscript and all associated files for tables, figures, and supplementary data via OSPREY or e-mail.

Text (including tables) should be provided in a word-processing format (any form of WordPerfect, Microsoft Word, or TeX is preferable, Windows or Macintosh platform). TeX macros for preparing accepted papers for submissions are available at ftp.tex.ac.uk/tex-archive/macros/latex/contrib/nrc/, ftp.dante.de/tex-archive/macros/latex/contrib/nrc/, and ctan.tug.org/tex-archive/macros/latex/contrib/nrc/.

To ensure the highest possible quality reproduction and printing of figures, authors should prepare figure files as follows.

(*i*) Upload figure files separately from the manuscript.

(*ii*) Ensure that the files are high resolution.

(*iii*) Ensure that figures are in their original file format (i.e., PhotoShop, Adobe Illustrator, Excel, CorelDraw, SigmaPlot, etc.) rather than embedded in a Word document or converted to a derived format. However, if figures are in a format that NRC Research Press does not accept, high-quality high-resolution PostScript or PDF files are acceptable. Sending files in more than one format is fine; the publisher will use the format that will reproduce the best.

(*iv*) Ensure that they are uploading the most recent, correct versions of the files.

Other information regarding submission

Cover letter

The corresponding author should send a cover letter with the submission that

(*i*) states the main points and significance of the work;

(*ii*) avows that all coauthors fully participated in and accept responsibility for the work;

(*iii*) avows that the manuscript is not being considered for publication elsewhere;

(*iv*) suggests potential referees;

(*v*) identifies other manuscripts, including "extended abstracts", containing the same, similar, or related information, from which other manuscripts may be generated;

(*vi*) includes the telephone and fax numbers, as well as e-mail and current mailing addresses, of all authors;

(*vii*) explains any real or perceived conflicts of interest (see Ethics section, Conflict of interest and disclosure).

Copyright assignment or license

If the Editors agree to consider a submitted manuscript for publication, the Editorial Office will request the return as soon as possible of copyright assignment and (or) license forms signed by all authors. Before a manuscript can be accepted for publication, all authors are required to complete a copyright assignment or license form assigning or licensing rights to NRC. Most authors will sign the assignment form, which transfers all rights to NRC. Employees of the government in Commonwealth countries will sign a license form that allows them to retain Crown copyright, and employees of the US government will sign a form agreeing to publication, since no US copyright exists. Copyright transfer forms are available from the Editors, in the first issue of the volume, or on the Web site of the Journal (pubs.nrc-cnrc.gc.ca/cgi-bin/rp/rp2_desc_e?cjfas).

Editorial process

Receipt of manuscripts

Once the Editors have decided to consider the manuscript for publication, the corresponding author of a submitted manuscript will receive a formal acknowledgement letter and will be requested by the Editorial Office to complete necessary forms as soon as possible. If the Editors have decided not to consider it for publication, then the corresponding author will be notified of this decision via e-mail.

The manuscript is read and examined for conformity to these *Instructions to Authors* by the technical editor. Failure to meet the criteria outlined may result in return of the manuscript for correction before evaluation.

Peer review/evaluation

Each manuscript is normally submitted to two referees for appraisal. However, the Senior Editor will return unreviewed those manuscripts that do not fall within the Journal's scope or character, and those that exceed the Journal's guidelines for prior publication as "extended abstracts" (guidelines available from the Editorial Office's Web site at uoguelph.ca/~cjfas/). Papers submitted for inclusion in supplements are treated with the same rigor of review as articles in regular issues.

Responses to referees and revisions to manuscripts should normally be completed within 90 days. Manuscripts not returned within 90 days of receipt may be treated as new submissions unless the authors contact the Editorial Office.

Resubmitted manuscripts

Authors resubmitting a manuscript after previous rejection or withdrawal must indicate the manuscript number assigned to the previous submission in their cover letter. Resubmitted

© 2007 NRC Canada

manuscripts are treated as new papers. Authors may submit the new manuscript by e-mail or via OSPREY, along with a detailed, point-by-point reply to all issues raised during the previous evaluation.

Publication process

General

The Editorial Office checks all accepted manuscripts for conformation to the *Instructions to Authors* and to ensure that all necessary paperwork is present. Any areas that are identified as problematic will be addressed by the Editorial Office in consultation with the corresponding author. Once the Editorial Office has resolved any problems with the manuscript and the original signed Assignment of Copyright forms have been received from all authors, the manuscript is forwarded to NRC Research Press in Ottawa for publication. The papers are prepared for publication by a professional copy editor responsible for ensuring that the final printed work is consistent in form and style.

Correspondence with NRC Research Press

Once the paper has been accepted, all correspondence should be with NRC Research Press, National Research Council of Canada, Ottawa, ON K1A 0R6, Canada (fax: 613-952-7656; e-mail: pubs@nrc-cnrc.gc.ca; URL: pubs.nrc-cnrc.gc.ca). NRC Research Press may make editorial changes as required, but will not make substantive changes in the content of a paper without consultation with the author and the Senoir Editor.

Galley proofs

A galley proof, illustration proofs, the copy-edited manuscript, and a reprint order form are sent to the corresponding author. **Galley proofs must be checked very carefully, as they will not be proofread by NRC Research Press,** and must be returned within 48 hours of receipt. The proof stage is not the time to make extensive corrections, additions, or deletions, and the cost of changes introduced at the proof stage and deemed to be excessive will be charged to the author.

Reprints

If reprints are desired, the reprint order form must be filled out completely and returned with payment (cheque, credit card number, purchase order number, or journal voucher) together with the corrected proofs and manuscript. Orders submitted after the Journal has been printed are subject to considerably higher prices. **The Journal does not provide free reprints, and reprints are not mailed until a purchase order number or payment is received**.

Permission to reproduce copyright material

Whenever a manuscript contains material (tables, figures, charts, etc.) that has been previously published and, hence, is protected by copyright, it is the obligation of the author to secure **written permission from the holder of the copyright** to reproduce the material **for both the print and electronic formats**. These letters must accompany the submitted manuscript; otherwise, publication may be delayed. All material designated as "taken from ..." must be accompanied by a letter of permission. If the material is not to be reproduced exactly as in the original, it should be designated as "modified from ...". In either case, the source of the material must be included in the reference list.

Permission to reprint material published in NRC journals

Requests for permission to reproduce or republish the paper, in whole or in part, should be sent to NRC Research Press, Roxanne Landriault (613-990-2254; e-mail: roxanne.landriault@nrc-cnrc.gc.ca).

Ethics

General

The ethical standards expected of authors, referees, and editors are described in the NRC Research Press Publication Policy (published in the January 1996 issue of the *Canadian Journal of Fisheries and Aquatic Sciences*, on the Journal Web site at pubs.nrc-cnrc.gc.ca/cgi-bin/rp/rp2_cust_e?pubpolicy, or upon request).

Duplicate and prior publication

It has long been a policy of the *Canadian Journal of Fisheries and Aquatic Sciences* to not publish manuscripts that have been published elsewhere. The Senior Editor considers a paper not eligible for publication if most of the content of the paper (*i*) is under consideration for publication or is published in a journal or book chapter; or (*ii*) is under consideration for publication or is published in a conference proceedings or a government publication, with a substantial circulation (distributed to 100 or more individuals over a wide area). Authors may place a draft of a submitted article on their Web site or their organization's server, provided that the draft is not amended once accepted for publication. We encourage authors to insert hyperlinks from preprints to the final published version on the NRC Research Press Web site (pubs.nrc-cnrc.gc.ca). Abstracts or extended abstracts related to conferences do not constitute prior publication. Extended abstracts are usually under 1000 words and do not include presentation of detailed tables and graphics of the results of the study. Further guidelines on extended abstracts are available from the Editorial Office's Web site (uoguelph.ca/~cjfas/).

Assurance of authorship

In the cover letter, the corresponding author must affirm that all of the authors have contributed substantially to the manuscript and approved the final submission.

Suggesting reviewers

Authors may suggest names of referees that may or may not be used, but the selection of the referees is at the discretion of the Editors. When suggesting referees, please provide full addresses, telephone and fax numbers, and e-mail if available.

Conflict of interest and disclosure

The Senior Editor recognizes that authors and peer reviewers may have real or perceived conflicts of interest arising from intellectual, personal, or financial circumstances of their research. Submitted manuscripts should include full disclosure of funding sources for the research and the letter of transmission should include an explanation of any real or per-

© 2007 NRC Canada

ceived conflicts of interest that may arise during the peer review process. Failure to disclose such conflicts may lead to refusal of a submitted manuscript.

Photos of people

If a person pictured in a photo is identifiable, his or her permission is required to publish the photo. The person must be asked to sign a letter or form allowing NRC Research Press to publish the photo.

Photo manipulation

Authors should be aware that the Journal considers digital images to be data. Hence, digital images submitted should contain the same data as the original image captured. Any manipulation using graphical software should be identified in the methods, including both the name of the software and the techniques used to enhance or change the graphic in any way. Such a disclaimer ensures that the methods are repeatable and ensures the scientific integrity of the work. The removal of artefacts or any (nonintegral) data held in the image is discouraged.

Parts of the manuscript

Format and organization

The manuscript should be typewritten, **double-spaced**, on paper 21.5 × 28 cm (8.5 × 11 in. or ISO A4). Each page should be numbered, beginning with the title page. Continuous line numbers should also be included for the text. For material that is to be set in italics, use an italic font; do not underline. Use capital letters only when the letters or words should appear in capitals.

Organize the manuscript on the basis of the purpose or scope of the study as stated in the Introduction. Ensure that the title and headings are in harmony with the statement of purpose.

Before writing any of the manuscript, list tentative headings in as few ranks as possible. Rework them until they appear to allow logical development for the reader; usually, chronological order is not effective. The findings will be more readily appreciated if methods, findings, and discussion are given in separate sections.

Organize tables and figures to facilitate comparisons, grouping related data in as few tables and figures as feasible. As far as possible, make the tables and figures clear without reference to the text.

Begin sections and paragraphs with topic sentences containing generalizations that lead readily to the particulars. Giving a conclusion first and then supporting it not only improves readability but also facilitates assessment by other scientists. Failure to give the most newsworthy generalizations first is one of the most prominent shortcomings in the presentation of manuscripts.

Assure that everything in each section is relevant to the heading and that everything in each paragraph is relevant to the topic (opening) sentence.

Before writing any paragraphs, try writing the topic sentences for all of them and arranging these in appropriate order.

Title

Limit the title to what is documented in the manuscript. It is the key to the article and should clearly and concisely reveal what appears in the paper itself. The title serves two functions: (*i*) it allows the reader to judge whether the article is of potential interest and (*ii*) it should provide enough information to permit the reader to judge the scope and potential importance of the article. Words in the title should convey a maximum amount of information and identify the nature of the research, organism used, and where appropriate, the technical approach (e.g., X-ray, chromatography, mathematical analysis). Titles should not begin with a numeral or introductory prepositions such as "On" or "Towards" or expressions such as "A contribution to ..." or "Investigations on ..." Good titles greatly assist scientists and librarians in using scientific literature and aid indexers in preparing titles for keyword indexes. Series titles should be avoided.

Title page

The title page should contain the following. (*i*) The full title of the paper. (*ii*) Authors listed in the order in which they are to appear at the head of the printed article. (*iii*) Affiliation and address (including e-mail address) for each author. This should reflect the affiliation and address at the time of the study. Indicate current affiliations and addresses (including e-mail addresses) that differ from those in the by-line in a footnote. (*iv*) Name, address, telephone number, fax number, and e-mail address of the author responsible for correspondence.

Authors' names

The Senior Editor urges all authors to use full forenames rather than initials and (or) one forename.

Abstract

An abstract is required for every contribution and should contain accurate descriptive words that will draw the reader to the content. This is particularly important because contemporary alerting services and search engines will search this text. It should not be more than 175 words and should appear on a separate page. The concise abstract should present the paper content accurately and should supplement, not duplicate, the title in this respect. Authors able to submit abstracts in both fluent English and French are encouraged to do so. Abstracts submitted in one language will be translated into the other official language by the Journal translator. References should not be cited in the abstract unless they are absolutely essential, in which case full bibliographic information must be provided.

Like the title, the abstract enables readers to determine the paper's content and decide whether they need to read the entire paper. Begin the abstract with the main conclusion from the study, and support it with the relevant findings. Limit details of methods to those needed in understanding what was done and work them into statements of findings. Avoid using phrases such as "... is discussed" or "... was found"; be specific. As the abstract is often divorced from the main body of the paper by abstracting and indexing services and is the only part of a paper some readers ever see, it is important that it accurately reflect the paper's contents and be completely self-contained (i.e., any *essential* references) in a retrievable form (e.g., R.B. Deriso. 1980. Can. J. Fish. Aquat. Sci. **37**: 268–282).

Introduction

Limit the Introduction largely to the scope, purpose, and rationale of the study. Restrict the literature review and other

© 2007 NRC Canada

background information to that needed in defining the problem or setting the work in perspective. Try beginning with the purpose or scope of the work, defining the problem next, and adding guideposts to orient the reader. An introduction generally need not exceed 375–500 words.

Materials and methods

Materials and methods provides the framework for getting answers to the questions posed in the purpose of the work.

Limit the information on materials and methods to what is needed in judging whether the findings are valid. To facilitate assessment, give all the information in one section when possible. Refer to the literature concerning descriptions of equipment or techniques already published, detailing only adaptations. Often, it helps to begin statements on procedures with a phrase indicating the purpose, such as "To determine ... we ...". If the section is long, consider using subheadings corresponding to headings for the findings.

Results

Limit the results to answers to the questions posed in the purpose of the work and condense them as comprehensively as possible. Give the findings as nearly as possible in the terms in which the observations or measurements were made so as to avoid confusion between facts and inferences. State noteworthy findings to be noted in each table and figure, and avoid restating in the text what is clear from the captions. Material supplementary to the text can be archived in the report literature or a recognized data depository and referenced in the text (see Supplementary material section).

Discussion

Limit the Discussion to giving the main contributions of the study and interpreting particular findings, comparing them with those of other workers. Emphasis should be maintained on synthesis and interpretation and exposition of broadly applicable generalizations and principles. If these are exceptions or unsettled points, note them and show how the findings agree or contrast with previously published work. Limit speculation to what can be supported with reasonable evidence. End the Discussion with a short summary of the significance of the work and conclusions drawn. If the Discussion is brief and straightforward, it can be combined with the Results section.

Acknowledgements

Acknowledgements should be written in the third person. We strongly urge authors to limit acknowledgments to those who contributed substantially to scientific and technical aspects of the paper, gave financial support, or improved the quality of the presentation. Avoid acknowledging those whose contribution was clerical only.

Footnotes

Footnotes to material in the text should not be used unless they are unavoidable, but their use is encouraged in tables. Where used in the text, footnotes should be cited in the manuscript by superscript Arabic numbers (except in the tables, see below) and should be numbered serially beginning with any that appear on the title page. Each footnote should be typed on the manuscript page upon which the reference is made; **footnotes should not be included in the list of references.**

Equations and list of symbols

Equations should be clearly typed; triple-spacing should be used if superscripts and (or) subscripts are involved. Superscripts and subscripts should be legible and carefully placed. Distinguish between lowercase *l* and the numeral *one*, and between capital *O* and the numeral *zero*. A letter or symbol should represent only one entity and be used consistently throughout the paper. Each variable must be defined in the text or in a **List of symbols** to appear after the reference list. Variables representing vectors, matrices, vector matrices, and tensors must be clearly identified. Numbers identifying equations must be in parentheses and placed flush with the **left margin**. In numbering, no distinction is made between mathematical and chemical equations.

References

General form

The author is responsible for verifying each reference against the original article. Each reference must be cited in the text using the surnames of the authors and the year, for example, (Walpole 1985) or Green and Brown (1990). Depending on the sentence construction, the names may or may not be in parentheses, but the year always is. If there are three or more authors, the citation should give the name of the first author followed by et al. (e.g., Green et al. 1991). If references occur that are not uniquely identified by the authors' names and year, use *a*, *b*, *c*, etc., after the year, for example, Green 1983*a*, 1983*b*; Green and Brown 1988*a*, 1988*b*, for the text citation and in the reference list.

Uniform reference locators (URLs) or digital object identifiers (DOIs) are useful in locating references on the Web, and authors are encouraged to include these; they should be added to the reference in the reference list (see example below).

Unpublished reports, private communications, and in-press references

References to unpublished data, manuscripts in preparation or submitted to other journals, progress reports, and unpublished papers given at annual meetings are not cited in the reference list but may be included as footnotes or in parentheses in the text, giving all authors' names and initials. For a private communication, year of communication should also be given (e.g., J.S. Jones (personal communication, 1999)). If consultants' reports or other documents of limited circulation must be cited, they should carry with them an availability statement explaining where the document can be obtained. If an unpublished book or article has been **accepted for publication**, include it in the reference list followed by the notation "In press". Do not include volume and page number in an in-press reference, as these are subject to change before publication.

Presentation of the list

The **reference list** must be double-spaced and placed at the end of the text. References must be listed in alphabetical order according to the name of the first author and not numbered. References with the same first author are listed in the following order. (*i*) Papers with **one author only** are listed first in chronological order, beginning with the earliest paper. (*ii*) Papers with **dual authorship** follow and are listed in alphabetical order by the last name of the second author.

© 2007 NRC Canada

(*iii*) Papers with **three or more authors** appear after the dual-authored papers and are arranged chronologically.

General guidelines on references

References should be selected judiciously and be largely restricted to significant, published literature. References should follow the form used in current issues of the Journal. The names of serials are abbreviated in the form given in *Chemical Abstracts Service Source Index* (*CASSI*) (Chemical Abstracts Service, 2540 Olentangy River Road, P.O. Box 3012, Columbus, OH 43210-0012, USA) or in *BIOSIS Serial Sources* (BIOSIS, 2100 Arch Street, Philadelphia, PA 19103-1399, USA). In doubtful cases, authors should write the name of the serial in full. The Journal encourages the inclusion of issue numbers which should be placed in parentheses after the volume number. The following bibliographic citations illustrate the punctuation, style, and abbreviations for references.

Examples of references types, including electronic references

Journal article with DOI:

Newbury, M.G., and Ashworth, A.C. 2004. A fossil record of colonization and response of lacustrine fish populations to climate change. Can. J. Fish. Aquat. Sci. **61**(10): 1807–1816. doi:10.1139/F04-113.

Journal article with URL:

Newbury, M.G., and Ashworth, A.C. 2004. A fossil record of colonization and response of lacustrine fish populations to climate change. Can. J. Fish. Aquat. Sci. **61**(10): 1807–1816. Available from pubs.nrc-cnrc.gc.ca/cgi-bin/rp/rp2_abst_e?cjfas_f04-113_61_ns_nf [accessed 28 October 2005].

Journal article available online only (with DOI):

van der Sanden, J.J., and Hoekman, D.H. 2005. Review of relationships between grey-tone co-occurrence, semivariance, and autocorrelation based image texture analysis approaches [online]. Can. J. Remote Sens. **31**(3): 207–213. doi:10.1139/rs03-011.

Entire issue of journal:

Gordon, D.C., Jr., and Hourston, A.S. (*Editors*). 1983. Proceedings of the Symposium on the Dynamics of Turbid Coastal Environments. Can. J. Fish. Aquat. Sci. **40**(Suppl. 1).

Report:

Sanders, W.W., Jr., and Elleby, H.A. 1970. Distribution of wheel loads in highway bridges. National Cooperative Highway Research Program Report 83, Transportation Research Board, National Research Council, Washington, D.C.

Book:

Williams, R.A. 1967. Communication systems analysis and design. Prentice-Hall, Inc., Englewood Cliffs, N.J.

Book in a series:

Scott, W.B., and Crossman, E.J. 1973. Freshwater fishes of Canada. Bull. Fish. Res. Board Can. No. 184.

Part of book:

Healey, M.C. 1980. The ecology of juvenile salmon in Georgia Strait, British Columbia. *In* Salmonid ecosystems of the North Pacific. *Edited by* W.J. McNeil and D.C. Himsworth. Oregon State University Press, Corvallis, Oreg. pp. 203–229.

Paper in conference proceedings:

Kemp, A.L.W. 1969. Organic matter in the sediments of Lakes Ontario and Erie. *In* Proceedings of the 12th Conference on Great Lakes Research, Ann Arbor, Mich., 5–7 May 1969. International Association for Great Lakes Research, Ann Arbor, Mich. pp. 237–249.

Institutional publications and pamphlets:

Dzikowski, P.A., Kirby, G., Read, G., and Richards, W.G. 1984. The climate for agriculture in Atlantic Canada. Available from the Atlantic Advisory Committee on Agrometeorology, Halifax, N.S. Publ. ACA 84-2-500. Agdex No. 070.

Corporate author:

American Public Health Association, American Water Works Association, and Water Pollution Control Federation. 1975. Standard methods for the examination of water and wastewater. 14th ed. American Public Health Association, American Water Works Association, and Water Pollution Control Federation, Washington, D.C.

Thesis:

Keller, C.P. 1967. The role of polysaccharidases in acid wall loosening of epidermal tissue from young *Phaseolus vulgaris* L. hypocotyls. M.Sc. thesis, Department of Botany, The University of British Columbia, Vancouver, B.C.

Web site citation:

Quinion, M.B. 1998. Citing online sources: advice on online citation formats [online]. Available from worldwidewords.org/articles/citation.htm [accessed 20 October 2005].

Translation:

Koike, A., and Ogura, B. 1977. Selectivity of meshes and entrances of shrimp traps and crab traps. J. Tokyo Univ. Fish. **64**: 1–11. [Translated from Japanese by Can. Transl. Fish. Aquat. Sci. 4950, 1983.]

Tables

Tables must be typed on separate pages, placed after the list of references, and numbered with Arabic numerals in the order cited in the text. The title of the table should be a concise description of the content, no longer than one sentence, that allows the table to be understood without detailed reference to the text. Column headings should be brief, but may be amplified by footnotes. Vertical rules should not be used. A copy of the Journal should be consulted to see how tables are set up and where the lines in them are placed. Footnotes in tables should be designated by symbols (in the order *, †, ‡, §, ||, ¶, #) or superscript lowercase italic letters. Descriptive material not designated by a footnote may be placed under a table as a **Note**. Numerous small tables should be avoided, and the number of tables should be kept to a minimum.

Figure captions

Figure captions should be listed on a **separate page** and placed after the tables. The caption should informatively describe the content of the figure, without need for detailed reference to the text. Experimental conditions should not be included, but should be adequately covered in the Methods. For graphs, captions should not repeat axis labels, but should

© 2007 NRC Canada

describe what the data show. A single caption can be provided for multipart (composite) figures, with necessary details on the separate parts, identified by their individual labels. If the separate parts require enough information to warrant separate captions, then the composite should be separated into individual figures.

Appendices

An appendix should be able to stand alone, as a separate, self-contained document. Figures and tables used in an appendix should be numbered sequentially but separately from those used in the main body of the paper, for example, Fig. A1, Table A1, etc. If references are cited in an appendix, they must be listed in an appendix reference list, separate from the reference list for the article. If there is more than one appendix, label as follows: Appendix A, Appendix B, etc.

Supplementary material

Supplementary material (or data) consists of extra tables, figures (maps), detailed calculations, and data sets produced by the authors as part of their research, but not essential for understanding or evaluating the paper, and not published with the article in the print edition of the Journal. Depending on the policy of the Journal, such material may or may not be peer reviewed with the article. Supplementary material should be submitted with the article. During Web submission (OSPREY), relevant files should be attached under "Supplementary data". For mail submission, supplementary material should be clearly marked as such. The National Research Council of Canada maintains a depository in which supplementary material may be placed, either at the request of the author or at the suggestion of the Senior Editor. In addition, supplementary material can be made available in its native file format on the Journal Web site. It will be linked from the Web page of the associated article. Tables and figures should be numbered in sequence separate from those published with the paper (e.g., Fig. S1, Table S1). The supplementary material should be referred to in the printed article by footnotes. Copies of material in the depository may be purchased from the Depository of Unpublished Data, CISTI, National Research Council of Canada, Ottawa, ON K1A 0R6, Canada.

Computer programs

It is not the policy of the Journal to publish detailed printouts of computer program statements. Where the availability of these details enhances the usefulness of the paper, the author should submit two copies of the program for deposit (see Supplementary material section).

Illustrations

General

Each figure or group of figures should be planned to fit, after appropriate reduction, into the area of either one or two columns of text. The maximum finished size of a one-column illustration is 8.6 × 23.7 cm (3.4 × 9.3 in.) and that of a two-column illustration is 18.2 × 23.7 cm (7.2 × 9.3 in.). The figures (including halftones) must be numbered consecutively in Arabic numerals, and each one must be referred to in the text and must be self-explanatory. All terms, abbreviations, and symbols must correspond with those in the text. Only essential labelling should be used, with detailed information given in the caption. Submission of noncontinuous (screened) photographs and scanned illustrations printed out on laser printers is not recommended, as moirés develop; a moiré is a noticeable, unwanted pattern generated by rescanning or rescreening an illustration that already contains a dot pattern.

Line drawings

All lines must be sufficiently thick (0.5 points minimum) to reproduce well, and all symbols, superscripts, subscripts, and decimal points must be in good proportion to the rest of the drawing and large enough to allow for any necessary reduction without loss of detail. Avoid small open symbols; these tend to fill in upon reproduction. **Lettering produced by dot matrix printers or typewriters, or by hand, is not acceptable**. The same font style and lettering sizes should be used for all figures of similar size in any one paper. Original recorder tracings of **NMR**, **IR**, **ESR spectra**, etc., are not acceptable for reproduction; they must be redrawn.

Maps

Maps must have very **clear, bold patterns** and must show longitudes and latitudes (or UTM coordinates) and a scale, to ensure proper identification of study locations. On **maps of Quebec**, the official name of municipalities must be used (e.g., Québec, Montréal, Clarke City) and physical features must be in French (e.g., Lac Bienville) except for those that are considered of pan-Canadian significance. Areas of pan-Canadian significance have an official form in English and French (e.g., Atlantic Ocean and Océan Atlantique) and should appear in the language of the paper. Quebec (the province) must also appear in the language of the paper. For a complete list of names of areas of pan-Canadian significance, see pp. 236–237 of *Le guide du rédacteur* (2nd ed., 1996), published by Public Works and Government Services Canada, Ottawa, ON K1A 0S5.

Photographs

Photographs should be continuous tone, of high quality, and with strong contrast. Only essential features should be shown. A photograph, or group of them, should be planned to fit into the area of either one or two columns of text **with no further reduction**. Electron micrographs or photomicrographs should include a scale bar directly on the print. The best results will be obtained if the authors match the contrast and density of all figures arranged as a single plate.

Colour illustrations

Colour illustrations will be at the author's expense. Further details on prices are available from Cecily Pearson, Managing Editor of the Journal (613-993-9099; fax: 613-952-7656; e-mail: cecily.pearson@nrc-cnrc.gc.ca).

Preparation of electronic graphic files

The preferred graphic application of NRC Research Press is CorelDraw! For other applications that can be used, see the electronic graphics list at pubs.nrc-cnrc.gc.ca/cgi-bin/rp/rp2_prog_e?jees_graphics_e.html.

PC or Macintosh versions of True Type or Type 1 fonts should be used. **Do not use bitmap or nonstandard fonts**.

All figures should be submitted at the desired published size. For figures with several parts (e.g., *a*, *b*, *c*, *d*, etc.) created using the same software application, assemble them into one file rather than sending several files.

© 2007 NRC Canada

Remember that the more complex your artwork becomes, the greater the possibility for problems at output time. Avoid complicated textures and shadings, especially in vector illustration programs; this increases the chance for a poor-quality final product.

Bitmap (raster) files are image files produced using a grid format in which each square (or pixel) is set to one level of black, colour, or grey. A bitmap (rasterized) file is broken down into the number of pixels or picture elements per inch (ppi). Pixels per inch is sometimes referred to as dots per inch (dpi). The higher the resolution of an image, the larger the number of pixels contained within the rectangular grid. The proper resolution should be used when submitting bitmap artwork. The minimum requirements for resolution are 600 dpi for line art, 1200 dpi for finelines (line art with fine lines or shading), 300 dpi for halftones and colour, and 600 dpi for combinations (halftones with lettering outside the photo area).

All **colour** files submitted must be as CMYK (cyan, magenta, yellow, and black). These colours are used in full-colour commercial printing. RGB graphics (red, green, and blue; colours specifically used to produce an image on a monitor) will not print correctly.

Vector files are image files produced using elements such as lines and shapes. Typically these files are used for line drawings.

Bitmaps can be imported into vector/draw applications only for the purpose of adding and overlaying information, lines, text, etc. Bitmaps should not be resized, cropped, rotated, or otherwise manipulated after importing.

Multimedia formats — Audio and video clips in the major multimedia formats are now accepted for NRC Research Press journals published in full-text HTML. For accepted formats, see the Electronic graphic list published on the Journal Web site.

Manuscript guidelines

Style guides

As a general guide for biological terms, *The CSE Manual for Authors, Editors, and Publishers: Scientific Style and Format* (7th ed., 2006) published by the Council of Science Editors, Reston, VA 20190, USA, is recommended.

Spelling

Spelling should follow *Webster's Third New International Dictionary* or the *Oxford English Dictionary*. Authors are responsible for consistency in spelling.

Nomenclature, abbreviations, and acronyms

Nomenclature and abbreviations should follow the rules recommended by the International Union of Biochemistry (IUB) Committee of Editors of Biochemical Journals with support of IUPAC. As a general guide for biological terms, *The CSE Manual for Authors, Editors, and Publishers: Scientific Style Format* (7th ed., 2006), published by the Council of Biology Editors, Reston, VA 20190, USA, is recommended. For enzyme nomenclature, *Enzyme Nomenclature (1992): Recommendations of the Nomenclature Committee of the International Union of Biochemistry and Molecular Biology* (Academic Press, San Diego, Calif.) should be followed.

Abbreviations and acronyms that are standard in the discipline need not be defined. All others must be defined when they are first mentioned in the text and those with more than one meaning should be avoided.

Units of measurement

SI units (Système international d'unités) should be used or SI equivalents should be given. Avoid ambiguous forms such as g C/m^2/day; use g C·m^{-2}·day^{-1}. This system is explained and other useful information is given in the *Metric Practice Guide* (2000) published by CSA International (178 Rexdale Blvd., Toronto, ON M9W 1R3, Canada). For practical reasons, some exceptions to SI units are allowed. Units such as kilocalorie, reciprocal centimetre (wave number), and atmosphere may be used for the foreseeable future.

Statistical analyses

The assumptions and (or) the model underlying any statistical analysis should be clearly stated. Symbols such as * and **, denoting levels of significance, should not be used except in conjunction with the actual values of the associated test statistic; actual *p* values are preferred.

Fish

The Journal follows the names and spelling for fishes recommended in *Common and Scientific Names of Fishes from the United States, Canada, and Mexico* (6th ed., Spec. Publ. No. 29, American Fisheries Society, 2004) and the gene nomenclature for protein-coding loci outlined in Shaklee et al. (Trans. Am. Fish. Soc. **119**: 2–15, 1990).

Writing numbers

In writing long numbers, the digits should be separated into groups of three, counted from the decimal marker to the left and right. The separator should be a space and not a comma, period, or any other mark, for example, 25 562 987 and not 25,562,987. In English text, the decimal marker should be a point, for example, 0.1 mL and not 0,1 mL. The decimal point in all numbers between 1 and –1, except 0, must be preceded by a 0. The sign × should be used to indicate multiplication, e.g., 3×10^5 and not $3 \cdot 10^5$.

NRC Research Press
National Research Council of Canada
Ottawa, ON K1A 0R6
Canada

E-mail: pubs@nrc-cnrc.gc.ca
URL: pubs.nrc-cnrc.gc.ca
Fax: 613-952-7656

Revised January 2007

© 2007 NRC Canada

Recommandations aux auteurs

Journal canadien des sciences halieutiques et aquatiques

Orientation du Journal et directives de soumission de manuscrits

La Rédaction encourage la soumission d'articles contribuant à l'enrichissement des connaissances des sciences halieutiques et aquatiques. Les articles peuvent porter sur les cellules, les organismes, les populations, les communautés, les écosystèmes ou les procédés qui affectent les systèmes aquatiques. Ils peuvent traiter de disciplines variées y compris la biologie et l'écologie des organismes d'eau douce et d'eau salée, la limnologie, l'océanographie, la physiologie, la toxicologie, la génétique, l'économie, les maladies et la gestion. Les articles sont choisis selon la portée et l'importance des nouvelles connaissances ou idées qu'ils contiennent. On accorde la préséance aux articles qui contribuent à la compréhension de phénomènes observés et à l'interprétation de résultats expérimentaux.

Nous invitons les auteurs à soumettre des articles ayant des objectifs précis ou relevant des hypothèses, concepts ou questions vérifiables et se terminant par de solides conclusions ou d'utiles synthèses. Ces articles enrichissent, changent, mettent en question ou réorientent les connaissances acquises sur divers aspects des sciences aquatiques. **La raison d'être de l'analyse et l'interprétation des résultats doivent être situées dans un vaste contexte disciplinaire ou interdisciplinaire.** Les articles de méthodologie et de modélisation doivent inclure des applications et prouver la supériorité de la méthodologie ou du modèle explicité.

La Rédaction décourage la soumission d'articles simplement descriptifs (à moins qu'il ne s'agisse de nouvelles disciplines), d'application très limitée (applicable à une seule année, une seule région ou un seul taxon, portant sur un unique composé chimique, etc.); d'articles qui ne font que reprendre les principes énoncés dans des articles précédents; ou d'articles rendant compte de l'application de normes sans gain de méthodologie. Les études préliminaires ou fragmentaires, ou dont la pertinence à grande échelle n'est pas démontrée, et les interprétations purement spéculatives sont carrément rejetées.

Les articles doivent être aussi complets que possible. S'il est impossible d'inclure toute les données pertinentes dans un seul article, l'auteur devra inclure des renvois à des articles connexes et soumettre ceux-ci avec son propre article.

Types de manuscrits

Le Journal publie le genre de textes suivants :

Articles — Études de vaste portée qui constituent de nouvelles contributions à la science.

Perspectives — Synthèses, synthèses critiques ou réévaluations de concepts ou de paradigmes couramment admis.

Discussions — Commentaire ou réplique sur des sujets récemment abordés dans le Journal.

Communications rapides — Présentations de nouveaux concepts, descriptions de nouvelles méthodologies ou courts textes sur des sujets d'actualité ou controversés.

On peut obtenir les caractéristiques précises de chacun de ces genres sur le site Web du Bureau de la rédaction (uoguelph.ca/~cjfas/).

Langue

Les manuscrits doivent être rédigés de manière claire et concise, **en français ou en anglais correct**. Les auteurs pour qui le français ou l'anglais est une langue seconde devraient faire réviser leur manuscrit par une personne dont la langue maternelle est celle du texte avant de soumettre leur manuscrit. Un style de qualité accélère et facilite l'examen et la publication des manuscrits.

Un résumé rédigé dans la langue du manuscrit doit accompagner chaque soumission. Les résumés sont traduits en anglais ou en français, selon le cas, par le traducteur du Journal. En revanche, les auteurs qui peuvent soumettre leur résumé en français et en anglais sont invités à le faire.

Frais d'impression par page

Il n'y a pas de frais d'impression par page dans le *Journal canadien des sciences halieutiques et aquatiques*.

Objectif des recommandations

Pour **faciliter la publication**, les auteurs doivent vérifier l'exactitude, l'uniformité et la lisibilité des symboles, des abréviations et des termes techniques. Les Presses scientifiques du CNRC se réservent le droit d'assurer la qualité technique du Journal. Les auteurs voudront consulter un récent numéro du Journal pour s'enquérir des exigences en matière de présentation, en particulier à l'égard des tableaux et de la bibliographie. **La non-conformité des manuscrits et des illustrations aux exigences décrites ci-dessous risque de retarder la publication.**

Soumission

Nouveaux manuscrits

Les auteurs peuvent soumettre leur manuscrit par le Web ou par courriel (cjfas@uoguelph.ca). On encourage la soumission Web par OSPREY (système de soumission et d'examen en direct des articles).

Par le Web

Les auteurs peuvent soumettre leur manuscrit par OSPREY, le système de soumission et d'examen en direct des articles (pubs.nrc-cnrc.gc.ca/jcsha/osprey). OSPREY est optimisé pour les fureteurs Netscape 7.0 et Internet Explorer 6.0 (ou toute version ultérieure). Au moment de l'inscription, les auteurs seront invités à choisir un nom d'utilisateur et un mot de passe. L'accès aux manuscrits est protégé par le système

© 2007 CNRC Canada

de nom d'utilisateur et de mot de passe. Les auteurs peuvent s'inscrire sur le site à tout moment; une seule inscription est nécessaire. Le profil des auteurs et des examinateurs ayant déjà utilisé le système OSPREY du Journal par le passé demeure actif. Pour accéder au système, il suffit alors d'entrer son adresse de courriel dans le champ « Mot de passe oublié » du site Web.

Les auteurs qui ont besoin d'une aide technique quant au processus de soumission sur le Web peuvent communiquer avec Louis Lafleur au (613) 998-9432 ou par courriel à louis.lafleur@nrc-cnrc.gc.ca, de 8 h 00 à 16 h 00 (HNE).

Un guide de l'utilisateur détaillé est offert sur le site Web.

Les auteurs doivent accompagner leur manuscrit d'une lettre de présentation. Les tableaux et les illustrations peuvent soit faire partie du fichier de manuscrit ou être téléchargés individuellement vers le serveur. OSPREY accepte la plupart des fichiers de format texte et graphique. (Visitez le site Web pour consulter la liste complète des formats acceptés.)

Actuellement, les Presses scientifiques du CNRC n'acceptent pas les documents Word de la version 12 de Microsoft Office (extension .docx). Veuillez noter que le fait de sauvegarder des documents .docx dans un autre format (tel que .doc, .rft ou .txt) pourrait avoir des répercussions sur le formatage ou entrainer une perte de données. Ainsi, nous demandons aux auteurs, qui convertissent leur manuscrit de format .docx à un autre, de le vérifier attentivement avant de le soumettre à des fins d'examen, et ce, pour éviter toute erreur ou perte de données éventuelle.

Lors de la première soumission d'un manuscrit à un examen par les pairs, une version à faible résolution des illustrations devrait être téléchargée afin de limiter la taille des fichiers. La soumission des manuscrits devrait se faire l'ordinateur qui contient tous les fichiers pertinents. Le processus de soumission de manuscrit exige environ 10 minutes, mais le temps de téléchargement vers le serveur variera en fonction du type de connexion Internet utilisé.

Toute correspondance relative au manuscrit soumis par OSPREY sera envoyée à la personne identifiée comme auteur correspondant au moment de la soumission du manuscrit. De plus, toute correspondance se fera par voie de courriel.

Manuscrits révisés

Quant aux révisions, l'auteur correspondant sera avisé par courriel d'une demande de révision.

Manuscrits acceptés

L'auteur sera avisé que son manuscrit a été accepté. On lui demandera alors de soumettre la version définitive du manuscrit et tous les fichiers connexes, y compris les tableaux, les illustrations et les données supplémentaires par OSPREY ou par courriel.

Le **texte** (y compris les tableaux) doit être soumis en format de traitement de texte (de préférence WordPerfect, Microsoft Word ou TeX, en version Windows ou Macintosh). Des macros TeX pour la préparation des manuscrits acceptés sont disponibles en direct à ftp.tex.ac.uk/tex-archive/macros/latex/contrib/nrc/, ftp.dante.de/tex-archive/macros/latex/contrib/nrc/ et ctan.tug.org/tex-archive/macros/latex/contrib/nrc/.

Lors de la soumission de la version définitive du manuscrit, pour assurer la qualité optimale de reproduction et d'impression des illustrations, les auteurs doivent :

(*i*) Télécharger les fichiers d'illustrations séparément du manuscrit.

(*ii*) S'assurer que la résolution des fichiers d'illustrations est élevée.

(*iii*) S'assurer que les illustrations sont dans leur format original (p. ex. PhotoShop, Adobe Illustrator, Excel, CorelDraw, SigmaPlot), et non intégrées à un document Word ou converties dans un autre format. Toutefois, si les illustrations sont dans un format que les Presses scientifiques du CNRC n'acceptent pas, les auteurs peuvent fournir les illustrations dans des fichiers PostScript ou PDF de haute qualité et à haute résolution. Il est aussi possible d'envoyer une illustration en différents formats; l'éditeur choisira le format qui donne les meilleurs résultats.

(*iv*) S'assurer de télécharger la bonne version et la version plus récente des fichiers.

Renseignements complémentaires sur la soumission

Lettre de présentation

L'auteur correspondant doit accompagner son manuscrit d'une lettre de présentation qui fait état :

(*i*) des principaux points et de l'importance du travail;

(*ii*) de la participation de tous les auteurs au manuscrit et de leur approbation de ce dernier;

(*iii*) de l'assurance que le manuscrit en question n'est pas en cours d'examen aux fins de publication dans une autre revue;

(*iv*) de suggestions quant aux arbitres éventuels;

(*v*) d'autres manuscrits, y compris de résumés détaillés, contenant une information identique ou similaire à celle contenue dans le manuscrit soumis;

(*vi*) des numéros de téléphone et de télécopieur ainsi que du courriel et de l'adresse de chaque auteur;

(*vii*) de tout conflit d'intérêts, réel ou perçu (cf. « Conflit d'intérêts et divulgation » sous la rubrique « Éthique »).

Cession ou licence de droits d'auteur

Si les directeurs scientifiques acceptent d'examiner un manuscrit à des fins de publication, le Bureau de la rédaction demandera aux auteurs de lui retourner dans les plus brefs délais les licences ou les formulaires de cession de droits d'auteur dûment signés. Pour que la publication d'un manuscrit soit autorisée, tous les auteurs doivent au préalable remplir un formulaire ou une licence qui cède leurs droits d'auteur au CNRC ou autorise le CNRC à publier leur document. La plupart des auteurs doivent signer le formulaire de cession de droits d'auteur, qui transfère tous les droits au CNRC. Les fonctionnaires des pays du Commonwealth doivent signer une licence qui leur permet de conserver les droits de la Couronne. Pour leur part, les fonctionnaires des États-Unis doivent signer une entente de publication, puisque leurs documents sont exclus de la protection des droits d'auteur des États-Unis. Les auteurs peuvent obtenir ces formulaires auprès du directeur scientifique, dans le premier numéro d'un volume ou dans le site Web du Journal (pubs.nrc-cnrc.gc.ca/cgi-bin/ps/rp2_desc_f?cjfas).

Processus de révision

Réception des manuscrits

Lorsque la directrice scientifique principale acceptera de prendre en considération un manuscrit à des fins de publication, l'auteur correspondant recevra un accusé de réception

© 2007 NRC Canada

officiel, et le Bureau de la rédaction lui demandera de remplir les formulaires nécessaires dans les plus brefs délais. Dans l'éventualité où un manuscrit soumis ne serait pas retenu pour examen en vue de publication, l'auteur correspondant serait avisé de cette décision par courriel.

La conformité du manuscrit aux *Recommandations aux auteurs* sera vérifiée par un lecteur technique. Les manuscrits non conformes ainsi que ceux qui ne réussissent pas à définir clairement l'objet de la recherche pourront être renvoyés à l'auteur correspondant pour que la présentation soit corrigée avant que le contenu n'en soit examiné.

Examen par les pairs/évaluation

Chaque article est habituellement soumis à une évaluation par deux réviseurs. Toutefois, la directrice scientifique principale renverra sans les évaluer tout article qui ne reflète pas la portée ou le caractère du Journal et les articles qui débordent des limites imposées pour la publication sous forme de « résumés approfondis ». On obtiendra les directives à cet égard sur le site Web du Bureau de la rédaction à uoguelph.ca/~cjfas/. Les articles soumis aux fins de publication dans un supplément sont soumis au même rigoureux exercice d'examen que les articles des numéros réguliers.

On demande habituellement aux auteurs d'examiner les commentaires des réviseurs et de modifier leur texte en conséquence en 90 jours, tout au plus. Faute de respecter ce délai, l'article renvoyé par l'auteur sera traité comme une nouvelle soumission à moins que l'auteur n'ait au préalable dûment communiqué avec le Bureau de la rédaction.

Manuscrits resoumis

Les auteurs qui soumettent un manuscrit précédemment refusé ou retiré doivent donner le numéro de manuscrit de leur première soumission. Les manuscrits resoumis sont traités comme de nouveaux manuscrits dans leur lettre de présentation. Les auteurs peuvent soumettre le nouveau manuscrit par courriel ou par OSPREY, accompagné d'une réponse détaillée et systématique à toutes les questions soulevées au cours de l'évaluation précédente.

Processus de publication

Généralités

La Rédaction vérifie tous les articles soumis afin de s'assurer qu'ils respectent les *Recommandations aux auteurs* et qu'ils sont accompagnés de toute la documentation d'appui nécessaire. Tout élément posant problème sera examiné par la Rédaction en consultation avec l'auteur correspondant. Une fois que tous les problèmes sont résolus par la Rédaction et que tous les formulaires de cession des droits d'auteur dûment signés par les auteurs sont reçus, le manuscrit est acheminé aux Presses scientifiques du CNRC, à Ottawa, en vue de sa publication. La préparation finale des manuscrits est assurée par un lecteur-rédacteur responsable de l'uniformité de la présentation et du style.

Correspondance avec les Presses scientifiques du CNRC

Après qu'un article a été accepté, toute correspondance doit être adressée aux Presses scientifiques du CNRC, Conseil national de recherches du Canada, Ottawa, ON K1A 0R6, Canada (télécopieur : 613-952-7656; courriel : pubs@nrc-cnrc.gc.ca; URL : pubs.nrc-cnrc.gc.ca). Les Presses scientifiques du CNRC se réservent le droit d'apporter des modifications rédactionnelles mais ne modifieront pas la substance d'un article sans préalablement consulter l'auteur et la directrice scientifique principale.

Épreuves en placard

Une épreuve en placard, les épreuves d'illustration, une copie de l'article annoté et un bon de commande de tirés à part seront envoyés à l'auteur correspondant. **Les épreuves en placard doivent être relues attentivement car elles ne seront pas revues par les Presses scientifiques du CNRC.** Elles doivent en outre être renvoyées dans les 48 heures suivant leur réception. Au stade des épreuves, il n'est plus temps d'apporter des modifications importantes ni de faire des ajouts ou des suppressions. Les frais occasionnés par des modifications excessives devront être assumés par les auteurs.

Tirés à part

Pour obtenir des tirés à part, il convient de remplir le bon de commande à cet effet, d'y annexer le paiement pertinent (chèque, numéro de carte de crédit, numéro de bon d'achat ou pièce de journal interne) et de renvoyer le tout en même temps que les épreuves et l'article corrigés. Le tarif des tirés à part commandés après la publication est fortement majoré. **Le Journal n'offre pas de tirés à part gratuits. Les tirés à part commandés ne sont postés qu'après réception d'un numéro du bon d'achat ou du paiement pertinent.**

Permission de reproduction de documents protégés par droits d'auteur

Les auteurs d'un manuscrit qui contient de la documentation déjà publiée (tableaux, illustrations, schémas, etc.), et donc assujettie aux droits d'auteur, doivent obtenir **une permission écrite, de la part du titulaire de ces droits d'auteur**, de reproduire l'information en question **en format imprimé et électronique**. Les permissions écrites doivent accompagner le manuscrit soumis, sans quoi le processus de publication pourra être retardé. Cette lettre sera exigée avec toute mention du type « tirée de… ». Si une illustration est modifiée, de sorte qu'une telle autorisation n'est pas requise, la formulation doit être explicit : « modifiée d'après… ». Si l'illustration est reconstituée à partir d'informations tirées d'autres auteurs la mention doit être du même type que pour une référence.

Permission de republication de documentation publiée dans les revues des Presses scientifiques du CNRC

Toute demande de permission de reproduction ou de republication partielle ou intégrale d'un manuscrit doit être adressée à Roxanne Landriault, des Presses scientifiques du CNRC (613-990-2254; courriel : roxanne.landriault@nrc-cnrc.gc.ca).

Éthique

Généralités

Les normes d'éthique auxquelles doivent se conformer les auteurs, les examinateurs et les directeurs scientifiques sont décrites dans la Politique éditoriale des Presses scientifiques du CNRC (publiée dans le numéro de janvier 1996 du *Journal*

© 2007 NRC Canada

canadien des sciences halieutiques et aquatiques, diffusée sur le site Web du Journal à pubs.nrc-cnrc.gc.ca/cgi-bin/ps/rp2_cust_f?pubpolicy ou disponible auprès des Presses scientifiques du CNRC).

Reproduction et rediffusion

En vertu d'une politique de longue date, le *Journal canadien des sciences halieutiques et aquatiques* refuse de publier des articles qui ont été publiés ailleurs. La Directrice scientifique principale juge un manuscrit inadmissible si le manuscrit en question (*i*) est en cours d'examen en vue d'être publié ou a déjà été publié dans un périodique ou dans un livre, ou (*ii*) est en cours d'examen en vue d'être publié ou a déjà été publié dans un compte rendu de conférence ou dans une publication officielle ouvertement distribuée à plus de 100 exemplaires. Les auteurs peuvent proposer, sur leur site Web ou sur le serveur de leur institution, une ébauche d'un article soumis, à condition que l'ébauche ne soit aucunement modifiée après l'acceptation du manuscrit. Les auteurs sont invités à inclure, sur la version préimprimée de leur manuscrit, un lien hypertexte vers sa version définitive sur le site Web des Presses scientifiques du CNRC (pubs.nrc-cnrc.gc.ca). Les résumés concis ou détaillés inclus dans les comptes rendus de conférences ne constituent pas une « publication antérieure ». Un « résumé détaillé » est un document de 1000 mots ou moins qui ne comprend ni tableaux détaillés ni illustrations des résultats de l'étude. Des renseignements supplémentaires sur les résumés détaillés sont disponibles sur le site Web du Bureau de la rédaction (uoguelph.ca/~cjfas/).

Déclaration de la paternité du manuscrit

Dans sa lettre de présentation, l'auteur correspondant doit garantir que les auteurs ont tous contribué de près au manuscrit et ont approuvé la version soumise.

Suggestion d'examinateurs

Les auteurs peuvent suggérer des examinateurs. Ils doivent fournir l'adresse complète, les numéros de téléphone et de télécopieur, ainsi que l'adresse de courriel (dans la mesure du possible) de ces personnes. Les directeurs scientifiques ne sont aucunement tenus de se limiter à ces suggestions.

Conflit d'intérêts et divulgation

La directrice scientifique principale reconnaît la possibilité que des conflits d'intérêts réels ou perçus surviennent à la suite de circonstances intellectuelles, personnelles ou financières liées aux travaux de recherche. Les manuscrits doivent inclure une divulgation de toute source de financement de la recherche. De plus, la lettre de présentation doit expliquer tout conflit d'intérêts, réel ou perçu, qui pourrait survenir lors du processus d'examen par les pairs. Si de tels conflits ne sont pas divulgués, le manuscrit pourrait être refusé.

Photos de personnes

La publication d'une photo qui montre une personne identifiable exige que la personne concernée signe une lettre ou un formulaire qui autorise les Presses scientifiques du CNRC à publier cette photo.

Retouche photographique

Le Journal estime que les photographies numériques font partie des données. Aussi est-il impératif que les images numériques soumises reproduisent fidèlement l'image d'origine. Toute retouche à l'aide d'un logiciel graphique doit être explicitée dans les méthodes, notamment quant au logiciel utilisé et aux techniques appliquées pour améliorer ou modifier l'illustration. Une telle explication assure la constance des méthodes et l'intégrité scientifique des travaux. La suppression des artéfacts ou de toute donnée non essentielle contenue dans l'image est découragée.

Sections du manuscrit

Disposition et organisation

Le manuscrit doit être composé à **double interligne**, d'un seul côté de feuilles de 21,5 sur 28 cm (8,5 po sur 11 po ou ISO A4). Chaque page doit être numérotée, en commençant par la page de titre. Les lignes du texte doivent aussi être numérotées. Le texte destiné à être publié en italique doit être présenté en italique, non pas souligné. Les auteurs utiliseront des caractères en majuscule seulement lorsque cela s'avèrera pertinent.

Les auteurs devraient structurer le manuscrit en fonction de l'énoncé des objectifs ou de la portée de l'étude présentée dans l'introduction. Il est particulièrement important que le titre et les en-têtes reflètent l'énoncé des objectifs.

Avant de commencer la rédaction du manuscrit, les auteurs devraient dresser une liste provisoire des en-têtes, avec le moins de subdivisions possible, et remanier cette liste jusqu'à ce qu'elle reflète une démarche logique, intelligible pour le lecteur. Habituellement, l'ordre chronologique ne sera pas satisfaisant. En effet, il sera plus facile de suivre le texte si les méthodes, les résultats et la discussion font partie de sections distinctes.

Les auteurs devraient organiser les tableaux et les illustrations de manière à faciliter les comparaisons et regrouper les données apparentées de façon à réduire au minimum le nombre de tableaux et d'illustrations. Dans la mesure du possible, les tableaux et les figures devraient être suffisamment explicites pour que le lecteur n'ait pas à se reporter au texte.

Les auteurs devraient commencer les sections et les paragraphes par des énoncés généraux qui aboutissent naturellement à des énoncés pointus. La présentation de la conclusion dans un premier temps et de sa justification dans un deuxième facilite considérablement la lecture et l'évaluation par les scientifiques. Lors de la rédaction des manuscrits, le défaut le plus courant consiste à omettre de présenter dès le début du texte les généralités les plus dignes de mention.

Les auteurs doivent veiller à ce que le contenu de chaque section soit pertinent à l'en-tête et que le contenu de chaque paragraphe se rapporte à la première phrase du paragraphe (la « phrase d'ouverture »).

Avant de rédiger les paragraphes, les auteurs devraient composer la phrase d'ouverture de chaque paragraphe et disposer chacune de celles-ci dans l'ordre approprié.

Titre

Les auteurs doivent limiter le titre à ce que démontre le manuscrit. Le titre est un élément fondamental de l'article et doit refléter clairement et brièvement le contenu du manuscrit. Le titre a deux fonctions : (*i*) il permet au lecteur de juger si, oui ou non, l'article est susceptible de l'intéresser et (*ii*) il devrait fournir suffisamment d'information pour permettre au lecteur de juger de la portée et de l'importance potentielle du contenu. Les mots du titre devraient fournir un maximum d'in-

© 2007 NRC Canada

formation et identifier la nature de la recherche, de l'organisme utilisé et, le cas échéant, la démarche technique (p. ex. radiographie, chromatographie, analyse mathématique). Les titres ne devraient pas commencer par un chiffre ou par des prépositions d'introduction telles que « Sur » ou « Vers », ou des expressions telles que « Contribution à ... » ou « Recherche sur ... ». Des titres judicieux facilitent considérablement le classement des publications et leur utilisation par les scientifiques et les bibliothécaires et de même que leur dépouillement par les indexateurs. Les titres en série devraient être évités.

Page de titre

La page de titre doit comprendre les suivants. (*i*) Le titre intégral du manuscrit. (*ii*) Le nom des auteurs, dans l'ordre dans lequel ces noms doivent apparaître dans l'intitulé de l'article imprimé. (*iii*) L'affiliation et l'adresse (y compris l'adresse de courriel) de chaque auteur pendant les recherches. Les changements d'affiliations et d'adresses (y compris d'adresse de courriel) devront être indiqués en note infrapaginale. (*iv*) Le nom, l'adresse, les numéros de téléphone et de télécopieur ainsi que l'adresse de courriel de l'auteur correspondant.

Noms des auteurs

La directrice scientifique principale encourage tous les auteurs à fournir leur prénom au complet plutôt qu'une simple initiale.

Résumé

Chaque contribution doit être accompagnée d'un résumé qui utilisera un vocabulaire évocateur, susceptible de capter l'intérêt des lecteurs visés. Ceci est particulièrement important en vue du dépouillement automatisé que font les services de repérage de l'information de même que les robots des moteurs de recherche. Un résumé comptera au plus 175 mots et sera présenté sur une page distincte. Le résumé concis doit refléter précisément le contenu du manuscrit et doit compléter le titre plutôt que simplement le reprendre. Les résumés sont traduits en anglais ou en français, selon le cas, par les traducteurs du Journal. En revanche, les auteurs qui peuvent soumettre leur résumé en français et en anglais sont invités à le faire. Le résumé ne devrait pas contenir de références à moins que cela ne soit essentiel. Dans ce dernier cas, il faudra fournir l'information bibliographique intégrale.

À l'instar du titre, le résumé permet au lecteur de prendre connaissance du contenu du manuscrit et de décider si, oui ou non, il lui faut le lire en entier. Les auteurs devraient présenter, au début du résumé, la principale conclusion de l'étude et l'appuyer par les résultats pertinents. Ils ne doivent donner que les détails des méthodes nécessaires à la compréhension de la démarche et les intégrer à l'énoncé des résultats. Il faut éviter l'emploi de phrases telles que « ... on y analyse » ou « ... a été trouvé » et être plus spécifique. Comme le résumé est souvent séparé du corps principal de l'article par les services d'analyse et les indexateurs et qu'il s'agit parfois de la seule partie de l'article que certains lecteurs auront l'occasion de voir, il importe qu'il reflète précisément le contenu du manuscrit et qu'il soit complet en lui-même, c.-à-d. qu'il contienne seulement des références absolument *essentielles* et facilement retraçables (p. ex. R.B. Deriso. 1980. Can. J. Fish. Aquat. Sci. **37** : 268–282).

Introduction

Les auteurs doivent limiter l'introduction à la portée, au but et à la raison de l'étude. Ils ne mentionneront que les travaux publiés et autres documents nécessaires à la définition du problème et du contexte. Les auteurs devraient tout d'abord décrire le but ou la portée de l'étude, définir ensuite le problème puis présenter des repères qui orienteront le lecteur. En général, une introduction comprendra de 375 à 500 mots.

Matériel et méthodes

La section « Matériel et méthodes » jette les fondations de la résolution du problème posé dans l'énoncé du travail.

Les auteurs limiteront les renseignements sur le matériel et les méthodes à ce qui est nécessaire pour juger de la validité des résultats. Cette évaluation sera facilitée si toute l'information connexe est présentée, autant que possible, dans une même section. S'il s'agit d'outillage ou de techniques connus, les auteurs incluront des références aux publications et ne décriront en détail que les adaptations. Il y a souvent avantage à commencer un énoncé des méthodes par une phrase qui en indique le but, comme : « Afin de déterminer ... nous ... ». Si la section est longue, les auteurs devraient la diviser à l'aide d'en-têtes correspondant aux en-têtes de la section des résultats.

Résultats

Les auteurs doivent limiter les résultats aux réponses apportées aux questions en rapport avec l'énoncé de travail et faire en sorte que ces réponses soient aussi complètes que possible tout en étant concises. Les résultats doivent être associés aussi étroitement que possible aux observations ou aux mesures, ceci afin que le lecteur ne confonde pas constations et spéculations. Les auteurs devraient dégager les principales constations mises en évidence par les tableaux et les illustrations et éviter de répéter dans le texte ce que les légendes expriment clairement. La documentation complémentaire au texte peut faire partie de la documentation du rapport intégral ou être versée dans un dépôt de données reconnu. Les auteurs peuvent y faire référence dans le texte (cf. section « Données supplémentaires »).

Discussion

Les auteurs devraient limiter la discussion à la présentation des principales contributions de l'étude et à l'interprétation de constatations particulières, en les comparant avec celles d'autres auteurs. Ils mettront l'accent sur la synthèse, l'interprétation et la présentation de généralisations et de principes largement applicables. S'il existe des exceptions ou des aspects douteux, les auteurs le souligneront et feront ressortir la manière dont les résultats corroborent ou contredisent les travaux déjà publiés. La spéculation doit se limiter à ce qui peut être appuyé sur des preuves raisonnables. Les auteurs devraient terminer cette section par un sommaire de l'importance du travail et par les conclusions qu'il a invitées. Si la discussion est brève et précise, elle peut être combinée avec les résultats en une seule section.

Remerciements

Les remerciements sont rédigés à la troisième personne. Les auteurs sont priés de limiter les remerciements aux personnes qui ont étroitement contribué aux aspects scientifiques et techniques de l'article, qui ont fourni une aide financière ou

© 2007 NRC Canada

qui ont sensiblement amélioré la qualité de la présentation. Les remerciements ne devraient pas viser les fournisseurs de service de soutien.

Notes infrapaginales

Les notes infrapaginales ne devraient figurer dans le corps du texte que lorsqu'elles sont indispensables; toutefois, leur utilisation dans les tableaux est encouragée. Lorsque des notes infrapaginales figurent dans le texte, les appels devraient être signalés à l'aide d'un chiffre arabe en exposant (sauf dans le cas des tableaux, cf. ci-dessous) et numérotés de façon consécutive à partir de la première note infrapaginale, y compris toute note apparaissant en page titre. Chaque note infrapaginale doit figurer au bas de la page où elle est signalée, **pas dans la bibliographie.**

Équations et liste de symboles

Les **équations** doivent être clairement dactylographiées et, si elles incluent des exposants ou des indices, être dactylographiées à triple interligne. Les exposants et les indices doivent être lisibles et correctement placés. Il convient de rendre évidente la distinction entre la lettre *l* et le chiffre *un*, et entre la lettre majuscule *O* et le chiffre *zéro*. Une lettre ou un symbole ne devrait être associé qu'à une seule réalité et devrait être utilisé de façon uniforme dans l'article. Chaque variable doit être définie dans le texte ou dans une **liste des symboles** qui succédera à la bibliographie. Les variables représentant des vecteurs, des matrices, des matrices vectorielles et des tenseurs doivent être clairement définies. Les équations doivent être identifiées à l'aide de chiffres arabes placés entre parenthèses, alignés avec la **marge de gauche**. Aucune distinction n'est faite entre la numérotation des formules mathématiques et celle des formules chimiques.

Références

Présentation générale

Il appartient aux auteurs d'assurer l'adéquation entre le contenu des références bibliographiques et l'information bibliographique des publications citées. Dans le texte, les références doivent être signalées à l'aide du nom des auteurs et de l'année de publication, p. ex. (Martial 1970) ou Dupont et Tremblay (1990), selon la structure de la phrase. Lorsqu'il y a trois auteurs ou plus, le nom du premier auteur est suivi de la mention et al. (p. ex. Dupont et al. 1991). Lorsque le nom et l'année ne suffisent pas à distinguer deux ouvrages, les lettres *a*, *b*, *c*, etc. sont ajoutées après l'année (à la fois dans le texte et dans la bibliographie), p. ex. Dupont 1983*a*, 1983*b*; Dupont et al. 1980*a*, 1980*b*).

Les adresses Web (adresses URL) ou les identificateurs d'objets numériques (système DOI) permettent de consulter les références qui sont accessibles sur le Web. Les auteurs sont invités à les utiliser et à les inclure avec les références dans la bibliographie (voir exemple ci-dessous).

Rapports non publiés, communications personnelles et documents sous presse

Les références bibliographiques à des rapports non publiés, à des communications personnelles ou à des articles en cours d'examen ne paraîtront pas dans la bibliographie. Elles seront plutôt signalées sous forme de notes infrapaginales ou entre parenthèses dans le texte. Elles devront contenir le nom des auteurs et leur initiale. Dans le cas des communications personnelles, il convient de préciser la nature de la source et l'année (p. ex. J.S. Ernst (communication personnelle, 1999)). Si l'on doit citer des rapports d'experts-conseils ou d'autres documents dont la distribution est limitée, on devra préciser l'endroit où l'on peut se les procurer. Si un livre ou un article non publié avéré est **en attente de publication**, sa référence doit apparaître dans la bibliographie et porter la mention « sous presse ». Dans ce cas, il ne faut pas préciser le volume et le numéro de la page, puisque cette information risque de changer lors du processus de publication.

Présentation de la bibliographie

Dans la **bibliographie**, qui apparaît à la suite du texte, les références sont composées à double interligne et classées par ordre alphabétique du nom du premier auteur, sans numérotation. Si la bibliographie comprend plusieurs publications d'un même premier auteur, les règles suivantes s'appliquent : (*i*) les articles avec **un seul auteur** sont signalés en premier, par ordre chronologique, en commençant par le plus ancien; (*ii*) viennent ensuite les articles avec **deux auteurs**, en ordre alphabétique du nom de famille du second auteur; (*iii*) puis viennent les articles de **trois auteurs et plus**, en ordre chronologique.

Directives générales quant aux références

On choisira les références avec soin, les limitant aux publications importantes. Les références doivent refléter le style des numéros récents du Journal. Le titre d'une revue doit être abrégé conformément au *Chemical Abstracts Service Source Index* (*CASSI*) (Chemical Abstracts Service, 2540 Olentangy River Road, P.O. Box 3012, Columbus, OH 43210-0012, É.-U.) ou à *BIOSIS Serial Sources* (BIOSIS, 2100 Arch Street, Philadelphia, PA 19103-1399, É.-U.). En cas de doute, les auteurs doivent écrire le nom de la revue au complet. Nous recommandons aux auteurs de préciser le numéro des revues citées et de l'indiquer entre parenthèses après le numéro du volume. La liste de références qui suit reflète les normes de ponctuation, de présentation et d'abréviation préconisées.

Exemples de divers types de références, y compris les références à des documents électroniques

Article de revue comprenant un système DOI :

Newbury, M.G., et Ashworth, A.C. 2004. A fossil record of colonization and response of lacustrine fish populations to climate change. Can. J. Fish. Aquat. Sci. **61**(10): 1807–1816. doi:10.1139/F04-113.

Article de revue comprenant une adresse Web :

Newbury, M.G., et Ashworth, A.C. 2004. A fossil record of colonization and response of lacustrine fish populations to climate change. Can. J. Fish. Aquat. Sci. **61**(10): 1807–1816. Disponible à pubs.nrc-cnrc.gc.ca/cgi-bin/rp/rp2_abst_f?cjfas_f04-113_61_ns_nf [cité 28 October 2005].

Article de revue disponible en ligne seulement (identificateur DOI) :

van der Sanden, J.J., et Hoekman, D.H. 2005. Review of relationships between grey-tone co-occurrence, semivariance, and autocorrelation based image texture analysis approaches [en ligne]. Can. J. Remote Sens. **31**(3): 207–213. doi:10.1139/rs03-011.

Numéro intégral d'une revue :

Gordon, D.C., Jr., et Hourston, A.S. (*Directeurs de la rédac-*

© 2007 NRC Canada

tion). 1983. Proceedings of the Symposium on the Dynamics of Turbid Coastal Environments. Can. J. Fish. Aquat. Sci. **40** (Suppl. 1).

Rapport :

Pigeon, M., et Langlois, M. 1987. Étude de la durabilité au gel d'un ciment avec fumée de silice. Ciments Saint-Laurent, Beauport (Québec). Rapp. GCT-87-09.

Livre :

Lacroix, P., et Lalonde, J. (*Directeurs de la rédaction*). 1992. Les grands barrages. Éditions Poly-Sciences, Montréal (Québec).

Livre faisant partie d'une collection :

Scott, W.B., et Crossman, E.J. 1973. Freshwater fishes of Canada. Bull. Fish. Res. Board Can. nº 184.

Section d'un livre :

Healey, M.C. 1980. The ecology of juvenile salmon in Georgia Strait, British Columbia. *Dans* Salmonid ecosystems of the North Pacific. *Sous la direction de* W.J. McNeil et D.C. Himsworth. Oregon State University Press, Corvallis (Oregon). p. 203–229.

Article d'un compte rendu de conférence :

Kemp, A.L.W. 1969. Organic matter in the sediments of Lakes Ontario and Erie. *Dans* Proceedings of the 12th Conference on Great Lakes Research, Ann Arbor (Michigan), du 5 au 7 mai 1969. Association internationale de recherche sur les Grands Lacs, Ann Arbor (Michigan). p. 237–249.

Publication ou brochure d'institution :

Dzikowski, P.A., Kirby, G., Read, G., et Richards, W.G. 1984. The climate for agriculture in Atlantic Canada. Disponible auprès du Atlantic Advisory Committee on Agrometeorology, Halifax (Nouvelle-Écosse). Publ. ACA 84-2-500. nº Agdex 070.

Auteur collectif :

American Public Health Association, American Water Works Association et Water Pollution Control Federation. 1975. Standard methods for the examination of water and wastewater. 14e éd. American Public Health Association, American Water Works Association et Water Pollution Control Federation, Washington (District de Columbia).

Mémoire :

Keller, C.P. 1987. The role of polysaccharidases in acid wall loosening of epidermal tissue from young *Phaseolus vulgaris* L. hypocotyls. Mémoire de maîtrise ès sciences, Département de botanique, The University of British Columbia, Vancouver (Colombie-Britannique).

Document sur un site Web :

Quinion, M.B. 1996. Citing online sources: advice on online citation formats [en ligne]. Disponible à worldwidewords.org/articles/citation.htm [cité le 20 octobre 2005].

Traduction :

Koike, A., et Ogura, B. 1977. Selectivity of meshes and entrances of shrimp traps and crab traps. J. Tokyo Univ. Fish. **64**: 1–11. [Traduit du japonais par Can. Transl. Fish. Aquat. Sci. 4950, 1983.]

Tableaux

Les tableaux, qui occuperont chacun une page distincte, doivent suivre la bibliographie, être numérotés de façon continue en chiffres arabes dans l'ordre de mention dans le manuscrit et comporter un bref titre descriptif, d'au plus une phrase, intelligible sans qu'il ne soit nécessaire de se reporter au texte. Les titres de colonne doivent être brefs, mais peuvent être étoffés à l'aide de notes infratabulaires. Les tableaux ne doivent pas contenir de traits verticaux. Les auteurs voudront consulter un exemplaire du Journal pour s'enquérir de la présentation souhaitable des tableaux. Les notes infratabulaires doivent être signalées par des symboles (selon l'ordre suivant : *, †, ‡, §, ||, ¶, #) ou des lettres minuscules en italique placées en exposant. Une note descriptive qui n'est pas introduite par un appel de note peut être inscrite au bas du tableau à titre de **Nota**. Les auteurs éviteront d'insérer de nombreux petits tableaux et garderont le nombre de tableaux au minimum.

Légendes des illustrations

Les légendes des illustrations doivent constituer une liste **sur une page distincte**, qui suivra les tableaux. Les légendes devraient être descriptives de sorte qu'il ne soit pas nécessaire de se reporter au texte. Elles ne devraient pas inclure d'information expérimentale : celle-ci aura plutôt été présentée comme il se doit dans la section « Méthodes ». Dans les graphiques, les légendes ne doivent pas reprendre le label des axes mais plutôt décrire ce que révèlent les données. Dans le cas de montages d'illustrations, les auteurs rédigeront une légende globale contenant suffisamment d'information pour décrire l'ensemble du montage. Si chaque élément mérite sa propre légende, le montage sera fractionné et les illustrations seront plutôt présentées de façon individuelle.

Annexes

Une annexe est un document distinct et complet. Les illustrations et les tableaux présentés dans les annexes doivent être numérotés de façon consécutive, distinctement des illustrations et tableaux du corps de l'article, p. ex. figure A1, tableau A1, etc. Si les annexes contiennent des références bibliographiques, ces dernières doivent apparaître dans une bibliographie distincte de la bibliographie du corps de l'article. S'il y a plus qu'une annexe, veuillez les identifier de la façon suivante : Annexe A, Annexe B, etc.

Données supplémentaires

Les données supplémentaires comprennent des tableaux, des figures (cartes), des calculs détaillés et des ensembles de données produits par les auteurs dans le cadre de leur recherche, mais qui ne sont pas essentiels à la compréhension ni à l'évaluation de l'article, et qui ne seront pas publiés dans la version imprimée du Journal. Selon la politique du Journal, les données de ce genre peuvent ou non être évaluées par les pairs. Les données supplémentaires doivent être soumises avec l'article. Pour la soumission en direct (OSPREY), joindre les fichiers concernés à la rubrique « Données supplémentaires ». Pour les envois postaux, indiquer clairement quelles sont les données supplémentaires. Le Conseil national de recherches du Canada administre un dépôt des données non publiées dans lequel les données supplémentaires peuvent être versées, à la demande des auteurs ou de la di-

© 2007 NRC Canada

rectrice scientifique principale. De plus, il est possible d'accéder à ces données dans leur format d'origine à partir du site Web du Journal, grâce aux hyperliens à cet effet apparaissant sur la version Web de l'article. Les tableaux et les illustrations doivent être numérotés de façon consécutive, distinctement de ceux destinés à la publication (p. ex. figure S1, tableau S1). Chaque ensemble de données supplémentaires doit faire l'objet d'une note infrapaginale dans l'article imprimé. Des exemplaires des données déposées peuvent être obtenus contre paiement auprès du Dépôt des données non publiées, ICIST, Conseil national de recherches Canada, Ottawa, ON K1A 0R6, Canada.

Programmes informatiques

La Rédaction ne publie habituellement pas les imprimés détaillés produits à l'aide de programmes informatiques. Si les données contenues dans un tel imprimé contribuent sensiblement à la valeur de l'article, l'auteur doit mettre deux copies du programme en dépôt (cf. section « Données supplémentaires »).

Illustrations

Généralités

Chaque illustration ou groupe d'illustrations doit être préparé de manière à occuper, après réduction, l'espace d'une ou deux colonnes du texte. Les dimensions définitives maximales d'une illustration sur une colonne sont de 8,6 sur 23,7 cm (3,4 sur 9,3 po) et celles d'une illustration sur deux colonnes de 18,2 sur 23,7 cm (7,2 sur 9,3 po). Les illustrations (y compris les similis) sont numérotées en chiffres arabes de façon consécutive. Elles doivent toutes être signalées dans l'article et être intelligibles sans qu'il ne soit nécessaire de se reporter au texte. Tous les termes, les abréviations et les symboles qu'elles contiennent doivent être identiques à ceux qui apparaissant dans le texte. Seuls les détails essentiels devraient être identifiés; l'information détaillée devrait figurer dans la légende. Les auteurs sont priés de ne pas soumettre de photographies en ton non continu (tramées) ni d'illustrations balayées puis imprimées au laser. En effet, la reproduction de ces documents cause souvent des moirures, c.-à-d. un effet visuel indésirable résultant du rebalayage ou du retramage d'une illustration formée de points.

Dessins au trait

L'épaisseur des traits doit être suffisante (au moins 0.5 point) pour que la reproduction soit nette; tous les symboles, les exposants, les indices et les signes décimaux doivent être proportionnés au reste du dessin et d'une dimension suffisante pour permettre la réduction nécessaire sans perte de détail. Il convient de ne pas utiliser de petits symboles ouverts, qui ont tendance à se refermer lorsqu'ils sont reproduits. **Les caractères d'imprimante à points, de machine à écrire ou écrits à la main ne sont pas acceptables.** Les illustrations de dimensions semblables doivent afficher le même style de police et la même dimension de caractère. Les imprimés originaux des **spectromètres RMN, IR, RPE,** etc. ne sont pas acceptables. Ils doivent être retracés au propre.

Cartes

Les cartes doivent avoir des **motifs clairs et gras**, et comporter les longitudes et latitudes (ou les coordonnées de Mercator transverses universelles) de même qu'une échelle graphique, ceci afin de pouvoir repérer avec exactitude l'emplacement du travail. Sur **les cartes du Québec**, le nom officiel des municipalités doit être utilisé (p. ex. Québec, Montréal, Clarke City). De plus, le nom des éléments topographiques doit systématiquement être en français (p. ex. Lac Bienville), à l'exception des noms d'intérêt pancanadien. En effet, ces noms ont une version officielle française et anglaise (p. ex. « Océan Atlantique » et « Atlantic Ocean ») et doivent donc être présentés dans la langue de l'article. La province de Québec, dans les cartes en anglais, doit être désignée « Quebec ». Les auteurs trouveront une liste complète des noms des régions d'intérêt pancanadien dans *Le guide du rédacteur* (p. 236–237, 2e édition, 1996), publié par Travaux publics et Services gouvernementaux Canada, Ottawa, ON K1A 0S5.

Photographies

Les photographies doivent être en ton continu, de première qualité, avec contrastes bien marqués, rognées de façon à ne laisser paraître que les éléments essentiels. Une photographie ou un groupe de photographies doit être préparé de manière à occuper, **sans réduction supplémentaire**, une ou deux colonnes du texte. Les micrographies électroniques et les photomicrographies doivent comporter une échelle graphique à même le cliché. Pour assurer un bon résultat de la reproduction, les auteurs uniformiseront le contraste et la densité de toutes les photographies montées sur une même planche.

Illustrations en couleur

Les illustrations en couleur sont reproduites aux frais de l'auteur. Les auteurs qui désirent en savoir davantage doivent communiquer avec la rédactrice administrative du Journal, Cecily Pearson (613-993-9099; télécopieur : 613-952-7656; courriel : cecily.pearson@nrc-cnrc.gc.ca).

Préparation des fichiers graphiques électroniques

Le logiciel graphique que préconisent les Presses scientifiques du CNRC est CorelDraw! Pour connaître les applications compatibles, les auteurs peuvent se reporter à la liste des programmes graphiques électroniques à pubs.nrc-cnrc.gc.ca/cgi-bin/ps/rp2_prog_f?jees_graphics_f.html.

Les versions PC ou Macintosh des polices True Type ou Type 1 doivent être utilisées. **Les auteurs ne doivent pas se servir des polices de caractères en mode point ou non standard**.

Toutes les illustrations doivent être soumises dans leur dimension de tirage final. Quant aux illustrations comportant plusieurs parties (p. ex., *a*, *b*, *c*, *d*, etc.) crées sur le même logiciel, elles doivent être regroupées dans un seul fichier plutôt que transmises individuellement.

Il convient de garder les illustrations le plus simple possible afin d'éviter les complications. Les auteurs voudront éviter les textures et les fonds grisés compliqués, particulièrement dans les programmes d'illustration vectorielle, puisque ceci risque d'altérer la qualité des illustrations au moment du tirage.

Les **fichiers d'images en mode point** sont produits selon une grille dans laquelle chaque carré (ou pixel) correspond à une nuance de noir, de couleur ou de gris. Un fichier en mode point (ou de données tramées) est défini par le nombre de pixels ou d'éléments d'image par pouce. Comme le pi-

© 2007 NRC Canada

xel est défini comme un point, on parle aussi de « points par pouce » ou « ppp ». Plus la résolution de l'image est élevée, plus le nombre de points sur une surface donnée est élevé. Les illustrations soumises en mode point doivent être de résolution suffisante. Les exigences minimales de résolution sont les suivantes : 600 ppp pour les dessins au trait, 1200 ppp pour les traits fins (les dessins au trait comportant des traits fins ou un fond grisé), 300 ppp pour les similis et les couleurs et 600 ppp pour les combinaisons (similis avec caractères à l'extérieur de l'espace réservé à la photo).

Tous les **fichiers en couleur** soumis doivent être en mode couleur CMJN (cyan, magenta, jaune et noir). Ces couleurs sont utilisées pour l'impression commerciale en polychromie. Les graphiques RVB (rouge, vert et bleu), soit le mode couleur pour la production d'images à l'écran, ne s'impriment pas correctement.

Les **fichiers vectoriels** sont des fichiers d'images composées d'éléments tels que des traits et des formes. Ce type de fichier est habituellement utilisé pour les dessins au trait.

Les éléments en mode point peuvent être importés dans un logiciel vectoriel ou de dessin pour ajouter ou superposer de l'information, des traits, du texte, etc. Les éléments d'image en mode point ne doivent pas être redimensionnés, recadrés, tournés ou manipulés de quelque façon après avoir été importés.

Formats multimédias — Il est maintenant possible d'inclure des extraits audio et vidéo dans les textes intégraux des revues des Presses scientifiques du CNRC publiées en HTML. Les principaux formats multimédias sont acceptés. Pour plus de détails, consultez la liste des fichiers acceptés dans le site Web du Journal.

Directives pour les manuscrits

Guides de style

Il est recommandé d'utiliser, comme guide général dans le domaine de la biologie, *The CSE Manual for Authors, Editors, and Publishers : Scientific Style and Format* (7e édition, 2006), publié par le Council of Science Editors (Reston, VA 20190, É.-U.).

Orthographe

L'orthographe doit respecter celle du *Petit Robert*. Les auteurs sont responsables de l'uniformité de l'orthographe dans l'ensemble du texte. Les accents doivent être insérés sur les majuscules.

Nomenclature, abréviations et acronymes

La nomenclature et les abréviations doivent être conformes aux règles proposées par la Commission des rédacteurs de revues de biochimie de l'Union internationale de biochimie (UIB) en collaboration avec l'UICPA. Il est recommandé d'utiliser, comme guide général dans le domaine de la biologie, *The CSE Manual for Authors, Editors, and Publishers : Scientific Style and Format* (7e édition, 2006), publié par le Council of Biology Editors (Reston, VA 20190, É.-U.). En matière de nomenclature des enzymes, il convient de consulter la publication *Enzymes nomenclature (1992): Recommendations of the Nomenclature Committee of the International Union of Biochemistry and Molecular Biology* (Academic Press, San Diego (Californie)).

Il n'est pas nécessaire de définir les abréviations et les acronymes d'usage courant dans le domaine. Toutes les autres doivent être définis à la première mention dans le texte et ceux ayant plus d'une signification ne devraient pas être utilisés.

Unités de mesure

Il est recommandé de se servir du **Système international d'unités** ou, à tout le moins, de fournir les équivalences en unités SI. Éviter les formes ambiguës, telles que g C/m^2/jour; utiliser plutôt g $C \cdot m^{-2} \cdot jour^{-1}$. Ce système est décrit dans le *Guide de familiarisation au système métrique*, CAN/CSA-Z234.1-00, publié par l'Association canadienne de normalisation (178, boulevard Rexdale, Toronto, ON M9W 1R3, Canada). Pour des raisons pratiques, la Rédaction admet parfois certaines exceptions à l'utilisation du Système international d'unités.

Analyses statistiques

Les hypothèses ou le modèle sous-jacent à toute analyse statistique doit être clairement énoncé. Les symboles * et **, indiquant les niveaux de signification, ne doivent être utilisés que s'ils sont accompagnés des valeurs réelles de la valeur à tester. Il est préférable d'utiliser les valeurs réelles de *p*.

Poissons

Pour le nom des poissons et leur orthographe, le Journal adhère aux recommandations contenues dans *Common and Scientific Names of Fishes from the United States, Canada, and Mexico* (6e éd., Spec. Publ. No. 29, American Fisheries Society, 2004). Pour la nomenclature génétique pour les loci de codage des protéines, le Journal adhère aux recommandations contenues dans Shaklee et al. (Trans. Am. Fish. Soc. **119** : 2–15, 1990).

Nombres

Les nombres de cinq chiffres ou plus sont répartis en groupes de trois à partir du signe décimal, à gauche comme à droite, puis séparés par un espace (pas un point, ni une virgule ou autre symbole); on aura ainsi 23 562 987 et non pas 23,562,987. En français, le signe décimal est la virgule (p. ex. 0,1 mL) et il est précédé d'un zéro pour les nombres entre 1 et –1, sauf pour le zéro. Le symbole × indique la multiplication (p. ex. 3×10^6 et non pas $3 \cdot 10^6$).

Presses scientifiques du CNRC
Conseil national de recherches du Canada
Ottawa, ON K1A 0R6
Canada

Courriel : pubs@nrc-cnrc.gc.ca
URL: pubs.nrc-cnrc.gc.ca
Télécopieur : 613-952-7656

Dernière révision : janvier 2007

© 2007 NRC Canada

Copyright Assignment or Licence

All authors of manuscripts accepted for publication by an NRC Research Press journal are required to assign copyright to the publisher, or to license the publisher to publish the manuscript. Each author should sign one of the following forms, as appropriate:

Assignment of Copyright (Manuscript)	Assigns copyright to the publisher. To be used by **most authors**.
Licence of Crown Copyright (Manuscript)	Licenses the publisher to publish and reuse the manuscript. To be used by authors who cannot assign copyright because they are **public servants in a Commonwealth country** (such as Canada, UK, Australia).
Publication Agreement (US Official)	Declares that the author is an **official of the US government**, in which case there is no US copyright on the manuscript.

These forms follow and are also available on the NRC Research Press website at http://pubs.nrc-cnrc.gc.ca/rp/rptemp/copyright_e.pdf.

National Research Council Canada | Conseil national de recherches Canada

Assignment of Copyright (Manuscript)

TO: **NATIONAL RESEARCH COUNCIL OF CANADA** (hereinafter "NRC")
Research Press, 1200 Montreal Road Ottawa, Ontario K1A 0R6

FROM: .....

.....

.....
(name and address of copyright holder or authorized signing officer of institution, government or corporation)

1. This refers to the manuscript entitled: .....
(hereinafter the "Manuscript"), manuscript number....., written by the following author(s):
.....
for publication in: .....

2. I declare that the authors qualify for authorship. I declare that the manuscript, or its equivalent, has not been submitted for publication elsewhere. If it is accepted for publication by the NRC, I will ensure that it, or its equivalent, is not submitted for publication elsewhere.

3. I further declare that I am:
(check only one option)

☐	the sole author of the Manuscript and the sole owner of the copyright in the Manuscript,	and→	I assign to NRC the entire copyright in the Manuscript.
☐	a co-author of the Manuscript and a part owner of the copyright in the Manuscript, in conjunction with interests held by co-authors, or their employers,	and→	I assign to NRC my entire interest in the copyright in the Manuscript, and I expect the co-authors to also sign a form like this one.
☐	an agent of my employer with authority to assign the copyright in the Manuscript owned by the employer, who is:	and→	I assign to NRC, on behalf of my employer, my employer's entire interest in the copyright in the Manuscript.

4. I also declare that, to the best of my knowledge and belief, the Manuscript does not infringe on the copyright or other proprietary rights of any third party.

5. I understand that my submission of this Manuscript does not guarantee publication. If the Manuscript is withdrawn, rejected, or not published within 2 years after acceptance, the assignment is revoked.

SIGNED at ..... on .....
(City, Province or State) *(Date)*

PER: .....
(Signature)

NAME & TITLE: .....
(Please Print)

.....

.....

(10/2005)

National Research Council Canada | Conseil national de recherches Canada

License of Crown Copyright (Manuscript)

TO: **NATIONAL RESEARCH COUNCIL OF CANADA** (hereinafter "NRC")
Research Press, 1200 Montreal Road Ottawa, Ontario K1A 0R6

FROM: .....

.....

.....

(name and address of copyright holder or authorized signing officer of government)

1. This refers to the manuscript entitled: .....

(hereinafter the "Manuscript"), manuscript number....., written by the following author(s):

.....

for publication in: .....

2. I declare that the authors qualify for authorship. I declare that the manuscript, or its equivalent, has not been submitted for publication elsewhere. If it is accepted for publication by the NRC, I will ensure that it, or its equivalent, is not submitted for publication elsewhere.

3. I further declare that I am a public servant in Canada (federal, provincial or territorial), the United Kingdom, or other Commonwealth country where the copyright in the Manuscript is owned by Her Majesty, and I have obtained the approval of my employer, according to the terms of my employment, to grant NRC a non-exclusive, perpetual, irrevocable, royalty-free, worldwide right and license to distribute, edit, publish, or re-publish the Manuscript in all media and all formats now known or hereafter devised on a world-wide basis, and to grant others the right to reproduce the published version.

4. I also declare that to the best of my knowledge and belief that the Manuscript does not infringe on the copyright or other proprietary rights of any third party.

5. I understand that my submission of this Manuscript does not guarantee publication. If the Manuscript is withdrawn, rejected, or not published within 2 years after acceptance, the license is revoked.

(To be signed by the author or by his/her copyright authority.)

SIGNED at ..... on .....
(City, Province or State) *(Date)*

PER: .....
(Signature)

NAME & TITLE: .....
(Please Print)

.....

.....

Publication Agreement (US official) (Manuscript)

TO: **NATIONAL RESEARCH COUNCIL OF CANADA** (hereinafter "NRC")
Research Press, 1200 Montreal Road Ottawa, Ontario K1A 0R6

FROM: .....

.....

.....
(name and address of authorized signing officer US government)

1. This refers to the manuscript entitled: .....
(hereinafter the "Manuscript"), manuscript number....., written by the following author(s):
.....
for publication in: .....

2. I declare that the authors qualify for authorship. I declare that the manuscript, or its equivalent, has not been submitted for publication elsewhere. If it is accepted for publication by the NRC, I will ensure that it, or its equivalent, is not submitted for publication elsewhere.

3. I declare that I am an official of the government of the United States of America, and I confirm that the Manuscript is a work created solely by U.S. government employees as part of their official duties and as such is expressly excluded from U.S. Copyright protection, and I assign to NRC, on behalf of my employer, my employer's entire interest in any copyright in the Manuscript that may exist outside the U.S.

4. I also declare that to the best of my knowledge and belief that the Manuscript does not infringe on the copyright or other proprietary rights of any third party.

5. I understand that my submission of this Manuscript does not guarantee publication. If the Manuscript is withdrawn, rejected, or not published within 2 years after acceptance, the license is revoked.

(To be signed by the author or by the authorized signing officer)

SIGNED at ..... on .....
(City, Province or State) *(Date)*

PER: .....
(Signature)

NAME & TITLE: .....
(Please Print)
.....
.....

L'auteur d'un manuscrit que les Presses scientifiques du CNRC acceptent de publier dans une de leurs revues doit céder son droit d'auteur à l'éditeur ou autoriser l'éditeur à publier le manuscrit. Chaque auteur doit signer un des formulaires décrits ci-après, selon le cas.

Cession du droit d'auteur (manuscrit)	Cède le droit d'auteur à l'éditeur. Formulaire utilisé par **la plupart des auteurs**.
Licence de droit d'auteur de la Couronne (manuscrit)	Autorise l'éditeur à publier et à réutiliser le manuscrit. Formulaire utilisé par les auteurs qui ne peuvent pas céder leur droit d'auteur parce qu'ils sont **fonctionnaires dans un pays du Commonwealth** (p. ex. le Canada, le Royaume-Uni ou l'Australie).
Entente de publication (fonctionnaire des États-Unis)	Déclare que l'auteur est **fonctionnaire du gouvernement des États-Unis**. Par conséquent, le manuscrit est exclu de la protection du droit d'auteur des États-Unis.

Vous trouverez ces formulaires ci-après ainsi que dans le site Web des Presses scientifiques du CNRC à http://pubs.nrc-cnrc.gc.ca/rp/rptemp/copyright_f.pdf.

National Research Council Canada | Conseil national de recherches Canada

Cession du droit d'auteur (manuscrit)

DESTINATAIRE : **CONSEIL NATIONAL DE RECHERCHES CANADA** (ci-après appelé CNRC)
Presses scientifiques, 1200, chemin Montréal, Ottawa (Ontario) K1A 0R6

EXPÉDITEUR : .....

.....

.....

(nom et adresse du titulaire du droit d'auteur ou de l'agent autorisé de l'institution, du gouvernement ou de la société)

1. La présente cession porte sur le manuscrit intitulé .....

(ci-après appelé Manuscrit), manuscrit numéro ....., rédigé par (inscrire le nom du ou des auteurs)

.....

à des fins de publication dans .....

2. Je déclare que la paternité du Manuscrit peut bel et bien être attribuée aux auteurs. Je déclare que le Manuscrit, ou son équivalent, n'a pas été soumis à quelque autre organisme à des fins de publication. Si le CNRC accepte de publier le Manuscrit, je veillerai à ce que celui-ci, ou son équivalent, ne soit soumis à aucun autre organisme à des fins de publication.

3. En outre, je déclare que je suis :
(ne cochez qu'une option)

☐ le seul auteur du Manuscrit et le seul titulaire de droit d'auteur afférent au Manuscrit,	et→	je cède au CNRC le droit d'auteur intégral afférent au Manuscrit.
☐ coauteur du Manuscrit et cotitulaire du droit d'auteur afférent au Manuscrit, de concert avec des coauteurs ou leurs employeurs,	et→	je cède au CNRC ma part entière du droit d'auteur afférent au Manuscrit et m'attends à ce que les coauteurs signent une entente semblable.
☐ un agent de mon employeur ayant le pouvoir de céder le droit d'auteur afférent au Manuscrit qui appartient à mon employeur, nommément	et→	je cède au CNRC, au nom de mon employeur, la part entière du droit d'auteur afférent au Manuscrit qui appartient à mon employeur.

4. Je déclare aussi que, au meilleur de mes connaissances, le Manuscrit ne viole aucun droit d'auteur ni aucun autre droit de propriété de toute tierce partie.

5. Je comprends que la soumission du Manuscrit ne garantit aucunement sa publication. Si le Manuscrit est retiré ou rejeté, ou s'il n'est pas publié dans les deux années qui suivent l'acceptation de la présente cession, cette dernière sera automatiquement révoquée.

SIGNÉ à ..... le .....
(ville, province ou État) *(date)*

PAR : .....
(signature)

NOM ET TITRE: .....
(en caractères d'imprimerie s.v.p.) .....

.....

National Research Council Canada | Conseil national de recherches Canada

Licence de droit d'auteur de la Couronne (manuscrit)

DESTINATAIRE : **CONSEIL NATIONAL DE RECHERCHES CANADA** (ci-après appelé CNRC)
Presses scientifiques, 1200, chemin Montréal, Ottawa (Ontario) K1A 0R6

EXPÉDITEUR : .....

.....

.....

(nom et adresse du titulaire du droit d'auteur ou de l'agent autorisé du gouvernement)

1. La présente licence porte sur le manuscrit intitulé .....

(ci-après appelé Manuscrit), manuscrit numéro .....rédigé par (inscrire le nom du ou des auteurs)

.....;

à des fins de publication dans .....

2. Je déclare que la paternité du Manuscrit peut bel et bien être attribuée aux auteurs. Je déclare que le Manuscrit, ou son équivalent, n'a pas été soumis à quelque autre organisme à des fins de publication. Si le CNRC accepte de publier le Manuscrit, je veillerai à ce que celui-ci, ou son équivalent, ne soit soumis à aucun autre organisme à des fins de publication.

3. En outre, je déclare que je suis fonctionnaire au Canada (gouvernement fédéral, provincial ou territorial), au Royaume-Uni ou dans tout autre pays du Commonwealth, où le droit d'auteur afférent au Manuscrit appartient à Sa Majesté. J'ai obtenu de mon employeur, conformément à mes conditions d'emploi, l'autorisation d'accorder au CNRC à l'échelle mondiale, sans paiement de redevances, un droit non exclusif, perpétuel, irrévocable et pouvant donner lieu à l'octroi d'une licence de distribution, d'édition, de publication ou de réédition du Manuscrit sur tous les supports et dans tous les formats connus actuellement ou conçus ultérieurement sur la scène internationale, ainsi qu'une permission de conférer à des tiers le droit de reproduire la version publiée.

4. Je déclare aussi que, au meilleur de mes connaissances, le Manuscrit ne viole aucun droit d'auteur ni aucun autre droit de propriété de toute tierce partie.

5. Je comprends que la soumission du Manuscrit ne garantit aucunement sa publication. Si le Manuscrit est retiré ou rejeté, ou s'il n'est pas publié dans les deux années qui suivent l'acceptation de la présente licence, cette dernière sera automatiquement révoquée.

(La présente doit être signée par l'auteur ou l'agent autorisé.)

SIGNÉ à ..... le .....
(ville, province ou État) *(date)*

PAR : .....
(signature)

NOM ET TITRE: .....
(en caractères d'imprimerie s.v.p.) .....

.....

National Research Council Canada | Conseil national de recherches Canada

Entente de publication (fonctionnaire des États-Unis) (manuscrit)

DESTINATAIRE : **CONSEIL NATIONAL DE RECHERCHES CANADA** (ci-après appelé CNRC)
Presses scientifiques, 1200, chemin Montréal, Ottawa (Ontario) K1A 0R6

EXPÉDITEUR : .....

.....

.....

(nom et adresse de l'agent autorisé du gouvernement des États-Unis)

1. La présente entente porte sur le manuscrit intitulé .....

(ci-après appelé Manuscrit), manuscrit numéro ....., rédigé par (inscrire le nom du ou des auteurs)

.....,

à des fins de publication dans .....

2. Je déclare que la paternité du Manuscrit peut bel et bien être attribuée aux auteurs. Je déclare que le Manuscrit, ou son équivalent, n'a pas été soumis à quelque autre organisme à des fins de publication. Si le CNRC accepte de publier le Manuscrit, je veillerai à ce que celui-ci, ou son équivalent, ne soit soumis à aucun autre organisme à des fins de publication.

3. Je déclare que je suis fonctionnaire du gouvernement des États-Unis et je confirme que le Manuscrit est l'œuvre exclusive d'employés du gouvernement des É.-U. dans le cadre de leurs fonctions officielles. Par conséquent, le Manuscrit est expressément exclu de la protection du droit d'auteur américain, et je cède au CNRC, au nom de mon employeur, la part entière de quelque droit d'auteur afférent au Manuscrit en vigueur ailleurs qu'aux É.-U.

4. Je déclare aussi que, au meilleur de mes connaissances, le Manuscrit ne viole aucun droit d'auteur ni aucun autre droit de propriété de toute tierce partie.

5. Je comprends que la soumission du Manuscrit ne garantit aucunement sa publication. Si le Manuscrit est retiré ou rejeté, ou s'il n'est pas publié dans les deux années qui suivent l'acceptation de la présente entente, cette dernière sera automatiquement révoquée.

(La présente doit être signée par l'auteur ou l'agent autorisé.)

SIGNÉ à ..... le .....
(ville, province ou État) *(date)*

PAR : .....
(signature)

NOM ET TITRE: .....
(en caractères d'imprimerie s.v.p.) .....

.....

Steven M. Seiler and Ernest R. Keeley	**127–135**	Morphological and swimming stamina differences between Yellowstone cutthroat trout (*Oncorhynchus clarkii bouvieri*), rainbow trout (*Oncorhynchus mykiss*), and their hybrids
Trond Kristiansen, Øyvind Fiksen, and Arild Folkvord	**136–151**	Modelling feeding, growth, and habitat selection in larval Atlantic cod (*Gadus morhua*): observations and model predictions in a macrocosm environment
Ronan Fablet, Françoise Daverat, and Hélène De Pontual	**152–165**	Unsupervised Bayesian reconstruction of individual life histories from otolith signatures: case study of Sr:Ca transects of European eel (*Anguilla anguilla*) otoliths
Nicolas Bez, David Reid, Suzanna Neville, Yves Vérin, Vidar Hjellvik, and Hans D. Gerritsen	**166–180**	Acoustic data collected during and between bottom trawl stations: consistency and common trends

National Research Council Canada
Ottawa, Canada K1A 0R6

Conseil national de recherches Canada
Ottawa, Canada K1A 0R6

Postage paid at Ottawa
Publications mail
Registration No. 40062591

Port payé à Ottawa
Poste-publication
Enregistrement n° 40062591

USPS periodical postage paid at Plattsburgh, NY 12901, USA

Canadian Journal of Fisheries and Aquatic Sciences

Volume 64, Number 1, January 2007

Journal canadien des sciences halieutiques et aquatiques

Volume 64, numéro 1, janvier 2007

RAPID COMMUNICATION		COMMUNICATION RAPIDE
Chris Gibbins, Damià Vericat, Ramon J. Batalla, and Carlos M. Gomez	**1–5**	Shaking and moving: low rates of sediment transport trigger mass drift of stream invertebrates
ARTICLES		ARTICLES
Steven E. Campana, Alexandra Valentin, Jean-Marie Sévigny, and Don Power	**6–18**	Tracking seasonal migrations of redfish (*Sebastes* spp.) in and around the Gulf of St. Lawrence using otolith elemental fingerprints
Rachel M. Cassoff, Steven E. Campana, and Sigmund Myklevoll	**19–29**	Changes in baseline growth and maturation parameters of Northwest Atlantic porbeagle, *Lamna nasus*, following heavy exploitation
Katherine A. Bucklin, Michael A. Banks, and Dennis Hedgecock	**30–42**	Assessing genetic diversity of protected coho salmon (*Oncorhynchus kisutch*) populations in California
Mark R. Loewen, Josef Daniel Ackerman, and Paul F. Hamblin	**43–57**	Environmental implications of stratification and turbulent mixing in a shallow lake basin
Katharine L. Pemberton, Ralph E.H. Smith, Greg M. Silsbe, Todd Howell, and Susan B. Watson	**58–73**	Controls on phytoplankton physiology in Lake Ontario during the late summer: evidence from new fluorescence methods
Blake Matthews and Asit Mazumder	**74–83**	Distinguishing trophic variation from seasonal and size-based isotopic (δ^{15}N) variation of zooplankton
Andrew Davie, Mark J.R. Porter, Niall R. Bromage, and Herve Migaud	**84–97**	The role of seasonally altering photoperiod in regulating physiology in Atlantic cod (*Gadus morhua*). Part I. Sexual maturation
Andrew Davie, Mark J.R. Porter, Niall R. Bromage, and Herve Migaud	**98–112**	The role of seasonally altering photoperiod in regulating physiology in Atlantic cod (*Gadus morhua*). Part II. Somatic growth
Fiona D. Johnston, John R. Post, Craig J. Mushens, Jim D. Stelfox, Andrew J. Paul, and Brian Lajeunesse	**113–126**	The demography of recovery of an overexploited bull trout, *Salvelinus confluentus*, population

Continued on inside back cover / Suite au verso

Front cover: Iboko Saito/Toshiyuki Tajima/Dex Image/Getty Images.

Page couverture : Iboko Saito/Toshiyuki Tajima/Dex Image/Getty Images.

Canada

Printed in Canada by / Imprimé au Canada par
NRC Reprographic Services / Service de reprographie CNRC
Page production by / Mise en page par
NRC Research Press / Presses scientifiques du CNRC

0706-652X(200701)64:1;1-B